CLASSICAL AND NOVEL BIOMARKERS FOR CARDIOVASCULAR DISEASE

EDITED BY: Maria Perticone, Alessio Molfino and Raffaele Maio
PUBLISHED IN: Frontiers in Cardiovascular Medicine

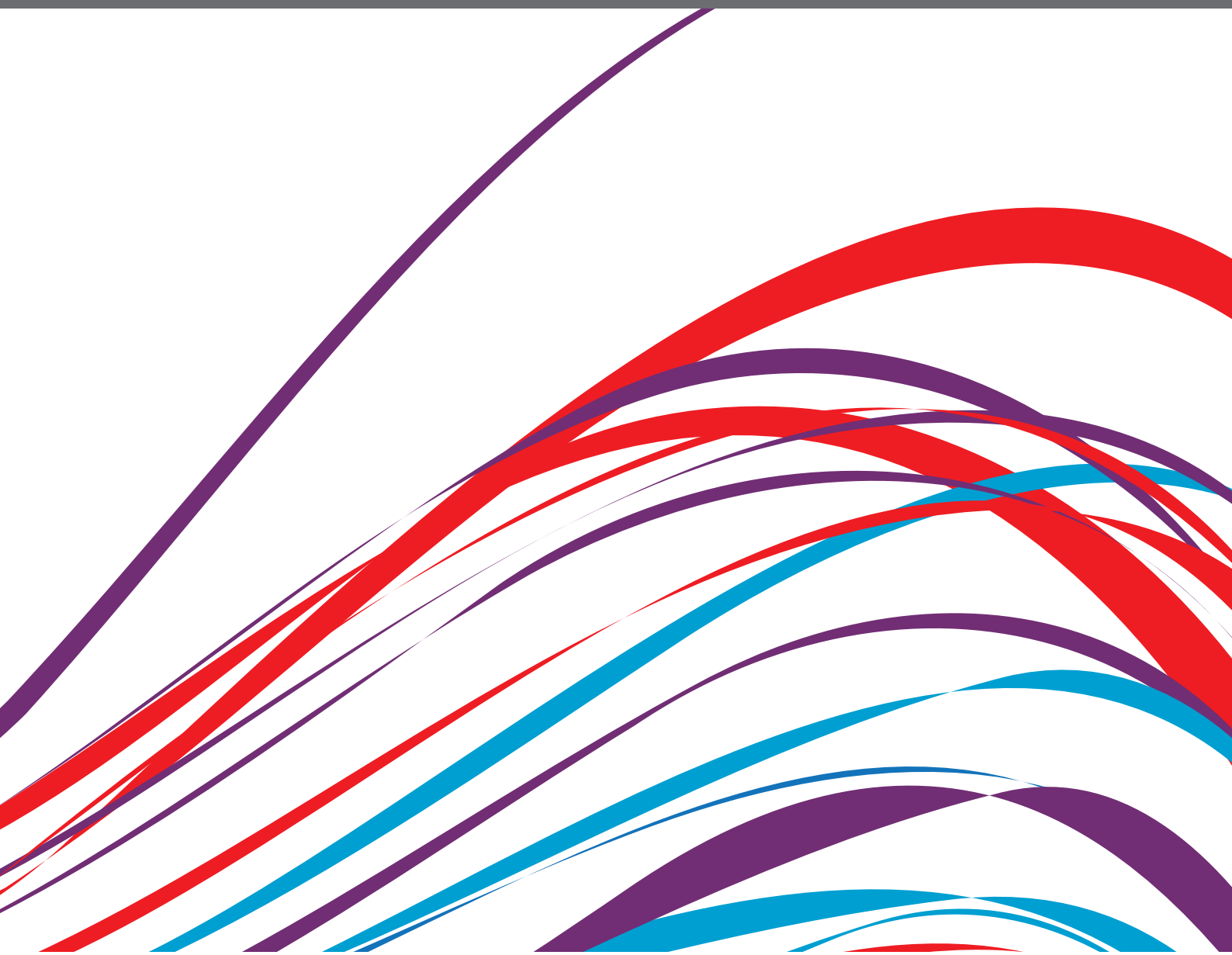

frontiers Research Topics

ISSN 1664-8714
ISBN 978-2-88976-534-8
DOI 10.3389/978-2-88976-534-8

About Frontiers

Frontiers is more than just an open-access publisher of scholarly articles: it is a pioneering approach to the world of academia, radically improving the way scholarly research is managed. The grand vision of Frontiers is a world where all people have an equal opportunity to seek, share and generate knowledge. Frontiers provides immediate and permanent online open access to all its publications, but this alone is not enough to realize our grand goals.

Frontiers Journal Series

The Frontiers Journal Series is a multi-tier and interdisciplinary set of open-access, online journals, promising a paradigm shift from the current review, selection and dissemination processes in academic publishing. All Frontiers journals are driven by researchers for researchers; therefore, they constitute a service to the scholarly community. At the same time, the Frontiers Journal Series operates on a revolutionary invention, the tiered publishing system, initially addressing specific communities of scholars, and gradually climbing up to broader public understanding, thus serving the interests of the lay society, too.

Dedication to Quality

Each Frontiers article is a landmark of the highest quality, thanks to genuinely collaborative interactions between authors and review editors, who include some of the world's best academicians. Research must be certified by peers before entering a stream of knowledge that may eventually reach the public - and shape society; therefore, Frontiers only applies the most rigorous and unbiased reviews.
Frontiers revolutionizes research publishing by freely delivering the most outstanding research, evaluated with no bias from both the academic and social point of view. By applying the most advanced information technologies, Frontiers is catapulting scholarly publishing into a new generation.

What are Frontiers Research Topics?

Frontiers Research Topics are very popular trademarks of the Frontiers Journals Series: they are collections of at least ten articles, all centered on a particular subject. With their unique mix of varied contributions from Original Research to Review Articles, Frontiers Research Topics unify the most influential researchers, the latest key findings and historical advances in a hot research area! Find out more on how to host your own Frontiers Research Topic or contribute to one as an author by contacting the Frontiers Editorial Office: frontiersin.org/about/contact

CLASSICAL AND NOVEL BIOMARKERS FOR CARDIOVASCULAR DISEASE

Topic Editors:
Maria Perticone, University of Magna Graecia, Italy
Alessio Molfino, Sapienza University of Rome, Italy
Raffaele Maio, Magna Græcia University, Italy

Citation: Perticone, M., Molfino, A., Maio, R., eds. (2022). Classical and Novel Biomarkers for Cardiovascular Disease. Lausanne: Frontiers Media SA.
doi: 10.3389/978-2-88976-534-8

Table of Contents

frontiers | Frontiers in Cardiovascular Medicine

EDITORIAL
published: 15 June 2022
doi: 10.3389/fcvm.2022.943227

Editorial: Classical and Novel Biomarkers for Cardiovascular Disease

Maria Perticone[1]*, *A. Molfino*[2] *and R. Maio*[3]

[1] Department of Medical and Surgical Sciences, Magna Graecia University, Catanzaro, Italy, [2] Department of Translational and Precision Medicine, Sapienza University, Rome, Italy, [3] Azienda Ospedaliero-Universitaria Mater Domini, Catanzaro, Italy

Keywords: cardiovascular disease, biomarkers, cardiovascular event, screening, follow-up

Editorial on the Research Topic

Classical and Novel Biomarkers for Cardiovascular Disease

Despite several efforts to prevent and treat atherosclerosis, cardiovascular disease (CVD) still remains a major cause of morbidity and mortality worldwide, and its prevalence is supposed to increase in the next years (1). In the last decades we observed a marked reduction in mortality rates for coronary heart disease (CHD) in Europe and United States of America, due to the improvements in acute care and prevention strategies; on the contrary, in the same period, both prevalence and mortality for CVD exponentially increased in low- and middle-income Countries, likely due to globalization (2).

In addition, CVD represents one of the most common comorbidities for several chronic diseases, including type 2 diabetes mellitus (T2DM), chronic kidney disease (CKD), and chronic obstructive pulmonary disease (COPD).

For these reasons, the use of biomarkers appears the most convenience option to screen and follow-up patients with CVD. The ideal biomarker should be widely available, low-cost and reliable. In the past decades several biomarkers have been proposed and used with this purpose (i.e., C-reactive protein, uric acid, troponin, natriuretic peptides, etc.) and several others are emerging (gamma-glutamyltransferase, miRNA, etc). The majority of these biomarkers are used to predict cardiovascular risk in specific settings of population.

To our knowledge, none of the existing biomarkers for cardiovascular disease are routinely used and scientifically validated among the general population and do not appear in cardiovascular risk scores. Thus, we proposed a Research Topic aimed to spread knowledge about useful novel biomarkers to predict and/or to manage cardiovascular risk, as well as to systematically analyze previously published data in order to draw robust conclusions on the use of specific biomarkers in the field of cardiovascular disease.

The Research Topic obtained a great success, since we received 28 submissions of which 15 have been published. Among these, we received 13 original articles and two reviews. The Research Topics of the published articles covered many of the most important and prevalent CVD, from heart failure, to light chain cardiac amyloidosis, pulmonary hypertension, acute myocardial infarction, etc.

The Research Topic collected both animal and human studies. In particular, Zaky et al. investigated the association of different echocardiographic, biochemical, and electrocardiographic correlates with progressive pulmonary arterial hypertension in rats. They demonstrated that, beyond classical invasive procedures used to assess myocardial and pulmonary vascular structure and function, also non-invasive methods (i.e., electrocardiogram and echocardiogram) can be used. Among biochemical biomarkers, authors identified plasma myosin light chain, cardiac

OPEN ACCESS

Edited and reviewed by:
Junjie Xiao,
Shanghai University, China

***Correspondence:**
Maria Perticone
mariaperticone@unicz.it

Specialty section:
This article was submitted to General Cardiovascular Medicine, a section of the journal Frontiers in Cardiovascular Medicine

Received: *13 May 2022*
Accepted: *16 May 2022*
Published: *15 June 2022*

Citation:
Perticone M, Molfino A and Maio R (2022) Editorial: Classical and Novel Biomarkers for Cardiovascular Disease. Front. Cardiovasc. Med. 9:943227. doi: 10.3389/fcvm.2022.943227

troponin T, and fatty acid-binding protein-3 as useful tools for monitoring pulmonary hypertension progression. On the contrary, Zhao et al. demonstrated, in a population of 232 patients affected by idiopathic pulmonary arterial hypertension, that echocardiographic attenuated right heart remodeling is an independent non-invasive determinant of prognosis in this setting.

Remaining in the field of pulmonary hypertension, Zhang et al. demonstrated the role of CA125 as a new predictor of clinical impairment in patients with pulmonary hypertension and their results allowed to establish a cut-off value of CA 125 > 35 U/ml that is associated with 2-folds increased risk of 1-year clinical worsening. CA 125 has also been associated with poor prognosis in patients with light-chain cardiac amyloidosis, as demonstrated in the study by Li et al. In particular, the authors found that patients with high levels of CA 125 had a median overall survival time of 5 months, compared with the 25 months of patients with normal values of CA 125. Of note, the ROC curve showed that the prediction accuracy of CA 125 was not inferior to that of cardiac troponin T, N-terminal pro-B-type natriuretic peptide and LDH in patients with light-chain cardiac amyloidosis.

Another rare disease, such as dilated cardiomyopathy, has been studied by Ma et al.; in this study the authors utilized the Robust Rank Aggregation method to identify expressed genes responsible of dilated cardiomyopathy, allowing to identify a 7-gene signature predictive of dilated cardiomyopathy.

Another important Research Topic addressed in this collection is the cardiovascular risk assessment of hemodialysis patients. Hwang et al. investigated the role of circulating neprilysin as a biomarker of cardiovascular events in a wide population of hemodialysis patients. The authors demonstrated that the cumulative event rate of cardiac events was higher in patients in the 3rd tertile of neprilysin values; in addition, circulating neprilysin resulted as an independent predictor of cardiovascular events in this setting of patients, opening new scenarios on the use of this molecule as a biomarker of cardiovascular events in hemodialysis patients. A study conducted by Kim et al. in the same population demonstrated the role of another molecule, vascular adhesion protein-1 (VAP-1), as a predictor of cardiovascular events in this setting of patients. Taken together, these studies represent an important step in the cardiovascular risk stratification of hemodialysis patients.

When considering coronary artery disease, two original research articles have been published in this Research Topic; the paper by Le et al. focused on the role of conventional indicators of lipid oxidation, in particular of oxylipins, in discriminating among the number of diseased coronary arteries and in predicting 5-year outcomes in symptomatic patients. Interestingly, the authors found that a panel of five oxylipins allows to diagnose three diseased arteries with 100% sensitivity and 70% specificity, thus helping clinicians in the diagnostic and therapeutic process of coronary artery disease. Similarly, the study by Yifan et al. investigated the role of ferroptosis (a novel type of programmed cell death and marker of cell injury usually studied in cancer development) as a biomarker of myocardial cell injury in circulating endothelial cells; they concluded that ferroptosis-related genes might be used as potential specific diagnostic markers for myocardial infarction. Remaining in the setting of acute cardiovascular disease, Yang S. et al. demonstrated that Neutrophil Extracellular Trap Levels show a significant diagnostic and predictive value of disease severity in patients with acute aortic dissection, while Zhai et al. used plasma osmolarity to predict in-hospital cardiac mortality in cardiac intensive care unit patients; interestingly, they observed that both hyposmolarity and hyperosmolarity were independently associated with an increased in-hospital cardiac mortality ("*U*"-shaped relationship).

Of note, this Research Topics also included the results of a multicenter prospective study conducted by Mise et al., that demonstrated that the urinary excretion of high-mannose glycan may be a valuable marker for predicting cardiovascular events in type 2 diabetes mellitus patients.

The two reviews of the Research Topic were both focused on heart failure. In particular, the meta-analysis by Yang C. et al. evaluated the diagnostic value of soluble suppression of tumorigenicity (sST2) in heart failure, with non-conclusive results. The review by Janssen et al. investigated another potential application of natriuretic peptides in heart failure; in particular, the authors analyzed the prognostic value of circulating natriuretic peptides before left ventricular assist device implantation for all-cause mortality and major adverse events, concluding that natriuretic peptides levels are of limited value in patients selection for left ventricular assist device therapy.

Taken together, all these papers underline the need to have simple, cost-effective and easily available biomarkers for the diagnosis and follow-up of CVD. The wide number of biomarkers investigated in this Research Topic can help physicians now and in the next future to better manage CVD, highly impacting on patient's prognosis and quality of life.

AUTHOR CONTRIBUTIONS

MP, AM, and RM wrote the Editorial and approved the last version. All authors contributed to the article and approved the submitted version.

REFERENCES

1. Bansilal S, Castellano JM, Fuster V. Global burden of CVD: focus on secondary prevention of cardiovascular disease. *Int J Cardiol.* (2015) 201(Suppl.1):S1–7. doi: 10.1016/S0167-5273(15)31026-3
2. Alwan A. *Global Status Report on Non-communicable Diseases 201*. Geneva: World Health Organization (2011).

Conflict of Interest: The authors declare that the research was conducted in the absence of any commercial or financial relationships that could be construed as a potential conflict of interest.

Publisher's Note: All claims expressed in this article are solely those of the authors and do not necessarily represent those of their affiliated organizations, or those of the publisher, the editors and the reviewers. Any product that may be evaluated in this article, or claim that may be made by its manufacturer, is not guaranteed or endorsed by the publisher.

frontiers in Cardiovascular Medicine

ORIGINAL RESEARCH
published: 21 April 2021
doi: 10.3389/fcvm.2021.645786

Plasma Oxylipins: A Potential Risk Assessment Tool in Atherosclerotic Coronary Artery Disease

D. Elizabeth Le[1†], Manuel García-Jaramillo[2,3,4†‡], Gerd Bobe[3,5†], Armando Alcazar Magana[3,6], Ashish Vaswani[3,6], Jessica Minnier[7], Donald B. Jump[2,3], Diana Rinkevich[1], Nabil J. Alkayed[1,8], Claudia S. Maier[3,6] and Sanjiv Kaul[1*]*

[1] Knight Cardiovascular Institute, Oregon Health and Science University, Portland, OR, United States, [2] Nutrition Program, School of Biological and Population Health Sciences, Oregon State University, Corvallis, OR, United States, [3] Linus Pauling Institute, Oregon State University, Corvallis, OR, United States, [4] Helfgott Research Institute, National University of Natural Medicine, Portland, OR, United States, [5] Department of Animal and Rangeland Sciences, Oregon State University, Corvallis, OR, United States, [6] Department of Chemistry, Oregon State University, Corvallis, OR, United States, [7] Department of Biostatistics and Knight Cancer Institute, Oregon Health and Science University, Portland, OR, United States, [8] Department of Anesthesiology and Perioperative Medicine, Oregon Health and Science University, Portland, OR, United States

Background: While oxylipins have been linked to coronary artery disease (CAD), little is known about their diagnostic and prognostic potential.

Objective: We tested whether plasma concentration of specific oxylipins may discriminate among number of diseased coronary arteries and predict median 5-year outcomes in symptomatic adults.

Methods: Using a combination of high-performance liquid chromatography (HPLC) and quantitative tandem mass spectrometry, we conducted a targeted analysis of 39 oxylipins in plasma samples of 23 asymptomatic adults with low CAD risk and 74 symptomatic adults (≥70% stenosis), aged 38–87 from the Greater Portland, Oregon area. Concentrations of 22 oxylipins were above the lower limit of quantification in >98% of adults and were compared, individually and in groups based on precursors and biosynthetic pathways, in symptomatic adults to number of diseased coronary arteries [(1) $n = 31$; (2) $n = 23$; (3) $n = 20$], and outcomes during a median 5-year follow-up (no surgery: $n = 7$; coronary stent placement: $n = 24$; coronary artery bypass graft surgery: $n = 26$; death: $n = 7$).

Results: Plasma levels of six quantified oxylipins decreased with the number of diseased arteries; a panel of five oxylipins diagnosed three diseased arteries with 100% sensitivity and 70% specificity. Concentrations of five oxylipins were lower and one oxylipin was higher with survival; a panel of two oxylipins predicted survival during follow-up with 86% sensitivity and 91% specificity.

Conclusions: Quantification of plasma oxylipins may assist in CAD diagnosis and prognosis in combination with standard risk assessment tools.

Keywords: coronary artery disease, oxylipins, diagnosis, prognosis, mass spectrometry, LCMS

OPEN ACCESS

Edited by:
Alessio Molfino, Sapienza University of Rome, Italy

Reviewed by:
Yuling Zhang, Sun Yat-Sen Memorial Hospital, China
Paulo M. Dourado, University of São Paulo, Brazil

***Correspondence:**
Sanjiv Kaul
kauls@ohsu.edu
Claudia S. Maier
claudia.maier@oregonstate.edu

[†] These authors have contributed equally to this work and share first authorship

‡Present address:
Manuel García-Jaramillo, Department of Environmental and Molecular Toxicology, Oregon State University, Corvallis, OR, United States

Specialty section:
This article was submitted to General Cardiovascular Medicine, a section of the journal Frontiers in Cardiovascular Medicine

Received: *24 December 2020*
Accepted: *15 March 2021*
Published: *21 April 2021*

Citation:
Le DE, García-Jaramillo M, Bobe G, Alcazar Magana A, Vaswani A, Minnier J, Jump DB, Rinkevich D, Alkayed NJ, Maier CS and Kaul S (2021) Plasma Oxylipins: A Potential Risk Assessment Tool in Atherosclerotic Coronary Artery Disease. Front. Cardiovasc. Med. 8:645786. doi: 10.3389/fcvm.2021.645786

INTRODUCTION

Coronary artery disease (CAD) is the leading cause of death worldwide (1–3). Traditional CAD risk factors such as diabetes, smoking, hypertension, hyperlipidemia, and family history of premature cardiovascular disease (CVD), as well as nontraditional risk factors of rheumatic inflammatory disease, human immunodeficiency disease, and gestational diabetes can assist clinicians in decisions for CAD primary prevention but have limited efficacy in high CAD risk patient management (4). This is currently done using expensive invasive tests, such as exercise stress testing (without or with concomitant imaging for myocardial perfusion and/or function) or measuring the coronary calcium score on X-ray computed tomography (CT). Our objective is to develop a point-of-care blood test that could assist in decision making regarding CAD patient management.

Ruptured arterial plaques are a major reason for adverse cardiac events with resultant thrombus formation that partially or completely impairs blood flow to the heart (5). The progression from asymptomatic to ruptured arterial plaques involves lipid oxidation and inflammation (6, 7). Conventional indicators of lipid oxidation include secondary products such as 4-hydroxynonenal (4-HNE) (8), malondialdehyde (MDA) (9), and oxidized low-density lipoproteins (Ox-LDL) (10), and its associated oxidized phospholipids (11). Technological advancements in soft ionization tandem mass spectrometry (MS/MS) have allowed multiplexed quantification of oxidized lipids in one analytical run and with it the emergence of isoprostanes and oxylipins as indicators of oxidative tissue injuries, implicating oxidative tissue injuries in the pathology of a variety of chronic diseases (3, 12).

Oxylipins are oxidized long and very long chain polyunsaturated fatty acids (PUFA), which are derived from phospholipids. Oxylipins can be classified based on their fatty acid (FA) precursor (**Figure 1**). The dominant precursors of oxylipins are the more proinflammatory omega-6 PUFA linoleic acid (LA; C18:2 $n-6$) and arachidonic acid (ARA; C20:4 $n-6$) and the more anti-inflammatory omega-3 PUFA linolenic acid (LNA; C18:3 $n-3$), eicosapentaenoic acid (EPA; C20:5 $n-3$), and docosahexaenoic acid (DHA; C22:6 $n-3$). The dominant oxylipin biosynthesis pathways are named after the enzymes involved, as follows: lipoxygenases (LOX), cyclooxygenases (COX), cytochrome P450 (CYP450) epoxygenases and hydroxylases, and soluble epoxide hydrolases. Reactive oxygen species (ROS) can initiate the formation of a few, specific oxylipins from PUFAs (13). Prior human studies with limited sample sizes reported elevated concentrations of ARA-derived oxylipins in unstable arterial plaques (14) and ischemic heart tissue (15). Elevated circulating concentrations were observed in individuals after cardiac surgery (16) and those experiencing adverse cardiac events on follow-up (17, 18). Furthermore, CAD patients had higher circulating concentrations of ARA-derived oxylipins than non-CAD adults (19–21).

In the present study, we evaluated whether plasma oxylipins, alone or in panels, may discriminate among number of diseased coronary arteries and predict median 5-year outcomes in high CAD risk symptomatic patients and ≥70% stenosis which, to our knowledge, has not been previously published. In doing so, a point-of-care plasma oxylipin test could assist in decision making regarding CAD patient management. Here, we report results of a small study confirming this hypothesis.

Abbreviations: ACN, acetonitrile; ARA, arachidonic acid; CAD, coronary artery disease; COX, cyclooxygenases; CUDA, 1-cyclohexyl ureido, 3-dodecanoic acid; CVD, cardiovascular diseases; CYP450, cytochrome P450; CYPEPOX, CYP epoxide; DHA, docosahexaenoic acid; EPA, eicosapentaenoic acid; FA, fatty acid; 4-HNE, 4-hydroxynonenal; HPLC-MS/MS, high-performance liquid chromatography tandem mass spectrometry; IMS, ionization mass spectrometry; IPA, isopropanol; LA, linoleic acid; LDL, low-density lipoproteins; LNA, linolenic acid; LOD, limit of detection; LOQ, limit of quantification; LOX, lipoxygenases; MDA, malondialdehyde; MRM, multi-reaction monitoring; PUFA, polyunsaturated fatty acids; ROS, reactive oxygen species; RT, retention time; sEH, soluble epoxide hydrolases.

MATERIALS AND METHODS

Participants and Study Design

The study was approved by the Institutional Review Board of the Oregon Health and Science University (OHSU) in Portland, Oregon. We prospectively enrolled 74 individuals from the greater Portland metropolitan area from October 2012 and January 2017 (IRB00008606) who were referred to OHSU for an invasive coronary angiography because of symptoms suggestive of CAD (median age: 66 years; range: 38–87 years). Inclusion criteria were inducible myocardial ischemia during stress (either on echocardiography or single-photon computed tomography) and ≥70% coronary luminal narrowing of one or more major coronary artery or its major branch on subsequent coronary angiography. Exclusion criteria were <70% coronary stenosis on angiography, prior myocardial infarction, hemodynamically significant valvular heart disease, prior revascularization, or congestive heart failure. The CAD patients were classified as having one-vessel ($n = 31$), two-vessel ($n = 23$), or three-vessel ($n = 20$) CAD and were followed up until November 2019 (**Figure 2**) for a median of 60 months (range: 25–84 months) for adverse events [i.e., coronary stent placement; coronary artery bypass graft (CABG) surgery; death]. Ten CAD patients were lost to follow-up (unable to contact: $n = 8$; declined to follow-up: $n = 2$).

To establish ranges of plasma oxylipin concentrations in low CAD risk populations, we established the Astoria cohort and prospectively enrolled 220 individuals from Astoria, a rural community within the same area as the CAD patients, from July 2016 to February 2017 (IRB00011193). For the current study, we selected individuals of the same age range (range: 38–71 years) that fulfilled all the exclusion criteria ($n = 23$). Exclusion criteria were self-reported history of hyperlipidemia, diabetes, myocardial infarction, ischemia, coronary artery revascularization surgery, coronary atherosclerosis on coronary angiography, active tobacco use, and family history of CAD. Participants from the Astoria and Portland were not age-matched.

Sample Collection and Preparation for Oxylipin Analysis

All participants fasted for at least 6 h before 4.5 mL blood was collected in tubes containing 0.01 M buffered sodium citrate and immediately placed on ice. Blood samples were collected 1–4 h

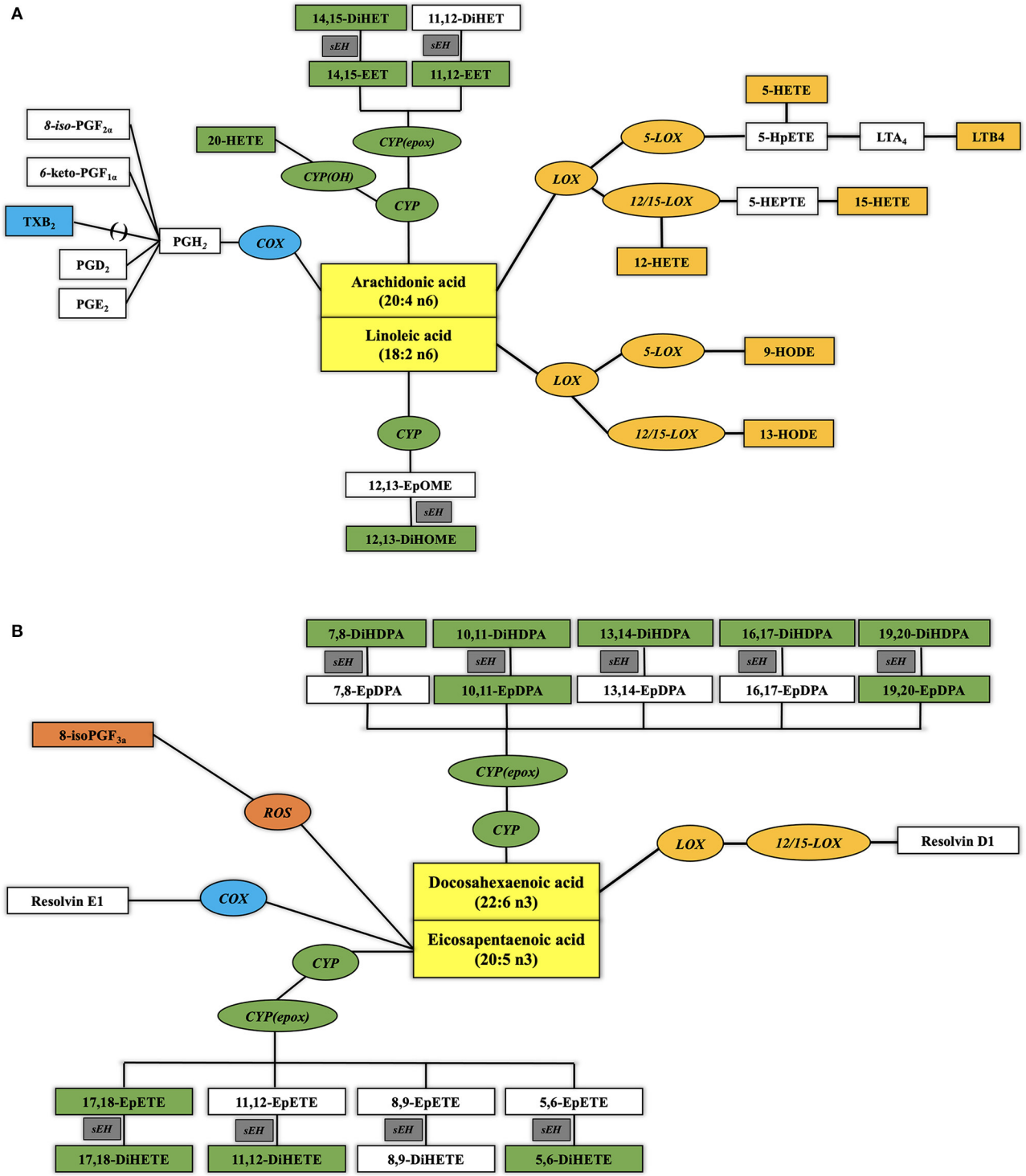

FIGURE 1 | Biosynthetic pathways of plasma oxylipins from omega-6 **(A)** and omega-3 **(B)** polyunsaturated fatty acids (PUFA). Normal text designates PUFA (yellow rectangular boxes) and oxylipins. Italic text designates enzymes involved in the metabolic transformation [blue oval boxes for cyclo-oxygenases or aspirin, orange oval boxes for lipoxygenases or CYP1B1, green oval boxes for cytochrome P450, and gray rectangular boxes for soluble epoxide hydrolase (sEH)] with their quantified oxylipins in the same color and oxylipins below the limit of quantification (LOQ) in noncolored squares. See Abbreviation Index and **Appendix** for full names description.

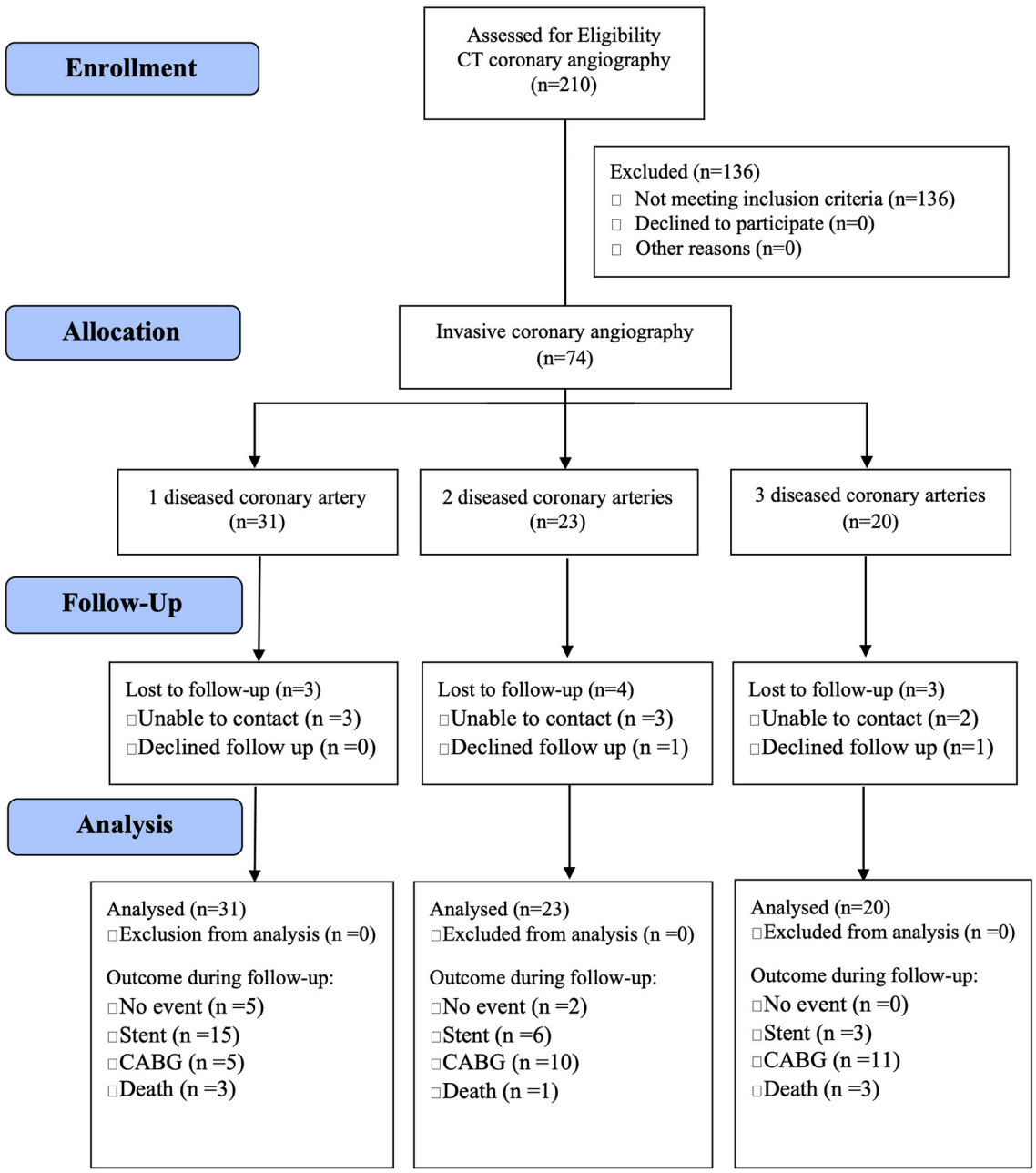

FIGURE 2 | Study flow diagram of adults with diseased coronary arteries (≥70% stenosis) from the greater Portland area, Oregon.

prior to coronary angiography of participants with CAD. Whole blood samples were then centrifuged at 3,000 rpm for 15 min in a refrigerated centrifuge at 4°C, after which the plasma was aliquoted into 1 mL Eppendorf tubes and immediately stored at −80°C until analysis.

Oxylipins from plasma were extracted as described in Pedersen et al. (22) with minor modifications. The internal oxylipin standards used during the extraction (**Supplementary Table 1**) were used to correct the recovery of the quantified oxylipins (23).

Chromatographic and Mass Spectrometric Analysis of Oxylipins

The high-performance liquid chromatography (HPLC) and mass spectrometry methods used for the analysis of plasma oxylipins was based on methods previously described for the analysis of oxylipins in liver (24). The analysis was performed using a Shimadzu Prominence HPLC system (Shimadzu, Columbia, MD) coupled to an Applied Biosystems 4000 QTRAP (AB SCIEX, Framingham, MA). Employing dynamic multireaction monitoring (dMRM), we evaluated 60 oxylipins

in a targeted approach (**Supplementary Figure 1**). For each compound, optimal transitions were determined by flow injection of pure standards using the optimizer application, and transitions were compared with literature when available. A detailed list of MRM transitions and experimental conditions is provided in **Supplementary Table 2**.

Compounds were separated using a Waters Acquity UPLC CSH C18 column (100 mm length × 2.1 mm id; 1.7 μm particle size) with an additional Waters Acquity VanGuard CSH C18 pre-column (5 mm × 2.1 mm id; 1.7 μm particle size). Column oven was set to 60°C. The mobile phase consisted of (A) water containing 0.1% acetic acid and (B) acetonitrile/isopropanol (ACN/IPA) (90/10, *v*/*v*) containing 0.1% acetic acid. Gradient elution (22) was carried out for 22 min at a flow rate of 0.15 ml min^{-1}. Gradient conditions were as follows: 0–1.0 min, 0.1–25% B; 1.0–2.5 min, 25–40% B; 2.5–4.5 min, 40–42% B; 4.5–10.5 min, 42–50% B; 10.5–12.5 min, 50–65% B; 12.5–14 min, 65–75% B; 14–14.5 min, 75–85% B; 14.5–20 min, 85–95% B; 20–20.5 min, 95–95% B; 20.5–22 min, 95–25% B. A 5-μl aliquot of each sample was injected. Limits of detection (LOD) and quantification (LOQ) (**Supplementary Table 1**) were calculated based on one concentration point (0.1 ng μl^{-1}) for each oxylipin and deuterated surrogate.

Data Processing and Statistical Analysis

Raw data from targeted oxylipin analyses were imported into MultiQuant 3.0.2 software (AB SCIEX) in order to perform the alignment and integration of the peaks (obtaining peak areas). This software allows for the correction of metabolite intensity with the intensity of the internal standards. Data obtained with MultiQuant were imported into MarkerView 1.3.1 software (AB SCIEX) for initial data visualization (25).

Data were analyzed using SAS version 9.2 (SAS Ins. Inc., Cary, NC). Demographic and clinical characteristics of groups were compared using Fisher's exact test for binary data and *t*-test for nonbinary data. Concentrations of oxylipins were compared using Wilcoxon rank sum test. To evaluate diagnostic and predictive efficacy of oxylipins, we used logistic regression analysis and calculated receiver operating characteristic (ROC) values, including area under the curves (AUC). Our goal was to identify oxylipin panels that could achieve an ROC of 0.90 or higher. To compare diagnostic and predictive efficacy of oxylipins with current standard risk assessment tool, we compared ROC values of our best oxylipin models with those of the 10-year Framingham general CVD risk scores using the ROCCONTRAST statement in PROC LOGISTIC. We were not able to use the 10-year atherosclerotic CVD risk score of the American College of Cardiology (ACC) because 41 of 74 CAD patient scores could not be calculated. All statistical tests were two sided. Significance was declared at $P \leq 0.05$.

RESULTS

Analysis of Oxylipins

In order to achieve a representative coverage of LA-, ARA-, EPA-, and DHA-derived oxylipins and the enzymatic and nonenzymatic pathways involved in their production, a library with 39 oxylipin standards was analyzed (**Supplementary Table 1**). Our LC-MRM method detected all 39 oxylipins in one 22-min run (**Supplementary Figure 1**). Of the 39 oxylipins, 24 were consistently above the LOD and 22 oxylipins were consistently above the LOQ. Oxylipin concentrations below the LOQ were set at 80% of the lowest quantifiable sample. The library included (i) four LA-derived oxylipins (two each from CYP450 and LOX pathways), of which three [CYP450: 12,13-DiHOME, LOX: 9(S) HODE, 13(S) HODE] were above the LOQ; (ii) 14 ARA-derived oxylipins (five from COX, five from CYP450, and four from LOX pathways), of which nine (COX: thromboxane B2; CYP450: 11,12-EET, 14,15-EET, 20-HETE, 14,15-DiHET; LOX: 5-HETE, 12-HETE, 15-HETE, leukotriene B4) were above the LOQ; (iii) 10 EPA-derived oxylipins (one from COX, eight from CYP450, and one from ROS pathways), of which three (CYP450: 11,12-DiHETE, 17,18-EpETE; ROS: 8-iso PGF3a) were above the LOQ; (iv) 11 DHA-derived oxylipins (10 CYP450 and one from LOX pathways) of which seven (CYP450: 10,11-EpDPA, 19,20 EpDPA, 7,8-DiHDPA, 10,11-DiHDPA, 13,14-DiHDPA, 16,17-DiHDPA, 19,20-DiHDPA) were above the LOQ.

Demographic, Clinical Characteristics, and Levels of Oxylipins of Adults With Diseased Coronary Arteries

Selected demographic and clinical characteristics of adults with diseased coronary arteries stratified by number of diseased arteries and adults of the same age range with a low CAD risk are listed in **Table 1**. Sixty-nine of 74 adults with CAD had multiple CVD risk factors (three CAD1 patients and one CAD2 patient had one CVD risk factor and one CAD2 patient had no CVD risk factor). Almost all adults with CAD had hypertension and hypercholesterolemia. Most adults with CAD were on aspirin, were overweight or obese, or had a history of smoking. About half adults with CAD had diabetes or a family history of CVD. Demographic and clinical characteristics of adults with CAD had a limited efficacy to diagnose number of diseased arteries. The 10-year Framingham general CVD risk score and the number of CAD risk factors increased with the number of diseased arteries; specifically, adults with multiple diseased arteries were more likely to be male, were overweight or obese, former smokers, or had lower plasma HDL cholesterol concentrations.

Ten of 22 (45%) individual oxylipin concentrations decreased with greater number of diseased arteries by at least 10%; six individual oxylipins (27%) had significantly lower concentrations in adults with three vs. one diseased artery (**Table 2**). For pattern detection, oxylipins were grouped in **Table 3** by (1) FA precursors (i.e., LA, ARA, EPA, and DHA), oxylipin groups (i.e., mid-chain HODE, EET, mid-chain HETE, EpDPA, DiHDPA), (2) enzymes involved in their synthesis [i.e., oxygenation of PUFAs by LOX followed by reduction or alternatively hydroxylation of PUFAs by CYP1B1; oxidation of PUFAs by CYP450 followed by hydroxylation of oxidized PUFAs by soluble epoxide hydrolase (sEH)], and (3) based on enzymatic product to substrate

TABLE 1 | Demographic and clinical characteristics of adults with diseased coronary arteries (≥70% stenosis) and adults of the same age range with a low coronary artery disease (CAD) risk.

Characteristics	Low	Number of diseased arteries			Contrast
	CAD risk (n = 23)	1 (n = 31)	2 (n = 23)	3 (n = 20)	CAD1/2 vs. CAD3
	Mean ± STD	Mean ± STD	Mean ± STD	Mean ± STD	*P*-value
Age (year)	49 ± 10[b]	65 ± 9[a]	67 ± 12[a]	66 ± 1[a]	0.89
Male [*n* (%)]	4 (17)[c]	17 (55)[b]	19 (83)[a]	17 (85)[a]	0.15
BMI (kg/m^2)	28.3 ± 6.7[ab]	28.1 ± 4.9[b]	31.0 ± 9.3[ab]	31.7 ± 6.1[a]	0.20
Overweight	3 (13)[ab]	15 (48)[a]	9 (39)[ab]	8 (40)[ab]	0.80
Obese	9 (39)	8 (26)	10 (43)	10 (50)	0.28
Blood pressure (mmHg)					
Systolic	124 ± 9	131 ± 20	133 ± 17	129 ± 17	0.58
Diastolic	79 ± 6[a]	71 ± 13[b]	69 ± 11[b]	70 ± 11[b]	0.89
Plasma					
Triacylglycerol (mg/dl)	88 ± 38[b]	136 ± 72[a]	165 ± 106[a]	218 ± 326[ab]	0.40
Total cholesterol (mg/dl)	195 ± 32	182 ± 49[a]	156 ± 33[b]	177 ± 60[ab]	0.62
HDL cholesterol (mg/dl)	65 ± 13[a]	52 ± 16[b]	46 ± 14[b]	40 ± 12[c]	0.03
LDL cholesterol (mg/dl)	126 ± 28[a]	101 ± 35[b]	76 ± 25[b]	104 ± 48[ab]	0.28
Hba1c (mmol/mol)	5.3 ± 0.4[b]	6.1 ± 1.1[a]	6.5 ± 1.3[a]	6.3 ± 1.1[a]	0.90
Medication	0[b]	30 (97)[a]	21 (91)[a]	18 (90)[a]	0.61
Blood pressure [total, *n* (%)]	0[b]	24 (77)[b]	21 (91)[ab]	20 (100)[a]	0.10
ACE inhibitor [*n* (%)]	0[b]	10 (32)[a]	8 (35)[a]	5 (25)[a]	0.58
Angiotension receptor blocker	0[b]	5 (16)[ab]	3 (13)[ab]	5 (25)[a]	0.32
Beta blocker [*n* (%)]	0[b]	18 (58)[a]	19 (83)[a]	13 (65)[a]	0.79
Calcium channel blocker [*n* (%)]	0[b]	7 (23)[a]	4 (17)[ab]	5 (25)[a]	0.75
Diabetes [total, *n* (%)]	0[b]	6 (19)[a]	6 (26)[a]	6 (30)[a]	0.55
Oral hyperglycemia [*n* (%)]	0[b]	3 (10)[ab]	3 (13)[ab]	4 (20)[a]	0.44
Insulin [*n* (%)]	0	3 (10)	3 (13)	2 (10)	1
Hyperlipidemia (total)					
Statin [*n* (%)]	0[b]	24 (77)[a]	16 (70)[a]	13 (65)[a]	0.56
Aspirin [*n* (%)]	0[b]	23 (74)[a]	19 (83)[a]	15 (75)[a]	0.77
CVD risk factors					
Tobacco use [*n* (%)]					
Former	6 (26)	8 (26)	9 (39)	6 (30)	1
Active	0[b]	4 (13)[ab]	2 (9)[ab]	5 (25)[a]	0.15
History of [*n* (%)]					
Hypertension	2 (9)[b]	25 (81)[a]	22 (96)[a]	20 (100)[a]	0.18
Diabetes	0[b]	8 (26)[a]	8 (49)[a]	9 (45)[a]	0.27
Hypercholesterolemia	0[b]	30 (97)[a]	21 (91)[a]	19 (95)[a]	1
CVD in family	0[b]	14 (45)[a]	12 (52)[a]	11 (55)[a]	0.79
Total risk (1–5)	0[c]	2.6 ± 0.9[b]	2.8 ± 0.9[ab]	3.2 ± 0.8[a]	0.04
Framingham 10-year CVD risk (%)	4.0 ± 2.3[c]	21.6 ± 16.2[b]	29.4 ± 17.5[ab]	35.7 ± 19.7[a]	0.04
ACC 10-year ASCVD risk (%)	1.8 ± 1.2[b]	15.6 ± 11.7[a]	18.6 ± 7.5[a]	25.7 ± 12.3[a]	0.05

The superscripts denote whether averages of specific groups in a row differed at $P \leq 0.05$. If none of the groups differed from each other, no superscripts are shown. If two groups differed from each other, the significantly higher group got a superscript a, and the significantly lower group got a superscript b, and the group that did not significantly differ from the higher or the lower group got a superscript ab. If three groups differed from each other, the significantly highest group got a superscript a, the significantly lower group got a superscript b, and the group that was significantly lower than the group with a superscript b, got a, c. Quantitative data were compared using Student's t-test. Proportions were compared using Fisher's exact test.

ACE, angiotension converting enzyme; ACC, American College of Cardiology; ASCVD, atherosclerotic cardiovascular disease.

ratio (i.e., hydroxylation of 10,11-EpDPA to 10,11-DiHDPA, 14,15-EET to 14,15-DiHET, or 19,20-EpDPA to 19,20-DiHDPA by sEH).

Total oxylipin concentrations significantly declined with number of diseased arteries, specifically omega-3 FA-derived oxylipins and within those hydroxylated DHA-epoxide

TABLE 2 | Plasma oxylipin concentrations of adults with diseased coronary arteries (≥70% stenosis) and adults of the same age range with a low coronary artery disease (CAD) risk.

Oxylipins (nM)	Low	Number of diseased arteries			Contrast
	CAD risk ($n = 23$)	1 ($n = 31$)	2 ($n = 23$)	3 ($n = 20$)	CAD1/2 vs. CAD3
	Median (IQR)	Median (IQR)	Median (IQR)	Median (IQR)	*P*-value
12,13-DiHOME	8.71[a] (5.27, 11.8)	6.97[ab] (4.76, 8.85)	5.59[bc] (4.07, 8.45)	5.11[c] (4.17, 5.89)	0.07
13(S)-HODE	29.1[b] (26.7, 33.8)	37.6[a] (25.5, 49.9)	34.1[ab] (23.4, 41.7)	31.0[ab] (24.4, 43.2)	0.64
9(S)-HODE	19.0 (17.6, 21.6)	22.3 (16.8, 28.8)	20.3 (16.9, 25.0)	20.5 (14.9, 26.7)	0.64
Leukotriene B4	0.19[ab] (0.15, 0.24)	0.23[a] (0.18, 0.28)	0.24[a] (0.16, 0.27)	0.18[b] (0.15, 0.21)	0.01
Thromboxane B2	0.05 (0.03, 0.08)	0.03 (0.02, 0.05)	0.04 (0.02, 0.04)	0.04 (0.03, 0.06)	0.10
20-HETE	9.18 (7.04, 11.2)	8.60 (7.39, 10.4)	9.37 (7.35, 10.7)	8.43 (6.98, 9.52)	0.36
14,15-EET	0.27[b] (0.18, 0.34)	0.34[a] (0.28, 0.45)	0.22[b] (0.18, 0.36)	0.35[a] (0.23, 0.40)	0.70
11,12-EET	0.25[b] (0.19, 0.30)	0.32[a] (0.26, 0.41)	0.32[a] (0.27, 0.37)	0.35[a] (0.28, 0.46)	0.35
14,15-DiHET	0.98[ab] (0.78, 1.13)	1.12[a] (0.93, 1.23)	0.99[ab] (0.84, 1.17)	0.90[b] (0.78,1.09)	0.08
5-HETE	2.69[b] (2.30, 3.14)	4.63[a] (3.37, 7.29)	4.37[a] (2.87, 6.86)	3.87[ab] (2.21, 6.65)	0.38
12-HETE	2.41[b] (1.13, 4.19)	8.14[a] (5.60, 20.8)	11.2[a] (6.51, 19.6)	7.92[a] (2.78, 12.0)	0.10
15-HETE	1.18[b] (1.02,1.53)	2.41[a] (1.84, 3.29)	2.39[a] (1.73, 3.49)	2.26[a] (1.47, 3.11)	0.47
8-iso PGF3a	0.93[a] (0.49, 1.58)	0.99[a] (0.55, 1.95)	0.87[ab] (0.40, 2.70)	0.58[b] (0.37, 0.81)	0.02
17,18-EpETE	0.29 (0.23, 0.35)	0.26 (0.20, 0.35)	0.26 (0.21, 0.34)	0.29 (0.24, 0.33)	0.51
11,12-DiHETE	0.08 (0.04, 0.11)	0.06 (0.04, 0.12)	0.09 (0.06, 0.12)	0.05 (0.01, 0.09)	0.07
19,20-EpDPA	0.53 (0.32, 0.95)	0.59 (0.43, 0.91)	0.50 (0.40, 0.76)	0.60 (0.48, 0.83)	0.37
10,11-EpDPA	0.11 (0.05, 0.16)	0.11 (0.07, 0.14)	0.12 (0.09, 0.20)	0.11 (0.07, 0.15)	0.16
19,20-DiHDPA	2.22[a] (1.40, 2.83)	1.92[a] (1.19, 2.76)	1.69[ab] (1.00, 2.63)	0.60[b] (0.48, 0.83)	0.04
13,14-DiHDPA	0.14[a] (0.07, 0.20)	0.11[ab] (0.07, 0.14)	0.09[ab] (0.07, 0.19)	0.09[b] (0.06, 0.12)	0.39
16,17-DiHDPA	0.24[ab] (0.15, 0.34)	0.24[a] (0.16, 0.28)	0.19[ab] (0.14, 0.27)	0.17[b] (0.14, 0.21)	0.04
10,11-DiHDPA	0.09 (0.06, 0.15)	0.11 (0.08, 0.17)	0.09 (0.06, 0.18)	0.08 (0.05, 0.11)	0.06
7,8-DiHDPA	0.12 (0.08, 0.14)	0.13 (0.09, 0.16)	0.11 (0.09, 0.17)	0.12 (0.10, 0.18)	0.74

The superscripts denote whether averages of specific groups in a row differed at $P \leq 0.05$ using Kruskal–Wallis test. If none of the groups differed from each other, no superscripts are shown. If two groups differed from each other, the significantly higher group got a superscript a, and the significantly lower group got a superscript b, and the group that did not significantly differ from the higher or the lower group got a superscript ab. If three groups differed from each other, the significantly highest group got a superscript a, the significantly lower group got a superscript b, and the group that was significantly lower than the group with a superscript b, got a, c.

DiHOME, dihydroxy-octadecenoic acid; HODE, hydroxy-octadecadienoic acid; HETE, hydroxy-eicosatetraenoic acid; EET, epoxy-eicosatrienoic acid; DiHET, dihydroxy-eicosatrienoic acid; EpDPA, epoxy-docosapentaenoic acid; DiHDPA, dihydroxy-docosapentaenoic acid.

TABLE 3 | Plasma concentrations of oxylipin groups in adults with diseased coronary arteries (≥70% stenosis) and adults of the same age range with a low coronary artery disease (CAD) risk.

Oxylipins (nM)	Low	Number of diseased arteries			Contrast
	CAD risk ($n = 23$)	1 ($n = 31$)	2 ($n = 23$)	3 ($n = 20$)	CAD1/2 vs. CAD3
	Median (IQR)	Median (IQR)	Median (IQR)	Median (IQR)	*P*-value
Total	80.3[b] (75.9, 102)	109[a] (85.8, 171)	97.9[ab] (82.0, 116)	85.4[b] (74.4, 108)	0.05
Fatty acid precursor					
C18:2 derived	47.7[b] (43.9, 54.7)	59.7[a] (41.7, 76.7)	54.1[ab] (47.4, 63.0)	55.5[ab] (45.0, 73.4)	0.64
C20:4 derived	18.5[b] (14.8, 21.3)	28.0[a] (22.0, 40.7)	28.6[a] (22.6, 42.8)	24.4[a] (18.5, 28.9)	0.11
C20:5 derived	1.35[a] (0.91, 2.01)	1.41[a] (0.83, 2.48)	1.14[ab] (0.76, 3.08)	0.94[b] (0.64, 1.24)	0.04
C22:6 derived	3.36[a] (2.26, 5.06)	3.36[ab] (2.16, 4.25)	3.14[ab] (2.01, 4.03)	2.59[b] (2.20, 3.19)	0.18
Oxylipin group					
Mid-chain HODE	47.7[b] (44.7, 54.7)	59.7[a] (41.7, 76.7)	54.1[ab] (47.4, 63.0)	51.2[ab] (40.1, 68.7)	0.64
EET	1.45[b] (1.28, 1.68)	1.77[a] (1.45, 2.16)	1.63[ab] (1.32, 1.87)	1.51[ab] (1.39, 1.89)	0.47
Mid-chain HETE	6.34[b] (5.06, 9.50)	17.1[a] (12.1, 27.0)	19.0[a] (10.6, 32.4)	13.2[a] (8.07, 19.8)	0.11
EpDPA	0.67 (0.36, 1.06)	0.75 (0.51, 1.13)	0.66 (0.50, 0.94)	0.74 (0.57, 0.99)	0.72
DiHDPA	2.84[a] (1.89, 3.70)	2.50[a] (1.63, 3.45)	2.34[ab] (1.37, 3.28)	1.89[b] (1.37, 2.33)	0.04
Enzyme products					
LOX/CYP1B1 products	55.8[b] (53.0, 68.0)	78.9[a] (60.7, 114)	79.1[a] (59.3, 92.3)	68.8[ab] (55.4, 89.4)	0.27
LOX12-15 products	32.9[b] (19.7, 40.4)	47.9[a] (37.2, 72.2)	53.8[a] (31.5, 62.5)	43.5[a] (31.6, 55.1)	0.26
LOX5 products	21.9[b] (20.1, 25.6)	27.2[a] (21.0, 37.3)	26.5[ab] (19.9, 30.2)	25.1[ab] (18.4, 31.4)	0.55
CYP epoxides	1.44 (1.19, 1.90)	1.70 (1.41, 2.19)	1.56 (1.22, 2.14)	1.94 (1.32, 2.11)	0.86
Hydroxylated CYP epoxides	11.8[a] (8.61, 20.8)	10.0[ab] (8.02, 14.1)	9.50[bc] (7.35, 11.9)	7.77[c] (6.40, 9.21)	0.008
sEH product to substrate ratios					
10,11-DiHDPA/10,11-EpDPA	0.90[a] (0.78, 1.30)	0.81[b] (0.63, 0.93)	0.79[b] (0.59, 1.04)	0.71[b] (0.52, 0.92)	0.21
14,15-DiHET/14,15-EET	4.03[a] (2.91, 5.34)	2.88[b] (2.39, 4.13)	3.76[a] (2.63, 5.37)	2.56[b] (2.29, 4.17)	0.08
19,20-DiHDPA/19,20-EpDPA	4.26[a] (2.48, 6.55)	2.97[a] (2.19, 3.92)	2.95[a] (2.13, 4.77)	1.91[b] (1.58, 2.98)	0.002

The superscripts denote whether averages of specific groups in a row differed at $P \leq 0.05$ using Kruskal–Wallis test. If none of the groups differed from each other, no superscripts are shown. If two groups differed from each other, the significantly higher group got a superscript a, and the significantly lower group got a superscript b, and the group that did not significantly differ from the higher or the lower group got a superscript ab. If three groups differed from each other, the significantly highest group got a superscript a, the significantly lower group got a superscript b, and the group that was significantly lower than the group with a superscript b, got a, c.

HODE, hydroxy-octadecadienoic acid; HETE, hydroxy-eicosatetraenoic acid; EET, epoxy-eicosatrienoic acid; DiHET, dihydroxy-eicosatrienoic acid; EpDPA, epoxy-docosapentaenoic acid; DiHDPA, dihydroxy-docosapentaenoic acid; LOX, lipoxygenase; CYP, cytochrome P450; sEH, soluble epoxide hydrolases.

DiHDPAs, which are generated by hydroxylation of oxidized PUFAs by sEH (**Table 3**). The strongest decline was observed for hydroxylation of 19,20-EpDPA to 19,20-DiHDPA.

Low CAD risk adults had lower total oxylipin concentrations than adults with CAD, specifically omega-6 FA-derived oxylipins and within those mid-chain HETEs (**Tables 2**, **3**). These include

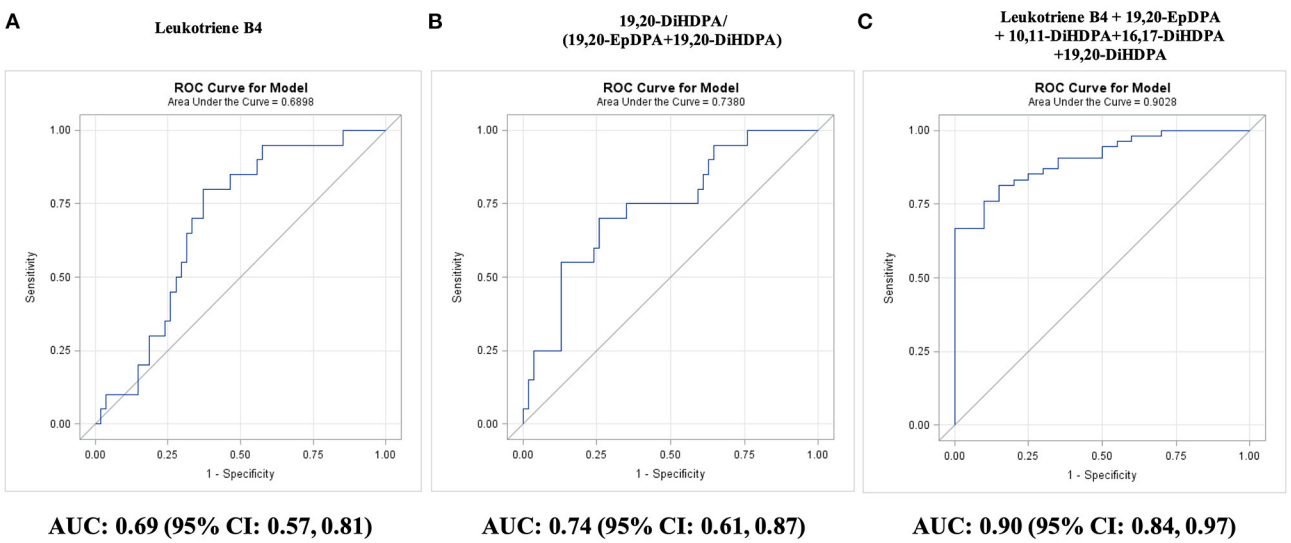

FIGURE 3 | Diagnosis of a number of diseased coronary arteries in adults with diseased coronary arteries (≥70% stenosis; $n = 74$), as shown by receiver operating characteristic (ROC) curves: **(A)** best single oxylipin model; **(B)** best single oxylipin group model; and **(C)** smallest oxylipin panel model achieving AUC ≥ 0.90.

the following three oxylipins that were significantly lower than in each CAD group: 11,12-EET, 12-HETE, and 15-HETE. We also observed less hydroxylation of 10,11-EpDPA to 10,11-DiHDPA, which is generated by sEH. Concentrations of LA-derived 12,13-DiHOME and DHA-derived DiHDPAs, specifically 19,20-DiHDPA and 16,17-DiHDPA, decreased gradually from adults with low CAD risk to those with three diseased arteries.

Diagnostic Efficacy of Oxylipins

Differences in plasma oxylipin concentrations were noted primarily between two and three diseased vessels. Among individual oxylipins, ARA-derived leukotriene B4 discriminated best three vs. less diseased arteries (AUC: 0.69; 95% CI: 0.57–0.81; $P = 0.003$; **Figure 3A**). Leukotriene B4 concentrations ≤0.21 nM diagnosed three diseased arteries in 80% of CAD3 adults and less diseased arteries in 65% CAD1 adults, 61% CAD2 adults, and 43% adults with low CAD risk.

Significant AUC values were also observed for EPA-derived 8-iso PGF3a (AUC: 0.67; 95% CI: 0.54–0.80; $P = 0.009$), three DHA-derived DiHDPA 19,20-DiHDPA (AUC: 0.66; 95% CI: 0.54–0.78; $P = 0.01$), 16,17-DiHDPA (AUC: 0.65; 95% CI: 0.52–0.79; $P = 0.02$), 10,11-DiHDPA (AUC: 0.64; 95% CI: 0.51–0.78; $P = 0.04$), and LA-derived 12,13-DiHOME (AUC: 0.64; 95% CI: 0.51–0.77; $P = 0.04$).

Among oxylipin groups and ratios, three diseased arteries were best diagnosed by the 19,20-DiHDPA fraction of the sum of 19,20-EpDPA and 19,20-DiHDPA (AUC: 0.74; 95% CI: 0.61–0.87; $P = 0.0003$; **Figure 3B**). A fraction of <72% diagnosed three diseased arteries in 70% of CAD3 adults and less diseased arteries in 74% CAD1 adults, 70% CAD2 adults, and 78% adults with low CAD risk. Adding 8-iso PGF3a to the fraction improved diagnosis of three diseased arteries to 80% but decreased diagnosis of less diseased arteries to 60% in CAD2 adults. An oxylipin panel of leukotriene B4, 19,20-EpDPA, 19,20-DiHDPA, 13,14-DiHDPA, and 10,11-DiHDPA diagnosed three diseased arteries in all CAD3 adults and less diseased arteries in 70% CAD1 and CAD2 adults (AUC: 0.90; 95% CI: 0.84–0.97; $P < 0.0001$; **Figure 3C**). The oxylipin panel improved ($P = 0.02$) diagnosis of three diseased arteries compared with the 10-year Framingham general CVD risk score (AUC: 0.68; 95% CI: 0.52–0.83; $P = 0.02$).

Prediction of Outcomes in Adults With Diseased Coronary Arteries

Adults with CAD were followed up until November 2019 for a median of 5 years (range: 25–84 months) and adverse events were recorded (i.e., coronary stent placement; CABG surgery; death). Ten participants (three women and seven men; median age: 61 years; range: 51–81 years) were lost to follow-up (**Figure 2**). Given the degree of stenosis, 52 of 64 adults with CAD underwent CABG surgery within 3 months of the angiography (CAD1: 19 of 28; CAD2: 16 of 19; CAD3: 17 of 17): 28 had a CABG surgery (CAD1: 5 of 19; CAD2: 10 of 16; CAD3: 13 of 17) and 26 had a coronary stent placement (CAD1: 16; CAD2: 6; CAD3: 4). Adults with multiple diseased coronary arteries were more likely to receive a CABG. Of the remaining 12 adults with CAD, seven had no further event, two adults with one diseased artery received a coronary artery stent during follow-up, and three died (CAD1: 2; CAD2: 1). In addition, four CAD adults that had undergone open-heart surgery within 3 months (two stents and two CABG) died during follow-up (CAD1: 1; CAD2: 0; CAD3: 3). Survival was not linked to the number of diseased coronary arteries.

Table 4 lists selected demographic and clinical characteristics of adults with diseased coronary arteries (≥70% stenosis) based on outcomes during follow-up. Survival was linked to lower systolic blood pressure or being a male, whereas

TABLE 4 | Demographic and clinical characteristics of adults with diseased coronary arteries (≥70% stenosis) stratified by outcome during 5-year follow-up.

Characteristics	Outcome during follow-up				Contrasts		
	No event (*n* = 7)	Stent (*n* = 24)	CABG (*n* = 26)	Death (*n* = 7)	No event vs. others	CABG/death vs. others	Death vs. Others
	Mean ± STD	Mean ± STD	Mean ± STD	Mean ± STD	*P*-value	*P*-value	*P*-value
Age (year)	65 ± 8	68 ± 8	67 ± 10	60 ± 17	0.71	0.52	0.31
Male [*n* (%)]	3 (43)^{bc}	19 (79)^{ab}	22 (85)^{a}	2 (29)^{c}	0.08	1	0.02
BMI (kg/m^2)	30.2 ± 8.5	29.9 ± 8.8	28.3 ± 3.3	29.9 ± 5.6	0.70	0.46	0.78
Overweight [*n* (%)]	1 (14)^{b}	9 (38)^{ab}	16 (62)^{a}	4 (57)^{ab}	0.11	0.03	0.70
Obese [*n* (%)]	3 (43)	9 (38)	7 (27)	2 (29)	0.67	0.43	1
Blood pressure (mmHg)							
Systolic	130 ± 16^{ab}	130 ± 16^{b}	130 ± 19^{ab}	147 ± 15^{a}	0.81	0.42	0.02
Diastolic	65 ± 12	72 ± 10	70 ± 11	67 ± 8	0.20	0.63	0.42
Plasma							
Triacylglycerol (mg/dl)	197 ± 131	167 ± 100	123 ± 59	89 ± 42	0.29	0.02	0.13
Total cholesterol (mg/dl)	174 ± 44	187 ± 50	162 ± 42	153 ± 46	0.91	0.06	0.29
HDL cholesterol (mg/dl)	48 ± 14	49 ± 12	44 ± 18	53 ± 14	0.94	0.51	0.39
LDL cholesterol (mg/dl)	92 ± 35	104 ± 37	94 ± 41	73 ± 39	0.79	0.29	0.17
Hba1c (mmol/mol)	5.9 ± 0.8	6.9 ± 0.4	6.2 ± 1.3	6.5 ± 2.5	0.61	0.74	0.95
Medication [*n* (%)]	7 (100)	23 (96)	25 (96)	7 (100)	1	1	1
Blood pressure (total)	6 (86)	22 (92)	22 (85)	6 (86)	1	0.71	1
ACE inhibitor	2 (29)	10 (42)	6 (23)	2 (29)	1	0.28	1
AR blocker	2 (29)	4 (17)	3 (12)	2 (29)	0.59	0.75	0.59
Beta blocker	3 (43)^{b}	20 (83)^{a}	17 (65)^{ab}	4 (57)^{ab}	0.19	0.43	0.67
Calcium channel blocker	3 (43)	4 (17)	6 (23)	1 (14)	0.17	1	1
Diabetes (total)	2 (29)	5 (21)	6 (23)	3 (43)	1	0.78	0.35
Oral hyperglycemia	2 (29)	3 (13)	3 (12)	1 (14)	0.25	0.73	1
Insulin	0	2 (8)	3 (12)	2 (29)	1	0.43	0.17
Hyperlipidemia (total)							
Statin	6 (86)	19 (79)	20 (77)	5 (71)	1	0.77	0.64
Aspirin	6 (86)	20 (83)	21 (81)	5 (71)	1	0.75	0.61
CAD risk factors							
Tobacco use [*n* (%)]							
Former	0	9 (40)	8 (31)	1 (14)	0.18	1	0.12
Active	1 (14)	2 (8)	4 (15)	3 (43)	1	0.30	0.07
History of [*n* (%)]							
Hypertension	6 (86)	22 (92)	22 (85)	7 (100)	0.57	1	1
Diabetes	3 (43)	6 (25)	8 (31)	4 (57)	0.67	0.60	0.20
Hypercholesterolemia	7 (100)	24 (100)	23 (88)	7 (100)	1	0.49	1
CVD in family	4 (57)	12 (50)	13 (50)	3 (43)	1	1	1
Total risk (1–5)	3.0 ± 0.8^{ab}	2.8 ±0.7^{b}	2.7 ± 1.0^{ab}	3.4 ± 1.0^{a}	0.60	0.85	0.06
Framingham 10-year CVD risk (%)	23.0 ± 18.8	28.0 ± 17.9	30.1 ± 18.3	28.4 ± 22.2	0.41	0.53	0.98
ACC 10-year ASCVD risk (%)	17.5 ± 11.9	18.9 ± 10.1	20.9 ± 13.8	9.0	0.77	0.77	ND

The superscripts denote whether averages of specific groups in a row differed at P ≤ 0.05. If none of the groups differed from each other, no superscripts are shown. If two groups differed from each other, the significantly higher group got a superscript a, and the significantly lower group got a superscript b, and the group that did not significantly differ from the higher or the lower group got a superscript ab. If three groups differed from each other, the significantly highest group got a superscript a, the significantly lower group got a superscript b, and the group that was significantly lower than the group with a superscript b, got a, c. Data were compared using Student's t-test. Proportions were compared using Fisher's exact test.

CABG, coronary artery bypass grafting; ACE, angiotension converting enzyme; AR, angiotension receptor; ACC, American College of Cardiology; ASCVD, Atherosclerotic Cardiovascular Disease.

survival without CABG was linked to higher plasma triacylglycerol concentrations. Unfavorable outcomes were linked to elevated oxylipin concentrations (**Table 5**), specifically omega-6 FA-derived oxylipins and within those LA-derived mid-chain HODEs and ARA-derived mid-chain HETEs, which are either generated by oxygenation of lipoxygenases

TABLE 5 | Plasma oxylipin concentrations of adults with diseased coronary arteries (≥70% stenosis) stratified by outcome during 5-year follow-up.

Oxylipins (nM)	Outcome during follow-up				Contrasts		
	No event ($n = 7$)	Stent ($n = 24$)	CABG ($n = 26$)	Death ($n = 7$)	No event vs. others	CABG/death vs. others	Death vs. others
	Median (IQR)	Median (IQR)	Median (IQR)	Median (IQR)	*P*-value	*P*-value	*P*-value
12,13-DiHOME	5.05 (3.81, 6.68)	5.71 (4.25, 7.64)	5.47 (4.29, 8.56)	5.69 (5.09, 6.93)	0.38	0.66	0.82
13(S)-HODE	33.9[cb] (18.5, 37.8)	27.4[b] (17.6, 40.2)	34.1[b] (25.2, 42.2)	46.2[a] (42.6, 58.9)	0.71	0.04	0.007
9(S)-HODE	19.4[cb] (12.2, 25.8)	20.0[b] (11.5, 22.4)	20.9[b] (17.1, 25.8)	30.6[a] (21.9, 56.9)	0.65	0.03	0.01
Leukotriene B4	0.22 (0.15, 0.24)	0.24 (0.17, 0.28)	0.22 (0.17, 0.25)	0.19 (0.16, 0.22)	0.47	0.36	0.14
Thromboxane B2	0.04[ab] (0.02, 0.11)	0.03[b] (0.02, 0.04)	0.04[a] (0.02, 0.06)	0.04[a] (0.04, 0.12)	0.89	0.04	0.08
20-HETE	8.03 (7.75, 9.93)	8.57 (6.88, 10.2)	8.62 (8.11, 10.4)	8.63 (5.66, 9.20)	0.54	0.44	0.58
14,15-EET	0.31 (0.22, 0.41)	0.28 (0.20, 0.38)	0.36 (0.22, 0.46)	0.29 (0.18, 0.38)	0.89	0.20	0.67
11,12-EET	0.35[ab] (0.27, 0.41)	0.29[b] (0.23, 0.38)	0.36[a] (0.22, 0.46)	0.32[ab] (0.24, 0.39)	0.72	0.08	0.92
14,15-DiHET	1.04 (0.87, 1.23)	0.97 (0.74, 1.13)	1.05 (0.89, 1.19)	1.03 (0.86, 1.18)	0.79	0.38	0.97
5-HETE	5.87[a] (4.12, 11.08)	3.68[b] (2.28, 5.00)	4.50[ab] (2.89, 5.98)	5.00[a] (4.43, 8.63)	0.07	0.31	0.04
12-HETE	8.14 (5.42, 11.2)	7.00 (4.60, 10.0)	10.9 (5.54, 20.8)	11.1 (5.48, 25.5)	0.97	0.09	0.38
15-HETE	2.92[ab] (1.84, 2.97)	1.86[b] (1.48, 2.34)	2.52[a] (2.05, 3.19)	2.44[a] (2.13, 4.17)	0.51	0.03	0.27
8-iso PGF3a	0.60[b] (0.29, 0.99)	1.48[a] (0.60, 14.6)	0.64[ab] (0.43, 1.95)	0.39[b] (0.34, 0.72)	0.28	0.08	0.06
17,18-EpETE	0.22 (0.19, 0.33)	0.28 (0.22, 0.35)	0.29 (0.19, 0.35)	0.31 (0.24, 0.39)	0.42	0.68	0.34
11,12-DiHETE	0.06 (0.04, 0.19)	0.05 (0.03, 0.13)	0.08 (0.04,0.12)	0.06 (0.04, 0.09)	0.67	0.81	0.57
19,20-EpDPA	0.70 (0.47, 1.04)	0.51 (0.28, 0.76)	0.64 (0.46, 0.83)	0.49 (0.40-0.56)	0.33	0.54	0.38
10,11-EpDPA	0.12 (0.10, 0.38)	0.10 (0.06, 0.19)	0.13 (0.06, 0.20)	0.09 (0.08, 0.11)	0.35	0.93	0.60
19,20-DiHDPA	1.61 (1.26, 2.81)	1.63 (0.91, 2.36)	1.44 (0.97, 2.18)	1.78 (1.19, 2.73)	0.63	0.64	0.45
13,14-DiHDPA	0.07 (0.06, 0.21)	0.10 (0.06, 0.15)	0.11 (0.08, 0.15)	0.08 (0.04, 0.12)	0.97	0.91	0.20
16,17-DiHDPA	0.20 (0.15, 0.41)	0.20 (0.13, 0.28)	0.18 (0.14, 0.24)	0.20 (0.15, 0.24)	0.43	0.43	0.99
10,11-DiHDPA	0.11 (0.04, 0.33)	0.09 (0.05, 0.13)	0.09 (0.06, 0.16)	0.08 (0.06, 0.11)	0.58	0.79	0.48
7,8-DiHDPA	0.15 (0.08, 0.20)	0.12 (0.08, 0.15)	0.12 (0.09, 0.17)	0.14 (0.11, 0.18)	0.48	0.82	0.67

The superscripts denote whether averages of specific groups in a row differed at $P \leq 0.05$ using Kruskal–Wallis test. If none of the groups differed from each other, no superscripts are shown. If two groups differed from each other, the significantly higher group got a superscript a, and the significantly lower group got a superscript b, and the group that did not significantly differ from the higher or the lower group got a superscript ab. If three groups differed from each other, the significantly highest group got a superscript a, the significantly lower group got a superscript b, and the group that was significantly lower than the group with a superscript b, got a, c.

CABG, coronary artery bypass grafting; DiHOME, dihydroxy-octadecenoic acid; HODE, hydroxy-octadecadienoic acid; HETE, hydroxy-eicosatetraenoic acid; EET, epoxy-eicosatrienoic acid; DiHET, dihydroxy-eicosatrienoic acid; EpDPA, epoxy-docosapentaenoic acid; DiHDPA, dihydroxy-docosapentaenoic acid.

TABLE 6 | Plasma concentrations of oxylipin groups in adults with diseased coronary arteries (≥70% stenosis) stratified by outcome during 5-year follow-up.

Oxylipins (nM)	Outcomes during follow-up				Contrasts		
	No event (*n* = 7)	Stent (*n* = 24)	CABG (*n* = 26)	Death (*n* = 7)	No event vs. others	CABG/death vs. others	Death vs. others
	Median (IQR)	Median (IQR)	Median (IQR)	Median (IQR)	*P*-value	*P*-value	*P*-value
Total	97.8[ab] (62.2, 112)	86.4[b] (69.4, 132)	103[ab] (81.4, 116)	119[a] (97.4, 180)	0.71	0.16	0.05
Fatty acid precursor							
C18:2 derived	59.7[b] (30.7, 62.4)	47.6[b] (28.9, 62.5)	54.9[b] (45.9, 65.8)	76.7[a] (64.5, 135)	0.76	0.04	0.004
C20:4 derived	28.0[ab] (24.9, 35.6)	23.3[b] (18.3, 30.5)	28.4[a] (23.6, 41.1)	29.0[a] (27.3, 44.9)	0.51	0.03	0.19
C20:5 derived	0.87[ab] (0.67, 1.37)	1.95[a] (0.87, 14.9)	0.97[ab] (0.74, 2.48)	0.86[b] (0.66, 1.07)	0.31	0.13	0.17
C22:6 derived	3.02 (2.25, 5.86)	2.95 (1.48, 4.21)	2.58 (2.13, 3.93)	2.96 (2.13, 3.66)	0.58	0.80	0.84
Oxylipin group							
Mid-chain HODE	59.7[b] (30.7, 62.4)	47.6[b] (28.9, 62.5)	54.9[b] (45.9, 65.8)	76.7[a] (64.5, 135)	0.76	0.04	0.004
EET	1.71 (1.45, 1.80)	1.51 (1.37, 1.83)	1.75 (1.44, 2.25)	1.46 (1.32, 1.99)	0.84	0.20	0.76
Mid-chain HETE	17.4[a] (15.2, 21.4)	12.9[b] (10.1, 18.4)	18.0[ab] (11.5, 30.8)	17.9[a] (17.1, 34.1)	0.36	0.08	0.17
EpDPA	0.82 (0.53, 1.42)	0.63 (0.33, 0.92)	0.77 (0.57, 0.97)	0.56 (0.50, 0.75)	0.32	0.59	0.35
DiHDPA	2.07 (1.72, 4.05)	2.13 (1.24, 3.01)	1.89 (1.35, 2.83)	2.26 (1.58, 3.27)	0.64	0.67	0.61
Enzyme products							
LOX/CYP1B1 products	77.7[ab] (47.2, 89.7)	62.6[b] (41.9, 89.6)	73.6[b] (61.7, 92.3)	96.4[a] (87.0, 154)	0.94	0.03	0.01
LOX12-15 products	46.2[bc] (30.3, 48.9)	37.4[c] (24.9, 58.4)	44.9[b] (38.0, 62.5)	57.1[a] (54.7, 72.2)	0.85	0.02	0.02
LOX5 products	26.7[ab] (18.3, 37.3)	23.9[b] (16.0, 28.7)	25.3[b] (21.4, 30.7)	37.1[a] (28.7, 64.8)	0.92	0.07	0.007
CYP epoxides	1.97 (1.41, 2.19)	1.57 (1.07, 1.95)	1.83 (1.34, 2.17)	1.56 (1.27, 1.97)	0.37	0.46	0.58
Hydroxylated CYP epoxides	10.0 (6.94, 10.4)	9.19 (7.50, 10.8)	9.22 (7.29, 12.0)	9.05 (7.96, 9.63)	0.89	0.91	0.94
sEH product to substrate ratios							
10,11-DiHDPA/10,11-EpDPA	0.79 (0.64, 0.94)	0.79 (0.60, 0.96)	0.79 (0.57, 1.04)	0.78 (0.58, 0.93)	0.89	0.88	0.96
14,15-DiHET/14,15-EET	2.83 (2.39, 5.27)	3.31 (2.54, 4.39)	2.79 (2.31, 4.17)	2.96 (2.51, 5.95)	0.99	0.66	0.71
19,20-DiHDPA/19,20-EpDPA	2.85[ab] (1.61, 3.11)	3.83[a] (2.13, 4.39)	2.57[b] (1.70, 3.31)	3.41[ab] (2.69, 4.86)	0.22	0.25	0.23

The superscripts denote whether averages of specific groups in a row differed at $P \leq 0.05$ using Kruskal–Wallis test. If none of the groups differed from each other, no superscripts are shown. If two groups differed from each other, the significantly higher group got a superscript a, and the significantly lower group got a superscript b, and the group that did not significantly differ from the higher or the lower group got a superscript ab. If three groups differed from each other, the significantly highest group got a superscript a, the significantly lower group got a superscript b, and the group that was significantly lower than the group with a superscript b, got a, c.

CABG, coronary artery bypass grafting; HODE, hydroxy-octadecadienoic acid; HETE, hydroxy-eicosatetraenoic acid; EET, epoxy-eicosatrienoic acid; DiHET, dihydroxy-eicosatrienoic acid; EpDPA, epoxy-docosapentaenoic acid; DiHDPA, dihydroxy-docosapentaenoic acid; LOX, lipoxygenase; CYP, cytochrome P450; sEH, soluble epoxide hydrolases.

or hydroxylation of CYP1B1 (**Table 6**). Concentrations of LA-derived 9(S)-HODE and 13(S)-HODE and ARA-derived thromboxane B2, 5-HETE, and 15-HETE increased gradually from stent placement to CABG to death. In contrast, concentrations of EPA-derived 8-iso PGF3α were lower with unfavorable outcomes.

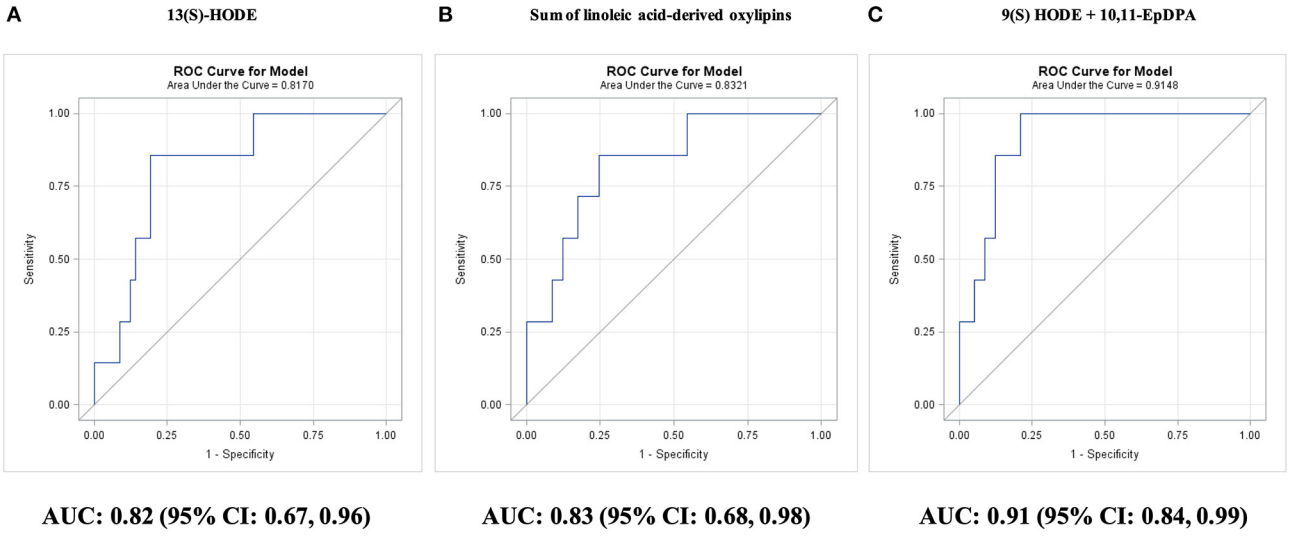

FIGURE 4 | Prediction of survival during 5-year follow-up in adults with diseased coronary arteries (≥70% stenosis; $n = 64$), as shown by receiver operating characteristic (ROC) curves: **(A)** best single oxylipin model; **(B)** best single oxylipin group model; and **(C)** smallest oxylipin panel model achieving AUC ≥ 0.90.

Predictive Efficacy of Oxylipins

Among individual oxylipins, survival was predicted best by LA-derived 13(S)-HODE (AUC: 0.82; 95% CI: 0.67–0.96; $P < 0.0001$); concentrations of 13(S)-HODE >42.5 nM predicted mortality in 86% nonsurviving adults with CAD and predicted survival in 81% surviving adults with CAD and 91% Astoria cohort adults (**Figure 4A**).

Adding 10,11-EpDPA concentrations <0.20 nM for classification, improved survival prediction to 91% surviving adults with CAD and 96% Astoria cohort adults (AUC: 0.90; 95% CI: 0.81–0.99; $P < 0.0001$). The two-oxylipin panel improved ($P = 0.02$) survival prediction compared with the 10-year Framingham general CVD risk score (AUC: 0.49; 95% CI: 0.16–0.83; $P = 0.97$).

The four remaining individual oxylipins that could significantly predict survival were ordered by *P*-value: EPA-derived 9(S)-HODE (AUC: 0.79; 95% CI: 0.62–0.96; $P = 0.0007$), ARA-derived 5-HETE (AUC: 0.73; 95% CI: 0.58–0.89; $P = 0.01$), EPA-derived 8-iso PGF3α (AUC: 0.72; 95% CI: 0.54–0.89; $P = 0.02$), and ARA-derived thromboxane B2 (AUC: 0.72; 95% CI: 0.54–0.89; $P = 0.03$). The best single predictor for survival was the sum of LA-derived oxylipins (AUC: 0.83; 95% CI: 0.68–0.98; $P < 0.0001$; **Figure 4B**). The targeted AUC value of at least 0.90 was achieved with a two-oxylipin panel of 9(S)-HODE and 10,11-EpDPA (AUC: 0.91; 95% CI: 0.84–0.99; $P < 0.0001$; **Figure 4C**).

Among individual oxylipins, survival without requiring CABG was best predicted by LA-derived 9(S)-HODE (AUC: 0.65; 95% CI: 0.52–0.79; $P = 0.03$; **Figure 5A**). The two-remaining individual oxylipins that could significantly predict survival without requiring CABG were ordered by *P*-value: ARA-derived 15-HETE (AUC: 0.65; 95% CI: 0.52–0.79; $P = 0.03$) and ARA-derived thromboxane B2 (AUC: 0.65; 95% CI: 0.51–0.79; $P = 0.03$). The best single predictor was the sum of LOX12/15-epoxygenated oxylipins (AUC: 0.67; 95% CI: 0.54–0.81; $P = 0.01$; **Figure 5B**). The targeted AUC value of ≥0.85 was achieved with a linear combination of 9(S)-HODE, 5-HETE, 14,15-DiHET, thromboxane B2, 19,20-EPDPA, and 16,17-DiHDPA (AUC: 0.85; 95% CI: 0.75–0.94; $P = 0.0001$; **Figure 5C**). The oxylipin panel improved predictive efficacy ($P = 0.004$) compared with the 10-year Framingham general CVD risk score (AUC: 0.55; 95% CI: 0.40–0.71; $P = 0.51$).

The only single oxylipin that could significantly predict no events in CAD adults was ARA-derived 5-HETE (AUC: 0.71; 95% CI: 0.52–0.91; $P = 0.03$). In general, patients without follow-up events had oxylipin values similar to patients who died during follow-up or had a surgery for a full blockage. The 10-year Framingham general CVD risk score had an AUC of 0.62 (95% CI: 0.38–0.87; $P = 0.33$).

DISCUSSION

In the current study, we provide evidence that in adults with diseased coronary arteries (>70% stenosis), plasma oxylipin panels may discriminate among the number of diseased coronary arteries and predict median 5-year outcomes, which, to our knowledge, has not been previously reported.

Analysis of Plasma Oxylipins

Novel analytical methods for extraction, detection, and data processing allow for the separation of a large number of diverse oxylipins in a short period of time (3, 12, 22, 23). In the present study, we detected and verified with standards 39 oxylipins of diverse origin and biosynthetic pathways in a 22-min LC-MS/MS run. Similar to inflammatory cytokines, low abundance, limited dynamic range, limited tissue specificity, very short half-life, significant daily fluctuation, and high inter- and intra-assay variation, limit the use of oxylipins as diagnostic biomarkers

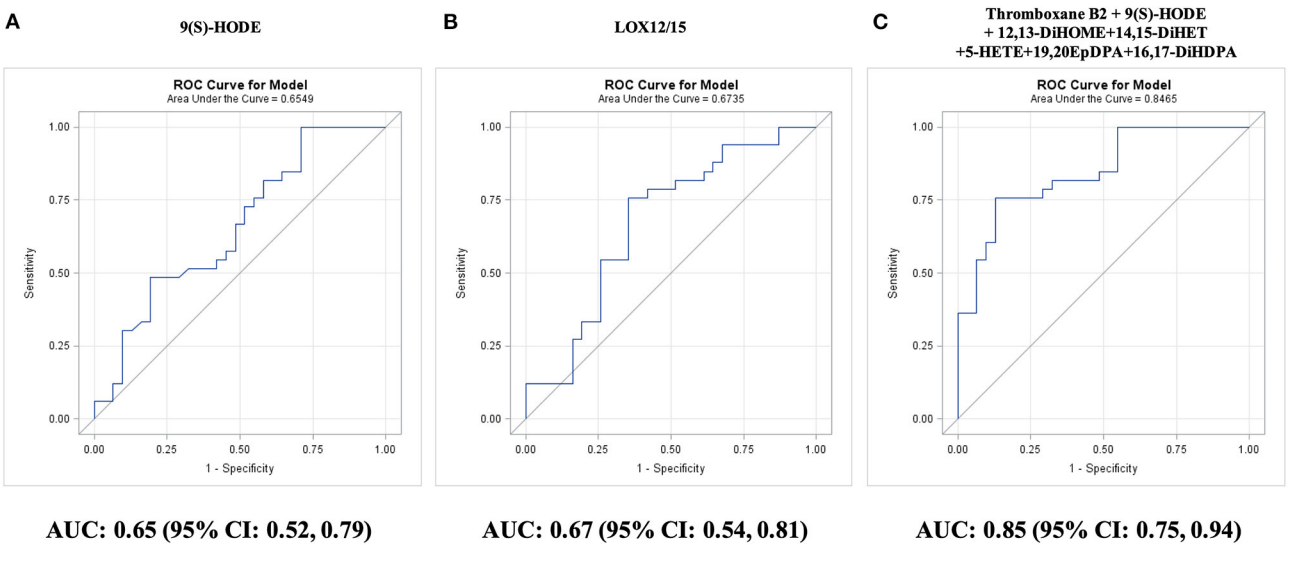

FIGURE 5 | Prediction of survival without coronary artery bypass graft (CABG) surgery during 5-year follow-up in adults with diseased coronary arteries (≥70% stenosis; $n = 64$), as shown by receiver operating characteristic (ROC) curves: **(A)** best single oxylipin model; **(B)** best single oxylipin group model; and **(C)** smallest oxylipin panel model achieving AUC ≥ 0.85.

(16). For diagnostic and prognostic research, a good biomarker must have a large dynamic range within the population. In the current study, 22 oxylipins had concentrations in the linear quantification range in at least 98% of sampled adults, which allowed us to evaluate the most abundant enzymatic oxylipin pathways; however, excluded pathways generated by COX or aspirin and ROS.

Diagnostic and Prognostic Efficacy of Oxylipins in CAD

Currently used risk assessment scores of CAD, such as the 10-year Framingham general CVD risk score, have been developed for the general population and have shown limited efficacy in high risk CAD adult management (4). In adults with significant diseased coronary arteries, a five-oxylipin panel diagnosed three diseased arteries with 100% sensitivity and 70% specificity. During a median 5-year survival, a panel of two oxylipins predicted survival with 86% sensitivity and 91% specificity. The oxylipin panels improved three diseased artery diagnosis and survival prognosis compared with the 10-year Framingham general CVD risk score.

Clinical Relevance of Oxylipins in CAD

Coronary artery disease (CAD) limits nutrient and oxygen supply to generate sufficient energy in cardiomyocytes, which becomes an even bigger challenge as the number and severity of diseased coronary arteries increase or plaques rupture with subsequent thrombus formation (5). In the present study, adults with more diseased coronary arteries (≥70% stenosis) had lower plasma concentrations of hydroxylated omega-3 PUFA-derived epoxides, specifically we observed lower levels of 19,20-DiHDPA (**Figure 6**). To our knowledge, the link between oxylipin concentrations and number of diseased coronary arteries has not been previously reported. The enzyme responsible for hydroxylation of epoxides is sEH, which is induced by hypoxia and has been proposed as potential pharmacological target for CAD (26–28). However, we cannot exclude the possibility that participants with CAD were already on medication that inhibited soluble CYP450 epoxide hydrolase. However, the gradual decrease in concentrations of LA-derived 12,13-DiHOME and DHA-derived DiHDPA with increasing diseased artery number support the hypothesis that the lower concentrations are a response to the hypoxia caused by arterial occlusions (29).

Five-year survival and no CABG surgery was linked to lower concentrations of oxygenated omega-6 PUFA LA and ARA, specifically lower concentrations of LA-derived mid-chain HODE and ARA-derived mid-chain HETE, which are either generated by oxygenation of lipoxygenases or hydroxylation of CYP1B1 (**Figure 6**). In support, elevated 15-HETE concentrations and LOX-15 enzymatic activity have been reported in ischemic heart disease and hypoxic human cardiomyocytes and cardiac endothelial cells (15), supporting our hypothesis that the elevated mid-chain HETE and HODE concentrations are a response to the hypoxia caused by the arterial occlusions. High concentrations of HETE, including 5-HETE, 12-HETE, and 15-HETE, were reported in atherosclerotic plaques, especially in those that were more likely to rupture (14). Elevated circulating concentrations of 5-HETE and 12-HETE were observed in individuals after cardiac surgery (16). Elevated concentrations of 5-HETE, 12-HETE, and 15-HETE were reported in individuals with acute cardiac syndrome (17). Elevated circulating concentrations of 5-HETE, 12-HETE, and 15-HETE were reported in individuals with CAD by Xu et al. (20), whereas only numerical increases were reported by Shishebor et al. (19) and Auguet

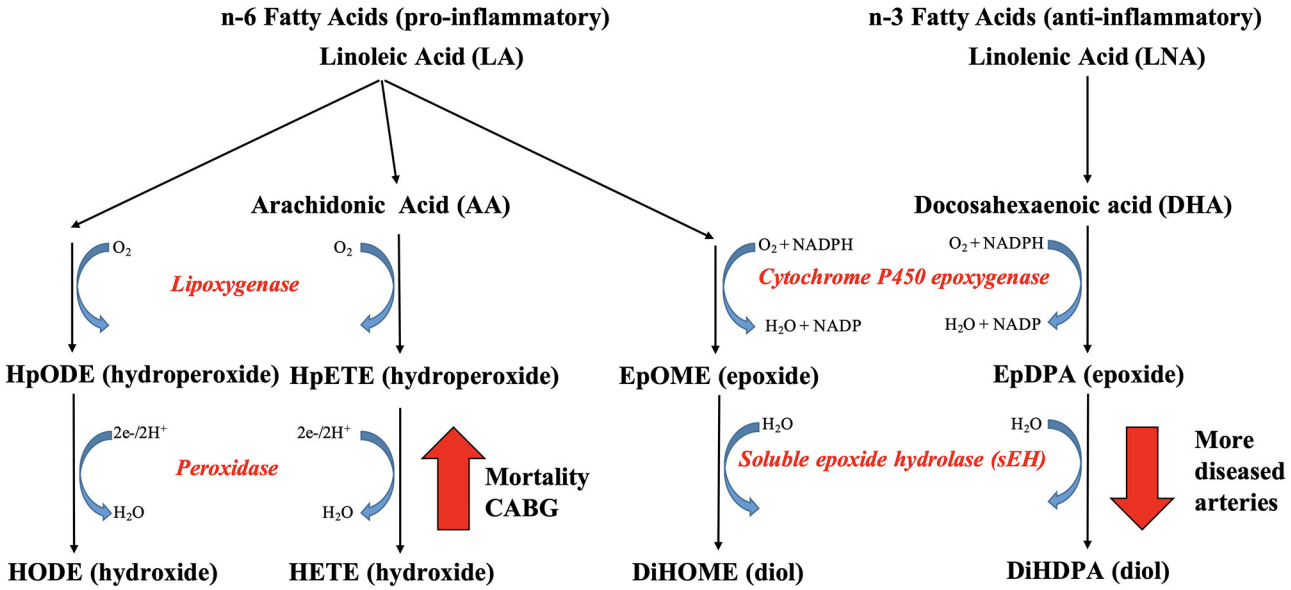

FIGURE 6 | The link between plasma oxylipins and coronary artery disease. Adults with more diseased coronary arteries (≥70% stenosis) had lower plasma concentrations of hydroxylated omega-3 fatty acid-derived epoxygenated oxylipins, which was linked to decreased soluble epoxide hydrolase (sEH) activity. Nonsurviving adults with diseased coronary arteries had higher plasma concentration of oxygenated omega-6 fatty acids, which was linked to increased lipoxygenase or CYP1B1 activity.

et al. (21); the latter did not quantify 5-HETE. The role of elevated mid-chain HETE in cardiovascular dysfunction has been well documented, whereas less is known of the role of mid-chain HODE (3, 30, 31). Inhibition of the oxygenation step of the LOX pathway has been proposed as treatment option for CAD management (30), suggesting clinical relevance of the identified oxylipins as indicator of chronic hypoxia.

Limitations of the Study

First, the number of adults with CAD were relatively small and came from a high-risk group, which underwent coronary angiography, but in whom the presence and extent of CAD was clearly defined. Second, all but five adults with CAD were on medical therapy for treatment for hypertension, hyperlipidemia, and/or diabetes, which could have influenced the levels of oxylipins. Third, differences in collateral blood flow may have impacted oxylipin concentration, which was not assessed in this cohort. Fourth, most adults with CAD had to undergo revascularization shortly after angiography, which may impact later outcomes. Fifth, follow-up time was limited to <6 years, which impacted the number of outcomes. Sixth, diagnostic and prognostic oxylipin panels could not be validated due to the limited clearly defined population size.

SUMMARY AND CONCLUSION

In summary, we observed a link between plasma oxylipin concentrations and CAD severity. Concentrations of six oxylipins decreased with the number of diseased arteries; a panel of five oxylipins diagnosed three diseased arteries with 100% sensitivity and 70% specificity. Concentrations of five oxylipins were lower and one oxylipin was higher with survival; a panel of two oxylipins predicted survival during follow-up with 86% sensitivity and 91% specificity. Plasma oxylipins may assist in diagnosis and prognosis of CAD in high-risk adults in combination with standard risk assessment tools. Our promising results require confirmation in larger unselected populations.

DATA AVAILABILITY STATEMENT

The original contributions presented in the study are included in the article/**Supplementary Material**, further inquiries can be directed to the corresponding author/s.

ETHICS STATEMENT

This study was approved by the Institutional Review Board of the Oregon Health and Science University (OHSU) in Portland, Oregon. The patients/participants provided their written informed consent to participate in this study.

AUTHOR CONTRIBUTIONS

DL, MG-J, GB, AA, DR, NA, CM, and SK: conceptualization. DL, MG-J, GB, AA, AV, JM, DJ, and CM: data curation. DL, MG-J, and GB: formal analysis and writing (original draft). MG-J, DJ, CM, and SK: funding acquisition. DL, MG-J, GB, AA, AV, JM, DJ, DR, NA, CM, and SK: investigation and writing (review and editing). DL, MG-J, GB, AA, DJ, CM, and SK: methodology. DL, MG-J, NA, CM, and SK: project administration. MG-J and GB: software and visualization. GB,

DJ, CM, and SK: supervision. DL, MG-J, GB, DJ, CM, and SK: validation. All authors contributed to the article and approved the submitted version.

FUNDING

This study was funded in part by grants (DK112360, 2R90AT008924-06, and S10RR022589) from the National Institutes of Health, Bethesda, Maryland. This work used facilities in OSU's Mass Spectrometry Center, Corvallis, Oregon.

ACKNOWLEDGMENTS

We thank Jeffrey Morrè (Operational Manager, Oregon State University Mass Spectrometry Center) for technical assistance and advice.

SUPPLEMENTARY MATERIAL

The Supplementary Material for this article can be found online at: https://www.frontiersin.org/articles/10.3389/fcvm.2021.645786/full#supplementary-material

REFERENCES

1. Roth GA, Johnson C, Abajobir A, Abd-Allah F, Abera SF, Abyu G, et al. Global, regional, and national burden of cardiovascular diseases for 10 causes, 1990 to 2015. *J Am Coll Cardiol.* (2017) 70:1–25. doi: 10.1016/j.jacc.2017.04.052
2. Pagidipati NJ, Gaziano TA. Estimating deaths from cardiovascular disease: a review of global methodologies of mortality measurement. *Circulation.* (2013) 127:749–56. doi: 10.1161/CIRCULATIONAHA.112.128413
3. Nayeem MA. Role of oxylipins in cardiovascular diseases. *Acta Pharmacol Sin.* (2018) 39:1142–54. doi: 10.1038/aps.2018.24
4. Hajar R. Risk factors for coronary artery disease: historical perspectives. *Heart Views.* (2017) 18:109–14. doi: 10.4103/HEARTVIEWS.HEARTVIEWS_106_17
5. Ambrose JA, Singh M. Pathophysiology of coronary artery disease leading to acute coronary syndromes. *F1000Prime Rep.* (2015) 7:8. doi: 10.12703/P7-08
6. Bentzon JF, Otsuka F, Virmani R, Falk E. Mechanisms of plaque formation and rupture. *Circ Res.* (2014) 114:1852–66. doi: 10.1161/CIRCRESAHA.114.302721
7. Rafieian-Kopaei M, Setorki M, Doudi M, Baradaran A, Nasri H. Atherosclerosis: process, indicators, risk factors and new hopes. *Int J Prev Med.* (2014) 5:927–46. https://www.ncbi.nlm.nih.gov/pubmed/25489440.
8. Zhong H, Yin H. Role of lipid peroxidation derived 4-hydroxynonenal (4-HNE) in cancer: focusing on mitochondria. *Redox Biol.* (2014) 4:193–9. doi: 10.1016/j.redox.2014.12.011
9. Gaweł S, Wardas M, Niedworok E, Wardas P. Dialdehyd malonowy (MDA) jako wskaźnik procesów peroksydacji w organizmie. *Wiad Lek.* (2004) 57:453–5.
10. Parthasarathy S, Raghavamenon A, Garelnabi MO, Santanam N. Oxidized low-density lipoprotein. *Methods Mol Biol.* (2010) 610:403–17. doi: 10.1007/978-1-60327-029-8_24
11. Catala A. Lipid peroxidation of membrane phospholipids generates hydroxy-alkenals and oxidized phospholipids active in physiological and/or pathological conditions. *Chem Phys Lipids.* (2009) 157:1–11. doi: 10.1016/j.chemphyslip.2008.09.004
12. Tourdot BE, Ahmed I, Holinstat M. The emerging role of oxylipins in thrombosis and diabetes. *Front Pharmacol.* (2014) 4:176. doi: 10.3389/fphar.2013.00176
13. Gabbs M, Leng S, Devassy JG, Monirujjaman M, Aukema HM. Advances in our understanding of oxylipins derived from dietary PUFAs. *Adv Nutr.* (2015) 6:513–540. doi: 10.3945/an.114.007732
14. Mallat Z, Nakamura T, Ohan J, Lesèche G, Tedgui A, Maclouf J, et al. The relationship of hydroxyeicosatetraenoic acids and F2-isoprostanes to plaque instability in human carotid atherosclerosis. *J Clin Invest.* (1999) 103:421–7. doi: 10.1172/JCI3985
15. Lundqvist A, Sandstedt M, Sandstedt J, Wickelgren R, Hansson GI, Jeppsson A, et al. The arachidonate 15-lipoxygenase enzyme product 15-HETE is present in heart tissue from patients with ischemic heart disease and enhances clot formation. *PLoS One.* (2016) 11:1–13. doi: 10.1371/journal.pone.0161629
16. Strassburg K, Huijbrechts AML, Kortekaas KA, Lindeman JH, Pedersen TL, Dane A, et al. Quantitative profiling of oxylipins through comprehensive LC-MS/MS analysis: application in cardiac surgery. *Anal Bioanal Chem.* (2012) 404:1413–26. doi: 10.1007/s00216-012-6226-x
17. Zu L, Guo G, Zhou B, Gao W. Relationship between metabolites of arachidonic acid and prognosis in patients with acute coronary syndrome. *Thromb Res.* (2016) 144:192–201. doi: 10.1016/j.thromres.2016.06.031
18. Caligiuri SPB, Aukema HM, Ravandi A, Lavallée R, Guzman R, Pierce GN. Specific plasma oxylipins increase the odds of cardiovascular and cerebrovascular events in patients with peripheral artery disease. *Can J Physiol Pharmacol.* (2017) 95:961–8. doi: 10.1139/cjpp-2016-0615
19. Shishehbor MH, Zhang R, Medina H, Brennan ML, Brennan DM, Ellis SG, et al. Systemic elevations of free radical oxidation products of arachidonic acid are associated with angiographic evidence of coronary artery disease. *Free Radic Biol Med.* (2006) 41:1678–83. doi: 10.1016/j.freeradbiomed.2006.09.001
20. Xu YJ, Ho WE, Xu F, Wen T, Ong CN. Exploratory investigation reveals parallel alteration of plasma fatty acids and eicosanoids in coronary artery disease patients. *Prostaglandins Other Lipid Mediat.* (2013) 106:29–36. doi: 10.1016/j.prostaglandins.2013.08.003
21. Auguet T, Aragonès G, Colom M, Aguilar C, Martín-Paredero V, Canela N, et al. Targeted metabolomic approach in men with carotid plaque. *PLoS One.* (2018) 13:1–11. doi: 10.1371/journal.pone.0200547
22. Pedersen TL, Newman JW. Establishing and performing targeted multi-residue analysis for lipid mediators and fatty acids in small clinical plasma samples. *Methods Mol Biol.* (2018) 1730:175–212. doi: 10.1007/978-1-4939-7592-1_13
23. La Frano MR, Hernandez-Carretero A, Weber N, Borkowski K, Pedersen TL, Osborn O, et al. Diet-induced obesity and weight loss alter bile acid concentrations and bile acid-sensitive gene expression in insulin target tissues of C57BL/6J mice. *Nutr Res.* (2017) 46:11–21. doi: 10.1016/j.nutres.2017.07.006
24. García-Jaramillo M, Lytle AK, Spooner HM, Jump BD. A lipidomic analysis of docosahexaenoic acid (22:6, ω3) mediated attenuation of western diet induced nonalcoholic steatohepatitis in male $Ldlr^{-/-}$ mice. *Metabolites.* (2019) 9:252. doi: 10.3390/metabo9110252
25. Housley L, Magana AA, Hsu A, Beaver LM, Wong CP, Stevens JF, et al. Untargeted metabolomic screen reveals changes in human plasma metabolite profiles following consumption of fresh broccoli sprouts. *Mol Nutr Food Res.* (2018) 62:e1700665. doi: 10.1002/mnfr.201700665
26. Morisseau C, Hammock BD. Impact of soluble epoxide hydrolase and epoxyeicosanoids on human health. *Annu Rev Pharmacol Toxicol.* (2012) 53:37–58. doi: 10.1146/annurev-pharmtox-011112-140244
27. Wagner KM, McReynolds CB, Schmidt WK, Hammock BD. Soluble epoxide hydrolase as a therapeutic target for pain, inflammatory and neurodegenerative diseases. *Pharmacol Ther.* (2017) 180:62–76. doi: 10.1016/j.pharmthera.2017.06.006

28. Imig JD. Prospective for cytochrome P450 epoxygenase cardiovascular and renal therapeutics. *Pharmacol Ther.* (2018) 192:1–19. doi: 10.1016/j.pharmthera.2018.06.015
29. Fleming I. The pharmacology of the cytochrome P450 epoxygenase/soluble epoxide hydrolase axis in the vasculature and cardiovascular disease. *Pharmacol Rev.* (2014) 66:1106–40. doi: 10.1124/pr.113.007781
30. Dobrian AD, Lieb DC, Cole BK, Taylor-Fishwick DA, Chakrabarti SK, Nadler JL. Functional and pathological roles of the 12- and 15-lipoxygenases. *Prog Lipid Res.* (2011) 50:115–31. doi: 10.1016/j.plipres.2010.10.005
31. Maayah ZH, El-Kadi AOS. The role of mid-chain hydroxyeicosatetraenoic acids in the pathogenesis of hypertension and cardiac hypertrophy. *Arch Toxicol.* (2016) 90:119–36. doi: 10.1007/s00204-015-1620-8

Disclaimer: The contents do not represent the views of the U.S. Department of Veterans Affairs or the United States Government.

Conflict of Interest: The authors declare that the research was conducted in the absence of any commercial or financial relationships that could be construed as a potential conflict of interest.

APPENDIX

8-iso PGF3a, 9S,11R,15S-trihydroxy-5Z,13E,17Z-prostatrienoate;
thromboxane B2, 9S,11,15S-trihydroxy-thromboxa-5Z;
17,18-DiHETE, 17,18-dihydroxy-5Z,8Z,11Z,14Z-eicosatetraenoic acid;
leukotriene B4, (5S,6Z,8E,10E,12R,14Z)-5,12-dihydroxyicosa-6,8,10,14-tetraenoic acid;
11,12-DiHETE, 11,12-dihydroxy-5Z,8Z,14Z,17Z-eicosatetraenoic acid;
12,13-DiHOME, 12,13-dihydroxy-9Z-octadecenoic acid;
5,6-DiHETE, 5,6-dihydroxy-8Z,11Z,14Z,17Z-eicosatetraenoic acid;
19,20-DiHDPA, 19,20-dihydroxy-4Z,7Z,10Z,13Z,16Z-docosapentaenoic acid;
14,15-DiHET or 14,15-DiHETrE, 14,15-dihydroxy-5Z,8Z,11Z-eicosatrienoic acid;
16,17-DiHDPA, 16,17-dihydroxy-4Z,7Z,10Z,13Z,19Z-docosapentaenoic acid;
13,14-DiHDPA, 13,14-dihydroxy-4Z,7Z,10Z,16Z,19Z-docosapentaenoic acid;
10,11-DiHDPA, 10,11-dihydroxy-4Z,7Z,13Z,16Z,19Z-docosapentaenoic acid;
7,8-DiHDPA, 7,8-dihydroxy-4Z,10Z,13Z,16Z,19Z-docosapentaenoic acid;
20-HETE, 20-hydroxy-5Z,8Z,11Z,14Z-eicosatetraenoic acid;
13(S)-HODE, 13S-hydroxy-9Z,11E-octadecadienoic acid;
9(S)-HODE, 9S-hydroxy-10E,12Z-octadecadienoic acid;
15-HETE, 15-hydroxy-5Z,8Z,11Z,13E-eicosatetraenoic acid;
17,18-EpETE, 17,18-epoxy-5Z,8Z,11Z,14Z-eicosatetraenoic acid;
12-HETE, 12-hydroxy-5Z,8Z,10E,14Z-eicosatetraenoic acid;
5-HETE, 5-hydroxy-6E,8Z,11Z,14Z-eicosatetraenoic acid;
19,20-EpDPA or 19,20-EpDPE, 19,20-epoxy-4Z,7Z,10Z,13Z,16Z-docosapentaenoic acid;
14,15-EET or 14,15-EpETrE, 14(15)-epoxy-5Z,8Z,11Z-eicosatrienoic acid;
10,11-EpDPA or 10,11-EpDPE, (4Z,7Z)-9-[3-(2Z,5Z,8Z)-2,5,8-undecatrien-1-yl-2-oxiranyl]-4,7-nonadienoic acid;
11,12-EET or 11,12-EpETrE, 11(12)-epoxy-5Z,8Z,14Z-eicosatrienoic acid.

frontiers in Cardiovascular Medicine

ORIGINAL RESEARCH
published: 07 May 2021
doi: 10.3389/fcvm.2021.650848

Echocardiographic Prognosis Relevance of Attenuated Right Heart Remodeling in Idiopathic Pulmonary Arterial Hypertension

Qin-Hua Zhao[1†], Su-Gang Gong[1†], Rong Jiang[1†], Chao Li[2], Ge-Fei Chen[3], Ci-Jun Luo[1], Hong-Ling Qiu[1], Jin-Ming Liu[1], Lan Wang[1,2] and Rui Zhang[1,2*]*

[1] Department of Pulmonary Circulation, Shanghai Pulmonary Hospital, Tongji University School of Medicine, Shanghai, China, [2] Tongji University School of Medicine, Shanghai, China, [3] Department of Biosciences and Nutrition, Karolinska Institutet, Stockholm, Sweden

OPEN ACCESS

Edited by:
Alessio Molfino, Sapienza University of Rome, Italy

Reviewed by:
Ran Miao, Capital Medical University, China
Ruijing Zhang, Second Hospital of Shanxi Medical University, China

****Correspondence:***
Rui Zhang
zgr1219@163.com
Lan Wang
wanglan198212@163.com

[†] These authors have contributed equally to this work

Specialty section:
This article was submitted to General Cardiovascular Medicine, a section of the journal Frontiers in Cardiovascular Medicine

Received: *08 January 2021*
Accepted: *22 March 2021*
Published: *07 May 2021*

Citation:
Zhao Q-H, Gong S-G, Jiang R, Li C, Chen G-F, Luo C-J, Qiu H-L, Liu J-M, Wang L and Zhang R (2021) Echocardiographic Prognosis Relevance of Attenuated Right Heart Remodeling in Idiopathic Pulmonary Arterial Hypertension. Front. Cardiovasc. Med. 8:650848. doi: 10.3389/fcvm.2021.650848

Background: Right ventricular (RV) function is a great determination of the fate in patients with pulmonary arterial hypertension (PAH). Monitoring RV structure back to normal or improvement should be useful for evaluation of RV function. The aims of this study were to assess the prognostic relevance of changed right heart (RH) dimensions by echocardiography and attenuated RH remodeling (ARHR) in idiopathic PAH (IPAH).

Methods: We retrospectively analyzed 232 consecutive adult IPAH patients at baseline assessment and included RH catheterization and echocardiography. ARHR at the mean 20 ± 12 months' follow-up was defined by a decreased right atrium area, RV mid-diameter, and left ventricular end-diastolic eccentricity index. The follow-up end point was all-cause mortality.

Results: At mean 20 ± 12 months' follow-up, 33 of 232 patients (14.2%) presented with ARHR. The remaining 199 surviving patients were monitored for another 25 ± 20 months. At the end of follow-up, the survival rates at 1, 3, and 5 years were 89, 89, and 68% in patients with ARHR, respectively, and 84, 65 and 41% in patients without ARHR (log-rank $p = 0.01$). ARHR was an independent prognostic factor for mortality. Besides, ARHR was available to further stratify patients' risk assessment through the French PAH non-invasive-risk criteria.

Conclusions: Echocardiographic ARHR is an independent determinant of prognosis in IPAH at long-term follow-up. ARHR might be a useful tool to indicate the RV morphologic and functional improvement associated with better prognostic likelihood.

Keywords: pulmonary arterial hypertension, right heart remodeling, echocardiography, biomarkers, prognosis

INTRODUCTION

Pulmonary arterial hypertension (PAH) was a progressive disease that affected both pulmonary vasculature and heart. Although the initial damage in PAH may involve the pulmonary vasculature, the prognosis of patients with PAH is closely related to the right ventricular (RV) function (1–3). RV function is a great clinical determinant of the fate in patients with severe pulmonary hypertension

(PH) (4, 5). The right heart (RH) failure may be a consequence of increased afterload in PH. An adapted right ventricle showed slightly dilated with preserved stroke volume and systolic function, whereas a maladapted right ventricle is dilated with reduced systolic function and increased dimensions (5, 6). Therefore, the changes of RV dimensions were inevitable and associated with pulmonary hemodynamics. Monitoring RV dimension could predict clinical worsening even at apparent clinical stability in PAH (7).

Echocardiography is an essential and non-invasive component estimated the role of RV function in PAH. Imaging modalities would be ideal to validate potential RV function and allow the creation of prediction scores to identify risk of mortality (8–10). Badagliacca et al. have reported the reversal of RH remodeling (RHRR) was associated with an improved outcome in idiopathic PAH (IPAH) patients by assessing right atrium (RA) area, left ventricular systolic eccentricity index (LV-EI), and RV end-diastolic area (11). Moreover, several clinical common echocardiographic variables were associated with mortality risk such as RV mid-diameter (RVMD) and tricuspid annular plane systolic excursion (12–14).

In the present study, we try to reassess and recalculate the efficacy of RH dimension's changes through general clinical echocardiographic parameters. Here, we defined a new model of attenuated RH remodeling (ARHR) using a decrease in RA area, RVMD, and left ventricular end-diastolic eccentricity index (LV-EId). Each of these echocardiographic parameters has been reported to be a determinant of prognosis in PAH (10, 11, 13). We proposed a hypothesis that ARHR created by a decrease in RA area, RVMD, and LV-EId would be associated with mortality and clinic outcomes.

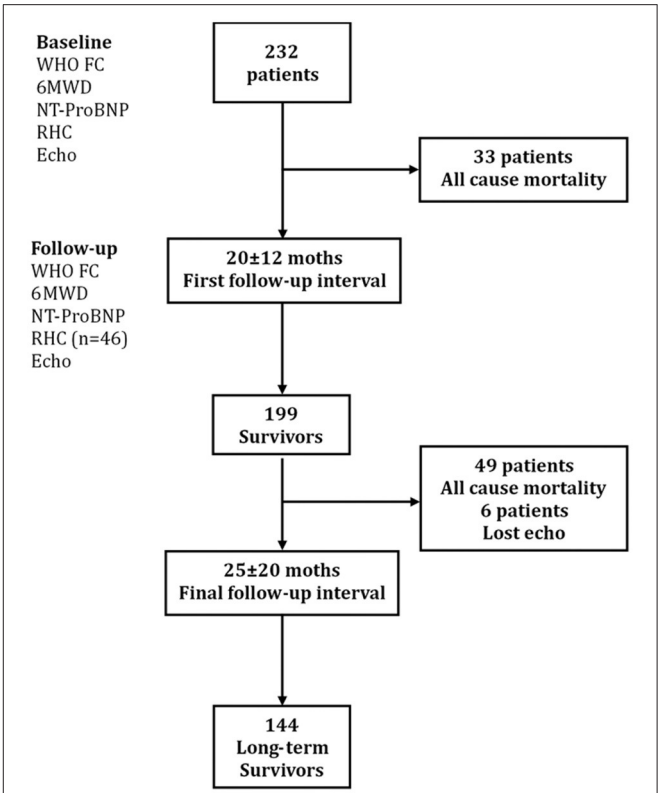

FIGURE 1 | Study design flowchart. Echo, echocardiography; 6MWD, 6-min walking distance; NT-proBNP, N-terminal fragmental of pro–brain natriuretic peptide; RHC, right heart catheterization; WHO FC, World Health Organization functional class.

MATERIALS AND METHODS

Study Subjects and Design

Two hundred thirty-two consecutive treatment-naive adult IPAH patients (≥18 years of age at diagnosis) were enrolled and monitored at the time of their first right heart catheterization (RHC) in Shanghai Pulmonary Hospital from November 2010 to January 2018. IPAH was diagnosed according to guideline standard: a mean pulmonary artery pressure (mPAP) ≥25 mmHg and pulmonary vascular resistance (PVR) >3 Woods units at rest in the presence of a normal pulmonary artery wedge pressure (≤15 mmHg) on RHC (15, 16). In accordance with criteria, the respiratory function tests, perfusion lung scan, computed tomography scan, and echocardiography were used. If patients had definite causes of PAH, such as connective tissue disease and congenital heart disease, portopulmonary hypertension, chronic pulmonary thromboembolism, PH due to left heart diseases and lung diseases, and/or hypoxemia, they could be excluded.

The baseline assessment at the time of diagnosis included medical history, physical examination, 6-min walking distance (6MWD), N-terminal fragmental of pro–brain natriuretic peptide (NT-proBNP), RHC, and echocardiography. During the first follow-up interval (mean follow-up time 20 ± 12 months), 33 patients died for all cause. The follow-up parameters included physical examination, 6MWD, NT-proBNP, echocardiography, and RHC (only 46 patients received RHC test). The 199 remaining survivors were reevaluated at a mean 25 ± 20 months until December 2018 (**Figure 1**). The major end point was all-cause mortality. The study was conformed according to the principles of the Declaration of Helsinki and was approved by the ethics committee of Shanghai Pulmonary Hospital (no. K16-293). Written informed consent signatures were obtained from all patients.

RHC and Echocardiographic Assessment

Pulmonary hemodynamics were examined in triplicate at end-expiration using triple-lumen balloon-tipped thermodilution

Abbreviations: BMI, body mass index; CI, cardiac index; IPAH, idiopathic pulmonary arterial hypertension; LAESD, left atrium end-systolic diameter; LV A wave PW, pulsed wave left ventricular A wave; LVEDD, left ventricular end-diastolic diameter; LVEF, left ventricular ejection fraction; LV-EId, left ventricular end-diastolic eccentricity index; LVESD, left ventricular end-systolic diameter; LV E wave PW, pulsed wave left ventricular E wave; mPAP, mean pulmonary arterial pressure; 6MWD, 6-min walking distance; NT-proBNP, N-terminal fragmental of pro–brain natriuretic peptide; PAWP, pulmonary artery wedge pressure; PASP, pulmonary arterial systolic pressure; PVR, pulmonary vascular resistance; RA area, right atrium area; RAP, right atrial pressure; RVLD, right ventricular longitudinal diameter; RVMD, right ventricular mid diameter; TAPSE, tricuspid annular plane systolic excursion; SvO_2, mixed venous oxygen saturation; WHO FC, World Health Organization functional class.

Swan–Ganz catheters. Cardiac output was detected by thermodilution (15, 16). Baseline echocardiographic measurements were performed within 24–48 h of the RHC. All echocardiographic data were acquired using commercially available equipment (Vivid 7, GE Healthcare) in standard views. The results were reviewed by at least three echocardiographic experts. Measurements were obtained from the mean of three consecutive beats based on the American Society of Echocardiography guidelines (17). The echo parameters and derived assessments that we focused on common and widely available for daily clinical practice, including RA area, RVMD, RV longitudinal diameter (RVLD), right atrial pressure (RAP), left atrium end-systolic diameter (LAESD), left ventricular end-diastolic diameter (LVEDD), left ventricular ejection fraction (LVEF), LV-EId, left ventricular end-systolic diameter (LVESD), pulmonary arterial systolic pressure (PASP), tricuspid annular plane systolic excursion (TAPSE), and presence of pericardial effusion. Spectral continuous-wave Doppler signal of tricuspid regurgitation corresponding to the RV-RA pressure gradient. SPAP was calculated as the sum of the estimated RAP and the peak pressure gradient between the peak RV and RA, as estimated by application of the modified Bernoulli equation to peak velocity represented by the tricuspid regurgitation Doppler signal. Early diastolic transmitral flow velocity (E) and late diastolic transmitral flow velocity (A) were measured by Doppler echocardiography. ARHR was defined by echocardiographic parameters of RA area, RVDM, and LV-EId, according to Cox proportional hazards regression for mortality risk at follow-up.

RVMD was defined as transversal RV diameter in the middle third of RV inflow, approximately hallway between the maximal basal diameter and the apex, at the level of papillary muscles at end-diastole (18). RA area is traced at the end of ventricular systole from the lateral aspect of the tricuspid annulus to the septal aspect, excluding the area between the leaflets and annulus, as well as the inferior vena cava, superior vena cava, and RA appendage (17). LV-EId was measured in the parasternal short-axis view at end-diastole. This index was calculated as D2/D1, where D2 is the minor-axis dimension of the left ventricle parallel to the septum, and D1 is the minor-axis dimension perpendicular to and bisecting the septum (3). TAPSE is measured by M-mode echocardiography with the cursor optimally aligned along the direction the tricuspid lateral annulus in the apical four-chamber view (18).

Statistical Analysis

Continuous variables were expressed as means with corresponding standard deviations, and categorical variables were expressed as numbers and percentages. The proportions were compared with the χ^2 test. If the data were normally distributed, two-group comparisons were performed with unpaired or paired, two-tailed *t*-test for means. If the data were not normally distributed, non-parametric two-sided Mann–Whitney *U* test was used. Bivariate linear analysis was to evaluate the correction between the change of NT-proBNP, 6MWD, and RA area, RVMD, and LV-EId during the follow-up, fitting curve was used a quadratic model with mean value 95% confidence interval.

Cox proportional hazards regression was used to determine risk factors for mortality at follow-up and to identify the association among patient characters and outcomes. For optimal cutoff value for mortality, RA area, RVMD, and LV-EId were generated by receiver operating characteristic (ROC) curves. The Cox proportional hazards regression used to derive a risk calculator assigning weighted for three echo parameters. An integer score of RA area was assigned a value of 1 for the β-coefficient associated with a hazard ratio (HR) of 1.009. Integer scores of 1.621 for RVMD and 2.033 for LV-EId were created assigning values of 1.5 and 2.0, respectively. The total sum of three echo parameters was used for each patient based on the number of the echo cutoff value. Univariate and multivariate logistic regression analyses were chosen to identify clinical and hemodynamic determinants of ARHR. Multivariate analysis to WHO FC I–II, 6MWD, and NT-proBNP for model 1 was created, and WHO FC I–II plus ARHR for model 2. The C-statistic was calculated for each model and model discrimination by R version 2.11.1 (19).

The French non-invasive low-risk criterion was calculated based on the number of non-invasive criteria to derive the original model 1, including WHO FC I–II, 6MWD >440 m, NT-proBNP <300 ng/L (20). The French non-invasive low-risk criteria score was used for Cox regression analysis to predict mortality (model 1), and model 2 was added the echo score. Survival analyses were performed using the Kaplan–Meier method and were compared by means of the log-rank test. For all analyses, $p < 0.05$ was considered statistically significant. All calculations were performed using the SPSS 14.0 statistical software package (Statistical Package for the Social Sciences, Chicago, IL, USA).

RESULTS

Baseline Clinical and Hemodynamic Characteristics of Patients

The baseline clinical, hemodynamic, and echocardiographic features of the IPAH patients are summarized in **Table 1**. Among 232 patients with IPAH, 147 (71%) were women, and 153 (66%) in WHO FC III and IV, with impaired exercise capacity and severe PH hemodynamic status. The echocardiography examination at baseline presented severe RV dilatation and systolic function reduction. Most patients had mild to moderate tricuspid regurgitation.

During mean 20 ± 12 follow-up interval, 33 patients (14%) died, including 26 deaths directly related to RH failure, 5 sudden deaths, and 2 cases not able to be ascertained. Compared with the remaining 199 patients, these patient deaths at baseline were more severe and had advanced disease, such as PVR (16 ± 10 vs. 13 ± 6 Woods unit, $p = 0.01$), RAP (9 ± 6 vs. 6 ± 5 mmHg, $p = 0.03$), S_VO_2 (60 ± 9 vs. 64 ± 9 %, $p = 0.02$), mPAP (62 ± 17 vs. 58 ± 15 mmHg, $p = 0.24$), CI (2.4 ± 0.8 vs. 2.7 ± 0.8 L/min per m^2, $p = 0.16$), NT-proBNP (1,341 ± 974 vs. 964 ± 1,092 ng/L, $p = 0.03$), WHO FC (3.0 ± 0.6 vs. 2.6 ± 0.6, $p = 0.04$), and 6MWD (356 ± 106 vs. 394 ± 110 m, $p = 0.09$).

TABLE 1 | Baseline clinical, hemodynamic, and echocardiographic characteristics of patients with IPAH.

Variable	Mean ± SD or no. (%) (*n* = 232)
Age, years	40 ± 15
Female, *n* (%)	147 (71)
BMI, kg/m^2	22 ± 4.7
WHO FC, *n* (%)	
Class I–II	79 (34)
Class III	142 (61)
Class IV	11 (5)
6MWD, m	390 ± 107
NT-proBNP, ng/L	997± 1,088
Hemodynamics	
RAP, mmHg	7 ± 4.9
mPAP, mmHg	59 ± 15
PAWP, mmHg	8 ± 3.1
CI, L/min per m^2	2.6 ± 0.8
PVR, Woods units	14 ± 6.5
S_VO_2, %	62 ± 9.1
Echocardiography	
RA area, cm^2	25 ± 11
RVMD, cm	4.5 ± 0.8
LV-EId	1.6 ± 0.4
RVLD, cm	6.5 ± 0.9
RA major axis dimension, cm	5.3 ± 1.0
RA minor axis dimension, cm	4.9 ± 1.2
LVESD, cm	2.2 ± 0.5
LVEDD, cm	3.8 ± 0.6
LAESD, cm	3.1 ± 0.5
TAPSE, mm	17 ± 3.4
LV-E wave PW, cm/s	54.9 ± 18.7
LV-A wave PW, cm/s	58.9 ± 17.1
LVEF, %	74 ± 8.4
PASP, mmHg	86 ± 23
RAP, mmHg	7 ± 3
Pericardial effusion, *n* (%)	63 (27)
Initial specific therapies, *n* (%)	
No specific/CCB therapy	16 (7)
Monotherapy	145 (63)
ERA	35 (15)
PDE5i	98 (42)
Prostanoid	12 (5)
Dual combination	71 (31)

Values are expressed as medians (interquartile range) or n (%), unless otherwise stated. BMI, body mass index; CCB, calcium channel blocker; CI, cardiac index; ERA, endothelin receptor antagonist; IPAH, idiopathic pulmonary arterial hypertension; LAESD, left atrium end-systolic diameter; LV A wave PW, pulsed wave left ventricular A wave; LVEDD, left ventricular end-diastolic diameter; LVEF, left ventricular ejection fraction; LV-EId, left ventricular end-diastolic eccentricity index; LVESD, left ventricular end-systolic diameter; LV E wave PW, pulsed wave left ventricular E wave; mPAP, mean pulmonary arterial pressure; 6MWD, 6-min walking distance; NT-proBNP, N-terminal fragmental of pro–brain natriuretic peptide; PAWP, pulmonary artery wedge pressure; PASP, pulmonary arterial systolic pressure; PDE5i, phosphodiesterase type 5 inhibitor; PVR, pulmonary vascular resistance; RA area, right atrium area; RAP, right atrial pressure; RVLD, right ventricular longitudinal diameter; RVMD, right ventricular mid diameter; TAPSE, tricuspid anular plane systolic excursion; SvO_2, mixed venous oxygen saturation; WHO FC, World Health Organization functional class.

Clinical and echocardiographic information was available for 199 survivors at the mean first follow-up interval.

Clinical and Echocardiographic Findings at First Follow-Up

At the first follow-up reevaluation, the 199 surviving patients had a relative improvement in clinical condition (6MWD, $+37 \pm 71$ m, $p = 0.02$; NT-proBNP, -361 ± 652 ng/L, $p = 0.025$; WHO FC, -0.2 ± 0.1, $p = 0.53$) and hemodynamics (PVR, -3.3 ± 1.9 Woods unit, $p = 0.004$; mPAP, -10.6 ± 9.3 mmHg, $p = 0.03$; CI, $+0.5 \pm 0.2$ L/min per m^2, $p = 0.005$; RAP, -2.0 ± 1.5 mmHg, $p = 0.39$; S_VO_2, $+5.9 \pm 4.0$ %, $p = 0.13$; follow-up RHC samples were from 46 patients). Importantly, these patients had a significant improvement of most echocardiographic parameters (RA area, -4.2 ± 3.8 cm^2, $p = 0.010$; RVMD, -0.3 ± 0.1 cm, $p = 0.015$; LV-EId, 0.09 ± 0.04, $p = 0.03$; TAPSE, $+0.24 \pm 0.49$, $p = 0.027$; RA major axis dimension, 0.17 ± 0.37 cm, $p = 0.001$; RA minor axis dimension, 0.19 ± 0.33 cm, $p = 0.011$; LVEF, 6.0 ± 3.0 %, $p < 0.001$; LV-E wave, 8.0 ± 3.4 cm/s, $p = 0.001$; LV-E wave, 2.2 ± 4.5 cm/s, $p = 0.51$; pericardial effusion 8% regression, $p = 0.002$) compared with their baseline data.

ARHR and Determinants

At univariate analysis, absolute changes from baseline to the first follow-up assessment in RA area (HR, 1.009; 95% confidence interval, 0.991–1.027; $p = 0.01$), RVMD (HR, 1.621; 95% confidence interval, 1.083–2.427; $p = 0.01$), and LV-EId (HR, 2.033; 95% confidence interval, 0.386–3.524; $p = 0.02$) were predictive of all-cause death in the subsequent period. The optimal cutoff points by ROC analysis protective against all-cause death were -5.8 cm^2 (sensitivity, 75%; specificity, 66%) for RA area change, -0.7 cm (sensitivity, 77%; specificity, 68%) for RVMD change, and -0.4 (sensitivity, 86%; specificity, 67%) for LV-EIs change.

A score was created deriving integers according to the HRs of the latter echo variables. Based on the achievement of change cutoff points of echo parameters, patients are categorized by the echo score. One hundred thirty-four patients (67.3%) had a score between 0 and 2.0 (0 or 1 protective changes cutoff point of echo parameters), 30 (15.1%) had a score between 2.5 and 3.5 (achievement of 2-echo-parameters cutoff point), and 35 (17.6%) had a score between 4.0 and 4.5 (achievement of all 3-echo-parameters cutoff point). The score between 4.0 and 4.5 was selected as a comprehensive criterion for ARHR. Conversely, a score <4.0 was defined as without ARHR. There were no significant differences in clinical and echocardiographic parameters between patients with or without subsequent ARHR at the first follow-up interval (**Table 2**). At the first follow-up, a significant correlation was present between the change of NT-proBNP and improvement of RA area ($r^2 = 0.51$, $p = 0.009$) and RVMD ($r^2 = 0.45$, $p = 0.001$) (**Figure 2**). Two examples of patients with and without ARHR at the first follow-up are demonstrated at **Figure 3**.

ARHR and Prognosis

After the first follow-up evaluation, the remaining 199 surviving patients were monitored for a mean of 25 ± 20 months. During

TABLE 2 | Clinical, hemodynamic, and echocardiographic characteristics of two patient groups based on ameliorative right heart remodeling at first follow-up interval.

Variable	No ARHR ($n = 164$)	ARHR ($n = 35$)	p-value
Age, years	42 ± 17	37 ± 11	0.16
Female, *n* (%)	131 (75)	18 (75)	0.89
WHO FC, *n* (%)			0.22
Class I–II	56 (32)	9 (38)	
Class III	108 (62)	14 (58)	
Class IV	11 (6)	1 (4)	
6MWD, m	415 ± 115	389 ± 131	0.92
NT-proBNP, ng/L	805 ± 1,141	1,023 ± 1,297	0.74
Echocardiography			
RA area, cm^2	28 ± 12	23 ± 13	0.06
RVMD, cm	5.1 ± 0.9	4.5 ± 0.8	0.28
LV-Eld	1.6 ± 0.5	1.5 ± 0.3	0.24
RVLD, cm	6.6 ± 0.8	6.5 ±0.7	0.59
RA major axis dimension, cm	5.5 ± 1.4	6.2 ± 1.3	0.72
RA minor axis dimension, cm	5.0 ± 1.4	5.3 ± 1.4	0.79
LVESD, cm	2.0 ± 0.6	1.5 ± 0.4	0.14
LVEDD, cm	3.7 ± 0.7	3.2 ±0.2	0.13
LAESD, cm	3.1 ± 0.5	3.0 ± 0.3	0.34
TAPSE, mm	17 ±4.2	13 ± 6.6	0.46
LV-E wave PW, cm/s	61.6 ± 18.1	58.2 ± 21.1	0.44
LV-A wave PW, cm/s	61.7 ± 19.4	71.7 ± 10.7	0.86
LVEF, %	78 ± 9.6	81 ± 6.7	0.40
PASP, mmHg	83 ± 24	90 ± 12	0.49
RAP, mmHg	7 ±3	8 ± 5	0.21
Pericardial effusion, *n* (%)	53 (30)	13 (54)	0.22
Initial specific therapies, *n* (%)			
No specific/CCB therapy	6 (3)	1 (4)	
Monotherapy			
ERA	25 (14)	4 (17)	
PDE5i	47 (27)	5 (21)	
Prostanoid	7 (4)	1 (4)	
Dual combination	88 (50)	13 (54)	

Values are expressed as medians (interquartile range) or n (%), unless otherwise stated. ARHR, attenuated right heart remodeling; CCB, calcium channel blocker; ERA, endothelin receptor antagonist; LAESD, left atrium end-systolic diameter; LV A wave PW, pulsed wave left ventricular A wave; LVEDD, left ventricular end-diastolic diameter; LVEF, left ventricular ejection fraction; LV-Eld, left ventricular end-diastolic eccentricity index; LVESD, left ventricular end-systolic diameter; LV E wave PW, pulsed wave left ventricular E wave; 6MWD, 6-min walking distance; NT-proBNP, N-terminal fragmental of pro–brain natriuretic peptide; PASP, pulmonary arterial systolic pressure; PDE5i, phosphodiesterase type 5 inhibitor; RA area, right atrium area; RVLD, right ventricular longitudinal diameter; RVMD, right ventricular mid diameter; TAPSE, tricuspid anular plane systolic excursion; WHO FC, World Health Organization functional class.

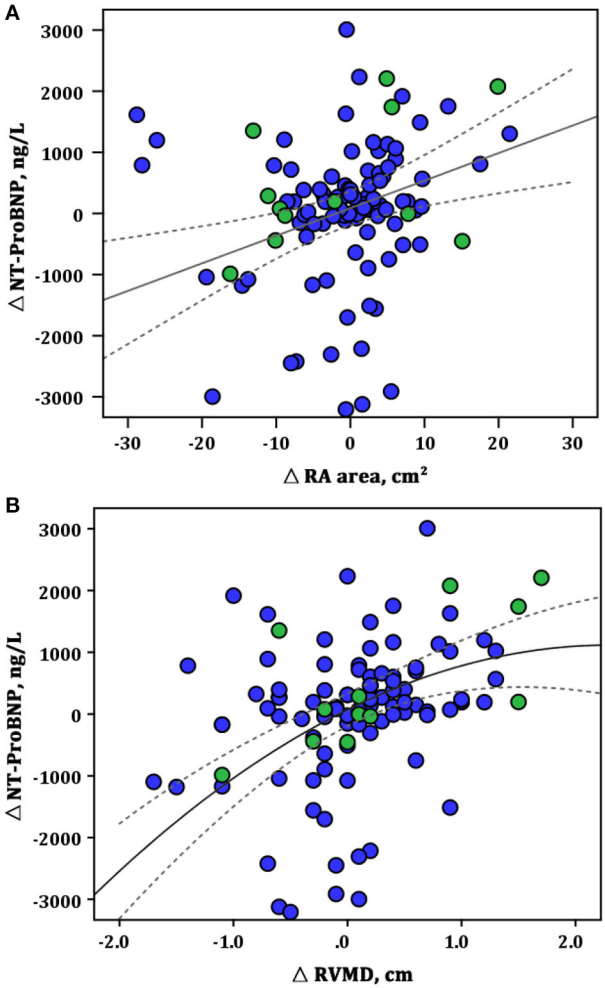

FIGURE 2 | Correlations between the changes in RA area, RVMD, and NT-proBNP at the first follow-up assessment. **(A)** ΔRA area vs. Δ NT-proBNP (linear model: $r^2 = 0.51$, $p = 0.009$); **(B)** ΔRVMD vs. Δ NT-proBNP (linear model: $r^2 = 0.45$, $p = 0.001$). Green circles represent the patients with ARHR; blue circles, without ARHR. NT-proBNP, N-terminal fragmental of pro–brain natriuretic peptide; RA, right area; RVMD, right ventricular mid diameter.

this period, there were 55 patient deaths. The total survival rate at the final follow-up assessment was 85, 70, and 53% at 1, 3, and 5 years of follow-up, respectively.

As shown in **Table 3**, we generated two Cox regression models at the follow-up assessment. Model 1 demonstrated that WHO FC I and II and NT-proBNP were independent predictors of death. Model 2 was created by adding the echo score according to the 3 echo parameters, showing the ARHR and WHO I and II were significantly protective factors independently from other variables. Accordingly, there were a greater proportion of patients attaining ARHR in WHO FC I–II group and lesser proportion of ARHR patients in WHO FC III ($p = 0.01$) (**Figure 4**). No ARHR patients were in the WHO FC IV group.

The survival curves at final follow-up of 199 surviving patients classified according to ARHR are shown in **Figure 5**. Patients with ARHR had a better long-term survival than others (log-rank $p = 0.01$). The cumulative survival rates at 1, 3, and 5 years of follow-up were 89, 89, and 68% in patients with ARHR, respectively, and 84, 65, and 41% in patients without ARHR.

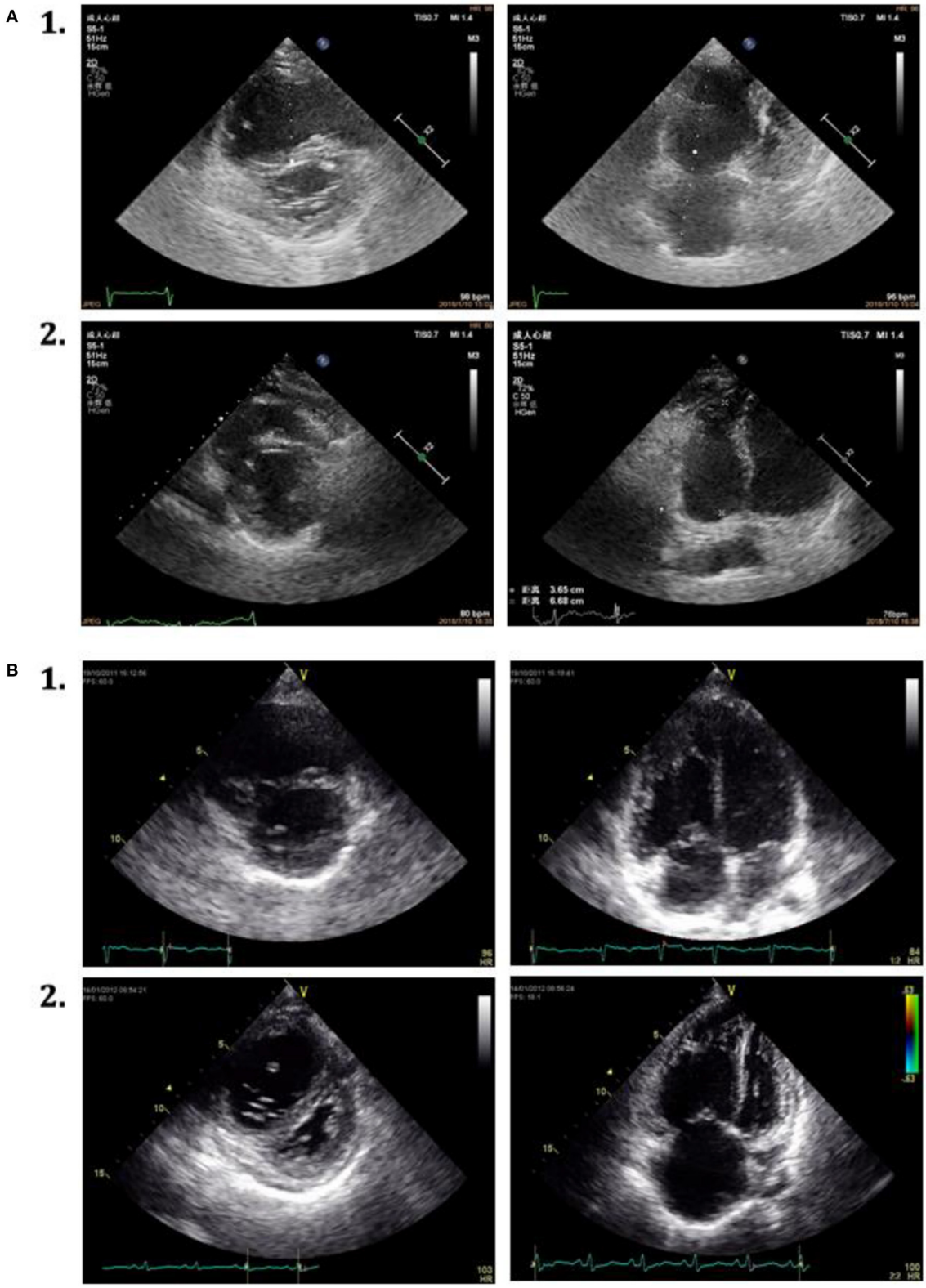

FIGURE 3 | Echocardiographic parasternal short-axis view and apical four-chamber view in 2 patients with IPAH. **(A)** 1. The characteristics at baseline. 2. Attenuated right heart remodeling of the same patient at the first follow-up assessment. **(B)** 1. The characters at baseline. 2. Without attenuated right heart remodeling of the same patient at the first follow-up assessment.

TABLE 3 | Cox regression models for dead prediction at the first follow-up evaluation: model 1 and model 2.

Variable	Unit	HR (95% confidence interval)	*p*-value	C-statistic (95% confidence interval)
Model 1				0.60 (0.52–0.73)
WHO I–II		0.46 (0.21–0.97)	0.0001	
6MWD	1	0.99 (0.98–1.02)	0.07	
NT-proBNP	1	1.46 (1.27–3.14)	0.002	
Model 2				0.75 (0.69–0.82)
WHO I–II		0.55 (0.21–0.98)	0.0001	
Echo score[a]				
0-2	REF			
2.5–3.5		0.80 (0.39–1.96)	0.45	
4–4.5 (ARHR)		0.42 (0.21–0.88)	0.004	

ARHR, attenuated right heart remodeling; CI, confidence interval; HR, hazard ratio; 6MWD, 6-min walking distance; NT-proBNP, N-terminal fragmental of pro–brain natriuretic peptide; WHO FC, World Health Organization functional class.
[a]Echo score, score based on protective changes in echo parameters by ROC curve analysis cutoff value.

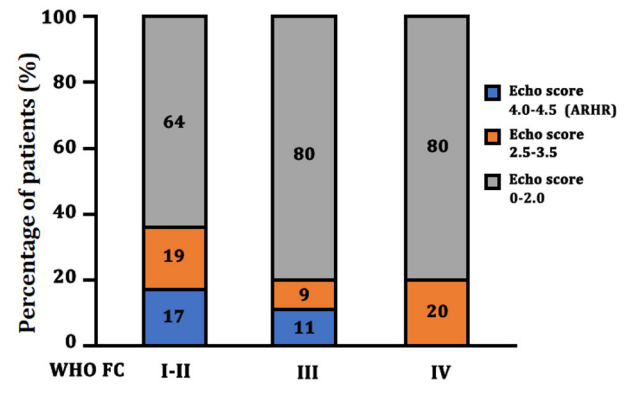

FIGURE 4 | Echo score in different WHO FC group at the follow-up assessment. ARHR, attenuated right heart remodeling; Echo, echocardiography; WHO FC, World Health Organization functional class.

ARHR Combined With French Non-invasive Low-Risk Criteria

To explore the adding value of ARHR on a well-generated risk evaluation tool, we repeated the analysis building a first model 1 according to the number of French non-invasive low-risk criteria (WHO FC I–II; 6MWD >440 m; NT-proBNP <300 ng/L). The ARHR echo score was then added to model 2 was and showed prognostic strength power (**Table 4**). The survival of the four groups are shown in **Figure 6**, based on the combination of French non-invasive low-risk criteria (3 criteria vs. 0–2 criteria) and ARHR (echo score 4.0–4.5 vs. <4.0). Patients with ARHR and French non-invasive criterion 0 had the best prognosis; 1-, 3-, and 5-year survival rates were all 100%. Patients without ARHR (score <4) and French non-invasive criteria 0–2 presented worst survival, and 1-, 3-, and 5-year survival rates were 78, 63, and 46%, respectively. However, we did not find significant difference between the combination of ARHR (score 4.0–4.5) and French non-invasive criterion 0–2 and those of non-ARHR (score <4.0) and French non-invasive criteria 3 (**Figure 6**).

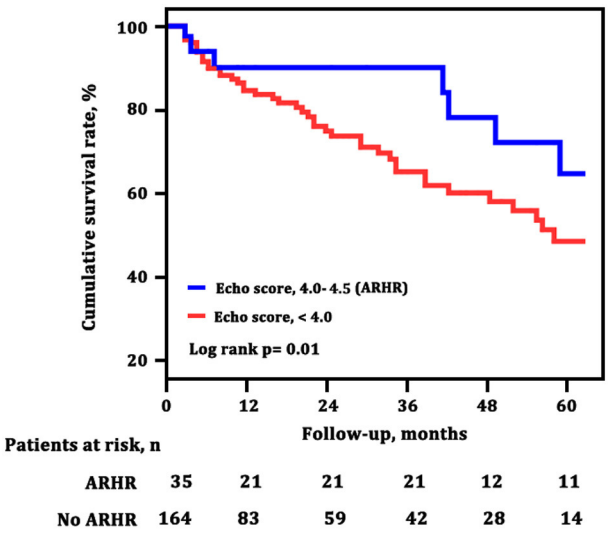

FIGURE 5 | Survival estimates of patients with and without attenuated right heart remodeling (ARHR). Green line (echo score, 4.0–4,5) represents the survival of patients with ARHR; blue line (echo score, <4.0) represents the survival of patients without ARHR.

TABLE 4 | Cox regression models for dead prediction according to the French non-invasive risk assessment and echo.

Variable	Unit	HR (95% confidence interval)	*p*-value	C-statistic (95% confidence interval)
Model 1				0.61 (0.53–0.73)
French non-invasive low-risk criteria[a]				
3 criteria	REF			
1–2 criteria		3.03 (1.10–4.28)	0.031	
0 criteria		2.77 (0.84–3.15)	0.041	
Model 2				0.72 (0.67–0.80)
French non-invasive low-risk criteria				
3 criteria	REF			
1–2 criteria		2.77 (1.06–3.04)	0.092	
0 criteria		2.97 (0.89–3.85)	0.042	
Echo score[b]				
0–2	REF			
2.5–3.5		0.83 (0.22–1.79)	0.655	
4–4.5 (ARHR)		0.39 (0.12–0.77)	0.012	

[a]French non-invasive low-risk criteria: based on the number of non-invasive criteria (WHO FC I–II; 6MWD >440 m; NT-proBNP <300 ng/L).
[b]Echo score: score based on protective changes in echo parameters by ROC curve analysis cutoff value.

DISCUSSION

Echocardiographic RV imaging combined with pulmonary hemodynamics was a good framework to interpret the prognosis

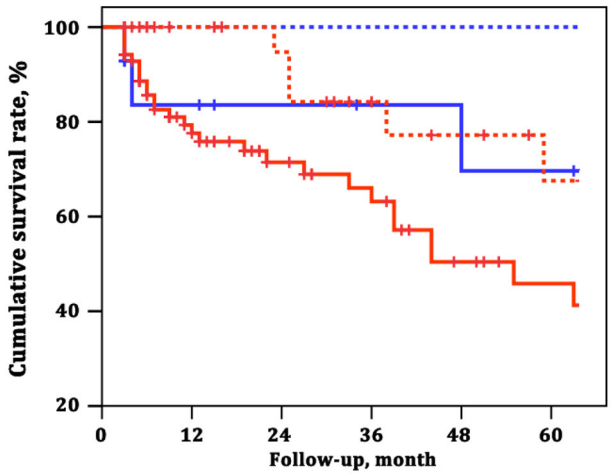

FIGURE 6 | Survival estimates of the four groups of patients based on the combination of French non-invasive low-risk criteria and attenuated right heart remodeling (ARHR). Blue dashed line represents French non-invasive criterion 3 and echo score 4.0–4.5. Red solid line represents French non-invasive criteria 0–2 and echo score 4.0–4.5. Blue solid line represents French non-invasive criterion 3 and echo score <4.0. Red dashed line represents French non-invasive criteria 0–2 and echo score <4.0.

of patients with IPAH (1, 4). Monitoring the change of RV dimensions back to normal or improvement should be useful for evaluation of the RV function. Therefore, it is noteworthy to find a practical echocardiographic predictor tool to remind prognosis. In our study, we defined an ARHR model and found that at the first reevaluation (a) ARHR was an independent predictor of mortality; and (b) ARHR combined with French non-invasive criterion could better predict the outcome of death. The RHRR might serve as a tool for pending prognosis in patients with IPAH.

RA area, RVMD, and LV-EId selected in this study were conventional and important echocardiography indices (12, 17, 21–24). For example, RA area >18 cm^2 was considered as one of the preferred parameters for end-diastole RA enlargement (17). RA enlargement reflected the severity of RH failure and predicted adverse outcomes in patients with severe primary PH (3). A study from Badagliacca's team used RA area as one of the determinants of RV reverse remodeling (10). Therefore, our findings supposed the change of RA area was also a marker of RA dilatation. If there is RV dilatation, RVMD should be measured to respond the chronic volume and/or pressure overload (22). In our study, RV size was measured from a four-chamber view, where RVMD was easily obtained and markers of RV dilatation. The third important parameter in this study is LV-EId, reflecting the degree of septal shift in diastole (3, 10). Echocardiography showed improved LV-EId in proportion to treatment-induced decrease in PVR (24). Taken together, the shift in RV remodeling during the development of PAH is not well elucidated. It is challenging to determine the best parameters for reflecting RV failure progression (25). ARHR in this study might be an indication with reversal of RH dimensions.

It is recognized that the change of RV structure is the main predictor of poor clinical outcomes in PAH (22). There was no more than 18% of IPAH patients presented with ARHR after a mean of 20 ± 12 months in our study, despite that more than 93% of patients had received PAH-specific therapies. This result is similar with the study on RHRR in IPAH patients after 1-year targeted treatment, which implies that the reversal of RV remodeling is hard and complex (10). At first follow-up time, both the disease severity and echocardiographic indicators seemed to have no significant difference between ARHR and no-ARHR group. However, the patients with ARHR had better long-term survival, as longstanding increase of RV afterload will overwhelm the compensatory mechanisms of the RV (26). Not surprisingly, the patients' hemodynamic status of pulmonary circulation is not always consistent with the changes of RV structure and function. Despite hemodynamics deterioration in patients with PAH, RV contractility is usually increased and not decreased (4, 27, 28). Consequently, the amount of work for the RV remained unaltered, leading to a clinical improvement but unchanged prognosis (29). Therefore, non-invasive imaging of RV dimensions and function is important to the longitudinal monitoring of patients with PAH and continued understanding of the response of RV to pulmonary vascular remodeling (30).

French PH registry permitted to use three non-invasive variables to assess the low-risk criteria score, such as WHO FC, 6MWD, and BNP/NT-proBNP (20). However, it remained unclear whether the addition of other non-invasive modes, such as echocardiography, to the three non-invasive criteria could further improve the prognostic utility (20, 31, 32). Notably, in our study, echocardiography-determined ARHR was able to further stratify patients assessed with French non-invasive low-risk criteria score, suggesting a better prognosis for those patients achieving ARHR. The 1-, 3-, and 5-year survival rates were all 100% in patients with ARHR and French non-invasive criterion 0, compared with 78%, 63%, and 46% in patients with no ARHR (score <4) and French non-invasive criteria 1–4, respectively. Therefore, our results indicated that non-invasive French low-risk criteria combined with echocardiography ARHR would be a preferable predictor model for mortality in patients with IPAH.

Certainly, several echocardiographic parameters were related to long-term prognosis, such as TAPSE, PASP, etc. (12, 33, 34). However, changes in TAPSE or PASP were not predictive of mortality at univariate analysis in our first follow-up time. This is attributable to the limitation of TAPSE assuming that the displacement of a single segment represents the function of a complex 3D, considering the RV shape is more "regular" (35, 36). Indeed, patients in our study underwent more pronounced increases in RV afterload (severe RV dilation), especially for non-ARHR patients who did not have significant improvement for systolic function. Thus, echocardiography is still a comprehensive and multiple tool for non-invasive assessment of the RH.

STUDY LIMITATIONS

There are several limitations to this study. First, this is a retrospectively study in a single center, and the sample size is not large enough with a potential selection bias. The follow-up

intervals of PAH patients were not fixed and varied. Second, the follow-up intervals of patients are not standardized and lack of RHC hemodynamic testing. It is different to further analyze the relationship between the change of hemodynamic parameters and ARHR. Then, we did not select the best ROC curve cutoff values for subsequent analysis to avoid the potential risk of a type I error. Finally, there are limitations to the quantification of RH morphology and function using two-dimensional echocardiography. In the future, we need more and accurate parameters to evaluate RV function.

CONCLUSIONS

In summary, our study demonstrated that echocardiographic ARHR created by RA area, RVMD, and LV-EId was an independent predictor of long-term prognosis in patients with IPAH. Similarly, ARHR integrated with French non-invasive criterion could better predict the risk for mortality. ARHR might be a useful tool to indicate RV morphologic and functional improvement associated with better prognostic likelihood. Whether this increases the proportion of patients with ARHR remained to be further confirmed in prospective and multicenter assessments.

DATA AVAILABILITY STATEMENT

The original contributions presented in the study are included in the article/supplementary material, further inquiries can be directed to the corresponding authors.

ETHICS STATEMENT

The studies involving human participants were reviewed and approved by Ethic Committee of Shanghai Pulmonary Hospital. The patients/participants provided their written informed consent to participate in this study. Written informed consent was obtained from the individual(s) for the publication of any potentially identifiable images or data included in this article.

AUTHOR CONTRIBUTIONS

RZ and LW were directly involved in the patients' recruitment and care, contributed to the study design, study conduct and supervision, scientific overview, data analysis, and editing of the manuscript. Q-HZ, S-GG, and RJ contributed to patient enrolment, data analysis, scientific interpretation, drafting, and editing the original manuscript. CL, G-FC, C-JL, H-LQ, and J-ML contributed to recruitment of participants, data collection and curation, and formal analysis. All authors have reviewed the manuscript and approved the final version for submission.

FUNDING

This study was supported in part by the Project of International Cooperation19410741000 (RZ) and 201409004100 (S-GG) in Science and Technology Commission Shanghai Municipality, Youth Scholar Program of Shanghai Pulmonary Hospital fkgg1804 (RZ), the National Natural Science Foundation of China 82000059, 81900050, and 81700045 (LW, Q-HZ, and RJ).

ACKNOWLEDGMENTS

The authors acknowledge the contribution of all investigators who participated in this study. We also thank the patients who participated in the study.

REFERENCES

1. van Wolferen SA, Marcus JT, Boonstra A, Marques KM, Bronzwaer JG, Spreeuwenbera MD, et al. Prognostic value of right ventricular mass, volume, and function in idiopathic pulmonary arterial hypertension. *Eur Heart J.* (2007) 28:1250–7. doi: 10.1093/eurheartj/ehl477
2. Sachdev A, Villarraga HR, Frantz RP, McGoon MD, Hsiao JF, Maalouf JF, et al. Right ventricular strain for prediction of survival in patients with pulmonary arterial hypertension. *Chest.* (2011) 139:1299–309. doi: 10.1378/chest.10-2015
3. Raymond RJ, Hinderliter AL, Willis PW, Palph D, Caldwell EJ, Williams W, et al. Echocardiographic predictors of adverse outcomes in primary pulmonary hypertension. *J Am Coll Cardiol.* (2002) 39:1214–9. doi: 10.1016/s0735-1097(02)01744-8
4. Vonk-Noordegraaf A, Chin KM, Haddad F, Hassoun PM, Hemnes AR, Hopkins SR, et al. Pathophysiology of the right ventricle and of the pulmonary circulation in pulmonary hypertension: an update. *Eur Respir J.* (2019) 53:1801900. doi: 10.1183/13993003.01900-2018
5. Vonk-Noordegraaf A, Haddad F, Chin KM, Forfia PR, Kwaut SM, Lumens J, et al. Right heart adaptation to pulmonary arterial hypertension: physiology and pathobiology. *J Am Coll Cardiol.* (2013) 62:D22–33. doi: 10.1016/j.jacc.2013.10.027
6. Badagliacca R, Poscia R, Pezzuto B, Nocioni M, Mezzapesa M, Francone M, et al. Right ventricular remodeling in idiopathic pulmonary arterial hypertension: adaptive versus maladaptive morphology. *J Heart Lung Transplant.* (2015) 34:395–403. doi: 10.1016/j.healun.2014.11.002
7. van de Veerdonk MC, Marcus JT, Westerhof N, Westerhof N, deMan FS, Boonstra A, et al. Signs of right ventricular deterioration in clinically stable patients with pulmonary arterial hypertension. *Chest.* (2015) 147:1063–71. doi: 10.1378/chest.14-0701
8. Amsallem M, Sweatt AJ, Aymami MC, Kuznetsova T, Selej M, Lu HQ, et al. Right heart end-systolic remodeling index strongly predicts outcomes in pulmonary arterial hypertension: comparison with validated models. *Circ Cardiovasc Imaging.* (2017) 10:e005771. doi: 10.1161/CIRCIMAGING.116.005771
9. Fine NM, Chen LB, Bastiansen PM, Frantz RP, Pellikka PA, Oh JK, et al. Outcome prediction by quantitative right ventricular function assessment in 575 subjects evaluated for pulmonary hypertension. *Circ Cardiovasc Imaging.* (2013) 6:711–21. doi: 10.1161/CIRCIMAGING.113.000640
10. Naeije R, Manes A. The right ventricle in pulmonary arterial hypertension. *Eur Respir Rev.* (2014) 23:476–87. doi: 10.1183/09059180.00007414
11. Badagliacca R, Poscia R, Pezzuto B, Papa S, Reali M, Pesce F, et al. Prognostic relevance of right heart reverse remodeling in idiopathic pulmonary arterial hypertension. *J Heart Lung Transplant.* (2017) 2498:32041–7. doi: 10.1016/j.healun.2017.09.026

12. Shelburne NJ, Parikh KS, Chiswell K, Shaw LK, Sivak J, Arges K, et al. Echocardiographic assessment of right ventricular function and response to therapy in pulmonary arterial hypertension. *Am J Cardiol.* (2019) 124:1298–304. doi: 10.1016/j.amjcard.2019.07.026
13. El-Yafawi R, Rancourt D, Hacobian M, Atherton D, Cohen MC, Wirth JA. Pulmonary hypertension subjects exhibit right ventricular transient exertional dilation during supine exercise stress echocardiography. *Pulm Circ.* (2019) 9:2045894019851904. doi: 10.1177/2045894019851904
14. Saeed S, Smith J, Grigoryan K, Lysne V, Rajani R, Chambers JB. The tricuspid annular plane systolic excursion to systolic pulmonary artery pressure index: association with all-cause mortality in patients with moderate or severe tricuspid regurgitation. *Int J Cardiol.* (2020) 317:176–80. doi: 10.1016/j.ijcard.2020.05.093
15. Galie N, Hoeper MM, Humbert M, Torbicki A, Vachiery JL, Barbera JA, et al. Guidelines for the diagnosis and treatment of pulmonary hypertension: the Task Force for the Diagnosis and Treatment of Pulmonary Hypertension of the European Society of Cardiology (ESC) and the European Respiratory Society (ERS), endorsed by the International Society of Heart and Lung Transplantation (ISHLT). *Eur Heart J.* (2009) 30:2493–537. doi: 10.1093/eurheartj/ehp297
16. Galie N, Humbert M, Vachiery JL, Gibbs S, Lang I, Torbicki A, et al. 2015 ESC/ERS Guidelines for the diagnosis and treatment of pulmonary hypertension: the Joint Task Force for the Diagnosis and Treatment of Pulmonary Hypertension of the European Society of Cardiology (ESC) and the European Respiratory Society (ERS): Endorsed by: Association for European Paediatric and Congenital Cardiology (AEPC), International Society for Heart and Lung Transplantation (ISHLT). *Eur Respir J.* (2015) 46:903–75. doi: 10.1183/13993003.01032-2015
17. Rudski LG, Lai WW, Afilalo J, Hua L, Handschumacher MD, Chandrasekaran K, et al. Guidelines for the echocardiographic assessment of the right heart in adults: a report from the American Society of Echocardiography endorsed by the European Association of Echocardiography, a registered branch of the European Society of Cardiology, and the Canadian Society of Echocardiography. *J Am Soc Echocardiogr.* (2010) 23:685–713. doi: 10.1016/j.echo.2010.05.010
18. Lang RM, Badano LP, Mor-Avi V, Afilalo J, Armstrong A, Ernande L, et al. Recommendations for cardiac chamber quantification by echocardiography in adults: an update from the American Society of Echocardiography and the European Association of Cardiovascular Imaging. *J Am Soc Echocardiogr.* (2015) 28:1–39. e14. doi: 10.1016/j.echo.2014.10.003
19. Jayaram N, Beekman RH, Benson L, Holzer R, Jenkins K, Kennedy KF, et al. Adjusting for risk associated with pediatric and congenital cardiac catheterization: a report from the NCDR IMPACT Registry. *Circulation.* (2015) 132:1863–70. doi: 10.1161/CIRCULATIONAHA.114.014694
20. Boucly A, Weatherald J, Savale L, Jais X, Cottin V, Prevot G, et al. Risk assessment, prognosis and guideline implementation in pulmonary arterial hypertension. *Eur Respir J.* (2017) 50:1700889. doi: 10.1183/13993003.00889-2017
21. D'Alto M, Scognamiglio G, Dimopoulos K, Bossone E, Vizza D, Romeo E, et al. Right heart and pulmonary vessels structure and function. *Echocardiography.* (2015) 32 Suppl1:S3–10. doi: 10.1111/echo.12227
22. Cassady SJ, Ramani GV. Right heart failure in pulmonary hypertension. *Cardiol Clin.* (2020) 38:243–55. doi: 10.1016/j.ccl.2020.02.001
23. Haddad F, Hunt S, Rosenthal DN, Murphy DJ. Right ventricular function in cardiovascular disease, part I: anatomy, physiology, aging, and functional assessment of the right ventricle. *Circulation.* (2008) 117:1436–48. doi: 10.1161/CIRCULATIONAHA.107.653576
24. D'Alto M, Badaliacca RB, Argiento P, Romeo E, Farro A, Papa S, et al. Risk redution and right heart reverse remodeling by upfront triple combination therapy in pulmonary arterial hypertension. *Chest.* (2020) 157:376–83. doi: 10.1016/j.chest.2019.09.009
25. Schuba B, Michel S, Guenther S, Weig T, Emaser J, Schneider C, et al. Lung transplatation in patients with severe pulmonary hypertension-focus on right ventricular remodelling. *Clin Transplant.* (2019) 33:e13586. doi: 10.1111/ctr.13586
26. van der Bruggen CEE, Tedford RJ, Handoko ML, van der Velden J, de Man FS. RV pressure overload: from hypertrophy to failure. *Cardiovasc Res.* (2017) 113:1423–32. doi: 10.1093/cvr/cvx145
27. Spruijt OA, de Man F, Groepenhoff H, Oosterveer F, Westerhof N, Vonk-Noordegraaf A, et al. The effects of exercise on right ventricular contractility and right ventricular-arterial coupling in pulmonary hypertension. *Am J Respir Crit Care Med.* (2015) 191:1050–7. doi: 10.1164/rccm.201412-2271OC
28. Moceri P, Bouvier P, Baudouy D, Dimopoulos K, Cerboni P, Wort SJ, et al. Cardiac remodelling amongst adults with various aetiologies of pulmonary arterial hypertension including Eisenmenger syndrome-implications on survival and the roe of right ventricular transverse strain. *Eur Heart J Cardiovasc Imaging.* (2017) 18:1262–70. doi: 10.1093/ehjci/jew277
29. Noordegraaf AV, Bogaard HJ. Restoring the right ventricle. *Chest.* (2020) 157:251–2. doi: 10.1016/j.chest.2019.10.022
30. Harrison A, Hatton N, Ryan JJ. The right ventricule under pressure: evaluating the adaptive and maladaptive changes in the right ventricle in pulmonary arterial hypertension using echocardiography (2013 Grover Conference series). *Pulm Circ.* (2015) 5:29–47. doi: 10.1086/679699
31. Hoeper MM, Pittrow D, Opitz C, Gibbs JS, Rosenkranz S, Grunig E, et al. Risk assessement in pulmonary arterial hypertension. *Eur Respir J.* (2018) 51:1702606. doi: 10.1183/13993003.02606-2017
32. Benza RL, Farber HW, Selej M, Gomberg-Maitland M. Assessing risk in pulmonary arterial hypertension: what we know, what we don't. *Eur Respir J.* (2017) 50:1701353. doi: 10.1183/13993003.01353-2017
33. Wright LM, Dwyer N, Celermajer D, Kritharides L, Marwick TH. Follow-up of pulmonary hypertension with echocardiography. *JACC Cardiovasc Imaging.* (2016) 9:733–46. doi: 10.1016/j.jcmg.2016.02.022
34. Wright LM, Dwyer N, Wahi S, Marwick TH. Relative importance of baselien and longitudinal evaluation in the follow-up of vasodilator therapy in pulmonary arterial hypertension. *JACC Cardiovasc Imaging.* (2019) 12:2103–11. doi: 10.1016/j.jcmg.2018.08.017
35. Mauritz GJ, Kind T, Marcus JT, Bogaard HJ, van deVeerdonk M, Postmus PE, et al. Progressive changes in right ventricular geometric shortening and long-term survival in pulmonary arterial hypertension. *Chest.* (2012) 141:935–43. doi: 10.1378/chest.10-3277
36. Hoette S, Creuze N, Gunther S, Montani D, Savale L, Jais X, et al. RV fractional area change and TAPSE as predictors of severe right ventricular dysfunction in pulmonary hypertension: a CMR study. *Lung.* (2018) 196:157–64. doi: 10.1007/s00408-018-0089-7

Conflict of Interest: The authors declare that the research was conducted in the absence of any commercial or financial relationships that could be construed as a potential conflict of interest.

frontiers in Cardiovascular Medicine

ORIGINAL RESEARCH
published: 24 May 2021
doi: 10.3389/fcvm.2021.668059

Novel Urinary Glycan Biomarkers Predict Cardiovascular Events in Patients With Type 2 Diabetes: A Multicenter Prospective Study With 5-Year Follow Up (U-CARE Study 2)

Koki Mise[1†], Mariko Imamura[1†], Satoshi Yamaguchi[1], Mayu Watanabe[1], Chigusa Higuchi[1], Akihiro Katayama[2], Satoshi Miyamoto[3], Haruhito A. Uchida[4], Atsuko Nakatsuka[1], Jun Eguchi[1], Kazuyuki Hida[5], Tatsuaki Nakato[6], Atsuhito Tone[6], Sanae Teshigawara[6], Takashi Matsuoka[7], Shinji Kamei[7], Kazutoshi Murakami[7], Ikki Shimizu[8], Katsuhiro Miyashita[9], Shinichiro Ando[10], Tomokazu Nunoue[11], Michihiro Yoshida[3], Masao Yamada[12], Kenichi Shikata[3] and Jun Wada[1*]*

[1] Department of Nephrology, Rheumatology, Endocrinology and Metabolism, Okayama University Graduate School of Medicine, Dentistry and Pharmaceutical Sciences, Okayama, Japan, [2] Diabetes Center, Okayama University Hospital, Okayama, Japan, [3] Center for Innovative Clinical Medicine, Okayama University Hospital, Okayama, Japan, [4] Department of Chronic Kidney Disease and Cardiovascular Disease, Okayama University Graduate School of Medicine, Dentistry and Pharmaceutical Sciences, Okayama, Japan, [5] Department of Diabetology and Metabolism, National Hospital Organization Okayama Medical Center, Okayama, Japan, [6] Okayama Saiseikai General Hospital, Okayama, Japan, [7] Kurashiki Central Hospital, Kurashiki, Japan, [8] The Sakakibara Heart Institute of Okayama, Okayama, Japan, [9] Japanese Red Cross Okayama Hospital, Okayama, Japan, [10] Okayama City General Medical Center, Okayama, Japan, [11] Nunoue Clinic, Tsuyama, Japan, [12] GlycoTechnica Ltd., Yokohama, Japan

Background: Although various biomarkers predict cardiovascular event (CVE) in patients with diabetes, the relationship of urinary glycan profile with CVE in patients with diabetes remains unclear.

Methods: Among 680 patients with type 2 diabetes, we examined the baseline urinary glycan signals binding to 45 lectins with different specificities. Primary outcome was defined as CVE including cardiovascular disease, stroke, and peripheral arterial disease.

Results: During approximately a 5-year follow-up period, 62 patients reached the endpoint. Cox proportional hazards analysis revealed that urinary glycan signals binding to two lectins were significantly associated with the outcome after adjustment for known indicators of CVE and for false discovery rate, as well as increased model fitness. Hazard ratios for these lectins (+1 SD for the glycan index) were UDA (recognizing glycan: mixture of Man5 to Man9): 1.78 (95% CI: 1.24–2.55, $P = 0.002$) and Calsepa [High-Man (Man2–6)]: 1.56 (1.19–2.04, $P = 0.001$). Common glycan binding to these lectins was high-mannose type of *N*-glycans. Moreover, adding glycan index for UDA to a model including known confounders improved the outcome prediction [Difference of Harrel's C-index: 0.028 (95% CI: 0.001–0.055, $P = 0.044$), net reclassification improvement at 5-year risk increased by 0.368 (0.045–0.692, $P = 0.026$), and the Akaike information criterion and Bayesian information criterion decreased from 725.7 to 716.5, and 761.8 to 757.2, respectively].

OPEN ACCESS

Edited by:
Alessio Molfino,
Sapienza University of Rome, Italy

Reviewed by:
Valdo Jose Dias Da Silva,
Universidade Federal Do Triângulo Mineiro, Brazil
Simone Meini,
Azienda USL Toscana Nord Ovest, Italy

***Correspondence:**
Koki Mise
kokims-frz@okayama-u.ac.jp
orcid.org/0000-0003-0296-7429
Jun Wada
junwada@okayama-u.ac.jp
orcid.org/0000-0003-1468-5170

[†] These authors have contributed equally to this work

Specialty section:
This article was submitted to General Cardiovascular Medicine, a section of the journal Frontiers in Cardiovascular Medicine

Received: 15 February 2021
Accepted: 07 April 2021
Published: 24 May 2021

Citation:
Mise K, Imamura M, Yamaguchi S, Watanabe M, Higuchi C, Katayama A, Miyamoto S, Uchida HA, Nakatsuka A, Eguchi J, Hida K, Nakato T, Tone A, Teshigawara S, Matsuoka T, Kamei S, Murakami K, Shimizu I, Miyashita K, Ando S, Nunoue T, Yoshida M, Yamada M, Shikata K and Wada J (2021) Novel Urinary Glycan Biomarkers Predict Cardiovascular Events in Patients With Type 2 Diabetes: A Multicenter Prospective Study With 5-Year Follow Up (U-CARE Study 2). Front. Cardiovasc. Med. 8:668059. doi: 10.3389/fcvm.2021.668059

Conclusion: The urinary excretion of high-mannose glycan may be a valuable biomarker for improving prediction of CVE in patients with type 2 diabetes, and provides the rationale to explore the mechanism underlying abnormal *N*-glycosylation occurring in patients with diabetes at higher risk of CVE.

Trial Registration: This study was registered with the University Hospital Medical Information Network on June 26, 2012 (Clinical trial number: UMIN000011525, URL: https://upload.umin.ac.jp/cgi-open-bin/ctr_e/ctr_view.cgi?recptno=R000013482).

Keywords: cardiovascular event, diabetes, lectins, N-glycans, urinary biomarkers

INTRODUCTION

Cardiovascular disease (CVD) is a global burden especially in low- and middle-income countries and the leading cause of disability and mortality (1). The understanding of CVD risk factors is quite important to establish the cardiovascular risk prediction models. The age, gender, body mass index (BMI), systolic blood pressure (SBP), diabetes mellitus, smoking, total cholesterol levels, and past cardiovascular events are established and also traditional risk factors in middle-aged and older individuals (2). Chronic kidney disease (CKD) is an emerging global health burden with prevalence of ∼15% of adult populations and is independently associated with increased cardiovascular event (CVE) including stroke and peripheral arterial disease (PAD) besides the traditional risk factors (3, 4). The addition of albuminuria and estimated glomerular filtration rate (eGFR) to traditional risk factors is significantly associated with cardiovascular outcomes in meta-analysis of general population cohort (5, 6). In type 2 diabetes, the CVE risk prediction is potentially improved by novel biomarkers involved in the biological process, not explained by the traditional risk factors (7). The improvement of risk prediction is statistically evaluated by discrimination ability and reclassification. The area under the receiver operating characteristic (AUROC) or c-index is a measurement for discrimination capacity of classification model, while the net reclassification improvement (NRI) is a commonly used measure for the prediction increment by the addition of new biomarkers. In the Second Manifestations of ARTertial disease (SMART) and the European Prospective Investigation into Cancer and Nutrition-NL (EPIC-NL) (8), Action in Diabetes and Vascular Disease: Preterax and Diamicron Modified Release Controlled Evaluation (ADVANCE) study (9), and the Outcome Reduction With Initial Glargine Intervention (ORIGIN) trial (10), the 23, 16, and 284 serum or plasma biomarkers were evaluated as to whether these biomarkers independently improve the AUROC and NRI, respectively. The three biomarkers in SMART/EPIC-NL, six in ADVANCE, and 10 in ORIGIN were identified in the prediction of CVD composite outcomes. N-terminal pro-B-type natriuretic peptide (NT-proBNP) was only the common biomarker in two studies for the prediction of composite CVE. In addition to the candidate approach for the identification of biomarkers, non-biased screening using metabolomic approach was also attempted such as amino acid (11) and lipid profiles (12).

The vigorous attempts were made for the identification of circulating biomarkers, and some of the urinary biomarkers were independently associated with CVE in patients with type 2 diabetes; however, they have failed to achieve significant incremental ability based on c-statistic and NRI (13–15). Urine albumin creatinine ratio (UACR) and eGFR are now regarded as the classical risk factors for CVE in type 2 diabetes; the concept of "cardiorenal syndrome" suggests that the identification of urinary biomarkers is promising approach. In the Urinary biomarker for Continuous And Rapid progression of diabetic nEphropathy (U-CARE) study, we performed urinary lectin microarray, measured urinary glycan signals binding to 45 lectins, and evaluated the potential for the prediction of 30% decline of eGFR or end-stage renal disease (ESRD) in the patients with type 2 diabetes (16). We found that the urinary glycan binding signals to *Sambucus nigra* (SNA), *Ricinus communis* (RCA120), *Dolichos biflorus* (DBA), *Agaricus bisporus* (ABA), *Artocarpus integrifolia* (Jacalin), and *Amaranthus caudatus* (ACA) improved the prediction of renal outcome in the models employing the known risk factors (16). The U-CARE study suggested that the global alterations of glycosylation of urinary protein are valuable disease progression markers and may be linked to disease mechanisms in diabetic kidney disease (DKD). The aim of this study (U-CARE Study 2) is to investigate in patients with type 2 diabetes the impact of urinary lectin microarray on the prediction of CVE by adding the glycan binding signals in the multivariate model containing the established risk factors of CVE.

MATERIALS AND METHODS

Study Design and Participants

This is a second report of the U-CARE Study, a prospective cohort study, which started in 2012. Precise study design was described previously (16). In the current study, among 688 patients with type 2 diabetes admitted to multi-institutions in Japan, 680 patients were enrolled. Eight patients were excluded in this study since they were diagnosed with slowly progressive type 1 diabetes during follow-up. The diagnosis of diabetes was based on the Japanese Diabetes Society criteria (17). This study was registered with the University Hospital Medical Information

Network in June 2012 (UMIN000011525). Written informed consent was obtained from all participants.

Laboratory Parameters and Definitions

Urinary glycans were measured by the evanescent-field fluorescence-assisted lectin microarray (18). In brief, we measured urinary levels of Cy3-labeled glycoprotein binding to 45 lectins coated on microplates. In a previous study, we demonstrated that net glycan intensity [Net-I; raw glycan intensity (Raw-I)—background intensity] more accurately predicted the 24-h urinary glycan in comparison with Net-I or Raw-I/urinary creatinine ratios (16, 19). Based on the evidence, we analyzed glycan indexes defined by Net-I and logarithmically transformed Net-I when they did not follow normal distribution.

In this study, CVD was defined as events requiring admission for treatment, excluding the events with arrhythmia, dilated cardiomyopathy, and valvular heart disease to focus attention on the atherosclerotic cardiovascular diseases. Stroke was defined as cerebral bleeding and infarction requiring admission for treatment, while PAD as an event requiring admission for open surgery and/or endovascular intervention. CVE was defined as any CVD, stroke, or PAD events. Mortality due to cardiovascular death or other causes was also assessed. BMI was calculated as weight divided by the square of height (kg/m^2). Hypertension was defined as a baseline blood pressure $\geq$140/90 mmHg or use of antihypertensive drugs. GFR was estimated by the Japanese coefficient-modified Chronic Kidney Disease Epidemiology Collaboration equation. The baseline UACR (mg/gCr) was measured in a spot urine specimen, and normoalbuminuria, microalbuminuria, and macroalbuminuria were defined as UACR $<$30 mg/gCr, 30 $\leq$ UACR $<$ 300 mg/gCr, and 300 mg/gCr $\leq$ UACR, respectively. Hemoglobin A1c (HbA1c) data are presented as National Glycohemoglobin Standardization Program values according to the recommendations of the Japanese Diabetes Society and the International Federation of Clinical Chemistry (20). The grade of diabetic retinopathy was determined by an ophthalmologist at baseline. The average annual values of clinical parameters including HbA1c, SBP, and diastolic blood pressure (DBP) were obtained. The administration of statin, angiotensin-converting enzyme (ACE) inhibitor or angiotensin II type I receptor blocker (ARB), glucagon-like peptide-1 receptor agonists (GLP1), and sodium glucose transporter 2 (SGLT2) inhibitor during follow-up were also recorded. These data and previous CVE were compared between patients with and without outcome.

Study Endpoint

The primary endpoint was defined as incidence of CVE, and follow-up period was defined as the period from the initiation of observation to the earliest CVE, death, or last observation of clinical variables.

Statistical Analysis

Data were presented as percentages or the mean $\pm$ standard deviation (SD), as appropriate. All skewed variables were subjected to natural logarithmic transformation to improve normality before analysis. Correlations among glycan indexes were evaluated by Pearson correlation analysis. The cumulative incidence rate of the primary outcome was estimated by Kaplan–Meier curves for urinary glycan quartiles in all patients, and incidence rates were compared with the log-rank test, including trend test among quartile groups. The Cox proportional hazards model was used to calculate the hazard ratio (HR) and 95% confidence interval (CI) for the event-censored endpoint. HR and 95% CI for the 1 SD increase of glycan index were individually calculated in each model. In the multivariate model, HRs were adjusted for age, gender, BMI, SBP, low-density lipoprotein (LDL) cholesterol, HbA1c, eGFR, and previous CVE at baseline. These covariates were selected as potential confounders on the basis of biological plausibility and previous reports (15, 21). False discovery rates (FDRs) for 45 glycan indexes were calculated by the Benjamini–Hochberg procedure in these Cox regression analyses to control the expected proportion of false rejections (22). The level of FDR was defined as 0.05. Time-dependent area under curve (AUC) in multivariate Cox regression analysis was obtained by integration of AUC in every 0.2 year from 0.5 year-observation calculated by 500 bootstrap sampling (23). We also compared Harrell's concordance index (c-index) between multivariate Cox proportional hazards models with or without glycan biomarkers. In addition, the Akaike information criterion (AIC) and Bayesian information criterion (BIC) in the multivariate Cox regression models were calculated to compare the model fitness. Furthermore, improvement in discriminating the 5-year risk of the study outcome was assessed by analyses of AUROC, category-free NRI, and absolute integrated discrimination improvement (IDI), as reported elsewhere (24, 25). The 95% CIs for the differences of the Harrell's c-index and AUROC, category-free NRI, and IDI were computed from 5,000 bootstrap samples to adjust for optimism bias. Two-tailed P-values $<$ 0.05 were considered as statistically significant. Analyses and creation of graphs were performed with Stata SE software (version 14.0, StataCorp LP) and Origin (version 2018, OriginLab).

RESULTS

Observation Period and Outcome Incidence

The median follow-up period was 4.8 years [interquartile range (IQR): 3.6–5.1 years]. During follow-up, the primary endpoint (CVE) occurred in 62 patients (9%), and 21 patients (3%) died. CVE was the cause of two patient deaths. Detailed information of CVE and other causes of death are shown in **Supplementary Tables 1**, **2**.

Clinical Characteristics

The clinical characteristics of all participants at baseline are displayed in **Table 1**. Their age was 63 $\pm$ 11 years (mean $\pm$ SD), 61% of the patients were men, and 24% of them had previous CVE. The median duration of diabetes was 11.1 years (IQR: 6.2–17.7), and baseline HbA1c was 7.1 $\pm$ 1.1% (54.3 $\pm$ 12.0 mmol/mol). Under 56% of statin use, the baseline LDL and non-high-density lipoprotein (non-HDL) cholesterol levels were 100.1 $\pm$ 25.3 and 126.5 $\pm$ 30.6 mg/dl, respectively.

TABLE 1 | Baseline clinical parameters.

Clinical parameters	All patients ($n = 680$)
Age (years)	63 ± 11
Male (%)	61
BMI (kg/m^2)	25.6 ± 4.6
Prior CVD/stroke/PAD (%)	17/9/1
Prior cardiovascular event (%)	24
Duration of DM (years)*	11.1 (6.2 > 17.7)
HbA1c (%)	7.1 ± 1.1
(mmol/mol)	54.3 ±12.0
Triglyceride (mg/dl)*	116 (81–163)
Total cholesterol (mg/dl)	180.5 ± 31.9
LDL cholesterol (mg/dl)	100.1 ± 25.3
Non-HDL cholesterol (mg/dl)	126.5 ± 30.6
Uric acid (mg/dl)	5.4 ± 1.4
SBP (mmHg)	131.0 ± 17.0
DBP (mmHg)	74.7 ± 10.9
Hypertension (%)†	70
Retinopathy (NDR/SDR/prePDR/PDR, %)‡	67/17/6/10
eGFR (ml/min/1.73 m^2)	71.0 ± 17.7
CKD GFR Categories (G1/G2/G3a/G3b/G4/G5, %)	10/69/11/6/3/1
UACR (mg/gCr)*	17.7 (7.8–74.1)
Normo/Micro/Macro (%)	63/25/12
Any type of antihypertensive agents (%)	62
ACE inihibitor or ARB (%)	53
Calcium channel blocker (%)	38
Number of antihypertensive agents*	1 (0–2)
Treatment for diabetes (Diet only/OHA/Insulin, %)	4/64/32
Drug treatment for hyperglycemia (SU/GLIN/BG/αGI/TZD/DPP4-I/GLP1, %)	32/10/35/28/15/49/7
Drug treatment for dyslipidemia/statin use (%)	64/56

BMI, body mass index; CVD, cardiovascular disease requiring admission for treatment; Stroke, cerebral bleeding or infarction requiring admission for treatment; PAD, peripheral arterial disease requiring admission for intervention or surgery; Cardiovasular event, any event of CVD, Stroke, and PAD; HbA1c, hemoglobin A1c; Duration of DM, estimated duration of diabetes mellitus; LDL cholesterol, low-density lipoprotein cholesterol; non-HDL cholesterol, non high-density lipoprotein cholesterol; SBP, systolic blood pressure; DBP, diastolic blood pressure; Retinopathy, diabetic retinopathy; NDR/SDR/prePDR/PDR, non diabetic retinopathy, simple diabetic retinopathy, pre proliferative diabetic retinopathy, and proliferative diabetic retinopathy, respectively; eGFR, estimated glomerular filtration rate, CKD GFR Categories; G1: ≥90 ml/min/1.73 m^2, G2: 60–90 ml/min/1.73 m^2, G3a: 45–59 ml/min/1.73 m^2, G3b: 30–44 ml/min/1.73 m^2, G4: 15–29 ml/min/1.73 m^2; UACR, urinary albumin creatinine ratio; Normo/Micro/Macro, normoalbuminuria, microalbuminuria, and macroalbuminuria, respectively; ACE inhibitor or ARB, treatment with an angiotensin-converting enzyme inhibitor or angiotensin II type I receptor blocker, respectively; Diet only, diet regimen only; OHA, oral hypoglycemic agent; Insulin therapy, treatment with insulin (including basal-supported oral therapy); SU, sulfonylurea; GLIN, meglitinide anologs; BG, biguanide (Metformin); αGI, alpha-glucosidase inhibitors; TZD, thiazolidinediones; DPP4-I, DPP-4 inhibitors; GLP1, glucagon-like peptide 1 receptor agonists; SGLT2, sodium glucose transporter 2.
**Median (interquartile range). †Hypertension was defined as blood pressure ≥140/90 mmHg or any antihypertensive drug treatment. ‡Data from 664 patients (98%) were available.*

Similarly, 62% of the patients received antihypertensive agents, average blood pressures were SBP (131.0 ± 17.0 mmHg) and DBP (74.7 ± 10.9 mmHg). The mean baseline eGFR was 71.0 ± 17.7 ml/min/1.73 m^2 and median UACR was 17.7 mg/gCr (IQR: 7.8–74.1). The average annual HbA1c, SBP, and DBP levels, and percentage of the use of ACE inhibitor or ARB, and GLP-1 receptor agonist during follow-up were not significantly different between the patients with and without outcome. Statin use during observation was significantly higher, and the use of SGLT2 inhibitor was significantly lower in patients with outcome compared with those without outcome (**Supplementary Table 3**).

Relation Between Primary Endpoint and Glycan Binding to the Lectin Panel

Unadjusted and adjusted HRs for glycan binding to the panel of 45 lectins with different specificities and the reported structure of the glycan binding to each lectin are shown in **Figure 1** and **Supplementary Table 4**. The urinary glycan binding signals to 13 lectins [*Pisum sativum* (PSA), *Lens culinaris* (LCA), *Aleuria aurantia* (AAL), SNA, *Tanthes japonica* (TJAI), RCA120, *Narcissus pseudonarcissus* (NPA), *Canavalia ensiformis* (ConA), *Galanthus nivalis* (GNA), *Hippeastrum hybrid* (HHL), *Tulipa gesneriana* (TxLCI), *Urtica dioica* (UDA), and *Calystegia sepium* (Calsepa)] were significantly associated with the outcome in either of the univariate and multivariate models. Among them, both glycan binding signals to UDA and Calsepa were selected based on the FDR <0.05 in the multivariate models. We fitted a series of multivariate Cox regression models, which include (i) only covariates, (ii) covariates + UACR, (iii) covariates + glycan signals (binding to UDA or Capsela), and (iv) covariates + UACR + glycan signal (**Table 2**). Then, the improvement of model fitness was evaluated based on the reduction of both AIC and BIC criteria. These criteria were minimized at model (iii) for both of UDA and Capsela, which were considered the best fitting model, that is, the two glycans were more substantially improved model fitness, and the addition of UACR did not exhibit improvement of model fitting. Glycan signals for UDA and Calsepa were not incorporated into the model at the same time to avoid multicolinearity because of the high correlation with each other ($r = 0.87$).

The relationships between the glycan indexes and outcome remained largely unchanged when treated of statin, ACE inhibitor or ARB, and SGLT2 inhibitor during the follow-up period, and the average annual HbA1c, average annual SBP, and baseline non-HDL cholesterol were incorporated into the multivariate model (**Supplementary Table 5**). As shown in **Supplementary Table 4**, UDA and Calsepa are known to bind to a mixture of Man5 to Man9 and to High-Man (Man2-6), respectively. The common recognized glycans are classified into intermediate and immature products of *N*-glycan synthesis (26).

Time-Dependent Area Under Curve and Harrell's C-Index in Cox Regression Model With or Without Urinary Glycans

Time-dependent AUCs and Harrell's C indexes in multivariate Cox regression model with or without glycan binding signals to UDA and Calsepa are displayed in **Figures 2A,B**. Overall, AUCs during observation were higher in models with those

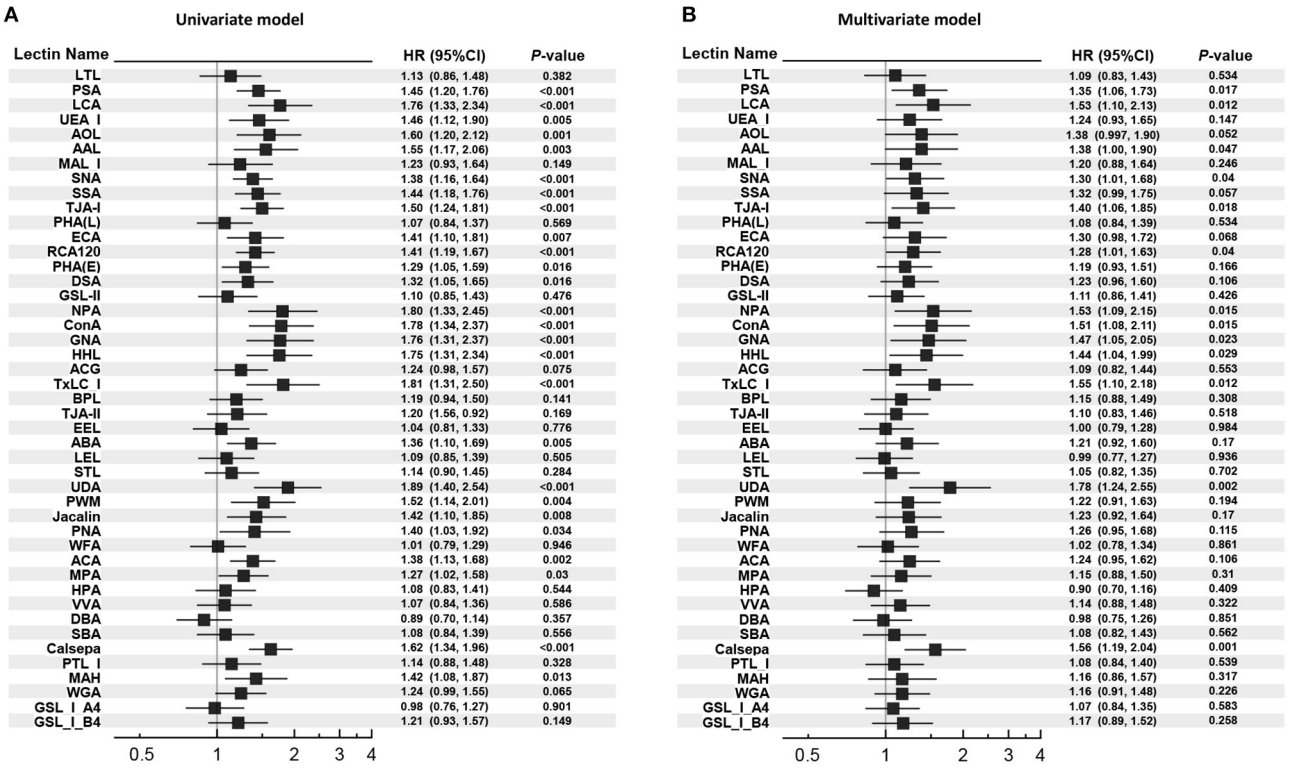

FIGURE 1 | Univariate and multivariate Cox proportional hazard models for the outcome. **(A)** Univariate Cox proportional hazard models. **(B)** Multivariate Cox proportional hazard models. HR per 1 SD increase in each glycan index is shown. In the multivariate model, HR was adjusted for age, gender, body mass index, systolic blood pressure, hemoglobin A1c, low-density lipoprotein cholesterol, estimated glomerular filtration rate, past cardiovascular event at baseline. HR, hazard ratio; 95% CI, 95% confidence interval.

TABLE 2 | Comparison of hazard ratio and model fitting between multivariate models with or without UACR and urinary glycans for UDA and Calsepa.

Markers	Multivariate model					Markers	Multivariate model with UACR				
	HR	95% CI	*P*-value	AIC	BIC		HR	95% CI	*P*-value	AIC	BIC
None	–	–	–	725.7	761.8	UACR	1.32	0.99–1.75	0.058	724.1	764.8
UDA	1.78	1.24–2.55	0.002	716.5	757.2	UDA	1.70	1.16–2.49	0.006	718.0	763.2
Calsepa	1.56	1.19–2.04	0.001	718.0	758.7	Calsepa	1.50	1.11–2.02	0.009	719.6	764.8

Covariates in multivariate model: age, gender, body mass index, systolic blood pressure, hemoglobin A1c, low density cholesterol levels, estimated glomerular filtration rate, and past cardiovascular event at baseline. Each glycan index was employed into the multivariate model with or without log transformed UACR. UACR, urinary albumin creatinine ratio; HR, hazard ratio; 95% CI, 95% confidence interval; AIC, Akaike's information criterion; BIC, Bayesian information criterion; UDA, Urtica dioica; Calsepa, Calystegia sepium.

glycan indexes than in model without them, while the Harrell's C-index was significantly higher only in the model containing glycan binding signal to UDA than in model without the glycans [Harrell's C-index for model without UDA: 0.766 (95% CI: 0.705–0.828), Harrell's C-index for model with UDA: 0.794 (0.739–0.850), and the difference in Harrell's C-index: 0.028 (0.001–0.055, $P = 0.044$)].

Cumulative Incidence Rate of the Primary Outcome in Urinary Glycan Quartiles

Kaplan–Meier curves stratified according to quartiles for baseline urinary glycan binding to UDA and Calsepa are shown in **Figure 3**. The cumulative incidence rate of the outcome was significantly higher in the higher quartile for urinary glycan binding to UDA and Calsepa than in the lower quartiles [*P* for trend: <0.001 for UDA (**Figure 3A**) and <0.0001 for Calsepa (**Figure 3B**)].

5-Year Risk Classification Ability of Urinary Glycan Binding to Urtica Dioica and Calystegia Sepium

The difference of AUROC between logistic regression models with or without urinary markers, category-free NRI, absolute IDI for predicting the primary outcome at 5-year follow-up time

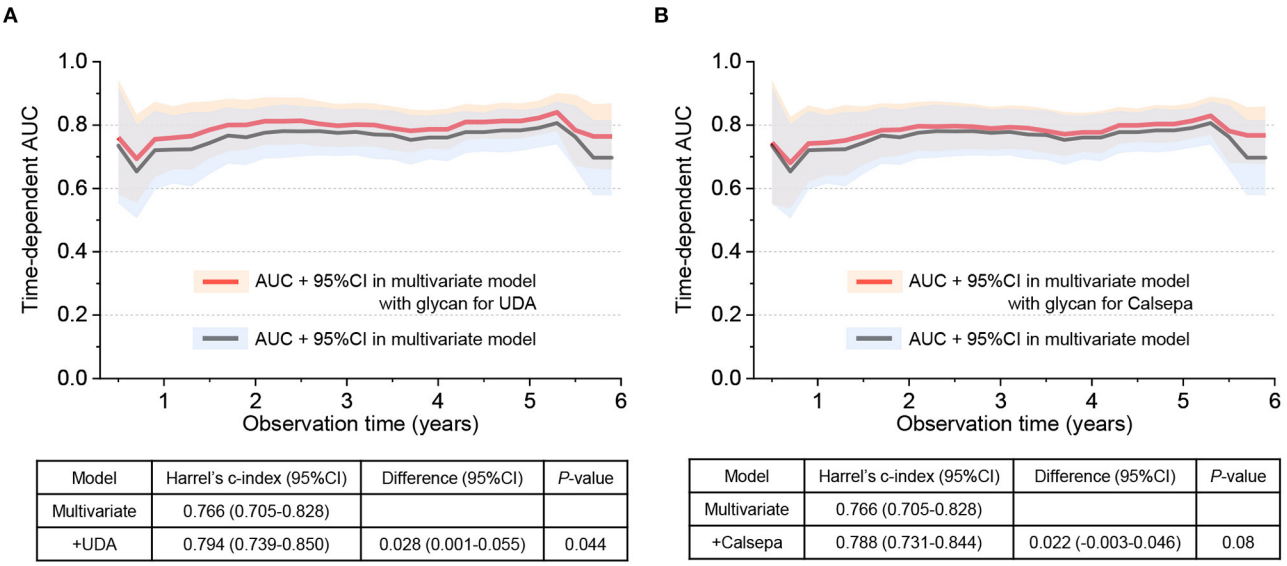

Model	Harrel's c-index (95%CI)	Difference (95%CI)	*P*-value
Multivariate	0.766 (0.705-0.828)		
+UDA	0.794 (0.739-0.850)	0.028 (0.001-0.055)	0.044

Model	Harrel's c-index (95%CI)	Difference (95%CI)	*P*-value
Multivariate	0.766 (0.705-0.828)		
+Calsepa	0.788 (0.731-0.844)	0.022 (-0.003-0.046)	0.08

FIGURE 2 | Time-dependent area under curve (AUC) and Harrell's C-index in Cox regression model with or without urinary glycans binding to UDA and Calsepa. **(A)** AUC and Harrell's C-index with or without urinary glycans binding to UDA. **(B)** AUC and Harrell's C-index with or without urinary glycans binding to Calsepa. In the multivariate Cox regression model without glycan, age, gender, body mass index, systolic blood pressure, hemoglobin A1c, low-density lipoprotein cholesterol, estimated glomerular filtration rate, past cardiovascular event at baseline were incorporated as adjusted variables. On the other hand, multivariate model with glycan includes the same covariates and any of two glycans binding to UDA and Calsepa. UDA, *Urtica dioica*; Calsepa, *Calystegia sepium*.

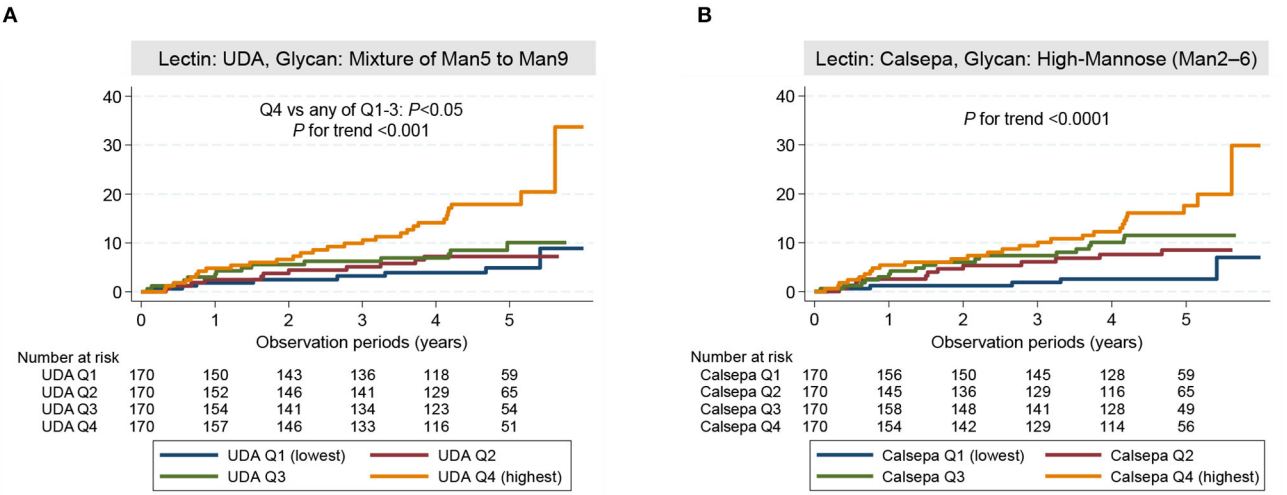

FIGURE 3 | Cumulative incidence rate of the outcome. **(A)** Cumulative incidence rate in patients stratified according to the quartiles of urinary glycan indexes for UDA. **(B)** Cumulative incidence rate in patients stratified according to the quartiles of urinary glycan indexes for Calsepa. The cumulative incidence rate was significantly higher in patients with higher glycan indexes than in those with lower glycan indexes (UDA: *P* for trend <0.001, Calsepa: *P* for trend <0.0001). Among quartile groups for UDA, cumulative incidence rate was significantly higher in highest quartile group (Q4) compared with lower quartile groups (Q1–3) ($P < 0.05$). The log-rank test was used for failure analysis. UDA, *Urtica dioica*; Calsepa, *Calystegia sepium*; Man, Mannose.

obtained by adding UACR and the glycan indexes for UDA and Calsepa are summarized in **Table 3**. Adding of either glycan indexes to the multivariate model significantly improved the ability of discrimination and reclassification such as AUROC and NRI [difference in AUROC: 0.031 (95% CI: 0.001–0.062, $P = 0.045$) for UDA, 0.027 (0.001–0.053, $P = 0.040$) for Calsepa, category-free NRI: 0.368 (0.045–0.692, $P = 0.026$) for UDA, and 0.388 (0.099–0.677, $P = 0.008$) for Calsepa], whereas either of the two glycan indexes did not significantly improve integrated discrimination [IDI: 0.024 (−0.009–0.056, $P = 0.16$) for UDA

TABLE 3 | AUROC, category-free NRI, and IDI for predicting the 5-year outcome with UACR and urinary glycan binding to UDA and Calsepa.

	AUROC (95% CI)	Difference of AUROC (95% CI)	*P*-value	Category-free NRI (95% CI)	*P*-value	IDI (95% CI)	*P*-value
Only covariates	0.774 (0.711–0.837)						
With UACR	0.790 (0.732–0.849)	0.017 (−0.002–0.035)	0.083	0.269 (−0.027–0.564)	0.075	0.005 (−0.014–0.024)	0.59
With glycan to UDA (Mixture of Man5 to Man9)	0.805 (0.748–0.862)	0.031 (0.001–0.062)	0.045	0.368 (0.045–0.692)	0.026	0.024 (−0.009–0.056)	0.16
With glycan to Calsepa [High-Man (Man2-6)]	0.801 (0.744–0.857)	0.027 (0.001–0.053)	0.040	0.388 (0.099–0.677)	0.008	0.021 (−0.010–0.053)	0.18

Covariates: age, gender, body mass index, systolic blood pressure, hemoglobin A1c, low density cholesterol levels, estimated glomerular filtration rate, and past cardiovascular event at baseline.

AUROC, The area under a receiver operating characteristic; NRI, net reclassification improvement; IDI, integrated discrimination improvement; UACR, urine albumin creatinine ratio; 95% CI, 95% confidence interval; UDA, Urtica dioica; Calsepa, Calystegia sepium; Man, Mannose.

and 0.021 (−0.010–0.053, $P = 0.18$) for Calsepa]. On the other hand, adding UACR did not show any significance on the incremental prediction [difference in AUROC: 0.017 (−0.002–0.035, $P = 0.083$), category-free NRI: 0.269 (−0.027–0.564, $P = 0.075$), and IDI: 0.005 (−0.014–0.024, $P = 0.59$)].

DISCUSSION

The urine glycan binding signals to UDA (mixture of Man5 to Man9) and Calsepa [High-Man (Man2-6)] improved model fitness scores for discrimination ability (Harrell's C index and AUROC), reclassification (NRI), and log-likelihood/complexity (AIC and BIC) when they were incorporated into the multivariate Cox and logistic regression model employing traditional risk factors. The strength of the current study was that the two urinary glycan signals were the novel urinary markers, which could provide the new mechanism of CVE in diabetes. They demonstrated the incremental predictive power with statistical significance, and they might be better markers than UACR. In previous studies of patients with type 2 diabetes, several urinary markers such as urinary kidney injury molecule 1, urinary neutrophil gelatinase-associated lipocalin, urinary liver-type fatty acid-binding protein, and urinary COOH-terminal propeptide of collagen VI, have been investigated for predicting CVE (13, 15, 27). However, none of them showed the statistical significance of model discrimination or reclassification in the multivariate model including known risk factors. Although it has been shown that UACR is associated with CVE independent of established confounders, its incremental predictive ability is limited (21). In our study, UACR had a marginal impact on the outcome in the multivariate Cox regression analysis [HR for logUACR: 1.32 (95% CI: 0.99–1.75), $P = 0.058$, **Table 2**], while it failed to demonstrate the significant values of AUROC, NRI, and IDI (**Table 3**) in the multivariate models, which was compatible with the previous results (21). In contrast to UACR, glycan indexes for UDA and Calsepa showed statistical significance of the incremental prediction as mentioned above. In addition, model fitness scores, i.e., AIC and BIC, were clearly better than that of UACR. Therefore, these novel glycan indexes might be superior to UACR for predicting CVE in patients with type 2 diabetes.

Interestingly, UDA and Calsepa recognize the high mannose glycan structures (**Supplementary Figure 1**). In endoplasmic reticulum (ER), Glc3Man9GlcNAc2 is transferred to the NXT/NXS sites of protein, Glc residues removed by glucosidases, and Man9GlcNAc2 converted to Man8GlcNAc2 by ER α-mannosidase I (MAN1B1). The glycoproteins are then transferred to *cis*-Golgi; the additional Man residues are removed until Man5GlcNAc2 is generated. Man5GlcNAc2 is a key intermediate for the pathway to hybrid and complex *N*-glycans in *trans*-Golgi and *trans*-Golgi network by the removal of mannose residues by Golgi mannosidases, while some of Man5GlcNAc2 also escapes further modification, and mature membrane or secreted glycoprotein carries Man5-9GlcNAc2, i.e., high mannose structures (**Supplementary Figure 1A**) (26). In the glycan analysis by urine lectin microarray, the elevation of high mannose and complex type of *N*-glycans in urine glycoproteins are tightly linked to the development of composite CVE.

The high-throughput plasma or serum *N*-glycan profiling studies using hydrophilic interaction liquid chromatography (HILIC) of peptide-*N*-glycosidase F digested and fluorescently labeled *N*-glycans were reported, and 46 *N*-glycan peaks (GP1-GP46) were demonstrated (28–32). In the patients with normo- and hyperglycemia during acute inflammation, the comparison of *N*-glycan profile demonstrated that increased branched, galactosylated, and sialylated tri- and tetraantennary *N*-glycans are associated with the development of type 2 diabetes (28). In Ghanaian population, branched, trigalactosylated, antennary fucosylated, and triantennary *N*-glycans (**Supplementary Figure 1B**) were increased in the patients with type 2 diabetes (29). A lower relative abundance of simple biantennary *N*-glycans and a higher abundance of branched, galactosylated, and sialylated complex *N*-glycans were increased both in type 1 (31) and type 2 (30) diabetes, and similar trends with increased levels of complex *N*-glycans (GP12, GP16, and GP22) were seen for higher UACR and greater annual loss of

eGFR (29, 31). Recently, in the prospective European Prospective Investigation of Cancer (EPIC)—Potsdam cohort ($n = 27{,}548$), the increased levels of complex *N*-glycans, GP5 in women, and GP16, GP23, and GP29 in men, improved the accuracy of risk prediction score for CVD (32).

Independent of serum or plasma *N*-glycan profiling, our efforts to identify the biomarkers to improve the prediction of DKD and CVD outcomes have been directed to the clinical studies using urinary glycan profiling by lectin microarray in the patients with type 2 diabetes (16, 33). Previously, we found that urinary glycan profiling by lectin microarray demonstrated the considerable changes in glycan binding signals during the progression of DKD in urine samples rather than serum samples (16, 33). The changes in glycan profile in urine samples may reflect the glycosylation changes in glycoproteins produced in kidney tissues or the changes in selective permeabilities of blood-derived glycoproteins through glomerular capillaries. In addition, the lectins are long-standing experimental tools to identify the glycan structures, which enable lectin microarray to detect the broad range of glycans compared with HILIC or other methods using mass analysis. For instance, the capture of *O*-glycans and neutral *N*-glycans such as high-mannose type and hybrid type *N*-glycans (**Supplementary Figure 1C**) are extremely difficult in HILIC (34). Furthermore, only 20 μl of urine samples is required, and the single step of Cy3 labeling without enzymatic treatments achieve the less-time consuming and high-throughput analyses. By taking these advantages of urine lectin microarray, we successfully identified that the glycan binding signals to high mannose or mannose-recognizing lectins, UDA and Calsepa, contributed the improvement of the prediction models using established risk factors for CVE. In the previous study, we identified that the glycan-binding signals to SNA, RCA120, DBA, ABA, Jacalin, and ACA significantly improved the prediction models for 30% decline in eGFR or ESRD, and these lectins mainly recognized the *O*-glycan structures, suggesting the specificity of the analyses with lectin microarray (16). Furthermore, the application of those eight lectins for the urine samples of the patients with type 2 diabetes provides a useful diagnostic tool for the future risk of the CVD and DKD progression.

Novel Mechanism of the Atherosclerotic Cardiovascular Event in Diabetes

The current clinical study provides the insight into the mechanism for the progression of atherosclerosis in type 2 diabetes. The detection of high mannose *N*-glycans, i.e., immature forms of *N*-glycans, in the urine samples in the patients with type 2 diabetes suggests the abnormalities in the processing and maturation of *N*-glycans in the ER and Golgi. In the ER, Glc1Man9GlcNAc2 *N*-glycans are properly folded by the assistance of calnexin and calreticulin, while the misfolded Man9GlcNAc2 is recognized by ER-degradation-enhancing α mannosidase I-like (EDEM) leading to ER degradation (26). The inhibition of ER α-mannosidase I (MAN1B1), which mediates the conversion of Man9GlcNAc2 to Man8GlcNAc2, was reported to enhance high mannose intercellular adhesion molecule-1 expression on endothelial cell surface (35). The impairment of quality control of glycoproteins and mannosidase activity in ER may cause the accumulation of high mannose *N*-glycans in ER. In addition, the knockout of the triple gene encoding Golgi α1,2-mannosidases (MAN1A1, MAN1A2, and MAN1B1) resulted in the production of high mannose *N*-glycans (36). The defects in the Golgi α1,2-mannosidases are also candidate mechanisms to produce high mannose *N*-glycans. The link between high mannose *N*-glycans and CVE further suggested the new mechanism for the progression of atherosclerosis in type 2 diabetes. High mannose *N*-glycans induced on endothelial cells by oscillatory shear stress, or tumor necrosis factor-α mediates the monocytic recruitment (37), and hypercholesterolemic patients exhibited higher plasma levels of a cluster of high-mannose and complex/hybrid *N*-glycans (38).

Study Limitations

One of the key limitations in this study is that this was a multi-center observational study, and the therapeutic strategy of diabetes and its complications in each participant was not exactly standardized, which might have affected the incidence of the outcome. However, the sensitivity analyses revealed that the impact of glycan indexes for UDA and Calsepa on the outcome did not largely change even when the various treatment factors during follow-up periods were incorporated into the multivariate Cox regression models (**Supplementary Table 5**). In addition, we might not be able to adjust for other possible confounders in the multivariate models. Several blood biomarkers, such as NT-proBNP and high-sensitivity troponin T, have been established as useful markers for predicting CVE (9, 39). It remains unknown whether glycan indexes for UDA and Calsepa are significantly associated with the outcome independent of those biomarkers. Nevertheless, we hope that these novel urinary markers predict CVE independent of other confounders since these glycan markers could reflect the novel mechanism of CVE as mentioned above.

CONCLUSIONS

The glycan profiling by urine lectin microarray demonstrated that the elevation of high mannose and complex type of *N*-glycans in urine glycoproteins is tightly linked to the development of CVE. UDA and Calsepa in lectin microarray may be a useful diagnostic tool for the prediction of CVD risk in patients with type 2 diabetes. The evidence linking the increased high mannose and complex type of *N*-glycans to the incidence of CVE in patients with diabetes suggests that the disease mechanisms and therapeutic targets are related to organellar dysfunction in the ER and Golgi, as well as to the progression of atherosclerosis.

DATA AVAILABILITY STATEMENT

The original contributions presented in the study are included in the article/**Supplementary Material**, further inquiries can be directed to the corresponding authors.

ETHICS STATEMENT

The studies involving human participants were reviewed and approved by Institutional Review Boards of the Okayama University. The patients/participants provided their written informed consent to participate in this study.

AUTHOR CONTRIBUTIONS

KMis conceived the study, formulated the analysis plan, performed the statistical analyses, collected the clinical data, performed the urinary lectin microarray, and wrote the manuscript. MI collected and assessed all the clinical data. SY measured the urinary glycan binding signals to lectins and collected the clinical data. MW, CH, AK, SM, HU, AN, JE, KH, TN, AT, ST, TM, SK, KMu, IS, KMiy, SA, TN, and KS recruited the patients and assessed the data. MYo supported the statistical analyses. MYa measured the urinary glycan binding signals to lectins, analyzed the urinary lectin microarray data, and wrote the manuscript. JW conceived the study, supervised the data collection, analyzed the data, and edited the manuscript. All authors contributed to the interpretation of the data, critical revision of the manuscript, and approval of the final version of the manuscript.

FUNDING

This work was partly supported by a Health Labor Sciences Grant (No. 201413003), the Japan Agency for Medical Research and development (AMED, Grant Nos. 17ek0210095h0001 and 20ek0109445h0001), the Novo Nordisk Pharma Ltd [Junior Scientist Development Grant (2016–2017)], the Okinaka Memorial Institute for Medical Research (a grant in 2017), and The Yukiko Ishibashi Foundation (a grant in 2016).

ACKNOWLEDGMENTS

We are grateful to Drs. Ichiro Nojima, Yuzuki Kano, Yuriko Yamamura, and Yasuhiro Onishi for collecting data. We are also grateful to Daniele Spinelli for helpful comments on the analyses.

SUPPLEMENTARY MATERIAL

The Supplementary Material for this article can be found online at: https://www.frontiersin.org/articles/10.3389/fcvm.2021.668059/full#supplementary-material

REFERENCES

1. Muthee TB, Kimathi D, Richards GC, Etyang A, Nunan D, Williams V, et al. Factors influencing the implementation of cardiovascular risk scoring in primary care: a mixed-method systematic review. *Implement Sci.* (2020) 15:57. doi: 10.1186/s13012-020-01022-x
2. van Bussel EF, Hoevenaar-Blom MP, Poortvliet RKE, Gussekloo J, van Dalen JW, van Gool WA, et al. Predictive value of traditional risk factors for cardiovascular disease in older people: a systematic review. *Prev Med.* (2020) 132:105986. doi: 10.1016/j.ypmed.2020.105986
3. Go AS, Chertow GM, Fan D, McCulloch CE, Hsu CY. Chronic kidney disease and the risks of death, cardiovascular events, and hospitalization. *N Engl J Med.* (2004) 351:1296–305. doi: 10.1056/NEJMoa041031
4. Tonelli M, Muntner P, Lloyd A, Manns BJ, Klarenbach S, Pannu N, et al. Risk of coronary events in people with chronic kidney disease compared with those with diabetes: a population-level cohort study. *Lancet.* (2012) 380:807–14. doi: 10.1016/S0140-6736(12)60572-8
5. Chronic Kidney Disease Prognosis, Matsushita K, van der Velde M, Astor BC, Woodward M, Levey AS, et al. Association of estimated glomerular filtration rate and albuminuria with all-cause and cardiovascular mortality in general population cohorts: a collaborative meta-analysis. *Lancet.* (2010) 375:2073–81. doi: 10.1016/S0140-6736(10)60674-5
6. Matsushita K, Coresh J, Sang Y, Chalmers J, Fox C, Guallar E, et al. Estimated glomerular filtration rate and albuminuria for prediction of cardiovascular outcomes: a collaborative meta-analysis of individual participant data. *Lancet Diabetes Endocrinol.* (2015) 3:514–25. doi: 10.1016/S2213-8587(15)00040-6
7. Bachmann KN, Wang TJ. Biomarkers of cardiovascular disease: contributions to risk prediction in individuals with diabetes. *Diabetologia.* (2018) 61:987–95. doi: 10.1007/s00125-017-4442-9
8. van der Leeuw J, Beulens JW, van Dieren S, Schalkwijk CG, Glatz JF, Hofker MH, et al. Novel biomarkers to improve the prediction of cardiovascular event risk in type 2 diabetes mellitus. *J Am Heart Assoc.* (2016) 5:e003048. doi: 10.1161/JAHA.115.003048
9. Looker HC, Colombo M, Agakov F, Zeller T, Groop L, Thorand B, et al. Protein biomarkers for the prediction of cardiovascular disease in type 2 diabetes. *Diabetologia.* (2015) 58:1363–71. doi: 10.1007/s00125-015-3535-6
10. Gerstein HC, Pare G, McQueen MJ, Haenel H, Lee SF, Pogue J, et al. Identifying novel biomarkers for cardiovascular events or death in people with dysglycemia. *Circulation.* (2015) 132:2297–304. doi: 10.1161/CIRCULATIONAHA.115.015744
11. Welsh P, Rankin N, Li Q, Mark PB, Wurtz P, Ala-Korpela M, et al. Circulating amino acids and the risk of macrovascular, microvascular and mortality outcomes in individuals with type 2 diabetes: results from the ADVANCE trial. *Diabetologia.* (2018) 61:1581–91. doi: 10.1007/s00125-018-4619-x
12. Alshehry ZH, Mundra PA, Barlow CK, Mellett NA, Wong G, McConville MJ, et al. Plasma lipidomic profiles improve on traditional risk factors for the prediction of cardiovascular events in type 2 diabetes mellitus. *Circulation.* (2016) 134:1637–50. doi: 10.1161/CIRCULATIONAHA.116.023233
13. Vaduganathan M, White WB, Charytan DM, Morrow DA, Liu Y, Zannad F, et al. Relation of serum and urine renal biomarkers to cardiovascular risk in patients with type 2 diabetes mellitus and recent acute coronary syndromes (from the EXAMINE trial). *Am J Cardiol.* (2019) 123:382–91. doi: 10.1016/j.amjcard.2018.10.035
14. Rotbain Curovic V, Hansen TW, Eickhoff MK, von Scholten BJ, Reinhard H, Jacobsen PK, et al. Urinary tubular biomarkers as predictors of kidney function decline, cardiovascular events and mortality in microalbuminuric type 2 diabetic patients. *Acta Diabetol.* (2018) 55:1143–50. doi: 10.1007/s00592-018-1205-0
15. Rasmussen DGK, Hansen TW, von Scholten BJ, Nielsen SH, Reinhard H, Parving HH, et al. Higher collagen VI formation is associated with all-cause mortality in patients with type 2 diabetes and microalbuminuria. *Diabetes Care.* (2018) 41:1493–500. doi: 10.2337/dc17-2392
16. Mise K, Imamura M, Yamaguchi S, Teshigawara S, Tone A, Uchida HA, et al. Identification of novel urinary biomarkers for predicting renal prognosis in patients with type 2 diabetes by glycan profiling in a multicenter prospective cohort study: U-CARE study 1. *Diabetes Care.* (2018) 41:1765–75. doi: 10.2337/dc18-0030
17. Seino Y, Nanjo K, Tajima N, Kadowaki T, Kashiwagi A, Araki E, et al. Report of the committee on the classification and diagnostic criteria of diabetes mellitus. *J Diabetes Invest.* (2010) 1:212–28. doi: 10.1111/j.2040-1124.2010.00074.x

18. Kuno A, Uchiyama N, Koseki-Kuno S, Ebe Y, Takashima S, Yamada M, et al. Evanescent-field fluorescence-assisted lectin microarray: a new strategy for glycan profiling. *Nat Methods.* (2005) 2:851–6. doi: 10.1038/nmeth803
19. Kawakita C, Mise K, Onishi Y, Sugiyama H, Yoshida M, Yamada M, et al. Novel urinary glycan profiling by lectin array serves as the biomarkers for predicting renal prognosis in patients with IgA nephropathy. *Sci Rep.* (2021) 11:3394. doi: 10.1038/s41598-020-77736-1
20. Kashiwagi A, Kasuga M, Araki E, Oka Y, Hanafusa T, Ito H, et al. International clinical harmonization of glycated hemoglobin in Japan: from Japan diabetes society to national glycohemoglobin standardization program values. *J Diabetes Invest.* (2012) 3:39–40. doi: 10.1111/j.2040-1124.2012.00207.x
21. Scirica BM, Mosenzon O, Bhatt DL, Udell JA, Steg PG, McGuire DK, et al. Cardiovascular outcomes according to urinary albumin and kidney disease in patients with type 2 diabetes at high cardiovascular risk: observations from the SAVOR-TIMI 53 trial. *JAMA Cardiol.* (2018) 3:155–63. doi: 10.1001/jamacardio.2017.4228
22. Benjamini Y, Hochberg Y. Controlling the false discovery rate: a practical and powerful approach to multiple testing. *J Roy Stat Soc B.* (1995) 57:289–300. doi: 10.1111/j.2517-6161.1995.tb02031.x
23. Cattaneo M, Malighetti P, Spinelli D. Estimating receiver operative characteristic curves for time-dependent outcomes: the stroccurve package. *Stata J.* (2018) 17:1015–23. doi: 10.1177/1536867X1701700415
24. Pencina MJ, D'Agostino RB Sr, D'Agostino RB Jr, Vasan RS. Evaluating the added predictive ability of a new marker: from area under the ROC curve to reclassification and beyond. *Stat Med.* (2008) 27:157–72; discussion 207–12. doi: 10.1002/sim.2929
25. Pencina MJ, D'Agostino RB, Pencina KM, Janssens AC, Greenland P. Interpreting incremental value of markers added to risk prediction models. *Am J Epidemiol.* (2012) 176:473–81. doi: 10.1093/aje/kws207
26. Stanley P, Taniguchi N, Aebi M. N-Glycans. In: Varki A, Cummings RD, Esko JD, Stanley P, Hart GW, Aebi M, et al., editors. *Essentials of Glycobiology*. Cold Spring Harbor Laboratory Press: Cold Spring Harbor, NY (2015). p. 99–111.
27. Panduru NM, Forsblom C, Saraheimo M, Thorn LM, Gordin D, Elonen N, et al. Urinary liver-type fatty acid binding protein is an independent predictor of stroke and mortality in individuals with type 1 diabetes. *Diabetologia.* (2017) 60:1782–90. doi: 10.1007/s00125-017-4328-x
28. Keser T, Gornik I, Vuckovic F, Selak N, Pavic T, Lukic E, et al. Increased plasma N-glycome complexity is associated with higher risk of type 2 diabetes. *Diabetologia.* (2017) 60:2352–60. doi: 10.1007/s00125-017-4426-9
29. Adua E, Memarian E, Russell A, Trbojevic-Akmacic I, Gudelj I, Juric J, et al. High throughput profiling of whole plasma N-glycans in type II diabetes mellitus patients and healthy individuals: a perspective from a Ghanaian population. *Arch Biochem Biophys.* (2019) 661:10–21. doi: 10.1016/j.abb.2018.10.015
30. Adua E, Anto EO, Roberts P, Kantanka OS, Aboagye E, Wang W. The potential of N-glycosylation profiles as biomarkers for monitoring the progression of type II diabetes mellitus towards diabetic kidney disease. *J Diabetes Metab Disord.* (2018) 17:233–46. doi: 10.1007/s40200-018-0365-3
31. Bermingham ML, Colombo M, McGurnaghan SJ, Blackbourn LAK, Vuckovic F, Pucic Bakovic M, et al. N-Glycan profile and kidney disease in type 1 diabetes. *Diabetes Care.* (2018) 41:79–87. doi: 10.2337/dc17-1042
32. Wittenbecher C, Stambuk T, Kuxhaus O, Rudman N, Vuckovic F, Stambuk J, et al. Plasma N-Glycans as emerging biomarkers of cardiometabolic risk: a prospective investigation in the EPIC-potsdam cohort study. *Diabetes Care.* (2020) 43:661–8. doi: 10.2337/dc19-1507
33. Inoue K, Wada J, Eguchi J, Nakatsuka A, Teshigawara S, Murakami K, et al. Urinary fetuin-A is a novel marker for diabetic nephropathy in type 2 diabetes identified by lectin microarray. *PLoS ONE.* (2013) 8:e77118. doi: 10.1371/journal.pone.0077118
34. Gargano AFG, Schouten O, van Schaick G, Roca LS, van den Berg-Verleg JH, Haselberg R, et al. Profiling of a high mannose-type N-glycosylated lipase using hydrophilic interaction chromatography-mass spectrometry. *Anal Chim Acta.* (2020) 1109:69–77. doi: 10.1016/j.aca.2020.02.042
35. Regal-McDonald K, Xu B, Barnes JW, Patel RP. High-mannose intercellular adhesion molecule-1 enhances CD16(+) monocyte adhesion to the endothelium. *Am J Physiol Heart Circ Physiol.* (2019) 317:H1028–H38. doi: 10.1152/ajpheart.00306.2019
36. Jin ZC, Kitajima T, Dong W, Huang YF, Ren WW, Guan F, et al. Genetic disruption of multiple alpha1,2-mannosidases generates mammalian cells producing recombinant proteins with high-mannose-type N-glycans. *J Biol Chem.* (2018) 293:5572–84. doi: 10.1074/jbc.M117.813030
37. Scott DW, Chen J, Chacko BK, Traylor JG, Jr., Orr AW, et al. Role of endothelial N-glycan mannose residues in monocyte recruitment during atherogenesis. *Arterioscler Thromb Vasc Biol.* (2012) 32:e51–9. doi: 10.1161/ATVBAHA.112.253203
38. Bai L, Li Q, Li L, Lin Y, Zhao S, Wang W, et al. Plasma high-mannose and complex/hybrid N-Glycans are associated with hypercholesterolemia in humans and rabbits. *PLoS ONE.* (2016) 11:e0146982. doi: 10.1371/journal.pone.0146982
39. Scirica BM, Bhatt DL, Braunwald E, Raz I, Cavender MA, Im K, et al. Prognostic implications of biomarker assessments in patients with type 2 diabetes at high cardiovascular risk: a secondary analysis of a randomized clinical trial. *JAMA Cardiol.* (2016) 1:989–98. doi: 10.1001/jamacardio.2016.3030

Conflict of Interest: MYa was a former employee of GP BioSciences Co., Ltd., and is currently an employee of GlycoTechnica Co., Ltd. JW received speaker honoraria from Astra Zeneca, Daiichi Sankyo, MSD, Novartis, Tanabe Mitsubishi, Taisho Toyama and received grant support from Baxter, Chugai, Dainippon Sumitomo, Ono, and Teijin. There are no other relevant declarations relating to employment, consultancy, patents, products in development, or marketed products. This does not alter the authors' adherence to all *Frontiers in Cardiovascular Medicine* policies on sharing data and materials.

The remaining authors declare that the research was conducted in the absence of any commercial or financial relationships that could be construed as a potential conflict of interest.

frontiers in Cardiovascular Medicine

ORIGINAL RESEARCH
published: 15 June 2021
doi: 10.3389/fcvm.2021.684297

Circulating Neprilysin Level Predicts the Risk of Cardiovascular Events in Hemodialysis Patients

Hyeon Seok Hwang[1], Jin Sug Kim[1], Yang Gyun Kim[1], Yu Ho Lee[2], Dong-Young Lee[3], Shin Young Ahn[4], Ju-Young Moon[1], Sang-Ho Lee[1], Gang-Jee Ko[4] and Kyung Hwan Jeong[1]**

[1] Division of Nephrology, Department of Internal Medicine, KyungHee University, Seoul, South Korea, [2] Division of Nephrology, Department of Internal Medicine, CHA Bundang Medical Center, CHA University, Seongnam, South Korea, [3] Division of Nephrology, Department of Internal Medicine, Veterans Health Service Medical Center, Seoul, South Korea, [4] Division of Nephrology, Department of Internal Medicine, Korea University College of Medicine, Seoul, South Korea

Background: Neprilysin inhibition has demonstrated impressive benefits in heart failure treatment, and is the current focus of interest in cardiovascular (CV) and kidney diseases. However, the role of circulating neprilysin as a biomarker for CV events is unclear in hemodialysis (HD) patients.

Methods: A total of 439 HD patients from the K-cohort were enrolled from June 2016 to April 2019. The plasma neprilysin level and echocardiographic findings at baseline were examined. The patients were prospectively followed up to assess the primary endpoint (composite of CV events and cardiac events).

Results: Plasma neprilysin level was positively correlated with left ventricular (LV) mass index, LV end-systolic volume, and LV end-diastolic volume. Multivariate linear regression analysis revealed that neprilysin level was negatively correlated with LV ejection fraction ($\beta = -2.14$; $p = 0.013$). The cumulative event rate of the composite of CV events was significantly greater in neprilysin tertile 3 ($p = 0.049$). Neprilysin tertile 3 was also associated with an increased cumulative event rate of cardiac events ($p = 0.016$). In Cox regression analysis, neprilysin tertile 3 was associated with a 2.61-fold risk for the composite of CV events [95% confidence interval (CI), 1.37–4.97] and a 2.72-fold risk for cardiac events (95% CI, 1.33–5.56) after adjustment for multiple variables.

Conclusions: Higher circulating neprilysin levels independently predicted the composite of CV events and cardiac events in HD patients. The results of this study suggest the importance of future studies on the effect of neprilysin inhibition in reducing CV events.

Keywords: cardiovascular disease, hemodialysis, neprilysin, atherosclerosis, left ventricular systolic dysfunction

OPEN ACCESS

Edited by:
Maria Perticone, University of Magna Graecia, Italy

Reviewed by:
Nicolas Vodovar, Institut National de la Santé et de la Recherche Médicale (INSERM), France
Jian Wu, Fudan University, China

****Correspondence:***
Gang-Jee Ko
lovesba@korea.ac.kr
Kyung Hwan Jeong
aprilhwan@naver.com

Specialty section:
This article was submitted to General Cardiovascular Medicine, a section of the journal Frontiers in Cardiovascular Medicine

Received: *23 March 2021*
Accepted: *24 May 2021*
Published: *15 June 2021*

Citation:
Hwang HS, Kim JS, Kim YG, Lee YH, Lee DY, Ahn SY, Moon J-Y, Lee S-H, Ko G-J and Jeong KH (2021) Circulating Neprilysin Level Predicts the Risk of Cardiovascular Events in Hemodialysis Patients. Front. Cardiovasc. Med. 8:684297. doi: 10.3389/fcvm.2021.684297

INTRODUCTION

Cardiovascular (CV) disease is a major cause of death in patients undergoing hemodialysis (HD) treatment, and an extremely high rate of CV complications has been reported in these patients (1, 2). HD patients are consistently exposed to risk factors for uremia, hemodynamic overload, and sympathetic and neurohumoral activation (3, 4). Furthermore, HD treatment itself induces metabolic derangement and electrolyte shift in cardiomyocytes, episodic cardiac ischemia, and

fibrosis (5, 6). Therefore, HD patients experience repetitive cardiac injuries, and these adverse processes induce cardiac dysfunction, structural changes, and remodeling, which are key factors for high CV morbidity and mortality rates.

Natriuretic peptides have been introduced into the dialysis setting, based on their pathophysiologic role in heart failure, to assess for myocardial ischemia, systolic dysfunction, and risk of future cardiac events (7, 8). Natriuretic peptides have a wide range of CV effects contributing to natriuresis, vasodilation, and blood pressure regulation. Neprilysin is the key enzyme responsible for their degradation, and its inhibition enhances the effect of natriuretic peptides on the CV system (9, 10). Previous reports have identified that neprilysin exists in soluble form in the bloodstream, and demonstrated that circulating neprilysin plays a central role in neurohormonal regulation, CV remodeling, and CV dysfunction (11–13). The neprilysin is also anticipated to be a promising biotarget for the reduction of CV risk in patients with chronic kidney disease (CKD) and cross-sectional study showed the usefulness of neprilysin for heart failure diagnosis in dialysis patients (14–18). However, almost studies exploring the neprilysin in patients with CKD enrolled the patients who were not receiving dialysis, and no evidence exists on circulating neprilysin as a pathologic surrogate to predict the incident CV events in patients undergoing HD treatment.

Therefore, we performed this study to test the hypothesis that plasma neprilysin levels are independently associated with an increased risk for future CV events in HD patients. We also investigated circulating neurohormonal markers and echocardiographic parameters to determine their relationships with neprilysin level.

MATERIALS AND METHODS

Study Population

All data in this study were obtained from the registry of the K-cohort, which is a multicenter, prospective cohort of HD patients in Korea. The inclusion and exclusion criteria have been previously described (19). A total of 637 patients were recruited between June 2016 and April 2019, and 439 patients with whole plasma samples at the time of study enrollment were included in this study.

The study protocol was approved by the local ethics committee (KHNMC 2016-04-039), and the study was conducted in accordance with the principles of the Second Declaration of Helsinki. All participants involved in the study signed written informed consent forms before enrollment.

Data Collection and Definitions

Demographic factors, comorbid conditions, laboratory data, dialysis information, and concomitant medication were collected at the time of inclusion. Information on patient comorbidities was derived to calculate the Charlson comorbidity index score (20). Blood samples for laboratory test and biomarkers were drawn before the start of HD in a mid-week dialysis session. Laboratory data were collected, and delivered *spKt/V* (*K*, dialyzer clearance; *t*, time; *V*, urea distribution volume) was assessed using the conventional method (21). Body mass index was calculated as body weight divided by the square of body height.

The patients were classified into three groups based on the circulating level of neprilysin: tertile 1, $<$ 107.0 pg/ml; tertile 2, 107.0–237.5 pg/ml; and tertile 3, $\geq$ 237.5 pg/ml. All patients were prospectively followed up after baseline assessments. The patient follow-up was censored at the time of transfer to peritoneal dialysis, kidney transplantation, follow-up loss, or patient consent withdrawal.

Laboratory Measures

Plasma samples for neurohormonal assessment were collected using ethylenediaminetetraacetic acid-treated tubes at the time of study entry. After centrifugation for 15 min at 1000 g at room temperature, the samples were stored at −80°C until use. Enzyme-linked immunosorbent assay was performed using Magnetic Luminex® Screening Assay multiplex kits (R&D Systems Inc., Minneapolis, MN, USA) to measure B-type natriuretic peptide (BNP), N-terminal-pro-B-type natriuretic peptide (NT-proBNP), interleukin-6 (IL-6), and galectin-3. Neprilysin levels were measured using a modified sandwich immunoassay (product no. SK00724-01; Aviscera Biosciences, Santa Clara, CA, USA). All patient samples were quantified for relevant markers; however, IL-6 was only measured in a subset of patients due to sample availability. IL-6 level was measured in 331 (75.4%) patients [128 (87.1%) patients in neprilysin tertile 1, 115 (78.8%) patients in neprilysin tertile 2, and 88 (60.3%) patients in neprilysin tertile 3]. The proportion of IL-6-measured patients was significantly lower in patients with neprilysin tertile 3 ($p <$ 0.001). hsCRP was measured using immunoturbidimetric method on Beckman Coulter AU5800 Analyzers (Brea, CA, USA).

Echocardiographic Measures

Of all patients, 355 (80.1%) patients received echocardiographic examination [123 (83.7%) in tertile 1, 113 (77.4%) in tertile 2, and 119 (81.5%) in tertile 3]. The echocardiographic data was collected from clinical report. M-mode and 2D measurements were conducted by trained sonographers or cardiologist in accord with methods recommended by the American Society of Echocardiography (22). Echocardiographic examiners were blinded to the clinical data and biomarker measurements and cardiologists adjudicate and confirm all echocardiographic findings. LV end-diastolic diameter (LVDd), LV end-systolic diameter (LVDs), LV posterior wall thickness (PWT), and interventricular septal thickness (IVST) was measured in M-mode plane. LV mass was estimated using the Devereux formula and body surface area was used to index the LV mass. LV end-diastolic volume (LVEVd), LV end-systolic volume (LVEVs), LV ejection fraction (LVEF), and left atrial dimensions were determined in apical two- and four-chamber views. Peak early diastolic flow velocity (E) and peak late diastolic flow velocity (A) were determined from the mitral valve inflow velocity curve in pulsed wave Doppler. Peak early diastolic tissue velocity (E') was measured from the septal aspect of the mitral annulus in

tissue Doppler. The ratio of E to A wave (E/A) and E to E′ (E/E′) was calculated.

Outcome Measures

The primary study endpoint was a composite of incident CV events, including cardiac and non-cardiac vascular events. Cardiac events were defined as acute coronary syndrome, heart failure, ventricular arrhythmia, cardiac arrest, and sudden death. Non-cardiac events included cerebral infarction, cerebral hemorrhage, and peripheral vascular occlusive diseases requiring revascularization or surgical intervention. All mortality events from any cause were recorded and carefully reviewed. The secondary endpoints were levels of circulating neurohormonal markers and echocardiographic parameters, and their correlations with neprilysin level were analyzed.

Statistical Analysis

Data are expressed as mean ± standard deviation (SD) or median [interquartile range (IQR)]. Kolmogorov-Smirnov test was used to assess the normality of the distribution of the variables. Differences among the three groups were identified using analysis of variance or Kruskal-Wallis test. Tukey *post hoc* test and Mann-Whitney *U*-test with Bonferroni correction were used to identify differences between more than two groups. Categorical variables were compared using the chi-square test or Fisher's exact test. Log-transformed values of high-sensitivity C-reactive protein (hsCRP) levels were used in regression analysis because of a skewed distribution. The values of neprilysin levels were log-transformed for linear regression analysis, and 1 SD was used for hazard ratio (HR) calculations. Spearman's analyses were used to evaluate the correlation between neprilysin level and continuous variables. The association between neprilysin level and LVEF was identified using linear regression analysis. A Cox proportional hazard model was constructed to identify independent variables related to CV events or patient death. Multivariate models included significantly associated parameters according to their weight in univariate testing and clinically fundamental parameters. Baseline characteristics and laboratory data was compared between patients with and without incident cardiac event to adjust the multivariate model (**Supplementary Table 1**). Charlson comorbidity score, prevalence of CV event history, hemoglobin level, and plasma NT-proBNP level was significantly different between two groups. All of these parameters were included in multivariate Cox model. We tried to adjust baseline cardiac remodeling status using NT-proBNP or BNP, because echocardiographic data is not fully investigated in this study. Statistical analyses were performed using SPSS software (version 22.0; SPSS, IBM Corp., Armonk, NY, USA). p-values < 0.05 were considered significant.

RESULTS

Baseline Demographic Characteristics and Laboratory Data

The median neprilysin level was 155.2 (IQR 88.6, 304.2) pg/ml in all studied patients. According to tertile, the median neprilysin level was 68.4 (IQR 45.2, 89.2) pg/ml in tertile 1 (n = 147), 155.9 (IQR 127.2, 184.4) pg/ml in tertile 2 (n = 146), and 424.0 (IQR 303.4, 741.6) pg/ml in tertile 3 (n = 146). The baseline patient demographics, clinical characteristics, and laboratory results are described in **Table 1**. Patients in tertile 3 of neprilysin level were younger and had a shorter duration of dialysis therapy than those in neprilysin tertile 1. Twenty (4.6%) patients with heart failure were enrolled in this study. Heart failure with preserved LVEF was observed in 6 (1.4%) patients and heart failure with reduced LVEF in 14 (3.2%) patients. Laboratory data and dialysis characteristics did not show significant differences. Among the circulating neurohormonal markers, galectin-3 showed a significantly higher level in patients in neprilysin tertile 3 than in patients in the other tertiles.

TABLE 1 | Baseline demographic and laboratory data of the study population.

	Tertiles of neprilysin level			
	Tertile 1 < 107.0 pg/ml (n = 147)	**Tertile 2 107.0–237.5 pg/ml (n = 146)**	**Tertile 3 ≥ 237.5 pg/ml (n = 146)**	***P*-value**
Age (years)	64.9 ± 12.1	61.5 ± 11.4*	58.7 ± 14.2*	<0.001
Male (%)	109 (74.1)	92 (63.0)	91 (62.3)	0.055
Body mass index (kg/m^2)	23.43 ± 3.82	22.99 ± 3.90	23.43 ± 4.55	0.567
HD duration (years)	4.66 ± 6.01	3.63 ± 5.07	2.91 ± 4.54*	0.017
Diabetes (%)	77 (52.4)	88 (60.3)	84 (57.5)	0.383
History of CV event (%)	64 (43.5)	62(42.5)	59 (40.4)	0.859
Charlson comorbidity score	4.10 ± 1.71	4.13 ± 1.21	3.97 ± 1.55	0.616
Hemoglobin (g/dl)	10.55 ± 1.28	10.46 ± 1.14	10.39 ± 1.26	0.529
Albumin (g/dl)	3.77 ± 0.33	3.82 ± 0.30	3.84 ± 0.34	0.156
LDL-cholesterol (mg/dl)	76.08 ± 25.62	77.72 ± 28.50	75.46 ± 24.84	0.752
hsCRP (mg/dl)	1.42 (0.20, 3.49)	0.92 (0.19, 3.54)	0.70 (0.19, 2.80)	0.149
Predialysis SBP (mmHg)	144.3 ± 18.9	141.3 ± 19.9	142.3 ± 21.8	0.421
Ultrafiltration (L)	2.25 ± 1.11	2.14 ± 1.07	2.29 ± 1.07	0.462
spKt/V	1.59 ± 0.46	1.55 ± 0.31	1.58 ± 0.25	0.634
ESA use (%)	131 (89.1)	132 (91.0)	136 (93.2)	0.479
BNP (pg/ml)	50.6 (16.3, 91.0)	37.3 (7.6, 86.6)	35.4 (7.6, 88.5)	0.384
NT-proBNP (pg/ml)	286 (200, 442)	330 (189, 475)	317 (198, 477)	0.542
IL-6 (pg/ml)	3.3 (2.2, 5.8)	3.0 (1.9, 4.8)	2.7 (2.1, 4.2)*	0.032
Galectin-3 (ng/ml)	17.2 (15.0, 19.8)	17.5 (15.0, 20.5)	19.0 (15.4, 22.0)*	0.029

IL-6 was measured in 331 (75.4%) patients.

**$p < 0.05$ vs. tertile 1.*

HD, hemodialysis; CV, cardiovascular; LDL, low-density lipoprotein; hsCRP, high-sensitivity C-reactive protein; SBP, systolic blood pressure; spKt/V, single-pool Kt/V; ESA, erythropoietin-stimulating agent; BNP, brain natriuretic peptide; NT-proBNP, N-terminal-pro-B-type natriuretic peptide; MMP-2, matrix metalloproteinase-2.

TABLE 2 | Correlation of neprilysin level with circulating cardiac markers and echocardiographic parameters.

	Correlation coefficient	*P*-value
Circulating neurohormonal marker		
BNP (pg/ml)	−0.092	0.055
NT-proBNP (pg/ml)	0.003	0.949
hsCRP (mg/dl)	−0.105	0.029
IL-6 (pg/ml)	−0.134	0.014
Galectin-3 (ng/ml)	0.124	0.009
Echocardiographic parameters		
LV mass index (g/m^2)	0.129	0.043
LVDs (mm)	0.068	0.235
LVDd (mm)	0.063	0.235
LVESV (ml)	0.137	0.035
LVEDV (ml)	0.137	0.035
LVEF (%)	−0.185	< 0.001
IVST (mm)	0.046	0.470
PWT (mm)	−0.023	0.690
E/E'	0.019	0.778
E/A	0.024	0.731
LA dimension (mm)	−0.048	0.445

Echocardiography was examined in 355 (80.9%) patients.
BNP, B-type natriuretic peptide; NT-proBNP, N-terminal-pro-B-type natriuretic peptide; MMP-2, matrix metalloproteinase-2; LV, left ventricle; LVDs, left ventricular end-systolic diameter; LVDd, left ventricular end-diastolic diameter; LVESV, left ventricular end-systolic volume; LVEDV, left ventricular end-diastolic volume; IVST, interventricular septal thickness in diastolic; PWT LV, posterior wall thickness in diastolic; LVEF, left ventricle ejection fraction; LA, left atrium.

Correlation of Neprilysin Level With Circulating Cardiac Markers and Echocardiographic Parameters

The correlations between the levels of neprilysin and circulating neurohormonal markers are shown in **Table 2** and **Supplementary Figure 1**. The plasma levels of BNP and NT-proBNP did not show a significant correlation with neprilysin level. A significant positive correlation was found between galectin-3 and neprilysin levels, and the circulating levels of hsCRP and IL-6 were negatively correlated with neprilysin level. However, all coefficient values and distribution patterns suggested that the correlation power was not strong.

The baseline echocardiographic measurements are described in **Supplementary Table 2**. LVEF was significantly different across tertiles, and the lowest LVEF was observed in patients in neprilysin tertile 3. Posterior wall thickness and the E/A ratio showed different mean values among the neprilysin tertiles. To investigate the relationship between neprilysin level and cardiac structures, the correlation between neprilysin level and echocardiographic parameters was evaluated (**Table 2**). LV systolic and diastolic diameters, LV wall thickness, and diastolic parameters were not correlated with circulating neprilysin level. A significant negative correlation was observed between LVEF and neprilysin level. LV mass index, LVESV, and LVEDV were positively correlated with neprilysin level. However, the coefficient values and distribution patterns of variables indicated weak correlation power (**Supplementary Figure 2**).

TABLE 3 | Relationship between the baseline parameters and LVEF.

	Unstandardized β	95% CI	*P*-value
Age (years)	0.03	−0.40, 0.10	0.417
Male	−0.57	−2.36, 1.22	0.531
History of CV event	−2.93	−4.68, −1.18	0.002
Hemoglobin (g/dl)	0.56	−0.12, 1.24	0.107
NT-proBNP (pg/ml)	−0.003	−0.007, 0.001	0.112
Ultrafiltration (L)	−0.54	−1.35, 0.27	0.193
Neprilysin (pg/ml)	−2.14	−3.83, −0.45	0.013

Of the all studied patients, 355 (80.9%) patients were examined with echocardiography. CV, cardiovascular; NT-proBNP, N-terminal-pro-B-type natriuretic peptide.

Relationship Between Plasma Neprilysin Level and Left Ventricular Ejection Fraction in Hemodialysis Patients

Univariate and multivariate linear regression models were constructed to determine the association between neprilysin level and LV systolic function. In univariate analysis, LVEF was significantly associated with history of CV events ($\beta = -2.89$; $p = 0.001$), NT-proBNP level ($\beta = -0.01$; $p = 0.023$), and neprilysin level ($\beta = -2.19$; $p = 0.011$). Hemoglobin level ($\beta = 0.50$; $p = 0.155$) and ultrafiltration volume ($\beta = -0.65$; $p = 0.115$) showed borderline significance in association with neprilysin level. The multivariate linear regression model is shown in **Table 3**. History of CV events ($\beta = -2.93$; $p = 0.002$) and neprilysin level ($\beta = -2.14$; $p = 0.013$) were independent determinants of LVEF in HD patients.

Prognostic Utility of Neprilysin Level in Hemodialysis Patients

During a mean follow-up of 30.1 months, 61 deaths (13.9%) and 66 CV events (15.0%) occurred. Of the CV events, acute coronary syndrome occurred in 27 patients, heart failure occurred in 6 patients, ventricular arrhythmia occurred in 4 patients, cardiac arrest occurred in 9 patients, sudden death occurred in 6 patients, cerebral vascular accidents occurred in 8 patients, and peripheral vascular occlusive diseases occurred in 6 patients. The cumulative event rate of the composite of CV events was significantly greater in neprilysin tertile 3 ($p = 0.049$; **Figure 1A**). Neprilysin tertile 3 was associated with a greater cumulative event rate of cardiac events ($p = 0.016$; **Figure 1B**). The cumulative event rate of patient death did not differ among patients in the different neprilysin tertiles ($p = 0.127$).

Univariable Cox regression analysis revealed that plasma neprilysin tertile 3 was significantly associated with an increased risk for the composite of CV events [HR, 2.10; 95% confidence interval (CI), 1.14–3.88; $p = 0.017$; **Table 4**]. This association remained significant after adjustment for multiple variables (HR, 2.61; 95% CI, 1.37–4.97; $p = 0.004$). Neprilysin increment per 1 SD also had an independent risk for composite events (HR, 1.40; 95% CI, 1.17–1.66; $p < 0.001$). To further investigate the risk for the composite of CV events, the HRs for cardiac events and non-cardiac vascular events were evaluated. Patients in neprilysin tertile 3 had a significant risk for cardiac events

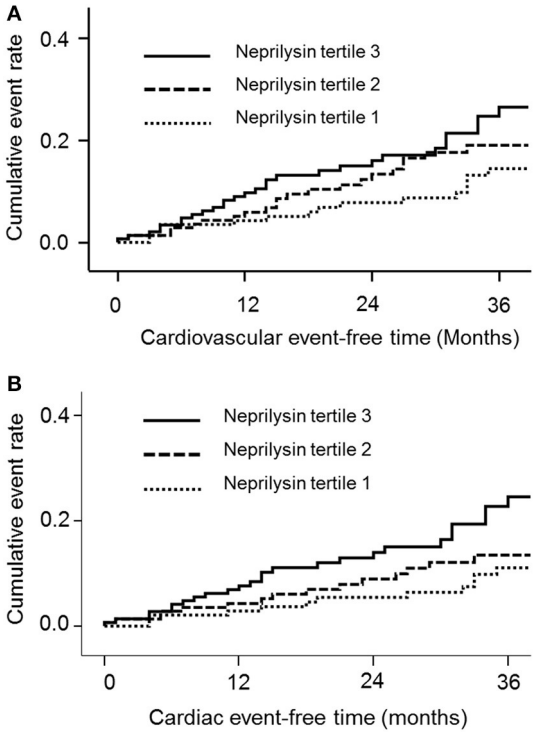

FIGURE 1 | Cumulative event rates of the composite of **(A)** cardiovascular events and **(B)** cardiac events according to neprilysin level.

TABLE 4 | Hazard ratios of neprilysin tertiles for cardiovascular events.

	No. event (%)	HR (95% CI), crude	HR (95% CI), adjusted
Composite of CVE			
Neprilysin tertile 1	16 (10.9)	Reference	Reference
Neprilysin tertile 2	21 (14.4)	1.46 (0.76, 2.81)	1.77 (0.90, 3.49)
Neprilysin tertile 3	29 (19.9)	2.10* (1.14, 3.88)	2.61* (1.37, 4.97)
Neprilysin per SD		1.32* (1.11, 1.57)	1.40* (1.17, 1.66)
Cardiac event			
Neprilysin tertile 1	12 (8.2)	Reference	Reference
Neprilysin tertile 2	16 (11.0)	1.45 (0.70, 2.98)	1.56 (0.72, 3.36)
Neprilysin tertile 3	26 (17.8)	2.54* (1.28, 5.05)	2.72* (1.33, 5.56)
Neprilysin per SD		1.37* (1.14, 1.64)	1.44* (1.20, 1.74)
Non-cardiac vascular event			
Neprilysin tertile 1	4 (2.7)	Reference	Reference
Neprilysin tertile 2	7 (4.8)	1.84 (0.54, 6.27)	2.56 (0.68, 9.72)
Neprilysin tertile 3	4 (2.7)	1.00 (0.25, 4.02)	1.47 (0.34, 6.30)
Neprilysin per SD		1.26 (0.89, 1.78)	1.27 (0.90, 1.78)
Patient death			
Neprilysin tertile 1	29 (19.7)	Reference	Reference
Neprilysin tertile 2	16 (11.0)	0.59 (0.32, 1.09)	0.75 (0.40, 1.42)
Neprilysin tertile 3	16 (11.0)	0.60 (0.33, 1.11)	0.81 (0.43, 1.55)
Neprilysin per SD		0.81 (0.52, 1.26)	0.88 (0.60, 1.29)

All analyses are adjusted for the following: age, sex, body mass index, Charlson comorbidity index, hemoglobin, hsCRP, NT-proBNP, ESA use, HD duration, spKt/V.
hsCRP, high-sensitivity C-reactive protein; NT-proBNP, N-terminal-pro-B-type natriuretic peptide; ESA, erythropoietin-stimulating agent; HD, hemodialysis; spKt/V, single-pool Kt/V.
$^{*}p < 0.05$.

after adjustment for multiple covariates (HR, 2.72; 95% CI, 1.33–5.56; $p = 0.006$) and neprilysin increment per 1 SD was also associated with the risk of cardiac events (HR, 1.44; 95% CI, 1.20–1.74; $p < 0.001$). However, neprilysin level per tertile or per 1 SD increment did not show a significant risk for non-cardiac events and patient death. We re-construct multivariate Cox hazard model including BNP as covariates, instead of NT-proBNP. Neprilysin tertile 3 and neprilysin increment per 1 SD was significantly associated with higher risk of CV composite and cardiac events (**Supplementary Table 3**).

DISCUSSION

Our prospective observational cohort study demonstrated that an increased level of neprilysin was associated with a greater cumulative event rate of CV composites and cardiac events. In addition, higher levels of neprilysin increased the risk for incident CV composites and cardiac events after adjustment for multiple covariates. Plasma neprilysin level was positively correlated with galectin-3 circulating level, LV dimension, and LV mass index. In addition, an independent negative relationship was observed between neprilysin level and LVEF. These findings suggest that neprilysin is a novel biomarker for assessing the risk of CV events, and that it is associated with cardiac structural and functional changes in HD patients.

Interestingly, we found a weakly negative correlation between neprilysin and the inflammatory markers hsCRP and IL-6. Inflammatory substrates are known to be degradable by neprilysin, and we presumed that higher levels of neprilysin are associated with a reduced inflammatory state. However, the correlation power between neprilysin and inflammatory marker was weak, suggesting that the inhibitory interaction was not substantial in HD patients (9, 23). The additional incidental finding was negative correlation between neprilysin levels and age ($\rho = -0.167$; $p < 0.001$). The reason of this finding is not clear, but we presumed that the correlation between circulating neprlysin level and age is dependent on population characteristics, because the correlations coefficients were changeable in different patient categories (11, 24, 25).

Galectin-3 is a contributing factor to cardiac fibrosis, and a biomarker for LV remodeling and heart failure progression (26–28). Our results showed that neprilysin level was positively correlated with galectin-3 level. In addition, LV internal volume and LV mass index increased as the plasma level of neprilysin increased. These findings suggest that circulating neprilysin level reflects the pathologic deformation of cardiac structures. However, correlation power indicated the weak relationship between neprilysin and echocardiographic parameters. Therefore, we construct linear regression model to find out independent relationship between neprilysin and LVEF. We observed that neprilysin level was associated with lower LVEF after multiple adjustment. These findings suggest that neprilysin is a noticeable indicator of LV systolic dysfunction and cardiac remodeling in HD patients.

The use of cardiac biomarkers in clinical practice allows clinicians to identify high-risk patients for incident CV events. Although BNP and NT-proBNP have been widely used in patients with heart failure, their use in HD patients is challenging because of high individual variations, increased plasma levels without any evidence of cardiac disease, more than normal values in 90% of HD patients, and wide differences in cutoff value for risk stratification in diverse studies (29–31). Therefore, alternative cardiac biomarkers are required in dialysis care, and neprilysin is of particular interest because it is a new biotarget for innovative therapeutic strategies in heart failure (10, 32). Our study revealed that plasma neprilysin levels were significantly associated with increased rates of CV composites and cardiac events. The association remained significant after adjustment for multiple established CV risk factors, including NT-proBNP. These findings suggest that higher neprilysin levels contribute to incident CV risk independently of traditional CV risk factors and that neprilysin is a valuable biomarker for CV risk prediction in patients undergoing HD treatment.

Although we found a significant predictive ability of neprilysin for adverse CV outcomes in HD patients, recent studies on non-dialysis-dependent CKD revealed that high neprilysin levels did not predict poor CV outcomes (33). We presumed that these divergent results might originate from the greater activation of natriuretic peptide systems in HD patients. Because HD patients usually have higher degrees of cardiac remodeling than non-dialysis-dependent CKD patients, the activation of natriuretic peptides is more pronounced in HD patients (34–36). Therefore, the clinical importance of neprilysin in HD patients may become larger with activated natriuretic peptides. This explanatory assumption is also supported by the discrepant results in different heart failure settings. Previous studies have reported that circulating neprilysin level is predictive of CV death in patients with heart failure with acute decompensation or reduced LVEF, but is not associated with CV outcomes in patients with heart failure with preserved LVEF (11, 12, 37, 38).

This study had some limitations. Echocardiographic parameters and IL-6 levels were not measured in some patients. The lower proportion of IL-6-measured patients in neprilysin tertile 3 may be possible to cause the bias in correlation analysis. Furthermore, given the limited number of events, we could not perform individual analyses for heart failure, although HD patients are at a higher risk for congestion (39). In addition, we measured neprilysin concentration only, and neprilysin activity was not measured. It was reported in a previous study that neprilysin activity, but not concentration, provided diagnostic information about heart failure in dialysis patients (18). Lower neprilysin activity combining with multi-markers helped to determine the presence of heart failure. Therefore, measurement of neprilysin activity might provide additional data on the risk of incident CV event. Further studies with neurohormonal peptides, neprilysin concentration and activity may improve predictability of CV complication in HD patients.

CONCLUSION

Circulating neprilysin level was correlated with pathologic remodeling of echocardiographic structures and independently associated with lower LVEF. Higher circulating neprilysin levels were associated with a greater risk of the composite of CV events and cardiac events in HD patients. Our results suggest the importance of future studies on the implication of neprilysin inhibition for HD patients.

DATA AVAILABILITY STATEMENT

The raw data supporting the conclusions of this article will be made available by the authors, without undue reservation.

ETHICS STATEMENT

The studies involving human participants were reviewed and approved by KyungHee University Hospital IRB. The patients/participants provided their written informed consent to participate in this study.

AUTHOR CONTRIBUTIONS

HSH conceived the research question conceived and designed the analysis. JSK, YGK, YHL, D-YL, J-YM, JYM, and S-HL undertook data collection conducted the study. HSH, G-JK, and KHJ drafted the manuscript. All authors reviewed the results and commented on the manuscript. All authors read and approved the final manuscript.

ACKNOWLEDGMENTS

This work was supported by Patient-Centered Clinical Research Coordinating Center funded by the Ministry of Health and Welfare, Republic of Korea (H19C0481, HC19C0041).

SUPPLEMENTARY MATERIAL

The Supplementary Material for this article can be found online at: https://www.frontiersin.org/articles/10.3389/fcvm.2021.684297/full#supplementary-material

REFERENCES

1. Cheung AK, Sarnak MJ, Yan G, Dwyer JT, Heyka RJ, Rocco MV, et al. Atherosclerotic cardiovascular disease risks in chronic hemodialysis patients. *Kidney Int*. (2000) 58:353-62. doi: 10.1046/j.1523-1755.2000.00173.x
2. Thompson S, James M, Wiebe N, Hemmelgarn B, Manns B, Klarenbach S, et al. Cause of death in patients with reduced kidney function. *J Am Soc Nephrol*. (2015) 26:2504-11. doi: 10.1681/ASN.2014070714
3. Meeus F, Kourilsky O, Guerin AP, Gaudry C, Marchais SJ, London GM. Pathophysiology of cardiovascular disease in hemodialysis patients. *Kidney Int Suppl*. (2000) 76:S140-7. doi: 10.1046/j.1523-1755.2000.07618.x

4. Rangaswami J, McCullough PA. Heart failure in end-stage kidney disease: pathophysiology, diagnosis, and therapeutic strategies. *Semin Nephrol*. (2018) 38:600-17. doi: 10.1016/j.semnephrol.2018.08.005
5. Odudu A, McIntyre CW. An update on intradialytic cardiac dysfunction. *Semin Dial*. (2016) 29:435-41. doi: 10.1111/sdi.12532
6. McIntyre CW. Effects of hemodialysis on cardiac function. *Kidney Int*. (2009) 76:371-5. doi: 10.1038/ki.2009.207
7. Wang AY, Lam CW, Yu CM, Wang M, Chan IH, Zhang Y, et al. N-terminal pro-brain natriuretic peptide: an independent risk predictor of cardiovascular congestion, mortality, and adverse cardiovascular outcomes in chronic peritoneal dialysis patients. *J Am Soc Nephrol*. (2007) 18:321-30. doi: 10.1681/ASN.2005121299
8. Wang AY. Clinical utility of natriuretic peptides in dialysis patients. *Semin Dial*. (2012) 25:326-33. doi: 10.1111/j.1525-139X.2012.01079.x
9. Bayes-Genis A, Barallat J, Richards AM. A test in context: neprilysin: function, inhibition, and biomarker. *J Am Coll Cardiol*. (2016) 68:639-53. doi: 10.1016/j.jacc.2016.04.060
10. McMurray JJ, Packer M, Desai AS, Gong J, Lefkowitz MP, Rizkala AR, et al. Angiotensin-neprilysin inhibition versus enalapril in heart failure. *N Engl J Med*. (2014) 371:993-1004. doi: 10.1056/NEJMoa1409077
11. Bayes-Genis A, Barallat J, Galan A, de Antonio M, Domingo M, Zamora E, et al. Soluble neprilysin is predictive of cardiovascular death and heart failure hospitalization in heart failure patients. *J Am Coll Cardiol*. (2015) 65:657-65. doi: 10.1016/j.jacc.2014.11.048
12. Bayes-Genis A, Barallat J, Pascual-Figal D, Nunez J, Minana G, Sanchez-Mas J, et al. Prognostic value and kinetics of soluble neprilysin in acute heart failure: a pilot study. *JACC Heart Fail*. (2015) 3:641-4. doi: 10.1016/j.jchf.2015.03.006
13. Wang Y, Zhou R, Lu C, Chen Q, Xu T, Li D. Effects of the angiotensin-receptor neprilysin inhibitor on cardiac reverse remodeling: meta-analysis. *J Am Heart Assoc*. (2019) 8:e012272. doi: 10.1161/JAHA.119.012272
14. Haynes R, Zhu D, Judge PK, Herrington WG, Kalra PA, Baigent C. Chronic kidney disease, heart failure and neprilysin inhibition. *Nephrol Dial Transplant*. (2020) 35:558-64. doi: 10.1093/ndt/gfz058
15. Judge P, Haynes R, Landray MJ, Baigent C. Neprilysin inhibition in chronic kidney disease. *Nephrol Dial Transplant*. (2015) 30:738-43. doi: 10.1093/ndt/gfu269
16. James M, Manns B. Neprilysin inhibition and effects on kidney function and surrogates of cardiovascular risk in chronic kidney disease. *Circulation*. (2018) 138:1515-8. doi: 10.1161/CIRCULATIONAHA.118.036523
17. Lyle MA, Iyer SR, Redfield MM, Reddy YNV, Felker GM, Cappola TP, et al. Circulating neprilysin in patients with heart failure and preserved ejection fraction. *JACC Heart Fail*. (2020) 8:70-80. doi: 10.1016/j.jchf.2019.07.005
18. Claus R, Berliner D, Bavendiek U, Vodovar N, Lichtinghagen R, David S, et al. Soluble neprilysin, NT-proBNP, and growth differentiation factor-15 as biomarkers for heart failure in dialysis patients (SONGBIRD). *Clin Res Cardiol*. (2020) 109:1035-47. doi: 10.1007/s00392-020-01597-x
19. Hwang HS, Kim JS, Kim YG, Lee SY, Ahn SY, Lee HJ, et al. Circulating PCSK9 level and risk of cardiovascular events and death in hemodialysis patients. *J Clin Med*. (2020) 9:244. doi: 10.3390/jcm9010244
20. Charlson ME, Pompei P, Ales KL, MacKenzie CR. A new method of classifying prognostic comorbidity in longitudinal studies: development and validation. *J Chronic Dis*. (1987) 40:373-83. doi: 10.1016/0021-9681(87)90171-8
21. Gotch FA. Kinetic modeling in hemodialysis. In: Nissenson AR, Fine RN, Gentile DE, editors. *Clinical Dialysis*. 3rd ed. Norwalk, CT: Appleton and Lange (1995). pp. 156–88.
22. Lang RM, Badano LP, Mor-Avi V, Afilalo J, Armstrong A, Ernande L, et al. Recommendations for cardiac chamber quantification by echocardiography in adults: an update from the American Society of Echocardiography and the European Association of Cardiovascular Imaging. *J Am Soc Echocardiogr*. (2015) 28:1-39.e14. doi: 10.1016/j.echo.2014.10.003
23. Chen Y, Burnett JC, Jr. Biochemistry, therapeutics, and biomarker implications of neprilysin in cardiorenal disease. *Clin Chem*. (2017) 63:108-15. doi: 10.1373/clinchem.2016.262907
24. Pavo N, Arfsten H, Cho A, Goliasch G, Bartko PE, Wurm R, et al. The circulating form of neprilysin is not a general biomarker for overall survival in treatment-naive cancer patients. *Sci Rep*. (2019) 9:2554. doi: 10.1038/s41598-019-38867-2
25. Reddy YNV, Iyer SR, Scott CG, Rodeheffer RJ, Bailey K, Jenkins G, et al. Soluble neprilysin in the general population: clinical determinants and its relationship to cardiovascular disease. *J Am Heart Assoc*. (2019) 8:e012943. doi: 10.1161/JAHA.119.012943
26. Ho JE, Liu C, Lyass A, Courchesne P, Pencina MJ, Vasan RS, et al. Galectin-3, a marker of cardiac fibrosis, predicts incident heart failure in the community. *J Am Coll Cardiol*. (2012) 60:1249-56. doi: 10.1016/j.jacc.2012.04.053
27. de Boer RA, Voors AA, Muntendam P, van Gilst WH, van Veldhuisen DJ. Galectin-3: a novel mediator of heart failure development and progression. *Eur J Heart Fail*. (2009) 11:811-7. doi: 10.1093/eurjhf/hfp097
28. Lok DJ, Lok SI, Bruggink-Andre de la Porte PW, Badings E, Lipsic E, van Wijngaarden J, et al. Galectin-3 is an independent marker for ventricular remodeling and mortality in patients with chronic heart failure. *Clin Res Cardiol*. (2013) 102:103-10. doi: 10.1007/s00392-012-0500-y
29. Vickery S, Price CP, John RI, Abbas NA, Webb MC, Kempson ME, et al. B-type natriuretic peptide (BNP) and amino-terminal proBNP in patients with CKD: relationship to renal function and left ventricular hypertrophy. *Am J Kidney Dis*. (2005) 46:610-20. doi: 10.1053/j.ajkd.2005.06.017
30. Booth J, Pinney J, Davenport A. N-terminal proBNP–marker of cardiac dysfunction, fluid overload, or malnutrition in hemodialysis patients? *Clin J Am Soc Nephrol*. (2010) 5:1036-40. doi: 10.2215/CJN.09001209
31. Fahim MA, Hayen A, Horvath AR, Dimeski G, Coburn A, Johnson DW, et al. N-terminal pro-B-type natriuretic peptide variability in stable dialysis patients. *Clin J Am Soc Nephrol*. (2015) 10:620-9. doi: 10.2215/CJN.09060914
32. Velazquez EJ, Morrow DA, DeVore AD, Duffy CI, Ambrosy AP, McCague K, et al. Angiotensin-neprilysin inhibition in acute decompensated heart failure. *N Engl J Med*. (2019) 380:539-48. doi: 10.1056/NEJMoa1812851
33. Emrich IE, Vodovar N, Feuer L, Untersteller K, Nougue H, Seiler-Mussler S, et al. Do plasma neprilysin activity and plasma neprilysin concentration predict cardiac events in chronic kidney disease patients? *Nephrol Dial Transplant*. (2019) 34:100-8. doi: 10.1093/ndt/gfy066
34. Roberts MA, Hare DL, Sikaris K, Ierino FL. Temporal trajectory of B-type natriuretic peptide in patients with CKD stages 3 and 4, dialysis, and kidney transplant. *Clin J Am Soc Nephrol*. (2014) 9:1024-32. doi: 10.2215/CJN.08640813
35. Horii M, Matsumoto T, Uemura S, Sugawara Y, Takitsume A, Ueda T, et al. Prognostic value of B-type natriuretic peptide and its amino-terminal proBNP fragment for cardiovascular events with stratification by renal function. *J Cardiol*. (2013) 61:410-6. doi: 10.1016/j.jjcc.2013.01.015
36. Paoletti E, De Nicola L, Gabbai FB, Chiodini P, Ravera M, Pieracci L, et al. Associations of left ventricular hypertrophy and geometry with adverse outcomes in patients with CKD and hypertension. *Clin J Am Soc Nephrol*. (2016) 11:271-9. doi: 10.2215/CJN.06980615
37. Goliasch G, Pavo N, Zotter-Tufaro C, Kammerlander A, Duca F, Mascherbauer J, et al. Soluble neprilysin does not correlate with outcome in heart failure with preserved ejection fraction. *Eur J Heart Fail*. (2016) 18:89-93. doi: 10.1002/ejhf.435
38. O'Connor CM, deFilippi C. PARAGON-HF - why we do randomized, controlled clinical trials. *N Engl J Med*. (2019) 381:1675-6. doi: 10.1056/NEJMe1912402
39. Campbell DJ. Long-term neprilysin inhibition - implications for ARNIs. *Nat Rev Cardiol*. (2017) 14:171-86. doi: 10.1038/nrcardio.2016.200

Conflict of Interest: The authors declare that the research was conducted in the absence of any commercial or financial relationships that could be construed as a potential conflict of interest.

frontiers in Cardiovascular Medicine

ORIGINAL RESEARCH
published: 28 June 2021
doi: 10.3389/fcvm.2021.663509

Development and Validation of a Random Forest Diagnostic Model of Acute Myocardial Infarction Based on Ferroptosis-Related Genes in Circulating Endothelial Cells

Chen Yifan[†‡], *Shi Jianfeng*[†] *and Pu Jun*[*‡]

State Key Laboratory for Oncogenes and Related Genes, Division of Cardiology, Renji Hospital, School of Medicine, Shanghai Jiao Tong University, Shanghai Cancer Institute, Shanghai, China

OPEN ACCESS

Edited by:
Maria Perticone, University of Magna Graecia, Italy

Reviewed by:
Alexander E. Berezin, Zaporizhia State Medical University, Ukraine
Hao Zhang, Shanghai Children's Medical Center, China

***Correspondence:**
Pu Jun
pujun310@hotmail.com

[†]*These authors have contributed equally to this work*

[‡]**ORCID:**
Chen Yifan
orcid.org/0000-0002-8889-1594
Pu Jun
orcid.org/0000-0003-2240-5108

Specialty section:
This article was submitted to General Cardiovascular Medicine, a section of the journal Frontiers in Cardiovascular Medicine

Received: *03 February 2021*
Accepted: *20 April 2021*
Published: *28 June 2021*

Citation:
Yifan C, Jianfeng S and Jun P (2021) Development and Validation of a Random Forest Diagnostic Model of Acute Myocardial Infarction Based on Ferroptosis-Related Genes in Circulating Endothelial Cells. Front. Cardiovasc. Med. 8:663509. doi: 10.3389/fcvm.2021.663509

The high incidence and mortality of acute myocardial infarction (MI) drastically threaten human life and health. In the past few decades, the rise of reperfusion therapy has significantly reduced the mortality rate, but the MI diagnosis is still by means of the identification of myocardial injury markers without highly specific biomarkers of microcirculation disorders. Ferroptosis is a novel reported type of programmed cell death, which plays an important role in cancer development. Maintaining iron homeostasis in cells is essential for heart function, and its role in the pathological process of ischemic organ damages remains unclear. Being quickly detected through blood tests, circulating endothelial cells (CECs) have the potential for early judgment of early microcirculation disorders. In order to explore the role of ferroptosis-related genes in the early diagnosis of acute MI, we relied on two data sets from the GEO database to first detect eight ferroptosis-related genes differentially expressed in CECs between the MI and healthy groups in this study. After comparing different supervised learning algorithms, we constructed a random forest diagnosis model for acute MI based on these ferroptosis-related genes with a compelling diagnostic performance in both the validation (AUC = 0.8550) and test set (AUC = 0.7308), respectively. These results suggest that the ferroptosis-related genes might play an important role in the early stage of MI and have the potential as specific diagnostic biomarkers for MI.

Keywords: ferroptosis, myocardial infarction, diagnostic model, random forest, supervised machine learning

INTRODUCTION

Myocardial infarction (MI), the most common and most precarious outcome of coronary heart disease, endangers the health of the majority (1). With the progress of interventional and reperfusion therapy in recent years, the mortality rate of acute MI has been significantly reduced. However, it cannot be ignored that there is still a lack of efficient tools and biomarkers for the early diagnosis of acute MI. Even in the early stage of acute MI, every hour of early diagnosis and timely treatment could increase the survival rate by about 15% (2, 3). Specific markers of myocardial injury, such as cardiac troponin T (cTnT) (4) and typical changes on an electrocardiogram (ECG) (5) take the top priority for MI diagnosis in recent clinical guidelines (6). However, such diagnostic

strategy still faces a lot of challenges. The cTnT in myocardial cells lacks timeliness for the early diagnosis of acute MI because it only reflects myocardial damage and even rupture caused by ischemia, hypoxia, and other factors without characterizing the early myocardial perfusion abnormalities. Moreover, the half-life of cTnT in the blood is too long to identify the reinfarction (7). What is more, typical changes on ECG of MI are not always stable and could be interfered with by other cardiomyopathy. Hence, measures should be taken immediately to explore novel biomarkers for early diagnosis.

Circulating endothelial cells (CECs) are derived from the metabolism of the vascular endothelium (8), which directly reflects the contractile function of blood vessels, the perfusion of capillaries, and the state of ischemia and hypoxia earlier than cardiomyocytes (9). Meanwhile, ischemia and hypoxia directly lead to abnormal metabolism and programmed death of vascular endothelial cells, which could also be obtained from the state of circulating endothelial cells through direct blood tests.

Ferroptosis is a newly discovered type of programmed cell death in recent years. It is well-known for its iron-dependent phospholipid peroxidation process to cause cell membrane damage and even cell death (10). In fact, iron metabolism is tightly regulated in the organism, and excessive Fe^{2+} could induce the production of active reactive oxygen species (ROS), which would trigger the oxidative stress. Meanwhile, glutathione peroxidase (GPX4) could reverse lipid peroxidation and ferroptosis by consuming glutathione. Recent studies show that the regulation of ferroptosis is associated with autophagy in cancer (11). And $CD8^+$ T cells activated by immunotherapy can exert their antitumor effects by enhancing the ferroptosis of tumor cells. Although this evidence demonstrates the importance of ferroptosis in cancer, few studies focus on its role in ischemic disease. In the field of cerebrovascular disease, it is reported that activating the expression of GPX4 could protect neurons in the ischemic stroke model (12). However, the underlying regulation of ferroptosis is still in the veil in the field of cardiovascular disease, especially in MI (13).

Here, we screened the differentially expressed genes in CECs of acute MI patients from the GEO database. Then, the ferroptosis-related genes collected from the FerrDb database (http://zhounan.org/ferrdb) (14) and other previous literature (15–18) were utilized to identify the differential ferroptosis-related genes in acute MI. Finally, we established and evaluated a random forest diagnostic model based on these genes and verified it in another data set in GEO after comparing three different supervised machine learning algorithms.

METHODS AND MATERIALS

Original Gene Expression Profiles Acquisition and Data Preprocessing

Two related CEC databases, GSE66360 (19) and GSE48060 (20), were selected and downloaded from the GEO database (https://www.ncbi.nlm.nih.gov/GEO/). Both of these data sets were updated on March 25, 2019. Although these two databases shared the same supplementary microarray probe platform GPL570, GSE66360 alone was selected as the training and validation sets. Meanwhile, GSE66360 is confirmed to be matched by both gender and age in the experimental and control groups (19). GSE48060 was treated as the test set to avoid the possible interference of a batch effect. Then, quality control and normalization of these two gene expression profiles were conducted through the scale function in R 4.0.3 software.

Differential Gene Expression

The latest version of the "stringr" and "limma" packages in R 4.0.3 software were used to perform differential expression analysis. The fold change (FC) was calculated based on the average gene expression of the acute MI and control groups, and the differentially expressed genes were defined by the cutoff values ($FC > 1.5$ and $P < 0.05$). Meanwhile, the gene probe IDs were matched with the "Gene Symbol" through "Gene ID Conversion" in the DAVID online database (http://david.ncifcrf.gov/) (21).

Functional Enrichment Analysis of Differential Genes

The DAVID online database was also adopted for the gene ontology (GO) enrichment analysis, including three aspects of biological process (BP), cell composition (CC), and molecular function (MF) for functional annotation (21). Meanwhile, the KEGG online database (http://genome.jp/kegg/pathway.html) (22) was used to analyze the KEGG signal pathway of those differentially expressed genes. In addition, hierarchical clustering of samples and differential genes were performed and visualized through the "heatmap" R package.

Collection of Ferroptosis-Related Genes

Ferroptosis-related genes were collected and retrieved from the FerrDb database (http://zhounan.org/ferrdb) (14), and other previous literature (15–18) was referenced for proofreading and completion. All the ferroptosis-related genes are provided in **Supplementary Table 1**.

Analysis of Differential Ferroptosis-Related Genes

The latest version of the "venneuler" package in R 4.0.3 software was applied to depict the intersection of differential and ferroptosis-related genes, and the "seaborn" library in Python 3.90 was used to visualize the expression of different ferroptosis-related genes between the MI and control groups, and Student's *t*-test was adopted as the statistical analysis by "scipy.stats" Python library. The *P*-value < 0.05 was considered statistically significant, and all *P*-values were two-tailed. Meanwhile, the STRING database (http://string-db.org/) (23) was used to perform a protein–protein interaction (PPI) network on the differentially expressed proteins of those ferroptosis-related genes. In addition, principal component analysis (PCA) was performed on the differentially expressed ferroptosis-related genes as a dimension-reduction strategy to distinguish the MI and control groups through the "sklearn" Python library.

Construction of Diagnostic Prediction Model Through Machine Learning

Differential expressions of ferroptosis-related genes were treated as independent variables to construct a prediction model for the diagnosis of acute MI based on CECs. In this study, we used the GSE66360 data set as the training and validation set (4:1), and the GSE48060 data set was treated as the test set. In order to prevent the overfitting phenomenon caused by the complex model, K-fold cross-validation with cv = 15 was adopted in this study to improve the generalization ability of the training set. Feature selection was implemented through the "sklearn.model_selection" Python library. Then, three different supervised machine learning algorithms were used to initially explore the diagnostic prediction model. The logistic regression, support vector classification, and random forest models were, respectively, built through the "sklearn.linear_model," "sklearn.svm," and "sklearn.ensemble" Python libraries. After comparing the performance of different models, the random forest algorithm was selected, and some parameters and structures were adjusted to optimize this algorithm. ROC curves were visualized through the "matplotlib" Python library. Then, the validation set was used to verify the prediction model, and the test set was applied to demonstrate the generalization ability of this diagnostic model.

RESULTS

Research Flow and the Collection of Ferroptosis-Related Genes

GSE66360, a CECs data set of acute MI with clinical information, was downloaded from the GEO database for further differential gene screening. This data set included 49 acute MI patients with strict diagnostic criteria and 50 healthy controls. Meanwhile, all the patient CECs were isolated from peripheral blood within 48 h of acute MI and identified with a $CD146^+$ specific antigen. Then, differential expression and functional enrichment analyses were performed after quality control and normalization of the gene expression matrix.

In addition, 259 ferroptosis-related genes were confirmed through the FerrDb database and other previous references after deduplication. Subsequently, the intersection of differentially expressed and ferroptosis-related genes were taken, and the expression differences of these genes were tested in the two groups. The PPI network of these differential ferroptosis-related genes was also built. Then, the GSE66360 data set was divided into the training and validation sets at a ratio of 4:1. Finally, a diagnostic prediction model of acute MI based on the random forest algorithm was constructed by those screened differential ferroptosis-related genes after K-fold cross-validation and algorithm comparison and verified on the test set GSE48060 including 26 acute MI patients with non-recurrent events and 21 normal controls (**Figure 1**).

Verification and Functional Analysis of Differentially Expressed Genes in Acute MI

The 99 samples in the MI and control groups of GSE66360 were normalized and the FC calculated through the "limma" R package. After setting the cutoff values (FC > 1.5 and $P < 0.05$), 256 differentially expressed genes of ECEs in the control and MI groups were screened, including 37 upregulated genes and 219 downregulated genes (**Figure 2A**). Meanwhile, the top five upregulated genes with huge significance were NR4A2, NLRP3, EFEMP1, CLEC7A, and CLEC4D in the MI group. The top five downregulated genes were XIST, TSIX, CTD-2528L19.6, LPAR5, and DAB1 in the MI group. Some of these genes were reported to be involved in various processes of the development of cardiovascular diseases, including hypoxia, autophagy, and oxidative stress (24–26).

In order to further explore the pathophysiology functions of these differentially expressed genes in acute MI, GO analysis according to the DAVID online database was adopted to cluster the BP, CC, and MF among them. The results were that most genes participated in the inflammatory response in BP, followed by extracellular space in CC and receptor activity in MF (**Figure 2B**).

In addition, the KEGG pathway analysis of these differentially expressed genes showed that the top three signal pathways with the largest number of enriched genes were the TNF signaling pathway, osteoclast differentiation, and Toll-like receptor signaling pathway (**Figure 2B**). All these pathway enrichments were also supported and echoed by corresponding literature (13, 27, 28).

What is more, hierarchical clustering was also applied to verify the reliability of these differential genes, and the two groups could be significantly distinguished according to a heat map (**Figure 2C**).

Expression and Functional Analysis of Differential Ferroptosis-Related Genes

By intersecting the collected ferroptosis-related genes with the differentially expressed genes described above, eight differentially expressed ferroptosis-related genes including C-X-C motif chemokine ligand 2 (CXCL2), endothelial PAS domain protein 1 (EPAS1), Jun dimerization protein 2 (JDP2), activating transcription factor 3 (ATF3), Toll-like receptor 4 (TLR4), ferritin heavy chain 1 (FTH1), AP-1 transcription factor subunit (JUN), and DNA damage-inducible transcript 3 (DDIT3) were obtained (**Figure 3A**). The relevant information of all these genes is demonstrated in **Table 1**. All these differentially expressed ferroptosis-related genes were shown to be significantly highly expressed in the acute MI group with P-values < 0.0001 (**Figure 3B**).

Although the specific mechanism of ferroptosis in cardiovascular disease was not clear, our results first confirmed the potential role of these ferroptosis-related genes in acute MI. CXCL2 occupied the most obvious difference in expression, which was thought to be associated with neutrophil-mediated inflammation (29). However, it is also gradually recognized as a key factor involved in cellular ferroptotic response in recent years. Meanwhile, it is also shown that CXCL2 is significantly highly expressed in the plaques and peripheral blood mononuclear cells of patients with coronary atherosclerosis, and it might be closely related to the prognosis (30). Another significant difference was shown on EPAS1, which played a critical role in ferroptosis through lipid peroxidation. It could

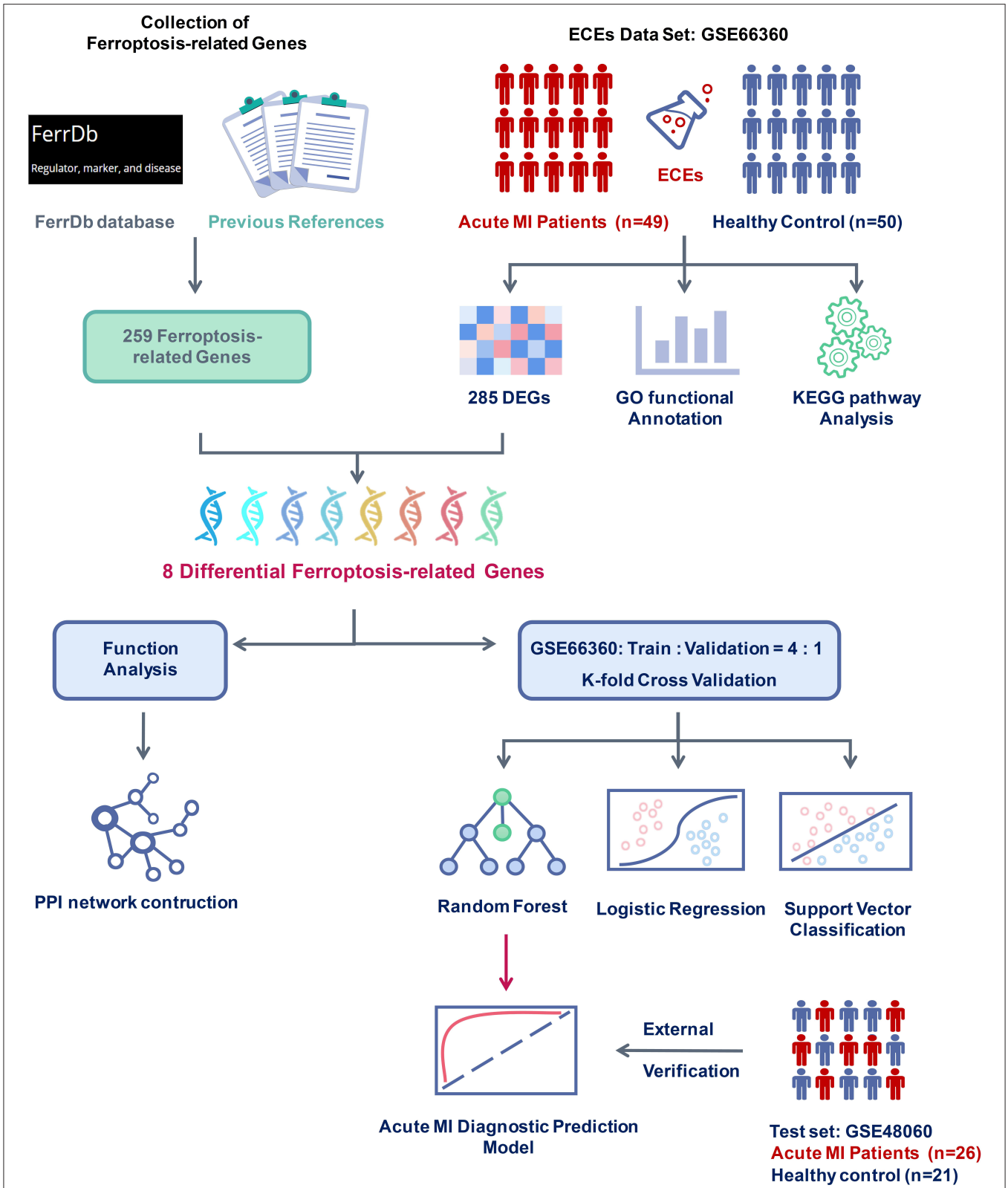

FIGURE 1 | Flow chart of research design and analysis. GSE66360 was applied to analyze differentially expressed genes (DEGs) between acute myocardial infarction (MI) and healthy controls. Ferroptosis-related genes were collected from the FerrDb database and other previous references. After checking the DEGs and the ferroptosis-related genes, eight differential ferroptosis-related genes were selected to perform functional analysis and construct a clinical diagnosis model. Compared with different supervised learning algorithms, including logistic regression and support vector classification, the random forest algorithm was determined to build the acute MI diagnostic model and was confirmed with the external verification of GSE48060.

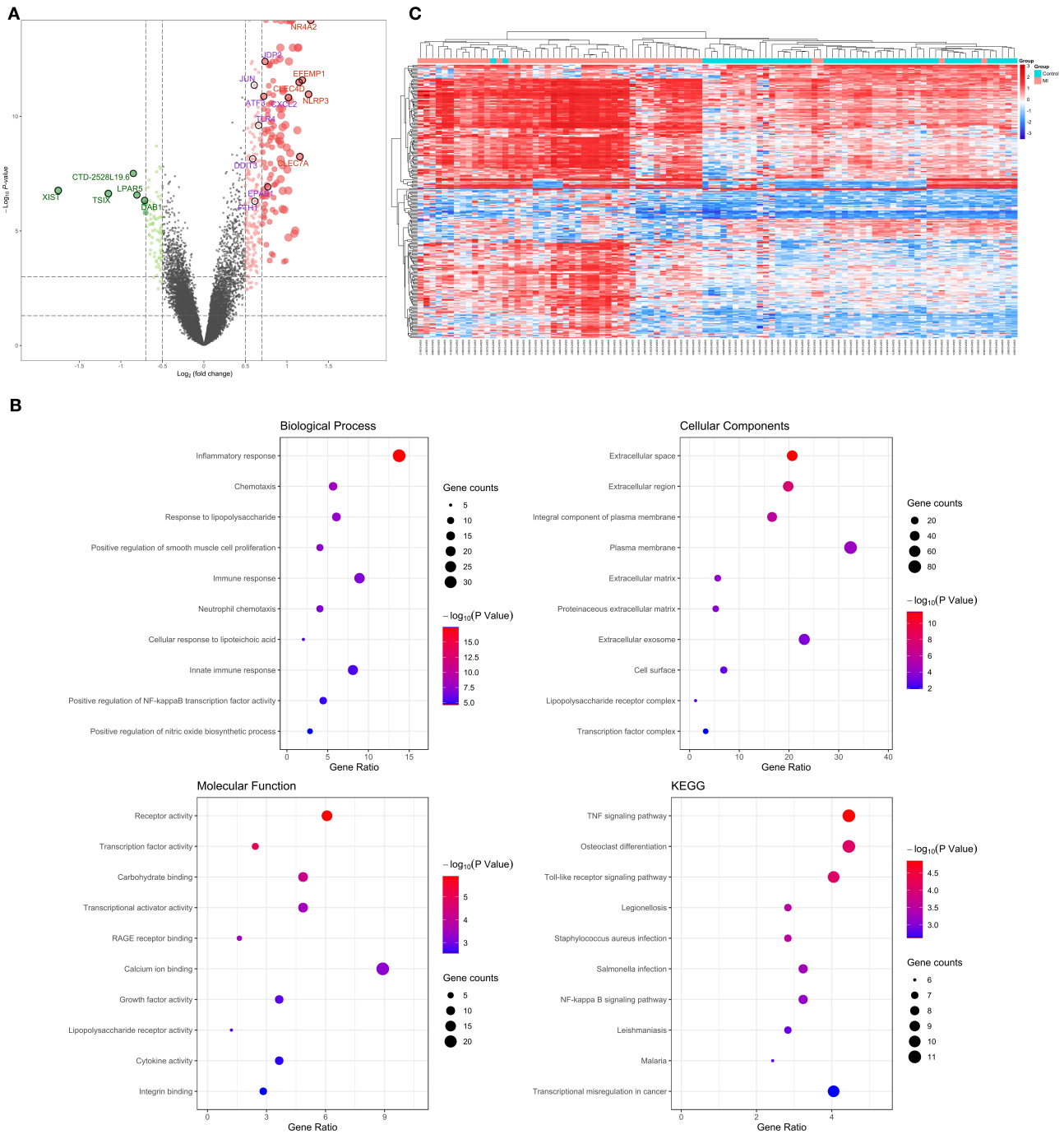

FIGURE 2 | Verification and functional analysis of differentially expressed genes (DEGs) in acute myocardial infarction (MI). **(A)** DEGs in acute MI and control group by the (FC > 1.5 and $P < 0.05$) cutoff value (top five upregulated genes are marked in red; top five downregulated genes are marked in green; the following differential ferroptosis-related genes are marked in purple); **(B)** gene ontology (GO) enrichment analysis among these DEGs, including biological process (BP), cell composition (CC), and molecular function (MF), and the KEGG pathway enriched by these DEGs; **(C)** the hierarchical clustering of all the DEGs and clinical status.

selectively enrich polyunsaturated lipids by upregulating hypoxia and lipid droplet-related protein. In some tumors, such as clear-cell carcinomas, EPAS1 may even promote the tumor-dependent ferroptotic death procession by recruiting some specific downstream factors (31). Another transcriptional regulator, JDP2, could activate the expression of inflammatory genes and promote fibrosis, which has been shown as a prognostic marker for MI patients to develop heart failure (32). As a key effector of ferroptosis, TLR4 plays an important role in reducing cardiomyocyte death and improving left ventricular remodeling.

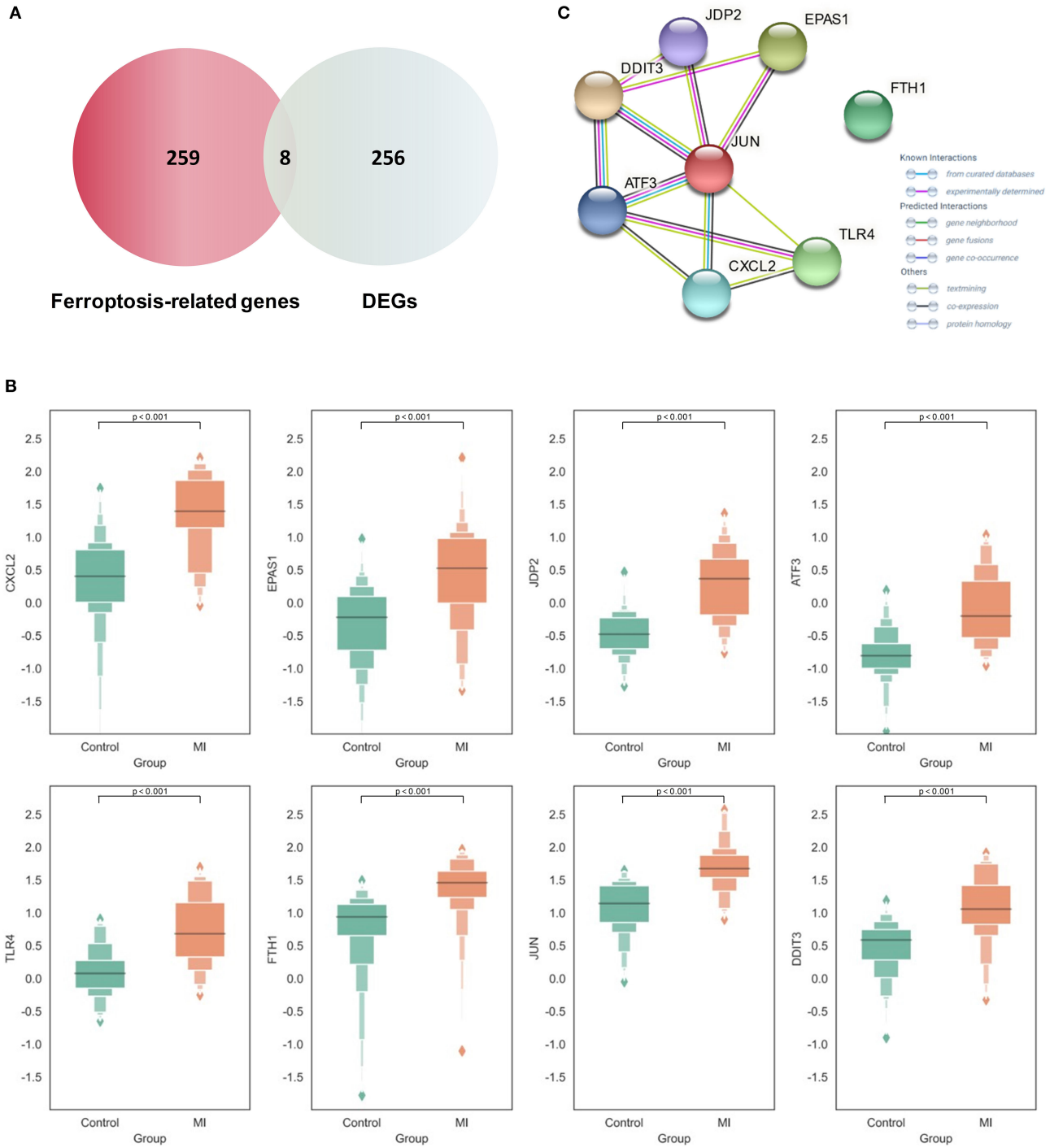

FIGURE 3 | Expression and functional analysis of differential Ferroptosis-related genes in acute myocardial infarction (MI). **(A)** The intersection between the collected ferroptosis-related genes and differentially expressed genes (DEGs) in acute MI; **(B)** the expression of different ferroptosis-related genes between the acute MI and control groups with the two-tailed Student's *t*-test ($P < 0.05$ as significance); **(C)** the protein–protein interaction (PPI) network on those ferroptosis-related genes.

After knocking down TLR4, autophagy and ferroptosis could be alleviated through the TLR4 and NADPH oxidase 4 (NOX4) pathway, which provides a potential treatment strategy for heart failure (33).

At the same time, the STRING database was used to construct the PPI interaction network of these differential ferroptosis-related proteins (**Figure 3C**). It was revealed that JUN might be the hub node in all eight differential ferroptosis-related

TABLE 1 | Summary of all these differential expressed ferroptosis-related genes in acute myocardial infarction (MI).

Gene	Full name	Role in Ferroptosis	logFC	*P*-value
CXCL2	C-X-C motif chemokine ligand 2	Marker	1.019	1.51×10^{-11}
EPAS1	Endothelial PAS domain protein 1	Driver	0.770	1.19×10^{-7}
JDP2	Jun dimerization protein 2	Marker	0.736	4.39×10^{-13}
ATF3	Activating transcription factor 3	Driver	0.722	1.33×10^{-11}
TLR4	Toll-like receptor 4	Driver	0.659	2.46×10^{-10}
FTH1	Ferritin heavy chain 1 (FTH1)	Marker	0.614	5×10^{-7}
JUN	AP-1 transcription factor subunit	Suppressor	0.606	4.27×10^{-12}
DDIT3	DNA damage-inducible transcript 3	Marker	0.588	7.1×10^{-9}

genes because it was related to almost all other genes except FTH1. In previous studies, Jun is shown to regulate the ferroptotic cell death with the help of hepatocyte nuclear factor 4 alpha (HNF4A) (16). Our results first report the potential role of Jun in acute MI by mediating abnormal ferroptosis. The following two key nodes are DDIT3 and ATF3, both of which are related to four other differential ferroptosis-related genes. The endoplasmic reticulum is an important organelle for maintaining cell homeostasis. As a key regulator of endoplasmic reticulum stress, DDIT3 is also reported to be involved in the ROS-dependent ferroptotic process (34), but its role in the pathological process of cardiovascular disease still remains unknown. In terms of ATF3, this famous common stress sensor could accelerate the progression of ferroptosis by inhibiting system Xc^- (35). Some studies also show that suppressing the expression of ATF3 could improve the prognosis of cardiovascular and cerebrovascular diseases through reducing cell death (36). Meanwhile, the isolation of FTH1 did not make sense. As a regulatory element of cellular iron storage, FTH1 is critical for maintaining intracellular iron homeostasis. Knockout of FTH1 is shown to induce ferroptosis through erastin, sorafenib, and other pathways in various disease models (37) while overexpression of FTH1 could restrain ferritinophagy to reduce ferroptosis (38). Moreover, FTH1-mediated iron metabolism disorder is shown to exacerbate myocardial damage during MI and reduce heart function (39).

Establishment of the Diagnostic Model Based on Differential Ferroptosis-Related Genes

First, PCA was performed on the above differentially expressed ferroptosis-related genes as a dimension reduction strategy. The results demonstrate that the MI and the control groups could be distinguished accurately (**Figure 4A**), which means that these differential genes might be treated as independent feature parameters for the diagnosis of acute MI. Then, the GSE66360 data set including 49 acute MI patients with strict diagnostic criteria and 50 healthy controls was taken as the training and validation sets (4:1), and the GSE48060 data set including 26 acute MI patients with non-recurrent events and 21 normal controls was treated as the test set.

After utilizing the K-fold cross-validation with cv = 15, the generalization ability of the training set was improved to prevent overfitting. Then, three different supervised machine learning algorithms, including logistic regression, support vector classification, and random forest, were attempted to construct the diagnostic prediction model of acute MI. The evaluating results of all three algorithms is shown in **Table 2**. The Kolmogorov–Smirnov (KS) values reflect the power of the binary model to classify positive and negative samples. The random forest algorithm is shown to take the leading advantage of distinguishing the two groups with KS = 0.70 in this study, and the KS values of the other two algorithms was 0.60. Admittedly, we also found that the diagnostic accuracy of the random forest model (accuracy = 0.75) was not as good as the other two models (accuracy = 0.80). However, it was far from enough to rely on accuracy to evaluate the diagnostic power, which was easily affected by the bias caused by the imbalance of categories. In other words, the recall rate was another evaluation feature that could not be ignored for diagnosing acute MI. The recall rate of the random forest algorithm (recall = 0.90) was higher than the other two models (recall = 0.80). It was indicated that the random forest model could minimize the missed cases of acute MI, which might provide a sufficient treatment window and significantly improve the prognosis of patients.

In addition, the ROC curves of the validation set from GSE66360 also described that the area under the curve (AUC) of the random forest model was 0.8550, which was higher than AUC = 0.80 and 0.81 of the other two groups (**Figure 4B**). Hence, the random forest algorithm was selected to further construct the acute MI diagnostic model after comprehensively analyzing all these parameters.

Simultaneously, GSE48060 was used as a test set to externally verify the diagnostic model based on the random forest algorithm. **Figure 4D** shows the ROC curve verified by external data, and its AUC is 0.7308 (**Figure 4C**), demonstrating a compelling diagnostic performance. What's more, the confusion matrix was visualized to evaluate the classification model (**Figure 4D**). Twenty-six patients with MI were correctly classified, and three healthy volunteers were identified as the control group. There was no misidentification of patients with MI as healthy people, which meant that this method could effectively reduce the false negative rate. Admittedly, we also noticed that some healthy people were misclassified as MI ($n = 18$).

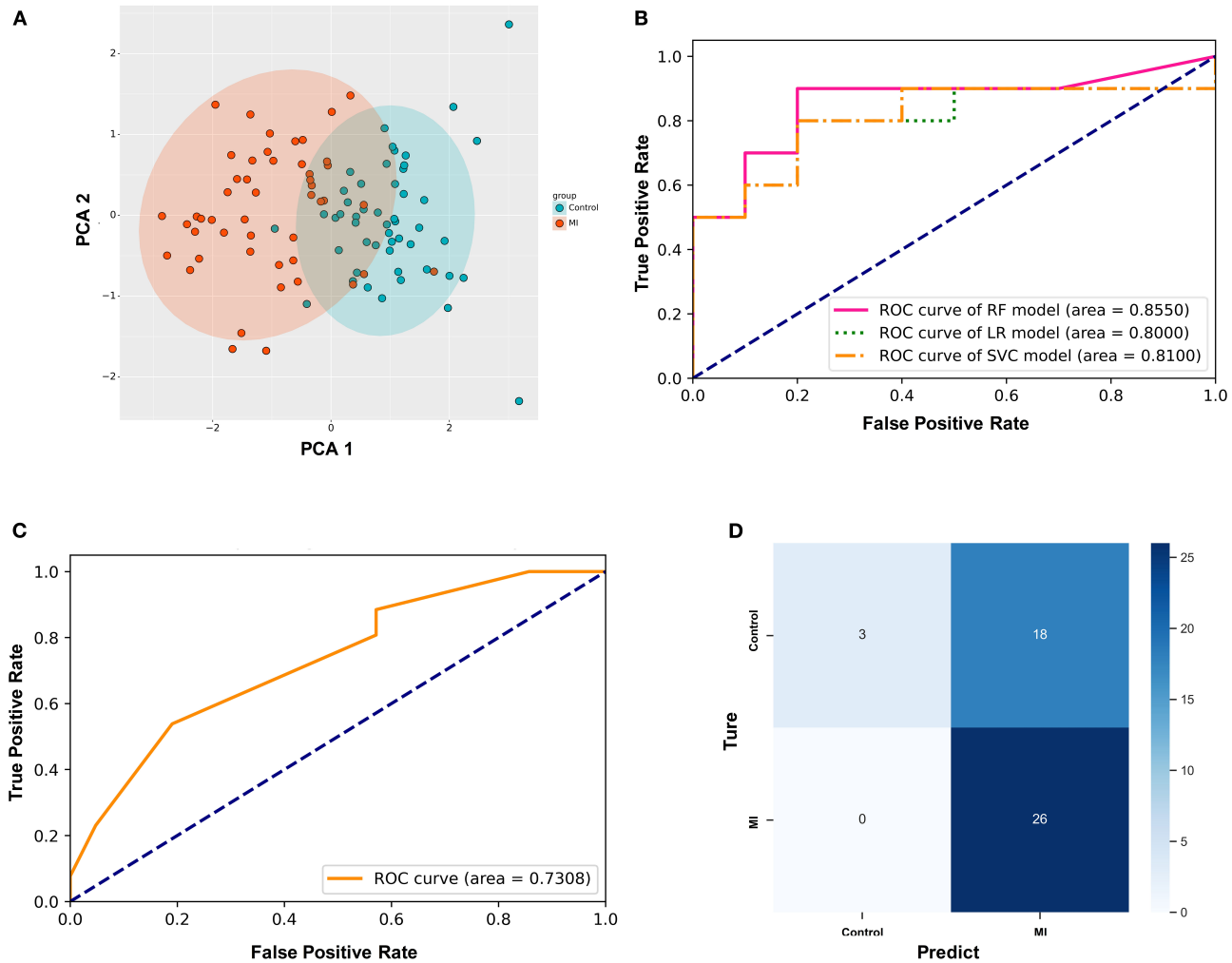

FIGURE 4 | Establishment of the random forest diagnostic model based on differential ferroptosis-related genes in acute myocardial infarction (MI). **(A)** Principal component analysis (PCA) of these differentially expressed ferroptosis-related genes as dimension reduction; **(B)** the comparison of three different supervised learning models (RF, random forest; LR, logistic regression; SVC, support vector classification); **(C)** the diagnostic performance of the predictive model in the test set; **(D)** the confusion matrix of the test set.

TABLE 2 | Comparison of the diagnostic efficacy of three different supervised learning models.

Model	Precision	Recall	F1-score	Accuracy	Error	KS
Random forest	0.69	0.90	0.78	0.75	0.25	0.70
Logistic regression	0.80	0.80	0.80	0.80	0.20	0.60
Support vector classification	0.80	0.80	0.80	0.80	0.20	0.60

CONCLUSION

In this study, we first identified eight differentially expressed ferroptosis-related genes in CECs of patients with acute MI and analyzed their potential functions by means of two GEO data sets. Compared with the performance of different supervised learning models, we established a random forest diagnostic models of MI based on these ferroptosis-related genes in CECs (AUC = 0.8550) through K-fold cross-validation and verified it with another data set (AUC = 0.7308).

DISCUSSION

With the increase of global aging, how to deal with the medical challenges brought about by aging is a topic of

general concern (40). Age-related diseases such as cardiovascular diseases, especially coronary artery diseases, continue to be a major threat to human health in the future. Advances in interventional technology and reperfusion therapy in recent years have effectively improved the prognosis of MI. However, there is still more attention that needs to be paid, and the early diagnosis of MI is still a key factor restricting mortality and prognosis.

As a kind of disease caused by insufficient myocardial perfusion, MI mainly contributes to coronary atherosclerosis. Although the current diagnostic methods are established on a series of biomarkers based on myocardial injury, which cannot give early warning when the myocardium has just appeared insufficient without yet being damaged. Not being a specific feature of MI, myocardial injury in many cardiomyopathies can also interfere with diagnosis in addition to the delayed diagnosis. Therefore, it is imperative to advance the diagnostic window of acute MI and develop diagnostic biomarkers that reflect myocardial hypoperfusion directly (9).

As a novel kind of iron-dependent programmed cell death, ferroptosis was first proposed in 2012 (41). The decrease in the activity of glutathione peroxidase (GPX4) and the depletion of glutathione interrupt the metabolic reaction of lipid oxides, which induces the Fe^{2+} to produce ROS, thereby promoting ferroptosis. Its sensitivity involves a large number of cellular metabolic processes, including amino acid, iron, and polyunsaturated fatty acid metabolism. Hence, the induction of ferroptosis leads to the increase of intracellular lipid ROS, and this regulating process could be inhibited by lipid antioxidants (17). As iron-rich and ROS production–based organelles, mitochondria are considered to be the critical place for ferroptosis with specific lipid precursors. Studies in recent years show that ferroptosis is associated with tumors (42), stroke (12), cerebral hemorrhage (43), and renal failure (44). However, the relationship between MI, especially the vascular endothelium and ferroptosis, still remains unknown.

Artificial intelligence and machine learning are important productivity tools in the twenty-first century (45). Different from traditional biomedical research, artificial intelligence, and machine learning are dedicated to learning natural laws from massive amounts of high-throughput data and then using the natural learned laws to predict unknown data, which are widely used in computer vision (46), natural language processing (47), biological features identification (48), and other fields. In the field of oncology research, a large number of machine learning diagnostic models based on gene expression have been widely developed and applied because samples of cancer can be obtained more conveniently through pathology. However, a majority of clinical prediction models are based on traditional risk factors and biomarkers for model fitting in non-tumor research fields. For example, a retrospective cohort study was used to construct a random forest model for atrial fibrillation diagnosis (49).

By means of machine learning and bioinformatics technology, our study first revealed the differential expression of ferroptosis genes in CECs of patients with acute MI. Meanwhile, all the results were verified in different data sets, which first implied that ferroptosis may be involved in regulating the metabolism of CECs in acute MI. On one hand, the eight ferroptosis-related genes described in this article have been verified and functionally confirmed through different bioinformatics technologies (GO enrichment analysis, PPI interaction analysis). Among them, CXCL2 (30), JDP2 (32), TLR4 (33), ATF3 (36), and FTH1 (39) are reported to participate in the regulation of a variety of cardiovascular diseases through different pathways, and Jun and DDIT3 were first described to be related to acute MI. All these results provide the direction and cornerstone for subsequent basic experiments to explore the role of ferroptosis regulation mechanism in the pathogenesis of acute MI.

On the other hand, this study constructed a random forest diagnostic model of acute MI through the above eight differentially expressed ferroptosis-related genes in CECs. The AUC of some clinical prediction models is extremely high, and their external verification has unsatisfactory results due to the overfitting caused by the small sample data. In this study, the K-fold cross-validation with cv = 15 was utilized to improve the generalization power. Hence, the variability of AUC between our validation and test sets was small enough to be satisfying. Meanwhile, we compared the performance of three supervised machine learning algorithms, including logistic regression, support vector classification, and random forest. After comprehensively evaluating KS, accuracy, recall, and AUC of all these three algorithms, this random forest model showed good diagnostic performance (AUC = 0.8550) and was validated in different data sets (AUC = 0.7308), which provides new ideas and directions for finding new MI-specific biomarkers in advance of the diagnosis window. What is more, the results of a confusion matrix indicate that this model has a strong ability to eliminate false negative interference, which is critical for MI with a very high fatality rate. Changes of gene expression level are the first step in the occurrence and development of diseases. The application of machine learning to analyze different gene expression levels can help explain the original mechanism of the disease and can build the first line of defense for disease diagnosis and early warning at the same time, which plays a strong guiding role of diseases such as acute MI with rapid disease development, high fatality rate, and no obvious symptoms in the early stage.

Compared with the traditional diagnostic model based on the detection of myocardial injury markers, the new model in this article based on the ferroptosis-related genes of CECs focuses more on reflecting the damage of endothelial function and the non-invasive screening for high-risk populations. Vascular endothelial injury is the key factor and initiating link of atherosclerosis. Normally, the anti-inflammatory system composed of cytokines and endothelial progenitor cells in the body repairs damaged endothelium and blood vessels. However, when the endothelial anti-inflammatory self-repair system is exhausted, endothelial cells develop a series of dysfunctions, including aging, autophagy, apoptosis, ferroptosis, etc. (50, 51), which causes endothelial cells to leave the blood vessel wall and enter circulation, which, in turn, leads to a series of undesirable consequences, such as vascular plaque formation, vascular remodeling, inflammation, vasoconstriction, thrombosis formation, and even plaque rupture. In fact, changes in CECs are important predictors of cardiovascular events before

the development of atherosclerotic morphological changes (52). At present, there have been a series of research on the evaluation of CEC functions (53, 54). So far, there is no reliable and recognized gold standard for the detection of functional changes of CECs (55). The identification and integrated analysis of ferroptosis-related genes in CECs in this model are helpful to reflect the early functional changes of CECs, which is ready for judging vascular endothelial function and predicting the occurrence of cardiovascular events, especially for early non-invasive detection of high-risk population screening.

It also cannot be ignored that coronary microcirculation dysfunction, an important independent prognostic factor for cardiovascular events, is inseparably related to functional changes in endothelial cells (56), which can lead to a decrease in coronary blood flow and myocardial perfusion. However, conventional coronary angiography cannot detect microcirculation cracks. At present, the methods for evaluating microcirculation disorders are mainly based on invasive methods, such as fractional flow reserve (FFR), and imaging detection, such as cardiovascular magnetic resonance (CMR). Studies suggest that microvascular occlusion (MVO) is inseparable from the swelling of capillary endothelial cells. The lack of endothelial integrity and functionality leads to the release of large amounts of cytokines, which, in turn, activates neutrophils and platelets, contributing to the formation of microthrombi. In this pathological process, the functional changes of CECs are considered to be an indispensable link. This model based on ferroptosis-related genes in CECs can directly reflect the regulation of ferroptosis-related networks in CECs, which may help determine whether the patient is in the process of MVO and the degree of MVO. In subsequent studies, the inclusion of more data related to MVO patients, such as FFR and CMR data collection, can help enhance the model's advantages in judging microcirculation lesions, which shows a large potential value in early non-invasive and accurate identification of patients with coronary microcirculation disorders.

Meanwhile, models based on CECs not only have important clinical significance for the diagnosis of endothelial function damage, but also play a crucial role in the risk stratification and prognosis of coronary heart disease. Early research on CECs focused on changes in their quantification, and the increase of CEC counts was shown to predict cardiovascular event risk to a large extent among patients with acute coronary syndrome (57), which suggests CECs would be applied for the judgment of long-term prognosis of MI. The development of more biomarker clusters with clinical application potential based on the internal genomics, transcriptomics, and secreted cytokines of CECs is still in its infancy, which is yet an unsolved mystery waiting for people to decipher. Due to the limitation of public data sets, data on patient severity is unfortunately not included in this model. However, according to the model constructed in this article and the support of the previous literature, it is very necessary in the subsequent cohort studies to associate the severity of coronary occlusion or the incidence of long-term cardiovascular events with ferroptosis-related genes in CECs to expand the scope of application of the model.

Of course, this study also has a few shortcomings. First, the biological functions of co-expressed genes have not been further explored through weighted gene co-expression network analysis and other technologies due to the small number of differentially expressed ferroptosis-related genes. Second, this model is not compared with some traditional clinical risk models because we cannot obtain individual specific clinical data from public data sets. This undoubtedly reduces the reliability of our results. However, every coin has two sides. Since the Framingham Study (58) proposed risk stratification for coronary heart disease, various risk scoring systems for coronary heart disease have been quickly built. The GRACE (59) and TIMI (60) risk scoring systems are two relatively representative scoring systems released in recent years. Several independent clinical predictive variables were screened out and applied to divide patients with different risk levels in these scoring systems through multivariate logistic regression analysis of large-scale clinical trials. However, most of the clinical predictive variables screened out rely on epidemiological evidence instead of the pathogenesis of the disease. Therefore, these traditional models can only perform macroscopic stratification without subtly reflecting the real endothelial function status of patients, not to mention achieving the purpose of precision medicine (61). In contrast, this diagnostic model based on ferroptosis-related genes has an irreplaceable advantage in reflecting the patient's immediate endothelial function status. It can provide diagnostic prediction models with pathological progress from the perspective of genetic and molecular pathology. In fact, these two kinds of diagnostic models are absolutely not opposite, and there is no sense comparing them in a single scale. On the contrary, they are complementary to pool their experiences. On one hand, the traditional model provides a macro-level risk assessment based on the past average body state of the patients. On the other hand, the novel gene–related score provides accurate evidence such as immediate and subtle molecular pathological changes for judging the pathological process of the patients. Under this cooperative consensus, future research directions should be to integrate traditional risk and novel gene–related scores and jointly develop a new model in order to help evaluate the patients and guide treatment in the mode of precision medicine. In addition, high-quality data determines the pros and cons of machine learning. The training and validation tests were built on the data set that was matched in both gender and age in the experimental and control groups so that the interference of potential confounding factors on our model could be eliminated. However, other data sources used in this study all come from the GEO database without additional clinical features. In future studies, traditional risk factors, such as age, gender, and hypertension in the cohort could be added to the existing models to construct new combined diagnostic model tools. Meanwhile, this diagnostic model can be further compared with myocardial markers such as cTnT, or a novel diagnostic model could be constructed by these ferroptosis-related genes in CECs combined with cTnT. What is more, there are different subtypes of acute MI (62), and different subtypes need different treatment measures. For example, acute ST-segment elevation MI (STEMI) requires immediate interventional treatment, and

some non-ST-segment elevation MI (NSTEMI) could choose selective intervention. Whether ferroptosis-related genes are differentially expressed in these different subtypes of MI and play different regulatory roles remains to be revealed. As is known to all, cardiovascular disease is a complex pathological process involving multiple factors and multilevel biomarkers should be established for different types or stages of the same disease to precise classification and treatment through various machine learning algorithms. In fact, the method of constructing clinical prediction models based on differentially expressed genes related to tumor incidence, metastasis, and prognosis risk via gene chip screening has been widely used in the research of different tumors (63–65). However, a model based on gene-related score in the research of cardiovascular diseases is still in its infancy due to the lack of traditional pathological specimens. Because CECs stand for changes in endothelial cell function to a large extent, enrichment and detection of differential genes may be helpful for assessing vascular endothelial dysfunction, especially identifying the risk of early coronary heart disease. Meanwhile, whether the diagnostic model based on ferroptosis-related gene labels could be practically accessible in clinical practice is worthy of attention. At present, relatively mature CEC rapid enrichment schemes have been constructed (66), and a rapid test kit based on the eight ferroptosis-related genes included in this model could be designed and produced with available test results within 4–6 h. In the next study, the cohort can be expanded to optimize and improve the model, which might reduce the missed diagnosis of early coronary heart disease and acute MI due to the heterogeneity of myocardial enzyme spectrum and the limitations of invasive coronary angiography. It is believed that integrating diverse molecular tags through machine learning can guide clinicians to more reasonable management and treatment of acute coronary syndromes in the future.

There is no doubt that the precision medicine bring about a revolution in the medical world and change the whole clinical practice. With the continuous development of artificial intelligence and machine learning, the discovery and confirmation of biomarker groups becomes possible under the maturity of massive biological information data analysis technology. Fully discovering and verifying the biomarker groups of different types and stages of MI help to comprehensively improve the prediction risk power of cardiovascular and cerebrovascular diseases, thereby reducing the mortality rate and improving the prognosis of MI.

DATA AVAILABILITY STATEMENT

The datasets presented in this study can be found in online repositories. The names of the repository/repositories and accession number(s) can be found in the article/**Supplementary Material**.

AUTHOR CONTRIBUTIONS

PJ and CY conceived the need for the article. CY finished the analysis and drafted the initial version. SJ helped revise the manuscript. PJ put forward many constructive comments for the final version. CY provided the production of the flowchart. All authors read and approved the manuscript.

FUNDING

This work was supported by grants from the National Science Fund for Distinguished Young Scholars (81625002), the National Natural Science Foundation of China (81930007, 81470389,81500221, and 81800307), the Shanghai Outstanding Academic Leaders Program (18XD1402400), the Science and Technology Commission of Shanghai Municipality (201409005200), and the Innovative research team of high-level local universities in Shanghai and the Shanghai Municipal Education Commission Gaofeng Clinical Medicine Grant Support (20152209).

SUPPLEMENTARY MATERIAL

The Supplementary Material for this article can be found online at: https://www.frontiersin.org/articles/10.3389/fcvm.2021.663509/full#supplementary-material

REFERENCES

1. Mehta LS, Beckie TM, DeVon HA, Grines CL, Krumholz HM, Johnson MN, et al. Acute myocardial infarction in women: a scientific statement from the American Heart Association. *Circulation.* (2016) 133:916–47. doi: 10.1161/CIR.0000000000000351
2. Auer J, Berent R, Lassnig E, Eber B. C-reactive protein and coronary artery disease. *Jpn Heart J.* (2002) 43:607–19. doi: 10.1536/jhj.43.607
3. Boeddinghaus J, Nestelberger T, Koechlin L, Wussler D, Lopez-Ayala P, Walter JE, et al. Early diagnosis of myocardial infarction with point-of-care high-sensitivity cardiac troponin I. *J Am Coll Cardiol.* (2020) 75:1111–24. doi: 10.1016/j.jacc.2019.12.065
4. Odqvist M, Andersson PO, Tygesen H, Eggers KM, Holzmann MJ. High-sensitivity troponins and outcomes after myocardial infarction. *J Am Coll Cardiol.* (2018) 71:2616–24. doi: 10.1016/j.jacc.2018.03.515
5. Thygesen K, Alpert JS, White HD. Universal definition of myocardial infarction. *J Am Coll Cardiol.* (2007) 50:2173–95. doi: 10.1016/j.jacc.2007.09.011
6. Collet JP, Thiele H, Barbato E, Barthelemy O, Bauersachs J, Bhatt DL, et al. 2020 ESC Guidelines for the management of acute coronary syndromes in patients presenting without persistent ST-segment elevation. *Eur Heart J.* (2020) 42:1289–367. doi: 10.1016/j.rec.2021.05.002
7. White HD, Chew DP. Acute myocardial infarction. *Lancet.* (2008) 372:570–84. doi: 10.1016/S0140-6736(08)61237-4
8. Rakic M, Persic V, Kehler T, Bastiancic AL, Rosovic I, Laskarin G, et al. Possible role of circulating endothelial cells in patients after acute myocardial infarction. *Med Hypotheses.* (2018) 117:42–6. doi: 10.1016/j.mehy.2018.06.005
9. Konijnenberg LSF, Damman P, Duncker DJ, Kloner RA, Nijveldt R, van Geuns RM, et al. Pathophysiology and diagnosis of coronary microvascular dysfunction in ST-elevation myocardial infarction. *Cardiovasc Res.* (2020) 116:787–805. doi: 10.1093/cvr/cvz301
10. Mou Y, Wang J, Wu J, He D, Zhang C, Duan C, et al. Ferroptosis, a new form of cell death: opportunities and challenges in cancer. *J Hematol Oncol.* (2019) 12:34. doi: 10.1186/s13045-019-0720-y
11. Song X, Zhu S, Chen P, Hou W, Wen Q, Liu J, et al. AMPK-mediated BECN1 phosphorylation promotes ferroptosis by directly blocking system Xc(-) activity. *Curr Biol.* (2018) 28:2388–99 e5. doi: 10.1016/j.cub.2018.05.094

12. Alim I, Caulfield JT, Chen Y, Swarup V, Geschwind DH, Ivanova E, et al. Selenium drives a transcriptional adaptive program to block ferroptosis and treat stroke. *Cell.* (2019) 177:1262–79 e25. doi: 10.1016/j.cell.2019.03.032
13. Yang Y, Yang J, Sui F, Huo P, Yang H. Identification of potential molecular mechanisms and candidate genes involved in the acute phase of myocardial infarction. *Cell J.* (2018) 20:435–42. doi: 10.22074/cellj.2018.5213
14. Zhou N, Bao J. FerrDb: a manually curated resource for regulators and markers of ferroptosis and ferroptosis-disease associations. *Database.* (2020) doi: 10.1093/database/baaa021
15. Hassannia B, Vandenabeele P, Vanden Berghe T. Targeting ferroptosis to iron out cancer. *Cancer Cell.* (2019) 35:830–49. doi: 10.1016/j.ccell.2019.04.002
16. Dai C, Chen X, Li J, Comish P, Kang R, Tang D. Transcription factors in ferroptotic cell death. *Cancer Gene Ther.* (2020) 27:645–56. doi: 10.1038/s41417-020-0170-2
17. Stockwell BR, Friedmann Angeli JP, Bayir H, Bush AI, Conrad M, Dixon SJ, et al. Ferroptosis: a regulated cell death nexus linking metabolism, redox biology, and disease. *Cell.* (2017) 171:273–85. doi: 10.1016/j.cell.2017.09.021
18. Bebber CM, Muller F, Prieto Clemente L, Weber J, von Karstedt S. Ferroptosis in cancer cell biology. *Cancers.* (2020) 12:164. doi: 10.3390/cancers12010164
19. Muse ED, Kramer ER, Wang H, Barrett P, Parviz F, Novotny MA, et al. A whole blood molecular signature for acute myocardial infarction. *Sci Rep.* (2017) 7:12268. doi: 10.1038/s41598-017-12166-0
20. Suresh R, Li X, Chiriac A, Goel K, Terzic A, Perez-Terzic C, et al. Transcriptome from circulating cells suggests dysregulated pathways associated with long-term recurrent events following first-time myocardial infarction. *J Mol Cell Cardiol.* (2014) 74:13–21. doi: 10.1016/j.yjmcc.2014.04.017
21. da Huang W, Sherman BT, Lempicki RA. Systematic and integrative analysis of large gene lists using DAVID bioinformatics resources. *Nat Protoc.* (2009) 4:44–57. doi: 10.1038/nprot.2008.211
22. Kanehisa M, Furumichi M, Tanabe M, Sato Y, Morishima K. KEGG: new perspectives on genomes, pathways, diseases and drugs. *Nucleic Acids Res.* (2017) 45:D353–61. doi: 10.1093/nar/gkw1092
23. Szklarczyk D, Franceschini A, Wyder S, Forslund K, Heller D, Huerta-Cepas J, et al. STRING v10: protein-protein interaction networks, integrated over the tree of life. *Nucleic Acids Res.* (2015) 43:D447–52. doi: 10.1093/nar/gku1003
24. Peng H, Luo Y, Ying Y. lncRNA XIST attenuates hypoxia-induced H9c2 cardiomyocyte injury by targeting the miR-122-5p/FOXP2 axis. *Mol Cell Probes.* (2020) 50:101500. doi: 10.1016/j.mcp.2019.101500
25. Li Z, Zhang Y, Ding N, Zhao Y, Ye Z, Shen L, et al. Inhibition of lncRNA XIST improves myocardial I/R injury by targeting mir-133a through inhibition of autophagy and regulation of SOCS2. *Mol Ther Nucleic Acids.* (2019) 18:764–73. doi: 10.1016/j.omtn.2019.10.004
26. Xiao L, Gu Y, Sun Y, Chen J, Wang X, Zhang Y, et al. The long noncoding RNA XIST regulates cardiac hypertrophy by targeting miR-101. *J Cell Physiol.* (2019) 234:13680–92. doi: 10.1002/jcp.28047
27. Aluganti Narasimhulu C, Singla DK. The role of bone morphogenetic protein 7 (BMP-7) in inflammation in heart diseases. *Cells.* (2020) 9:280. doi: 10.3390/cells9020280
28. Li Y, Chen B, Yang X, Zhang C, Jiao Y, Li P, et al. S100a8/a9 signaling causes mitochondrial dysfunction and cardiomyocyte death in response to ischemic/reperfusion injury. *Circulation.* (2019) 140:751–64. doi: 10.1161/CIRCULATIONAHA.118.039262
29. Girbl T, Lenn T, Perez L, Rolas L, Barkaway A, Thiriot A, et al. Distinct compartmentalization of the chemokines CXCL1 and CXCL2 and the atypical receptor ACKR1 determine discrete stages of neutrophil diapedesis. *Immunity.* (2018) 49:1062–76 e6. doi: 10.1016/j.immuni.2018.09.018
30. Yang J, Liu H, Cao Q, Zhong W. Characteristics of CXCL2 expression in coronary atherosclerosis and negative regulation by microRNA-421. *J Int Med Res.* (2020) 48:300060519896150. doi: 10.1177/0300060519896150
31. Zou Y, Palte MJ, Deik AA, Li H, Eaton JK, Wang W, et al. A GPX4-dependent cancer cell state underlies the clear-cell morphology and confers sensitivity to ferroptosis. *Nat Commun.* (2019) 10:1617. doi: 10.1038/s41467-019-09277-9
32. Heger J, Bornbaum J, Wurfel A, Hill C, Brockmann N, Gaspar R, et al. JDP2 overexpression provokes cardiac dysfunction in mice. *Sci Rep.* (2018) 8:7647. doi: 10.1038/s41598-018-26052-w
33. Chen X, Xu S, Zhao C, Liu B. Role of TLR4/NADPH oxidase 4 pathway in promoting cell death through autophagy and ferroptosis during heart failure. *Biochem Biophys Res Commun.* (2019) 516:37–43. doi: 10.1016/j.bbrc.2019.06.015
34. Lee YS, Lee DH, Choudry HA, Bartlett DL, Lee YJ. Ferroptosis-induced endoplasmic reticulum stress: cross-talk between ferroptosis and apoptosis. *Mol Cancer Res.* (2018) 16:1073–76. doi: 10.1158/1541-7786.MCR-18-0055
35. Wang L, Liu Y, Du T, Yang H, Lei L, Guo M, et al. ATF3 promotes erastin-induced ferroptosis by suppressing system Xc(.). *Cell Death Differ.* (2020) 27:662–75. doi: 10.1038/s41418-019-0380-z
36. Huang CY, Chen JJ, Wu JS, Tsai HD, Lin H, Yan YT, et al. Novel link of anti-apoptotic ATF3 with pro-apoptotic CTMP in the ischemic brain. *Mol Neurobiol.* (2015) 51:543–57. doi: 10.1007/s12035-014-8710-0
37. Sun X, Ou Z, Chen R, Niu X, Chen D, Kang R, et al. Activation of the p62-Keap1-NRF2 pathway protects against ferroptosis in hepatocellular carcinoma cells. *Hepatology.* (2016) 63:173–84. doi: 10.1002/hep.28251
38. Tian Y, Lu J, Hao X, Li H, Zhang G, Liu X, et al. FTH1 inhibits ferroptosis through ferritinophagy in the 6-OHDA model of Parkinson's disease. *Neurotherapeutics.* (2020) 17:1796–812. doi: 10.1007/s13311-020-00929-z
39. Nishizawa H, Matsumoto M, Shindo T, Saigusa D, Kato H, Suzuki K, et al. Ferroptosis is controlled by the coordinated transcriptional regulation of glutathione and labile iron metabolism by the transcription factor BACH1. *J Biol Chem.* (2020) 295:69–82. doi: 10.1074/jbc.RA119.009548
40. Yifan C, Jun P. Understanding the clinical features of coronavirus disease 2019 from the perspective of aging: a systematic review and meta-analysis. *Front Endocrinol.* (2020) 11:557333. doi: 10.3389/fendo.2020.557333
41. Dixon SJ, Lemberg KM, Lamprecht MR, Skouta R, Zaitsev EM, Gleason CE, et al. Ferroptosis: an iron-dependent form of nonapoptotic cell death. *Cell.* (2012) 149:1060–72. doi: 10.1016/j.cell.2012.03.042
42. Liang C, Zhang X, Yang M, Dong X. Recent progress in ferroptosis inducers for cancer therapy. *Adv Mater.* (2019) 31:e1904197. doi: 10.1002/adma.201904197
43. Wan J, Ren H, Wang J. Iron toxicity, lipid peroxidation and ferroptosis after intracerebral haemorrhage. *Stroke Vasc Neurol.* (2019) 4:93–5. doi: 10.1136/svn-2018-000205
44. Friedmann Angeli JP, Schneider M, Proneth B, Tyurina YY, Tyurin VA, Hammond VJ, et al. Inactivation of the ferroptosis regulator Gpx4 triggers acute renal failure in mice. *Nat Cell Biol.* (2014) 16:1180–91. doi: 10.1038/ncb3064
45. Goecks J, Jalili V, Heiser LM, Gray JW. How machine learning will transform biomedicine. *Cell.* (2020) 181:92–101. doi: 10.1016/j.cell.2020.03.022
46. Murphy RR. Computer vision and machine learning in science fiction. *Sci Robot.* (2019) 4:eaax7421. doi: 10.1126/scirobotics.aax7421
47. Esteva A, Robicquet A, Ramsundar B, Kuleshov V, DePristo M, Chou K, et al. A guide to deep learning in healthcare. *Nat Med.* (2019) 25:24–9. doi: 10.1038/s41591-018-0316-z
48. Captur G, Heywood WE, Coats C, Rosmini S, Patel V, Lopes LR, et al. Identification of a multiplex biomarker panel for hypertrophic cardiomyopathy using quantitative proteomics and machine learning. *Mol Cell Proteomics.* (2020) 19:114–27. doi: 10.1074/mcp.RA119.001586
49. Hu WS, Hsieh MH, Lin CL. A novel atrial fibrillation prediction model for Chinese subjects: a nationwide cohort investigation of 682 237 study participants with random forest model. *Europace.* (2019) 21:1307–12. doi: 10.1093/europace/euz036
50. Damani S, Bacconi A, Libiger O, Chourasia AH, Serry R, Gollapudi R, et al. Characterization of circulating endothelial cells in acute myocardial infarction. *Sci Transl Med.* (2012) 4:126ra33. doi: 10.1126/scitranslmed.3003451
51. Boos CJ, Balakrishnan B, Blann AD, Lip GY. The relationship of circulating endothelial cells to plasma indices of endothelial damage/dysfunction and apoptosis in acute coronary syndromes: implications for prognosis. *J Thromb Haemost.* (2008) 6:1841–50. doi: 10.1111/j.1538-7836.2008.03148.x
52. Erdbruegger U, Dhaygude A, Haubitz M, Woywodt A. Circulating endothelial cells: markers and mediators of vascular damage. *Curr Stem Cell Res Ther.* (2010) 5:294–302. doi: 10.2174/157488810793351721
53. Chen S, Sun Y, Neoh KH, Chen A, Li W, Yang X, et al. Microfluidic assay of circulating endothelial cells in coronary artery disease patients with angina pectoris. *PLoS ONE.* (2017) 12:e0181249. doi: 10.1371/journal.pone.0181249
54. Budzyn M, Gryszczynka B, Boruczkowski M, Kaczmarek M, Begier-Krasinska B, Osinska A, et al. The potential role of circulating

endothelial cells and endothelial progenitor cells in the prediction of left ventricular hypertrophy in hypertensive patients. *Front Physiol.* (2019) 10:1005. doi: 10.3389/fphys.2019.01005
55. Lanuti P, Simeone P, Rotta G, Almici C, Avvisati G, Azzaro R, et al. A standardized flow cytometry network study for the assessment of circulating endothelial cell physiological ranges. *Sci Rep.* (2018) 8:5823. doi: 10.1038/s41598-018-24234-0
56. Bekkers SC, Yazdani SK, Virmani R, Waltenberger J. Microvascular obstruction: underlying pathophysiology and clinical diagnosis. *J Am Coll Cardiol.* (2010) 55:1649–60. doi: 10.1016/j.jacc.2009.12.037
57. Boos CJ, Soor SK, Kang D, Lip GY. Relationship between circulating endothelial cells and the predicted risk of cardiovascular events in acute coronary syndromes. *Eur Heart J.* (2007) 28:1092–1. doi: 10.1093/eurheartj/ehm070
58. Sheridan S, Pignone M, Mulrow C. Framingham-based tools to calculate the global risk of coronary heart disease: a systematic review of tools for clinicians. *J Gen Intern Med.* (2003) 18:1039–52. doi: 10.1111/j.1525-1497.2003.30107.x
59. Granger CB, Goldberg RJ, Dabbous O, Pieper KS, Eagle KA, Cannon CP, et al. Global registry of acute coronary events, Predictors of hospital mortality in the global registry of acute coronary events. *Arch Intern Med.* (2003) 163:2345–53. doi: 10.1001/archinte.163.19.2345
60. Antman EM, Cohen M, Bernink PJ, McCabe CH, Horacek T, Papuchis G, et al. The TIMI risk score for unstable angina/non-ST elevation MI: a method for prognostication and therapeutic decision making. *JAMA.* (2000) 284:835–42. doi: 10.1001/jama.284.7.835
61. Yan AT, Jong P, Yan RT, Tan M, Fitchett D, Chow CM, et al. Canadian Acute Coronary Syndromes registry, Clinical trial–derived risk model may not generalize to real-world patients with acute coronary syndrome. *Am Heart J.* (2004) 148:1020–7. doi: 10.1016/j.ahj.2004.02.014
62. Sandoval Y, Jaffe AS. Type 2 myocardial infarction: JACC review topic of the week. *J Am Coll Cardiol.* (2019) 73:1846–60. doi: 10.1016/j.jacc.2019.02.018
63. Wang J, Chen X, Tian Y, Zhu G, Qin Y, Chen X, et al. Six-gene signature for predicting survival in patients with head and neck squamous cell carcinoma. *Aging.* (2020) 12:767–83. doi: 10.18632/aging.102655
64. Yang H, Liu H, Lin HC, Gan D, Jin W, Cui C, et al. Association of a novel seven-gene expression signature with the disease prognosis in colon cancer patients. *Aging.* (2019) 11:8710–27. doi: 10.18632/aging.102365
65. Chen L, Lu D, Sun K, Xu Y, Hu P, Li X, et al. Identification of biomarkers associated with diagnosis and prognosis of colorectal cancer patients based on integrated bioinformatics analysis. *Gene.* (2019) 692:119–25. doi: 10.1016/j.gene.2019.01.001
66. Bethel K, Luttgen MS, Damani S, Kolatkar A, Lamy R, Sabouri-Ghomi M, et al. Fluid phase biopsy for detection and characterization of circulating endothelial cells in myocardial infarction. *Phys Biol.* (2014) 11:016002. doi: 10.1088/1478-3975/11/1/016002

Conflict of Interest: The authors declare that the research was conducted in the absence of any commercial or financial relationships that could be construed as a potential conflict of interest.

frontiers in Cardiovascular Medicine

ORIGINAL RESEARCH
published: 02 July 2021
doi: 10.3389/fcvm.2021.692764

The Association Between Plasma Osmolarity and In-hospital Mortality in Cardiac Intensive Care Unit Patients

*Guangyao Zhai, Jianlong Wang, Yuyang Liu and Yujie Zhou**

Beijing Anzhen Hospital, Capital Medical University, Beijing, China

OPEN ACCESS

Edited by:
Maria Perticone,
University of Magna Graecia, Italy

Reviewed by:
Vishnu Vardhan R.,
Pondicherry University, India
Jingyi Ren,
China-Japan Friendship Hospital, China
Zhuozhong Wang,
The Second Affiliated Hospital of Harbin Medical University, China

****Correspondence:***
Yujie Zhou
azzyj12@163.com

Specialty section:
This article was submitted to General Cardiovascular Medicine, a section of the journal Frontiers in Cardiovascular Medicine

Received: *09 April 2021*
Accepted: *09 June 2021*
Published: *02 July 2021*

Citation:
Zhai G, Wang J, Liu Y and Zhou Y (2021) The Association Between Plasma Osmolarity and In-hospital Mortality in Cardiac Intensive Care Unit Patients. Front. Cardiovasc. Med. 8:692764. doi: 10.3389/fcvm.2021.692764

Objectives: Plasma osmolarity is a common marker used for evaluating the balance of fluid and electrolyte in clinical practice, and it has been proven to be related to prognosis of many diseases. The purpose of this study was to identify the association between plasma osmolarity and in-hospital mortality in cardiac intensive care unit (CICU) patients.

Method: All of the patients were divided into seven groups stratified by plasma osmolarity, and the group with 290–300 mmol/L osmolarity was used as a reference group. Primary outcome was in-hospital mortality. The local weighted regression (Lowess) smoothing curve was drawn to determine the "U"-shaped relationship between plasma osmolarity and in-hospital mortality. Binary logistic regression analysis was performed to determine the effect of plasma osmolarity on the risk of in-hospital mortality.

Result: Overall, 7,060 CICU patients were enrolled. A "U"-shaped relationship between plasma osmolarity and in-hospital mortality was observed using the Lowess smoothing curve. The lowest in-hospital mortality (7.2%) was observed in the reference group. whereas hyposmolarity (<280 mmol/L vs. 290–300 mmol/L: 13.0 vs. 7.2%) and hyperosmolarity (≥330 mmol/L vs. 290–300 mmol/L: 31.6 vs. 7.2%) had higher in-hospital mortality. After adjusting for possible confounding variables with binary logistic regression analysis, both hyposmolarity (<280 mmol/L vs. 290–300 mmol/L: OR, 95% CI: 1.76, 1.08–2.85, $P = 0.023$) and hyperosmolarity (≥330 mmol/L vs. 290–300 mmol/L: OR, 95% CI: 1.65, 1.08–2.52, $P = 0.021$) were independently associated with an increased risk of in-hospital mortality. Moreover, lengths of CICU and hospital stays were prolonged in patients with hyposmolarity or hyperosmolarity.

Conclusion: A "U"-shaped relationship between plasma osmolarity and in-hospital mortality was observed. Both hyposmolarity and hyperosmolarity were independently associated with the increased risk of in-hospital mortality.

Keywords: cardiac care intensive unit, cardiovascular, in-hospital mortality, "U"-shaped, plasma osmolarity

INTRODUCTION

Although the prognosis of cardiovascular diseases has greatly improved due to technological advances and innovative drug use, cardiovascular diseases still remain the leading cause of death and disability worldwide (1). Much research is still needed in the field of cardiovascular diseases, especially for severe cardiovascular diseases with high mortality (2). Cardiac intensive care unit (CICU) has been established to manage severe cardiovascular diseases, and patients admitted to the CICU are usually at great risk of adverse outcomes (3). For CICU patients, readily available risk factors are always welcomed by clinicians, which will help doctors in assessment of the patients' condition and prognosis.

As a common marker used for evaluating the balance of fluid and electrolyte in clinical practice (4–7), plasma osmolarity can be calculated easily from serum sodium, potassium, glucose, and blood nitrogen urea (8). Previous clinical studies have shown that plasma osmolarity is associated with prognosis of many diseases, such as stroke (9), intracerebral hemorrhage (10), and gastrointestinal diseases (11). Plasma osmolarity is also tightly related to a higher rate of mortality and adverse cardiac events in patients with heart failure (12, 13). Likewise, in patients with coronary artery disease undergoing percutaneous coronary intervention (PCI), higher plasma osmolarity was shown to be associated with higher mortality and acute kidney injury (14, 15). Plasma osmolarity is also closely associated with the severity of disease, in-hospital mortality, and other adverse outcomes in critically ill patients (11). However, no research has been done to explore the influence of plasma osmolarity on the prognosis of CICU patients. Therefore, the purpose of this study was to identify the association between plasma osmolarity and in-hospital mortality in CICU patients.

METHOD

Population Selection Criteria and Definition of Plasma Osmolarity

As shown in **Figure 1**, all adult CICU patients at their first admission were eligible. Patients meeting the following criteria were excluded: (1) age under 18 years; (2) hospital admission for non-heart disease; (3) insufficient data to calculate plasma osmolarity; and (4) Acute Physiology and Chronic Health Evaluation IV (APACHE IV) data missing. A total of 7,060 CICU patients were included.

Plasma osmolarity was calculated as follows: $2 \times$ [serum sodium concentration (mmol/L)] $+ 2 \times$ [serum potassium concentration (mmol/L)] + [blood glucose (mmol/L)] + [blood nitrogen urea (mmol/L)] (8). Initial plasma osmolarity referred to the plasma osmolarity obtained from the first blood test after admission, while maximum osmolarity referred to the maximum plasma osmolarity during hospitalization. Plasma osmolarity was calculated from the serum sodium, potassium, glucose, and blood nitrogen urea levels measured at the same time.

Data Extraction

The data used in this study were taken from eICU Collaborative Research Database (16), which collected information on 200,859 admissions from 208 hospitals in the United States between 2014 and 2015. This database is available at: https://doi.org/10.13026/C2WM1R, and the author was granted access to the database through Protecting Human Research Participants exam (certificate number: 9,728,458).

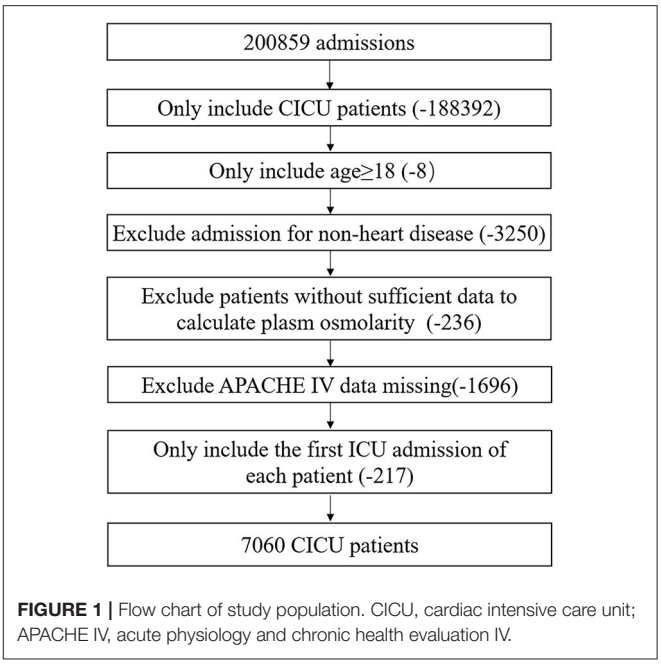

FIGURE 1 | Flow chart of study population. CICU, cardiac intensive care unit; APACHE IV, acute physiology and chronic health evaluation IV.

The following data were collected: demographics (age, gender, and race), vital signs (blood pressure, heart rate, respiration rate, oxygen saturation), body mass index, diagnoses and comorbidities [coronary artery disease, acute coronary syndrome, ST-elevation myocardial infarction (STEMI), non-ST-elevation myocardial infarction (NSTEMI), congestive heart failure, arrhythmias, cardiac arrest, atrial fibrillation, ventricular arrhythmias, atrioventricular block, cardiomyopathy, valve disease, shock, pulmonary embolism, pulmonary hypertension, hypertension, diabetes, chronic obstructive pulmonary disease (COPD), respiratory failure, chronic kidney disease, acute kidney injury, malignancy, stroke, sepsis], laboratory parameters (white blood cells, red blood cells, platelets, hemoglobin, hematocrit, glucose, creatinine, blood nitrogen urea, sodium, potassium), medication use [antiplatelet, oral anticoagulants, beta-blockers, angiotensin-converting enzyme inhibitor/angiotensin receptor blocker (ACEI/ARB), statins], acute physiology score (APS), and Acute Physiology and Chronic Health Evaluation IV (APACHE IV) (17).

Grouping and Outcomes

In clinical practice, we usually consider 285–307 mmol/L as a normal range of plasma osmolarity (8); however, according to the Lowess smoothing curve (**Figure 2**), we found that in-hospital mortality was the lowest when plasma osmolarity ranged from 290 to 300 mmol/L. Therefore, we decided to use osmolarity of 290–300 mmol/L as the reference group in binary logistic regression analysis. In order to better explore the association

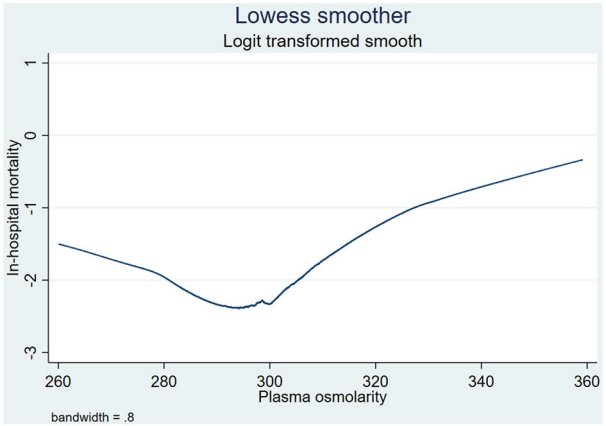

FIGURE 2 | Association between plasma osmolarity and in-hospital mortality presented through Lowess smoothing. Lowess, local weighted regression.

between plasma osmolarity and in-hospital mortality of CICU patients, all of the enrolled patients were divided into seven groups according to their initial plasma osmolarity: group 1 (< 280 mmol/L), group 2 (280–290 mmol/L), group 3 (290–300 mmol/L), group 4 (300–310 mmol/L), group 5 (310–320 mmol/L), group 6 (320–330 mmol/L), and group 7 (≥ 330 mmol/L).

The primary outcome was in-hospital mortality. Secondary outcomes were length of CICU stay and length of hospital stay.

Statistical Analysis

Normally distributed continuous variables were expressed as mean ± standard deviation (SD) and compared between the groups using Student's *t*-test. Skewed data were expressed as median and interquartile range (IQR) and were compared using the Kruskal–Wallis test or the Mann–Whitney *U*-test. Categorical variables were expressed as a number (percentage) and compared between the groups using the chi-square test.

The relationship between plasma osmolarity and in-hospital mortality was identified by binary logistic regression analysis, and the results were expressed as odds ratio (OR) with 95% confidence interval (CI). Covariates were selected on basis of statistical analysis and clinical suspicion that the factors may modulate the result. The curve in line with overall trend was drawn by local weighted regression (Lowess). All the tests were two-sided, and $P < 0.05$ was considered statistically significant. All of the data analyses were performed in Stata V.15.1.

RESULTS

Subjects and Baseline Characteristics

As shown in **Figure 1**, a total of 7,060 CICU patients were enrolled after screening step by step; most of them were White and male. Baseline characteristics of survivors and non-survivors are shown in **Table 1**. Initial plasma osmolarity and maximum plasma osmolarity of all the patients were 302.2 ± 14.4 and 308.4 ± 15.6 mmol/L, respectively. Non-survivors had higher initial plasma osmolarity (308.1 ± 18.1 vs. 301.4 ± 13.7, $P < 0.001$) and maximum plasma osmolarity (321.0 ± 19.9 vs. 306.7 ± 14.1, $P < 0.001$) than survivors. Non-survivors were more likely to have lower blood pressure, oxygen saturation, and body mass index, but higher heart rate and respiration rate. Moreover, non-survivors more often presented congestive heart failure, cardiac arrest, atrial fibrillation, ventricular arrhythmias, shock, COPD, respiratory failure, chronic kidney disease, acute kidney injury, malignancy, stroke, and sepsis, but less commonly coronary artery disease, acute coronary syndrome, STEMI, and hypertension. Non-survivors also had higher white blood cell count, glucose, creatinine, blood nitrogen urea, sodium, and potassium levels, but lower red blood cell and platelet counts, hemoglobin, and hematocrit. Non-survivors less often received oral anticoagulant, antiplatelet, beta-blocker, ACEI/ARB, and statin therapy. APS and APACHE IV of non-survivors were significantly higher than those of survivors.

Association Between Osmolarity and Outcomes

The primary outcome was in-hospital mortality. Through the Lowess smoothing curve shown in **Figure 2**, a "U"-shaped relationship between in-hospital mortality and plasma osmolarity was found. When plasma osmolarity ranged from 290 to 300 mmol/L, in-hospital mortality of CICU patients was the lowest. Therefore, we decided to use osmolarity of 290–300 mmol/L as the reference group in binary logistic regression analysis.

Table 2 shows crude outcomes by plasma osmolarity categories. The lowest in-hospital mortality (7.2%) was observed in the group with 290–300 mmol/L osmolarity. When plasma osmolarity was >290 mmol/L, as plasma osmolarity increased, in-hospital mortality increased significantly (≥330 vs. 290–300 mmol/L: 31.6 vs. 7.2%, respectively). When plasma osmolarity was below 300 mmol/L, as plasma osmolarity decreased, in-hospital mortality increased significantly (<280 vs. 290–300 mmol/L: 13.0 vs. 7.2%, respectively). Higher in-hospital mortality was confirmed in both lower and higher plasma osmolarity group, which was similar with the conclusion drawn by Lowess smoothing shown in **Figure 2**. Moreover, the lengths of CICU and hospital stays were the lowest in the 290–300 mmol/L group; in contrast, the lengths of CICU and hospital stays were prolonged in both hyposmolarity and hyperosmolarity groups (**Table 2**).

As shown in **Table 3**, in unadjusted logistic regression model, with the 290–300 mmol/L group serving as the reference group, both hyposmolarity (<280 vs. 290–300 mmol/L: OR, 95% CI: 1.92, 1.27–2.90, $P = 0.002$) and hyperosmolarity (≥330 mmol/L vs. 290–300 mmol/L: OR, 95% CI: 5.92, 4.33–8.09, $P < 0.001$) were related to the increased risk of in-hospital mortality. When plasma osmolarity was >290 mmol/L, the risk of in-hospital mortality increased gradually as plasma osmolarity increased. When plasma osmolarity was below 300 mmol/L, the risk of in-hospital mortality increased gradually as plasma osmolarity decreased. After adjusting for age, gender, and ethnicity in the model 1, the conclusion was basically consistent with that

TABLE 1 | Baseline characteristics between survivors and non-survivors.

Characteristics	Total (n = 7,060)	Survivors (n = 6,207)	Non-survivors (n = 853)	P-value
Age (years)	65.6 ± 15.2	65.1 ± 15.3	69.4 ± 13.7	<0.001
Gender, *n* (%)				0.701
Male	3,958 (56.1)	3,485 (56.2)	473 (55.5)	
Female	3,102 (43.9)	2,722 (43.9)	380 (44.6)	
Ethnicity, *n* (%)				<0.001
Caucasian	4,989 (70.7)	4,366 (70.3)	623 (73.0)	
African American	1,185 (16.8)	1,022 (16.5)	163 (19.1)	
Other	886 (12.6)	819 (13.2)	67 (7.9)	
Vital signs				
Systolic blood pressure (mmHg)	122.3 ± 19.7	123.7 ± 19.3	111.7 ± 19.4	<0.001
Diastolic blood pressure (mmHg)	66.1 ± 11.3	66.7 ± 11.2	61.3 ± 10.8	<0.001
Mean blood pressure (mmHg)	82.3 ± 13.0	83.1 ± 12.9	76.0 ± 12.3	<0.001
Heart rate (beats/min)	87.4 ± 22.4	86.4 ± 21.9	95.0 ± 24.1	<0.001
Respiration rate (beats/min)	21.0 ± 6.7	20.7 ± 6.5	22.9 ± 7.7	<0.001
Oxygen saturation (%)	96.3 ± 5.3	96.5 ± 4.4	94.4 ± 9.5	<0.001
Body mass index (kg/m^2)	29.1 ± 7.5	29.2 ± 7.4	28.4 ± 8.1	0.006
Diagnoses and comorbidities, *n* (%)				
Congestive heart failure	1,396 (19.8)	1,200 (19.3)	196 (23.0)	0.012
Coronary artery disease	2,619 (37.1)	2,417 (38.9)	202 (23.7)	<0.001
Acute coronary syndrome	1,646 (23.3)	1,518 (24.5)	128 (15.0)	<0.001
STEMI	688 (9.8)	641 (10.3)	47 (5.5)	<0.001
NSTEMI	499 (7.1)	441 (7.1)	58 (6.8)	0.774
Arrhythmias	2,205 (31.2)	1,935 (31.2)	270(32.7)	0.777
Cardiac arrest	577 (8.2)	270 (4.4)	307 (36.0)	<0.001
Atrial fibrillation	1,260 (17.9)	1,077 (17.4)	183 (21.5)	0.003
Ventricular arrhythmias	114 (1.6)	83 (1.3)	31 (3.6)	<0.001
Atrioventricular block	176 (2.5)	161 (2.6)	15 (1.8)	0.142
Cardiomyopathy	419 (5.9)	370 (6.0)	49 (5.7)	0.802
Valve disease	182 (2.6)	157 (2.5)	25 (2.9)	0.488
Shock	1,951 (27.6)	1,534 (24.7)	417 (48.9)	<0.001
Pulmonary embolism	143 (2.0)	122 (2.0)	21 (2.5)	0.335
Pulmonary hypertension	76 (1.1)	65 (1.1)	11 (1.3)	0.520
Hypertension	2,019 (28.6)	1,868 (30.1)	151 (17.7)	<0.001
Diabetes	1,306 (18.5)	1,146 (18.5)	160 (18.8)	0.836
COPD	717 (10.2)	610 (9.8)	107 (12.5)	0.014
Respiratory failure	1,894 (26.8)	1,416 (22.8)	478 (56.0)	<0.001
Chronic kidney disease	982 (13.9)	821 (13.2)	161 (18.9)	<0.001
Acute kidney injury	1,178 (16.7)	895 (14.4)	283 (33.2)	<0.001
Malignancy	371 (5.3)	294 (4.7)	77 (9.0)	<0.001
Stroke	262 (3.7)	212 (3.4)	50 (5.9)	<0.001
Sepsis	1,396 (19.8)	1,113 (17.9)	283 (33.2)	<0.001
Laboratory parameters				
White blood cell (10^9/L)	11.7 ± 8.4	11.3 ± 7.9	14.6 ± 11.1	<0.001
Red blood cell (10^9/L)	4.1 ± 0.8	4.1 ± 0.8	3.9 ± 0.8	<0.001
Platelet (10^9/L)	226.6	227.8 ± 96.4	217.4 ± 108.3	0.004
Hemoglobin (g/dL)	12.1 ± 2.5	12.2 ± 2.5	11.5 ± 2.5	<0.001
Hematocrit (%)	36.7 ± 7.0	36.9 ± 7.0	35.4 ± 7.4	<0.001
Glucose (mmol/L)	8.9 ± 5.1	8.7 ± 5.0	10.2 ± 6.0	<0.001
Creatinine (mg/dL)	1.69 ± 1.48	1.64 ± 1.48	2.02 ± 1.47	<0.001

(Continued)

TABLE 1 | Continued

Characteristics	Total (n = 7,060)	Survivors (n = 6,207)	Non-survivors (n = 853)	P-value
Blood nitrogen urea (mmol/L)	28.7 ± 21.7	27.4 ± 20.6	38.1 ± 26.3	<0.001
Sodium (mmol/L)	137.2 ± 5.3	137.2 ± 5.2	137.6 ± 6.4	0.043
Potassium (mmol/L)	4.2 ± 0.8	4.2 ± 0.7	4.4 ± 0.9	<0.001
Medication use, n (%)				
Antiplatelet	3,396 (48.1)	3,078 (49.6)	318 (37.3)	<0.001
Oral anticoagulants	767 (10.9)	710 (11.4)	57 (6.7)	<0.001
Beta-blockers	3,034 (43.0)	2,795 (45.0)	239 (28.0)	<0.001
ACEI/ARB	1,914 (27.1)	1,805 (29.1)	109 (12.8)	<0.001
Statin	2,150 (30.5)	1,999 (32.2)	151(17.7)	<0.001
APS	38 (27–55)	36 (25–49)	76 (52–106)	<0.001
APACHE IV	52 (38–70)	49 (36–64)	92 (67–121)	<0.001
Initial osmolarity (mmol/L)	302.2 ± 14.4	301.4 ± 13.7	308.1 ± 18.1	<0.001
Maximum osmolarity (mmol/L)	308.4 ± 15.6	306.7 ± 14.1	321.0 ± 19.9	<0.001

Normally distributed continuous variables were presented as mean ± SD or median (IQR). Categorical variables were presented as number (percentage). STEMI, ST-elevation myocardial infarction; NSTEMI, non-ST-elevation myocardial infarction; COPD, chronic obstructive pulmonary disease; ACEI, angiotensin-converting enzyme inhibitor; ARB, angiotensin receptor blocker; APS, acute physiology score; APACHE IV, acute physiology and chronic health evaluation IV.

TABLE 2 | Outcomes by osmolarity categories in CICU patients.

Outcome	Osmolarity (mmol/L)							
	<280 (n = 231)	280–290 (n = 732)	290–300 (n = 2,283)	300–310 (n = 2290)	310–320 (n = 917)	320–330 (n = 363)	≥330 (n = 244)	P-value
In-hospital mortality, n (%)	30 (13.0)	71 (9.7)	165 (7.2)	243 (10.6)	173 (18.9)	94 (25.9)	77 (31.6)	<0.001
Length of CICU stay (days)	2.2 (1.4–4.6)	2.0 (1.1–3.9)	1.8 (1.0–3.1)	1.9 (1.1–3.4)	2.2 (1.2–4.1)	2.7 (1.5–5.0)	3.3 (1.6–6.0)	<0.001
Length of hospital stay (days)	5.7 (3.0–10.7)	5.2 (2.9–9.9)	4.6 (2.5–8.9)	5.0 (2.8–9.2)	5.9 (3.1–10.3)	7.4 (3.6–12.2)	7.9 (4.3–14.9)	<0.001

Lengths of CICU and hospital stays were skewed. Therefore, they were presented as median (IQR). Categorical variables were presented as number (percentage). CICU, cardiac intensive care unit.

of the unadjusted model. After adjusting for more possible confounding variables in the model 2, the association between osmolarity and in-hospital mortality was attenuated but still remained statistically significant. Both hyposmolarity (<280 vs. 290–300 mmol/L: OR, 95% CI: 1.76, 1.08–2.85, $P = 0.023$) and hyperosmolarity (≥330 mmol/L vs. 290–300 mmol/L: OR, 95% CI: 1.65, 1.08–2.52, $P = 0.021$) were independently associated with the increased risk of in-hospital mortality. OR values increased gradually as plasma osmolarity increased when plasma osmolarity was >290 mmol/L; when plasma osmolarity was below 300 mmol/L, OR values increased gradually as plasma osmolarity decreased. **Figure 3** vividly presents the change of OR with the change of osmolarity groups in the unadjusted model, model 1, and model 2.

DISCUSSION

This study identified the association between plasma osmolarity and in-hospital mortality in CICU patients. A "U"-shaped relationship between plasma osmolarity and in-hospital mortality was observed. With the group of 290–300 mmol/L serving as the reference group, both hyposmolarity and hyperosmolarity were associated with the increased risk of in-hospital mortality, even after adjusting for possible confounding variables. The lengths of CICU and hospital stays were prolonged in both hyposmolarity and hyperosmolarity groups.

As a common clinical marker to evaluate the balance of fluid and electrolytes (4–7), plasma osmolarity can be easily calculated from the concentrations of serum sodium, potassium, glucose, and blood nitrogen urea (8). Plasma osmolarity is the most commonly used indicator of hydration (18), which can influence cell size and function (19). Therefore, changes in plasma osmolarity can reflect changes in cell function. A great number of studies have been done on plasma osmolarity, and there is sufficient evidence that plasma osmolarity is associated with the prognosis of many diseases, such as stroke (9), intracerebral hemorrhage (10), and acute pulmonary embolism (20). Moreover, recent studies have shown a correlation between

TABLE 3 | The association between in-hospital mortality and osmolarity (mmol/L).

	Unadjusted		Model 1		Model 2	
	OR(95% CIs)	***P*-value**	**OR(95% CIs)**	***P*-value**	**OR(95% CIs)**	***P*-value**
Osmolarity (<280)	1.92 (1.27–2.90)	0.002	1.85 (1.22–2.80)	0.004	1.76 (1.08–2.85)	0.023
Osmolarity (280–290)	1.38 (1.03–1.85)	0.031	1.39 (1.04–1.87)	0.027	1.20 (0.85–1.69)	0.289
Osmolarity (290–300)	1.0 (reference)		1.0 (reference)		1.0 (reference)	
Osmolarity (300–310)	1.52 (1.24–1.87)	<0.001	1.45 (1.18–1.78)	<0.001	1.13(0.88–1.45)	0.351
Osmolarity (310–320)	2.98 (2.37–3.75)	<0.001	2.80 (2.22–3.53)	<0.001	1.46 (1.09–1.96)	0.012
Osmolarity (320–330)	4.49 (3.38–5.95)	<0.001	4.16 (3.13–5.53)	<0.001	1.46 (1.00–2.13)	0.052
Osmolarity (≥330)	5.92 (4.33–8.09)	<0.001	5.58 (4.07–7.65)	<0.001	1.65 (1.08–2.52)	0.021

Models were derived from binary logistic regression analysis. Unadjusted model: unadjusted. Model 1: adjusted for age, gender, ethnicity. Model 2: adjusted for age, gender, ethnicity, systolic blood pressure, diastolic blood pressure, mean blood pressure, heart rate, respiration rate, congestive heart failure, coronary artery disease, acute coronary syndrome, STEMI, NSTEMI, cardiac arrest, ventricular arrhythmias, shock, hypertension, diabetes, respiratory failure, acute kidney injury, sepsis, stroke, malignancy, white blood cell, red blood cell, hemoglobin, creatinine, ACEI/ARB, beta-blockers, statin, and oral anticoagulants, APS, APACHE IV. OR, odds ratio; CI, confidence interval.

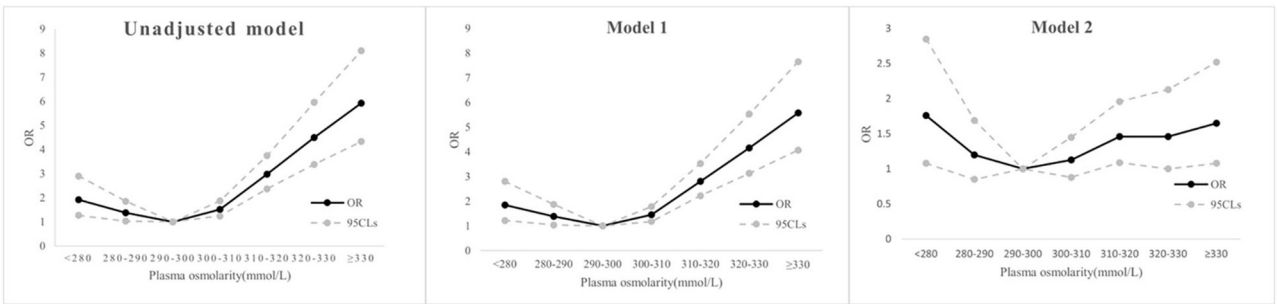

FIGURE 3 | Line graphs reflecting the trend of change in OR of in-hospital mortality in unadjusted model, model 1, and model 2. OR, odds ratio; CI, confidence interval.

plasma osmolarity and cardiovascular diseases. A single-center retrospective study with 1,927 patients after PCI showed that the rate of acute kidney injury and 1-year mortality increased significantly as plasma osmolarity increased (14). Another study, which enrolled 985 patients with acute coronary syndrome undergoing PCI, confirmed higher mortality in the higher osmolarity group (15). In patients with STEMI, higher rates of all-cause mortality, recurrent myocardial infarction, and revascularization were found in those with higher plasma osmolarity (21). Previous studies also showed that both low and high plasma osmolarity were related to more cardiovascular deaths, deterioration of cardiac function, and rehospitalization in patients with heart failure (12, 13). In this study exploring the relationship between plasma osmolarity and in-hospital mortality in CICU patients, we came to a similar conclusion that plasma osmolarity was closely associated with in-hospital mortality. Moreover, through Lowess smoothing, we found a "U"-relationship between in-hospital mortality and osmolarity, which provided a more graphic description of the overall trend.

Plasma osmolarity is mainly determined by serum sodium, chloride, potassium, blood glucose, and blood nitrogen urea. Hypernatremia, hyperchloremia, hyperkalemia, hyperglycemia, and high urea contribute to high plasma osmolarity. Hypernatremia was shown to be associated with higher mortality and more cardiovascular diseases in older men (22). Another study confirmed that increased hypernatremia was associated with higher perioperative 30-day mortality (23). For patients with intracranial hemorrhage, hypernatremia was associated with more adverse cardiac events (24). Patel et al. found that hyperchloremia was independently associated with acute kidney injury in patients with STEMI undergoing PCI (25). Hyperkalemia can lead to malignant arrhythmia and increase mortality (26). Hyperglycemia is very common in clinical practice and it is related to higher mortality and more adverse cardiac events in patients with or without diabetes (27). A prospective study with 1,667 patients diagnosed with acute coronary syndrome showed that high blood nitrogen was associated with more adverse cardiac events and higher mortality (28). These studies can explain why high plasma osmolarity leads to high mortality, which can also explain the results of our study. The lengths of CICU and hospital stays were prolonged in both the hyposmolarity and the hyperosmolarity groups, indicating that patients with hyposmolarity or hyperosmolarity had a more complex condition and therefore required a longer treatment. The increased lengths of CICU and hospital stays imposed not only the financial but also mental burden on patients. In

exceptional cases, some patients may abandon treatment because of financial problems. Therefore, more attention to plasma osmolarity of CICU patients is needed.

Changes in plasma osmolarity can provide guidance for clinical practice. Usually, the clinicians tend to pay more attention to the outliers, but when all the variables are within the normal range but close to the upper limit of the normal value, plasma osmolarity will increase significantly. At this time, plasma osmolarity can better reflect the patient's condition and give the clinician a hit. The independent association between in-hospital mortality and plasma osmolarity was confirmed in this study. As a readily accessible and inexpensive prognostic marker, plasma osmolarity is clinically valuable for critically ill patients admitted to CICU, especially in some cases that more complex prognostic score can't be calculated, for example, the patient is unable to undergo complex examination or the patient is in a remote area without the means to do so, plasma osmolarity may alert the clinicians.

We confirmed the association between plasma osmolarity and in-hospital mortality in CICU patients in this study, which is convenient for clinical use. The multicenter and large sample size makes the conclusion more reliable. However, some limitations in this study should be noted. First, bias was inevitable due to the retrospective nature of the study. Second, some important information, such as left ventricular ejection fraction and information about smoking and alcohol, could not be collected. In general, the variables included in the model determine the accuracy of the model; thus, the accuracy of the model was likely affected by the missing variables. Third, we were not able to dynamically observe plasma osmolarity. Fourth, although the optimal equation was used, the calculated plasma osmolarity cannot be the exactly the same as the real plasma osmolarity.

CONCLUSION

A "U"-shaped relationship between plasma osmolarity and in-hospital mortality was observed. The lowest in-hospital mortality was shown in the group with 290–300 mmol/L osmolarity; patients with hyposmolarity or hyperosmolarity had higher in-hospital mortality. With the group with 290–300 mmol/L osmolarity serving as the reference group, both hyposmolarity and hyperosmolarity were shown to be independently associated with the increased risk of in-hospital mortality.

DATA AVAILABILITY STATEMENT

The original contributions presented in the study are included in the article/**Supplementary Materials**, further inquiries can be directed to the corresponding author/s.

ETHICS STATEMENT

Ethical review and approval was not required for the study on human participants in accordance with the local legislation and institutional requirements. The ethics committee waived the requirement of written informed consent for participation.

AUTHOR CONTRIBUTIONS

GZ and YZ contributed to study design, data analysis, and article writing. JW and YL contributed to data collection. All authors contributed to the article and approved the submitted version.

FUNDING

This study was supported by grants from Beijing Municipal Health Commission (Grant Nos. PXM2020_026272_000002 and PXM2020_026272_000014) and Natural Science Foundation of Beijing, China (Grant No. 7212027) to YZ.

SUPPLEMENTARY MATERIAL

The Supplementary Material for this article can be found online at: https://www.frontiersin.org/articles/10.3389/fcvm.2021.692764/full#supplementary-material

Results of covariates in multiple logistic regression analysis (Model 2) were presented in the **Supplementary Materials**.

REFERENCES

1. GBD 2017 DALYs and HALE Collaborators. Global, regional, and national disability-adjusted life-years (DALYs) for 359 diseases and injuries and healthy life expectancy (HALE) for 195 countries and territories, 1990–2017: a systematic analysis for the Global Burden of Disease Study 2017. *Lancet*. (2018) 392:1859–922. doi: 10.1016/S0140-6736(18)32335-3
2. Vervoort D. Global cardiac surgery: a wake-up call. *Eur J Cardio Thoracic Surg*. (2019) 55:1022–3. doi: 10.1093/ejcts/ezy319
3. Katz JN, Shah BR, Volz EM, Horton JR, Shaw LK, Newby LK, et al. Evolution of the coronary care unit: clinical characteristics and temporal trends in healthcare delivery and outcomes. *Crit Care Med*. (2010) 38:375–81. doi: 10.1097/CCM.0b013e3181cb0a63
4. Earley LE, Sanders CA. The effect of changing serum osmolality on the release of antidiuretic hormone in certain patients with decompensated cirrhosis of the liver and low serum osmolality. *J Clin Invest*. (1959) 38:545–50. doi: 10.1172/JCI103832
5. Rasouli M. Basic concepts and practical equations on osmolality: biochemical approach. *Clin Biochem*. (2016) 49:936–41. doi: 10.1016/j.clinbiochem.2016.06.001
6. Gennari FJ. Current concepts. Serum osmolality. Uses and limitations. *N Engl J Med*. (1984) 310:102–5. doi: 10.1056/NEJM198401123100207
7. Cheuvront SN, Kenefick RW, Sollanek KJ, Ely BR, Sawka MN. Water-deficit equation: systematic analysis and improvement. *Am J Clin Nutr*. (2013) 97:79–85. doi: 10.3945/ajcn.112.046839
8. Heavens KR, Kenefick RW, Caruso EM, Spitz MG, Cheuvront SN. Validation of equations used to predict plasma osmolality in a healthy adult cohort. *Am J Clin Nutr*. (2014) 100:1252–6. doi: 10.3945/ajcn.114.091009
9. Bhalla A, Sankaralingam S, Dundas R, Swaminathan R, Wolfe CD, Rudd AG. Influence of raised plasma osmolality on clinical outcome after acute stroke. *Stroke*. (2000) 31:2043–8. doi: 10.1161/01.STR.31.9.2043
10. Nag C, Das K, Ghosh M, Khandakar MR. Plasma osmolality in acute spontanious intra-cerebral hemorrhage: does it influence hematoma volume and clinical outcome? *J Res Med Sci*. (2012) 17:548–51.

11. Shen Y, Cheng X, Ying M, Chang HT, Zhang W. Association between serum osmolarity and mortality in patients who are critically ill: a retrospective cohort study. *BMJ Open.* (2017) 7:e015729. doi: 10.1136/bmjopen-2016-015729
12. Vaduganathan M, Marti CN, Mentz RJ, Greene SJ, Ambrosy AP, Subacius HP, et al. Serum osmolality and postdischarge outcomes after hospitalization for heart failure. *Am J Cardiol.* (2016) 117:1144–50. doi: 10.1016/j.amjcard.2015.12.059
13. Kaya H, Yücel O, Ege MR, Zorlu A, Yücel H, Güneş H, et al. Plasma osmolality predicts mortality in patients with heart failure with reduced ejection fraction. Kardiologia polska. (2017) 75:316–22. doi: 10.5603/KP.a2016.0168
14. Farhan S, Vogel B, Baber U, Sartori S, Aquino M, Chandrasekhar J, et al. Calculated serum osmolality, acute kidney injury, and relationship to mortality after percutaneous coronary intervention. *Cardiorenal Med.* (2019) 9:160–7. doi: 10.1159/000494807
15. Rohla M, Freynhofer MK, Tentzeris I, et al. Plasma osmolality predicts clinical outcome in patients with acute coronary syndrome undergoing percutaneous coronary intervention. *Eur Heart J Acute Cardiovasc Care.* (2014) 3:84–92. doi: 10.1177/2048872613516018
16. Pollard TJ, Johnson AEW, Raffa JD, Celi LA, Mark RG, Badawi O. The eICU collaborative research database, a freely available multi-center database for critical care research. *Sci Data.* (2018) 5:180178. doi: 10.1038/sdata.2018.178
17. Zimmerman JE, Kramer AA, McNair DS, Malila FM. Acute physiology and chronic health evaluation (APACHE IV) IV: hospital mortality assessment for today's critically ill patients. *Crit Care Med.* (2006) 34:1297–310. doi: 10.1097/01.CCM.0000215112.84523.F0
18. Francesconi RP, Hubbard RW, Szlyk PC, Schnakenberg D, Carlson D, Leva N, et al. Urinary and hematologic indexes of hypohydration. *J Appl Physiol.* (1987) 62:1271–6. doi: 10.1152/jappl.1987.62.3.1271
19. Danziger J, Zeidel ML. Osmotic homeostasis. *Clin J Am Soc Nephrol.* (2015) 10:852–62. doi: 10.2215/CJN.10741013
20. Öz A, Çinar T, Hayiroglu M, Avşar S, Keskin M, Orhan AL. The predictive value of plasma osmolality for in-hospital mortality in patients with acute pulmonary embolism. *Clin Respir J.* (2019) 13:174–83. doi: 10.1111/crj.13001
21. Tatlisu MA, Kaya A, Keskin M, Uzman O, Borklu EB, Cinier G, et al. Can we use plasma hyperosmolality as a predictor of mortality for ST-segment elevation myocardial infarction? *Coron Artery Dis.* (2017) 28:70–6. doi: 10.1097/MCA.0000000000000426
22. Wannamethee SG, Shaper AG, Lennon L, Papacosta O, Whincup P. Mild hyponatremia, hypernatremia and incident cardiovascular disease and mortality in older men: a population-based cohort study. *Nutr Metab Cardiovasc Dis.* (2016) 26:12–9. doi: 10.1016/j.numecd.2015.07.008
23. Leung AA, McAlister FA, Finlayson SR, Bates DW. Preoperative hypernatremia predicts increased perioperative morbidity and mortality. *Am J Med.* (2013) 126:877–6. doi: 10.1016/j.amjmed.2013.02.039
24. Fisher LA, Ko N, Miss J, Tung PP, Kopelnik A, Banki NM, et al. Hypernatremia predicts adverse cardiovascular and neurological outcomes after SAH. *Neurocrit Care.* (2006) 5:180–5. doi: 10.1385/NCC:5:3:180
25. Patel N, Baker SM, Walters RW, Kaja A, Kandasamy V, Abuzaid A, et al. Serum hyperchloremia as a risk factor for acute kidney injury in patients with ST-segment elevation myocardial infarction undergoing percutaneous coronary intervention. Proc (Bayl Univ Med Cent). (2016) 29:7–11. doi: 10.1080/08998280.2016.11929341
26. Dunn JD, Benton WW, Orozco-Torrentera E, Adamson RT. The burden of hyperkalemia in patients with cardiovascular and renal disease. *Am J Manag Care.* (2015) 21(15 Suppl):s307–15.
27. Capes SE, Hunt D, Malmberg K, Gerstein HC. Stress hyperglycaemia and increased risk of death after myocardial infarction in patients with and without diabetes: a systematic overview. *Lancet.* (2000) 355:773–8. doi: 10.1016/S0140-6736(99)08415-9
28. Saygitov RT, Glezer MG, Semakina SV. Blood urea nitrogen and creatinine levels at admission for mortality risk assessment in patients with acute coronary syndromes. *Emerg Med J.* (2010) 27:105–9. doi: 10.1136/emj.2008.068155

Conflict of Interest: The authors declare that the research was conducted in the absence of any commercial or financial relationships that could be construed as a potential conflict of interest.

frontiers in Cardiovascular Medicine

SYSTEMATIC REVIEW
published: 07 July 2021
doi: 10.3389/fcvm.2021.699492

Prognostic Value of Natriuretic Peptides for All-Cause Mortality, Right Ventricular Failure, Major Adverse Events, and Myocardial Recovery in Advanced Heart Failure Patients Receiving a Left Ventricular Assist Device: A Systematic Review

*Eva Janssen, J. Wouter Jukema, Saskia L. M. A. Beeres, Martin J. Schalij and Laurens F. Tops**

Department of Cardiology, Leiden University Medical Center, Leiden, Netherlands

OPEN ACCESS

Edited by:
Maria Perticone,
University of Magna Graecia, Italy

Reviewed by:
Kevin Shah,
The University of Utah, United States
Judith Cuypers,
Erasmus Medical Center, Netherlands

****Correspondence:***
Laurens F. Tops
l.f.tops@lumc.nl

Specialty section:
This article was submitted to General Cardiovascular Medicine, a section of the journal Frontiers in Cardiovascular Medicine

Received: *23 April 2021*
Accepted: *01 June 2021*
Published: *07 July 2021*

Citation:
Janssen E, Jukema JW, Beeres SLMA, Schalij MJ and Tops LF (2021) Prognostic Value of Natriuretic Peptides for All-Cause Mortality, Right Ventricular Failure, Major Adverse Events, and Myocardial Recovery in Advanced Heart Failure Patients Receiving a Left Ventricular Assist Device: A Systematic Review. Front. Cardiovasc. Med. 8:699492. doi: 10.3389/fcvm.2021.699492

Aims: Major adverse event (MAE) rates during left ventricular assist device (LVAD) therapy in advanced heart failure (HF) patients are high, and impair quality of life and survival. Prediction and risk stratification of MAEs in order to improve patient selection and thereby outcome during LVAD therapy is therefore warranted. Circulating natriuretic peptides (NPs) are strong predictors of MAEs and mortality in chronic HF patients. However, whether NPs can identify patients who are at risk of MAEs and mortality or tend toward myocardial recovery after LVAD implantation is unclear. The aim of this systematic review is to analyze the prognostic value of circulating NP levels before LVAD implantation for all-cause mortality, MAEs and myocardial recovery after LVAD implantation.

Methods and Results: Electronic databases were searched for studies analyzing circulating NP in adults with advanced HF before LVAD implantation in relation to mortality, MAEs, or myocardial recovery after LVAD implantation. Twenty-four studies published between 2008 and 2021 were included. Follow-up duration ranged from 48 hours to 5 years. Study sample size ranged from 14 to 15,138 patients. Natriuretic peptide levels were not predictive of all-cause mortality. However, NPs were predictive of right ventricular failure (RVF) and MAEs such as ventricular arrhythmias, moderate or severe aortic regurgitation, and all-cause rehospitalization. No relation between NPs and myocardial recovery was found.

Conclusion: This systematic review found that NP levels before LVAD implantation are not predictive of all-cause mortality after LVAD implantation. Thus, NP levels may be of limited value in patient selection for LVAD therapy. However, NPs help in risk stratification of MAEs and may be used to identify patients who are at risk for RVF, ventricular arrhythmias, moderate or severe aortic regurgitation, and all-cause rehospitalization after LVAD implantation.

Keywords: left ventricular assist device, circulating biomarkers, natriuretic peptides, adverse events, prognosis

INTRODUCTION

The prognosis of advanced heart failure (HF) is poor, with annual mortality rates over 50%, and limited treatment options (1). Cardiac transplantation is the most effective treatment, although its availability is limited due to insufficient number of donor organs and strict eligibility criteria. Left ventricular assist devices (LVADs) are an alternative treatment option through mechanical unloading of the failing left ventricle (LV). To date, LVAD therapy is increasingly used as destination therapy in patients not eligible for transplantation. Patient selection and timing of LVAD implantation is guided by the profiles of the Interagency Registry for Mechanically Assisted Circulatory Support (INTERMACS) classifying patients with advanced heart failure (2).

The most recent INTERMACS report has shown a 1-year survival rate of 79–80% in patients receiving continuous flow (CF)-LVAD therapy (3, 4). Major adverse event (MAE) and rehospitalization rates are high, and impair quality of life and survival (4, 5). These MAEs include neurologic event (defined as stroke or transient ischemic attack), gastrointestinal bleeding, major infection, and right heart failure (RVF) occurring 13–20, 20–25, 40–43, and 29–38% at 1 year after CF-LVAD implantation, respectively (4). All-cause rehospitalization rates were 21–23% (4). Device explantation for LV myocardial recovery is rare with 3.1% at 3 years, and <5% at 5 years follow-up (3, 6). It would be beneficial to identify patients prone to myocardial recovery, and consider adjustments of their pharmacological treatment (7). To identify patients at risk of MAEs and early mortality would be of great importance. Treatment options for MAEs are limited and often ineffective, having corresponding high mortality rates. Thus, prediction and risk stratification of MAEs before LVAD implantation is warranted in order to improve patient selection, and thereby outcome of LVAD therapy. Measurement of circulating biomarkers such as natriuretic peptides (NPs) may help in risk stratification.

Three subtypes of NP are known; atrial natriuretic peptide (ANP), B-type natriuretic peptide (BNP), and C-type natriuretic peptide (CNP) (8, 9). Natriuretic peptides mainly reflect the hemodynamic burden of the failing heart, and are regulated by volume overload and neuro-hormonal stimulation. Prehormone pro-BNP is released by cardiomyocytes in reaction to mechanical stretch and myocardial ischemia. Upon secretion into the circulation it is cleaved in biologically active BNP and its inactive remnant N-terminal proBNP (NT-proBNP) (**Figure 1**) (8–12). Levels of NP are influenced by various factors including age, gender, comorbidities, renal function, pulmonary disease, and obesity (13–15). Heart failure medication, including beta-blockers, diuretics, and inotropes affect NP levels, reflecting the improvement in hemodynamic state induced by these therapies. The novel HF drug sacubitril/valsartan influences BNP and NT-proBNP levels differently, in particular during the first 8–10 weeks after initiation. Whereas, the use of sacubitril/valsartan, a neprilysin inhibitor, may increase the circulating levels of BNP, it does not affect the circulating levels of NT-proBNP since the latter is not a substrate of neprilysin inhibition. Nonetheless, both BNP and NT-proBNP have prognostic value during treatment with sacubitril/valsartan (8, 16). Finally, it has been demonstrated that a large percentage of measured circulating BNP or NT-proBNP is in fact their prehormone proBNP. Therefore, BNP, NT-proBNP, and proBNP measurements from different assays are not reliably comparable due to their differences in cross-reactivity (17, 18).

In the American College of Cardiology/American Heart Association guideline, BNP and NT-proBNP have a class IA recommendation to establish disease severity and prognosis of patients with chronic HF (2). Hutfless et al. showed that preoperative BNP levels are strong predictors of postoperative need for intra-aortic balloon pump, longer postoperative hospital stay, and higher 1-year mortality in patients undergoing open heart surgery (19). Furthermore, the prognostic value of NP levels related to all-cause mortality, adverse events, and rehospitalization in chronic HF patients has been well-established (20–24).

Whether preoperative NP levels can improve patient selection for LVAD therapy by identifying patients who are at risk for early all-cause mortality, right ventricular failure (RVF), or MAEs, and can identify patients who tend toward myocardial recovery after LVAD implantation, is not yet systematically evaluated. In this review, we sought to systematically evaluate the prognostic value of circulating NP levels in advanced HF patients before LVAD implantation for all-cause mortality, RVF, MAEs including rehospitalization, and myocardial recovery after successful LVAD implantation.

METHODS

This systematic review is written in accordance with the Preferred Reporting Items for Systematic Reviews and Meta-analyses (PRISMA) guideline (**Supplementary Material 1**). Since individual patient data are not included, institutional review board approval was not required.

Literature Search and Selection

Seven electronic databases were searched: MEDLINE, Web of Science Core Collection, Cochrane Reviews, Cochrane Trials, PubMed, Factiva, and Embase. The following (MeSH) terms were used: "left ventricular assist device," "ventricular assist device," "mechanical circulatory support," "biomarkers," "natriuretic peptide," "B-type natriuretic peptide," "brain natriuretic peptide," "pro B-type natriuretic peptide," "pro brain natriuretic peptide," "NT-pro B-type natriuretic peptide," "N-terminal pro B-type natriuretic peptide," and "N-terminal pro brain natriuretic peptide." The search was restricted to human studies published in English up to January 1st, 2021. Study selection criteria were predefined as described in **Table 1**.

The authors of this manuscript screened the titles and abstracts of all studies retrieved from the literature search. Potentially relevant studies, or studies whose relevance could not be ascertained based on the abstract, were screened full text. A single assessor screened each article full text for inclusion. Corresponding authors were contacted to obtain full data not covered in the publication.

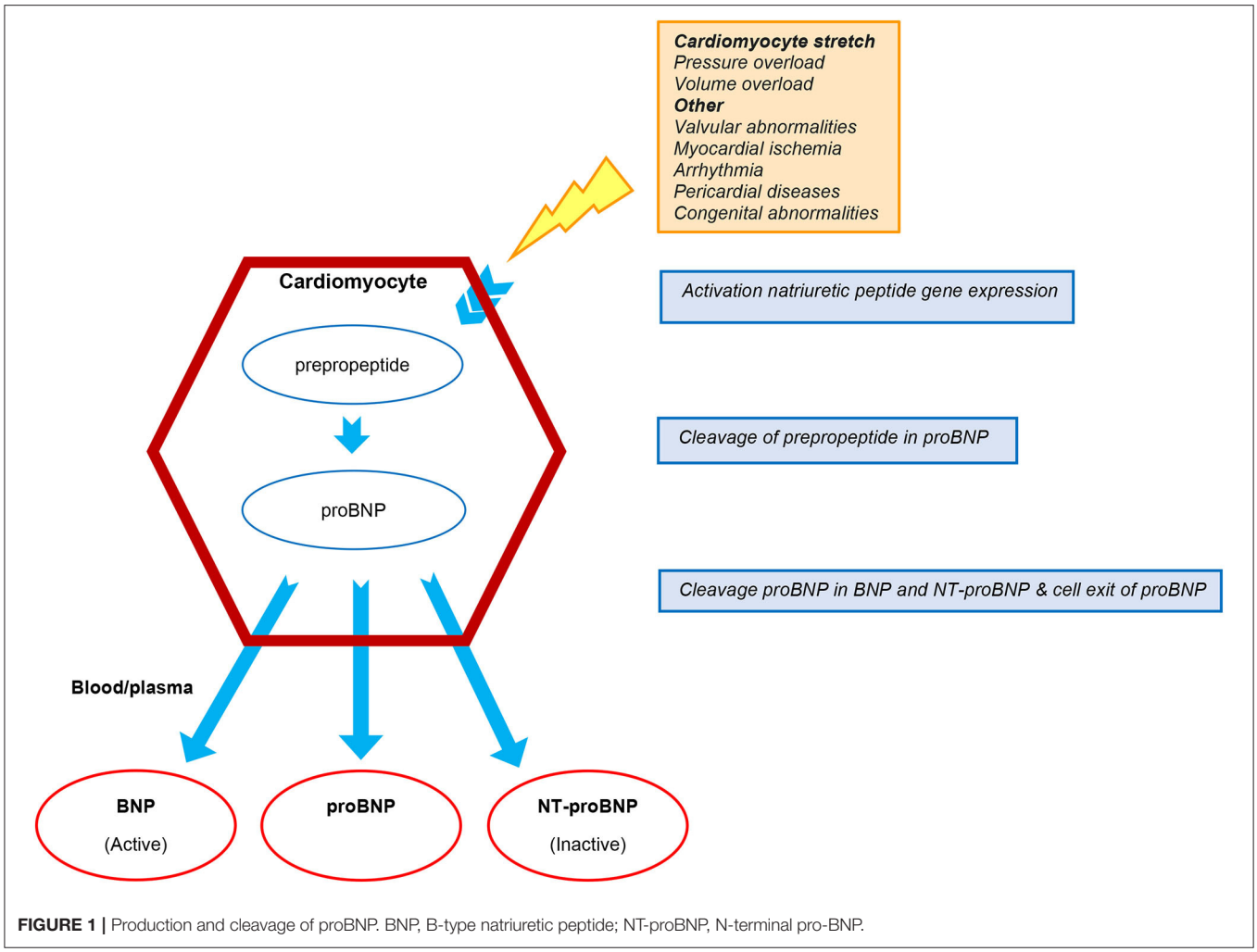

FIGURE 1 | Production and cleavage of proBNP. BNP, B-type natriuretic peptide; NT-proBNP, N-terminal pro-BNP.

TABLE 1 | Inclusion–and exclusion criteria.

Inclusion
Patient population: humans > 18 years with advanced HF who will receive left ventricular assist device therapy
Outcome(s): all-cause mortality, right ventricular failure, major adverse events, myocardial recovery
Prognostic factor: circulating natriuretic peptide levels measured before LVAD implantation
Language: English
Exclusion
Reviews, editorials, case reports, abstracts

Data Collection

Extracted data included details of the patient population, etiology of HF, type of VAD, device strategy, timing of blood sampling for NPs measurement, type of NPs, cut-off points of NPs (when available), type of statistical analysis, adjusted variables for multivariate analysis, and duration of follow-up. The outcomes all-cause mortality, RVF, MAEs (including all-cause planned and unplanned rehospitalization) and myocardial recovery, and their describing definitions were extracted. Major adverse events were defined according to the "2020 Updated definitions of adverse events for trials and registries of mechanical circulatory support" (25). In the current review, the following MAEs were included: ventricular arrhythmia (VA), aortic regurgitation (AR), "combined adverse events" (including episode of VA, HF, chest pain, bleeding, infection, thrombosis, pump-related problems, biliary disfunction, elective procedures), complicated postoperative stay, and all-cause rehospitalization.

Study Quality

The Newcastle–Ottawa Scale (NOS) for observational cohorts was used to assess the quality of all included studies (26). The NOS score was then converted into Agency for Healthcare Research and Quality standards (AHRQ); good, fair, and poor (27).

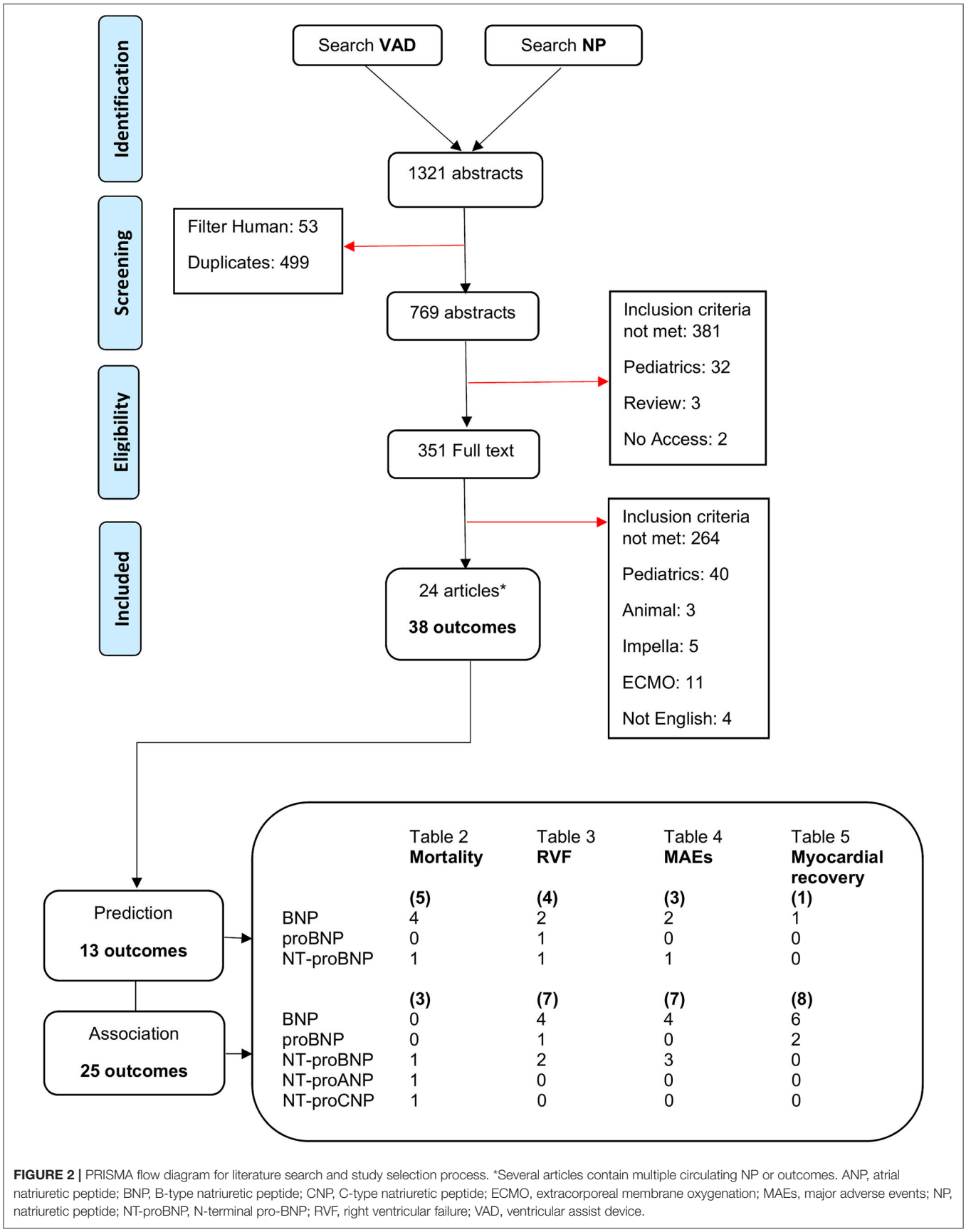

FIGURE 2 | PRISMA flow diagram for literature search and study selection process. *Several articles contain multiple circulating NP or outcomes. ANP, atrial natriuretic peptide; BNP, B-type natriuretic peptide; CNP, C-type natriuretic peptide; ECMO, extracorporeal membrane oxygenation; MAEs, major adverse events; NP, natriuretic peptide; NT-proBNP, N-terminal pro-BNP; RVF, right ventricular failure; VAD, ventricular assist device.

RESULTS

Literature Search

The literature search and selection process is presented in the PRISMA flow diagram in **Figure 2**. The literature search retrieved 1,321 citations from the seven electronic databases. After duplicates were removed, 769 citations went through title and abstract screening, of which 351 articles were screened full text. A total of 745 citations were excluded; the majority did not meet the inclusion criteria regarding advanced HF, reporting any kind of endpoint, receiving LVAD therapy, or measurement of circulating NPs prior to device implantation. Eventually, 24 articles passed full text screening and were included in this review.

Study Characteristics

The included studies were published between 2008 and 2020, and were from countries in Europe, the United States of America, and Japan. Twenty-three of the included studies were retrospective cohort studies. The 24 studies were fairly heterogenous reporting on multiple subtypes of NP, and various and multiple outcomes. This resulted in a total of 38 outcomes in all studies, where predictive relations were studied in 13 and associative relations in 25 (**Figure 2**). Follow-up duration ranged from 48 hours up to 5 years after LVAD implantation. Study sample sizes ranged from 14 to 15,138 patients. Natriuretic peptides were extracted from various materials (blood or plasma), measured with different assays, and presented in diverse measuring units. The upper

TABLE 2 | Baseline characteristics and outcomes of included studies for all-cause mortality.

References	NP	Timing NP days	Design *N*	LVAD/CF *N (%)*	DT/BTT *N (%)*	Male gender *N (%)*	Age years	ICM *N (%)*	FU days	Definition outcome mortality	Statistics	Relation NPs—mortality
Predictive relation												
Papathanasiou et al. (28)	BNP- Log pg/ml	2	RS 103	103 (100) 103 (100)	69 (67) 34 (33)	82 (80)	59 (11)†	56 (54)	180	All-cause mortality	HR, 95%CI HR, 95%CI	1.27 (0.94–1.71) $p = 0.12$ 1.35 (0.92–1.96)‡ $p = 0.12$
										All-cause mortality or rehospitalization	HR, 95%CI HR, 95%CI	*1.10 (0.87–1.37)* *$p = 0.45$* *1.00 (0.76–1.33)*‡ *$p = 0.98$*
Sato et al. (29)	BNP- Log pg/ml	1	RS 83	83 (100) 18 (22)	83 (100) 0 (0)	63 (76)	39 ± 12	3 (4)	90	All-cause mortality	HR, 95%CI	1.00 (0.99–1.00) $p = 0.673$
Yoshioka et al. (30)	BNP pg/ml	-	RS 41	41 (100) 6 (15)	0 (0) 41 (100)	29 (71)	39 ± 2	3 (7)	90	All-cause mortality	OR, 95%CI	1.00 (0.99–1.00) $p = 0.246$
Shiga et al. (31)	BNP pg/ml	-	RS 47	47 (100) 0 (0)	0 (0) 47 (100)	35 (75)	39 ± 15	12 (26)	730	All-cause mortality	OR, 95%CI	1.000 (1.000–1.001) $p = 0.576$
	BNP ≥1,000 pg/ml										OR, 95%CI	1.143 (0.382–3.421) $p = 0.812$
Topilsky et al. (32)	NT-proBNP per 100 increase pg/ml	1	R- 83	83 (100) 83 (100)	56 (67) 27 (23)	81 (98)	63 ± 12	45 (54)	30	Mortality	OR, 95%CI	1.03 (1.01–1.06) **$p = 0.003$**
Associative relation												**Survivors vs. non-survivors Median (range)**
Cabiati et al. (33)	NT-proBNP pg/ml	Hospital admission	RS 17	17 (100) 17 (100)	- -	16 (94)	51 (47–63)†	5 (28)	28	All-cause mortality	*χ2* test	986.10 vs. 5721.00 **$p = 0.028$**
	NT-proANP nmol/l	Hospital admission	RS 17	17 (100) 17 (100)	- -	16 (94)	51 (47–63)†	5 (28)	28	All-cause mortality	*χ2* test	8.04 vs. 11.20 $p = 0.832$
	NT-proCNP pg/ml	Hospital admission	RS 17	17 (100) 17 (100)	- -	16 (94)	51 (47–63)†	5 (28)	28	All-cause mortality	*χ2* test	85.92 vs. 52.07 $p = 0.322$

Age in years is described in Mean ± SD, except for † Median (range).

‡ Adjusted for age, male gender, DT, EF, creatinine, CKD, ECLS, IABP, invasive ventilation, inotropes.

BNP, B-type natriuretic peptide; BTT, bridge to transplant; CKD, chronic kidney disease; CF, continuous flow; CI confidence interval; DT, destination therapy; ECLS, Extra Corporeal Life Support; EF, ejection fraction; FU, follow up; HR, hazards ratio; IABP, intra-aortic balloon pump; ICM, ischemic cardiomyopathy; Log, log transformed, LVAD, left ventricular assist device; NP, natriuretic peptide; NT-proBNP; N-terminal pro-B-type NP; N, number; OR, odds ratio; R, retrospective cohort; S, single center; SD, standard deviation; vs., versus.
The bold p-values indicate statistical significance.

TABLE 3 | Baseline characteristics and outcomes of included studies for right ventricular failure.

References	NP	Timing NP days	Design *N*	LVAD/CF *N (%)*	DT/BTT *N (%)*	Male gender *N (%)*	Age years	ICM *N (%)*	FU *Days*	Definition outcome RVF	Statistics	Relation NPs—RVF
Predictive relation												
Shiga et al. (34)	BNP- Log pg/ml BNP ≥1,200 pg/ml	-	RS 79	79 (100) 20 (25)	0 (0) 79 (100)	58 (73)	39 ± 14	14 (18)	PO	ECMO, or need for RVAD	OR, 95%CI OR, 95%CI	1.001 (1.000–1.001) **$p = 0.043$** 8.409 (0.922–76.73) $p = 0.059$
Kato et al. (35)	BNP >1,232 ng/ml	≤5	RS 61	61 (100) 30 (49)	- -	52 (85)	54 ± 13	25 (41)	2–14	NO inhalation >48 h, and/or restarting/ inotropic support >14 days, or need for RVAD	OR, 95%CI OR, 95%CI	1.021 (1.000–1.042) **$p = 0.035$** 1.021(1.000–1.027)‡ **$p = 0.0357$**
Loghmanpour et al. (36)	proBNP -	-	RM 10909	10909 (100) 10909 (100)	3811 (35) 6901 (63)	8,606 (78)	(50–69)†	4,466 (41)	2–14	Pharmacological management of RVF/PVR, or need for RVAD	Bayesian model; 176 variables	**6th most powerful predictor out of 176**
Potapov et al. (37)	NT-proBNP >10,000 pg/ml	1	R- 54	54 (100) 37 (69)	- -	49 (91)	52 (32–69)†	6 (11)	2	In absence of cardiac tamponade 2 criteria, MAP ≤55 mmHg, CVP ≥16 mmHg, mixed VS ≤55%, CI <2 L/min/m^2, IS >20 h, or need for RVAD	OR, 95%CI	1 (1–1.002) $p = 0.1$
Associative relation												**RVF vs. no RVF Mean ± SD**
Kapelios et al. (38)	BNP pg/ml	-	RS 20	20 (100) 20 (100)	20 (100) 0 (100)	19 (95)	54 ± 10	12 (60)	1,241 ± 694*	>1 year: inotrope: iv or inhaled vasodilator (>7days), tqo of the four criteria; CVP >18 mmHg or mean RAP >18 mmHg, CI <2.3 L/min/m^2, ascites/ peripheral edema, CVP>, or need for RVAD	Paired t-test	1,819 ± 1,492 vs. 1,359 ± 1,611 $p = 0.52$
Kato et al. (35)	BNP pg/ml	≤5	RS 61	61 (100) 30 (49)	- -	52 (85)	54 ± 13	25 (41)	2–14	NO inhalation >48 h, and/or restarting/ inotropic support >14 days, or need for RVAD	Paired t-test	1895.1 ± 1551.1 vs. 1250.5 ± 1045.2 $p = 0.0572$
Shiga et al. (34)	BNP- Log pg/ml	-	RS 79	79 (100) 20 (25)	0 (0) 79 (100)	58 (73)	39 ± 14	14 (18)	PO	ECMO, or need for RVAD	$\chi 2$ test	7.55 ± 0.60 vs. 6.76 ± 0.90 **$p = 0.041$**
Deswarte et al. (39)	BNP pg/ml	-	RM 14	14 (100) 14 (100)	14 (100) 0 (0)	-	63 (37–69)†	7 (50)	30	Inotropic support ≤14days, death caused by RVF, or need for RVAD	Mann-Whitney *U*-test	1,792 (992–8,500) vs. 1,710 (701–3,643)§ $p > 0.05$#
Pettinari et al. (40)	proBNP -	-	R- 59	59 (100) 59 (100)	4 (7) 55 (93)	53 (90)	48 ± 15	31 (52)	PO	Need for RVAD	Mann-Whitney *U*-test	11,034 ± 9,620 vs. 4,667 ± 3,082 $p = 0.06$

(Continued)

TABLE 3 | Continued

References	NP	Timing NP days	Design N	LVAD/CF N (%)	DT/BTT N (%)	Male gender N (%)	Age years	ICM N (%)	FU Days	Definition outcome RVF	Statistics	Relation NPs—RVF
Hennig et al. (41)	NT-proBNP pg/ml	1	RS	40 (100)	0 (0)	38 (95)	54 ± 13	-	2	In absence of cardiac tamponade two criteria: MAP ≤55 mmHg, CVP ≥16 mmHg, mixed VS ≤55%, CI <2 L/min/m^2, IS >20 h; or need for RVAD	Mann-Whitney *U*-test or $\chi 2$ test	17,174 vs. 6,322[†] ***p* = 0.032**
			40	22 (55)	40 (100)							
Potapov et al. (37)	NT-proBNP pg/ml	1	R-	54 (100)	–	49 (91)	52 (32–69)[†]	6 (11)	2	In absence of cardiac tamponade two criteria: MAP ≤55 mmHg, CVP ≥16 mmHg, mixed VS ≤55%, CI <2 L/min/m^2, IS >20 h; or need for RVAD	Mann-Whitney *U*-test or t-test	13,026 (8,800–17,566) vs. 4,699 (925–10,433)[†] ***p* = 0.003**
			54	37 (69)	–							

Age in years is described in Mean ± SD, except for [†]Median (range).
[‡]Adjusted for PAP, RAP, RVSWI, tBili, RV FAC, serum OPN.
[*]Mean ± SD.
[§]Mean (interquartile range).
[#]Exact p-value unknown.
BNP, B-type natriuretic peptide; BTT, bridge to transplant; CF, continuous flow; CI, cardiac index; CI confidence interval; CVP, central venous pressure; DT, destination therapy; ECMO, Extracorporeal membrane oxygenation; FU, follow up; h, hours; HR, hazards ratio; ICM, ischemic cardiomyopathy; IS, inotropic support; Log, log transformed, LVAD, left ventricular assist device; M, multicenter; MAP, mean arterial pressure; N, number; NO, nitric oxide; NP, natriuretic peptide; NT-proBNP; N-terminal pro-B-type NP; OPN, osteopontin; OR, odds ratio; PAP, pulmonary artery pressure; PO, postoperative; PVR, pulmonary vascular resistance; R, retrospective cohort; RVAD, right ventricular assist device; RVF, right ventricular failure; RV FAC, right ventricular fractional area change; RVSWI, right ventricular stroke work index; S, single center; SD, standard deviation; tBili, total bilirubin concentration; vs., versus; VS, venous saturation.
The bold p-values indicate statistical significance.

cut off levels for normal NP levels varied from one study to the other. It should be pointed out that NP levels, unless log transformed, are non-normal distributed. Nevertheless, several studies included in this review chose to report NP levels non-log transformed. Descriptive statistic, mean ± standard deviation (SD), was used for log transformed NP measurements. Median and (interquartile) range was used for non-log transformed NP measurements. Groups were compared using various analyses depending on how continuous variables were expressed and how many groups were compared. Univariate and multivariate Cox regression was used for survival analyses expressed in hazard ratio. Univariate and multivariate logistic regression was used to estimate the strength of the effect of NPs expressed in odds ratio. The quality assessed by the NOS was "good" in all studies (**Supplementary Material 2**).

Study Results

The 24 studies assessing the relation between NP levels before LVAD implantation and all-cause mortality, RVF, MAEs, and myocardial recovery after implantation are summarized in **Tables 2–5**.

All-Cause Mortality

Five studies analyzed the predictive value of NPs for all-cause mortality, of which 4 studies included BNP and 1 study included NT-proBNP (**Table 2**). None of the studies found BNP levels before LVAD implantation predictive of all-cause mortality (28–31). In contrast, NT-proBNP levels before LVAD implantation were predictive of 30-days all-cause mortality (32). The study by Cabiati et al. looked at an associative relation and found that NT-proBNP was associated with 4-weeks all-cause mortality, while NT-proANP and NT-proCNP were not (33).

Right Ventricular Failure

Four studies assessed the predictive value of NPs for RVF (two studies BNP, one study proBNP, and one study NT-proBNP) (**Table 3**) (34–37). All studies had at least the outcome "need for right ventricular assist device (RVAD)." Study sample size was 54–79, with the exception of the study by Loghmanpour et al. with a large study population of $N = 10{,}909$ (34–37). The two studies analyzing BNP demonstrated that BNP levels before LVAD implantation were predictive of the need of RVAD postoperatively up to 14 days (34, 35). In the study of Shiga et al. it was demonstrated that BNP levels ≥1,200 pg/ml were not predictive of RVF, while in the study by Kato et al. BNP levels ≥1,232 ng/ml were an independent predictor of RVF after 2–14 days (34, 35). In a Bayesian prediction model, proBNP levels had high predictive value for RVF in 2–14 days after LVAD implantation (36). NT-proBNP levels before LVAD implantation were not predictive of RVF within 48 hours post-operatively (37). Importantly, this study by Potapov et al. used a cut-off value of NT-proBNP >10,000 pg/ml (37). Of the seven studies analyzing an associative relation, four analyzed BNP, one analyzed proBNP, and two analyzed NT-proBNP (34, 35, 37–41). Shiga et al. found that BNP levels were associated with "need for RVAD" within the postoperative period (34). Both Hennig et al. and Potapov et al. found that NT-proBNP was associated with RVF within 48 hours

TABLE 4 | Baseline characteristics and outcomes of included studies for major adverse events.

References	NP	Timing NP days	Design *N*	LVAD/CF *N (%)*	DT/BTT *N (%)*	Male gender *N (%)*	Age years	ICM *N (%)*	FU *Days*	Definition outcome MAEs	Statistics	Relation NPs—MAEs
Predictive Relation												
Truby et al. (42)	BNP >500 ng/l	-	RM 10603	10,279 (97) 10,603 (100)	4,474 (42) 6,047 (57)	8,246 (78)	>60 (45)*	4,738 (45)	730	Moderate or severe AR	HR, 95%CI	1.48 (1.23–1.77) **$p < 0.001$**
Hellman et al. (43)	BNP max. pg/ml	122	RS 74	74 (100) 74 (100)	- -	49 (66)	56	30 (41)	15	VA: VF, VT, or asymptomatic NSVT	OR, 95%CI	1.5–5.1‡ **$p = 0.0008$**
Hasin et al. (44)	NT-proBNP per 1,000 increase pg/ml	Hospital admission	RS 88	115 (100) 115 (100)	73 (63) 42 (37)	96 (83)	62 (53–69)†	56 (49)	511 ± 329#	**Less** rehospitalization: Cardiac (VA, HF, chest pain), bleeding, infection, thrombosis, pump related, biliary, elective, other	HR, 95%CI HR, 95%CI	0.98 (0.96–0.99) **$p = 0.022$** 0.98 (0.96–1.00)§ **$p = 0.022$**
Associative Relation												**Outcome vs. no outcome Median (range)**
Truby et al. (42)	BNP ng/l	-	RM 10603	10,279 (97) 10,603 (100)	4,474 (42) 6047 (57)	8,246 (78)	>60 (45)*	4,738 (45)	730	Moderate or severe AR	Kruskal-Wallis test	915 (489–1783) vs. 756 (382–1421) **$p = 0.001$**
Hegarova et al. (45)	BNP ng/l	1	PS 136	136 (100) 136 (100)	0 (0) 136 (100)	121 (89)	51 (23–72)†	54 (40)	298 (159–456)†	**Less** adverse events; HF, infection, pump thrombosis	Mann-Whitney *U*-test	1440.4 vs. 2405.5# **$p = 0.001$**
	BNP ng/l	1	PS 59	59 (100) 59 (100)	0 (0) 59 (100)	51 (86)	51 (23–72)†	23 (39)	298 (159–456)†	Rehospitalization	Mann-Whitney *U*-test	1118.7 vs. 1762.1# $p = 0.056$
Hellman et al. (43)	BNP pg/ml	122	RS 74	74 (100) 74 (100)	- -	49 (66)	56	30 (41)	15	VA: VF, VT, or asymptomatic NSVT	Mann-Whitney *U*-test	2,373 vs. 1,309 **$p = 0.0016$**
Hasin et al. (46)	NT-proBNP pg/ml	Hospital admission	RS 72	72 (100) 72 (100)	- 21 (29)	63 (87)	63 (53–69)†	36 (50)	14	Complicated postoperative stay: IC > 5days, ventilator support > 2days, total hospital stay >14 days	Mann-Whitney *U*-test	4,786 (2,232–13,790) vs. 3,199 (869–11,803) $p = 0.224$
	NT-proBNP Log pg/ml											1.14 (0.46–2.16) vs. 1.09 (0.32–3.30)‡‡ $p = 0.725$
	NT-proBNP pg/ml	1	RS 72	72 (100) 72 (100)	- 21 (29)	63 (87)	63 (53–69)†	36 (50)	14	Complicated postoperative stay: IC >5 days, ventilator support >2 days, total hospital stay >14 days	Mann-Whitney *U*-test	3,446 (1,801–8,101) vs. 3,431 (932–5,113) $p = 0.187$
	NT-proBNP Log pg/ml											1.11 (0.52–2.72) vs. 0.98 (0.49–2.16)‡‡ $p = 0.410$
Hasin et al. (44)	NT-proBNP Per 1,000 expressed pg/ml	Hospital admission	RS 115‡	115 (100) 115 (100)	73 (63) 42 (37)	96 (83)	62 (53–69)†	56 (49)	511 ± 329#	**Less** rehospitalization: Cardiac (VA, HF, chest pain), bleeding, infection, thrombosis, pump related, biliary, elective, other	Wilcoxon signed rank test	4.3 (2.4–8.3) vs. 4.7 (3.0–8.1) $p = 0.022$

*Age in years is described in Mean ± SD, except for *Percentage with age > 60 years and †Median (range).*

‡Adjusted for VT in the past, ICD, CAD, and age.

§Adjusted for referral zone, neighboring states, and hemoglobin.

#Mean ± SD.

‡‡Adjusted for age, gender, and glomerular filtration rate.

AR, aortic regurgitation; BNP, B-type natriuretic peptide; BTT, bridge to transplant; CAD, coronary artery disease; CF, continuous flow; CI confidence interval; DT, destination therapy; FU, follow up; HF, heart failure; HR, hazards ratio; IC, intensive care; ICD, internal cardiac defibrillator; ICM, ischemic cardiomyopathy; Log, log transformed, LVAD, left ventricular assist device; M, multicenter; MAEs, major adverse events; Max, maximal level measured; NP, natriuretic peptide; NT-proBNP; N-terminal pro-B-type NP; N, number; OR, odds ratio; P, prospective cohort; R, retrospective cohort; S, single center; SD, standard deviation; VA, ventricular arrhythmia; VF, ventricular fibrillation; (NS)VT, non-sustained ventricular tachycardia; vs., versus.

The bold p-values indicate statistical significance.

TABLE 5 | Baseline characteristics and outcomes of included studies for left ventricular (LV) myocardial recovery.

References	NP	Timing NP Days	Design *N*	LVAD/CF *N (%)*	DT/BTT *N (%)*	Male gender *N (%)*	Age *Years*	ICM *N (%)*	FU *Days*	Definition outcome Myocardial recovery	Statistics	Relation NPs—Myocardial recovery
Predictive relation												
Imamura et al. (47)	BNP- Log pg/ml	1	RS 27	27 (100) 22 (81)	0 (0) 27 (100)	21 (78)	35 ± 14	0 (0)	183	LVRR (EF ≥35%)	OR, 95%CI	0.753 (0.021–27.17) $p = 0.877$
Associative relation												**Myocardial recovery vs. no myocardial recovery Mean ± SD**
Topkara et al. (6)	BNP pg/ml	-	RM 13454	13,454 (100) 13,454 (100)	5,257 (39) 3,714 (28)	10,567 (79)	51.5 ± 13	6,241 (46)	1,096	Device explant vs. no device explant	Unpaired *t*-test	926.7 ± 860.9 vs. 1169.9 ± 1097.6 **$p = 0.024$**
			RM 8805	8,805 (100) 8,805 (100)	351 (46)	6,918 (79)	57.1 ± 14	3942 (29)	1,096	LVRR (EF ≥40%) vs. no LVRR (EF <30%)	Unpaired *t*-test	1240.9 ± 149.5 vs. 1157.4 ± 1086.1 $p = 0.199$
	proBNP pg/ml	-	RM 13454	13,454 (100) 13,454 (100)	241 (32) 5,257(39)	10,567 (79)	51.5 ± 13	6241 (46)	1,096	Device explant vs. no device explant	Unpaired *t*-test	4642.4 ± 7323.3 vs. 6787.2 ± 7887.3 $p = 0.153$
			RM 8805	8,805 (100) 8,805 (100)	3,714 (28) 351 (46) 241 (32)	6,918 (79)	57.1 ± 14	3942 (29)	1,096	LVRR (EF ≥40%) vs. no LVRR (EF <30%)	Unpaired *t*-test	9880.8 ± 11664.4 vs. 6617.3 ± 7737.5 **$p = 0.003$**
Wever-Pinzon et al. (48)	BNP pg/ml	-	RM 15138	14,287 (94) 13,987 (92)	5601 (37) 4,284 (28)	11,877 (78)	50	27 (14)	1,826	Device explant or deactivation	X^2 test	742 (377-1090) vs. 825 (412-1565)* $p = 0.10$
Imamura et al. (47)	BNP- Log pg/ml	1	RS 27	27 (100) 22 (81)	0 (0) 27 (100)	21 (78)	35 ± 14	0 (0)	183	LVRR (EF ≥35%)	Unpaired *t*-test	2.8 ± 0.2 vs. 2.8 ± 0.3 $p = 0.882$
Imamura et al. (49)	BNP- Log pg/ml	1	R-60	60 (100) 34 (57)	0 (0) 60 (100)	48 (80.0)	40.1 ± 12	0 (0)	183	LVRR (EF ≥35%) or device explant	Unpaired *t*-test	2.92 ± 0.30 vs. 2.89 ± 0.36 $p = 0.793$
Mano et al. (50)	BNP pg/ml	–	RS 41	41 (100) 0 (0)	0 (0) 41 (100)	28 (68)	30.1 ± 10	0 (0)	365	Device explant	Unpaired *t*-test	1140 ± 660 vs. 1282 ± 1074 $p = 0.76$

Age in years is described in Mean ± SD.

**Median (IRQ).*

BNP, B-type natriuretic peptide; BTT, bridge to transplant; CF, continuous flow; CI confidence interval; DT, destination therapy; FU, follow up; HR, hazards ratio; IQR, inter quartile range; ICM, ischemic cardiomyopathy; Log, log transformed, LVAD, left ventricular assist device; LVRR, left ventricular reverse remodeling; M, multicenter; NP, natriuretic peptide; NT-proBNP; N-terminal pro-B-type NP; N, number; OR, odds ratio; R, retrospective cohort; S, single center; SD, standard deviation; vs., versus.

The bold p-values indicate statistical significance.

postoperatively (37, 41). The remaining studies did not find an association between NP levels and RVF, although in some studies results were close to statistical significance (35, 38–40).

Major Adverse Events

A total of five studies assessed the predictive or associative relation between NPs and MAEs. The following MAEs were identified in these studies: VA, AR, "combined adverse events" (including episode of VA, HF, chest pain, bleeding, infection, thrombosis, pump-related problems, biliary disfunction, elective procedures), complicated postoperative stay, and all-cause rehospitalization. Three studies analyzed whether NPs were predictive of MAEs, of which two studies assessed BNP and one study assessed NT-proBNP (**Table 4**). All studies found that BNP and NT-proBNP levels before LVAD implantation were predictive of MAEs (42–44). Hellman et al. demonstrated that BNP was an independent predictor for VA within 15 days post-operative (43). In a large study by Truby et al. BNP >500 ng/l was predictive of the development of moderate or severe AR (42). NT-proBNP measured at "hospital admission" before LVAD implantation was an independent predictor for rehospitalization due to cardiac, bleeding, infection, thrombosis, pump related, biliary, or "elective" events (44). Of the studies reporting on associative relations, three studies analyzed BNP levels and two studies analyzed NT-proBNP levels (42, 44–46). In these studies, BNP levels before LVAD implantation were associated with MAEs between 2 weeks up to 2 years (42, 43, 45). In a sub-analysis, Hegarova et al. demonstrated that although BNP was associated with adverse events up to 1.5 years after initial discharge, it was not associated with subsequent rehospitalizations (45). The two studies analyzing NT-proBNP levels found that it was not associated with complicated post-operative stay. However, it was associated with less rehospitalization for combined adverse events (44, 46).

Myocardial Recovery

Only one study assessed the predictive value of NP for myocardial recovery (**Table 5**). This study found that BNP levels before LVAD implantation were not predictive of LV recovery after 6 months (47). Five studies reported on associative relations between NP and myocardial recovery. All studies analyzed BNP levels, whereas Topkara et al. additionally investigated proBNP levels. Besides the large study by Topkara et al. none of the included studies found an association between BNP and LV recovery (6, 47–50).

DISCUSSION

To the best of our knowledge, this is the first systematic review assessing the prognostic value of circulating NP levels in advanced HF patients receiving LVAD therapy. The main findings are as follows:

1. B-type natriuretic peptide is not predictive of all-cause mortality at a follow-up of 3 months or longer. Evidence regarding NT-proBNP is insufficient to draw a reliable conclusion.
2. B-type natriuretic peptide is predictive of RVF in the postoperative period after the first 48 hours. In contrast, NT-proBNP seems associated with RVF within 48 hours after LVAD implantation.
3. B-type natriuretic peptide and NT-proBNP levels appear to be predictive of various MAEs, and related to rehospitalization up to 1.5 years after LVAD implantation.
4. B-type natriuretic peptide is not predictive of, and most likely not associated with, myocardial recovery.

All-Cause Mortality

None of the studies found that BNP levels before LVAD implantation are predictive of all-cause mortality up to 2 years after implantation. In contrast, Topilsky et al. demonstrated that preoperative NT-proBNP levels are predictive of 1-month mortality after LVAD implantation (32). The study by Papathanasiou et al. analyzing BNP, had a similar study sample size and baseline characteristics compared to the study by Topilsky et al., but did not report a significant predictive relation (28). The differences in type of NPs and length of follow-up may have contributed to this contradictory finding. The follow-up duration may be an important factor, as both studies analyzing 1-month mortality found a significant relation (32, 33). This may suggest that NPs are related to early postoperative mortality, but lose their prognostic value for all-cause mortality at longer follow-up. Of note, both studies analyzed NT-proBNP, and to date no studies are available analyzing BNP levels in relation to 1-month mortality after LVAD implantation. Whether BNP and NT-proBNP have different prognostic power regarding all-cause mortality after LVAD implantation needs to be investigated in future prospective studies.

In the studies included in this review, BNP levels are not predictive of all-cause mortality after LVAD implantation. This is an interesting finding, since NPs (including BNP and NT-proBNP) are strong predictors of all-cause mortality in HF patients (2, 20–22). In addition, BNP levels are independent predictors of mortality in advanced HF patients receiving cardiac resynchronization defibrillator (CRT-D) therapy (51, 52). It may well be that NPs are not so much a predictor of mortality risk after LVAD implantation, but rather a reflection of disease severity. Furthermore, the change in prognostic value of NPs may be caused by several mechanisms related to the LVAD itself. The device unloads the LV, thereby reducing pressure and stretch of cardiomyocytes. Reduced myocardial stretch may lead to lower NP levels. Decreased NP levels are related to a lower mortality risk (53). In parallel with the improvements in hemodynamics and prognosis provided by the LVAD, NT-proBNP levels decrease after LVAD implantation (27, 49). However, they remain abnormal and elevated compared to the levels in chronic HF patients, suggesting that key pathological changes on cellular myocardial level remain, despite LVAD support (49). This may partly be explained by the fact that the flow mechanisms of the devices, including lack of pulsatility and high rotation speed of the LVAD disc or propeller, influence several physiological processes connected to NPs, like neurohormonal changes and sympathetic and renin-angiotensin-aldosterone activity (27, 49, 51). These processes may result in altered NP release. Therefore,

the prognostic value of NP levels before LVAD implantation may be changed by the therapy itself. Nonetheless, several studies have shown that NP measurements and their fluctuations during LVAD therapy are strongly related to adverse outcome including mortality (28, 29, 45). These findings may suggest, that NP levels before implantation and during LVAD support may not have similar predictive value for all-cause mortality, as the hemodynamic support provided by the LVAD may change NP levels and the accompanied mortality risk.

Finally, another explanation for the lack of predictive value of NPs regarding all-cause mortality could be the erratic course of LVAD therapy. Major adverse event rates are high and correspond to high mortality rates. The studies included in this review that found no relation between NPs and all-cause mortality had a follow-up duration of 90, 180, and 730 days after LVAD implantation. Competing risk analyses should have been performed to account for the effect of MAEs on mortality. However, none of the studies included in this review provided these analyses. This statistic error could explain why in the included studies NPs are not predictive for mortality, but appear to have predictive value for various MAEs.

Right Ventricular Failure

Four studies investigated whether NP levels were predictive of RVF after LVAD implantation. Due to the large study by Loghmanpour et al. the sample size of the studies (BNP, proBNP) reporting a positive predictive value for RVF was 11.049 patients, whereas the total sample size of the studies (NT-proBNP) which reported no predictive value was 54 patients (34–37). All studies analyzing BNP and proBNP were predictive, whereas the study by Potapov et al. analyzing NT-proBNP was not. It should be noted that this is only one study with a small study population (37). Nevertheless, this finding may be linked to the type of NPs that was investigated. In addition, this could be explained by the follow-up duration. Potapov et al. investigated RVF within 48 hours postoperatively, whereas all other studies analyzed RVF after the first 48 hours post LVAD implantation (34–37). Furthermore, it should be noted that in all studies, the definition of RVF included "need for RVAD." Since the decision to use an RVAD after LVAD implantation may vary based on clinical practice, this may change the definition of outcome and thereby the prognostic value of NPs for prediction of RVF.

It is well-known that RVF after LVAD implantation severely impairs prognosis. In the INTERMACS registry, RVF represented the specific cause of death in 4% of all patients (4). The interaction between the LVAD, the right ventricle (RV), and NP system is complex. Preoperative elevated NP levels, inflammatory markers and cytokines may represent a worse hemodynamic status and therefore a higher susceptibility to RVF after LVAD implantation (41). At the same time, it has been suggested that elevations in neurohumoral markers and cytokines may directly influence RV function, contributing to the development of RVF (41).

One study included in our review analyzed late RVF after LVAD implantation, and found no relation of BNP levels before LVAD implantation to late RVF (mean follow-up of 3.4 years) (38). This may be explained by the fact that development of RVF during long-term support is most likely multi-factorial. Different from the LV, the RV does not exhibit significant reverse structural remodeling despite reduced RV afterload during LVAD support (54–56). Kato et al. demonstrated that the CF-LVAD impairs the physiological contractility of cardiomyocytes by the non-pulsatile mode of LV unloading, which over time could lead to decreased RV compliance and contractility (40, 57). Furthermore, interventricular septum displacement caused by suction of the CF-LVAD may result in RV dysynchrony and also reduced cooptation of the tricuspid valve. In long-term LVAD therapy, this may gradually increase tricuspid regurgitation and subsequent increase RV preload. Over time these factors could contribute to the development of late RVF (38). Future studies should address preoperative circulating NP levels in relation to these different factors, in order to better predict RVF during long-term LVAD support.

Major Adverse Events

In the INTERMACS registry, the most frequently reported MAEs after LVAD implantation are infection, neurologic events, RVF, device malfunction including pump thrombosis, and multiple system organ failure (4). However, apart from RVF, there were no studies available that assessed the relation between NPs and these specific MAEs. The studies included in this review assessed the relation between NP levels before LVAD implantation and MAEs including VA, AR, "combined adverse events," complicated postoperative stay, and all-cause rehospitalization. All studies that were included found that NP (BNP and NT-proBNP) levels before LVAD implantation are predictive of diverse MAEs occurring in the postoperative period within 15 days up to 2 years follow-up, and rehospitalizations within 1.5 year after LVAD implantation (42–44).

Ventricular Arrhythmia

Hellman et al. demonstrated that high BNP levels before LVAD implantation are a powerful predictor for VA up to 15 days (43). Several mechanisms may explain this finding. BNP levels reflect ventricular stretch and hypertrophy, which over time results in tissue fibrosis and other changes of the myocardium that may be a substrate for VA (58). The LVAD unloads the failing heart, but cannot initiate reverse remodeling within 15 days. Thus, the substrate for VA remains, as does the prognostic value of BNP before LVAD implantation. Another possible explanation may be that high BNP levels are associated with elevated levels of cytokines and catecholamines, resulting in prolongation of the action potential and enhanced calcium entry, causing QTc prolongation and promoting arrhythmogenesis, eventually triggering VA (43, 59).

Aortic Regurgitation

During CF-LVAD therapy, up to 15% of the patients may develop moderate to severe AR, with significant impact on morbidity and mortality (42). The study by Truby et al. identified BNP levels >500 ng/L as a predictor in a univariate analysis of a cox proportional hazard model for the development of moderate or severe AR after 2 years of LVAD therapy. However, BNP levels were not taken into account in the multivariate analysis

of AR development (42). Factors like body mass index, sex, and destination therapy strategy appear to be stronger predictors of development of moderate or severe AR than BNP levels (42). Nevertheless, this study points out that BNP identifies patients who are vulnerable for adverse events. In patients with AR, NPs are predictive of the development of HF and mortality (60). However, no studies are available that assess the prognostic value of NPs in relation to AR in (advanced) HF patients. Therefore, more studies are needed to get mechanistic insights into the relation between NPs and AR in HF patients receiving LVAD therapy.

Rehospitalization and Combined Adverse Events

Two studies analyzed rehospitalization after initial discharge, of which Hasin et al. found higher NT-proBNP before LVAD implantation predictive for, and associated with, less rehospitalization for any MAE (44). Hegarova et al. demonstrated that higher BNP levels were associated with less or no combined adverse events that required outpatient care or rehospitalization. In a sub-analysis, the authors found that BNP levels were not able to differentiate between combined adverse events that required rehospitalization and those that did not (45). Interestingly, both studies demonstrated that higher NP levels before LVAD implantation were related to less combined adverse events (44, 45). This finding may be related to the kind of MAE. Hasin et al. found that cardiac events (30.4%) including VA, HF, and chest pain, and bleeding events (29.6%) were the main reasons for rehospitalization, whereas Hegarova et al. found that pump thrombosis (29%) and decompensated HF (26%) were the most frequent adverse events (44, 45). These findings suggest that NP levels before LVAD implantation within a certain range may be predictive for rehospitalization of specific MAEs.

Myocardial Recovery

Among the articles considered in this systematic review, five studies investigated the relation of NPs with myocardial recovery. Imamura et al. demonstrated that BNP before LVAD implantation was not predictive for LV ejection fraction recovery (47). The study by Topkara et al. demonstrated that NP levels (BNP, proBNP) were associated with myocardial recovery, while the other studies did not (6, 47–50). The total sample size in the four studies that found no association was just slightly larger than the sample size of the one study that did, mainly due to the large studies by Topkara et al. (6) and Wever-Pinzon et al. (48). Both authors extracted their data from the INTERMACS registry, had comparable inclusion criteria, baseline characteristics, outcome and median follow-up. Nevertheless, they found conflicting results. This may be related to the fact that Wever-Pinzon et al. additionally included patients implanted with pulsatile-flow LVADs, and a relatively high number of INTERMACS level 1 patients, who were in critical cardiogenic shock at time of device implantation (48). The higher number of INTERMACS level 1 patients may explain the higher levels of BNP found within the recovery group, and may diminish the associative relation between lower levels of BNP and myocardial recovery. Taken together, these reports are indicative for the fact that NPs may not be a specific marker for cardiac recovery, but rather reflect the general physical condition and the severity of HF in advanced HF patients receiving LVAD therapy.

Limitations

Although we systematically assessed the evidence for NP and its role as prognostic biomarker in advanced HF patients who receive LVAD therapy, our study is not devoid of its own limitations. According to the NOS score, most studies included in our review were of good quality. However, a number of these studies had a small patient population and therefore low statistical power. The heterogenous nature of the data in terms of timing of NP measurements, subtypes of NP, follow-up time, statistical analyses, and end-points pre-empted us from performing a meta-analysis and derive definitive conclusions. In addition, in a number of studies included in this review, the predictive value of NPs in LVAD patients was not the main hypothesis. We were not able to asses all end-points because of limited literature, and several end-points had heterogenous and subjective definitions, such as "need for RVAD" for the definition of RVF. Although it is generally accepted that NP levels are influenced by gender, age, BMI, comorbidities, kidney disease, and HF medication, most studies did not take all variables into account. In addition, some bias was created as the manuscripts from the same authors, and several studies analyzing multiple subtypes of NP or end-points, were included.

Future Perspective

Given the high incidence of MAEs after LVAD implantation, optimization of patient selection is crucial in order to improve outcome after LVAD implantation. Circulating NP levels may have some power predicting MAEs, RVF and rehospitalization during LVAD therapy. However, new, more promising, circulating biomarkers have been identified for prognostication of MAEs and mortality in HF patients (15, 61–64). Multi-biomarker panels seem to improve the prognostic power of these biomarkers. Emdin et al. compared a multi-biomarker panel [NT-proBNP, soluble suppression of tumorigenicity-2 (sST2), high-sensitive troponin T (hs-TnT)] with a single biomarker (NT-proBNP). Relative risk for all-cause mortality was higher among patients with elevated levels of all multi-panel biomarkers compared to patients with elevated levels of a single biomarker (NT-proBNP, sST2, hs-TnT; RR 9.5 vs. NT-proBNP; RR 2.3, respectively) (65). Ahmad et al. showed that novel biomarkers, such as galectin-3 (GAL-3), ST2, growth differentiation factor-15 (GDF-15), high sensitive C-reactive protein (hs-CRP), and copeptin, when stratified by baseline NT-proBNP levels in their cohort of advanced HF patients, were more sensitive of maladaptive processes than traditional laboratory markers with established prognostic significance, such as red blood cell distribution width, creatinine, blood urea nitrogen, and sodium, which remained within normal limits (66). These studies show that novel biomarkers and their multi-biomarker panels may reflect disease severity more accurately than currently used metrics (65–67). In addition, these novel biomarkers provide a unique insight into the pathophysiologic changes of HF as they reflect the different maladaptive processes involved e.g., oxidative stress, fibrosis, and inflammation (68).

Therefore, novel biomarkers may be considered for screening of patients with advanced HF requiring CF-LVAD therapy, and monitoring of LVAD patients. The present systematic review demonstrates that in order to improve generalizability and interpretation, large prospective studies with predefined outcome, and follow-up duration analyzing preimplantation NPs, multi-biomarker panels and their changes over time are warranted. Validated assays in consecutive patients should be used, and detailed cardiovascular profiles should be created to systematically define pathologies contributing to the levels of NP and other circulating biomarkers.

CONCLUSIONS

This systematic review demonstrates that BNP levels before LVAD implantation are not predictive of all-cause mortality after LVAD implantation. The implantation of an LVAD appears to alter prognosis and NP levels to such an extent that prognosis for mortality stratified by NP levels before LVAD implantation is not applicable after LVAD implantation. However, NP levels appear to identify advanced HF patients who are at risk for postoperative RVF and MAEs, such VA, AR, and rehospitalization. More studies regarding the timing of NP measurements, using different subtypes of NPs within prospective cohorts with predetermined end-points and follow-up are needed to confirm the prognostic value of NPs in advanced HF patients who will receive LVAD therapy.

DATA AVAILABILITY STATEMENT

The original contributions presented in the study are included in the article/**Supplementary Material**, further inquiries can be directed to the corresponding author.

AUTHOR CONTRIBUTIONS

EJ: conceptualization: lead, formal analysis: lead, investigation: equal, methodology: equal, project administration: lead, software: equal, writing–original draft: lead, writing–review & editing: equal. JJ: conceptualization: lead, investigation: equal, methodology: equal, supervision: lead, writing-original draft: equal, writing–review & editing: equal. SB: conceptualization: lead, methodology: equal, supervision: equal, writing–original draft: equal, writing–review & editing: equal. MS: conceptualization: equal, supervision: equal, writing-original draft: equal, writing–review & editing: equal. LT: conceptualization: lead, formal analysis: equal, methodology: equal, supervision: lead, writing- original draft: lead, writing–review & editing: lead. All authors contributed to the article and approved the submitted version.

SUPPLEMENTARY MATERIAL

The Supplementary Material for this article can be found online at: https://www.frontiersin.org/articles/10.3389/fcvm.2021.699492/full#supplementary-material

REFERENCES

1. Ahmad T, Patel CB, Milano CA, Rogers JG. when the heart runs out of heartbeats: treatment options for refractory end-stage heart failure. *Circulation*. (2012) 125:2948–55. doi: 10.1161/CIRCULATIONAHA.112.097337
2. Yancy CW, Jessup M, Bozkurt B, Butler J, Casey DE Jr, Colvin MM, et al. 2017 ACC/AHA/HFSA focused update of the 2013 ACCF/AHA guideline for the management of heart failure: a report of the American college of cardiology/American heart association task force on clinical practice guidelines and the heart failure society of America. *J Am Coll Cardiol*. (2017) 70:776–803. doi: 10.1016/j.jacc.2017.04.025
3. Teuteberg JJ, Cleveland JC Jr, Cowger J, Higgins RS, Goldstein DJ, Keebler M, et al. The society of thoracic surgeons intermacs 2019 annual report: the changing landscape of devices and indications. *Ann Thorac Surg*. (2020) 109:649–60. doi: 10.1016/j.athoracsur.2019.12.005
4. Kormos RL, Cowger J, Pagani FD, Teuteberg JJ, Goldstein DJ, Jacobs JP, et al. The society of thoracic surgeons intermacs database annual report: evolving indications, outcomes, and scientific partnerships. *Ann Thorac Surg*. (2019) 107:341–53. doi: 10.1016/j.athoracsur.2018.11.011
5. Kirklin JK, Pagani FD, Kormos RL, Stevenson LW, Blume ED, Myers SL, et al. Eighth annual INTERMACS report: special focus on framing the impact of adverse events. *J Heart Lung Transplant*. (2017) 36:1080–6. doi: 10.1016/j.healun.2017.07.005
6. Topkara VK, Garan AR, Fine B, Godier-Furnemont AF, Breskin A, Cagliostro B, et al. Myocardial recovery in patients receiving contemporary left ventricular assist devices: results from the interagency registry for mechanically assisted circulatory support (INTERMACS). *Circ Heart Fail*. (2016) 9 e003157.doi: 10.1161/CIRCHEARTFAILURE.116.003157
7. Hon JK, Yacoub MH. Bridge to recovery with the use of left ventricular assist device and clenbuterol. *Ann Thorac Surg*. (2003) 75:S36–41. doi: 10.1016/S0003-4975(03)00460-0
8. Motiwala SR, Januzzi JL. The role of natriuretic peptides as biomarkers for guiding the management of chronic heart failure. *Clin Pharmacol Ther*. (2013) 93:57–67. doi: 10.1038/clpt.2012.187
9. Levin ER, Gardner DG, Samson WK. Natriuretic peptides. *NEJM*. (1998) 339:321–8. doi: 10.1056/NEJM199807303390507
10. Kinnunen P, Vuolteenaho O, Ruskoaho H. Mechanisms of atrial and brain natriuretic peptide release from rat ventricular myocardium: effect of stretching. *Endocrinology*. (1993) 132:1961–70. doi: 10.1210/endo.132.5.8477647
11. Weber M, Hamm C. Role of B-type natriuretic peptide (BNP) and NT-proBNP in clinical routine. *Heart*. (2006) 92:843–9. doi: 10.1136/hrt.2005.071233
12. Piek A, Du W, de Boer RA, Sillje HHW. Novel heart failure biomarkers: why do we fail to exploit their potential? *Crit Rev Clin Lab Sci*. (2018) 55:246–63. doi: 10.1080/10408363.2018.1460576
13. Savic-Radojevic A, Pljesa-Ercegovac M, Matic M, Simic D, Radovanovic S, Simic T. Novel biomarkers of heart failure. *Adv Clin Chem*. (2017) 79:93–152. doi: 10.1016/bs.acc.2016.09.002
14. Madamanchi C, Alhosaini H, Sumida A, Runge MS. Obesity and natriuretic peptides, BNP and NT-proBNP: mechanisms and diagnostic implications for heart failure. *Int J Cardiol*. (2014) 176:611–7. doi: 10.1016/j.ijcard.2014.08.007
15. Chow SL, Maisel AS, Anand I, Bozkurt B, de Boer RA, Felker GM, et al. Role of biomarkers for the prevention, assessment, and management of heart failure: a scientific statement from the American heart association. *Circulation*. (2017) 135:e1054–91. doi: 10.1161/CIR.0000000000000490
16. Myhre PL, Vaduganathan M, Claggett B, Packer M, Desai AS, Rouleau JL, et al. B-Type natriuretic peptide during treatment with sacubitril/valsartan:

the PARADIGM-HF trial. *J Am Coll Cardiol*. (2019) 73:1264–72. doi: 10.1016/j.jacc.2019.01.018
17. Saenger AK, Rodriguez-Fraga O, Ler R, Ordonez-Llanos J, Jaffe AS, Goetze JP, et al. Specificity of B-type natriuretic peptide assays: cross-reactivity with different BNP, NT-proBNP, and proBNP peptides. *Clin Chem*. (2017) 63:351–8. doi: 10.1373/clinchem.2016.263749
18. Lam CS, Burnett JC Jr, Costello-Boerrigter L, Rodeheffer RJ, Redfield MM. Alternate circulating pro-B-type natriuretic peptide and b-type natriuretic peptide forms in the general population. *J Am Coll Cardiol*. (2007) 49:1193–202. doi: 10.1016/j.jacc.2006.12.024
19. Hutfless R, Kazanegra R, Madani M, Bhalla MA, Tulua-Tata A, Chen A, et al. Utility of B-type natriuretic peptide in predicting postoperative complications and outcomes in patients undergoing heart surgery. *J Am Coll Cardiol*. (2004) 43:1873–9. doi: 10.1016/j.jacc.2003.12.048
20. Oremus M, Don-Wauchope A, McKelvie R, Santaguida PL, Hill S, Balion C, et al. BNP and NT-proBNP as prognostic markers in persons with chronic stable heart failure. *Heart Failure Rev*. (2014) 19:471–505. doi: 10.1007/s10741-014-9439-6
21. Doust JA, Pietrzak E, Dobson A, Glasziou PP. How well does B-type natriuretic peptide predict death and cardiac events in patients with heart failure: systematic review. *Brit Med J*. (2005) 330:625–7. doi: 10.1136/bmj.330.7492.625
22. Huang YT, Tseng YT, Chu TW, Chen J, Lai MY, Tang WR, et al. N-terminal pro b-type natriuretic peptide (NT-pro-BNP)–based score can predict in-hospital mortality in patients with heart failure. *Sci Rep*. (2016) 6:29590. doi: 10.1038/srep29590
23. Januzzi JL Jr, Maisel AS, Silver M, Xue Y, DeFilippi C. Natriuretic peptide testing for predicting adverse events following heart failure hospitalization. *Congest Heart Fail*. (2012) 18:S9–13. doi: 10.1111/j.1751-7133.2012.00306.x
24. Savarese G, Musella F, D'Amore C, Vassallo E, Losco T, Gambardella F, et al. Changes of natriuretic peptides predict hospital admissions in patients with chronic heart failure: a meta-analysis. *JACC: Heart Failure*. (2014) 2:148–58. doi: 10.1016/S0735-1097(14)60737-3
25. Kormos RL, Antonides CFJ, Goldstein DJ, Cowger JA, Starling RC, Kirklin JK, et al. Updated definitions of adverse events for trials and registries of mechanical circulatory support: a consensus statement of the mechanical circulatory support academic research consortium. *J Heart Lung Transplant*. (2020) 39:735–50. doi: 10.1016/j.healun.2020.03.010
26. Moskalewicz A, Oremus M. No clear choice between newcastle-ottawa scale and appraisal tool for cross-sectional studies to assess methodological quality in cross-sectional studies of health-related quality of life and breast cancer. *J Clin Epid*. (2020) 120:94–103. doi: 10.1016/j.jclinepi.2019.12.013
27. Berkman ND, Lohr KN, Morgan LC, Richmond E, Kuo TM, Morton S, et al. *Reliability Testing of The Ahrq Epc Approach to Grading The Strength of Evidence in Comparative Effectiveness Reviews*. Rockville: AHRQ Methods for Effective Health Care (2012).
28. Papathanasiou M, Pizanis N, Tsourelis L, Koch A, Kamler M, Rassaf T, et al. Dynamics and prognostic value of B-type natriuretic peptide in left ventricular assist device recipients. *J Thorac Dis*. (2019) 11:138–44. doi: 10.21037/jtd.2018.12.43
29. Sato T, Seguchi O, Iwashima Y, Yanase M, Nakajima S, Hieda M, et al. Serum brain natriuretic peptide concentration 60 days after surgery as a predictor of long-term prognosis in patients implanted with a left ventricular assist device. *ASAIO J*. (2015) 61:373–8. doi: 10.1097/MAT.0000000000000234
30. Yoshioka D, Sakaguchi T, Saito S, Miyagawa S, Nishi H, Yoshikawa Y, et al. Predictor of early mortality for severe heart failure patients with left ventricular assist device implantation: significance of INTERMACS level and renal function. *Circ J*. (2012) 76:1631–8. doi: 10.1253/circj.CJ-11-1452
31. Shiga T, Kinugawa K, Hatano M, Yao A, Nishimura T, Endo M, et al. Age and preoperative total bilirubin level can stratify prognosis after extracorporeal pulsatile left ventricular assist device implantation. *Circ J*. (2011) 75:121–8. doi: 10.1253/circj.CJ-10-0770
32. Topilsky Y, Oh JK, Shah DK, Boilson BA, Schirger JA, Kushwaha SS, et al. Echocardiographic predictors of adverse outcomes after continuous left ventricular assist device implantation. *JACC: Cardiovasc Imaging*. (2011) 4:211–22. doi: 10.1016/j.jcmg.2010.10.012
33. Cabiati M, Caruso R, Caselli C, Frigerio M, Prescimone T, Parodi O, et al. The natriuretic peptide time-course in end-stage heart failure patients supported by left ventricular assist device implant: focus on NT-proCNP. *Peptides*. (2012) 36:192–8. doi: 10.1016/j.peptides.2012.05.018
34. Shiga T, Kinugawa K, Imamura T, Kato N, Endo M, Inaba T, et al. Combination evaluation of preoperative risk indices predicts requirement of biventricular assist device. *Circ J*. (2012) 76:2785–91. doi: 10.1253/circj.CJ-12-0231
35. Kato TS, Chokshi A, Singh P, Khawaja T, Iwata S, Homma S, et al. Markers of extracellular matrix turnover and the development of right ventricular failure after ventricular assist device implantation in patients with advanced heart failure. *J Heart Lung Transplant*. (2012) 31:37–45. doi: 10.1016/j.healun.2011.10.007
36. Loghmanpour NA, Kormos RL, Kanwar MK, Teuteberg JJ, Murali S, Antaki JF. A bayesian model to predict right ventricular failure following left ventricular assist device therapy. *JACC Heart Fail*. (2016) 4:711–21. doi: 10.1016/j.jchf.2016.04.004
37. Potapov EV, Stepanenko A, Dandel M, Kukucka M, Lehmkuhl HB, Weng Y, et al. Tricuspid incompetence and geometry of the right ventricle as predictors of right ventricular function after implantation of a left ventricular assist device. *J Heart Lung Transplant*. (2008) 27:1275–81. doi: 10.1016/j.healun.2008.08.012
38. Kapelios CJ, Charitos C, Kaldara E, Malliaras K, Nana E, Pantsios C, et al. Late-onset right ventricular dysfunction after mechanical support by a continuous-flow left ventricular assist device. *J Heart Lung Transplant*. (2015) 34:1604–10. doi: 10.1016/j.healun.2015.05.024
39. Deswarte G, Kirsch M, Lesault PF, Trochu JN, Damy T. Right ventricular reserve and outcome after continuous-flow left ventricular assist device implantation. *J Heart Lung Transplant*. (2010) 29:1196–8. doi: 10.1016/j.healun.2010.05.026
40. Pettinari M, Jacobs S, Rega F, Verbelen T, Droogne W, Meyns B. Are right ventricular risk scores useful? *Eur J Cardiothorac Surg*. (2012) 42:621–6. doi: 10.1093/ejcts/ezs104
41. Hennig F, Stepanenko AV, Lehmkuhl HB, Kukucka M, Dandel M, Krabatsch T, et al. Neurohumoral and inflammatory markers for prediction of right ventricular failure after implantation of a left ventricular assist device. *Gen Thorac Cardiovasc Surg*. (2011) 59:19–24. doi: 10.1007/s11748-010-0669-9
42. Truby LK, Garan AR, Givens RC, Wayda B, Takeda K, Yuzefpolskaya M, et al. Aortic insufficiency during contemporary left ventricular assist device support: analysis of the INTERMACS registry. *JACC Heart Fail*. (2018) 6:951–60. doi: 10.1016/j.jchf.2018.07.012
43. Hellman Y, Malik AS, Lin H, Shen C, Wang IW, Wozniak TC, et al. B-type natriuretic peptide levels predict ventricular arrhythmia post left ventricular assist device implantation. *Artificial Organs*. (2015) 39:1051–5. doi: 10.1111/aor.12486
44. Hasin T, Marmor Y, Kremers W, Topilsky Y, Severson CJ, Schirger JA, et al. Readmissions after implantation of axial flow left ventricular assist device. *J Am Coll Cardiol*. (2013) 61:153–63. doi: 10.1016/j.jacc.2012.09.041
45. Hegarova M, Kubanek M, Netuka I, Maly J, Dorazilova Z, Gazdic T, et al. Clinical correlates of b-type natriuretic peptide monitoring in outpatients with left ventricular assist device. *Biomed Pap Med Fac Univ Palacky Olomouc Czech Repub*. (2017) 161:68–74. doi: 10.5507/bp.2017.003
46. Hasin T, Kushwaha SS, Lesnick TG, Kremers W, Boilson BA, Schirger JA, et al. Early trends in N-terminal pro-brain natriuretic peptide values after left ventricular assist device implantation for chronic heart failure. *Am J Cardiol*. (2014) 114:1257–63. doi: 10.1016/j.amjcard.2014.07.056
47. Imamura T, Kinugawa K, Nitta D, Kinoshita O, Nawata K, Ono M. Preoperative iodine-123 meta-iodobenzylguanidine imaging is a novel predictor of left ventricular reverse remodeling during treatment with a left ventricular assist device. *J Artif Organs*. (2016) 19:29–36. doi: 10.1007/s10047-015-0857-6
48. Wever-Pinzon O, Drakos SG, McKellar SH, Horne BD, Caine WT, Kfoury AG, et al. Cardiac recovery during long-term left ventricular assist device support. *J Am Coll Cardiol*. (2016) 68:1540–53. doi: 10.1016/j.jacc.2016.07.743
49. Imamura T, Kinugawa K, Hatano M, Fujino T, Muraoka H, Inaba T, et al. Preoperative beta-blocker treatment is a key for deciding left ventricular assist device implantation strategy as a bridge to recovery. *J Artificial Organs*. (2014) 17:23–32. doi: 10.1007/s10047-013-0748-7
50. Mano A, Nakatani T, Oda N, Kato T, Niwaya K, Tagusari O, et al. Which factors predict the recovery of natural heart function after insertion of a

left ventricular assist system? *J Heart Lung Transplant*. (2008) 27:869–74. doi: 10.1016/j.healun.2008.05.007
51. El-Saed A, Voigt A, Shalaby A. Usefulness of brain natriuretic peptide level at implant in predicting mortality in patients with advanced but stable heart failure receiving cardiac resynchronization therapy. *Clin Cardiol*. (2009) 32:E33–8. doi: 10.1002/clc.20490
52. Shalaby AA, Abraham WT, Fonarow GC, Bersohn MM, Gorcsan J III, Lee LY, et al. Association of BNP and troponin levels with outcome among cardiac resynchronization therapy recipients. *Pacing Clin Electrophysiol*. (2015) 38:581–90. doi: 10.1111/pace.12610
53. Zile MR, Claggett BL, Prescott MF, McMurray JJ, Packer M, Rouleau JL, et al. Prognostic implications of changes in n-terminal pro-B-type natriuretic peptide in patients with heart failure. *J Am Coll Cardiol*. (2016) 68:2425–36. doi: 10.1016/j.jacc.2016.09.931
54. Maybaum S, Mancini D, Xydas S, Starling RC, Aaronson K, Pagani FD, et al. Cardiac improvement during mechanical circulatory support–a prospective multicenter study of the LVAD working group. *Circulation*. (2007) 115:2497–505. doi: 10.1161/CIRCULATIONAHA.106.633180
55. Klotz S, Naka Y, Oz MC, Burkhoff D. Biventricular assist device-induced right ventricular reverse structural and functional remodeling. *J Heart Lung Transplant*. (2005) 24:1195–201. doi: 10.1016/j.healun.2004.08.005
56. Drakos SG, Wever-Pinzon O, Selzman CH, Gilbert EM, Alharethi R, Reid BB, et al. Magnitude and time course of changes induced by continuous-flow left ventricular assist device unloading in chronic heart failure: insights into cardiac recovery. *J Am Coll Cardiol*. (2013) 61:1985–94. doi: 10.1016/j.jacc.2013.01.072
57. Kato TS, Chokshi A, Singh P, Khawaja T, Cheema F, Akashi H, et al. Effects of continuous-flow versus pulsatile-flow left ventricular assist devices on myocardial unloading and remodeling. *Circulation Heart Fail*. (2011) 4:546–53. doi: 10.1161/CIRCHEARTFAILURE.111.962142
58. Tapanainen JM, Lindgren KS, Makikallio TH, Vuolteenaho O, Leppaluoto J, Huikuri HV. natriuretic peptides as predictors of non-sudden and sudden cardiac death after acute myocardial infarction in the beta-blocking era. *J Am Coll Cardiol*. (2004) 43:757–63. doi: 10.1016/j.jacc.2003.09.048
59. Vrtovec B, Knezevic I, Poglajen G, Sebestjen M, Okrajsek R, Haddad F. Relation of B-type natriuretic peptide level in heart failure to sudden cardiac death in patients with and without QT interval prolongation. *Am J Cardiol*. (2013) 111:886–90. doi: 10.1016/j.amjcard.2012.11.041
60. Pizarro R, Bazzino OO, Oberti PF, Falconi ML, Arias AM, Krauss JG, et al. Prospective validation of the prognostic usefulness of b-type natriuretic peptide in asymptomatic patients with chronic severe aortic regurgitation. *J Am Coll Cardiol*. (2011) 58:1705–14. doi: 10.1016/j.jacc.2011.07.016
61. Aimo A, Januzzi JL Jr, Bayes-Genis A, Vergaro G, Sciarrone P, Passino C, et al. Clinical and prognostic significance of sST2 in heart failure: JACC review topic of the week. *J Am Coll Cardiol*. (2019) 74:2193–203. doi: 10.1016/j.jacc.2019.08.1039
62. Barutaut M, Fournier P, Peacock WF, Evaristi MF, Dambrin C, Caubère C, et al. sST2 adds to the prognostic value of Gal-3 and BNP in chronic heart failure. *Acta Cardiol*. (2019) 75:739–47. doi: 10.1080/00015385.2019.1669847
63. Bettencourt P, Ferreira-Coimbra J, Rodrigues P, Marques P, Moreira H, Pinto MJ, et al. Towards a multi-marker prognostic strategy in acute heart failure: a role for GDF-15. *ESC Heart Fail*. (2018) 5:1017–22. doi: 10.1002/ehf2.12301
64. Salah K, Stienen S, Pinto YM, Eurlings LW, Metra M, Bayes-Genis A, et al. Prognosis and NT-proBNP in heart failure patients with preserved versus reduced ejection fraction. *Heart*. (2019) 105:1182–9. doi: 10.1136/heartjnl-2018-314173
65. Emdin M, Aimo A, Vergaro G, Bayes-Genis A, Lupón J, Latini R, et al. sST2 predicts outcome in chronic heart failure beyond NT-proBNP and high-sensitivity troponin T. *J Am Coll Cardiol*. (2018) 72:2309–20. doi: 10.1016/j.jacc.2018.08.2165
66. Ahmad T, Fiuzat M, Felker GM, O'Connor C. Novel biomarkers in chronic heart failure. *Nat Rev Cardiol*. (2012) 9:347–59. doi: 10.1038/nrcardio.2012.37
67. Mathieu K, Ibrahim E-B, Michael B, Martin B, Ibrahim A. Biomarkers in cardiomyopathies and prediction of sudden cardiac death. *Curr Pharm Biotechnol*. (2017) 18:472–81. doi: 10.2174/1389201018666170623125842
68. Frangogiannis NG. Cardiac fibrosis: cell biological mechanisms, molecular pathways and therapeutic opportunities. *Mol Aspects Med*. (2019) 65:70–99. doi: 10.1016/j.mam.2018.07.001

Conflict of Interest: The authors declare that the research was conducted in the absence of any commercial or financial relationships that could be construed as a potential conflict of interest.

frontiers in Cardiovascular Medicine

SYSTEMATIC REVIEW
published: 13 July 2021
doi: 10.3389/fcvm.2021.685904

The Diagnostic Value of Soluble ST2 in Heart Failure: A Meta-Analysis

Chaojun Yang[1†], Zhixing Fan[1†], Jinchun Wu[2†], Jing Zhang[1], Wei Zhang[3], Jian Yang[4†] and Jun Yang[1*]*

[1] Central Laboratory, Department of Cardiology, The First College of Clinical Medical Science, China Three Gorges University and Yichang Central People's Hospital, Yichang, China, [2] Department of Cardiology, Qinghai Provincial People's Hospital, Xining, China, [3] Department of Cardiology, Renmin Hospital of Wuhan University, Wuhan, China, [4] Department of Cardiology, The People's Hospital of Three Gorges University and The First People' s Hospital of Yichang, Yichang, China

OPEN ACCESS

Edited by:
Raffaele Maio,
University of Catanzaro, Italy

Reviewed by:
Zengjun Wang,
Nanjing Medical University, China
Chen Gao,
UCLA Department of Anesthesiology & Perioperative Medicine, United States

***Correspondence:**
Jian Yang
yangjian@ctgu.edu.cn
Jun Yang
yangjun@ctgu.edu.cn

[†] These authors have contributed equally to this work and share first authorship

Specialty section:
This article was submitted to General Cardiovascular Medicine, a section of the journal Frontiers in Cardiovascular Medicine

Received: 07 April 2021
Accepted: 10 June 2021
Published: 13 July 2021

Citation:
Yang C, Fan Z, Wu J, Zhang J, Zhang W, Yang J and Yang J (2021) The Diagnostic Value of Soluble ST2 in Heart Failure: A Meta-Analysis. Front. Cardiovasc. Med. 8:685904. doi: 10.3389/fcvm.2021.685904

Objective: The diagnostic performance of soluble suppression of tumorigenicity (sST2) in heart failure (HF) had been investigated in multiple studies, but the results were inconsistent. This meta-analysis evaluated the diagnostic value of sST2 in HF.

Methods: Pubmed, Web of Science, Embase, and Cochrane Library databases were searched until March 2021. Cohort studies or case-control studies relevant to the diagnostic value of sST2 in HF were screened, and true positive (TP), false positive (FP), false negative (FN), and true negative (TN) data were extracted for calculating sensitivity, specificity, positive likelihood ratio (PLR), negative likelihood ratio (NLR), diagnostic odds ratio (DOR), and area under the curve (AUC). The quality of the included studies was evaluated using the Quality Assessment of Diagnostic Accuracy Studies (QUADAS), the threshold effect was determined by calculating Spearman correlation coefficients and summary receiver operating characteristic (SROC) curve patterns, the heterogeneity was evaluated using the I^2 statistic and the Galbraith radial plot, and sensitivity analysis was also performed. Deeks' test was used to assess publication bias.

Results: A total of 11 studies from 10 articles were included in this meta-analysis. The Spearman correlation coefficient was 0.114, $p = 0.739$, and the SROC curve did not show a "shoulder-arm" shape, which suggests that there was no threshold effect, but study heterogeneity existed because of non-threshold effects. The combined sensitivity was 0.72 [95% confidence interval (CI): 0.65–0.78], specificity was 0.65 (95% CI: 0.45–0.81), PLR was 1.75 (95% CI: 1.33–2.31), NLR was 0.48 (95% CI: 0.37–0.63), DOR was 3.63 (95% CI: 2.29–5.74), and AUC was 0.75. The Deeks' test suggested no significant publication bias in the included studies ($P = 0.94$).

Conclusion: sST has some diagnostic value in HF, but this should be further evaluated in additional studies with rigorous design and high homogeneity.

Keywords: soluble suppression of tumorigenicity, heart failure, diagnostic value, sensitivity, specificity, meta-analysis

INTRODUCTION

Heart failure (HF) is a clinical syndrome of cardiac blood flow impairment caused by ventricular systolic or diastolic insufficiency. It is a global health concern with high morbidity and mortality and has seriously endangered human health (1). Currently, HF is diagnosed based on clinical symptoms, medical history, echocardiography, B-type natriuretic peptide (BNP), and N-terminal (NT)-proBNP (2). However, because of the atypical symptoms and signs of HF, the ancillary tests such as echocardiography and invasive hemodynamics are often limited by factors such as medical condition, and BNP or NT-proBNP levels are easily affected by age, sex, body size, and renal function, which makes the diagnosis and management of HF still a clinical challenge (3). Simple, sensitive, and specific techniques are required to assist in the diagnosis of HF, and HF-related biological markers are the current focus of HF diagnosis (4). Soluble suppression of tumorigenicity 2 (sST2), a marker associated with cardiomyocyte traction, is a potential pathophysiological mediator of myocardial hypertrophy and myocardial fibrosis and an important biomarker of HF (5). Several trials have now confirmed that sST2 levels are significantly elevated in patients with HF and that the elevated levels of sST2 correlate significantly with the degree of HF (6, 7). In recent years, more studies have been reported on the diagnosis of HF using sST2, but the results of these studies vary significantly. In this study, we intend to systematically evaluate the diagnostic value of sST2 in HF using meta-analysis.

DATA AND METHODS

Literature Search Strategy

For English databases Pubmed, Web of Science, Embase, and Cochrane Library, Heart failure, ST2, and diagnostic test were searched as the key words by the combination of medical subject headings (MeSH) and entry term. The literature search start date was not restricted, and the search end date was March 2021. The search language was only English. The following search strategy was used for pubmed and modified to suit other databases (the detailed retrieval strategy of other databases in **Supplementary Documents**):

#1 heart failure[MeSH Terms]
#2 ((((((((((((Cardiac Failure[Title/Abstract]) OR (Heart Decompensation[Title/Abstract])) OR (Decompensation, Heart[Title/Abstract])) OR (Heart Failure, Right-Sided[Title/Abstract])) OR (Heart Failure, Right Sided[Title/Abstract])) OR (Right-Sided Heart Failure[Title/Abstract])) OR (Right Sided Heart Failure[Title/Abstract])) OR (Myocardial Failure[Title/Abstract])) OR (Congestive Heart Failure[Title/Abstract])) OR (Heart Failure, Congestive[Title/Abstract])) OR (Heart Failure, Left-Sided[Title/Abstract])) OR (Heart Failure, Left Sided[Title/Abstract])) OR (Left-Sided Heart Failure[Title/Abstract])) OR (Left Sided Heart Failure[Title/Abstract]))) OR (HF)
#3 #1 OR #2
#4 ((((((Soluble suppression of tumorigenicity 2[Title/Abstract]) OR (Soluble suppression of tumorigenicity-2[Title/Abstract])) OR (suppression of tumorigenicity 2[Title/Abstract])) OR (suppression of tumorigenicity-2[Title/Abstract])) OR (sST2[Title/Abstract])) OR (ST2[Title/Abstract])) OR (soluble ST2[Title/Abstract])
#5 "sensitiv*"[Title/Abstract] OR "sensitivity and specificity"[MeSH Terms] OR ("predictive"[Title/Abstract] AND "value*"[Title/Abstract]) OR ("predictive value of tests"[MeSH Terms] OR ("predictive"[All Fields] AND "value"[All Fields] AND "tests"[All Fields]) OR "predictive value of tests"[All Fields]) OR "accuracy*"[Title/Abstract]
#6 #3 AND #4 AND #5.

Literature Inclusion and Exclusion Criteria

Literature inclusion criteria: (1) cohort studies or case-control studies investigating sST2 for the diagnosis of HF; (2) valid data available in the literature for the calculation of true positives (TPs), false positives (FPs), false negatives (FNs), and true negatives (TNs) to obtain information for a four-grid table; and (3) high quality studies using quality evaluation (see below). Exclusion criteria: (1) reviews, conference papers, and letters; (2) literature that cannot provide valid data for a four-grid table; (3) literature with duplicate data; (4) literature reporting results from animals or cellular models; (5) literature with too small a sample size ($n < 100$); (6) literature of low quality using quality evaluation. This systematic evaluation was performed by two authors who independently judged whether the retrieved literature could be included in the study, and the third author made an independent judgment whether to include it in case of disagreement.

Literature Quality Evaluation Criteria

The quality assessment of diagnostic accuracy studies (QUADAS) tool provided by the Cochrane Collaboration system was used to evaluate the quality of the literature. The QUADAS tool evaluates the four biases in terms of case selection, trials to be evaluated, gold standard, and flow, and it evaluates the quality of the literature by assessing 11 landmark questions and three types of clinical applicability questions. The 11 landmark issues were evaluated as "Yes" for clear fit, "Unclear" for unclear, and "No" for not meeting the conditions; the four biases were evaluated as "High risk" for clear bias, "Unclear" for unclear bias, and "Low risk" for no clear bias; and the three types of clinical applicability were evaluated as "High concern" for good matches, "Unclear" for unclear matches, and "Low concern" for poor matches. For each included study, two authors evaluated the quality independently, and the third author made an independent judgment in case of disagreement.

Data Extraction

The extracted information included the basic information of the study and the four-grid table information. The basic information included authors, year of publication, country, sample size, mean age, sST2 detection method, sST2 cut-off, HF diagnostic criteria, HF type, control population, and study type. TP, FP, TN, and

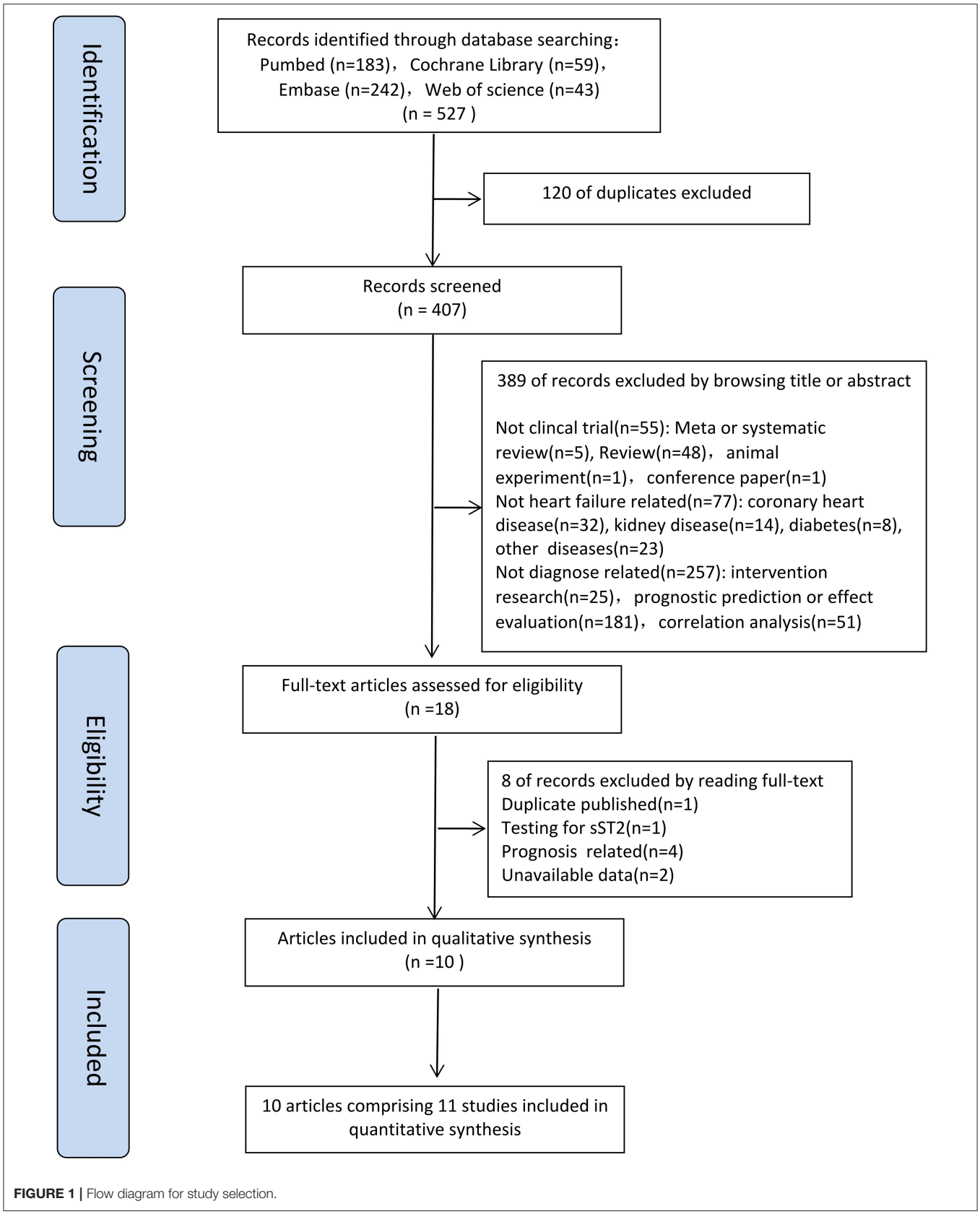

FIGURE 1 | Flow diagram for study selection.

TABLE 1 | Characteristics of the studies included in this meta-analysis.

No	References	Year	Country	Sample size	Male	Average age (year) HF/no HF	sST2 ELISAS kit source	Cut-off value	HF diagnostic criteria	Type of HF	Medical history of HF	Treatment history	Characteristics of controls	Type of research
1	Dieplinger et al. (8)	2009	Australia	251	234	72.82	MBL	121 ng/L	Framingham	HF	Arterial hypertension, diabetes mellitus	ACEI, ARB, calcium antagonist, β-blockers, digitalis, diuretics, amiodarone	ED patients with dyspnea	Cohort
2	Aldous et al. (9)	2012	New Zealand	995	591	66.00	-	34.3 U/mL	Chest radiograph evidence of pulmonary edema or symptoms of HF with raised BNP	HF	Ischemic heart disease, lung disease, stroke, Hypertension, dyslipidemia	-	ED patients with ischemic type pain	Cohort
3	Santhanakrishnan et al. (10)	2012	Singapore	100	52	66.00	Presage™	26.47 ng/mL	Framingham	HFPEF	Diabetes mellitus, hypertension, coronary artery disease, stroke	ACEI/ARB, Spironolactone, β-blocker, diuretics, digoxin, statin, aspirin,	Community adults	Case-Control
4	Santhanakrishnan et al. (10)	2012	Singapore	101	66	60.98	Presage™	30.32 ng/mL	Framingham	HFREF			Community adults	Case-Control
5	Wang et al. (11)	2013	Taiwan	107	57	65.08	R&D	13.5 ng/mL	Framingham	HFPEF	Diabetes, dyslipidemia, coronary artery disease, atrial fibrillation	Aspirin, nitrates, calcium channel blockers, ACEI/ARB, β-Blockers, diuretics, statins, antiarrythmic agents	Outpatients with hypertension	Cohort

(Continued)

TABLE 1 | Continued

No	References	Year	Country	Sample size	Male	Average age (year) HF/no HF	sST2 ELISAS kit source	Cut-off value	HF diagnostic criteria	Type of HF	Medical history of HF	Treatment history	Characteristics of controls	Type of research
6	Jakob et al. (12)	2016	Austria and UK	203		7.5	Presage™	44.4 pg/mL	Presence of HF symptoms and abnormal ventricular systolic function	HF	Dilated cardiomyopathy, functional single ventricle, pulmonary/right-sided obstruction, aortic/left-sided obstruction, ventricular septal defect, tetralogy of fallot, atrioventricular septal defect, patent arterial duct, hypertrophic cardiomyopathy, restrictive cardiomyopathy, atrial septal defect, mixed lesion/other	-	children without heart disease undergoing phlebotomy prior to an elective procedure	Case-Control
7	Mueller et al. (13)	2016	Austria	251	234	76/69	Presage™	26.5 ng/mL	Framingham	HF	Arterial hypertension, diabetes mellitus, atrial fibrillation, coronary artery disease	ACEI/ARB, calcium antagonists, β-blockers, digitalis, diuretics, amiodarone	dyspnoea attributed to other reasons	Cohort
8	Sinning et al. (14)	2016	Germany	4,972	2,526	67/55	Presage™	-	NYHA	HF	Diabetes, hypertension, dyslipidemi	-	Recruitment with no HF	Cohort

(Continued)

TABLE 1 | Continued

No	References	Year	Country	Sample size	Male	Average age (year) HF/no HF	sST2 ELISAS kit source	Cut-off value	HF diagnostic criteria	Type of HF	Medical history of HF	Treatment history	Characteristics of controls	Type of research
9	Jin et al. (15)	2017	China	303	200	61.89/60.31	Shanghai Research Institute for Enzyme-linked Biology	-	ESC Guidelines	HF	-	-	Healthy people	Case-Control
10	Luo et al. (16)	2017	China	876	460	67.49/65.93	–	0.159 μg/L	China Guidelines	HFPEF	Coronary heart disease, diabetes mellitus, hypertension, fatty liver, carotid plaque, gout	Antiplatelet drugs, ACEI/ARB, β-blockers, trimetazidine, diuretics, statins, digitalis	healthy individuals	Case-Control
11	Cui et al. (17)	2018	China	202	135	73/67	Shanghai Qiyi Biological Co.	68.6 pg/mL	ESC Guidelines	HFPEF	Hypertension, diabetes mellitus, coronary heart disease, Atrial fibrillation	β-blocker, ARB, dioxin, aldosterone antagonist, statin	Health examiner	Case-Control

TABLE 2 | Main findings of the included studies.

References	TP	FP	FN	TN	SEN	SPE
Dieplinger et al. (8)	123	89	14	25	0.90	0.22
Aldous et al. (9)	25	196	9	765	0.74	0.80
Santhanakrishnan et al. (10)	35	26	15	24	0.70	0.48
Santhanakrishnan et al. (10)	35	16	16	34	0.69	0.68
Wang et al. (11)	50	10	18	29	0.74	0.74
Jakob et al. (12)	65	39	49	50	0.57	0.56
Mueller et al. (13)	104	58	33	56	0.76	0.49
Sinning et al. (14)	81	2,882	27	1,982	0.75	0.41
Jin et al. (15)	154	0	43	106	0.78	1.00
Luo et al. (16)	267	166	109	334	0.71	0.67
Cui et al. (17)	83	13	89	17	0.48	0.57

TP, True positive; FP, False positive; FN, False negative; TN, True negative; SEN, Sensitivity; SPE, Specificity.

FN data were extracted from the included studies, and data that could not be extracted directly could be obtained by data transformation or by contacting the authors.

Statistical Methods

Statistical analysis of the data was performed using Stata 15 and Meta-Disc (version 14.0) software. First, threshold effects were determined using Spearman correlation coefficient and the pattern of the summary receiver operating characteristic cure (SROC) curve. Then, the combined effect indicators—sensitivity, specificity, positive likelihood ratio (PLR), negative likelihood ratio (NLR), diagnostic odds ratio (DOR), and area under the curve (AUC) of SROC—were calculated. Heterogeneity was tested with the chi-square test using the I^2 of Q statistic, and $I^2 < 50\%$ or $P > 0.05$ indicated no significant heterogeneity among studies, and the effect indicators were combined using the fixed effect model (FEM); $I^2 > 50\%$ or $P < 0.05$ indicated a significant heterogeneity among studies, so the effect indicators were combined using the randomized effect model (REM), and heterogeneity analysis and sensitivity analysis were conducted. The Deeks' test was used to assess publication bias. $P < 0.05$ was considered a statistically significant difference.

RESULTS

Literature Search Results

Five hundred and twenty-seven articles were obtained by searching with the proposed input, and a total of 407 articles were retrieved after removing duplicates. By reading the titles and abstracts, 389 articles were initially excluded (55 were not clincal trial; 77 were not heart failure related; 257 were not diagnose related) according to the inclusion and exclusion criteria. A total of 18 articles was investigated, and eight of them were excluded by reading full-text. For the eight excluded articles, one was duplicate publication, one was testing for sST2, four were prognosis related and two with no access to the four-grid table information. Finally, 10 articles with 11 studies were included in the meta-analysis (8–17) (**Figure 1**).

Basic Characteristics of the Included Literature

A total of 11 studies were included. Santhanakrishnan et al. (9) divided HF patients into HF with preserved ejection fraction (HFPEF) and HF with reduced ejection fraction (HFREF) and studied them separately, and thus this literature was considered as two studies. The basic information of the included studies is shown in **Table 1**. The total sample size of 8,361 patients was included, involving cases from Australia, New Zealand, Singapore, the United Kingdom, Germany, and China. Ten studies investigated middle-aged and elderly populations, and one study focused on children. There were five cohort studies and six case-control studies. sST2 was detected using enzyme-linked immunosorbent assays (ELISAs), and sST2 kits were available from five manufacturers, including MBL, Presage^{TM}, and R&D. Regarding the type of HF, four studies included patients with HFPEF, one included patients with HFREF, and the other six studies did not distinguish between reduced and preserved ejection fractions. The control population included people with dyspnea unrelated to HF, children with hypertension unrelated to HF, healthy populations, and community populations. TP, FP, FN, and TN data were extracted from each study for the meta-analysis (**Table 2**), and the quality evaluation of the included studies is shown in **Figure 2**.

Threshold Effect Analysis

Meta-disc analysis showed that the Spearman correlation coefficient between the log of sensitivity and the log of (1-specificity) was 0.114, $P = 0.739$, and the SROC curve showed no "shoulder-arm" pattern, which suggests that there was no threshold effect in this study.

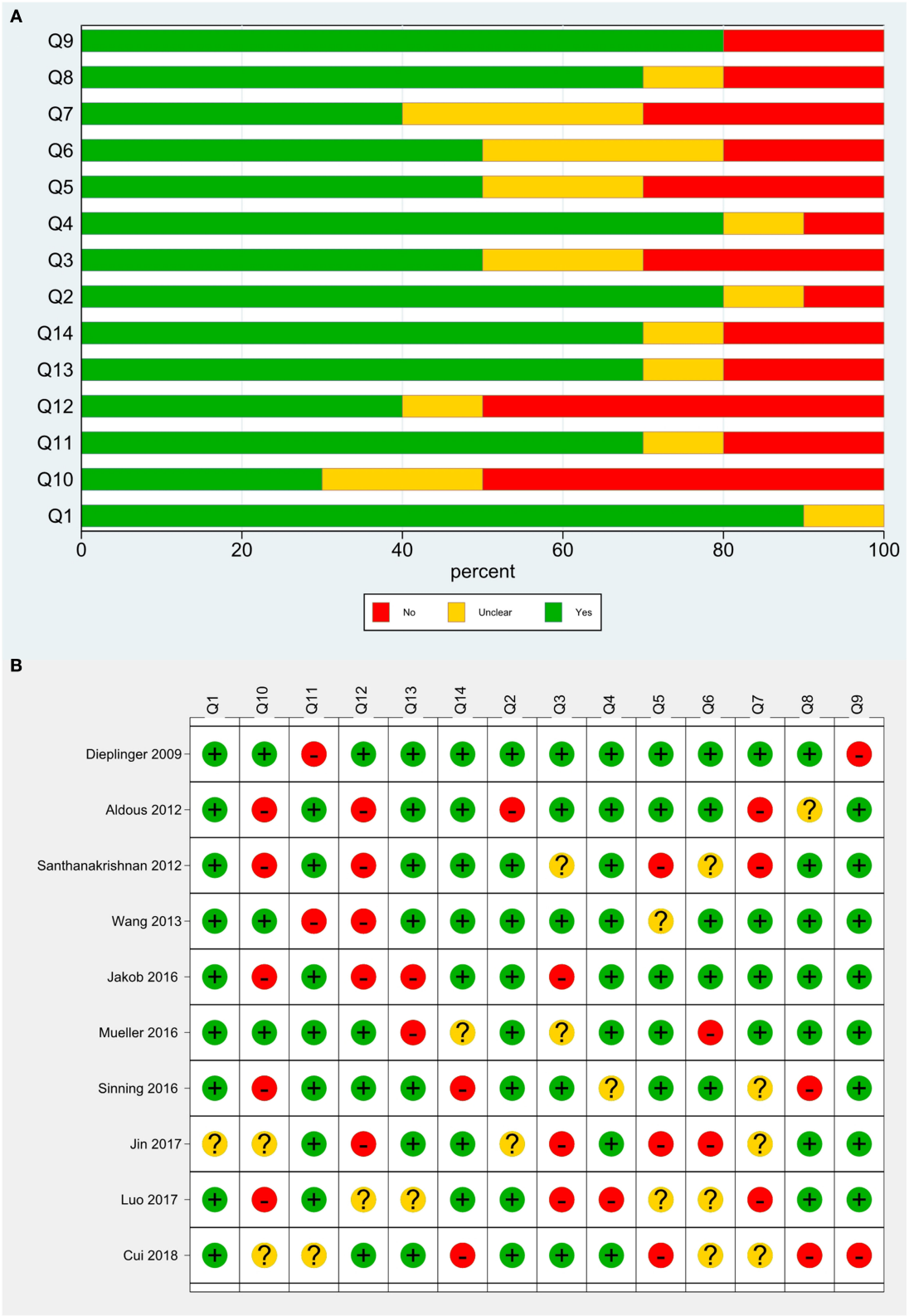

FIGURE 2 | Quality evaluation of the included studies. **(A)** Review authors' judgments presented as percentages for the included studies; **(B)** Review authors' judgements for each included study.

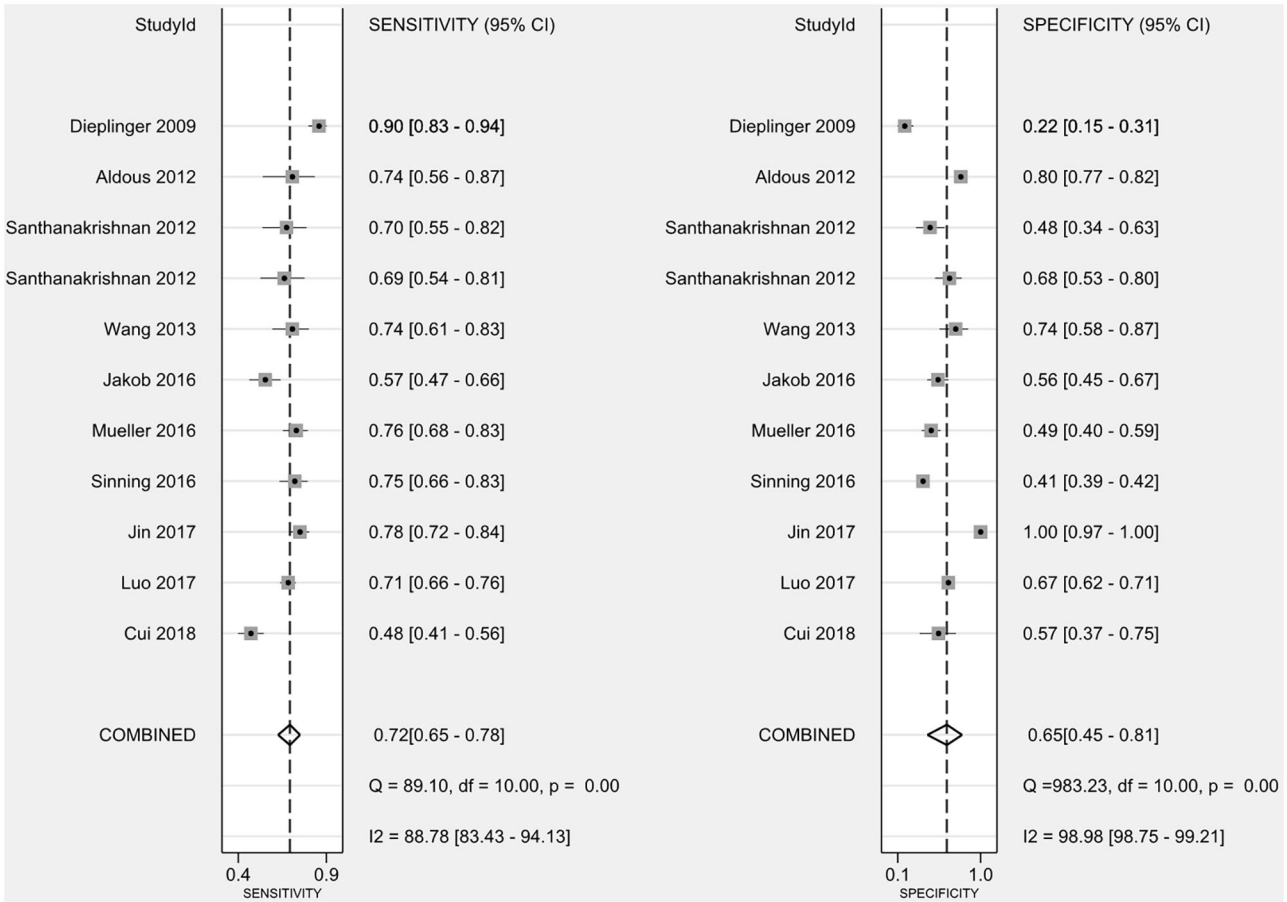

FIGURE 3 | The combined sensitivity and specificity of sST2 for the diagnosis of HF. sST2, soluble suppression of tumorigenicity; HF, heart failure.

Diagnostic Value of sST2 in Patients With HF

The combined sensitivity of sST2 for the diagnosis of HF was 0.72 (95% confidence interval (CI): 0.65–0.78) (**Figure 3**), the combined specificity was 0.65 (95% CI: 0.45–0.81) (**Figure 3**), the combined PLR was 1.75 (95% CI: 1.33–2.31) (**Figure 4A**), the combined NLR was 0.48 (95% CI: 0.37–0.63) (**Figure 4B**), and the combined DOR was 3.63 (95% CI: 2.29–5.74) (**Figure 4C**). The AUC of the SROC curve was 0.75 (**Figure 4D**).

Heterogeneity Analysis

Heterogeneity tests showed that $I^2 = 88.78\%$ ($P < 0.0001$) for sensitivity, $I^2 = 98.98\%$ ($P < 0.0001$) for specificity, $I^2 = 94.0\%$ ($P < 0.0001$) for PLR, $I^2 = 84.7\%$ ($P < 0.0001$) for NLR, and $I^2 = 82.2\%$ ($P < 0.0001$) for DOR, which suggests the presence of heterogeneity unrelated to threshold effects in this study, so the effect sizes were combined using a randomized effect model and the source of heterogeneity was analyzed. The Galbraith radial plot (**Figure 5**) showed that four studies conducted by Dieplinger et al., Santhanakrishnan et al., Jakob et al., and Cui et al. were the sources of the heterogeneity.

Sensitivity Analysis

Sensitivity analysis of the data from this study showed that the studies conducted by Santhanakrishnan et al. and Cui et al. had the most impact on the calculation of the results of this study (**Figure 6A**), while the other original studies had no impact on the calculation of the study results. Taken together, the results of this study were relatively stable. Sensitivity analysis of the impact of individual studies showed that the exclusion of the study conducted by Cui et al. had the most effect on the calculation of results in this meta-analysis (**Figure 6B**).

Publication Bias

The Deeks' test was performed using Stata software to assess publication bias (**Figure 7**); it showed a $P = 0.94$, which suggests that there was no significant publication bias in the included studies.

DISCUSSION

HF is a common outcome of multiple cardiovascular diseases. Cardiac overload and myocardial cell injury can lead to reduced cardiac function, which results in compensatory changes

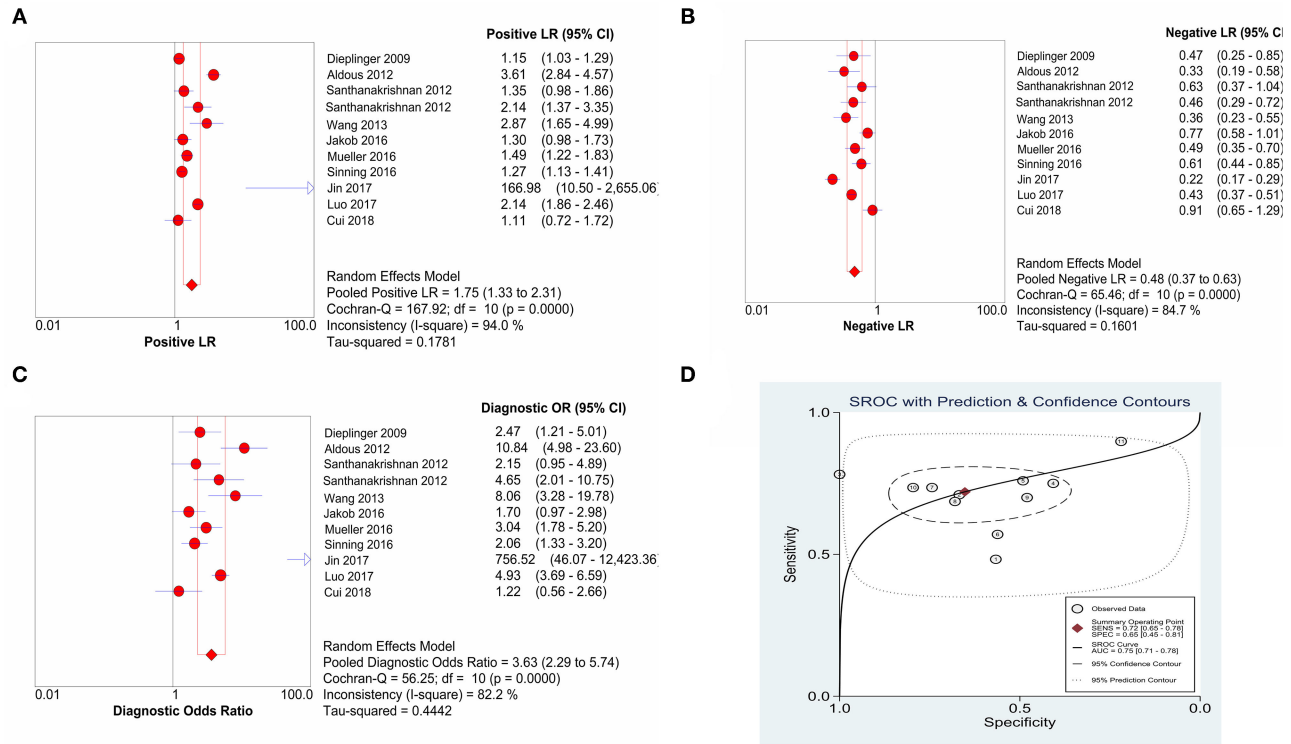

FIGURE 4 | The forest plots of **(A)** PLR, **(B)** NLR, **(C)** DOR, and **(D)** AUC of SROC. PLR, positive likelihood ratio; NLR, negative likelihood ratio; DOR, diagnostic odds ratio; AUC, area under curve; SROC, summary receiver operating characteristic.

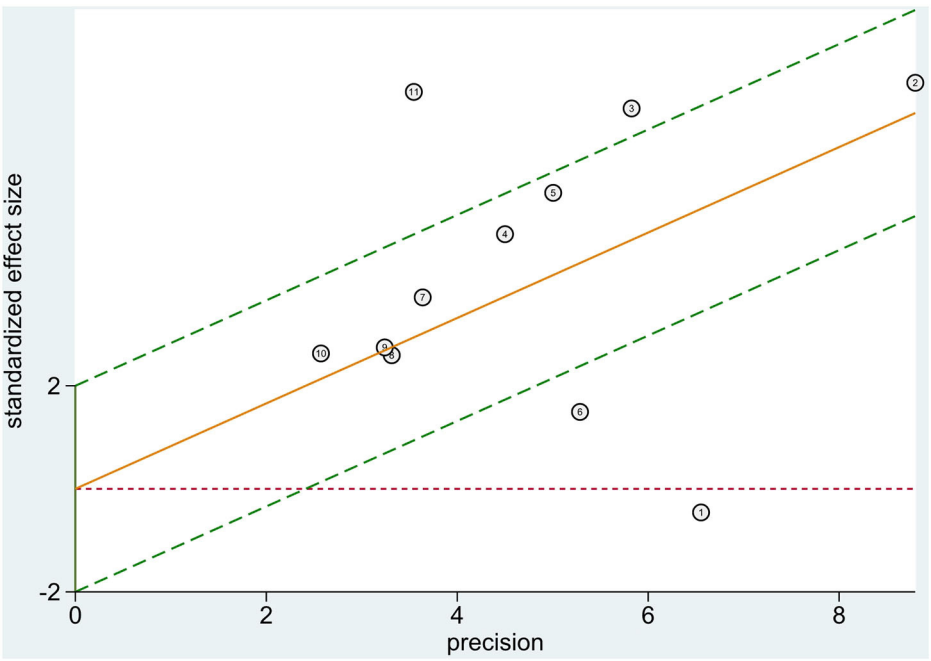

FIGURE 5 | Heterogeneity analysis. Heterogeneity was evaluated by Galbraith radial plot.

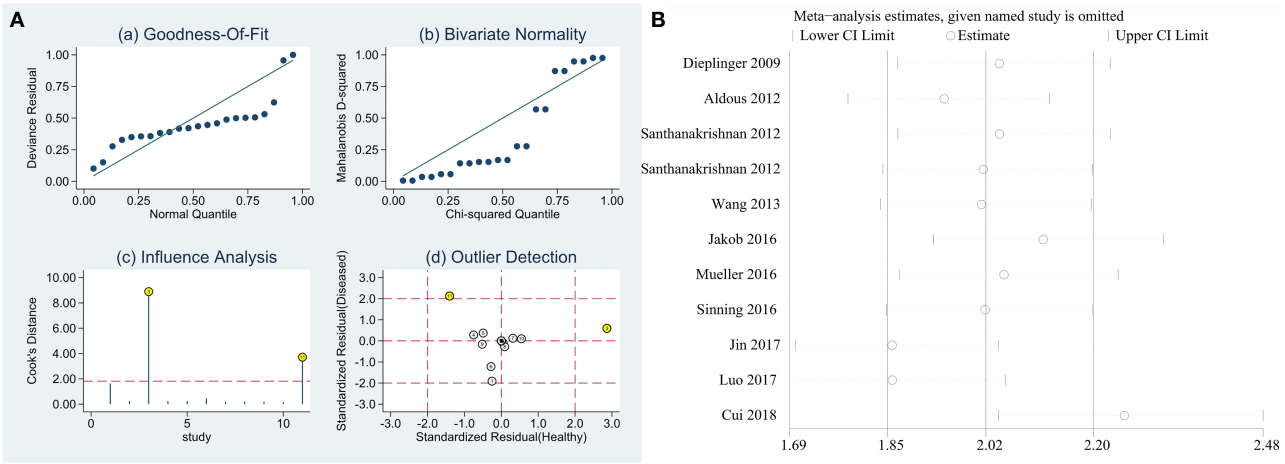

FIGURE 6 | Sensitivity analysis diagram. **(A)** Sensitivity analysis, **(B)** Individual study exclusion.

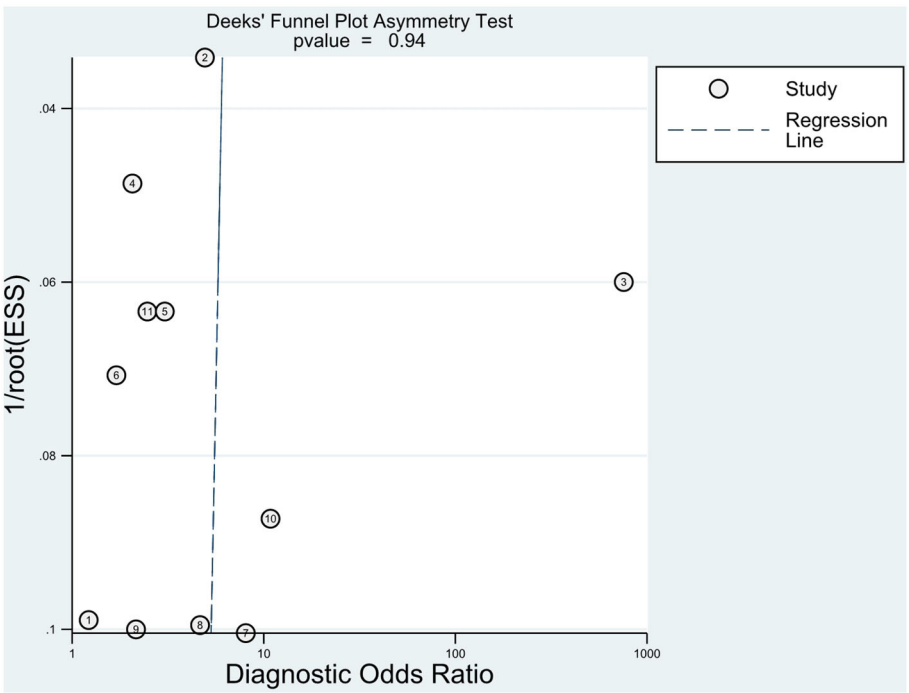

FIGURE 7 | Publication bias. The Deek's test was established to evaluate publication bias.

such as ventricular hypertrophy and chamber enlargement, as well as corresponding changes in cardiomyocytes, extracellular matrix, and collagen fiber networks followed by ventricular remodeling, leading to further deterioration of cardiac function (18). Multiple factors are involved in the progression of HF, such as myocardial necrosis, apoptosis, autophagy, fibrosis, oxidative stress, inflammatory response, and neurohumoral regulatory disorders, as well as changing levels in a series of biomarkers (19). The American College of Cardiology/American Heart Association/Heart Failure Society of America (ACC/AHA/HFSA) guidelines released in 2017 stated that BNP and NT-proBNP provide clear diagnostic value in patients with chronic HF (20). BNP or NT-proBNP has been used clinically as a routine test for HF, but it is susceptible to various factors such as age, sex, and disease condition. Among these biomarkers, the myocardial

fibrosis marker sST2 is not affected by factors like age, sex, renal function, and weight (21). Meanwhile, the 2017 ACC/AHA/HFSA guidelines recommend measuring sST2 for risk stratification of patients with chronic HF (20). This suggests that sST2 has some value in the diagnosis and prognosis of HF.

ST2 is a member of the interleukin-1 (IL-1) receptor superfamily, which is encoded by the *ST2* gene in cardiomyocytes during myocardial stretch and under mechanical stress. The *ST2* gene is located on human chromosome 2q12 and can encode two isoforms of sST2 and the transmembrane receptor form of ST2 (ST2L). Interleukin-33 (IL-33) is a functional ligand for ST2, and the ST2/IL-33 signaling pathway exerts cardioprotective effects by activating ST2L receptors to reduce myocardial fibrosis, inhibit cardiomyocyte hypertrophy, and improve cardiac function, which does not require the sST2 receptor (22). During HF, the increased cardiac load exposes the myocardium to excessive stretch stimulation, and the overproduced sST2 can compete with ST2L for binding IL-33, abrogating the cardioprotective effect of the ST2/IL-33 signaling pathway; this leads to apoptosis, hypertrophy and fibrosis of cardiomyocytes, and further deterioration of cardiac function, aggravating the HF process (23). This suggests that sST2 plays an important role in the development of HF. Clinical studies on the diagnostic value of sST2 in HF have gradually increased in recent years (24). In this study, the clinical diagnostic value of sST2 in HF was evaluated using meta-analysis.

Meta-analysis showed that the combined sensitivity was 0.72, specificity was 0.65, DOR was 3.63, and AUC was 0.75, which indicates that sST2 has a good diagnostic value for HF. The meta-analysis conducted by Huang et al. (24) included 10 original studies, all of which were conducted before 2014 and published in either Chinese or English, and their combined sensitivity was 0.84, specificity was 0.74, DOR was 8.49, and AUC was 0.81. Both the sensitivity and specificity in this study were about 10% lower than those in the Huang et al. (24), which may be related to the inclusion of recent literature and more stringent quality screening performed in this study, but both meta-analyses had a high degree of heterogeneity. Diagnostic studies are generally more heterogeneous than other types of clinical studies because of a possible bias in case selection, trials to be evaluated, gold standards, and flow. This study showed that four studies, those conducted by Dieplinger et al., Santhanakrishnan et al., Jakob et al., and Cui et al. may be the source of heterogeneity in this meta-analysis, and the study conducted by Cui et al. had the most impact on the results of the meta-analysis. The analysis revealed that Dieplinger et al. used a sST2 kit from MBL, Santhanakrishnan et al. conducted a case-control study, Jakob et al. focused on children, and Cui et al. performed a case-control study on patients with HFPEF using a sST2 kit from Shanghai Qiyi Biological Co.; thus, the above-mentioned differences may have contributed to the large heterogeneity observed in this study. In addition, the heterogeneity of this study may have also been caused by the disease typing (different degrees of HF in different studies), the composition of the disease spectrum (the patient group may be combined with other diseases, and the control group includes patients with various cardiovascular diseases without HF), the diagnostic thresholds (the thresholds were not uniform among studies), and differences in the sST2 detection methods. Moreover, there was also heterogeneity because of mixed bias caused by the HF type, control population, sST2 kit, HF diagnostic criteria, study type, and other biases.

Although this meta-analysis included a relatively comprehensive literature search, there were still some limitations. First, the heterogeneity of the included studies was high, and the potential sources include HF type, control population, sST2 kit, HF diagnostic criteria, and study type, with possible heterogeneity between subgroups and from other sources. Second, most of the included studies were case-control studies, which could cause selection bias in the selection of study subjects and increase diagnostic sensitivity. Third, the diagnostic cut-off values of sST2 were not uniform, and the diagnostic cut-off values of sST2 varied among the 11 included studies, which may have been related to factors such as kits, test conditions, and sample-handling methods.

In general, sST2 has some diagnostic value for HF, but factors such as HF type, control population, sST2 kits, HF diagnostic criteria, and study type in the original studies may have affected its diagnostic value. Therefore, we still need to design prospective cohort studies with high quality, large sample sizes, uniform study populations, uniform control populations, and uniform test methods to further explore and validate the reliability of the results of this analysis; we also need to establish an accurate cut-off value for sST2 to provide clinical guidance for the diagnosis of HF.

DATA AVAILABILITY STATEMENT

The original contributions presented in the study are included in the article/**Supplementary Material**, further inquiries can be directed to the corresponding author/s.

AUTHOR CONTRIBUTIONS

This study was designed by ZF and JuY. CY and JiY contributed data to the paper. Statistical analysis and interpretation of data were performed by JiY, JZ, WZ, and JW. All authors were involved in drafting and revision of the manuscript for important intellectual content and approved the final version to be published.

FUNDING

This work was supported by the National Natural Science Foundation of China (Grant Nos. 81800258, 81770360, and 81670333), Hubei Province Health and Family Planning Scientific Research Project (WJ2019Z004), Hubei Provincial Natural Science Foundation of China (2018CFA044), Hubei Province's Outstanding Medical Academic Leader program, and

the Medical and Health Research Project of Yichang city, China (Grant No. A20-2-004).

ACKNOWLEDGMENTS

We thank Mark Abramovitz, PhD, from Liwen Bianji, Edanz Group China (www.liwenbianji.cn/ac), for editing the English text of a draft of this manuscript.

SUPPLEMENTARY MATERIAL

The Supplementary Material for this article can be found online at: https://www.frontiersin.org/articles/10.3389/fcvm.2021.685904/full#supplementary-material

Supplementary Document 1 | Literature searches and search strategy.

Supplementary Table 1 | Included and excluded reference.

REFERENCES

1. Agbor VN, Ntusi NAB, Noubiap JJ. An overview of heart failure in low- and middle-income countries. *Cardiovasc Diagn Ther*. (2020) 10:244–51. doi: 10.21037/cdt.2019.08.03
2. Shiraishi Y, Kawana M, Nakata J, Sato N, Fukuda K, Kohsaka S. Time-sensitive approach in the management of acute heart failure. *ESC Heart Fail*. (2021) 8:204–21. doi: 10.1002/ehf2.13139
3. Sabanayagam A, Cavus O, Williams J, Bradley E. Management of heart failure in adult congenital heart disease. *Heart Fail Clin*. (2018) 14:569–77. doi: 10.1016/j.hfc.2018.06.005
4. Sarhene M, Wang Y, Wei J, Huang Y, Li M, Li L, et al. Biomarkers in heart failure: the past, current and future. *Heart Fail Rev*. (2019) 24:867–903. doi: 10.1007/s10741-019-09807-z
5. Lotierzo M, Dupuy AM, Kalmanovich E, Roubille F, Cristol JP. sST2 as a value-added biomarker in heart failure. *Clin Chim Acta*. (2020) 501:120–30. doi: 10.1016/j.cca.2019.10.029
6. Sobieszek G, Powrózek T, Jaroszyński A, Skwarek-Dziekanowska A, Rahnama-Hezavah M, Małecka-Massalska T. Soluble ST2 proteins in male cachectic patients with chronic heart failure. *Nutr Metab Cardiovasc Dis*. (2021) 31:886–93. doi: 10.1016/j.numecd.2020.11.014
7. Crnko S, Printezi MI, Jansen TPJ, Leiteris L, van der Meer MG, Schutte H, et al. Prognostic biomarker soluble ST2 exhibits diurnal variation in chronic heart failure patients. *ESC Heart Fail*. (2020) 7:1224–33. doi: 10.1002/ehf2.12673
8. Dieplinger B, Gegenhuber A, Haltmayer M, Mueller T. Evaluation of novel biomarkers for the diagnosis of acute destabilised heart failure in patients with shortness of breath. *Heart*. (2009) 95:1508–13. doi: 10.1136/hrt.2009.170696
9. Aldous SJ, Richards AM, Troughton R, Than M. ST2 has diagnostic and prognostic utility for all-cause mortality and heart failure in patients presenting to the emergency department with chest pain. *J Card Fail*. (2012) 18:304–10. doi: 10.1016/j.cardfail.2012.01.008
10. Santhanakrishnan R, Chong JP, Ng TP, Ling LH, Sim D, Leong KT, et al. Growth differentiation factor 15, ST2, high-sensitivity troponin T, and N-terminal pro brain natriuretic peptide in heart failure with preserved vs. reduced ejection fraction. *Eur J Heart Fail*. (2012) 14:1338–47. doi: 10.1093/eurjhf/hfs130
11. Wang YC, Yu CC, Chiu FC, Tsai CT, Lai LP, Hwang JJ, et al. Soluble ST2 as a biomarker for detecting stable heart failure with a normal ejection fraction in hypertensive patients. *J Card Fail*. (2013) 19:163–8. doi: 10.1016/j.cardfail.2013.01.010
12. Hauser JA, Demyanets S, Rusai K, Goritschan C, Weber M, Panesar D, et al. Diagnostic performance and reference values of novel biomarkers of paediatric heart failure. *Heart*. (2016) 102:1633–9. doi: 10.1136/heartjnl-2016-309460
13. Mueller T, Gegenhuber A, Leitner I, Poelz W, Haltmayer M, Dieplinger B. Diagnostic and prognostic accuracy of galectin-3 and soluble ST2 for acute heart failure. *Clin Chim Acta*. (2016) 463:158–64. doi: 10.1016/j.cca.2016.10.034
14. Sinning C, Kempf T, Schwarzl M, Lanfermann S, Ojeda F, Schnabel RB, et al. Biomarkers for characterization of heart failure-Distinction of heart failure with preserved and reduced ejection fraction. *Int J Cardiol*. (2017) 227:272–7. doi: 10.1016/j.ijcard.2016.11.110
15. Jin XL, Huang N, Shang H, Zhou MC, Hong Y, Cai WZ, et al. Diagnosis of chronic heart failure by the soluble suppression of tumorigenicity 2 and N-terminal pro-brain natriuretic peptide. *J Clin Lab Anal*. (2018) 32:e22295. doi: 10.1002/jcla.22295
16. Luo NS, Zhang HF, Liu PM, Lin YQ, Huang TC, Yang Y, et al. Diagnostic value of combining serum soluble ST2 and interleukin-33 for heart failure patients with preserved left ventricular ejection fraction. *Zhonghua Xin Xue Guan Bing Za Zhi*. (2017) 45:198–203. doi: 10.3760/cma.j.issn.0253-3758.2017.03.006
17. Cui Y, Qi X, Huang A, Li J, Hou W, Liu K. Differential and predictive value of galectin-3 and soluble suppression of tumorigenicity-2 (sST2) in heart failure with preserved ejection fraction. *Med Sci Monit*. (2018) 24:5139–46. doi: 10.12659/MSM.908840
18. Hieda M, Sarma S, Hearon CM Jr, Dias KA, Martinez J, Samels M, et al. Increased myocardial stiffness in patients with high-risk left ventricular hypertrophy: the hallmark of stage-b heart failure with preserved ejection fraction. *Circulation*. (2020) 141:115–23. doi: 10.1161/CIRCULATIONAHA.119.040332
19. Mitic VT, Stojanovic DR, Deljanin Ilic MZ, Stojanovic MM, Petrovic DB, Ignjatovic AM, et al. Cardiac remodeling biomarkers as potential circulating markers of left ventricular hypertrophy in heart failure with preserved ejection fraction. *Tohoku J Exp Med*. (2020) 250:233–42. doi: 10.1620/tjem.250.233
20. Yancy CW, Jessup M, Bozkurt B, Butler J, Casey DE Jr, Colvin MM, et al. 2017 ACC/AHA/HFSA focused update of the 2013 ACCF/AHA guideline for the management of heart failure: a report of the American college of cardiology/american heart association task force on clinical practice guidelines and the heart failure society of America. *Circulation*. (2017) 136:e137–61. doi: 10.1161/CIR.0000000000000509
21. Homsak E, Gruson D. Soluble ST2: a complex and diverse role in several diseases. *Clin Chim Acta*. (2020) 507:75–87. doi: 10.1016/j.cca.2020.04.011
22. Weinberg EO, Shimpo M, De Keulenaer GW, MacGillivray C, Tominaga S, Solomon SD, et al. Expression and regulation of ST2, an interleukin-1 receptor family member, in cardiomyocytes and myocardial infarction. *Circulation*. (2002) 106:2961–6. doi: 10.1161/01.CIR.0000038705.69871.D9
23. Sanada S, Hakuno D, Higgins LJ, Schreiter ER, McKenzie AN, Lee RT. IL-33 and ST2 comprise a critical biomechanically induced and cardioprotective signaling system. *J Clin Invest*. (2007) 117:1538–49. doi: 10.1172/JCI30634
24. Huang DH, Sun H, Shi JP. Diagnostic value of soluble suppression of tumorigenicity-2 for heart failure. *Chin Med J*. (2016) 129:570–7. doi: 10.4103/0366-6999.177000

Conflict of Interest: The authors declare that the research was conducted in the absence of any commercial or financial relationships that could be construed as a potential conflict of interest.

frontiers in Cardiovascular Medicine

ORIGINAL RESEARCH
published: 20 July 2021
doi: 10.3389/fcvm.2021.699904

Carbohydrate Antigen 125 Is a Biomarker of the Severity and Prognosis of Pulmonary Hypertension

Yi Zhang[1†], Qi Jin[1,2†], Zhihui Zhao[1], Qing Zhao[1], Xue Yu[1,3], Lu Yan[1], Xin Li[1], Anqi Duan[1], Chenhong An[1], Xiuping Ma[1], Changming Xiong[1], Qin Luo[1] and Zhihong Liu[1*]*

[1] Center for Pulmonary Vascular Diseases, Fuwai Hospital, National Center for Cardiovascular Diseases, Chinese Academy of Medical Sciences and Peking Union Medical College, Beijing, China, [2] Department of Cardiology, Shanghai Institute of Cardiovascular Diseases, Zhongshan Hospital, Fudan University, Shanghai, China, [3] Department of Cardiology, Qingdao Municipal Hospital, Qingdao, China

OPEN ACCESS

Edited by:
Maria Perticone,
University of Magna Graecia, Italy

Reviewed by:
Qian Yang,
First Affiliated Hospital of Chinese PLA General Hospital, China
Xiaohu Li,
First Affiliated Hospital of Anhui Medical University, China

***Correspondence:**
Qin Luo
luoqin2009@163.com
Zhihong Liu
zhihongliufuwai@163.com

[†] These authors have contributed equally to this work

Specialty section:
This article was submitted to General Cardiovascular Medicine, a section of the journal Frontiers in Cardiovascular Medicine

Received: 24 April 2021
Accepted: 17 June 2021
Published: 20 July 2021

Citation:
Zhang Y, Jin Q, Zhao Z, Zhao Q, Yu X, Yan L, Li X, Duan A, An C, Ma X, Xiong C, Luo Q and Liu Z (2021) Carbohydrate Antigen 125 Is a Biomarker of the Severity and Prognosis of Pulmonary Hypertension. Front. Cardiovasc. Med. 8:699904. doi: 10.3389/fcvm.2021.699904

Background: Emerging evidence has showed that serum carbohydrate antigen 125 (CA 125) levels are associated with the severity and prognosis of heart failure. However, its role in pulmonary hypertension remains unclear. This study aimed to investigate the clinical, echocardiographic, hemodynamic, and prognostic associations of CA 125 in pulmonary hypertension.

Methods and Results: We conducted a retrospective cohort study of all idiopathic pulmonary arterial hypertension and chronic thromboembolic pulmonary hypertension patients receiving CA 125 measurement in Fuwai Hospital (January 1, 2014–December 31, 2018). The primary end-point was cumulative 1-year clinical worsening-free survival rate. Linear regression was performed to assess the association between CA 125 and clinical, echocardiographic, and hemodynamic parameters. Cox proportional hazards models were used to assess the association between CA 125 and clinical worsening events. Receiver operating characteristic (ROC) curve analysis was performed to determine the predictive performance of CA 125. A total of 231 patients were included. After adjustment, CA 125 still positively correlated with World Health Organization functional class, NT-proBNP, right ventricular end-diastolic diameter, pericardial effusion, mean right atrial pressure and pulmonary arterial wedge pressure; negatively correlated with 6-min walk distance, left ventricular end-diastolic diameter, mixed venous oxygen saturation, and cardiac index. After adjustment, CA 125 $>$ 35 U/ml was associated with over 2 folds increased risk of 1-year clinical worsening. Further, ROC analysis showed that CA 125 provided additional predictive value in addition to the established pulmonary hypertension biomarker NT-proBNP.

Conclusion: CA 125 was associated with functional status, echocardiography, hemodynamics and prognosis of pulmonary hypertension.

Keywords: pulmonary hypertension, carbohydrate antigen 125, biomarkers, prognosis, severity

INTRODUCTION

Carbohydrate antigen 125 (CA 125), also known as mucin 16, is a glycoprotein synthesized by serosal cells in response to mechanical stress (congestion) or inflammatory stimuli (1–3). High serum CA 125 levels have been identified in malignancies such as ovarian, lung and gastrointestinal cancer (4). Currently, CA 125 is a widely used biomarker for the screening (5), monitoring (6) and risk stratification (7) of ovarian cancer. In addition, emerging evidence has linked serum CA 125 levels to non-malignant conditions such as cardiovascular disease (e.g., heart failure, pericardial diseases, and coronary artery disease) (8). More specifically, serum CA 125 levels were found to be associated with functional class (9), echocardiography (10), and hemodynamics (11) in heart failure. Furthermore, some studies have demonstrated the diagnostic and prognostic value of CA 125 in heart failure (12, 13). The capability of CA 125 to serve as a therapeutic target for heart failure has also been investigated, and the results were promising (14, 15).

As the release of CA 125 is irrelevant to the etiology of cardiac aggression, it should be considered a final organ damage marker (8). Thus, it may also play a role in pulmonary hypertension (PH). Unfortunately, there is still limited knowledge on this topic. Rahimi-Rad et al. reported that patients with PH had higher serum CA 125 levels than those without PH in chronic obstructive pulmonary disease (16). A similar phenomenon was also observed in congenital heart disease (17). Whether serum CA 125 levels are correlated with the severity and prognosis of PH remains unclear. In the present study, we aimed to investigate the correlations between CA125 and the functional status, echocardiography, hemodynamics, and prognosis of PH in a retrospective cohort.

MATERIALS AND METHODS

Study Design and Participants

This observational retrospective cohort study was conducted at Fuwai Hospital, Chinese Academy of Medical Sciences (Beijing, China). We screened all patients with idiopathic pulmonary arterial hypertension (IPAH) and chronic thromboembolic pulmonary hypertension (CTEPH) who underwent right heart catheterization (RHC) from January 1, 2014, to December 31, 2018. Patients with CA 125 data and multiple clinical visit/hospitalization records were enrolled as long as they had a minimum of 1 year of follow-up data for outcomes. In addition, echocardiography-suspected PH patients with normal invasive pulmonary arterial pressure and CA 125 data were also recruited as the control group. The establishment of IPAH and CTEPH was based on the 2009 (before January 2016) or 2015 European Society of Cardiology/European Respiratory Society (ERS) guidelines (18, 19). Normal pulmonary arterial pressure was defined as the mean pulmonary arterial pressure (mPAP) <25 mm Hg (18, 19). By design, patients were excluded if they had (1) any malignancy, (2) inflammatory diseases, or (3) active infection. The following clinical data were collected via an electronic medical record system by two independent reviewers: demographics, etiology of PH, 6-minute walk distance (6MWD), N-terminal pro-brain natriuretic peptide (NT-proBNP) levels, smoking history, alcohol consumption, World Health Organization functional class (WHO-FC), PH-specific medication, history of balloon pulmonary angioplasty/pulmonary endarterectomy, comorbidities, parameters derived from echocardiography and RHC, serum CA 125 levels, and follow-up data. The study protocol was approved by the Ethics Committee of Fuwai Hospital. Written informed consent was obtained from each patient.

CA 125 Measurement

Fasting venous blood samples were collected for CA 125 measurement on the first day of admission. Serum levels of CA125 were measured using a chemiluminescent microparticle immunoassay (product name: Access OV Monitor; Cat. No. 386357; Beckman Coulter Inc., Brea, CA, USA). Please refer to the manufacturer's website for the detailed methodology of the Access OV Monitor (https://mms.mckesson.com/product/586335/Beckman-Coulter-386357). The upper limit of normal for CA 125 was 35 U/ml with the Access OV Monitor. Accordingly, the included patients were divided into either the CA 125 $>$ 35 U/ml group or the CA 125 $\leq$ 35 U/ml group.

RHC and Echocardiographic Examination

The detailed protocol for RHC has been provided in our previous publications (20–23). Briefly, with local anesthesia under continuous electrocardiographic monitoring, a 6 French pigtail catheter or 7 French Swan-Ganz catheter (Edwards Lifesciences World Trade Co., Ltd, Irvine, CA, USA) was advanced into the pulmonary artery through the right femoral vein or right internal jugular vein by placement of a 6 or 7 French vascular sheath. Correct catheter positioning was verified by fluoroscopy. Transducers were positioned at the midaxillary line and zeroed at atmospheric pressure. Transthoracic echocardiography was performed by experienced ultrasonologists in the Department of Echocardiography under the current guidelines (24).

Outcome

We considered the cumulative 1-year clinical worsening-free survival rate as the primary endpoint. Clinical worsening was defined as the occurrence of any of the following events: deteriorated WHO-FC, escalation of PH-specific therapy and rehospitalization due to heart failure or progression of PH. Endpoint events were adjudicated by two senior clinicians. Any discordance was resolved by the supervisors (QL and ZHL).

Statistical Analysis

Continuous variables are presented as the mean $\pm$ standard deviation. Categorical variables are given as counts. Comparisons between two groups were performed using an independent-sample *t*-test, the Mann–Whitney *U*-test or the chi-square test, as appropriate. Correlations between CA 125 and other variables were examined using the Spearman correlation coefficient. To adjust for potential confounding factors, associations with $P <$ 0.100 were further assessed using multivariate linear regression analysis (enter method).

The Kaplan–Meier method was used to assess differences in the rate of 1-year clinical worsening events between patients with values above or below 35 U/ml; curves were compared with the log-rank test. The association between serum CA 125 levels and clinical worsening events was evaluated by a Cox proportional hazards model. Univariate Cox analysis was first performed to screen all prognostic factors. Variables with clinical significance or $P < 0.100$ in univariate analysis were selected for multivariate Cox analysis (enter method). We tested the Cox proportional hazards assumption for each covariate using Schoenfeld residuals. The linearity assumption for CA 125 was evaluated by restricted cubic splines with four knots. Collinearity diagnostics were examined for the potential presence of collinearity between independent variables in multivariate linear regression analysis and multivariate Cox analysis. Receiver operating characteristic (ROC) curve analysis was performed to assess the predictive performance of CA 125. Internal validation was performed using 500 bootstrap resamples (25, 26).

Values of CA 125 and NT-proBNP were logarithmically transformed (ln) and then used in correlation analysis, linear regression and the Cox proportional hazards model. No single missing value was replaced. A two-sided $P < 0.05$ was considered indicative of statistical significance. Data analysis was performed using SPSS (version 23.0), R-studio (version 1.4.1106), R (version 4.0.5), and MedCalc (version 19.7.2).

RESULTS

Patient Enrolment

We identified 231 (45.9%) eligible records for IPAH/CTEPH patients from the 503 records assessed; of the patients, 164 were IPAH and 67 were CTEPH. Furthermore, 84 patients with normal invasive pulmonary arterial pressure and CA 125 data were included as controls. A flow chart displaying the enrolment process is shown in **Figure 1**.

Baseline Characteristics

The baseline characteristics of all included patients are presented in **Table 1**. Among 231 patients with PH, 191 were categorized into the CA 125 $\leq$ 35 U/ml group and 40 into the CA 125 $>$ 35 U/ml group. At baseline, 111 (48.1%) of 231 patients presented with WHO-FC III/IV, and 40 (17.3%) patients did not receive PH-specific medication. During the follow-up period, 73 (31.6%) patients experienced clinical worsening events. More specifically, 20 patients had deteriorated WHO-FC, 16 patients escalated their PH-specific therapy, and 37 patients were rehospitalized due to heart failure or progression of pulmonary hypertension. Among patients who experienced clinical worsening, 23 were in the CA 125>35 U/ml group, and 50 were in the CA 125 $\leq$ 35 U/ml group.

Patients With PH vs. Control Group

Compared to those in the control group, patients with PH were younger (40.0 $\pm$ 15.3 vs. 50.4 $\pm$ 16.2 years, $P <$ 0.001), had worse WHO-FC, 6MWD, echocardiographic and haemodynamic parameters, and had higher serum levels of NT-proBNP and CA 125 [17.3 (11.3, 25.8) vs. 9.5 (6.1, 18.2) U/ml, $P < 0.001$].

PH Patients With CA 125 > 35 U/ml vs. Those With CA 125 ≤ 35 U/ml

Compared to those with CA 125 $\leq$ 35 U/ml, patients with CA 125 $>$ 35 U/ml had lower mixed venous oxygen saturation (S_VO_2), lower cardiac index (CI) values, a larger right ventricular end-diastolic diameter (RVED), higher prevalence rates of hyperlipidaemia and pericardial effusion, higher mean right atrial pressure (mRAP), and higher serum levels of NT-proBNP and CA 125 [55.9 (43.7, 83.0) vs. 14.5 (10.6, 21.1) U/ml, $P < 0.001$]. In addition, patients with CA 125 $>$ 35 U/ml tended to have a smaller left ventricular end-diastolic diameter (LVED) (36.2 $\pm$ 6.6 vs. 38.2 $\pm$ 6.2 mm, $P = 0.064$).

CA 125 Is Weakly Associated With Established Markers of PH Severity

As shown in **Table 2**, ln(CA 125) was weakly correlated with 6MWD, WHO-FC, ln(NT-proBNP), echocardiographic parameters (LVED, RVED, and pericardial effusion), and haemodynamic parameters [S_vO_2, mRAP, CI and pulmonary vascular resistance (PVR)]. In addition, ln(CA 125) tended to correlate with pulmonary arterial wedge pressure (PAWP) ($r = 0.123$, $P = 0.062$). However, no correlations were observed between ln(CA 125) and left atrial dimension ($r = -0.066$, $P = 0.318$), left ventricular ejection fraction ($r = 0.034$, $P = 0.605$), systolic pulmonary arterial pressure ($r = -0.037$, $P = 0.585$), or mPAP ($r = 0.106$, $P = 0.109$). Similar results were observed in the CTEPH and IPAH subgroups (**Supplementary Tables 1, 2**).

In multivariate linear regression analysis (enter method), we further assessed correlations between CA 125 and functional status (6MWD, WHO-FC, and NT-proBNP) and echocardiographic (LVED, RVED and pericardial effusion) and haemodynamic (S_vO_2, mRAP, CI, PVR, and PAWP) parameters by adjusting for age, sex, and body mass index. The results showed that ln(CA 125) was still positively correlated with WHO-FC, ln(NT-proBNP), RVED, pericardial effusion, mRAP, and PAWP and negatively correlated with 6MWD, LVED, S_vO_2, and CI (**Table 2**). Similar results were observed in the CTEPH and IPAH subgroups (**Supplementary Tables 1, 2**). No problems with collinearity were detected in multivariate linear regression analysis (variance inflation factor < 5).

CA 125 Is Associated With Prognosis of PH

Kaplan–Meier analysis showed that IPAH/CTEPH patients with CA 125 $>$ 35 U/ml had a lower cumulative one-year clinical worsening-free survival rate than those with CA 125 $\leq$ 35 U/ml (42.5 vs. 73.8%, $P < 0.0001$; **Figure 2**).

In univariate Cox analysis, 6MWD, ln(NT-proBNP), S_VO_2, mRAP, PAWP, and CA 125 $>$ 35 U/ml had a $P < 0.100$ (**Table 3**). Considering their clinical importance, age, WHO-FC and pericardial effusion were also selected for multivariate Cox analysis (enter method). Events per variable are often used to estimate the sample size needed in multiple Cox analyses, and the lowest acceptable number of events per

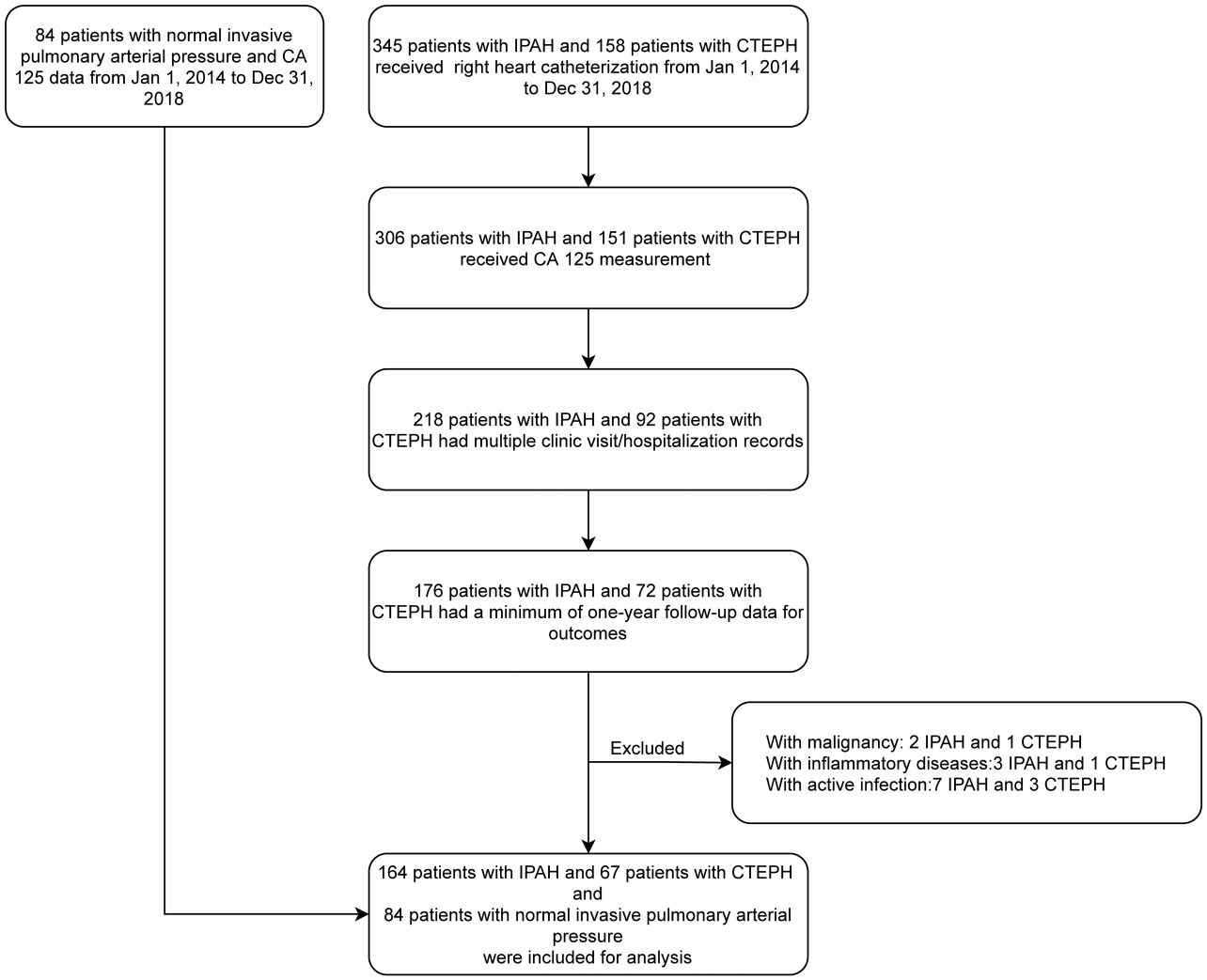

FIGURE 1 | Flow diagram of patient enrollment and exclusion. CA 125, Carbohydrate antigen 125; CTEPH, Chronic thromboembolic pulmonary hypertension; IPAH, Idiopathic pulmonary arterial hypertension.

variable is usually considered to be 10 (27). Given that 73 patients reached the primary endpoint in the present study, it was relatively safe for us to include a maximum of 7 independent variables into multivariate Cox analysis. Model 1 was adjusted for S_vO_2, 6MWD, ln(NT-proBNP), mRAP, and PAWP. Model 2 was adjusted for the variables in model 1 plus age. Model 3 was adjusted for the variables in model 1 plus hyperlipidemia. Model 4 was adjusted for the variables in model 1 plus WHO-FC. Model 5 was adjusted for the variables in model 1 plus pericardial effusion. In all 5 Cox models, CA 125 was found to be an independent predictor of clinical worsening (**Table 4**). The C statistic was 0.648 [95% CI: 0.577–0.718] for model 1, 0.652 [95% CI: 0.582–0.722] for model 2, 0.649 [95% CI: 0.578–0.720] for model 3, 0.649 [95% CI: 0.579–0.720] for model 4 and 0.647 [95% CI: 0.576–0.718] for model 5. Using bootstrap validation, the optimism-corrected C statistic was 0.609 for model 1, 0.606 for model 2, 0.603 for model 3, 0.604 for model 4 and 0.602 for model 5, indicating that the predictive ability of the models is relatively stable in future patients. We did not observe statistically significant deviations from the proportional hazards assumption in any of the Cox models (**Supplementary Table 3**). When modeled as restricted cubic splines, CA 125 showed a linear association with the HR for clinical worsening (**Supplementary Figure 1**). No problems with collinearity were detected in multivariate Cox analysis (variance inflation factor < 5). Subgroup analysis also showed that CA 125 was an independent predictor of clinical worsening in CTEPH and IPAH (**Supplementary Tables 4–7**).

CA 125 Provided Additional Predictive Value in Combination With NT-proBNP

To provide better insight into the predictive value of CA 125 for clinical worsening, we benchmarked it against the established

TABLE 1 | Basic characteristics of control group and patients with PH.

Variables	Control ($n = 84$)	IPAH/CTEPH			*P*-value*
		Total ($n = 231$)	CA 125 ≤ 35 U/ml ($n = 191$)	CA 125 > 35 U/ml ($n = 40$)	
Age, years	50.4 ± 16.2	40.0 ± 15.30‡	40.2 ± 15.2‡	38.9 ± 16.0‡	0.500
Female gender, no.	62 (73.8%)	158 (68.4%)	131 (68.6%)	27 (67.5%)	0.893
BMI, kg/m^2	23.0 ± 3.9	23.2 ± 3.5	23.3 ± 3.5	22.8 ± 3.4	0.354
IPAH/CTEPH, no.	–	164/67	136/55	28/12	0.879
6 MWD, m	454.4 ± 96.2	420.4 ± 100.4†	424.0 ± 101.0	398.3 ± 95.2‡	0.259
NT-proBNP, pg/ml	135.0 (53.3, 314.9)	880.0 (170.3, 1908.0)‡	712.9 (151.5, 1705.0)‡	1,375.0 (888.7, 3206.5)‡	**0.002**
Smoking, no.	12 (14.3%)	29 (12.6%)	21 (11.0%)	8 (20.0%)	0.118
Alcohol intake, no.	13 (15.5%)	22 (9.5%)	16 (8.4%)	6 (15.0%)	0.194
WHO-FC		‡	‡	‡	**0.007**
I or II, no.	71 (84.5%)	120 (51.9%)	107 (56.0%)	13 (32.5%)	
III or IV, no.	13 (15.5%)	111 (48.1%)	84 (44.0%)	27 (67.5%)	
PH specific medication					0.376
None, no.	–	40 (17.3%)	35 (18.3%)	5 (12.5%)	
Mono or combination therapy, no.	–	191 (82.7%)	156 (81.7%)	35 (87.5%)	
PEA or BPA#, no.	–	24 (10.4%)	23 (12.0%)	1 (2.5%)	**0.044**
Co-morbidities					
Systemic hypertension, no.	25 (29.8%)	45 (19.5%)	40 (20.9%)	5 (12.5%)†	0.220
Diabetes mellitus, no.	4 (4.8%)	11 (4.8%)	9 (4.7%)	2 (5.0%)	1.000
Hyperlipidemia, no.	15 (17.9%)	22 (9.5%)†	22 (11.5%)	0†	**0.017**
Echocardiography					
LVEF, %	63.4 ± 6.4	63.3 ± 5.8	63.3 ± 5.8	63.0 ± 5.7	0.785
LA, mm	34.3 ± 5.9	31.0 ± 5.5‡	30.8 ± 5.0‡	31.8 ± 7.5‡	0.722
LVED, mm	44.5 ± 4.7	37.8 ± 6.3‡	38.2 ± 6.2‡	36.2 ± 6.6‡	**0.064**
RVED, mm	25.6 ± 6.6	32.2 ± 6.6‡	31.2 ± 6.4‡	33.7 ± 6.5‡	**<0.001**
sPAP, mm Hg	47.0 ± 10.0	86.7 ± 26.0‡	87.85 ± 27.2‡	81.1 ± 18.9‡	**0.096**
Pericardial effusion, no.	7 (8.3%)	32 (13.9%)	18 (9.4%)	14 (35.0%)‡	**<0.001**
Hemodynamics					
S_VO_2, %	76.0 ± 5.8	67.1 ± 6.5‡	67.8 ± 6.2‡	63.9 ± 7.4‡	**<0.001**
mRAP, mm Hg	3.0 (1.0, 5.0)	5.0 (2.0, 8.0)‡	4.0 (2.0, 7.0)‡	7.0 (3.3, 13.8)‡	**0.001**
mPAP, mm Hg	15.2 ± 3.2	51.2 ± 13.4‡	51.3 ± 13.5‡	50.9 ± 13.3‡	0.791
CI, L/min/m^2	3.7 ± 0.8	3.0 ± 1.0‡	3.1 ± 1.0‡	2.7 ± 0.9‡	**0.018**
PVR, Wood units	1.2 ± 0.8	10.7 ± 5.1‡	10.6 ± 5.2‡	11.3 ± 4.4‡	0.227
PAWP, mm Hg	8.3 ± 3.3	7.7 ± 3.4	7.6 ± 3.2	8.5 ± 4.2	0.138
CA125, U/ml	9.5 (6.1, 18.2)	17.3 (11.3, 25.8)‡	14.5 (10.6, 21.1)‡	55.9 (43.7, 83.0)‡	**<0.001**

*Data are presented as mean ± standard deviation, median (range) or number (percentage). BMI, Body mass index; BPA, balloon pulmonary angioplasty; CA 125, Carbohydrate antigen 125; CI, Cardiac index; CTEPH, Chronic thromboembolic pulmonary hypertension; IPAH, Idiopathic pulmonary arterial hypertension; LA, Left atrium dimension; LVED, Left ventricular end-diastolic diameter; LVEF, Left ventricular ejection fraction; mPAP, Mean pulmonary arterial pressure; mRAP, Mean right atrial pressure; NT-proBNP, N-terminal pro-brain natriuretic peptide; PAWP, Pulmonary arterial wedge pressure; PAH, Pulmonary arterial hypertension; PEA, Pulmonary endarterectomy; PH, Pulmonary hypertension; PVR, Pulmonary vascular resistance; RVED, Right ventricular end-diastolic diameter; 6MWD, 6-min walk distance; sPAP, Systolic pulmonary arterial pressure; S_VO_2, Mixed venous oxygen saturation; WHO-FC, World Health Organization functional class. #Only for patients with CTEPH. *CA 125 > 35 U/ml compared with CA 125 ≤ 35 U/ml. †P < 0.05, compared with control group. ‡P <0.001, compared with control group. Bold values means their P value < 0.100.*

PH biomarker NT-proBNP (18). The areas under the curve for CA 125, NT-proBNP, and combined CA 125 and NT-proBNP were 0.604 (95% CI 0.537–0.667), 0.573 (95% CI 0.507–0.638), and 0.637 (0.571–0.699), respectively. The area under the curve of CA 125 + NT-proBNP was significantly higher than that of NT-proBNP alone ($P = 0.0233$), as shown in **Figure 3**. No significant differences were observed between CA 125 and NT-proBNP ($P = 0.5108$) or CA 125 and CA 125 + NT-proBNP ($P = 0.2710$).

DISCUSSION

In the present study, we found that serum CA 125 levels were weakly correlated with functional status (6MWD, WHO-FC, and NT-proBNP) and echocardiographic (LVED, RVED, and pericardial effusion) and haemodynamic (S_vO_2, mRAP, and CI) parameters of PH after adjustment. Moreover, CA 125>35 U/ml was found to be an independent predictor of 1-year clinical worsening in PH.

TABLE 2 | Correlations between carbohydrate antigen 125 and established markers of PH severity.

Variables	Coefficient (r)	*P*-value	Adjusted coefficient (r)*	*P*-value
6MWD	−0.168	**0.018**	−0.208	**0.004**
WHO-FC	0.277	**<0.001**	0.293	**<0.001**
ln (NT-proBNP)	0.309	**<0.001**	0.284	**<0.001**
Echocardiography				
LVEF	0.034	0.605		
LA	−0.066	0.318		
LVED	0.215	**0.001**	−0.173	**0.017**
RVED	0.306	**<0.001**	0.382	**<0.001**
sPAP	−0.037	0.585		
Pericardial effusion	0.251	**<0.001**	0.290	**<0.001**
Hemodynamics				
S_vO_2	−0.230	**<0.001**	−0.312	**<0.001**
mRAP	0.244	**0.001**	0.372	**<0.001**
mPAP	0.106	0.109		
Cardiac index	−0.243	**<0.001**	−0.208	**0.002**
PVR	0.198	**0.003**	0.127	**0.068**
PAWP	0.123	**0.062**	0.157	**0.018**

*ln, Logarithmically transformed; LA, Left atrium dimension; LVED, Left ventricular end-diastolic diameter; LVEF, Left ventricular ejection fraction; mRAP, Mean right atrial pressure; NT-proBNP, N-terminal pro-brain natriuretic peptide; PAWP, Pulmonary arterial wedge pressure; PH, Pulmonary hypertension; PVR, Pulmonary vascular resistance; RVED, Right ventricular end-diastolic diameter; 6MWD, 6-min walk distance; S_vO_2, Mixed venous oxygen saturation; WHO-FC, World Health Organization functional class. *Each variable is adjusted for age, gender, body mass index by multivariate linear regression analysis. Bold values means their P value < 0.100.*

CA 125 Is Weakly Associated With Established Markers of PH Severity

Compared to patients with normal invasive pulmonary arterial pressure, patients with PH had higher serum CA 125 levels, which was consistent with the results seen in chronic obstructive pulmonary disease (16) and congenital heart disease (17).

WHO-FC, 6MWD, NT-proBNP, pericardial effusion, mRAP, CI, and S_vO_2 are well-established prognostic markers of IPAH (18). We demonstrated that CA 125 was positively correlated with WHO-FC (9), NT-proBNP (28), RVED (10), pericardial effusion (10), mRAP (9, 11), and PAWP (9, 11) in PH, which was consistent with the results seen in heart failure. Additionally, we also found that CA 125 was negatively correlated with 6MWD, LVED, S_vO_2, and CI in PH. Therefore, CA 125 may serve as a novel biomarker of severity in PH.

To date, it remains unclear what leads to CA125 overproduction in heart failure (29, 30). It has been hypothesized to correlate with so-called "stressed" mesothelial cells: (1) mesothelial cells are stimulated by tissue stretching/mechanical stress induced by fluid overload due to heart failure. (2) mesothelial cells are stimulated by inflammatory cytokine network activation (interleukin-1, tumor necrosis factor-α, lipopolysaccharides) (29, 31). PH is characterized by increased mPAP and high PVR, which cause right ventricular hypertrophy, and finally result in right-sided heart failure. Based on our results, we hereby offered a hypothesis to explain the relationship between CA 125 elevation and right heart failure. Elevated PVR increased the afterload of right ventricle, which would further cause right ventricular dilation and elevation of right atrial filling pressure, leading to elevated hydrostatic pressure and congestion, which would further cause both serosal mechanical stretch and third space fluid retention with resultant inflammation and cytokines release (8), ultimately resulting in the elevation of CA 125 (29).

CA 125 Is Associated With Prognosis of PH

Compared to those with CA 125 $\leq$ 35 U/ml, patients with CA 125 $>$ 35 U/ml had higher serum levels of NT-proBNP and worse echocardiographic and haemodynamic parameters at baseline. In all 5 Cox models we constructed, CA125 $>$ 35 U/ml was associated with an over 2-fold increased risk of 1-year clinical worsening, which was similar to the results seen in heart failure (32, 33). Furthermore, ROC analysis showed that CA 125 provided additional predictive value in addition to the established PH biomarker NT-proBNP (18). Due to its close relationship with congestion (8), CA 125 should be considered a final organ damage marker in cardiovascular diseases. This may explain why we found that CA 125 was a severe and prognostic marker in PH.

Clinical Implications

Based on the current knowledge, CA 125 has several merits for use as a biomarker in clinical practice: (1) it is inexpensive, widely available, and measurable with standard methods and has a relatively long half-life (5–7 days) (34–36). (2) It correlates with the severity and prognosis of PH, providing additional information in combination with established risk factors. Therefore, CA 125 may become a valuable tool in the management of PH in the near future. Further studies are needed to evaluate its capacity to monitor response to treatment, serving as a therapeutic target and predicting hard outcomes (such as mortality).

Limitations

As a retrospective cohort study, follow-up bias is our biggest concern. Two hundred nine patients with CA 125 data were excluded for not having a minimum of 1 year of follow-up data for outcomes (**Figure 1**). Among these 209 patients, 29 had CA 125 $>$ 35 U/ml, and 180 had CA 125 $\leq$ 35 U/ml. In other words, these two groups had similar rates of loss to follow-up [29/(40 + 29), 42.0% for CA 125 $>$ 35 U/ml; 180/(191 + 180), 48.5% for CA 125 $\leq$ 35 U/ml]. Moreover, the percentage of patients who reached the endpoint was higher in the CA 125 $>$ 35 U/ml group (57.5 vs. 26.2%). Taken together, these results indicate that the effect size (e.g., hazard ratio) in the present study would be underestimated rather than exaggerated. Follow-up bias should not undermine our conclusion. The present study included only patients with IPAH/CTEPH, which may limit its generalizability to other etiologies of PH. We planned to conduct a comprehensive retrospective study to investigate the correlations between CA 125 and functional status and echocardiographic and hemodynamic parameters in all five groups of PH patients.

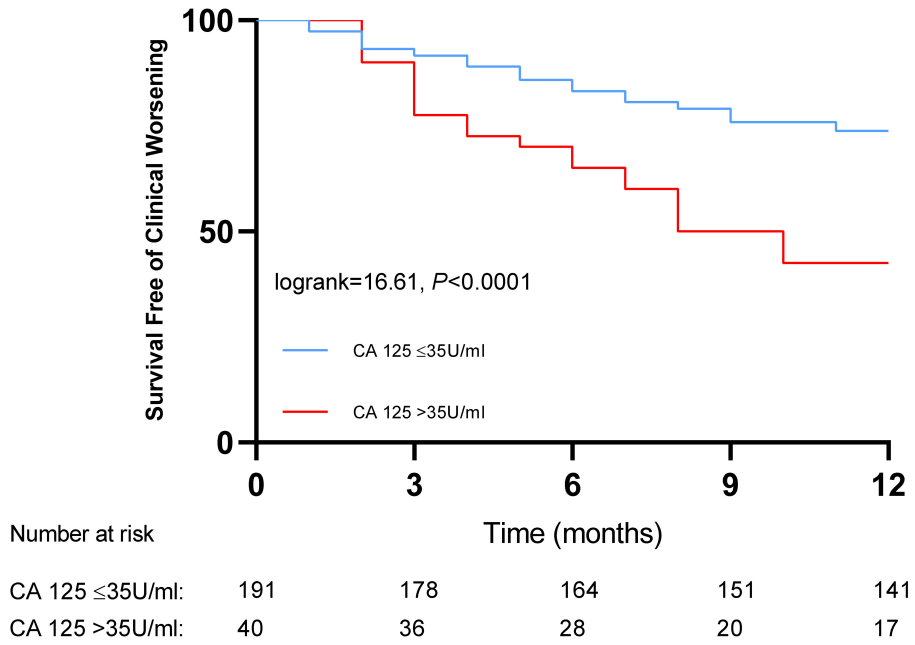

FIGURE 2 | Kaplan-Meier curves for patients with pulmonary hypertension classified by baseline serum levels of carbohydrate antigen 125.

TABLE 3 | Univariate cox analysis of proportional risks for 1-year clinical worsening.

Variable	β	Standard error	HR (95% CI)	Wald	*P*-value
Age	0.009	0.007	1.009 (0.994–1.024)	1.470	0.225
Female gender	−0.094	0.249	0.910 (0.559–1.484)	0.811	0.707
6MWD	−0.002	0.001	0.998 (0.995–1.000)	3.840	**0.050**
ln (NT-proBNP)	0.146	0.085	1.157 (0.979–1.368)	2.918	**0.088**
WHO-FC	0.177	0.234	1.193 (0.754–1.888)	0.568	0.451
Smoking	0.289	0.327	1.335 (0.703–2.535)	0.778	0.378
Alcohol intake	0.048	0.398	1.105 (0.482–2.288)	0.015	0.903
Systemic hypertension	−0.123	0.306	0.884 (0.485–1.611)	0.162	0.687
Diabetes mellitus	−0.662	0.717	0.516 (0.127–2.104)	0.852	0.356
Hyperlipidemia	−0.380	0.463	0.684 (0.276–1.695)	0.674	0.412
LVEF	0.000	0.020	0.982 (0.961–1.041)	0.001	0.982
LA	0.004	0.021	1.004 (0.963–1.047)	0.034	0.854
LVED	−0.016	0.019	0.985 (0.949–1.021)	0.695	0.404
RVED	0.016	0.017	1.017 (0.983–1.051)	0.949	0.330
sPAP	0.005	0.004	1.005 (0.998–1.013)	1.829	0.176
Pericardial effusion	0.410	0.306	1.507 (0.827–2.746)	1.797	0.180
S_VO_2	−0.061	0.018	0.941 (0.909–0.974)	12.023	**0.001**
mRAP	0.090	0.023	1.095 (1.047–1.145)	15.558	**<0.001**
mPAP	0.004	0.008	1.004 (0.988–1.020)	0.218	0.641
CI	−0.145	0.135	0.865 (0.664–1.127)	1.156	0.282
PVR	0.016	0.022	1.016 (0.974–1.061)	0.568	0.451
PAWP	0.064	0.035	1.067 (0.996–1.142)	3.411	**0.065**
CA 125 (category[#])	0.975	0.253	2.650 (1.615–4.349)	14.866	**<0.001**

CA 125, Carbohydrate antigen 125; CI, Cardiac index; HR, Hazard ratio; LA, Left atrium dimension; LVED, Left ventricular end-diastolic diameter; LVEF, Left ventricular ejection fraction; ln, Logarithmically transformed; mPAP, Mean pulmonary arterial pressure; mRAP, Mean right atrial pressure; NT-proBNP, N-terminal pro-brain natriuretic peptide; PAWP, Pulmonary arterial wedge pressure; PVR, Pulmonary vascular resistance; RVED, Right ventricular end-diastolic diameter; 6MWD, 6-min walk distance; sPAP, Systolic pulmonary arterial pressure; S_VO_2, Mixed venous oxygen saturation; WHO-FC, World Health Organization functional class. [#]CA 125 is classified into two groups, namely CA 125 ≤35 U/ml and CA 125 >35 U/ml. Bold values means their P value < 0.100.

TABLE 4 | Multivariate cox analysis of proportional risks for 1-year clinical worsening.

Model	Variable	β	HR (95% CI)	*P*-value
1	CA 125 (category#)	0.860	2.362 (1.286–4.340)	**0.006**
	S_VO_2	−0.052	0.949 (0.904–0.996)	**0.035**
	6MWD	−0.001	0.999 (0.996–1.002)	0.576
	ln (NT-proBNP)	−0.042	0.959 (0.800–1.150)	0.650
	mRAP	0.009	1.009 (0.942–1.080)	0.802
	PAWP	0.040	1.041 (0.967–1.120)	0.282
2	CA 125 (category#)	0.876	2.401 (1.303–4.422)	**0.005**
	S_VO_2	−0.049	0.952 (0.906–1.000)	**0.050**
	6MWD	−0.001	0.999 (0.997–1.002)	0.691
	ln (NT-proBNP)	−0.037	0.964 (0.802–1.158)	0.692
	mRAP	0.011	1.011 (0.944–1.083)	0.759
	PAWP	0.037	1.037 (0.965–1.115)	0.323
	Age	0.007	1.007 (0.990–1.024)	0.424
3	CA 125 (category#)	1.474	4.366 (1.306–14.590)	**0.017**
	S_VO_2	−0.028	0.972 (0.883–1.071)	0.570
	6MWD	−0.003	0.997 (0.991–1.002)	0.225
	ln (NT-proBNP)	−0.153	0.858 (0.603–1.221)	0.396
	mRAP	−0.013	0.987 (0.878–1.110)	0.826
	PAWP	0.003	1.003 (0.883–1.138)	0.969
	Hyperlipidemia	−0.856	0.425 (0.088–2.043)	0.285
4	CA 125 (category#)	0.914	2.494 (1.339–4.645)	**0.004**
	S_VO_2	−0.054	0.948 (0.902–0.995)	**0.031**
	6MWD	−0.001	0.999 (0.996–1.002)	0.526
	ln (NT-proBNP)	−0.020	0.980 (0.810–1.186)	0.835
	mRAP	0.012	1.012 (0.944–1.084)	0.741
	PAWP	0.037	1.038 (0.963–1.118)	0.331
	WHO-FC	−0.244	0.784 (0.441–1.393)	0.406
5	CA 125 (category#)	0.843	2.323 (1.245–4.333)	**0.008**
	S_VO_2	−0.053	0.949 (0.904–0.996)	**0.034**
	6MWD	−0.001	0.999 (0.996–1.002)	0.607
	ln (NT-proBNP)	−0.048	0.953 (0.789–1.151)	0.616
	mRAP	0.010	1.010 (0.943–1.081)	0.783
	PAWP	0.040	1.040 (0.967–1.120)	0.289
	Pericardial effusion	0.095	1.100 (0.516–2.342)	0.806

CA 125, Carbohydrate antigen 125; HR, Hazard ratio; ln, logarithmically transformed; mRAP, Mean right atrial pressure; NT-proBNP, N-terminal pro-brain natriuretic peptide; PAWP, Pulmonary arterial wedge pressure; 6MWD, 6-min walk distance; S_VO_2, Mixed venous oxygen saturation; WHO-FC, World Health Organization functional class. #CA 125 is classified into two groups, namely CA 125 ≤35 U/ml and CA 125 >35 U/ml. Bold values means their P value < 0.100.

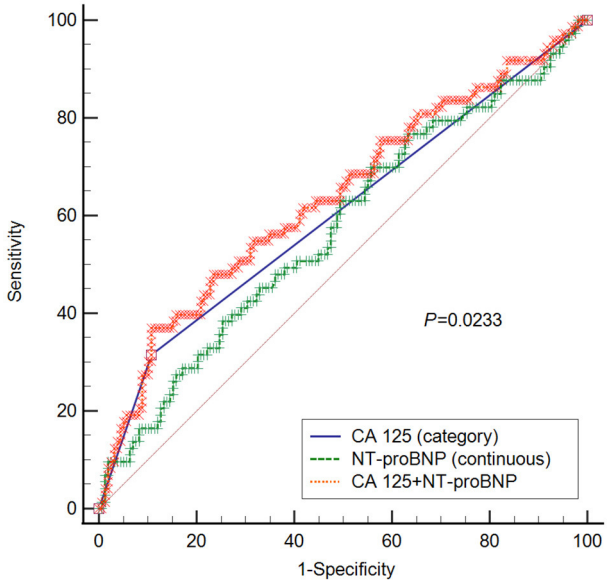

FIGURE 3 | ROC curve for CA 125, NT-proBNP, and CA 125+ NT-proBNP in predicting clinical worsening. *P*-value refers to the comparison between NT-proBNP and NT-proBNP + CA 125. No statistical significances were observed between CA 125 and NT-proBNP ($P = 0.5108$), or CA 125 and CA 125 + NT-proBNP ($P = 0.2710$). CA 125 is classified into two groups, namely CA 125 ≤ 35 U/ml and CA 125 > 35 U/ml; CA 125, Carbohydrate antigen 125; NT-proBNP, N-terminal pro-brain natriuretic peptide.

CONCLUSION

CA 125 was associated with the functional status, echocardiography and hemodynamics of PH. It was found to be an independent predictor of 1-year clinical worsening in PH. Moreover, it provided additional predictive value in combination with the established PH biomarker NT-proBNP. Given that the number of patients with elevated CA 125 levels was low, our results, despite being promising, need to be confirmed in a large prospective study.

DATA AVAILABILITY STATEMENT

The original contributions presented in the study are included in the article/**Supplementary Material**, further inquiries can be directed to the corresponding author/s.

ETHICS STATEMENT

The studies involving human participants were reviewed and approved by the Ethics Committee of Fuwai Hospital. The patients/participants provided their written informed consent to participate in this study.

AUTHOR CONTRIBUTIONS

ZL and QL contributed to the conception of the study. YZ and QJ performed the data analyses and wrote the manuscript. ZZ, QZ, and CX contributed significantly to analysis and manuscript preparation. XY, LY, XL, AD, CA, and XM contributed to data collection. All authors critically reviewed the manuscript for intellectual content and had final responsibility for the decision to submit for publication.

FUNDING

This research article was supported by National Natural Science Foundation of China (81370326 and 81641005); Beijing

Municipal Science and Technology Project (Z181100001718200); Beijing Municipal Natural Science Foundation (7202168); and National Precision Medical Research Program of China (2016YFC0905602).

ACKNOWLEDGMENTS

We are especially thankful to Dr. Yang Wang and Yanyan Zhao (Department of Statistics, National Center for Cardiovascular Diseases, Beijing, China) for their invaluable and dedicated assistance with the statistics.

SUPPLEMENTARY MATERIAL

The Supplementary Material for this article can be found online at: https://www.frontiersin.org/articles/10.3389/fcvm.2021.699904/full#supplementary-material

REFERENCES

1. O'Brien TJ, Tanimoto H, Konishi I, Gee M. More than 15 years of CA 125: what is known about the antigen, its structure and its function. *Int J Biol Markers.* (1998) 13:188–95. doi: 10.1177/172460089801300403
2. Barbieri RL, Niloff JM, Bast RC Jr, Scaetzl E, Kistner RW, Knapp RC. Elevated serum concentrations of CA-125 in patients with advanced endometriosis. *Fertil Steril.* (1986) 45:630–4. doi: 10.1016/S0015-0282(16)49333-7
3. Halila H, Stenman UH, Seppälä M. Ovarian cancer antigen CA 125 levels in pelvic inflammatory disease and pregnancy. *Cancer.* (1986) 57:1327–9. doi: 10.1002/1097-0142(19860401)57:7<1327::AID-CNCR2820570713>3.0.CO;2-Z
4. Lee G, Ge B, Huang TK, Zheng G, Duan J, Wang IH. Positive identification of CA215 pan cancer biomarker from serum specimens of cancer patients. *Cancer Biomark.* (2010) 6:111–7. doi: 10.3233/CBM-2009-0134
5. Clarke-Pearson DL. Clinical practice. Screening for ovarian cancer. *N Engl J Med.* (2009) 361:170–7. doi: 10.1056/NEJMcp0901926
6. Bouanène H, Miled A. [Tumor marker CA125: biochemical and molecular properties]. *Bull Cancer.* (2009) 96:597–601. doi: 10.1684/bdc.2009.0859
7. Burger RA, Darcy KM, DiSaia PJ, Monk BJ, Grosen EA, Gatanaga T, et al. Association between serum levels of soluble tumor necrosis factor receptors/CA 125 and disease progression in patients with epithelial ovarian malignancy: a gynecologic oncology group study. *Cancer.* (2004) 101:106–15. doi: 10.1002/cncr.20314
8. Falcão F, de Oliveira FRA, da Silva M, Sobral Filho DC. Carbohydrate antigen 125: a promising tool for risk stratification in heart diseases. *Biomark Med.* (2018) 12:367–81. doi: 10.2217/bmm-2017-0452
9. D'Aloia A, Faggiano P, Aurigemma G, Bontempi L, Ruggeri G, Metra M, et al. Serum levels of carbohydrate antigen 125 in patients with chronic heart failure: relation to clinical severity, hemodynamic and doppler echocardiographic abnormalities, short-term prognosis. *J Am Coll Cardiol.* (2003) 41:1805–11. doi: 10.1016/S0735-1097(03)00311-5
10. Yilmaz MB, Zorlu A, Tandogan I. Plasma CA-125 level is related to both sides of the heart: a retrospective analysis. *Int J Cardiol.* (2011) 149:80–2. doi: 10.1016/j.ijcard.2009.12.003
11. Nägele H, Bahlo M, Klapdor R, Schaeperkoetter D, Rödiger W. CA 125 and its relation to cardiac function. *Am Heart J.* (1999) 137:1044–9. doi: 10.1016/S0002-8703(99)70360-1
12. Núñez J, Núñez E, Bayés-Genís A, Fonarow GC, Miñana G, Bodí V, et al. Long-term serial kinetics of N-terminal pro B-type natriuretic peptide and carbohydrate antigen 125 for mortality risk prediction following acute heart failure. *Euro Heart J Acute Cardiovasc Care.* (2017) 6:685–96. doi: 10.1177/2048872616649757
13. Hung CL, Hung TC, Liu CC, Wu YJ, Kuo JY, Hou CJ, et al. Relation of carbohydrate antigen-125 to left atrial remodeling and its prognostic usefulness in patients with heart failure and preserved left ventricular ejection fraction in women. *Am J Cardiol.* (2012) 110:993–1000. doi: 10.1016/j.amjcard.2012.05.030
14. Núñez J, Sanchis J, Núñez E, Fonarow GC, Bodí V, Bertomeu-González V, et al. [Benefits of statin therapy based on plasma carbohydrate antigen 125 values following an admission for acute heart failure]. *Rev Esp Cardiol.* (2011) 64:1100–8. doi: 10.1016/j.rec.2011.05.033
15. Núñez J, Llàcer P, Bertomeu-González V, Bosch MJ, Merlos P, García-Blas S, et al. Carbohydrate antigen-125-Guided therapy in acute heart failure: CHANCE-HF: a randomized study. *JACC Heart Failure.* (2016) 4:833–43. doi: 10.1016/j.jchf.2016.06.007
16. Rahimi-Rad MH, Rahimi P, Rahimi B, Gholamnaghad M. Serum CA-125 level in patients with chronic obstructive pulmonary disease with and without pulmonary hypertension. *Pneumologia.* (2014) 63:164–6.
17. Pektaş A, Olguntürk R, Kula S, Çilsal E, Oguz AD, Tunaoglu FS. Biomarker and shear stress in secondary pediatric pulmonary hypertension. *Turk J Med Sci.* (2017) 47:1854–60. doi: 10.3906/sag-1609-13
18. Galiè N, Humbert M, Vachiery JL, Gibbs S, Lang I, Torbicki A, et al. 2015 ESC/ERS guidelines for the diagnosis and treatment of pulmonary hypertension: the joint task force for the diagnosis and treatment of pulmonary hypertension of the European society of cardiology (ESC) and the European respiratory society (ERS): endorsed by: association for European paediatric and congenital cardiology (AEPC), international society for heart and lung transplantation (ISHLT). *Eur Respir J.* (2015) 46:903–75. doi: 10.1093/eurheartj/ehv317
19. Galiè N, Hoeper MM, Humbert M, Torbicki A, Vachiery JL, Barbera JA, et al. Guidelines for the diagnosis and treatment of pulmonary hypertension: the task force for the diagnosis and treatment of pulmonary hypertension of the European society of cardiology (ESC) and the European respiratory society (ERS), endorsed by the international society of heart and lung transplantation (ISHLT). *Eur Heart J.* (2009) 30:2493–537. doi: 10.1093/eurheartj/ehp297
20. Tang Y, Luo Q, Liu Z, Ma X, Zhao Z, Huang Z, et al. Oxygen uptake efficiency slope predicts poor outcome in patients with idiopathic pulmonary arterial hypertension. *J Am Heart Assoc.* (2017) 6:e005037. doi: 10.1161/JAHA.116.005037
21. Zhang HL, Liu ZH, Wang Y, Xiong CM, Ni XH, He JG, et al. Acute responses to inhalation of iloprost in patients with pulmonary hypertension. *Chin Med J.* (2012) 125:2826–31. doi: 10.3760/cma.j.issn.0366-6999.2012.16.005
22. Yu X, Luo Q, Liu Z, Zhao Z, Zhao Q, An C, et al. Prevalence of iron deficiency in different subtypes of pulmonary hypertension. *Heart Lung.* (2018) 47:308–13. doi: 10.1016/j.hrtlng.2018.05.002
23. Jin Q, Luo Q, Yang T, Zeng Q, Yu X, Yan L, et al. Improved hemodynamics and cardiopulmonary function in patients with inoperable chronic thromboembolic pulmonary hypertension after balloon pulmonary angioplasty. *Respir Res.* (2019) 20:250. doi: 10.1186/s12931-019-1211-y
24. Rudski LG, Lai WW, Afilalo J, Hua L, Handschumacher MD, Chandrasekaran K, et al. Guidelines for the echocardiographic assessment of the right heart in adults: a report from the American society of echocardiography endorsed by the European association of echocardiography, a registered branch of the European society of cardiology, and the Canadian society of echocardiography. *J Am Soc Echocardiogr.* (2010) 23:685–713; quiz 786–688. doi: 10.1016/j.echo.2010.05.010
25. Harrell FE, Jr., Califf RM, Pryor DB, Lee KL, Rosati RA. Evaluating the yield of medical tests. *JAMA.* (1982) 247:2543–6. doi: 10.1001/jama.1982.03320430047030
26. Harrell FE, Jr., Lee KL, Mark DB. Multivariable prognostic models: issues in developing models, evaluating assumptions and adequacy, and measuring and reducing errors. *Stat Med.* (1996) 15:361–87. doi: 10.1002/(SICI)1097-0258(19960229)15:4<361::AID-SIM168>3.0.CO;2-4
27. Pavlou M, Ambler G, Seaman SR, Guttmann O, Elliott P, King M, et al. How to develop a more accurate risk prediction model when there are few events. *BMJ.* (2015) 351:h3868. doi: 10.1136/bmj.h3868

28. Duman D, Palit F, Simsek E, Bilgehan K. Serum carbohydrate antigen 125 levels in advanced heart failure: relation to B-type natriuretic peptide and left atrial volume. *Eur J Heart Fail.* (2008) 10:556–9. doi: 10.1016/j.ejheart.2008.04.012
29. Hung CL, Hung TC, Lai YH, Lu CS, Wu YJ, Yeh HI. Beyond malignancy: the role of carbohydrate antigen 125 in heart failure. *Biomark Res.* (2013) 1:25. doi: 10.1186/2050-7771-1-25
30. Núñez J, Miñana G, Núñez E, Chorro FJ, Bodí V, Sanchis J. Clinical utility of antigen carbohydrate 125 in heart failure. *Heart Fail Rev.* (2014) 19:575–584. doi: 10.1007/s10741-013-9402-y
31. Frigy A, Belényi B, Kirchmaier Á, Fekete N, Szabó IA. Elevated CA-125 as humoral biomarker of congestive heart failure: illustrative cases and a short review of literature. *Case Rep Cardiol.* (2020) 2020:1642914. doi: 10.1155/2020/1642914
32. Shi C, van der Wal HH, Silljé HHW, Dokter MM, van den Berg F, Huizinga L, et al. Tumour biomarkers: association with heart failure outcomes. *J Intern Med.* (2020) 288:207–18. doi: 10.1111/joim.13053
33. Chen YX, Wang XQ, Fang CF, Wang JF, Tang LJ. Value of BNP and tumour marker CA125 in patients with heart failure. *Acta Cardiol.* (2008) 63:501–6. doi: 10.2143/AC.63.4.2033050
34. Schmidt T, Rein DT, Foth D, Eibach HW, Kurbacher CM, Mallmann P, et al. Prognostic value of repeated serum CA 125 measurements in first trimester pregnancy. *Eur J Obstet Gynecol Reprod Biol.* (2001) 97:168–73. doi: 10.1016/S0301-2115(00)00533-9
35. Colaković S, Lukiç V, Mitroviç L, Jeliç S, Susnjar S, Marinkoviç J. Prognostic value of CA125 kinetics and half-life in advanced ovarian cancer. *Int J Biol Markers.* (2000) 15:147–52. doi: 10.1177/172460080001500204
36. Bidart JM, Thuillier F, Augereau C, Chalas J, Daver A, Jacob N, et al. Kinetics of serum tumor marker concentrations and usefulness in clinical monitoring. *Clin Chem.* (1999) 45:1695–707. doi: 10.1093/clinchem/45.10.1695

Conflict of Interest: The authors declare that the research was conducted in the absence of any commercial or financial relationships that could be construed as a potential conflict of interest.

frontiers in Cardiovascular Medicine

ORIGINAL RESEARCH
published: 20 July 2021
doi: 10.3389/fcvm.2021.705666

Echocardiographic, Biochemical, and Electrocardiographic Correlates Associated With Progressive Pulmonary Arterial Hypertension

*Ahmed Zaky[1], Iram Zafar[1], Juan Xavier Masjoan-Juncos[1], Maroof Husain[1], Nithya Mariappan[1], Charity J. Morgan[2], Tariq Hamid[3], Michael A. Frölich[1], Shama Ahmad[1] and Aftab Ahmad[1]**

[1] Department of Anesthesiology and Perioperative Medicine, University of Alabama at Birmingham, Birmingham, AL, United States, [2] Department of Biostatistics, University of Alabama at Birmingham, Birmingham, AL, United States, [3] Division of Cardiovascular Disease, Department of Medicine, University of Alabama at Birmingham, Birmingham, AL, United States

OPEN ACCESS

Edited by:
Maria Perticone, University of Magna Graecia, Italy

Reviewed by:
Owais Bhat, Virginia Commonwealth University, United States
Hao Zhang, Shanghai Children's Medical Center, China

***Correspondence:**
Aftab Ahmad
aftabahmad@uabmc.edu

Specialty section:
This article was submitted to General Cardiovascular Medicine, a section of the journal Frontiers in Cardiovascular Medicine

Received: *05 May 2021*
Accepted: *09 June 2021*
Published: *20 July 2021*

Citation:
Zaky A, Zafar I, Masjoan-Juncos JX, Husain M, Mariappan N, Morgan CJ, Hamid T, Frölich MA, Ahmad S and Ahmad A (2021) Echocardiographic, Biochemical, and Electrocardiographic Correlates Associated With Progressive Pulmonary Arterial Hypertension. Front. Cardiovasc. Med. 8:705666. doi: 10.3389/fcvm.2021.705666

Background: Pulmonary arterial hypertension (PAH) is a progressive proliferative vasculopathy associated with mechanical and electrical changes, culminating in increased vascular resistance, right ventricular (RV) failure, and death. With a main focus on invasive tools, there has been an underutilization of echocardiography, electrocardiography, and biomarkers to non-invasively assess the changes in myocardial and pulmonary vascular structure and function during the course of PAH.

Methods: A SU5416-hypoxia rat model was used for inducing PAH. Biventricular functions were measured using transthoracic two-dimensional (2D) echocardiography/Doppler (echo/Doppler) at disease onset (0 week), during progression (3 weeks), and establishment (5 weeks). Similarly, electrocardiography was performed at 0, 3, and 5 weeks. Invasive hemodynamic measurements and markers of cardiac injury in plasma were assessed at 0, 3, and 5 weeks.

Results: Increased RV systolic pressure (RVSP) and rate of isovolumic pressure rise and decline were observed at 0, 3, and 5 weeks in PAH animals. EKG showed a steady increase in QT-interval with progression of PAH, whereas P-wave height and RS width were increased only during the initial stages of PAH progression. Echocardiographic markers of PAH progression and severity were also identified. Three echocardiographic patterns were observed: a steady pattern (0–5 weeks) in which echo parameter changed progressively with severity [inferior vena cava (IVC) expiratory diameter and pulmonary artery acceleration time (PAAT)], an early pattern (0–3 weeks) where there is an early change in parameters [RV fractional area change (RV-FAC), transmitral flow, left ventricle (LV) output, estimated mean PA pressure, RV performance index, and LV systolic eccentricity index], and a late pattern (3–5 weeks) in which there is only a late rise at advanced stages of PAH (LV diastolic eccentricity index). RVSP correlated with PAAT, PAAT/PA ejection times, IVC diameters, RV-FAC, tricuspid systolic excursion, LV systolic eccentricity and output, and transmitral flow. Plasma myosin light chain (Myl-3) and cardiac troponin I (cTnI) increased progressively across the three time points. Cardiac

troponin T (cTnT) and fatty acid-binding protein-3 (FABP-3) were significantly elevated only at the 5-week time point.

Conclusion: Distinct electrocardiographic and echocardiographic patterns along with plasma biomarkers were identified as useful non-invasive tools for monitoring PAH progression.

Keywords: pulmonary arterial hypertension, echocardiography, disease progression, electrocardiography, SU5416, cardiac troponin T, cardiac troponin I, FABP-3

INTRODUCTION

Pulmonary arterial hypertension (PAH) is a progressive proliferative vasculopathy affecting small pulmonary arterioles culminating in increased vascular resistance and right ventricular afterload (1). According to a recent task force report, assessing RV function is an ongoing challenge (2).

Failure of the RV to adapt to increased afterload is the principal cause of death in patients with pulmonary hypertension (PH) (3, 4). Factors reflecting RV dysfunction by cardiac catheterization such as cardiac index and mean right atrial pressure are significant predictors of survival in patients with PAH (3). Additionally, a failing RV causes poor prognosis even if pulmonary vascular resistance is reduced (5), demonstrating the importance of evaluating and maintaining RV function in PAH patients.

Despite the prognostic significance of the RV status in PH, gaps still remain in the assessment of RV function and structure both during the course of the disease and during treatment (6). This stems in part from the lack of well-established clinical determinants of RV function, and the complex structure and orientation of the RV in the anterior chest that hampers a straightforward assessment using conventional imaging modalities (2, 7). Previous attempts to evaluate progression of PAH in animal models were limited in that invasive measurements were carried out at one time point with an underutilization of echocardiography to assess the pulmonary vasculature and the left ventricle during the course of PAH (6). While advanced imaging techniques can provide a better assessment of RV function, a vast number of clinicians still rely on conventional imaging modalities. Furthermore, less attention has been given to the assessment of the electrical function and trend of biomarker progression during the course of PAH. Understanding the biochemical, electrocardiographic, and echocardiographic patterns during the course of PAH may guide clinical management of patients with PAH and help identify patients at an early stage of the disease when therapies could potentially be more effective (8). Furthermore, recent change in the clinical diagnosis of PAH using a threshold of mean pulmonary artery pressure (mPAP) from >25 to >20 mmHg underscores the efforts in diagnosing PAH at an early stage (9, 10).

To address these gaps, we sought to perform a comprehensive analysis to assess electrical, biochemical, and mechanical changes that occur in the heart and in the pulmonary circulation during the progression of PAH in a SU5416-hypoxia rat model. Our objective is to identify sensitive indices that can be obtained and monitored non-invasively in the early diagnosis of PAH and during the course of PAH.

Abbreviations: HV D, hepatic vein diastolic; HV S/D, hepatic vein systolic/diastolic; IVC_EXP, inferior vena cava expiratory diameter; IVC_INSP, inferior vena cava inspiratory diameter; LV CO, left ventricle cardiac output; LVSV, left ventricle stroke volume; LV-EIs, left ventricle eccentricity index systolic; LV-Eid, left ventricle eccentricity index diastolic; LV-VCFr, left ventricle circumferential shortening; MPAP, mean pulmonary artery pressure; MV(E/A), early diastolic mitral velocity/late diastolic mitral velocity; PAAT, pulmonary artery acceleration time; PAET, pulmonary artery ejection time; RVEDV, right ventricle end diastolic volume; RVESV, right ventricle end systolic volume; RVEDP, right ventricle end diastolic pressure; RVESP, right ventricle end systolic pressure; RV-EF, right ventricle ejection fraction; RV-FAC, right ventricle fractional area change; RV-FWT, right ventricle free wall thickness; RV-MPI, right ventricle myocardial performance index; RV-CO, right ventricle cardiac output; RVSV, right ventricle stroke volume; TAPSE, tricuspid annular plane systolic excursion; TV-Sa, tricuspid valve systolic wave.

METHODS

Animal Model of Pulmonary Arterial Hypertension

All animal experiments were performed under the University of Alabama Institutional Animal Care and Use Committee approval and in accordance with the National Institutes of Health Guide for the care and use of laboratory animals. This manuscript adheres to the ARRIVE guidelines. PAH was induced in rats using an established model (11). Briefly, adult male Sprague–Dawley rats weighing 160–200 g were injected subcutaneously with SU-5416 (20 mg/kg), a vascular endothelial growth factor receptor 2 (VEGFR-2) inhibitor, and exposed to normobaric hypoxia (10% O_2) for 3 weeks (SuHyx rats). They were then returned to normoxia (21% O_2, room air) for two additional weeks. For invasive measurements, separate sets of animals were used for the control, 3- and 5-week time points groups. For echocardiographic measurements, the same animals were used for the control (0 week), 3- and 5-week measurements. The number of animals used in each measurement is indicated in the figure legends. Experiments in each group were carried out independently for a minimum of two times.

Hemodynamic Measurements

Hemodynamic measurements were performed in rats under 2% isoflurane anesthesia using a 1.4 F high-fidelity Millar catheter as described by us before (12). Using a Biopac data acquisition system and AcqKnowledge III software (ACQ 3.2), the rate of

rise of ventricular pressure during systole ($dP/dT_{maximum}$) and subsequent fall during diastole ($dP/dT_{minimum}$) were measured. Systemic blood pressure was also monitored using the same catheter inserted in the carotid artery. In animals where echocardiography was carried out, invasive measurements were performed at the end of the 5-week protocol before the animals ($n = 10$) were euthanized. Separate sets of animals were used for invasive measurements of naïve ($n = 17$) and 3-week exposed animals ($n = 11$).

Immunofluorescence Staining

Animals were euthanatized, and the left lung was inflation fixed with low-melting agarose and immersed in a solution of 10% formalin in ethanol for up to 48 h. The tissues were then processed for paraffin embedding. Five-micrometer-thick sections were cut on positively charged slides, and deparaffinization and antigen retrieval was performed. Sections were then blocked in 5% normal goat serum and incubated overnight with anti-von Willebrand factor (vWF) antibody (Dako cat# A0082) and anti-alpha smooth muscle actin (α-SMA) (Abcam cat# 18147). After washing with TBST (Tris-buffered saline with 0.025% Triton-X100), fluorescence tagged secondary antibodies, anti-rabbit Alexa fluor 488 (vWF), and anti-mouse Alexa fluor 594 (α-SMA) were applied, and sections were incubated for 1 h. Sections were then washed, rinsed with PBS, and mounted with VECTASHIELD containing DAPI (Vector laboratories). Images were captured at ×20 using the BZ-X800 Keyence microscope.

Cardiac Biomarker Measurements

Levels of cardiac and skeletal muscle markers of injury were measured in the plasma of rats from 0-, 3-, and 5-week time points using the meso scale discovery (Rockville, MD, USA) muscle injury panel 1 kit. A multiplex assay to quantitate plasma levels of cTnI (cardiac troponin I), cTnT (cardiac troponin T), FABP3 (fatty acid-binding protein 3), Myl3 (myosin light chain 3), and sTnI (skeletal troponin I) were carried out using standards and as per protocol of the manufacturer.

Echocardiography and Electrocardiography

Transthoracic echocardiography and electrocardiography were performed in anesthetized animals (2% isoflurane) as described by us before (12). Echocardiography was performed prior to, at 3 and 5 weeks post exposure using a Vevo2100 high-resolution ultrasound system (Visual Sonics Inc., Toronto, ON, Canada) using a 13- to 24-MHz linear transducer (MS-250). Rats were placed supine on the warmed stage (37°C) of the echocardiography system. Two-dimensional cardiac images were acquired from the parasternal long- and short-axis, apical, subcostal, and suprasternal views using M-mode and B-modes at mid papillary level and averaged to determine the RV and LV dimensions at end systole and end diastole as described (13).

The RV and LV volumes, cardiac output, fractional shortening, fractional area of change, and ejection fraction were obtained according to guidelines (14). The LV systolic and diastolic eccentricity index was calculated as the ratio of the LV anteroposterior dimension and the septolateral dimension. The parasternal pulmonary artery view was obtained, and pulsed wave Doppler was used to measure flow across the RV outflow tract. End systolic diameter of the pulmonary artery was measured, and the end systolic diameter of the pulmonary artery to the end systolic diameter of ascending aorta ratio (stiffness index) was calculated. Apical four-chamber views with B- and M-modes were obtained to determine tricuspid annular plane systolic excursion (TAPSE). Pulsed wave Doppler was used to determine transmitral and transtricuspid early (E) and atrial (A) wave peak velocities, isovolumic relaxation time (IVRT), E-wave deceleration time, and isovolumic contraction time, with the ratio of E to A calculated across both the mitral and tricuspid valves. A tricuspid regurgitant jet was sought to estimate the RVSP when discernable (15). Tissue Doppler imaging was used to determine lateral mitral and tricuspid annular diastolic peak early (E'), late atrial (A'), systolic (S') annular velocities, and (E) to (E') ratios were calculated. Myocardial performance index (MPI) for both ventricles was calculated from the spectral Doppler tracing of transmitral and transtricuspid flows as described (16). A subcostal inferior vena caval view was obtained, and the inferior vena caval diameter was measured at end inspiration and end exhalation. Pulsed wave Doppler was used to assess hepatic venous blood flow.

For electrocardiography, a two-channel electrocardiography was performed on anesthetized rats prior to, at 3 and 5 weeks post exposure. To obtain ECG tracings, bipolar platinum electrodes were positioned in the thorax (subcutaneous tissue) directly in derivation DII. To determine the intervals RR, PR, QT, corrected QT (QTc), and QRS complex, a period of 10 s was analyzed in the ECG tracing of each animal. The QT interval was measured starting from the onset of the QRS complex until the end of the T wave, which is the return of the T wave to the baseline. QTc was obtained using Bazett's formula ($QTc = QT/HRR$) (17). Parameters were analyzed using previously described procedures (18).

Statistical Analyses

Values were expressed as mean ±SEM. Statistical analyses were performed using Prism software. Repeated measures one-way ANOVA was used to test for differences in each parameter at 0, 3, and 5 weeks. For statistically significant parameters, *post-hoc* pairwise t-tests were conducted using Tukey's method for correcting for multiple comparisons. To assess the relationship between invasively measured RVSP and echocardiographic parameters, control and study animals were pooled, and Pearson correlations were calculated. Fisher's z transformation was used to calculate 95% confidence intervals. Due to the large number of tested parameters, a Bonferroni correction was applied to adjust for multiple comparisons.

RESULTS

Invasive Hemodynamics

A rat SuHyx model of PAH was used as described before (11). Right ventricular systolic pressure (RVSP) and hypertrophy were measured at 0, 3, and 5 weeks to confirm progression and

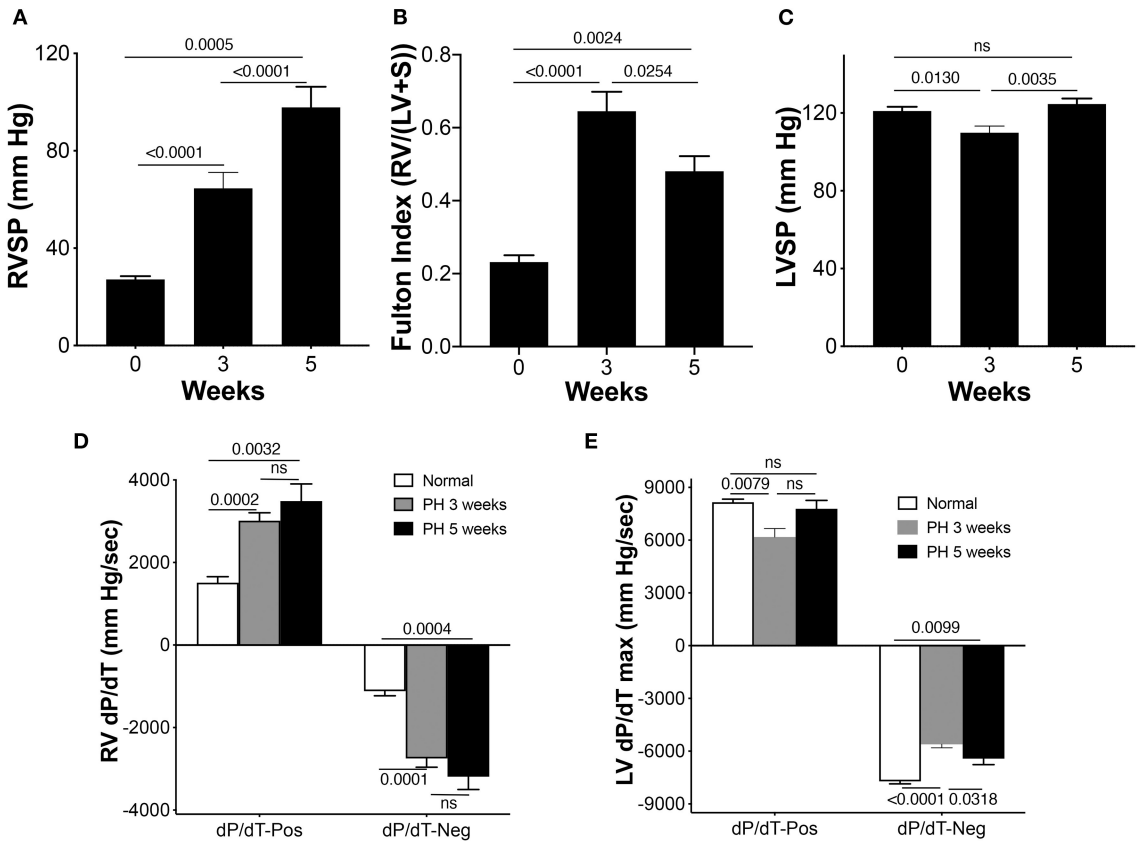

FIGURE 1 | Right ventricle (RV) pressures and electrocardiographic parameters in pulmonary arterial hypertension (PAH) rats. Pulmonary arterial hypertension was induced in rats as described in the Methods section. **(A)** The RV systolic pressure (RVSP) was measured in separate sets of control animals and animals at 3 and 5 weeks during the development of PAH, $n = 10–17$ animals/group. **(B)** Fulton Index ($n = 6–9$ animals/group). **(C)** Left ventricle systolic pressure (LVSP), $n = 10–17$ animals/group. **(D)** Rates of rise and decline of the RV pressure in systole (above baseline) and in diastole (below baseline) (dP/dT) were recorded, $n = 10–17$ animals/group. **(E)** Rates of rise and decline of the LV pressure in systole (above baseline) and in diastole (below baseline) (dP/dT) were recorded, $n = 9–17$ animals/group.

establishment of PH. **Figure 1A** demonstrates a steady increase in RVSP in the PAH rats at 3 and 5 weeks, when compared with the controls. As expected in this model, the chronic increase in RV afterload led to RV hypertrophy shown by an increase in the Fulton index both at 3 and 5 weeks compared with controls (**Figure 1B**). Hypertrophy was more at the 3-week time point compared with the 5-week time point. LV systolic pressure (LVSP) remained unaltered in the PAH group at 5 weeks but was decreased at the 3-week time point (**Figure 1C**). The rate of rise of RV pressure during ejection and post ejection phases of the cardiac cycle was used to assess the contractile and relaxation properties of the RV. RV $dP/dT_{maximum}$ was substantially elevated in the PAH animals at 3 and 5 weeks when compared with the controls (**Figure 1D**). Similarly, the RV $dP/dT_{minimum}$ at 3 and 5 weeks were increased in the PAH animals when compared with the controls (**Figure 1D**). Since RV dysfunction can alter LV contractility, we measured the LV dP/dT. Interestingly, LV dP/dT positive did not differ from the control at 5 weeks, but there was a decrease at the 3-week time point (**Figure 1E**). However, the LV dP/dT negative in the PAH group at 3 and 5 weeks were both diminished when compared with the controls (**Figure 1E**).

Electrocardiography

Polarization characteristics of the heart chambers resulting from adaptation and maladaptation were assessed using electrocardiography (EKG). Representative tracing at all three time points shows changes with progression of PAH (**Figure 2A**). A significant prolongation in the corrected QT interval (QTc), an increase in the amplitude of P and T waves, and a widening of the QRS complex were observed in the PAH animals across the three time points, 0, 3, and 5 weeks (**Figures 2B–G**).

Lung Histology and Cardiac Markers of Injury

To validate PAH pathology, the lung sections were stained for vWF and α-SMA to highlight changes in the intima and media of the arteries, respectively, during disease progression. As

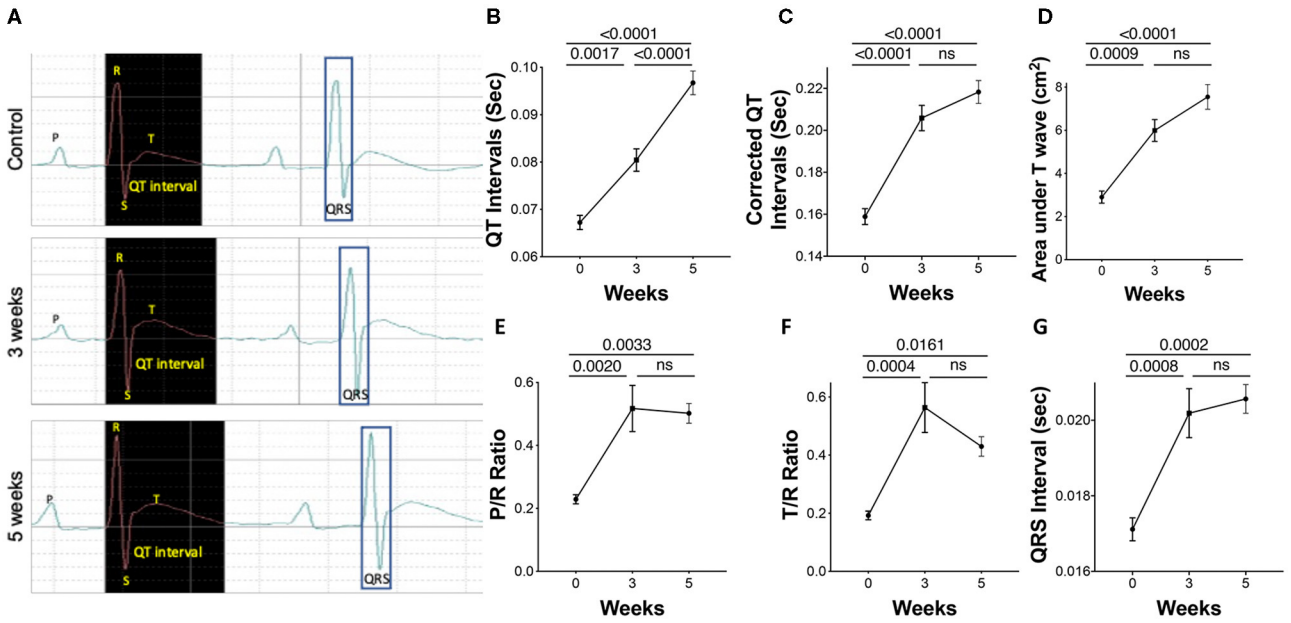

FIGURE 2 | Electrocardiographic parameters during PAH progression in rats. Pulmonary arterial hypertension was induced in rats as described in the Methods. A 2-channel electrocardiography (EKG) was utilized to record parameters. **(A)** Representative EKG tracings, showing **(B)** uncorrected QT intervals, **(C)** corrected QT intervals, **(D)** area under the T wave, **(E)** P/R ratio, **(F)** T/R ratio, and **(G)** QRS interval was also performed. *N* = 7–10 animals/group.

expected, the lung histology showed increased muscularization of the arteries with time demonstrating the progressive nature of the disease in this model (**Figures 3A–C**). Markers of cardiac injury are known to increase in pulmonary hypertension. cTnI increased linearly with disease progression (**Figure 3D**). Similarly, myosin light chain 3 (Myl3), a ventricular and slow skeletal muscle isoform, also increased linearly with disease progression (**Figure 3H**). Cardiac troponin T, however, increased only at the 5-week time point (**Figure 3E**). As expected, sTnI did not change with disease severity (**Figure 3F**). FABP3 (aka: H-FABP; heart type fatty acid-binding protein) increased only at the 5-week time point (**Figure 3G**).

Echocadiographic Estimation of Pulmonary Pressures and Pulmonary Vascular Resistance

In addition to the invasive RVSP, we also measured non-invasive surrogates of PH using echo Doppler across three time points. PAAT and PAAT/PAET were reduced with disease progression (**Figures 4A,C**). A non-significant reduction in PAET from baseline to 3 weeks occurred (**Figure 4B**). Calculated values of mPAP using PAAT increased significantly at 3 weeks of PH. Although, mPAP was expected to increase with progression of PH, calculated values did not increase further between 3 and 5 weeks (**Figure 4D**). The PA diameter as assessed by echocardiography progressively increased across the three time points. The PA distensibility index was significantly increased at 3 weeks with no further increase at 5 weeks (**Figure 4E**). Increased PA resistance and a reduction in compliance of large PAs cause premature systolic PA wave reflection resulting in flow deceleration and a mid-systolic notch. A mid-systolic notch was discernable with progressive PAH at 5 weeks (**Figure 4F**).

Right Ventricle Function and Structure

RV fractional area of change (RV-FAC) and ejection fraction (EF) reflect global RV systolic function. Tricuspid annular plane systolic excursion (TAPSE) and tricuspid valve systolic wave (TV-Sa) can serve as surrogates of the systolic function of the RV. Although, variable, RV systolic function was significantly reduced with progression of PAH. RV-FAC was significantly reduced at 3 weeks and continued to decline over 5 weeks (**Figure 4G**). Both EF and TAPSE, as measured by M-mode echocardiography tended to decrease with PH but were not statistically significant (**Figures 4H,I**). TV-Sa was significantly reduced starting at 3 weeks (**Figure 4J**). Similarly, RV myocardial performance index (RV-MPI), a measure of global systolic and diastolic RV function (19), was also increased at 3 weeks with no further change from 3 to 5 weeks (**Figure 4K**). Interestingly, RVSV did not change across the three time points (**Figure 4L**). However, a non-statistical reduction in RV cardiac output (RV-CO) at an early time point was observed (**Figure 4M**).

Increased RV pressure overload results in RV hypertrophy. The RV free wall thickness (RV-FWT), an indicator of RV hypertrophy, was significantly increased at 3 weeks. Furthermore, modest non-significant FWT changes occurred at 3- to 5-week time point (**Figure 4N**). An increase in FWT is consistent

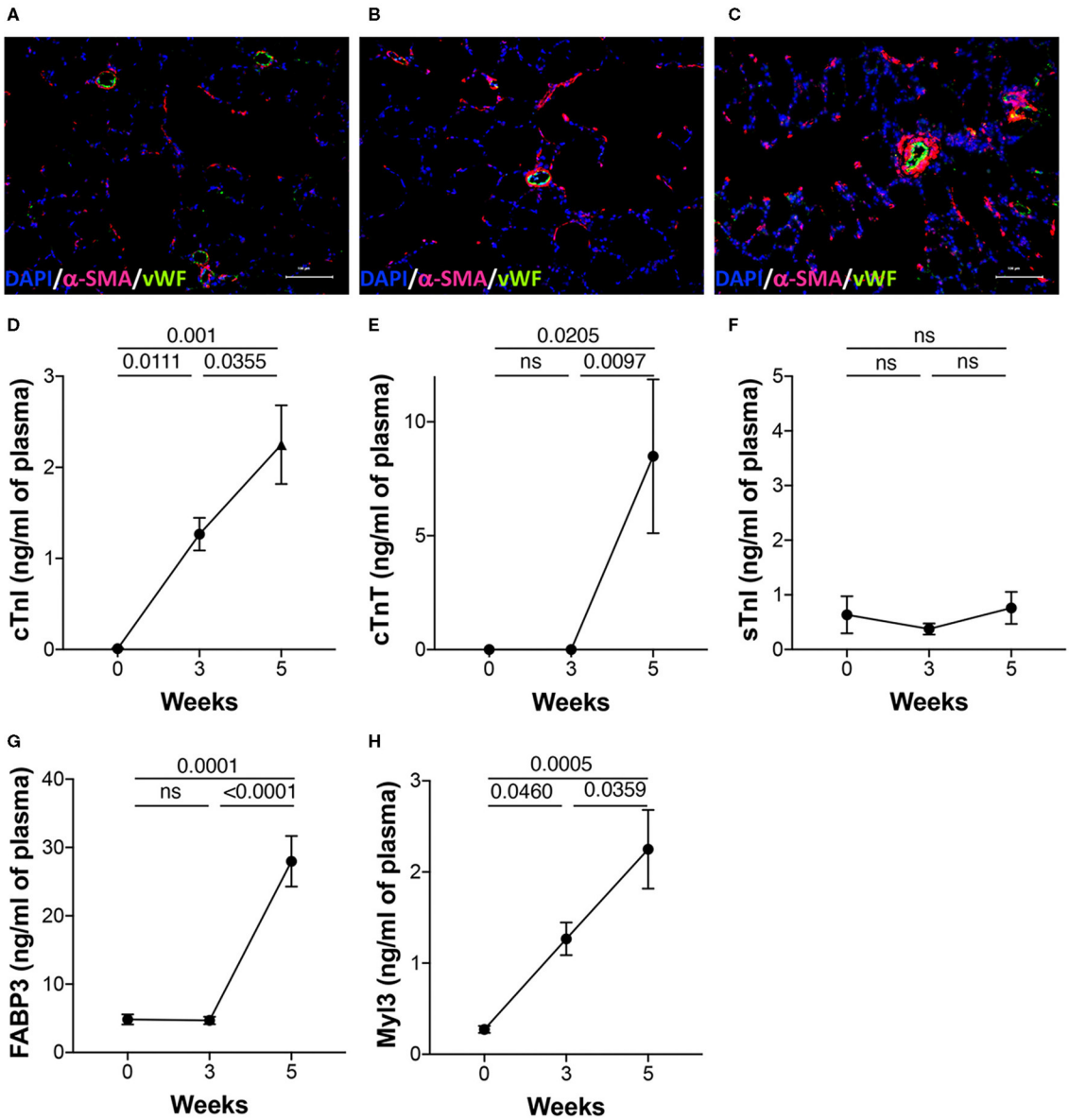

FIGURE 3 | Lung histology and plasma biomarkers of cardiac injury. PAH was induced in rats over a 5-week period as described in the Methods. **(A–C)** Representative images of the lung sections from the three time points stained for anti-vWF and anti-αSMA as described in details in the Methods. DAPI was used as a counterstain to visualize nuclei in tissue. Plasma was collected from separate sets of animals from naïve (0 day), 3 and 5 weeks post-induction of PAH. Markers of injury were estimated in the plasma using a multiplexed, meso scale discovery platform for **(D)** cardiac troponin I (cTnI), **(E)** cardiac troponin T (cTnT), **(F)** skeletal troponin I (sTnI), **(G)** fatty acid binding protein 3 (FABP3), and **(H)** myosin light chain 3 (Myl3). $N = 5–9$ animals/group.

with increased Fulton index at 3 and 5 weeks. No significant change in the RV diastolic function (RV E/A ratio, E′, or E/E′) was noticed across the three time points (data not shown).

Inferior Vena Cava and Hepatic Venous Flows

The hepatic venous (HV) flows and IVC diameter indicate the flow upstream from the PA and can be altered in PAH. The IVC diameters progressively increased from 0 to 5 weeks (**Figures 5A,B**). An increase in RV-EDP can lead to an increase in the amplitude of the HV atrial reversal waveform. A non-significant reduction in the S/D over time was observed (**Figure 5C**). Peak velocity of the HV atrial reversal wave was also increased (**Figure 5D**).

Left Ventricle Function and Structure

The progressive increase in RV afterload can compromise LV function, structure, and filling. The inter-ventricular septum

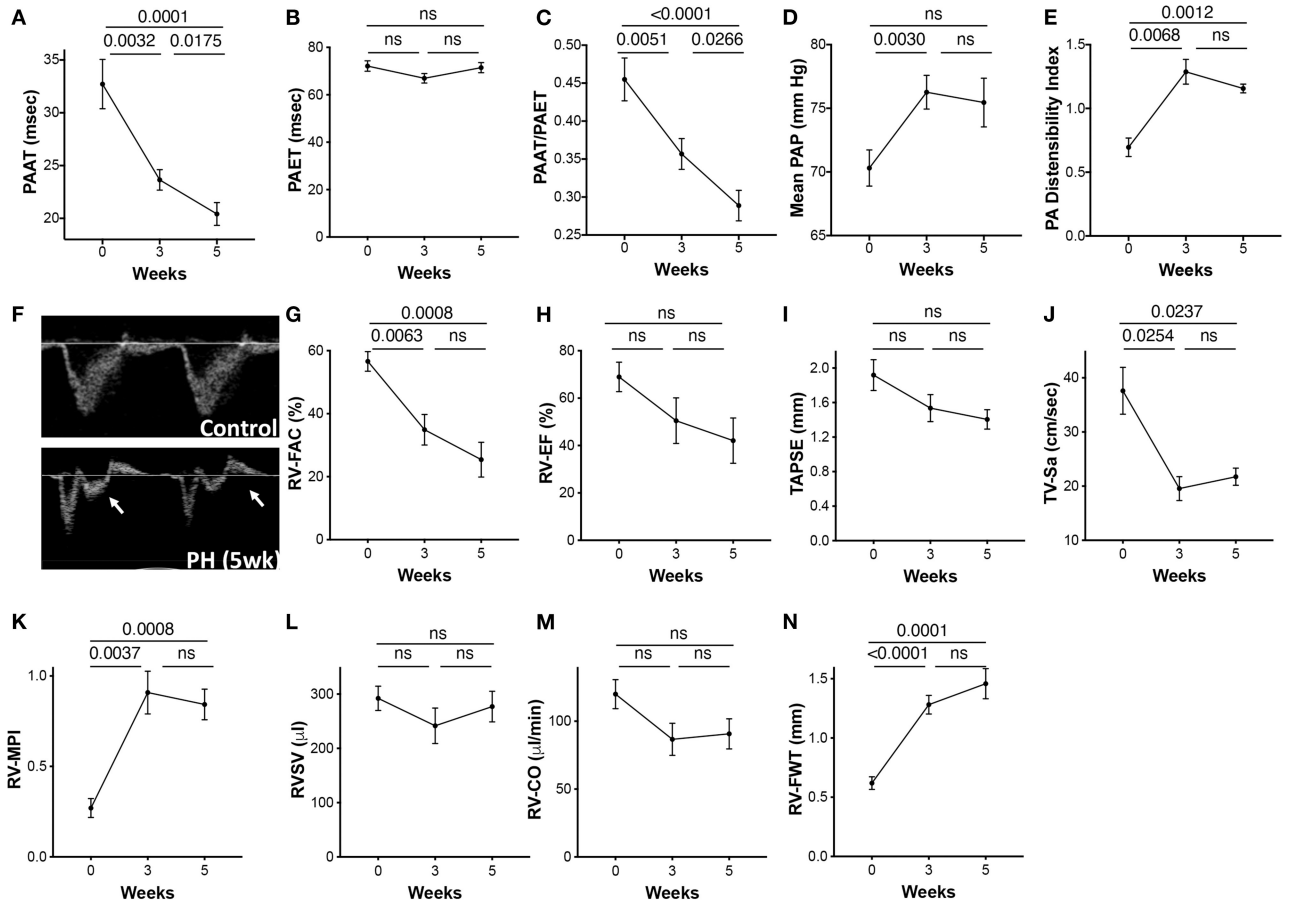

FIGURE 4 | Echocardiographic parameters of the pulmonary artery and the RV during progression of PAH. PAH was induced in rats over a 5-week period as described in the Methods. Echocardiographic images were acquired prior to induction of PH (0 day) and at 3 and 5 weeks post-induction. **(A)** Pulmonary artery acceleration time (PAAT), **(B)** pulmonary artery ejection time (PAET), **(C)** PAAT/PAET ratio, **(D)** calculated mean pulmonary artery pressure (mPAP), and **(E)** PA distensibility index, calculated as the ratio of the PA diameter (obtained from parasternal RV outflow tract view) to ascending aortic diameter from parasternal long axis flow at end diastole. **(F)** Pulse wave Doppler tracings showing the PA flow obtained from parasternal RV outflow view. Arrow shows the PA mid systolic notch. Each animal served as its own control at previous time points. A 2-dimensional echocardiographic examination of the RV was also performed from multiple acoustic views. **(G)** RV fractional area of change (RV-FAC) was measured from the transgastric midpapillary view, **(H)** RV-EF, **(I)** Tricuspid annular plane systolic excursion (TAPSE), **(J)** Tricuspid peak annular systolic velocity (TV-Sa), and **(K)** RV myocardial performance index (RV-MPI). **(L)** RVSV and **(M)** RV-CO were calculated from the parasternal long axis view. **(N)** RV free wall thickness (FWT) was measured from the apical four-chamber views. $N = 10$ animals/group.

was flattened with a leftward shift (**Figure 6A**). The LV eccentricity index systolic (LV-EIs) and the LV eccentricity index diastolic (LV-EId) increased progressively from baseline to 5 weeks (**Figures 6B,C**). A significant reduction in the LV filling was demonstrated by a reduced E and E/A from baseline to week 3, with a trend toward further reduction afterward (**Figures 6D,H**). LV cardiac output (LV-CO) was significantly reduced at week 3 with modest changes thereafter (**Figure 6E**). LV-SV was reduced at 3 weeks with no additional change with increased severity of PAH (**Figure 6F**). There was a significant reduction in the LV velocity of circumferential shortening (LV-VCFr) at 5 weeks (**Figure 6G**). In summary, reduced LV filling and output early in the disease was followed by reduction in the LV contractility at more advanced stage of PAH.

Correlation Between Echocardiographic Variables and Invasively Measured Right Ventricular Systolic Pressure

Pooled analyses of the study and control animals revealed significant correlation between invasively measured RVSP and each of the following parameters: pulmonary artery acceleration time (PAAT), PAAT/PAET (pulmonary artery ejection time), IVC diameter, RV-FAC, TAPSE, LV-EIs, LV-CO, LV-SV, and trans-mitral E/A (**Table 1**).

DISCUSSION

Using serial measurements, we identified distinct patterns of EKG, and biochemical and echocardiographic parameters that

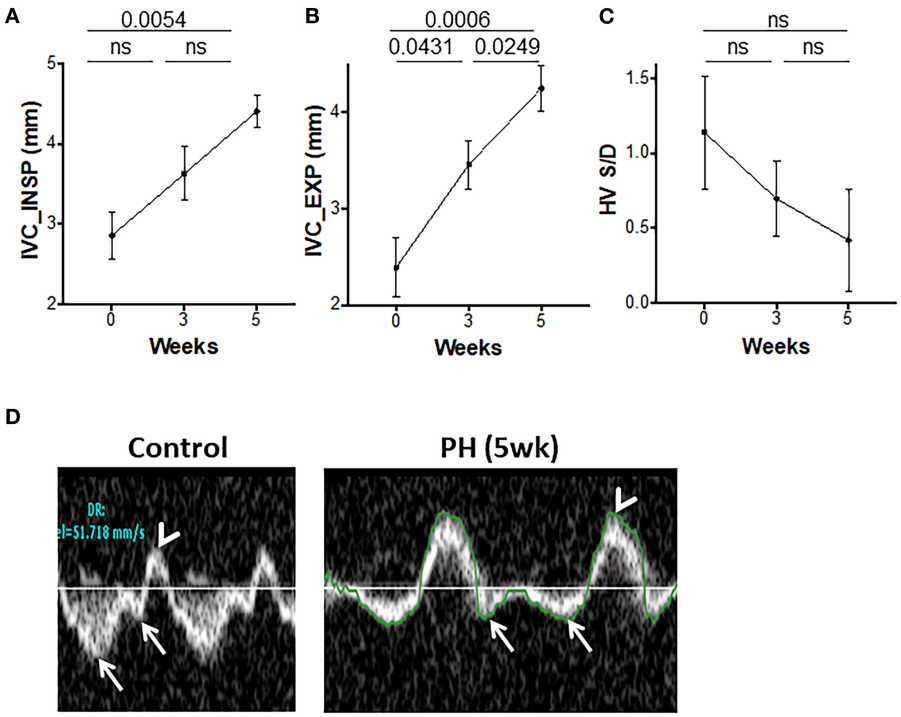

FIGURE 5 | Inferior vena cava (IVC) and hepatic venous flows during progression of PAH. IVC diameters at end inspiration **(A)** and end expiration **(B)** and the ratio of hepatic venous systolic to diastolic peak velocities **(C)** were measured from the subcostal view. **(D)** Representative echocardiographic images showing hepatic venous flow pattern with a reversal of systolic to diastolic peak velocity ratio (arrows) and prominent atrial reversal peak velocity wave (arrowhead) in control and animals with PH. *N* = 10 animals/group.

together can potentially be used to detect PAH early, monitor PAH progression, and assess RV dysfunction and its response to treatment. Knowledge of these patterns addresses the current gap in practice that focuses primarily on PAP reduction rather than on holistically reversing myocardial and vascular remodeling (2). Echocardiographic markers showed three different patterns representative of the pulmonary vascular and cardiac remodeling that takes place during the course of PAH; a steady pattern in which there is a progressive change of the echo parameters across the three time points of PAH (IVC end inspiratory, IVC end expiratory diameter, and PAAT), an early change in which there is an early reduction [RV-FAC, TV-Sa, MV(E/A), LV-CO, LVSV] or increase (mPAP by PAAT, RV-MPI, LV-EIs) followed by a plateau at severe PH, and a late pattern in which there is only a late rise at severe stages of PAH (LV-EId). In the same animal model, plasma biomarkers of cardiac injury showed two different patterns. Plasma levels of Myl-3 and cTnI steadily increased across the three time points compared with FABP-3 and cTnT that showed only a late rise at the 5-week time point. Grouping these variables into "patterns" overcomes some of their individual limitations in terms of their temporal relationship to the severity and progression of PAH.

PAH is characterized by a decrease in pulmonary vascular compliance and an increase in PVR causing initial adaptive compensation followed by a maladaptive decompensatory phase of the RV failure (20). The patterns identified in our study capture some of these mechanisms. The presence of mid-systolic notching on the RV outflow tract spectral Doppler observed at the 5-week time point can be used as a qualitative marker of the reduction in the PA compliance responsible for the increase in pulsatile load of the RV, which precedes the increase in PVR. It can also be used as a qualitative surrogate of the RV/PA uncoupling, an important measure in determining the RV maladaptation in PAH (21).

With progressive increase in mPAP, less time is spent during ejection, and a faster rise in peak systolic pressure occurs due to a rapid closure of the pulmonary valve, causing reduction in PAAT and PAAT/PAET ratio (22). The reduction in PAAT is indicative of increased PVR and is a consistent finding in preclinical and clinical PH, further supporting its reliability in monitoring the disease progression (22). Although, there has been some success in echocardiographically estimated mPAP, consistent determination of estimates remain a challenge (23, 24).

RV hypertrophy is the hallmark of PAH, and an increase in the RV free wall thickness (FWT) signifies an important compensatory mechanism by which the RV reduces its wall stress induced by the increase in pressure overload. Here we used the RV-FWT as a surrogate of RV hypertrophy rather than measuring the RV mass, given the limitations of measuring the RV mass by M-mode echocardiography (14). These findings were confirmed by Fulton index measurements and are consistent with other reports (25) and may represent a compensatory mechanism. The

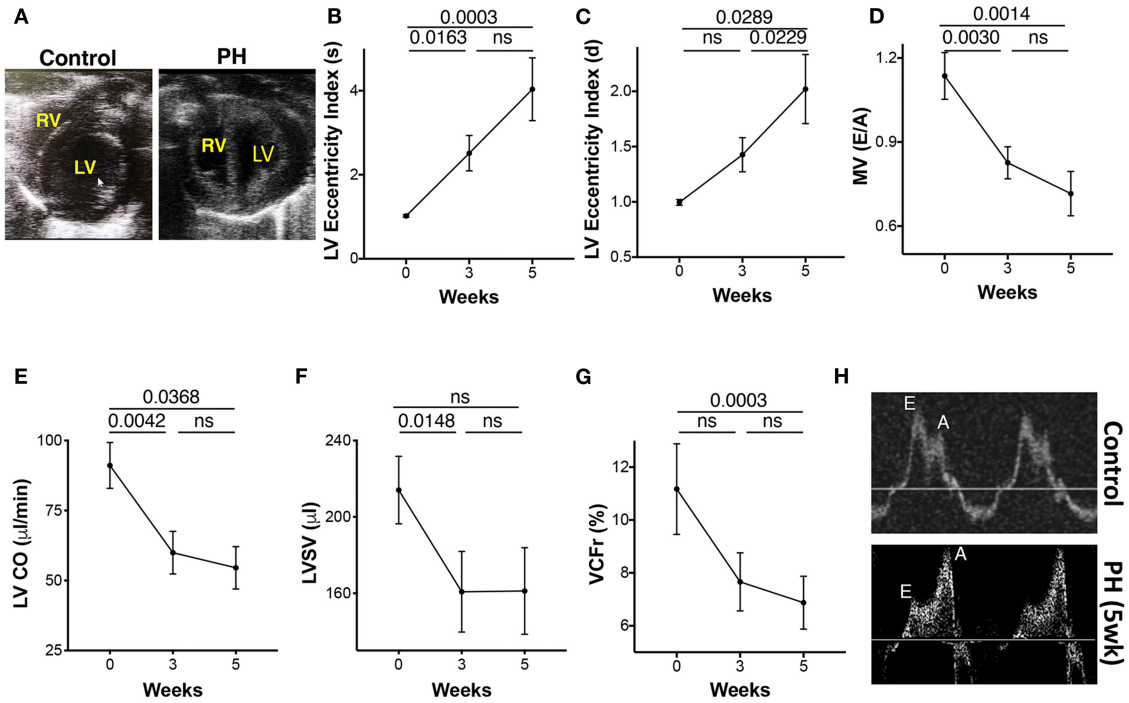

FIGURE 6 | Echocardiographic parameters of the left ventricle (LV) during progression of PAH. **(A)** Apical view of the chambers showing the RV and LV. LV eccentricity index image showing a reduction in the septolateral diameter in relation to the antero-inferior diameter of the LV. Eccentricity index was calculated from the transgastric midpapillary short axis view as the ratio of the antero-inferior diameter to the septolateral diameter of the LV. **(B)** LV eccentricity index in systole, **(C)** LV eccentricity index in diastole, **(D)** Transmitral ratio of peak early to late diastolic wave velocity, **(E)** CO, **(F)** SV, and **(G)** LV velocity of circumferential shortening as measured from the parasternal long axis view at 0, 3, and 5 weeks of PH induction. **(H)** Echocardiographic tracings showing mitral valve flow in control (top) and PH (bottom) animals. $N = 10$ animals/group.

RV contractility as measured by dP/dT_{max} increased significantly during the early phase of PAH development and consistent with other reports (26, 27). However, changes from 3 to 5 weeks were not significant despite a significant increase in RVSP and may represent the maladaptive phase of PAH. High RV dP/dT_{max} positive values were observed in PH patients even with evidence of RV failure (28). In advanced stages of PAH, dP/dT may be more dependent on the RV mass, HR, and intracavitary pressure rather than myocardial contractility (29).

Increased PA pressures can alter hepatic venous (HV) flows and IVC diameter leading to a reduction in the forward flow from the HV to the RV. An increase in IVC diameter reflects an increase in back pressure from the right atrium as a result of increase in RV afterload and can serve as a prognostic indicator of PH (30). Hepatic venous flow was shown to plateau after 3 weeks reflecting sensitivity only during the initial phases of development of PAH. This reflects the variable presentation of PAH in terms of the development of RV failure, elevation of the RV-EDP, occurrence of significant TR, and occurrence of atrial fibrillation (AF). Although, TR is a consistent finding in humans with PH, we were unable to discern a consistent tricuspid regurgitant jet due to technical limitations in image acquisition in rats.

We analyzed the correlation between the echocardiographic markers of progression of PAH and RVSP in order to assess their association with the severity of PAH. Markers associated with severity of PAH may be used for prognostication, whereas those associated with progression of PAH may be sought for monitoring of the disease progression and response to therapy. The correlation of TAPSE with RVSP confirms its prognostic significance and is consistent with previous reports. However, its failure to reduce beyond 3 weeks of PAH progression can be explained by the RV assuming a more spherical configuration during advanced stages of PAH and that TAPSE, being representative of the longitudinal motion of the RV and only of the free wall of the TV annulus, may be less contributing to RV ejection at this advanced stage of PAH. We are aware of the limitations of M-mode echocardiography in measuring RVEF compared with 3D echocardiography, which we did not possess at the time of the study. Similarly, RV-FAC, while being a prognostic marker of PAH, may not be an ideal marker of progression since it lacks representation of the RV outflow tract and may not represent the intrinsic contractility of the RV. Overall, echocardiography is a valuable tool in monitoring the severity and progression of PAH and may be helpful in its early diagnosis.

In the model, serial changes in the LV with progressive PAH were also characterized. The rise in LVSP pattern is consistent with previous reports (31). Flattening of the inter-ventricular septum with a leftward shift is also consistent with other studies

TABLE 1 | Correlation of echocardiographic variable with right ventricular systolic pressure (RVSP).

Variable	Correlation coefficient	*p*-Value
HV D	−0.44	0.053
HV S/D	−0.45	0.044
HV S2	−0.06	0.792
IVC_INSP	0.31	0.185
IVC-EXP	0.56	0.010
LV CO	−0.65	0.002
LV eccentricity index d	0.52	0.027
LV eccentricity index s	0.58	0.013
MPAP (common)	−0.62	0.055
MPAP (PAAT <120 ms)	−0.39	0.271
MV (E/A)	−0.77	<0.001
PA distensibility index	0.56	0.045
PAAT	−0.63	0.004
PAET	0.26	0.266
PAAT/PAET	−0.64	0.003
RV-EF	−0.34	0.208
RV-FAC	−0.60	0.005
RV mass	0.12	0.671
RV-MPI	0.48	0.053
RV-CO	−0.51	0.075
RVSV	−0.52	0.066
LVSV	−0.58	0.007
TAPSE	−0.50	0.025
TV-Sa	−0.09	0.714

(32). This reduces LV septo-lateral dimension compared with antero-inferior dimension at end systole and diastole reflecting ventricular interdependence (33). The initial pattern of reduced filling is evidenced by a decrease in transmitral E/A and an increase in LV-EIs and LV-EId, followed by a reduction in LV-CO and LV-SV, and ending with a reduction in contractility as shown by reduced VCFr. The latter is considered a less load-dependent index of systolic function compared with LV-EF (34).

In our EKG studies, progressive prolongation in QT-interval reflects an abnormality in ventricular depolarization or repolarization, which may predispose to ventricular arrhythmias reportedly common in PH (35). Prolongation of QT-interval has been shown to correlate with cardiac remodeling, in addition to being an independent predictor of mortality in PH (36). Increased QT-interval and wide RS-interval observed in our studies were also consistent with other reports where QRS prolongation was associated with clinical severity and mortality in patients with PH (37, 38). An increase in the QRS interval is a sign of intraventricular electrical conduction delay, likely due to ventricular dys-synchrony resulting from RV hypertrophy and dilation. Increased amplitude of the P wave is a sign of atrial enlargement likely related to right atrial enlargement secondary to elevated RVSP and secondary to PH (18). These EKG findings of raised right atrial pressure, intraventricular conduction delay, and propensity for ventricular arrhythmias are consistent with adverse outcomes in PH (39).

Makers of cardiac injury are frequently used in stratification of disease. Our findings of increased levels of cTnT and FABP3 only during the late stages of PAH suggests their potential use as markers of disease severity. It is therefore not surprising that both of these markers were shown to correlate with major adverse events and were also predictors of mortality (40, 41). On the other hand, cTnI levels increased linearly with PAH progression suggesting its potential use as a sensitive marker of disease progression and in response to therapies. We also found that Myl3, another marker of cardiotoxicity (42, 43), also increased with disease severity and can also be potentially used as a sensitive marker of PH progression.

In summary, recognizing biochemical, electrocardiographic, and echocardiographic patterns of PAH progression and severity may help in the monitoring and prognostication of RV function in PAH. Despite limitations, echocardiography is invaluable not only in diagnosing PAH but also in follow-up. There is a need for a "collective" assessment of the entire cardiovascular system in PAH. More studies are needed to mechanistically correlate electrical, vascular, and mechanical remodeling to non-invasive echo- and electrocardiographic findings.

DATA AVAILABILITY STATEMENT

The original contributions presented in the study are included in the article/supplementary material, further inquiries can be directed to the corresponding author/s.

ETHICS STATEMENT

The animal study was reviewed and approved by Institutional Animal Care and Use Committee (IACUC), University of Alabama at Birmingham, Birmingham, Alabama, USA.

AUTHOR CONTRIBUTIONS

AZ and AA helped conceive the idea, design the study, analyze the data, and write the manuscript. IZ, MH, and NM helped acquire and analyze the data and review and write the manuscript. JM-J and TH helped analyze the data and review and write the manuscript. CM and MF helped with the statistical analysis of the data and reviewed and edited the manuscript. All authors contributed to the article and approved the submitted version.

FUNDING

Grant support from NIH (R01HL114933, U01ES025069, R01HL137046) is gratefully acknowledged.

ACKNOWLEDGMENTS

The authors are grateful to Wayne Bradley for performing the echocardiography measurements. We thank Dr. Dan Berkowitz for providing valuable feedback.

REFERENCES

1. van de Veerdonk MC, Bogaard HJ, Voelkel NF. The right ventricle and pulmonary hypertension. *Heart Fail Rev.* (2016) 21:259–71. doi: 10.1007/s10741-016-9526-y
2. Lahm T, Douglas IS, Archer SL, Bogaard HJ, Chesler NC, Haddad F, et al. Assessment of right ventricular function in the research setting: knowledge gaps and pathways forward. An Official American Thoracic Society research statement. *Am J Respir Crit Care Med.* (2018) 198:e15–43. doi: 10.1164/rccm.201806-1160ST
3. Boucly A, Weatherald J, Savale L, Jais X, Cottin V, Prevot G, et al. Risk assessment, prognosis and guideline implementation in pulmonary arterial hypertension. *Eur Respir J.* (2017) 50:e1700889. doi: 10.1183/13993003.00889-2017
4. Hemnes AR, Champion HC. Right heart function and haemodynamics in pulmonary hypertension. *Int J Clin Pract Suppl.* (2008) 160:11–9. doi: 10.1111/j.1742-1241.2008.01812.x
5. van de Veerdonk MC, Kind T, Marcus JT, Mauritz GJ, Heymans MW, Bogaard HJ, et al. Progressive right ventricular dysfunction in patients with pulmonary arterial hypertension responding to therapy. *J Am Coll Cardiol.* (2011) 58:2511–9. doi: 10.1016/j.jacc.2011.06.068
6. Voelkel NF, Quaife RA, Leinwand LA, Barst RJ, McGoon MD, Meldrum DR, et al. Right ventricular function and failure: report of a National Heart, Lung, and Blood Institute working group on cellular and molecular mechanisms of right heart failure. *Circulation.* (2006) 114:1883–91. doi: 10.1161/CIRCULATIONAHA.106.632208
7. Badano LP, Ginghina C, Easaw J, Muraru D, Grillo MT, Lancellotti P, et al. Right ventricle in pulmonary arterial hypertension: haemodynamics, structural changes, imaging, and proposal of a study protocol aimed to assess remodelling and treatment effects. *Eur J Echocardiogr.* (2010) 11:27–37. doi: 10.1093/ejechocard/jep152
8. Galie N, Humbert M, Vachiery JL, Gibbs S, Lang I, Torbicki A, et al. 2015 ESC/ERS Guidelines for the diagnosis and treatment of pulmonary hypertension: the joint task force for the diagnosis and treatment of pulmonary hypertension of the European Society of Cardiology (ESC) and the European Respiratory Society (ERS): Endorsed by: Association for European Paediatric and Congenital Cardiology (AEPC), International Society for Heart and Lung Transplantation (ISHLT). *Eur Respir J.* (2015) 46:903–75. doi: 10.1183/13993003.01032-2015
9. Maron BA, Kovacs G, Vaidya A, Bhatt DL, Nishimura RA, Mak S, et al. Cardiopulmonary hemodynamics in pulmonary hypertension and heart failure: JACC review topic of the week. *J Am Coll Cardiol.* (2020) 76:2671–81. doi: 10.1016/j.jacc.2020.10.007
10. Simonneau G, Montani D, Celermajer DS, Denton CP, Gatzoulis MA, Krowka M, et al. Haemodynamic definitions and updated clinical classification of pulmonary hypertension. *Eur Respir J.* (2019) 53:e1801913. doi: 10.1183/13993003.01913-2018
11. Taraseviciene-Stewart L, Kasahara Y, Alger L, Hirth P, Mc Mahon G, Waltenberger J, et al. Inhibition of the VEGF receptor 2 combined with chronic hypoxia causes cell death-dependent pulmonary endothelial cell proliferation and severe pulmonary hypertension. *FASEB J.* (2001) 15:427–38. doi: 10.1096/fj.00-0343com
12. Ahmad S, Masjoan Juncos JX, Ahmad A, Zaky A, Wei CC, Bradley WE, et al. Bromine inhalation mimics ischemia-reperfusion cardiomyocyte injury and calpain activation in rats. *Am J Physiol Heart Circ Physiol.* (2019) 316:H212–23. doi: 10.1152/ajpheart.00652.2017
13. Liu J, Rigel DF. Echocardiographic examination in rats and mice. *Methods Mol Biol.* (2009) 573:139–55. doi: 10.1007/978-1-60761-247-6_8
14. Rudski LG, Lai WW, Afilalo J, Hua L, Handschumacher MD, Chandrasekaran K, et al. Guidelines for the echocardiographic assessment of the right heart in adults: a report from the American Society of Echocardiography endorsed by the European Association of Echocardiography, a registered branch of the European Society of Cardiology, and the Canadian Society of Echocardiography. *J Am Soc Echocardiogr.* (2010) 23:685–713; quiz 86–8. doi: 10.1016/j.echo.2010.05.010
15. Steckelberg RC, Tseng AS, Nishimura R, Ommen S, Sorajja P. Derivation of mean pulmonary artery pressure from non-invasive parameters. *J Am Soc Echocardiogr.* (2013) 26:464–8. doi: 10.1016/j.echo.2013.01.006
16. Tei C, Ling LH, Hodge DO, Bailey KR, Oh JK, Rodeheffer RJ, et al. New index of combined systolic and diastolic myocardial performance: a simple and reproducible measure of cardiac function–a study in normals and dilated cardiomyopathy. *J Cardiol.* (1995) 26:357–66. doi: 10.1016/S0894-7317(05)80111-7
17. Tattersall ML, Dymond M, Hammond T, Valentin JP. Correction of QT values to allow for increases in heart rate in conscious Beagle dogs in toxicology assessment. *J Pharmacol Toxicol Methods.* (2006) 53:11–9. doi: 10.1016/j.vascn.2005.02.005
18. Konopelski P, Ufnal M. Electrocardiography in rats: a comparison to human. *Physiol Res.* (2016) 65:717–25. doi: 10.33549/physiolres.933270
19. Levy PT, Sanchez Mejia AA, Machefsky A, Fowler S, Holland MR, Singh GK. Normal ranges of right ventricular systolic and diastolic strain measures in children: a systematic review and meta-analysis. *J Am Soc Echocardiogr.* (2014) 27:549–60.e3. doi: 10.1016/j.echo.2014.01.015
20. Vonk-Noordegraaf A, Haddad F, Chin KM, Forfia PR, Kawut SM, Lumens J, et al. Right heart adaptation to pulmonary arterial hypertension: physiology and pathobiology. *J Am Coll Cardiol.* (2013) 62(Suppl. 25):D22–33. doi: 10.1016/j.jacc.2013.10.027
21. Ghuysen A, Lambermont B, Kolh P, Tchana-Sato V, Magis D, Gerard P, et al. Alteration of right ventricular-pulmonary vascular coupling in a porcine model of progressive pressure overloading. *Shock.* (2008) 29:197–204. doi: 10.1097/shk.0b013e318070c790
22. Tossavainen E, Soderberg S, Gronlund C, Gonzalez M, Henein MY, Lindqvist P. Pulmonary artery acceleration time in identifying pulmonary hypertension patients with raised pulmonary vascular resistance. *Eur Heart J Cardiovasc Imaging.* (2013) 14:890–7. doi: 10.1093/ehjci/jes309
23. Parasuraman S, Walker S, Loudon BL, Gollop ND, Wilson AM, Lowery C, et al. Assessment of pulmonary artery pressure by echocardiography-A comprehensive review. *Int J Cardiol Heart Vasc.* (2016) 12:45–51. doi: 10.1016/j.ijcha.2016.05.011
24. Naing P, Kuppusamy H, Scalia G, Hillis GS, Playford D. Non-invasive assessment of pulmonary vascular resistance in pulmonary hypertension: current knowledge and future direction. *Heart Lung Circ.* (2017) 26:323–30. doi: 10.1016/j.hlc.2016.10.008
25. Vitali SH, Hansmann G, Rose C, Fernandez-Gonzalez A, Scheid A, Mitsialis SA, et al. The Sugen 5416/hypoxia mouse model of pulmonary hypertension revisited: long-term follow-up. *Pulm Circ.* (2014) 4:619–29. doi: 10.1086/678508
26. Hsu S, Houston BA, Tampakakis E, Bacher AC, Rhodes PS, Mathai SC, et al. Right ventricular functional reserve in pulmonary arterial hypertension. *Circulation.* (2016) 133:2413–22. doi: 10.1161/CIRCULATIONAHA.116.022082
27. Wang Z, Schreier DA, Hacker TA, Chesler NC. Progressive right ventricular functional and structural changes in a mouse model of pulmonary arterial hypertension. *Physiol Rep.* (2013) 1:e00184. doi: 10.1002/phy2.184
28. Stein PD, Sabbah HN, Anbe DT, Marzilli M. Performance of the failing and non-failing right ventricle of patients with pulmonary hypertension. *Am J Cardiol.* (1979) 44:1050–5. doi: 10.1016/0002-9149(79)90168-1
29. Levine HJ, Gaasch WH. *The Ventricle : Basic and Clinical Aspects*. Boston: Nijhoff; Hingham, MA: Distributors for North America, Kluwer Academic (1985). p. ix, 345. doi: 10.1007/978-1-4613-2599-4
30. Watanabe R, Amano H, Saito F, Toyoda S, Sakuma M, Abe S, et al. Echocardiographic surrogates of right atrial pressure in pulmonary hypertension. *Heart Vessels.* (2019) 34:477–83. doi: 10.1007/s00380-018-1264-8
31. Sztuka K, Jasinska-Stroschein M. Animal models of pulmonary arterial hypertension: a systematic review and meta-analysis of data from 6126 animals. *Pharmacol Res.* (2017) 125(Pt. B):201–14. doi: 10.1016/j.phrs.2017.08.003
32. Kim BS, Heo R, Shin J, Lim YH, Park JK. E/E' and D-shaped left ventricle severity in patients with increased pulmonary artery pressure. *J Cardiovasc Imaging.* (2018) 26:85–92. doi: 10.4250/jcvi.2018.26.e6
33. Egemnazarov B, Schmidt A, Crnkovic S, Sydykov A, Nagy BM, Kovacs G, et al. Pressure overload creates right ventricular diastolic dysfunction in a mouse model: assessment by echocardiography. *J Am Soc Echocardiogr.* (2015) 28:828–43. doi: 10.1016/j.echo.2015.02.014

34. Mizuno R, Fujimoto S, Saito Y, Okamoto Y. Detection of latent anthracycline-induced cardiotoxicity using left ventricular end-systolic wall stress-velocity of circumferential fiber-shortening relationship. *Heart Vessels.* (2014) 29:384–9. doi: 10.1007/s00380-013-0375-5
35. Smith B, Genuardi MV, Koczo A, Zou RH, Thoma FW, Handen A, et al. Atrial arrhythmias are associated with increased mortality in pulmonary arterial hypertension. *Pulm Circ.* (2018) 8:1–9. doi: 10.1177/2045894018790316
36. Rich JD, Thenappan T, Freed B, Patel AR, Thisted RA, Childers R, et al. QTc prolongation is associated with impaired right ventricular function and predicts mortality in pulmonary hypertension. *Int J Cardiol.* (2013) 167:669–76. doi: 10.1016/j.ijcard.2012.03.071
37. Sun PY, Jiang X, Gomberg-Maitland M, Zhao QH, He J, Yuan P, et al. Prolonged QRS duration: a new predictor of adverse outcome in idiopathic pulmonary arterial hypertension. *Chest.* (2012) 141:374–80. doi: 10.1378/chest.10-3331
38. Temple IP, Logantha SJ, Absi M, Zhang Y, Pervolaraki E, Yanni J, et al. Atrioventricular node dysfunction and ion channel transcriptome in pulmonary hypertension. *Circ Arrhythm Electrophysiol.* (2016) 9:e003432. doi: 10.1161/CIRCEP.115.003432
39. Raymond RJ, Hinderliter AL, Willis PW, Ralph D, Caldwell EJ, Williams W, et al. Echocardiographic predictors of adverse outcomes in primary pulmonary hypertension. *J Am Coll Cardiol.* (2002) 39:1214–9. doi: 10.1016/S0735-1097(02)01744-8
40. Qian HY, Huang J, Yang YJ, Yang YM, Li ZZ, Zhang JM. Heart-type fatty acid binding protein in the assessment of acute pulmonary embolism. *Am J Med Sci.* (2016) 352:557–62. doi: 10.1016/j.amjms.2016.08.018
41. Filusch A, Giannitsis E, Katus HA, Meyer FJ. High-sensitive troponin T: a novel biomarker for prognosis and disease severity in patients with pulmonary arterial hypertension. *Clin Sci.* (2010) 119:207–13. doi: 10.1042/CS20100014
42. Schultze AE, Main BW, Hall DG, Hoffman WP, Lee HY, Ackermann BL, et al. A comparison of mortality and cardiac biomarker response between three outbred stocks of Sprague Dawley rats treated with isoproterenol. *Toxicol Pathol.* (2011) 39:576–88. doi: 10.1177/0192623311402219
43. Berna M, Ackermann B. Increased throughput for low-abundance protein biomarker verification by liquid chromatography/tandem mass spectrometry. *Anal Chem.* (2009) 81:3950–6. doi: 10.1021/ac902744

Conflict of Interest: The authors declare that the research was conducted in the absence of any commercial or financial relationships that could be construed as a potential conflict of interest.

frontiers in Cardiovascular Medicine

ORIGINAL RESEARCH
published: 07 September 2021
doi: 10.3389/fcvm.2021.701079

Circulating Vascular Adhesion Protein-1 Level Predicts the Risk of Cardiovascular Events and Mortality in Hemodialysis Patients

Dae Kyu Kim[1†], Yu Ho Lee[2†], Jin Sug Kim[3], Yang Gyun Kim[3], So-Young Lee[2], Shin Young Ahn[4], Dong-Young Lee[5], Kyung Hwan Jeong[3], Sang-Ho Lee[3], Hyeon Seok Hwang[3] and Ju-Young Moon[3*]*

[1] Department of Medicine, Graduate School, Kyung Hee University, Seoul, South Korea, [2] Division of Nephrology, Department of Internal Medicine, CHA Bundang Medical Center, CHA University, Seongnam, South Korea, [3] Division of Nephrology, Department of Internal Medicine, Kyung Hee University, Seoul, South Korea, [4] Division of Nephrology, Department of Internal Medicine, Korea University College of Medicine, Seoul, South Korea, [5] Division of Nephrology, Department of Internal Medicine, Veterans Health Service Medical Center, Seoul, South Korea

OPEN ACCESS

Edited by:
Alessio Molfino,
Sapienza University of Rome, Italy

Reviewed by:
Pan Gao,
Fudan University, China
Lizhe Sun,
Xi'an Jiaotong University, China

***Correspondence:**
Hyeon Seok Hwang
hwanghsne@gmail.com
Ju-Young Moon
jymoon@khu.ac.kr

[†]These authors have contributed equally to this work and share first authorship

Specialty section:
This article was submitted to General Cardiovascular Medicine, a section of the journal Frontiers in Cardiovascular Medicine

Received: 27 April 2021
Accepted: 13 August 2021
Published: 07 September 2021

Citation:
Kim DK, Lee YH, Kim JS, Kim YG, Lee S-Y, Ahn SY, Lee D-Y, Jeong KH, Lee S-H, Hwang HS and Moon J-Y (2021) Circulating Vascular Adhesion Protein-1 Level Predicts the Risk of Cardiovascular Events and Mortality in Hemodialysis Patients. Front. Cardiovasc. Med. 8:701079. doi: 10.3389/fcvm.2021.701079

Background: Vascular adhesion protein-1 (VAP-1) is an oxidative enzyme of primary amines that facilitates the transmigration of inflammatory cells. Its oxidative and inflammatory effects are prominently increased in pathological conditions, such as metabolic, atherosclerotic, and cardiac diseases. However, the clinical significance of circulating VAP-1 levels in hemodialysis (HD) patients is unclear.

Methods: A total of 434 HD patients were enrolled in a prospective multicenter cohort study between June 2016 and April 2019. Plasma VAP-1 levels were measured at the time of data entry, and the primary endpoint was defined as a composite of cardiovascular (CV) and cardiac events.

Results: Circulating VAP-1 levels were positively correlated with plasma levels of cardiac remodeling markers, including brain natriuretic peptide, galectin-3, and matrix metalloproteinase-2. Multivariable logistic regression analysis revealed that patients with higher circulating VAP-1 levels were more likely to have left ventricular diastolic dysfunction [odds ratio, 1.40; 95% confidence interval [CI], 1.04–1.88]. The cumulative event rate of the composite of CV events was significantly greater in VAP-1 tertile 3 than in VAP-1 tertiles 1 and 2 ($P = 0.009$). Patients in tertile 3 were also associated with an increased cumulative event rate of cardiac events ($P = 0.015$), with a 2.06-fold higher risk each for CV (95% CI, 1.10–3.85) and cardiac (95% CI, 1.03–4.12) events after adjusting for multiple variables.

Conclusions: Plasma VAP-1 levels were positively associated with left ventricular diastolic dysfunction and the risk of incident CV and cardiac events in HD patients. Our results indicate that VAP-1 may aid clinicians in identifying HD patients at a high risk of CV events.

Keywords: vascular adhesion protein-1, hemodialysis, cardiovascular disease, endothelial dysfunction, diastolic dysfunction

INTRODUCTION

Patients receiving hemodialysis (HD) have substantial retention of uremic toxins, which lead to a number of adverse metabolic processes (1). Oxidative stress and inflammation are representative pathophysiologic processes of uremic complications and are major contributors of cardiovascular (CV) complications in HD patient (2–5), by promoting myocardial stiffening and left ventricular (LV) hypertrophy and inducing endothelial dysfunction and progression of atherosclerosis (5–7). These conditions severely increase the risk of CV complications, which have become leading causes of death in HD patients (8).

Vascular adhesion protein-1 (VAP-1) is a semicarbazide-sensitive amine oxidase that catalyzes the oxidative deamination of primary amines, which generates free radicals and causes oxidative stress (9, 10). It also facilitates the transmigration of inflammatory cells and worsens injuries in inflamed tissues (9, 11). These deleterious roles are prominently enhanced in pathological conditions. Circulating VAP-1 levels are increased in septic, metabolic, and autoimmune diseases, and higher VAP-1 levels increase the risk of atherosclerotic events and CV mortality (12–14). In patients with impaired renal function, excessive concentrations and abundant substrates of VAP-1 were observed, the latter of which undergo uncontrolled deamination and oxidative stress (14, 15). Furthermore, VAP-1 is suggested to play a pivotal role in HD patients because many dialysis-specific factors upregulate inflammatory processes (15, 16). Therefore, VAP-1 may be critically involved in the occurrence of adverse CV events in HD patients through oxidative stress and inflammation.

However, the clinical significance of VAP-1 has rarely been evaluated in HD patients, and no reports have investigated the prognostic significance of VAP-1. In this study, we investigated the association between circulating VAP-1 levels and risk of incident adverse CV events in HD patients, along with the relationship of echocardiographic parameters and circulating cardiac biomarkers with VAP-1 levels.

MATERIALS AND METHODS

Study Population

All data in this study were obtained from the K-cohort registry, which is a multicenter, internet-based, prospective cohort of HD patients in Korea designed to investigate the prognostic markers of CV complications and mortality. Patients from six general hospitals were enrolled if they were aged >18 years and received regular 4-h HD prescriptions per session that occurred thrice a week for at least 3 months. The exclusion criteria were as follows: pregnancy, hematological malignancy, presence of a solid tumor, and a life expectancy of <6 months. A total of 637 patients were recruited between June 2016 and April 2019, and 434 patients with whole plasma samples at the time of enrollment were included. The study protocol was approved by the local ethics committee (KHNMC 2016-04-039), and the study was conducted in accordance with the principles of the Declaration of Helsinki. All involved participants signed written informed consent forms before enrollment.

The patients were classified into three groups based on the circulating VAP-1 levels as follows: tertile 1, <343.2 ng/mL; tertile 2, 343.2–<438.2 ng/mL; and tertile 3, ≥438.2 ng/mL. All patients were prospectively followed up for specific clinical events after baseline assessments. Patient follow-up was censored at the time of transfer to peritoneal dialysis, kidney transplantation, loss of follow-up, or patient consent withdrawal.

Data Collection and Outcome Measures

Information on baseline demographic factors, laboratory data, dialysis, and concomitant medications were collected from medical records and interviews. Information on comorbidities were investigated and used to calculate the Charlson comorbidity index score (17). Fasting blood samples for laboratory data and enzymatic measurements were collected before the start of HD in a midweek session.

The primary endpoint was a composite of incident CV events and mortality, which included cardiac events such as coronary artery disease requiring coronary artery bypass surgery or percutaneous intervention, myocardial infarction, heart failure, ventricular arrhythmia, cardiac arrest, and sudden death, as well as cerebral infarction, cerebral hemorrhage, and peripheral vascular occlusive diseases requiring revascularization or surgical intervention. All-cause mortality events were recorded. The secondary endpoints were the correlation of VAP-1 levels with LV diastolic dysfunction, which was defined as peak early diastolic flow velocity (E)/peak early diastolic tissue velocity (E') of >15 on echocardiography, and levels of circulating cardiac markers.

Echocardiographic Measurements

Among the enrolled patients, 214 (49.3%) underwent echocardiography [61 (42.4%) in tertile 1, 75 (51.7%) in tertile 2, and 78 (53.8%) in tertile 3]. Cardiologists and trained sonographers examined two-dimensional and M-mode echocardiographs based on the recommendations of the American Society of Echocardiography (18). LV end-diastolic diameter (LVDd), LV end-systolic diameter, LV posterior wall thickness, and interventricular septal thickness were measured in the M-mode echocardiogram. LV mass was estimated using the Devereux formula, with the body surface area as the index. LV end-diastolic and LV end-systolic volumes, LV ejection fraction, and left atrial dimensions were determined in apical two- and four-chamber views. E and peak late diastolic flow velocity (A) was determined from the mitral valve inflow velocity curve using pulsed-wave Doppler ultrasonography. E' was measured from the septal aspect of the mitral annulus using tissue Doppler. The E/A and E/E' ratios were calculated.

Measurements of Circulating Cardiac Markers and VAP-1 Levels

Baseline plasma samples for the measurement of N-terminal pro-B-type natriuretic peptide (NT-proBNP), brain natriuretic peptide (BNP), matrix metalloproteinase-2 (MMP-2), and VAP-1 were collected using ethylenediaminetetraacetic acid-treated tubes. After centrifugation for 15 min at 1,000 × g at room temperature, the samples were stored at 80°C until use. Enzyme-linked immunosorbent assay was performed using Magnetic

Luminex® Screening Assay multiplex kits (R&D Systems, Inc., Minneapolis, MN, USA).

Statistical Analysis

Data are expressed as means ± standard deviations (SDs) or medians (interquartile ranges). Differences among the three groups were identified using analysis of variance or Kruskal-Wallis test. Tukey *post-hoc* test and Mann-Whitney *U*-test with Bonferroni correction were used to identify intergroup differences. Chi-square test or Fisher's exact test was used to compare the categorical variables. Log-transformed high-sensitivity C-reactive protein (hsCRP) values were used because of the skewed data distribution. Correlation between the VAP-1 levels and continuous variables was evaluated using Spearman's analyses. Binary logistic regression analysis was used to assess the association between the VAP-1 levels and LV diastolic dysfunction. A Cox proportional hazards model was constructed to identify independent variables related to CV and cardiac events and all-cause mortality. Parameters significantly associated with weight in the univariable analysis and clinically fundamental parameters were included in the multivariable models. Formal tests for the interaction between VAP-1 levels and predefined subgroups were conducted in addition to the main effects of the fully adjusted models. We modeled the association between VAP-1 levels and the hazard ratio to predict CV events. We used three knots and restricted cubic spline transformations to continuous measures. We calculated the sample size using standard formulas based on the number of patients to obtain the adequate statistical power for the primary endpoint and show a different composite event-free survival rate with an α-level of 0.05, β error of 0.20, and hazard ratio of 1.5. The minimum required sample size in each group was 98 patients. Statistical significance was set at $P < 0.05$. Statistical analyses were performed using the SPSS software (version 22.0; SPSS, IBM Corp., Armonk, NY, USA) and R software (version 3.6.2).

RESULTS

Baseline Demographic Characteristics and Laboratory Data

The mean VAP-1 level was 386.0 (range, 318.1–484.6) ng/mL, with mean VAP-1 levels in tertiles 1, 2, and 3 of 281.8 ng/mL (range, 242.6–318.5 ng/mL), 385.5 ng/mL (range, 365.6–411.0 ng/mL), and 523.6 ng/mL (range, 484.6–601.4 ng/mL), respectively. The baseline clinical characteristics, demographics, and laboratory results are shown in **Table 1**. Patients in tertile 3 had a shorter HD history, higher prevalence of diabetes mellitus, higher Charlson comorbidity index, higher pre-dialysis systolic blood pressure (SBP), and lower intact parathyroid hormone (i-PTH) than those in tertile 1. Regarding the circulating cardiac markers, patients in tertile 3 showed the highest BNP and MMP-2 levels. Plasma MMP-2 levels were moderately correlated with plasma VAP-1 levels, whereas BNP and galectin-3 showed weak positive correlations (**Supplementary Table S1**). In contrast, hsCRP levels demonstrated a weak negative correlation with circulating VAP-1 levels.

Relationship Between Plasma VAP-1 Levels and LV Diastolic Dysfunction in Hemodialysis Patients

Baseline echocardiographic measurements are presented in **Supplementary Table S2**. LVDd was significantly different among the tertiles, with the highest E wave and E/A and E/E' ratios observed in patients in VAP-1 tertile 3. We constructed univariable and multivariable binary logistic regression models to determine the association between VAP-1 and LV diastolic dysfunction (**Table 2**). In the univariable analysis, circulating VAP-1 level increment per SD [dds ratio [OR], 1.51; 95% confidence interval [CI], 1.15–2.00; $P = 0.004$] and Charlson comorbidity index (OR, 1.32; 95% CI, 1.08–1.62; $P = 0.006$) were significantly associated with an increased risk of LV diastolic dysfunction. Age, male sex, pre-dialysis SBP, and NT-proBNP increments per SD showed a borderline significant association with LV diastolic dysfunction. In the multivariable binary logistic regression model, the Charlson comorbidity index (OR, 1.24; 95% CI, 1.01–1.53; $P = 0.045$) and serum VAP-1 level (OR, 1.40; 95% CI, 1.04–1.88; $P = 0.028$) remained statistically significant as independent determinants of LV diastolic dysfunction in HD patients.

Prognostic Utility of the VAP-1 Level in Hemodialysis Patients

During a mean follow-up of 30.3 months, 61 deaths (14.1%) and 77 adverse CV events (17.7%) occurred. Regarding CV events, coronary artery disease occurred in 36 patients, heart failure in 7, ventricular arrhythmia in 1, cardiac arrest in 9, sudden death in 9, CV events in 9, and peripheral vascular occlusive diseases in 6. VAP-1 tertile 3 had the highest cumulative CV event rate ($P = 0.009$; **Figure 1A**) and a greater cumulative rate of cardiac events ($P = 0.015$; **Figure 1B**). The cumulative event rate of patient mortality did not differ among VAP-1 tertiles ($P = 0.747$).

Univariable Cox regression analysis revealed that VAP-1 tertile 3 was significantly associated with an increased risk of the composite of CV events [hazard ratio [HR], 2.51; 95% CI, 1.39–4.54; $P = 0.002$] (**Table 3**). In the multivariable Cox regression analysis, VAP-1 tertile 3 was significantly associated with a 2.06-fold higher risk of CV events (95% CI, 1.10–3.85; $P = 0.025$) and VAP-1 increment per SD was significantly associated with a 1.31-fold higher risk of CV events (95% CI, 1.05–1.64; $P = 0.019$). The risk of cardiac events and patient mortality was further investigated. Patients in VAP-1 tertile 3 had a 2.06-fold higher risk of cardiac disease after adjustment for multiple variables (95% CI, 1.03–4.12; $P = 0.041$). VAP-1 increment per SD was also significantly associated with the risk of cardiac events (HR, 1.29; 95% CI, 1.01–1.64; $P = 0.038$). However, among patients in VAP-1 tertile 3, VAP-1 levels were not significantly associated with the risk of mortality. To evaluate potential linear associations, we evaluated the association between VAP-1 and the risk of composite of CV events and cardiac events during follow-up. The restricted cubic spline model after multiple adjustments showed gradually increasing HRs for both CV and cardiac events with increasing VAP-1 levels (**Figure 2**).

TABLE 1 | Baseline demographic and laboratory data of the study population.

	Tertiles of circulating VAP-1 levels			
	Tertile 1 (<343.2 ng/mL)	**Tertile 2 (343.2–438.2 ng/mL)**	**Tertile 3 (≥438.2 ng/mL)**	***P*-value**
Age (years)	60.5 ± 14.9	63.0 ± 12.1	61.6 ± 11.2	0.262
Males, n (%)	93 (64.6)	102 (70.3)	96 (66.2)	0.561
Body mass index (kg/m^2)	23.3 ± 4.1	23.1 ± 3.7	23.5 ± 4.5	0.725
HD duration (years)	4.4 ± 5.8	4.1 ± 5.6	2.7 ± 4.1[a,b]	0.014
History of CV events, n (%)	81 (84)	20 (86)	18 (87)	0.747
Diabetes mellitus, n (%)	45 (31.7)	82 (56.6)[a]	120 (82.8)[a,b]	< 0.001
Charlson comorbidity index	3.6 ± 1.6	4.2 ± 1.6[a]	4.5 ± 1.2[a]	< 0.001
Pre-dialysis SBP (mm Hg)	138.7 ± 20.8	142.0 ± 19.0	147.0 ± 20.1[a]	0.002
Hemoglobin (g/dL)	10.4 ± 1.4	10.6 ± 1.1	10.3 ± 1.1	0.338
Glucose (mg/dL)	139.3 ± 57.9	150.1 ± 61.9	172.6 ± 66.5[a,b]	< 0.001
Albumin (g/dL)	3.8 ± 0.4	3.8 ± 0.3	3.8 ± 0.3	0.515
LDL-C (mg/dL)	79.0 ± 26.9	75.4 ± 26.5	74.3 ± 23.7	0.276
hsCRP (mg/dL)	1.4 (0.2–5.5)	0.8 (0.2–2.9)	0.9 (0.2–2.7)	0.062
i-PTH (pg/mL)	287.0 ± 244.1	292.5 ± 232.3	233.9 ± 165.0[a,b]	0.040
spKt/V	1.6 ± 0.5	1.6 ± 0.3	1.5 ± 0.3	0.219
Catheter as vascular access, *n* (%)	8 (5.6)	5 (3.4)	7 (4.8)	0.679
Follow-up years	30.8 ± 14.8	29.9 ± 14.4	29.9 ± 14.0	0.823
NT-proBNP (pg/mL)	286 (165–466)	311 (207–431)	335 (226–508)	0.076
BNP (pg/mL)	33.4 (7.6–68.4)	33.4 (6.7–88.3)	55.6 (13.4–108.2)[a]	0.015
Galectin-3 (ng/mL)	16.8 (15.0–20.0)	17.8 (15.1–20.6)	18.2 (15.3–21.4)	0.057
MMP-2 (ng/mL)	577 (478–678)	665 (568–763)	746 (626–897)[a,b]	< 0.001

Data are expressed as means ± standard deviations or medians (interquartile ranges), unless otherwise specified. VAP, vascular adhesion protein; HD, hemodialysis; CV, cardiovascular; LDL-C, low-density lipoprotein cholesterol; i-PTH, intact parathyroid hormone; hsCRP, high-sensitivity C-reactive protein; SBP, systolic blood pressure; NT-proBNP, N-terminal pro-B-type natriuretic peptide; BNP, brain natriuretic peptide; MMP, matrix metalloproteinase.

[a] *P < 0.05 vs. tertile 1.*

[b] *P < 0.05 vs. tertile 2.*

The relationship between VAP-1 levels and the composite of incident CV events was further investigated in subgroups stratified by the presence of diabetes mellitus and NT-proBNP levels, with cut-offs defined as median values in each parameter (>386.5 ng/mL for VAP-1 and >313.3 pg/mL for NT-proBNP, respectively; **Table 4**). Multivariable analysis showed that higher VAP-1 levels were associated with an increased risk of CV events both in patients with (HR, 2.39; 95% CI, 1.14–5.03; $P = 0.022$) and without (HR, 2.57; 95% CI, 1.05–6.30; $P = 0.039$) diabetes mellitus. There was a significant interaction between higher VAP-1 levels and diabetes mellitus in association with CV events (HR, 0.51; 95% CI, 0.29–0.90; P for interaction = 0.02). Compared to those with low NT-proBNP levels, patients with high VAP-1 and NT-proBNP levels showed an increased risk of CV events (HR, 1.99; 95% CI, 1.01–3.89; $P = 0.046$), whereas those with isolated high NT-proBNP levels did not show this association. There was no significant interaction between VAP-1 and NT-proBNP levels (HR, 1.57; 95% CI, 0.59–4.18; P for interaction = 0.36).

DISCUSSION

In this prospective cohort study, we investigated the associations of plasma VAP-1 levels with cardiac dysfunction and CV outcomes in HD patients. Plasma VAP-1 levels were positively associated with circulating cardiac biomarker levels and LV diastolic dysfunction. Patients in VAP-1 tertile 3 had the greatest risk of a higher composite of CV events, and this association remained significant after adjusting for established CV risk factors. Taken together, our findings suggest that plasma VAP-1 may be a novel biomarker of incident CV events in HD patients.

High blood pressure and hyperglycemia were representative metabolic disorders that increased plasma VAP-1 levels in individuals without renal impairment (13, 19–23). In the present study, serum glucose level and pre-dialysis SBP were the highest among patients in VAP-1 tertile 3, suggesting that the relationship among blood pressure, serum glucose, and VAP-1 levels is consistent in HD patients. Because VAP-1 promoted the inflammatory process, the positive correlation between plasma VAP-1 levels and hsCRP was expected. However, we showed that the correlation between VAP-1 and hsCRP was negative and the correlation power was highly weak, implying that higher plasma VAP-1 levels may not merely be a secondary reflection of systemic inflammation in HD patients.

LV diastolic dysfunction is commonly identified in HD patients and is associated with high CV mortality (24–28). In this study, the E/E' ratio was used as a criterion for LV diastolic dysfunction because an E/E' ratio of >15 has been reported as a strong predictor of CV events in HD patients (29, 30). We found

TABLE 2 | Relationship between vascular adhesion protein-1 levels and left ventricle diastolic dysfunction.

	Univariable analysis		Multivariable analysis	
	OR (95% CI)	***P*-value**	**OR (95% CI)**	***P*-value**
Age	1.02 (1.00–1.04)	0.057	1.02 (1.00–1.05)	0.078
Male sex	0.59 (0.33–1.04)	0.066	0.58 (0.32–1.07)	0.083
BMI	1.01 (0.94–1.07)	0.880	–	–
Hemodialysis duration	1.04 (0.96–1.19)	0.362	–	–
Charlson comorbidity index	1.32 (1.08–1.62)	0.006	1.24 (1.01–1.53)	0.045
Pre-dialysis SBP	1.01 (1.00–1.03)	0.063	1.01 (0.99–1.02)	0.327
Hemoglobin	1.08 (0.85–1.37)	0.544	–	–
Albumin	0.62 (0.26–1.48)	0.281	–	–
LDL-C	1.00 (0.99–1.01)	0.365	–	–
hsCRP	1.05 (0.75–1.48)	0.765	–	–
NT-proBNP per SD	1.28 (0.95–1.73)	0.109	1.15 (0.83–1.60)	0.393
VAP-1 per SD	1.51 (1.15–2.00)	0.004	1.40 (1.04–1.88)	0.028

OR, odds ratio; CI, confidence interval; BMI, body mass index; LDL-C, low-density lipoprotein cholesterol; hsCRP, high-sensitivity C-reactive protein; NT-proBNP, N-terminal pro-B-type natriuretic peptide; SD, standard deviation; VAP, vascular adhesion protein.

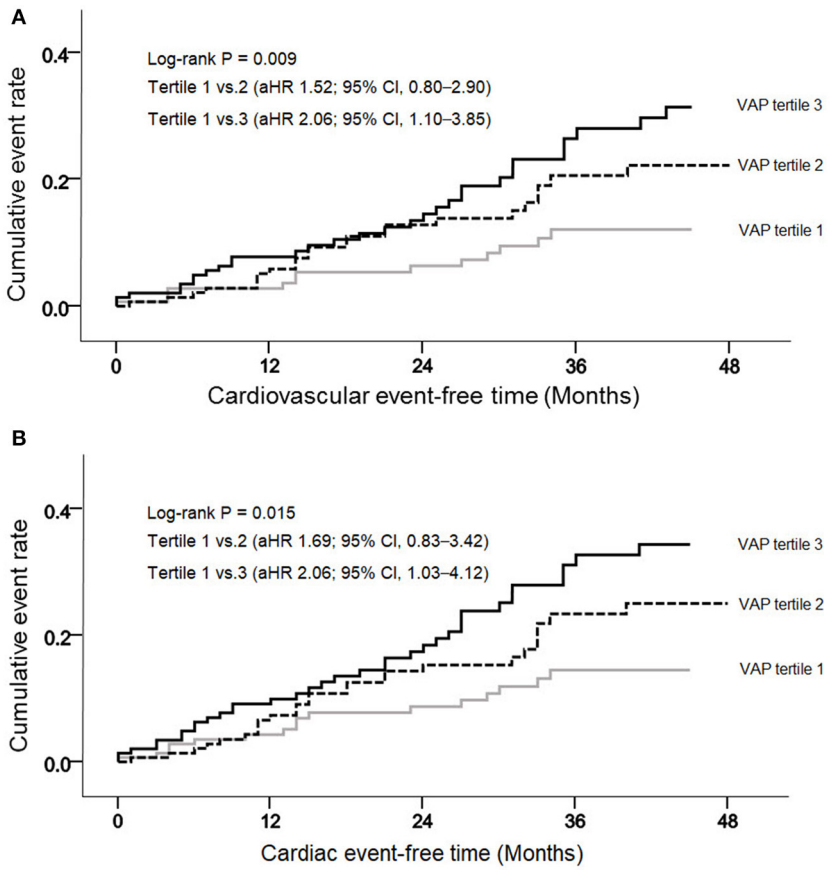

FIGURE 1 | Cumulative cardiovascular **(A)** and cardiac **(B)** event rates, according to the vascular adhesion protein-1 (VAP-1) levels.

that a higher VAP-1 level was independently associated with an increased risk of LV diastolic dysfunction. In addition, higher VAP-1 levels were correlated with an increased risk of cardiac events after adjusting for multiple confounders, indicating that VAP-1 levels may reflect structural changes in cardiac pathology and that VAP-1 could be a potential biomarker of incident cardiac events in HD patients. Furthermore, we found a significant correlation between plasma VAP-1 and MMP-2, one of the main

TABLE 3 | Hazard ratios of plasma vascular adhesion protein-1 levels for cardiovascular events, cardiac events, and mortality.

	Number of events (%)	Univariable analysis HR (95% CI)	Multivariable analysis HR (95% CI)
Composite of CV events			
VAP-1 tertile 1	16 (11.1)	Reference	
VAP-1 tertile 2	26 (17.9)	1.74 (0.93–3.24)	1.52 (0.80–2.90)
VAP-1 tertile 3	35 (24.1)	2.51 (1.39–4.54)	2.06 (1.10–3.85)
VAP-1 per SD	–	1.40 (1.14–1.71)	1.31 (1.05–1.64)
Cardiac events			
VAP-1 tertile 1	13 (9.0)	Reference	
VAP-1 tertile 2	23 (15.9)	1.90 (0.96–3.75)	1.69 (0.83–3.42)
VAP-1 tertile 3	30 (20.7)	2.66 (1.38–5.10)	2.06 (1.03–4.12)
VAP-1 per SD	–	1.42 (1.14–1.77)	1.29 (1.01–1.64)
Patient deaths			
VAP-1 tertile 1	23 (16.0)	Reference	
VAP-1 tertile 2	20 (13.8)	0.90 (0.50–1.64)	0.85 (0.44–1.65)
VAP-1 tertile 3	18 (12.4)	0.81 (0.44–1.50)	0.86 (0.43–1.72)
VAP-1 per SD	–	0.96 (0.74–1.26)	0.98 (0.72–1.33)

HR, hazard ratio; CI, confidence interval; CV, cardiovascular; SD, standard deviation; VAP, vascular adhesion protein. All analyses were adjusted for the following covariates: age, sex, body mass index, hemodialysis duration, Charlson comorbidity index, pre-dialysis systolic blood pressure, hemoglobin, low-density lipoprotein cholesterol, high-sensitivity C-reactive protein, spKt/V, catheter use, and N-terminal pro-B-type natriuretic peptide.

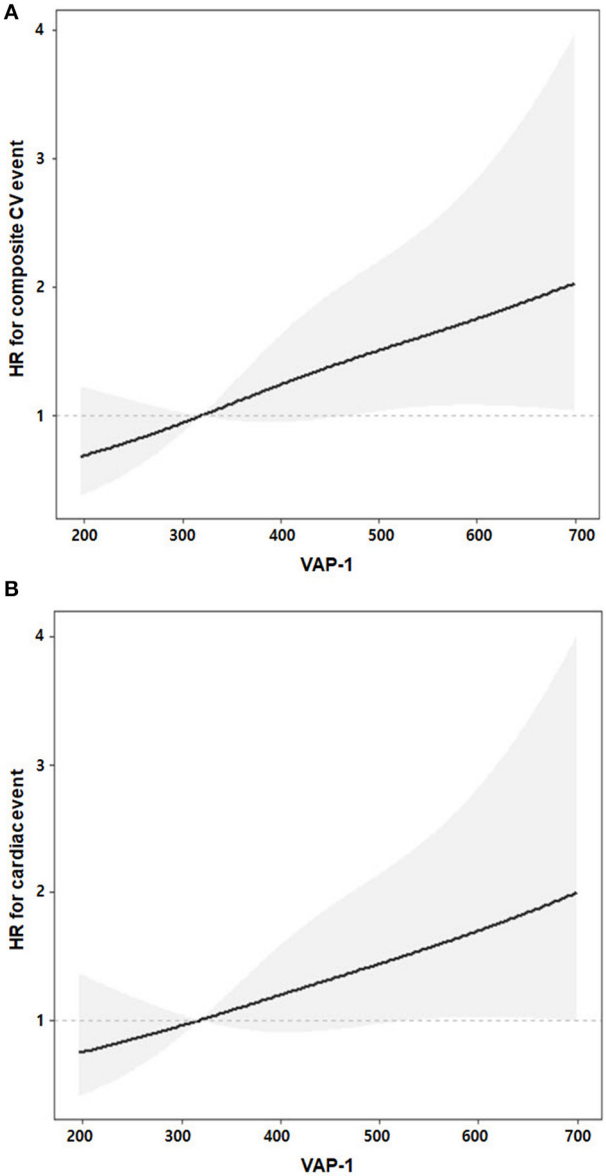

FIGURE 2 | Linear associations of VAP-1 and adjusted risks of the composite of cardiovascular **(A)** and cardiac **(B)** events. Gray shaded areas represent 95% confidence intervals. The adjusted multiple variables were age, sex, body mass index, hemodialysis duration, Charlson comorbidity index, pre-dialysis systolic blood pressure, hemoglobin, low-density lipoprotein cholesterol, high-sensitivity C-reactive protein, spKt/V, catheter use, and N-terminal pro-B-type natriuretic peptide.

mediators of pathologic extracellular matrix remodeling and fibrosis in several cardiac diseases (31–33). Previous studies have reported that MMP-2 is involved in LV diastolic dysfunction because circulating MMP-2 levels were correlated with the E/E' ratio (32, 33).

Patients in VAP-1 tertile 3 had a higher cumulative incidence of the composite of CV events than those in VAP-1 tertile 1. In addition, Cox regression analysis showed that high plasma VAP-1 levels were independently associated with a significantly increased risk of CV events, even after adjustments for possible confounders, including SBP and the Charlson comorbidity index. These findings suggest that VAP-1 may be a useful indicator for screening HD patients at a high risk of CV events. Positive correlations of plasma VAP-1 with traditional risk factors, including glucose levels, pre-dialysis SBP, and LV diastolic dysfunction, further support its usefulness in predicting CV outcomes. Notably, plasma VAP-1 levels did not predict all-cause mortality, despite their significant association with CV events. A possible explanation for this discrepancy might be that more than two-third (65.6%) of mortalities in this study were not attributed to CV events.

Subgroup analysis showed that higher plasma VAP-1 levels were associated with an increased risk of CV events in both patients with and without diabetes mellitus. However, the HR of higher VAP-1 levels was lower in HD patients with diabetes mellitus than in HD patients without diabetes mellitus (P for interaction = 0.02), indicating that the predictive power of VAP-1 may differ based on the presence of diabetes mellitus. Considering that more HD patients are developing diabetes mellitus (34, 35), a lower predictive power of plasma VAP-1 levels in this subpopulation could be a disadvantage as a prognostic biomarker of CV events. Although the underlying mechanism of this phenomenon could not be assessed in this study, we speculate that hyperglycemia-induced upregulation of unfavorable molecules, such as plasma proinflammatory cytokines and advanced glycation end products, reduce the relative contributions of plasma VAP-1 to the incidence of CV events (36, 37).

TABLE 4 | Hazard ratios of plasma vascular adhesion protein-1 levels for the composite of cardiovascular events according to predefined subgroups.

	Number of CV events (%)	Univariable analysis HR (95% CI)	Multivariable analysis HR (95% CI)	*P* for interaction
Diabetes mellitus				0.02
Low VAP-1, without DM	11 (8.1)	Reference		
High VAP-1, without DM	9 (17.6)	2.34 (0.97–5.66)	2.57 (1.05–6.30)	
Low VAP-1, with DM	15 (18.5)	2.45 (1.13–5.34)	1.68 (0.73–3.84)	
High VAP-1, with DM	42 (25.3)	3.67 (1.89–7.14)	2.39 (1.14–5.03)	
NT-proBNP				0.36
Low VAP-1, low NT-proBNP	14 (12.7)	Reference		
High VAP-1, low NT-proBNP	19 (17.8)	1.66 (0.83–3.30)	1.43 (0.71–2.89)	
Low VAP-1, high NT-proBNP	12 (11.2)	0.97 (0.45–2.09)	0.88 (0.40–1.96)	
High VAP-1, high NT-proNBP	32 (29.1)	2.64 (1.41–4.95)	1.99 (1.01–3.89)	

CV, cardiovascular; HR, hazard ratio; CI, confidence interval; VAP, vascular adhesion protein; DM, diabetes mellitus; NT-proBNP, N-terminal pro-B-type natriuretic peptide. High VAP-1 was defined as median value > 386.5 ng/mL, and criteria for predefined subgroups were also based on medians; high NT-proBNP > 313.3 pg/mL. All analyses were adjusted for the following covariates (except for the variable used to define the subgroup in each case): age, sex, body mass index, hemodialysis duration, Charlson comorbidity index, pre-dialysis systolic blood pressure, hemoglobin, low-density lipoprotein cholesterol, high-sensitivity C-reactive protein, spKt/V, catheter use, and N-terminal pro-B-type natriuretic peptide.

The clinical utility of NT-proBNP as a cardiac biomarker in HD patients had been inconclusive, partly because of intra-patient variations and different cut-off values used across studies (38–40). An observational study also reported that elevated NT-proBNP levels are likely caused by intravascular volume expansion rather than cardiac dysfunction in stable HD patients, further complicating the interpretations of its clinical value in HD patients with hypervolemia (41). Our subgroup analysis showed that increased VAP-1 and NT-proBNP levels were associated with a significantly higher risk of composite CV events, whereas isolated NT-proBNP levels were not (**Table 4**). These findings indicate that plasma VAP-1 levels can help differentiate those at a high risk of adverse CV outcomes among HD patients exhibiting increased baseline NT-proBNP levels.

Our study had some limitations. Analyses for individual CV events could not be performed because of the limited number of events and short follow-up period. Echocardiographic data were obtained in a small proportion of enrolled patients (49.3%), although the analysis of available data revealed an evident association between high plasma VAP-1 levels and LV diastolic dysfunction. Moreover, multivariable analysis might not have controlled all relevant confounding factors, and thus these were not thoroughly assessed in this study.

In conclusion, our study demonstrated that plasma VAP-1 levels were associated with circulating markers of cardiac remodeling, as well as a greater risk of LV diastolic dysfunction. In addition, higher plasma VAP-1 levels were correlated with an increased risk of future CV events in HD patients. Our results indicate that VAP-1 might help overcome the limitations of traditional risk factors in the setting of end-stage renal disease and help clinicians identify HD patients at a high risk of CV events.

DATA AVAILABILITY STATEMENT

The raw data supporting the conclusions of this article will be made available by the authors, without undue reservation.

ETHICS STATEMENT

The studies involving human participants were reviewed and approved by KyungHee University Hospital IRB. The patients/participants provided their written informed consent to participate in this study.

AUTHOR CONTRIBUTIONS

DKK, YHL, and HSH constructed the research questions and designed the analysis. JSK, YGK, S-YL, SYA, D-YL, KHJ, S-HL, and J-YM conducted the data collection. DKK, YHL, J-YM, and HSH drafted the manuscript. All authors reviewed the results, commented on the manuscript, read, and approved the final manuscript.

FUNDING

This research was supported by grants from the Patient-Centered Clinical Research Coordinating Center, which was funded by the Ministry of Health & Welfare, Republic of Korea (H19C0481 and HC19C0041).

ACKNOWLEDGMENTS

All authors acknowledge the support from Patient-Centered Clinical Research Coordinating Center funded by the Ministry of Health and Welfare, Republic of Korea (H19C0481 and HC19C0041).

SUPPLEMENTARY MATERIAL

The Supplementary Material for this article can be found online at: https://www.frontiersin.org/articles/10.3389/fcvm.2021.701079/full#supplementary-material

REFERENCES

1. Rysz J, Franczyk B, Lawinski J, Gluba-Brzozka A. Oxidative stress in ESRD patients on dialysis and the risk of cardiovascular diseases. *Antioxidants.* (2020) 9:1079. doi: 10.3390/antiox9111079
2. Russa D, Pellegrino D, Montesanto A, Gigliotti P, Perri A, Russa A, et al. Oxidative balance and inflammation in hemodialysis patients: biomarkers of cardiovascular risk? *Oxid Med Cell Longev.* (2019) 2019:8567275. doi: 10.1155/2019/8567275
3. Hwang HS, Kim JS, Kim YG, Lee SY, Ahn SY, Lee HJ, et al. Circulating PCSK9 level and risk of cardiovascular events and death in hemodialysis patients. *J Clin Med.* (2020) 9:244. doi: 10.3390/jcm9010244
4. Verma S, Singh P, Khurana S, Ganguly NK, Kukreti R, Saso L, et al. Implications of oxidative stress in chronic kidney disease: a review on current concepts and therapies. *Kidney Res Clin Pract.* (2021) 40:183–93. doi: 10.23876/j.krcp.20.163
5. Sasaki K, Shoji T, Kabata D, Shintani A, Okute Y, Tsuchikura S, et al. Oxidative stress and inflammation as predictors of mortality and cardiovascular events in hemodialysis patients: the DREAM cohort. *J Atheroscler Thromb.* (2021) 28:249–60. doi: 10.5551/jat.56069
6. Ren H, Zhou X, Luan Z, Luo X, Han S, Cai Q, et al. The relationship between carotid atherosclerosis, inflammatory cytokines, and oxidative stress in middle-aged and elderly hemodialysis patients. *Int J Nephrol.* (2013) 2013:835465. doi: 10.1155/2013/835465
7. Hwang HS, Kim JS, Kim YG, Lee YH, Lee DY, Ahn SY, et al. Circulating neprilysin level predicts the risk of cardiovascular events in hemodialysis patients. *Front Cardiovasc Med.* (2021) 8:684297. doi: 10.3389/fcvm.2021.684297
8. Cozzolino M, Mangano M, Stucchi A, Ciceri P, Conte F, Galassi A. Cardiovascular disease in dialysis patients. *Nephrol Dial Transplant.* (2018) 33:iii28–34. doi: 10.1093/ndt/gfy174
9. Noonan T, Lukas S, Peet GW, Pelletier J, Panzenbeck M, Hanidu A, et al. The oxidase activity of vascular adhesion protein-1 (VAP-1) is essential for function. *Am J Clin Exp Immunol.* (2013) 2:172–85.
10. Salmi M, Jalkanen S. VAP-1: an adhesin and an enzyme. *Trends Immunol.* (2001) 22:211–6. doi: 10.1016/S1471-4906(01)01870-1
11. Salmi M, Jalkanen S. Vascular adhesion protein-1: a cell surface amine oxidase in translation. *Antioxid Redox Signal.* (2019) 30:314–32. doi: 10.1089/ars.2017.7418
12. Aalto K, Havulinna AS, Jalkanen S, Salomaa V, Salmi M. Soluble vascular adhesion protein-1 predicts incident major adverse cardiovascular events and improves reclassification in a finnish prospective cohort study. *Circ Cardiovasc Genet.* (2014) 7:529–35. doi: 10.1161/CIRCGENETICS.113.000543
13. Boomsma F, de Kam PJ, Tjeerdsma G, van den Meiracker AH, van Veldhuisen DJ. Plasma semicarbazide-sensitive amine oxidase (SSAO) is an independent prognostic marker for mortality in chronic heart failure. *Eur Heart J.* (2000) 21:1859–63. doi: 10.1053/euhj.2000.2176
14. Pannecoeck R, Serruys D, Benmeridja L, Delanghe JR, van Geel N, Speeckaert R, et al. Vascular adhesion protein-1: role in human pathology and application as a biomarker. *Crit Rev Clin Lab Sci.* (2015) 52:284–300. doi: 10.3109/10408363.2015.1050714
15. Wong MY, Saad S, Pollock C, Wong MG. Semicarbazide-sensitive amine oxidase and kidney disease. *Am J Physiol Renal Physiol.* (2013) 305:F1637–44. doi: 10.1152/ajprenal.00416.2013
16. Nemcsik J, Szoko E, Soltesz Z, Fodor E, Toth L, Egresits J, et al. Alteration of serum semicarbazide-sensitive amine oxidase activity in chronic renal failure. *J Neural Transm.* (2007) 114:841–3. doi: 10.1007/s00702-007-0698-4
17. Charlson ME, Pompei P, Ales KL, MacKenzie CR. A new method of classifying prognostic comorbidity in longitudinal studies: development and validation. *J Chronic Dis.* (1987) 40:373–83. doi: 10.1016/0021-9681(87)90171-8
18. Lang RM, Badano LP, Mor-Avi V, Afilalo J, Armstrong A, Ernande L, et al. Recommendations for cardiac chamber quantification by echocardiography in adults: an update from the American Society of Echocardiography and the European Association of Cardiovascular Imaging. *J Am Soc Echocardiogr.* (2015) 28:1–39.e14. doi: 10.1016/j.echo.2014.10.003
19. Aalto K, Maksimow M, Juonala M, Viikari J, Jula A, Kahonen M, et al. Soluble vascular adhesion protein-1 correlates with cardiovascular risk factors and early atherosclerotic manifestations. *Arterioscler Thromb Vasc Biol.* (2012) 32:523–32. doi: 10.1161/ATVBAHA.111.238030
20. Boomsma F, van den Meiracker AH, Winkel S, Aanstoot HJ, Batstra MR, Man in 't Veld AJ, et al. Circulating semicarbazide-sensitive amine oxidase is raised both in type I (insulin-dependent), in type II (non-insulin-dependent) diabetes mellitus and even in childhood type I diabetes at first clinical diagnosis. *Diabetologia.* (1999) 42:233–7. doi: 10.1007/s001250051143
21. Boomsma F, van Veldhuisen DJ, de Kam PJ, Man in't Veld AJ, Mosterd A, Lie KI, et al. Plasma semicarbazide-sensitive amine oxidase is elevated in patients with congestive heart failure. *Cardiovasc Res.* (1997) 33:387–91. doi: 10.1016/S0008-6363(96)00209-X
22. Koc-Zorawska E, Malyszko J, Zbroch E, Malyszko J, Mysliwiec M. Vascular adhesion protein-1 and renalase in regard to diabetes in hemodialysis patients. *Arch Med Sci.* (2012) 8:1048–52. doi: 10.5114/aoms.2012.32413
23. Maciorkowska D, Zbroch E, Malyszko J. Circulating renalase, catecholamines, and vascular adhesion protein 1 in hypertensive patients. *J Am Soc Hypertens.* (2015) 9:855–64. doi: 10.1016/j.jash.2015.08.002
24. Antlanger M, Aschauer S, Kopecky C, Hecking M, Kovarik JJ, Werzowa J, et al. Heart failure with preserved and reduced ejection fraction in hemodialysis patients: prevalence, disease prediction and prognosis. *Kidney Blood Press Res.* (2017) 42:165–76. doi: 10.1159/000473868
25. Unger ED, Dubin RF, Deo R, Daruwalla V, Friedman JL, Medina C, et al. Association of chronic kidney disease with abnormal cardiac mechanics and adverse outcomes in patients with heart failure and preserved ejection fraction. *Eur J Heart Fail.* (2016) 18:103–12. doi: 10.1002/ejhf.445
26. Han JH, Han JS, Kim EJ, Doh FM, Koo HM, Kim CH, et al. Diastolic dysfunction is an independent predictor of cardiovascular events in incident dialysis patients with preserved systolic function. *PLoS ONE.* (2015) 10:e0118694. doi: 10.1371/journal.pone.0118694
27. Smith DH, Thorp ML, Gurwitz JH, McManus DD, Goldberg RJ, Allen LA, et al. Chronic kidney disease and outcomes in heart failure with preserved versus reduced ejection fraction: the Cardiovascular Research Network PRESERVE Study. *Circ Cardiovasc Qual Outcomes.* (2013) 6:333–42. doi: 10.1161/CIRCOUTCOMES.113.000221
28. Hillege HL, Nitsch D, Pfeffer MA, Swedberg K, McMurrayJJ, Yusuf S, et al. Renal function as a predictor of outcome in a broad spectrum of patients with heart failure. *Circulation.* (2006) 113:671–8. doi: 10.1161/CIRCULATIONAHA.105.580506
29. Nagueh SF, Smiseth OA, Appleton CP, Byrd BF III, Dokainish H, Edvardsen T, et al. Recommendations for the evaluation of left ventricular diastolic function by echocardiography: an update from the american society of echocardiography and the european association of cardiovascular imaging. *J Am Soc Echocardiogr.* (2016) 29:277–314. doi: 10.1016/j.echo.2016.01.011
30. Han SS, Cho GY, Park YS, Baek SH, Ahn SY, Kim S, et al. Predictive value of echocardiographic parameters for clinical events in patients starting hemodialysis. *J Korean Med Sci.* (2015) 30:44–53. doi: 10.3346/jkms.2015.30.1.44
31. Ahmed SH, Clark LL, Pennington WR, Webb CS, Bonnema DD, Leonardi AH, et al. Matrix metalloproteinases/tissue inhibitors of metalloproteinases: relationship between changes in proteolytic determinants of matrix composition and structural, functional, and clinical manifestations of hypertensive heart disease. *Circulation.* (2006) 113:2089–96. doi: 10.1161/CIRCULATIONAHA.105.573865
32. Zile MR, Jhund PS, Baicu CF, Claggett BL, Pieske B, Voors AA, et al. Plasma biomarkers reflecting profibrotic processes in heart failure with a preserved ejection fraction: data from the prospective comparison of ARNI with ARB on management of heart failure with preserved ejection fraction study. *Circ Heart Fail.* (2016) 9:e002551 doi: 10.1161/CIRCHEARTFAILURE.115.002551
33. Kobusiak-Prokopowicz M, Krzysztofik J, Kaaz K, Jolda-Mydlowska B, Mysiak A. MMP-2 and TIMP-2 in patients with heart failure and chronic kidney disease. *Open Med.* (2018) 13:237–46. doi: 10.1515/med-2018-0037
34. Oh KH, Kang M, Kang E, Ryu H, Han SH, Yoo TH, et al. The KNOW-CKD study: what we have learned about chronic kidney diseases. *Kidney Res Clin Pract.* (2020) 39:121–35. doi: 10.23876/j.krcp.20.042
35. Jeon HJ, Bae HJ, Ham YR, Choi DE, Na KR, Ahn MS, et al. Outcomes of end-stage renal disease patients on the waiting list for deceased donor

kidney transplantation: a single-center study. *Kidney Res Clin Pract.* (2019) 38:116–23. doi: 10.23876/j.krcp.18.0068
36. Schottker B, Herder C, Rothenbacher D, Roden M, Kolb H, Muller H, et al. Proinflammatory cytokines, adiponectin, and increased risk of primary cardiovascular events in diabetic patients with or without renal dysfunction: results from the ESTHER study. *Diabetes Care.* (2013) 36:1703–11. doi: 10.2337/dc12-1416
37. Hegab Z, Gibbons S, Neyses L, Mamas MA. Role of advanced glycation end products in cardiovascular disease. *World J Cardiol.* (2012) 4:90–102. doi: 10.4330/wjc.v4.i4.90
38. Fahim MA, Hayen A, Horvath AR, Dimeski G, Coburn A, Johnson DW, et al. N-terminal pro-B-type natriuretic peptide variability in stable dialysis patients. *Clin J Am Soc Nephrol.* (2015) 10:620–9. doi: 10.2215/CJN.09060914
39. Madsen LH, Ladefoged S, Corell P, Schou M, Hildebrandt PR, Atar D. N-terminal pro brain natriuretic peptide predicts mortality in patients with end-stage renal disease in hemodialysis. *Kidney Int.* (2007) 71:548–54. doi: 10.1038/sj.ki.5002087
40. Vickery S, Price CP, John RI, Abbas NA, Webb MC, Kempson ME, et al. B-type natriuretic peptide (BNP) and amino-terminal proBNP in patients with CKD: relationship to renal function and left ventricular hypertrophy. *Am J Kidney Dis.* (2005) 46:610–20. doi: 10.1053/j.ajkd.2005.06.017
41. Booth J, Pinney J, Davenport A. N-terminal proBNP–marker of cardiac dysfunction, fluid overload, or malnutrition in hemodialysis patients? *Clin J Am Soc Nephrol.* (2010) 5:1036–40. doi: 10.2215/CJN.09001209

Conflict of Interest: The authors declare that the research was conducted in the absence of any commercial or financial relationships that could be construed as a potential conflict of interest.

Publisher's Note: All claims expressed in this article are solely those of the authors and do not necessarily represent those of their affiliated organizations, or those of the publisher, the editors and the reviewers. Any product that may be evaluated in this article, or claim that may be made by its manufacturer, is not guaranteed or endorsed by the publisher.

frontiers in Cardiovascular Medicine

ORIGINAL RESEARCH
published: 28 October 2021
doi: 10.3389/fcvm.2021.692083

High Serum Carbohydrate Antigen (CA) 125 Level Is Associated With Poor Prognosis in Patients With Light-Chain Cardiac Amyloidosis

Muzheng Li[1†], Zhijian Wu[1†], Ilyas Tudahun[1], Na Liu[1], Qiuzhen Lin[1], Jiang Liu[2], Yingmin Wang[1], Mingxian Chen[1], Yaqin Chen[1], Nenghua Qi[1], Qingyi Zhu[1], JunLi Li[3], Wei Li[4], Jianjun Tang[1] and Qiming Liu[1*]*

[1] Department of Cardiovascular Medicine, The Second Xiangya Hospital of Central South University, Changsha, China, [2] Department of Cardiovascular Surgery, The Second Xiangya Hospital of Central South University, Changsha, China, [3] Department of Radiology, The Second Xiangya Hospital of Central South University, Changsha, China, [4] Department of Cardiology, Huaihua Hospital of Traditional Chinese Medicine, Huaihua, China

OPEN ACCESS

Edited by:
Alessio Molfino,
Sapienza University of Rome, Italy

Reviewed by:
Wenming Yao,
Nanjing Medical University, China
Xiao Huang,
Second Affiliated Hospital of Nanchang University, China

***Correspondence:**
Jianjun Tang
tom200210@csu.edu.cn
Qiming Liu
qimingliu@csu.edu.cn

[†]These authors have contributed equally to this work

Specialty section:
This article was submitted to General Cardiovascular Medicine, a section of the journal Frontiers in Cardiovascular Medicine

Received: 07 April 2021
Accepted: 24 September 2021
Published: 28 October 2021

Citation:
Li M, Wu Z, Tudahun I, Liu N, Lin Q, Liu J, Wang Y, Chen M, Chen Y, Qi N, Zhu Q, Li J, Li W, Tang J and Liu Q (2021) High Serum Carbohydrate Antigen (CA) 125 Level Is Associated With Poor Prognosis in Patients With Light-Chain Cardiac Amyloidosis. Front. Cardiovasc. Med. 8:692083. doi: 10.3389/fcvm.2021.692083

Background and Aims: Patients with light-chain cardiac amyloidosis (AL-CA) are characterized by high levels of serum carbohydrate antigen 125 (CA 125). However, studies have not explored the correlation between CA 125 and AL-CA. The aim of this study was to explore the clinical implications of an increase in CA 125 in patients with AL-CA.

Methods and Results: A total of 95 patients diagnosed with AL-CA at the Second Xiangya Hospital were enrolled in this study. Out of the 95 patients with AL-CA, 57 (60%) patients had elevated serum CA 125 levels. The mean age was 59.7 ± 10.0 years with 44 (77.2%) men in the high serum CA 125 group, and 61.8 ± 9.6 years with 28 (73.7%) men in the normal group. Patients with high CA 125 showed higher rates of polyserositis (79.3% vs. 60.5%, $p = 0.03$), higher levels of hemoglobin (117.4 ± 21.9 g/L vs. 106.08 ± 25.1 g/L, $p = 0.03$), serum potassium (4.11 ± 0.47 mmol/L vs. 3.97 ± 0.40 mmol/L, $p = 0.049$), low-density lipoprotein-cholesterol (3.0 ± 1.6 mmol/L vs. 2.3 ± 1.10 mmol/L, $p = 0.01$), and cardiac troponin T (96.0 pg/mL vs. 91.9 pg/mL, $p = 0.005$). The median overall survival times for patients with high or normal serum CA 125 were 5 and 25 months, respectively ($p = 0.045$). Multivariate Cox hazard analysis showed that treatment without chemotherapy (HR 1.694, 95% CI 1.121–2.562, $p = 0.012$) and CA 125 (HR 1.002, 95% CI 1.000–1.004, $p = 0.020$) was correlated with high all-cause mortality. The time-dependent receiver operating characteristic (t-ROC) curve showed that the prediction accuracy of CA 125 was not inferior to that of cardiac troponin T, N-terminal pro-B-type natriuretic peptide (NT-proBNP), and lactate dehydrogenase (LDH) based on the area under the curve.

Conclusions: CA 125 is a novel prognostic predictor. High serum CA 125 values are correlated with low overall survival, and the accuracy of predicting prognosis is similar to that of traditional biomarkers in AL-CA.

Keywords: light-chain cardiac amyloidosis, CA 125, prognostic predictor, overall survival, biomarkers

INTRODUCTION

Cardiac amyloidosis is a condition of systemic amyloidosis with myocardial involvement. It is caused by the deposition of amyloid proteins derived from misfolded transthyretin or immunoglobulin light-chain in the myocardial interstitium, small vessels, and conduction system. These changes lead to increased ventricular wall thickness, diastolic dysfunction, and arrhythmia. Although more than 30 types of amyloids have been characterized, there are three main types of cardiac amyloidosis, including, acquired monoclonal immunoglobulin light-chain cardiac amyloidosis (AL-CA), wild-type transthyretin amyloidosis (wtTTR-CA), and hereditary transthyretin amyloidosis (hTTR-CA) (1–3). The natural course, treatment, and prognosis of different types of cardiac amyloidosis are different and the diagnosis is performed in late stages and maybe missed (4, 5). Despite the advance in diagnostic and treatment approaches, the exact pathophysiological mechanism of AL-CA has not been elucidated, and the prognosis is extremely poor. Therefore, studies should explore the pathophysiology and clinical aspects of AL-CA.

Previous studies indicated that several biomarkers have a demonstrated diagnostic and/or prognostic value in patients with AL-CA such as cardiac troponin T (6, 7), N-terminal pro-B-type natriuretic peptide (NT-proBNP) (7), D-dimer (8), and lactate dehydrogenase (LDH) (9). However, these biomarkers are easily affected by other conditions such as end-stage liver disease and renal failure. Moreover, the biomarkers staging system cannot accurately stratify the risk of subjects. Therefore, a better prediction biomarker is needed to evaluate the condition of patients and predict the prognosis in clinical practice.

Carbohydrate antigen 125 (CA 125) is a tumor marker associated with ovarian cancer, which is a high-molecular-weight soluble glycoprotein produced by serosal epithelium (10, 11). Increased serum CA 125 levels have also been reported in other malignancies, such as hematological malignant tumors like leukemia and non-Hodgkin's lymphoma, breast and lung cancers, melanoma, and gastrointestinal carcinoma, as well as non-malignant conditions including abdominal surgery, bacterial peritonitis, and tuberculosis (12). Previous studies (13–16) reported that elevated serum CA 125 values are associated with the clinical severity, hemodynamic status, and short-term prognosis of patients with heart failure (HF).

Patients with AL-CA are characterized by a high level of CA125. Currently, the prevalence and implications of increased CA 125 levels in AL-CA are unknown. Therefore, the present study sought to explore the associations between serum CA 125 levels and AL-CA, and systematically evaluated the clinical implications of CA 125 elevation in patients with AL-CA.

PATIENTS AND METHODS

A retrospective analysis was conducted on 170 patients diagnosed with AL-CA in the Second Xiangya Hospital of Central South University, from June 2012 to September 2020. The diagnostic criteria for suspected cardiac amyloidosis are symptoms of HF; echocardiography that indicated the interventricular septum and/or the posterior thickness of left ventricular $\geq$ 12 mm without any other causes of left ventricular hypertrophy; electrocardiogram that showed low voltage in the limb leads; and positive serum free light chain or blood/urine Bence Jones protein. If the suspected criteria are met, cardiac magnetic resonance (CMR) or tissue biopsies will be performed to confirm the diagnosis. The diagnosis of AL-CA was confirmed based on previous literature reports (5) and described as below: (1) positive serum free light chain or blood/urine Bence Jones protein; (2) the presence of apple-green appearance viewed under cross-polarized light with Congo red staining and tissue typing by immunohistochemistry on tissue biopsies from endocardial myocardial tissue or at least one clinically involved organ, including abdominal fat tissue, bone marrow, kidney, and intestinal mucosa; (3) a typical diffuse subendocardial or transmural late gadolinium enhancement pattern on CMR. The compliance of patients with 1+2 or 1+3 was included in this study. The CA 125 test was completed in 102 patients, and four patients with cancer history (except multiple myeloma [MM]), and three patients with incomplete information were excluded. The demographic and clinical characteristics, comorbidities, baseline data of laboratory tests, electrocardiogram and echocardiography data, and treatment of 95 patients with AL-CA were included as the test group (**Figure 1**). To explore the levels of CA 125 in other diseases, 52 patients with chronic HF (CHF) in the same period were included as one group. AL amyloidosis and MM are plasma cell diseases, and AL amyloidosis is mostly associated with MM (5), therefore, 48 patients who had been diagnosed with MM in the corresponding period were included as another group. Patients with non-cardiac amyloidosis in the two groups, who had a history of cancer diseases and missed CA 125 level data, were excluded. Consequently, the population of the final two groups consisted of 41 and 39 patients.

The study protocol was performed following the ethical guidelines of the Declaration of Helsinki (17). The study was approved by the human research committee of the Second Xiangya Hospital of Central South University.

All patients have undergone venous blood samples for serum levels of CA 125 on the day of admission. Serum CA 125 levels were determined by using electrochemiluminescence (Relia Biotechnology [Jiangsu, China] Co., Ltd), and the cutoff value was set at 35 KU/L.

Follow-up started at the time of diagnosis of AL-CA. The primary endpoint for this study was death from any cause. The survival time (months) was defined as the duration between the diagnosis to the date of death. If the survival time was more than 15 days and <30 days, it would be calculated as 1 month. Data were obtained from medical records or from telephone interviews with patients or relatives by four trained physicians. The last date of follow-up was November 16, 2020. Patients were censored if they were still alive at the end of the research period or were lost to follow-up, on which occasion their last clinic visit or correspondence time was used.

Normally distributed parameters were expressed as mean $\pm$ SD, whereas non-normally distributed parameters were expressed as median with interquartile range (Q3-Q1).

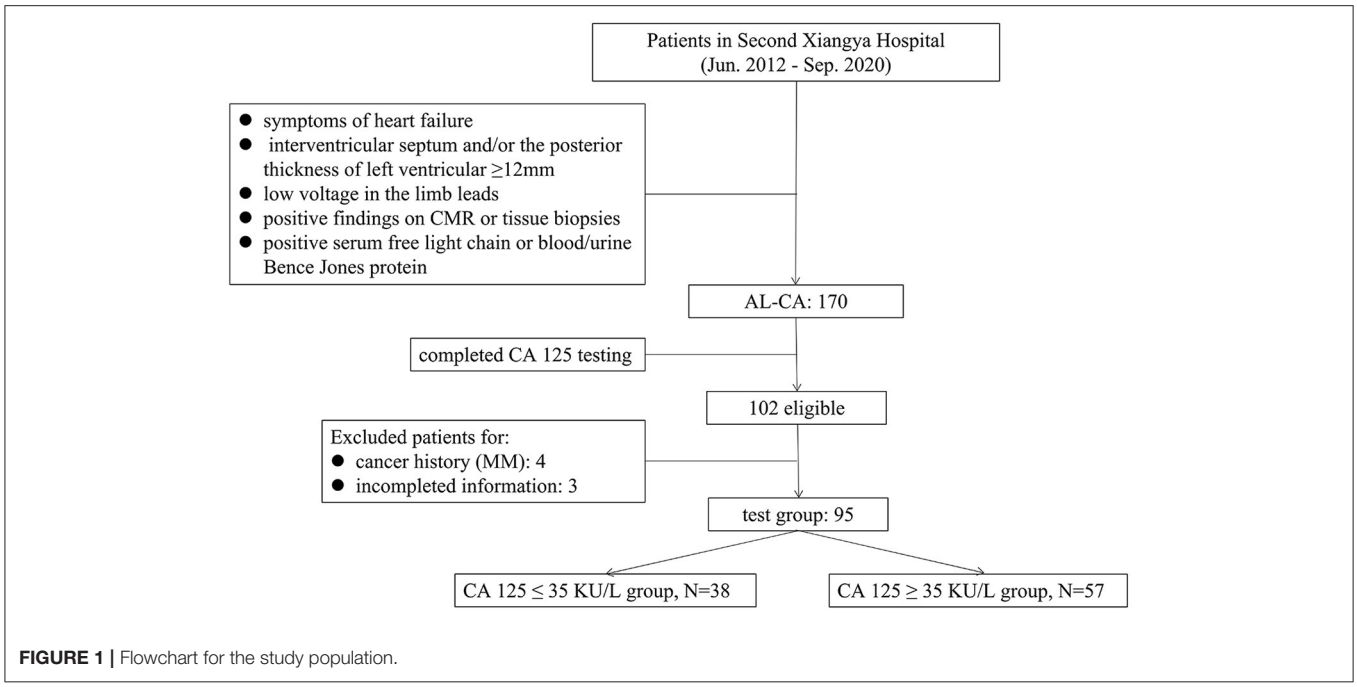

FIGURE 1 | Flowchart for the study population.

Categorical values were presented as numbers (percentages). Categorical variables were compared either with Chi-squared or Fisher's exact test. Comparison of continuous variables between two independent groups was performed using unpaired Student's *t*-test (if normally distributed) or Mann–Whitney U-test (non-normally distributed variables). One-way ANOVA or Kruskal-Wallis test was used for comparison of more than two groups. Prognostic factors with *p*-values < 0.05 after univariate Cox regression analysis were subjected to multivariate regression analysis to determine the independent factors of predicting survival according to the forward likelihood ratio method. The overall survival was evaluated with Kaplan-Meier curves, and the log-rank test was used to assess the significance of differences between groups. Time-dependent receiver operating characteristic (t-ROC) was used to reflect the accuracy of different biomarkers in predicting the overall survival at various time points based on the area under the curve (AUC). All tests were two-tailed and a *p*-value of <0.05 was considered to be statistically significant. Statistical analysis was performed using Statistical Product and Service Solutions (SPSS) 26.0 (IBM Software Inc), Empower Stats 3.0 software, and R (version 3.3.2) software.

RESULTS

Baseline and Characteristics of Patients With AL-CA

The characteristics of 95 patients in the test group were presented in **Table 1**. Out of the 95 patients, 57 (60%) and 38 (40%) patients were placed into high (CA 125 > 35 KU/L) and normal (CA 125 ≤ 35 KU/L) serum CA 125 groups, respectively. The mean age was 59.7 ± 10.0 years with 44 (77.2%) men in the high serum CA 125 group, and 61.8 ± 9.6 years with 28 (73.7%) men in the normal group. Among all patients with elevated CA 125, 14 (24.5%) patients belonged to New York Heart Association (NYHA) class I-II, whereas 43 (75.5%) patients were at class III-IV. Analysis showed no significant difference in New York Heart Association classification compared with the normal serum CA 125 group ($p = 0.156$). Polyserositis was observed in 46 (80.7%) patients with high serum CA 125 group, compared with 20 (52.6%) patients in the normal CA 125 group ($p = 0.004$). Use of aspirin and furosemide was significantly different between normal and high serum CA 125 groups (28.9% vs. 10.5%, $p = 0.022$; 81.6% vs. 94.7%, $p = 0.041$, respectively). Patients with high serum CA 125 were more likely to present with higher median levels of hemoglobin (117.4 ± 21.9 g/L vs. 106.8 ± 25.1 g/L, $p = 0.032$), serum potassium (4.11 ± 0.47 mmol/L vs. 3.97 ± 0.40 mmol/L, $p = 0.049$), low-density lipoprotein-cholesterol (3.0 ± 1.6 mmol/L vs. 2.3 ± 1.1 mmol/L, $p = 0.031$), cardiac troponin T [96.0 pg/mL (83.3–144.8) vs. 91.6 pg/mL (41.7–96.0), $p = 0.008$], and serum CA 125 [165.4 (114.5–265.9) KU/L vs. 17.9 (11.8–27.3) KU/L, $p < 0.001$] compared with patients with normal serum CA 125. Analysis showed no statistically significant difference in the diameter of atriums and ventricles, the thickness of the ventricular wall, and the ejection fraction. Analysis of ECG showed that patients with elevated CA 125 had lower limb voltage compared with normal CA 125 (76.4% vs. 52.6%, $p = 0.017$).

Level of Serum CA 125 in Different Groups

The level of serum CA 125 in the polyserositis group was higher compared with that in the non-polyserositis group (150.2 ± 150.6 vs. 100.0 ± 140.4, $p = 0.015$). In the palliative care group, the CA 125 level was higher than the chemotherapy group

TABLE 1 | Characteristics of 95 patients with AL-cardiac amyloidosis.

	CA 125 ≤ 35 KU/L ***N* = 38**	**CA 125 > 35 KU/L** ***N* = 57**	***P*-value**
Age, years	61.8 (9.6)	59.7 (10.0)	0.329
Male, n (%)	28 (73.7%)	44 (77.2%)	0.696
SBP, mmHg	119.2 (27.7)	109.4 (23.5)	0.067
DBP, mmHg	73.7 (14.0)	69.8 (13.0)	0.179
NYHA, n (%)			0.156
Class I-II	13 (34.2%)	14 (24.5%)	-
Class III-IV	25 (65.8%)	43 (75.5%)	-
Mayo AL 2004 stage, n (%)			0.097
I	2 (5.3%)	0 (0.0%)	-
II	13 (34.2%)	14 (24.6%)	-
IIIa	12 (31.6%)	14 (24.6%)	-
IIIb	11 (28.9%)	29 (50.98%)	-
Comorbidities, n (%)			
Multiple myeloma	15 (39.5%)	14 (24.6%)	0.122
Hypertension	15 (39.5%)	16 (28.1%)	0.246
Hyperlipidaemia	9 (23.7%)	15 (26.3%)	0.772
Polyserositis	20 (52.6%)	46 (80.7%)	**0.004**
T2DM	4 (10.5%)	9 (15.8%)	0.465
Medications, n (%)			
Pacemaker	4 (10.5%)	2 (3.5%)	0.168
Aspirin	11 (28.9%)	6 (10.5%)	**0.022**
Statins	17 (44.7%)	15 (26.3%)	0.063
ACEI or ARB	11 (28.9%)	16 (28.1%)	0.926
Furosemide	31 (81.6%)	54 (94.7%)	**0.041**
Digitalis	7 (18.4%)	12 (21.1%)	0.753
Chemotherapy regimens, n (%)			
Thalidomide	18 (47.4%)	16 (28.1%)	**0.055**
Prednisone or dexamethasone	19 (50.0%)	16 (28.1%)	**0.030**
Bortezomib-based	13 (34.2%)	9 (15.8%)	**0.037**
Melphalan-based	1 (2.6%)	4 (7.0%)	0.348
Palliative care, n (%)	18 (47.4%)	39 (68.4%)	**0.043**
Laboratory results			
Hemoglobin, g/L	106.8 (25.1)	117.4 (21.9)	**0.032**
ALB, g/L	29.7 (6.6)	28.5 (7.1)	0.402
LDH, U/L	261.8 (225.7–317.3)	255.3 (216.8–331.5)	0.258
Potassium, mmol/L	3.97 (0.40)	4.11 (0.47)	**0.049**
Calcium, mmol/L	2.1 (0.2)	2.0 (0.2)	0.064
LDL-C, mmol/L	2.3 (1.1)	3.0 (1.6)	**0.031**
TC, mmol/L	3.8 (1.6)	4.5 (2.5)	0.115
CRP, mg/L	18.6 (25.5)	25.6 (36.9)	0.480
ESR, mm/h	57.7 (39.6)	35.8 (30.8)	**0.011**
Cardiac troponin T, pg/mL	91.9 (41.7–96.0)	96.0 (83.3–144.8)	**0.008**
NT-proBNP, pg/mL	5618.6 (3309.0–10309.5)	8987.0 (4970.3–11649.0)	0.164
D-Dimer, ug/mL	1.52 (1.92)	2.13 (2.40)	0.221
CA 125, KU/L	17.9 (11.8–27.3)	165.4 (114.5–265.9)	**<0.001**
eGFR, mL/(min × 1.73 m^2)	62.8 (35.5)	58.6 (31.8)	0.567
24-h urine protein ≥ 1.0 g/24 h	26 (68.4%)	36 (63.2%)	0.598
Echocardiography			
LVEDd, mm	45.5 (7.2)	43.5 (6.4)	0.160

(Continued)

TABLE 1 | Continued

	CA 125 ≤ 35 KU/L N = 38	CA 125 > 35 KU/L N = 57	*P*-value
RVEDd, mm	32.6 (5.7)	32.9 (5.1)	0.560
LAESd, mm	40.6 (8.1)	41.2 (9.0)	0.759
RAESd, mm	37.9 (9.1)	39.3 (10.6)	0.514
IVS, mm	13.2 (3.1)	14.1 (3.8)	0.213
LVPW, mm	12.8 (2.9)	13.6 (3.3)	0.238
LVEF (%)	54.9 (8.1)	53.0 (10.2)	0.338
Electrocardiogram			
Atrial fibrillation, n (%)	6 (15.8%)	11 (20.0%)	0.606
Low limb voltage, n (%)	20 (52.6%)	42 (76.4%)	**0.017**
PRWP, n (%)	29 (76.3%)	47 (85.5%)	0.262

Data are (N) Mean (SD) or (N) n (%), Median (Q3–Q1), where N is the total number of patients with available data.
ACEI, Angiotensin-Converting Enzyme Inhibitor; AL-CA, Light-Chain amyloidosis; ALB, Albumin; ARB, Angiotensin Receptor Blocker; ThD/LeD, Thalidomide/Lenalidomide; CA 125, Carbohydrate Antigen 125; T2DM, Type 2 Diabetes Mellitus; ESR, Erythrocyte Sedimentation Rate; CRP, C-Reactive Protein; DBP, Diastolic Blood Pressure; eGFR, estimated Glomerular Filtration Rate; ESR, Erythrocyte Sedimentation Rate; IVS, Interventricular Septum; LAESd, Left Atrium End Systolic diameter; LDH, Lactate Dehydrogenase; LDL-C, Low Density Lipoprotein-Cholesterol; LVEDd, Left Ventricular End Diastolic diameter; LVEF, Left Ventricular Ejection Fraction; LVPW, Left Ventricular Posterior Wall; NT-proBNP, N-terminal pro–B-type Natriuretic Peptide; NYHA, New York Heart Association; PCT, Procalcitoin; PRWP, Poor R-wave progression; RAESd, Right Atrium End Systolic diameter; RVEDd, Right Ventricular End Diastolic diameter; SBP, Systolic Blood Pressure; TC, Total Cholesterol. Bold values are statistical significance $p < 0.05$.

(150.8 ± 153.7 vs. 109.9 ± 138.7, $p = 0.053$) as well. CA 125 levels varied among different Mayo AL 2004 stages and were statistically different, with higher Mayo stage associated with higher CA 125 levels [I (6.5 ± 2.6), II (117.1 ± 134.4), IIIa (84.4 ± 77.7), IIIb (185.3 ± 178.0)]. Serum CA 125 levels were not statistically different among different NYHA classifications [I (169.6 ± 175.6), II (134.2 ± 151.5), III (150.6 ± 202.5), IV (119.1 ± 92.2); **Figure 2**].

Further, the levels of CA 125 in different diseases were explored. Clinical characteristics of the test group and the other three groups were shown in **Supplementary Table 1**. Elevated serum CA 125 values were observed in 57 (60.0%) patients in the AL-CA group, with a mean value of 134.9 ± 148.6 KU/L, in 6 (54.5%) patients in the TTR-CA group, with a mean value of 112.4 ± 134.7 KU/L, in 16 (39.0%) patients in the CHF group with a mean value of 45.7 ± 44.9 KU/L and in 3 (7.7%) patients in the MM group with a mean value of 18.9 ± 20.9 KU/L ($p < 0.01$), **Supplementary Figure 1**.

Univariate and Multivariate Predictors of All-Cause Mortality

Prognostic factors for all-cause mortality were explored using univariate and multivariate Cox hazard analyses (**Table 2**). Univariate analysis showed that systolic blood pressure (HR 0.988, 95% CI 0.976–0.997, $p = 0.010$), diastolic blood pressure (HR 0.981, 95% CI 0.965–0.998, $p = 0.025$), palliative care (HR 2.259, 95% CI 1.309–3.898, $p = 0.003$), low-density lipoprotein-cholesterol (HR 1.232, 95% CI 1.039–1.461, $p = 0.017$), total cholesterol (HR 1.163, 95% CI 1.033–1.310, $p = 0.013$), CA 125 (HR 1.002, 95% CI 1.001-1.004, $p = 0.001$), interventricular septum (HR 1.049, 95% CI 1.000–1.136, $p = 0.048$), and left ventricular posterior wall (HR 1.085, 95% CI 1.004–1.174, $p = 0.040$) were statistically significant predictors of overall survival. However, multivariate analysis showed that the only independent predictors were palliative care (HR 2.613, 95% CI 1.300–5.251, $p = 0.007$) and CA 125 (HR 1.002, 95% CI 1.000–1.004, $p = 0.033$).

Kaplan–Meier Analyses of Overall Survival

Patients with high levels of CA 125 were followed up for a median period of 7 months (IQR 1.0–10.2) and those with normal levels were followed-up for a period of 9 months (IQR 1.5–19.0, $p = 0.10$). Forty-six (80.7%) patients died in elevated CA 125 group and 22 (57.9%) patients died in patients with normal CA 125 ($p = 0.016$) during the follow-up period. The median overall survival in patients with high level CA 125 was 5 months (95% CI 3.881–6.119) and 25 months (95% CI 0.602–39.398) in patients with normal CA 125 levels ($p = 0.012$, **Figure 3A**). Patients with palliative care had a median overall survival of only 5 months (95% CI 4.823–7.177). The overall survival was significantly shorter for patients with palliative care compared with 13 months (95% CI 2.103–23.897) in patients receiving chemotherapy ($p = 0.035$, **Figure 3B**).

Biomarkers for Predicting Overall Survival Using t-ROC Analysis

The accuracy of the four biomarkers for predicting overall survival was explored by t-ROC analysis. The AUC of 3-months, 6-months, 12-months, and 24-months overall survival for CA 125 were 0.60, 0.75, 0.75, and 0.77, respectively (**Figure 4A**), compared with NT-proBNP (**Figure 4B**), cardiac troponin T (**Figure 4C**), and LDH (**Figure 4D**).

DISCUSSIONS

AL-CA is the most common type of infiltrative cardiomyopathy. It is characterized by various clinical manifestations such as congestive HF, arrhythmia, orthostatic hypotension, syncope, or

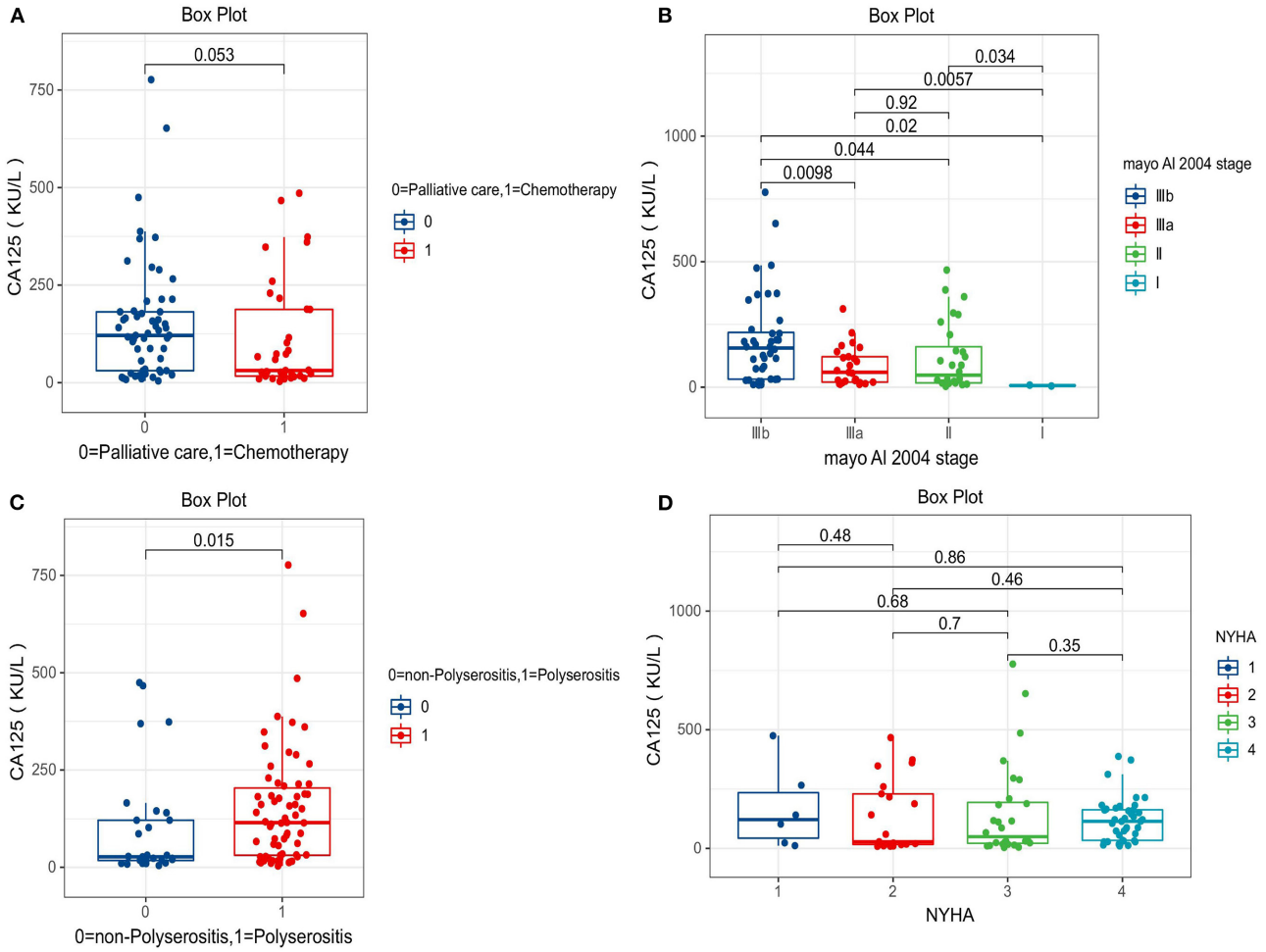

FIGURE 2 | Comparison of serum carbohydrate antigen 125 (CA 125) levels between different groups. **(A)** Palliative care group vs. chemotherapy group (150.8 ± 153.7 vs. 109.9 ± 138.7). **(B)** Mayo AL 2004 stage I (6.5 ± 2.6), II (117.1 ± 134.4), IIIa (84.4 ± 77.7), IIIb (185.3 ± 178.0). **(C)** Polyserositis group vs. non-Polyserositis group (150.2 ± 150.6 vs. 100.0 ± 140.4). **(D)** NHYA I (169.6 ± 175.6), II (134.2 ± 151.5), III (150.6 ± 202.5), IV (119.1 ± 92.2).

even other system expressions like gastrointestinal symptoms, albuminuria, and carpal tunnel syndrome leading to a high rate of missed diagnosis (1). In the present study, we analyzed serum CA 125 levels in 95 consecutive patients with AL-CA at an expertise center in China. To the best of our knowledge, this is the first study to explore the prevalence and evaluate the clinical significance of increased CA 125 levels in patients with AL-CA. The principal results of this study were as follows: (1) serum CA 125 levels were elevated in more than half of patients with AL-CA, compared with those with normal CA 125 levels. Patients who exhibited high serum CA 125 showed higher levels of hemoglobin, LDL-C, TC, and cardiac troponin T, and showed higher rates of polyserositis and low limb voltage compared with those with normal levels of CA 125; (2) patients with polyserositis or those who treated with palliative care seemed to express higher CA 125 levels in AL-CA, and higher Mayo stage was associated with higher CA 125 levels; (3) the values of CA 125 in patients with AL-CA were significantly higher compared with those in patients with CHF and MM; (4) CA 125 was a significant independent predictor of survival, with higher levels independently correlated with lower overall survival; (5) the prediction accuracy of CA 125 was not inferior to that of cardiac troponin T, NT-proBNP, and LDH based on the AUC. In addition, CA 125 seemed to be not affected by the estimated Glomerular Filtration Rate (eGFR) status of patients.

Serum CA 125 values are used for diagnosis and follow-up of patients with ovarian cancer and to evaluate the response to therapy (18, 19). An increase in serum CA 125 has also been observed in other malignancies (20–24) and non-malignant diseases (25–28). The first study on the relationship between CA 125 and the cardiovascular system investigated the association between serum CA 125 levels and pericardial effusion in 1993 (29). Following this, Nägele et al. (16) first revealed that CA 125 may be a valuable tool for monitoring the status and clinical course of patients with HF. A previous study (15) demonstrated that only CA 125 levels were correlated with baseline clinical status in CHF compared with CA 19-9, CA 15-3, carcinoembryonic antigen (CEA), and alpha-fetoprotein

TABLE 2 | Univariate and multivariate Cox hazard analyses of predictors for all-cause mortality.

Variables	Univariate			Multivariate		
	HR	95% CI	*p*-value	HR	95% CI	*p*-value
Male	0.797	0.452–1.407	0.435	-	-	-
Age	1.008	0.986–1.031	0.473	-	-	-
NYHA	1.210	0.941–1.580	0.295	-	-	-
SBP	0.988	0.976–0.997	**0.010**	0.988	0.964–1.011	0.302
DBP	0.981	0.965–0.998	**0.025**	0.995	0.953–1.038	0.995
MM	1.352	0.796–2.298	0.265	-	-	-
Hyperlipidemia	1.650	0.931–2.277	0.105	-	-	-
Polyserositis	1.060	0.633–1.776	0.824	-	-	-
Hemoglobin	1.008	0.999–1.018	0.464	-	-	-
ALB	0.973	0.999–1.019	0.078	-	-	-
Calcium	0.987	0.326–2.985	0.981	-	-	-
eGFR	0.998	0.991–1.006	0.672	-	-	-
Palliative care	2.259	1.309–3.898	**0.003**	2.613	1.300–5.251	**0.007**
LDL-C	1.232	1.039–1.461	**0.017**	0.822	0.439–1.539	0.539
TC	1.163	1.033–1.310	**0.013**	1.365	0.894–2.085	0.149
D-Dimer	1.097	0.989–1.216	0.079	-	-	-
CA 125	1.002	1.001–1.004	**0.001**	1.002	1.000–1.004	**0.033**
IVS	1.049	1.000–1.136	**0.048**	1.033	0.834–1.280	0.767
LVPW	1.085	1.004–1.171	**0.040**	1.029	0.804–1.316	0.820
LVEF	0.979	0.958–1.012	0.280	-	-	-
Low voltage	0.681	0.404–1.148	0.150	-	-	-
PRWP	0.687	0.339–1.392	0.297	-	-	-

HR, hazard ratio; CI, Confidence Interval.
*For other abbreviations, see **Table 1**. Bold values are statistical significance $p < 0.05$.*

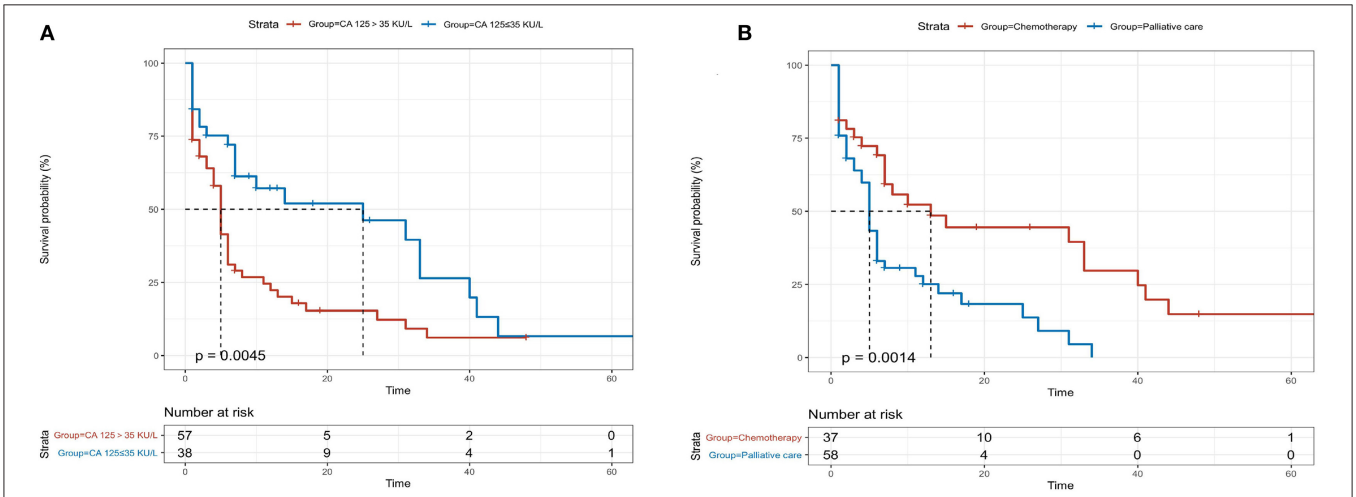

FIGURE 3 | Kaplan-Meier analysis for patients with light-chain cardiac amyloidosis (AL-CA) classified according to serum levels of CA 125 **(A)** and treatment with/without chemotherapy **(B)**. The median overall survival in elevated and normal CA 125 values were 5 months and 25 months, respectively (log rank, $p = 0.0045$). Patients with palliative care had a median overall survival of 5 months while the patients receiving chemotherapy had a median overall survival of 13 months (log-rank, $p = 0.0014$).

(AFP), and the serum CA 125 levels of patients with CHF were significantly higher in NYHA class III/IV compared with those in NYHA class I/II. In addition to CHF, elevated CA 125 values were observed in acute HF (AHF) and have been used to assess 6-months risk stratification in patients admitted with AHF (30). Studies have confirmed that cardiac troponin T and NT-proBNP have significant clinical values in determining the prognosis for newly diagnosed patients with AL-CA. Therefore,

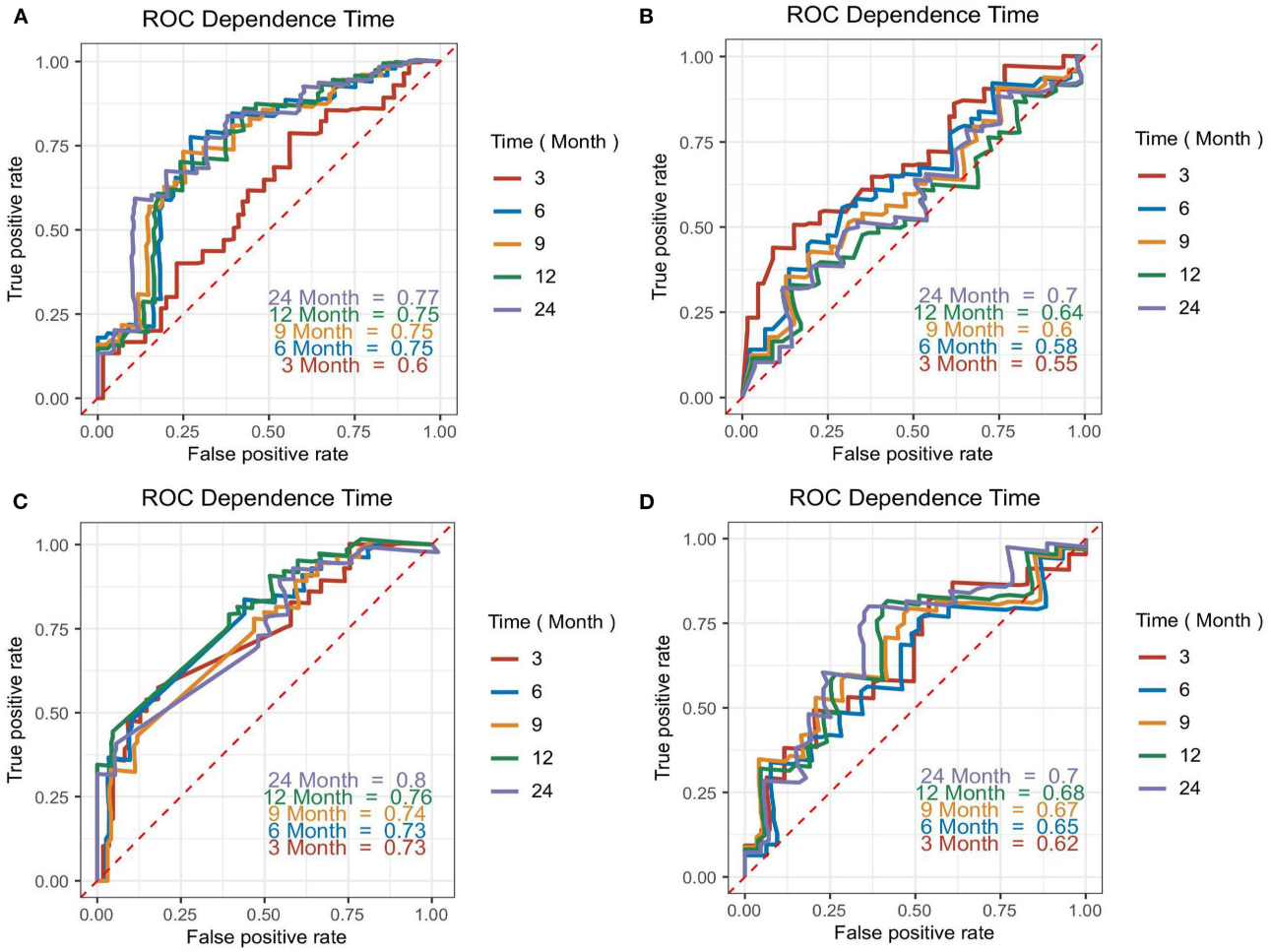

FIGURE 4 | Time-dependent ROC (t-ROC) curves for CA 125 **(A)**, N-terminal pro-B-type natriuretic peptide (NT-proBNP) **(B)**, cardiac troponin T **(C)**, and lactate dehydrogenase (LDH) **(D)** models. The area under the curve (AUC) presented the accuracy of predicting overall survival time (from diagnosis confirmed) for each biomarker at various time points.

the Mayo Clinic established a staging system using the two biomarkers (as well as free light chain) to predict patient outcomes (31, 32). This risk stratification system is also the most commonly used in clinical practice. However, the Mayo AL-stage is tremendously affected by renal function. The values of troponin and NT-proBNP in patients with decreased eGFR are severely overestimated, which leads to the conclusion that this system does not truly reflect the prognosis of patients with AL-CA, and novel prognostic biomarkers need to be continuously explored in clinical practice.

The potential mechanism of serum CA 125 levels elevation in AL-CA remains unclear. Seo et al. (29) reported that among 57 patients with different etiologies of pericardial effusion, 65% of the patients had significantly higher serum CA 125 levels compared with normal patients. Moreover, the levels of CA 125 decreased or normalized with the reduction or disappearance of effusion. In addition, the study used anti-CA 125 antibodies to stain the pericardial tissue obtained through autopsy of 17 patients and showed higher serum CA 125 levels in the CA 125-positive-stained pericardium compared with those in negative-stained for CA 125. Except for pericardial effusion, elevated serum CA 25 levels have been reported in pleural and peritoneal effusions with non-malignant diseases and reported that CA 125 may be produced from the mesothelial cells of pleura and peritoneum (33–35). These findings were consistent with findings from our study that polyserositis was observed in 80.7% of 57 patients with AL-CA with elevated CA 125 levels, and we also found that patients with polyserositis were more likely to show higher CA 125 values ($p = 0.015$). Studies reported that blood levels of cytokines and/or their receptors, including Interleukin (IL)-6, IL-10, and tumor necrosis factor (TNF)-α, were more likely to be increased in patients with HF, and cytokine network activation is one of the main factors for serum CA 125 elevation in patients with CHF dependent on inflammation (36–38). Serum CA 125 levels with AL-CA were significantly higher in our study compared with those of patients with CHF ($p < 0.01$), although the blood mean levels of CA 125 in CHF were above normal. Analysis showed that only three patients

with MM had a mild elevated serum CA 125 levels ($p < 0.01$). Therefore, the effect of plasma cell diseases on CA 125 was excluded. Previous findings and findings from the current study showed that the reasons for the elevation of serum CA 125 levels in AL-CA may be as follows: (1) abnormal deposition of amyloid in the serosal tissue and increased chronic right ventricular filling pressure caused by CHF leading to tissue stretching and stimulation of secretion by mesothelial cells; (2) amyloid activates the cytokine network by inflammation excitation and stimulates the mesothelial cells to produce and secrete CA 125. However, the underlying mechanism linked between CA 125, cytokines, CA 125-producing cells, and AL-CA should be explored further.

Our study revealed that the levels of cardiac troponin T were associated with the serum CA 125 levels. Higher cardiac troponin T levels were observed in the high serum CA 125 group compared with the level in the normal CA 125 group. Patients with elevated serum CA 125 may have more fluid accumulation leading to increased left ventricular filling pressure and polyserositis, thus causing increased wall stress due to diastolic dysfunction and compressed myocardial capillaries, inducing deficient myocardial blood supply and myocardial ischemia (6). In addition, patients with high serum CA 125 values had higher levels of hemoglobin, potassium, LDL-C, and TC. These findings imply that in most of the patients with AL-CA with elevated CA 125 levels, the kidney is involved, and combined with nephrotic syndrome (39), resulting in entry of body fluid to the interstitial space or serous cavity, leading to blood concentration and dyslipidemia. The significant difference between the serum CA 125 levels of low limb voltage can be attributed to serous effusion. However, the pathophysiological mechanisms should be explored in subsequent studies.

CA 125 was significantly correlated with prognosis after adjusting for systolic blood pressure, diastolic blood pressure, treatment without chemotherapy, low-density lipoprotein-cholesterol, total cholesterol, interventricular septum, and left ventricular posterior wall. The median overall survival of high levels of patients with CA 125 was only 5 months, whereas the median overall survival in normal CA 125 levels was 25 months. This finding implies that high levels of serum CA 125 are independently correlated with high mortality in patients with AL-CA. The accuracy of CA 125 in predicting the overall survival was not inferior compared with the classical prognostic biomarkers including cardiac troponin T, NT-proBNP, and LDH. The possible advantages of CA 125 compared with these biomarkers include being easy to obtain, repeatable, no preparations required, and inexpensive cost (<4 dollars per determination in China compared with more than 40 dollars for NT-proBNP). Notably, CA 125-guided therapy (keeping CA 125 levels at 35 KU/L or less by optimizing the use of a diuretic, enforcing the use of statins, and increasing the frequency of monitoring visits) is superior compared with the standard of care for AHF by reducing the risk of 1-year death and the rate of rehospitalization (40). Further studies should adjust the treatment strategy for patients with AL-CA to reduce the myocardial injury, improve the clinical condition of patients, assist chemotherapy, and decrease the rate of mortality and readmission based on serum CA 125 values.

LIMITATIONS

Several limitations of the study need to be addressed. First, the small sample size and information bias may affect the results of our study. Further research should be conducted with a larger sample size and minimize the information bias for more reliable results. Second, the effect of therapies including chemotherapy and palliative care on serum CA 125 levels was not explored, which may have a crucial influence on the evaluation of treatment outcome and short-term prognosis. Third, although analysis showed no significant difference in eGFR between different serum CA 125 levels groups, CA 125 levels were not evaluated in different renal function stages of patients with AL-CA. Notably, a nephrotic syndrome caused by renal involvement of AL-CA leads to fluid retention and polyserositis and may have caused increased serum CA 125. Therefore, further studies should explore the relationship between CA 125 and nephrotic syndrome.

CONCLUSION

The prevalence of elevated serum CA 125 levels is more than 50% in patients with AL-CA. CA 125 is a novel independent prognostic predictor. High serum CA 125 values are correlated with low overall survival and the accuracy of predicting prognosis was not inferior compared with conventional biomarkers.

DATA AVAILABILITY STATEMENT

The raw data supporting the conclusions of this article will be made available by the authors, without undue reservation.

ETHICS STATEMENT

The studies involving human participants were reviewed and approved by the Human Research Committee of the Second Xiangya Hospital of Central South University. The patients/participants or their legal guardian/next of kin provided their written informed consent to participate in this study.

AUTHOR CONTRIBUTIONS

QLiu and JT designed this study and performed quality control of data authenticity. ML drafted the manuscript. ZW and ML collected and analyzed these data. ML, ZW, IT, and NQ performed follow-up visits. JLi, WL, and QZ provided study guidance and revised the paper. QLin, JLiu, NL, YW, MC, YC, QLiu, and JT revised the paper and all authors approved the final version.

FUNDING

Financial support was obtained from the National Natural Science Foundation of China (Nos. 81770337 and 81800302),

China International Medical Foundation (Z-2016-23-2001-14), and Provincial Natural Science Foundation of Hunan (No. 2019JJ50871).

ACKNOWLEDGMENTS

We would like to thank the Home for the research editorial team (www.home-for-researchers.com) provided language emollient assistance during the writing of the manuscript.

SUPPLEMENTARY MATERIAL

The Supplementary Material for this article can be found online at: https://www.frontiersin.org/articles/10.3389/fcvm.2021.692083/full#supplementary-material

Supplementary Figure 1 | Comparison of serum CA 125 levels between different groups. CHF, Chronic Heart Failure; AL-CA, Light-chain Cardiac Amyloidosis; TTR-CA, Transthyretin Amyloidosis; CA 125, Carbohydrate Antigen 125; MM, Multiple Myeloma.

Supplementary Table 1 | Clinical characteristics of several control groups.

REFERENCES

1. Banypersad SM, Moon JC, Whelan C, Hawkins PN, Wechalekar AD. Updates in cardiac amyloidosis: a review. *J Am Heart Assoc.* (2012) 1:e364. doi: 10.1161/JAHA.111.000364
2. Wechalekar AD, Gillmore JD, Hawkins PN. Systemic amyloidosis. *Lancet (London, England).* (2016) 387:2641–54. doi: 10.1016/S0140-6736(15)01274-X
3. Rapezzi C, Merlini G, Quarta CC, Riva L, Longhi S, Leone O, et al. Systemic cardiac amyloidoses: disease profiles and clinical courses of the 3 main types. *Circulation.* (2009) 120:1203–12. doi: 10.1161/CIRCULATIONAHA.108.843334
4. Ruberg FL, Grogan M, Hanna M, Kelly JW, Maurer MS. Transthyretin amyloid cardiomyopathy: JACC state-of-the-art review. *J Am Coll Cardiol.* (2019) 73:2872–91. doi: 10.1016/j.jacc.2019.04.003
5. Falk RH, Alexander KM, Liao R, Dorbala S. AL (Light-Chain) cardiac amyloidosis: a review of diagnosis and therapy. *J Am Coll Cardiol.* (2016) 68:1323–41. doi: 10.1016/j.jacc.2016.06.053
6. Takashio S, Yamamuro M, Izumiya Y, Hirakawa K, Marume K, Yamamoto M, et al. Diagnostic utility of cardiac troponin T level in patients with cardiac amyloidosis. *ESC Heart Failure.* (2018) 5:27–35. doi: 10.1002/ehf2.12203
7. Pregenzer-Wenzler A, Abraham J, Barrell K, Kovacsovics T, Nativi-Nicolau J. Utility of biomarkers in cardiac amyloidosis. JACC. *Heart Fail. (*2020). 8:701–11. doi: 10.1016/j.jchf.2020.03.007
8. Pudusseri A, Sanchorawala V, Sloan JM, Bever KM, Doros G, Kataria S, et al. Prevalence and prognostic value of D-dimer elevation in patients with AL amyloidosis. *Am J Hematol.* (2019) 94:1098–103. doi: 10.1002/ajh.25576
9. He H, Liu J, Jiang H, Du J, Li L, Lu J, et al. High serum lactate dehydrogenase adds prognostic value to cardiac biomarker staging system for light chain amyloidosis. *J Cancer.* (2019) 10:5622–7. doi: 10.7150/jca.30345
10. Kenemans P, Yedema CA, Bon GG, von Mensdorff-Pouilly S. CA 125 in gynecological pathology—a review. *Eur J Obstet Gynecol Reprod Biol.* (1993) 49:115–24. doi: 10.1016/0028-2243(93)90135-Y
11. Högberg T, Kågedal B. Long-term follow-up of ovarian cancer with monthly determinations of serum CA 125. *Gynecol Oncol.* (1992) 46:191–8. doi: 10.1016/0090-8258(92)90254-G
12. Kouris NT, Zacharos ID, Kontogianni DD, Goranitou GS, Sifaki MD, Grassos HE, et al. The significance of CA125 levels in patients with chronic congestive heart failure. Correlation with clinical and echocardiographic parameters. *Eur J Heart Fail.* (2005) 7:199–203. doi: 10.1016/j.ejheart.2004.07.015
13. Duman D, Palit F, Simsek E, Bilgehan K. Serum carbohydrate antigen 125 levels in advanced heart failure: relation to B-type natriuretic peptide and left atrial volume. *Eur J Heart Fail.* (2008) 10:556–9. doi: 10.1016/j.ejheart.2008.04.012
14. D'Aloia A, Faggiano P, Aurigemma G, Bontempi L, Ruggeri G, Metra M, et al. Serum levels of carbohydrate antigen 125 in patients with chronic heart failure: relation to clinical severity, hemodynamic and Doppler echocardiographic abnormalities, and short-term prognosis. *J Am Coll Cardiol.* (2003) 41:1805–11. doi: 10.1016/S0735-1097(03)00311-5
15. Varol E, Ozaydin M, Dogan A, Kosar F. Tumour marker levels in patients with chronic heart failure. *Eur J Heart Fail.* (2005) 7:840–3. doi: 10.1016/j.ejheart.2004.12.008
16. Nägele H, Bahlo M, Klapdor R, Schaeperkoetter D, Rödiger W. CA 125 and its relation to cardiac function. *Am Heart J.* (1999) 137:1044–9. doi: 10.1016/S0002-8703(99)70360-1
17. World Medical Association declaration of Helsinki. Recommendations guiding physicians in biomedical research involving human subjects. *JAMA.* (1997) 277:925–6. doi: 10.1001/jama.277.11.925
18. Canney PA, Moore M, Wilkinson PM, James RD. Ovarian cancer antigen CA125: a prospective clinical assessment of its role as a tumour marker. *Br J Cancer.* (1984) 50:765–9. doi: 10.1038/bjc.1984.254
19. Bates SE. Clinical applications of serum tumor markers. *Ann Intern Med.* (1991) 115:623–38. doi: 10.7326/0003-4819-115-8-623
20. Camera A, Villa MR, Rocco S, De Novellis T, Costantini S, Pezzullo L, et al. Increased CA 125 serum levels in patients with advanced acute leukemia with serosal involvement. *Cancer Am Cancer Soc.* (2000) 88:75–8. doi: 10.1002/(sici)1097-0142(20000101)88:1<75::aid-cncr11>3.0.co;2-#
21. Wu JZ, Tian T, Huang Y, Liang JH, Miao Y, Wang L, et al. Serum carbohydrate antigen 125 concentration as a superior predictor for serosal effusion at diagnosis and a prognostic factor in diffuse large B-cell lymphoma. *Cancer Biomark Sect A Dis Mark.* (2016) 17:205–12. doi: 10.3233/CBM-160632
22. Sakamoto K, Haga Y, Yoshimura R, Egami H, Yokoyama Y, Akagi M. Comparative effectiveness of the tumour diagnostics, CA 19-9, CA 125 and carcinoembryonic antigen in patients with diseases of the digestive system. *GUT.* (1987) 28:323–9. doi: 10.1136/gut.28.3.323
23. Lei Y, Zang R, Lu Z, Zhang G, Huang J, Liu C, et al. ERO1L promotes IL6/sIL6R signaling and regulates MUC16 expression to promote CA125 secretion and the metastasis of lung cancer cells. *Cell Death Dis.* (2020) 11:853. doi: 10.1038/s41419-020-03067-8
24. Yerushalmi R, Tyldesley S, Kennecke H, Speers C, Woods R, Knight B, et al. Tumor markers in metastatic breast cancer subtypes: frequency of elevation and correlation with outcome. *Ann Oncol Off J Eur Soc Med Oncol.* (2012) 23:338–45. doi: 10.1093/annonc/mdr154
25. Talbot RW, Jacobsen DJ, Nagorney DM, Malkasian GD, Ritts RE. Temporary elevation of CA 125 after abdominal surgical treatment for benign disease and cancer. *Surg Gynecol Obstet.* (1989) 168:407–412.
26. Devarbhavi H, Kaese D, Williams AW, Rakela J, Klee GG, Kamath PS. Cancer antigen 125 in patients with chronic liver disease. *Mayo Clin Proc.* (2002) 77:538–41. doi: 10.4065/77.6.538
27. Halila H, Stenman UH, Seppälä M. Ovarian cancer antigen CA 125 levels in pelvic inflammatory disease and pregnancy. *Cancer Am Cancer Soc.* (1986) 57:1327–9.
28. Shin HP, Lee JI, Seo HM, Lim SJ, Jung SW, Cha JM, et al. Laparoscopic appearance in a case of peritoneal tuberculosis with elevated cancer antigen 125 levels. *Gastrointest Endosc.* (2009) 69:180–2. doi: 10.1016/j.gie.2008.03.1079
29. Seo T, Ikeda Y, Onaka H, Hayashi T, Kawaguchi K, Kotake C, et al. Usefulness of serum CA125 measurement for monitoring pericardial effusion. *Jpn Circ J.* (1993) 57:489–94. doi: 10.1253/jcj.57.489
30. Núñez J, Sanchis J, Bodí V, Fonarow GC, Núñez E, Bertomeu-González V, et al. Improvement in risk stratification with the combination of the tumour marker antigen carbohydrate 125 and brain natriuretic peptide in patients with acute heart failure. *Eur Heart J.* (2010) 31:1752–63. doi: 10.1093/eurheartj/ehq142
31. Kumar S, Dispenzieri A, Lacy MQ, Hayman SR, Buadi FK, Colby C, et al. Revised prognostic staging system for light chain amyloidosis incorporating

cardiac biomarkers and serum free light chain measurements. *J Clin Oncol Off J Am Soc Clin Oncol.* (2012) 30:989–95. doi: 10.1200/JCO.2011.38.5724
32. Lilleness B, Ruberg FL, Mussinelli R, Doros G, Sanchorawala V. Development and validation of a survival staging system incorporating BNP in patients with light chain amyloidosis. *Blood.* (2019) 133:215–23. doi: 10.1182/blood-2018-06-858951
33. Bergmann JF, Bidart JM, George M, Beaugrand M, Levy VG, Bohuon C. Elevation of CA 125 in patients with benign and malignant ascites. *Cancer Am Cancer Soc.* (1987) 59:213–7.
34. Epiney M, Bertossa C, Weil A, Campana A, Bischof P. CA125 production by the peritoneum: *in-vitro* and in-vivo studies. *Hum Reprod (Oxford, England).* (2000) 15:1261–5. doi: 10.1093/humrep/15.6.1261
35. Sevinc A, Buyukberber S, Sari R, Kiroglu Y, Turk HM, Ates M. Elevated serum CA-125 levels in hemodialysis patients with peritoneal, pleural, or pericardial fluids. *Gynecol Oncol.* (2000) 77:254–7. doi: 10.1006/gyno.2000.5776
36. Deswal A, Petersen NJ, Feldman AM, Young JB, White BG, Mann DL. Cytokines and cytokine receptors in advanced heart failure: an analysis of the cytokine database from the Vesnarinone trial (VEST). *Circulation.* (2001) 103:2055–9. doi: 10.1161/01.CIR.103.16.2055
37. Kosar F, Aksoy Y, Ozguntekin G, Ozerol I, Varol E. Relationship between cytokines and tumour markers in patients with chronic heart failure. *Eur J Heart Fail.* (2006) 8:270–4. doi: 10.1016/j.ejheart.2005.09.002
38. Stanciu AE, Stanciu MM, Vatasescu RG. NT-proBNP and CA 125 levels are associated with increased pro-inflammatory cytokines in coronary sinus serum of patients with chronic heart failure. *Cytokine.* (2018) 111:13–9. doi: 10.1016/j.cyto.2018.07.037
39. Sevinc A, Buyukberber S, Sari R, Turk HM, Ates M. Elevated serum CA-125 levels in patients with nephrotic syndrome-induced ascites. *Anticancer Res.* (2000) 20:1201–3. doi: 10.1006/gyno.1999.5670
40. Núñez J, Llàcer P, Bertomeu-González V, Bosch MJ, Merlos P, García-Blas S, et al. Carbohydrate antigen-125-guided therapy in acute heart failure: CHANCE-HF: a randomized study. JACC. *Heart Fail.* (2016). 4:833–43. doi: 10.1016/j.jchf.2016.06.007

Conflict of Interest: The authors declare that the research was conducted in the absence of any commercial or financial relationships that could be construed as a potential conflict of interest.

Publisher's Note: All claims expressed in this article are solely those of the authors and do not necessarily represent those of their affiliated organizations, or those of the publisher, the editors and the reviewers. Any product that may be evaluated in this article, or claim that may be made by its manufacturer, is not guaranteed or endorsed by the publisher.

frontiers in Cardiovascular Medicine

REVIEW
published: 08 November 2021
doi: 10.3389/fcvm.2021.709396

Aortic Stiffness: Epidemiology, Risk Factors, and Relevant Biomarkers

Rebecca Angoff[1], *Ramya C. Mosarla*[2] *and Connie W. Tsao*[1]*

[1] Cardiovascular Division, Department of Medicine, Beth Israel Deaconess Medical Center, Boston, MA, United States,
[2] Division of Cardiology, Department of Medicine, New York University Langone Health, New York, NY, United States

Aortic stiffness (AoS) is a maladaptive response to hemodynamic stress and both modifiable and non-modifiable risk factors, and elevated AoS increases afterload for the heart. AoS is a non-invasive marker of cardiovascular health and metabolic dysfunction. Implementing AoS as a diagnostic tool is challenging as it increases with age and varies amongst races. AoS is associated with lifestyle factors such as alcohol and smoking, as well as hypertension and comorbid conditions including metabolic syndrome and its components. Multiple studies have investigated various biomarkers associated with increased AoS, and this area is of particular interest given that these markers can highlight pathophysiologic pathways and specific therapeutic targets in the future. These biomarkers include those involved in the inflammatory cascade, anti-aging genes, and the renin-angiotensin aldosterone system. In the future, targeting AoS rather than blood pressure itself may be the key to improving vascular health and outcomes. In this review, we will discuss the current understanding of AoS, measurement of AoS and the challenges in interpretation, associated biomarkers, and possible therapeutic avenues for modulation of AoS.

Keywords: aortic stiffness, pulse wave velocity, cardiovascular health, risk factors, biomarkers

OPEN ACCESS

Edited by:
Maria Perticone,
University of Magna Graecia, Italy

Reviewed by:
Muhammad Tarek Abdel Ghafar,
Tanta University, Egypt
Richard Yang Cao,
Shanghai Xuhui Central Hospital, China

***Correspondence:**
Connie W. Tsao
ctsao1@bidmc.harvard.edu

Specialty section:
This article was submitted to General Cardiovascular Medicine, a section of the journal Frontiers in Cardiovascular Medicine

Received: *13 May 2021*
Accepted: *30 September 2021*
Published: *08 November 2021*

Citation:
Angoff R, Mosarla RC and Tsao CW (2021) Aortic Stiffness: Epidemiology, Risk Factors, and Relevant Biomarkers. Front. Cardiovasc. Med. 8:709396. doi: 10.3389/fcvm.2021.709396

INTRODUCTION

Aortic stiffness (AoS) is a measure of the elasticity of the blood vessel wall, and elevated AoS may result from and contribute to increased stress on the vessel walls. It is a non-invasive method of measuring maladaptive change and remodeling to aortic properties and is a promising marker of subclinical disease. Its measurement is based on principles of physics. The arterial tree has varying mechanical properties along its length, primarily determined by different contributions of collagen and elastin to its structure, in addition to varying degrees of modulation by smooth muscle. Pulse waves generated from pulsatile hemodynamics of the cardiac cycle travel down the large conduit arteries to the mid-sized arteries where they incur increased resistance due to branch points and increased arterial tone. The incident waves are then reflected back toward the central arteries from the periphery. The stiffness of the central conduit arteries determines the velocity with which the reflected waves return, with increased AoS resulting in more rapid propagation of reflected waves, determining the measured pulse wave velocity (PWV) (1). Pathologically increased AoS allows waves reflected from the periphery to return in phase with cardiac systole, augmenting central systolic pressure and increasing hemodynamic load on the left ventricle. AoS is able to capture a unique measure of central hemodynamics not reflected by

simply the blood pressure alone, likely explaining the ability of carotid-femoral PWV (cfPWV) to serve as an independent predictor of cardiovascular outcomes. Further, the processes implicated in AoS, which include activation of oxidative stress pathways and inflammation may be reflective of underlying vascular risk (2).

The purpose of this review is to discuss the clinical implications of AoS, its measurements including PWV and augmentation index (AI), and the factors that contribute to and alter AoS. We will also review AoS involvement in disease processes as well as biomarkers involved in AoS. The goal is to gain a better understanding of AoS as a subclinical marker of chronic disease.

CLINICAL SIGNIFICANCE

Stiffening of the aorta is a marker of subclinical disease and has been demonstrated to precede the onset of hypertension in a longitudinally followed cohort (3). Earlier studies first implicated elevated PWV to be associated with atherosclerosis (4) and as a predictor of worse cardiovascular outcomes and mortality in high-risk conditions such as diabetes mellitus (DM), chronic kidney disease, and hypertension, as well as coronary artery disease post-myocardial infarction (5–7). AoS was later demonstrated in healthy community dwelling individuals to predict incident events including coronary disease, heart failure, stroke, and cardiovascular mortality independently of adjustment for cardiovascular risk factors (8–11). Further, there is evidence that AoS reflects the presence of composite end-organ damage and has been shown to have superior prognostic value to measurements of office and ambulatory systolic blood pressures in patients with advanced kidney disease (12).

The adverse outcomes related to elevated AoS suggested by the prior studies have been corroborated and further evaluated through meta-analyses. In such a 2010 study by Vlachopoulos et al. an increase in PWV of 1 m/s conferred an increased risk of cardiovascular events, cardiovascular mortality, and all-cause mortality (13). Moreover, a meta-analysis of over 17,000 participants showed that a 1-standard deviation difference in log-transformed cfPWV was associated with an increased risk of future cardiovascular events over 5 years even after adjusting for more traditional risk factors; furthermore, this same meta-analysis showed that using cfPWV in addition to traditional risk factors was able to reclassify patient risk for cardiovascular disease (CVD) for those who had an intermediate 10 year CVD risk (14). Therefore, by measuring AoS in patients, practitioners may be able to detect patients at risk for CVD at an early, subclinical stage. This early detection may provide the opportunity for early intervention, patient education on risk factors, and potentially help to decrease the incidence of overt disease.

MEASUREMENT

Several modalities are available to measure AoS by PWV including recording the pulse waves by a tonometer transducer, standard blood pressure cuff, doppler ultrasound, and magnetic resonance imaging (MRI) (15). The transducer methods consist of placing a tonometer over the carotid and femoral arteries and monitoring an ECG signal for timing of the pressure waveforms. These methods have historically been the gold standard but can be a challenging learning curve for the operator. Thus, there has been increased interest in comparing the various AoS measurement methods to determine which is most accurate and easiest to implement. Pulse wave doppler ultrasound allows measurement of AoS without the need for a specific measurement device, is quicker, and has been shown to be comparable to transducer methods (16, 17). While blood pressure cuff measured cfPWV may be easier to acquire than the doppler approach, it often requires correction (18). MRI based techniques also offer promise due to their ability to directly and accurately visualize path-length and ability to quantify AoS in more proximal aortic segments but lack practicality (19).

cfPWV is the gold standard measure of aortic wall stiffness (2). cfPWV is obtained via transcutaneous measurement of the pressure waveform at the common carotid artery and at the femoral artery by either probes or blood pressure cuffs; alternatively, this can be measured from Doppler or MRI flow waveforms (20). The distance between the two surface sites and the time delay between the waveforms is used to determine the velocity component (2). **Figure 1** depicts how the cfPWV is calculated. It is important to note that blood pressure and PWV are closely intertwined with higher mean arterial pressures correlated with increased AoS (15, 22).

However, there are additional challenges to measuring cfPWV. The surface distance between carotid and femoral sites of measurement may not represent true arterial path-length, especially in patients with obesity. Therefore, proposed correction factor equations account for these systematic inaccuracies such as multiplying the distance from the carotid artery to the femoral artery by 0.8 (23). In addition, there are challenges with measuring pressure waveforms in obese patients and in controlling for existing atherosclerotic disease in vessels. Furthermore, conditions during time of measurements such as patient positioning, temperature in the room, and white coat hypertension can all confound the results (2). Brachial PWV methods also exist, but because of PWV amplification in peripheral arteries, it is considered a less reliable measure of central artery stiffness (24).

Augmentation index (AI) is another measurement of AoS (**Figure 1**). It is measured by dividing the augmentation pressure by the pulse pressure and multiplying by 100 to provide a number (percentage). AI is a stronger predictor of left ventricular mass reduction in response to lowering the blood pressure compared to other more conventional measures such as brachial blood pressure (25), and increased AI is independently associated with increased cardiovascular events in those undergoing percutaneous coronary interventions (26). Furthermore, more recent data has shown that higher augmentation index is associated with poor exercise capacity after heart transplant (27). However, AI is impacted by other factors such as age, systolic blood pressure, heart rate, left ventricular ejection time, and height to a greater extent than PWV (28, 29). Therefore, PWV, and in particular cfPWV, is used more often in trials.

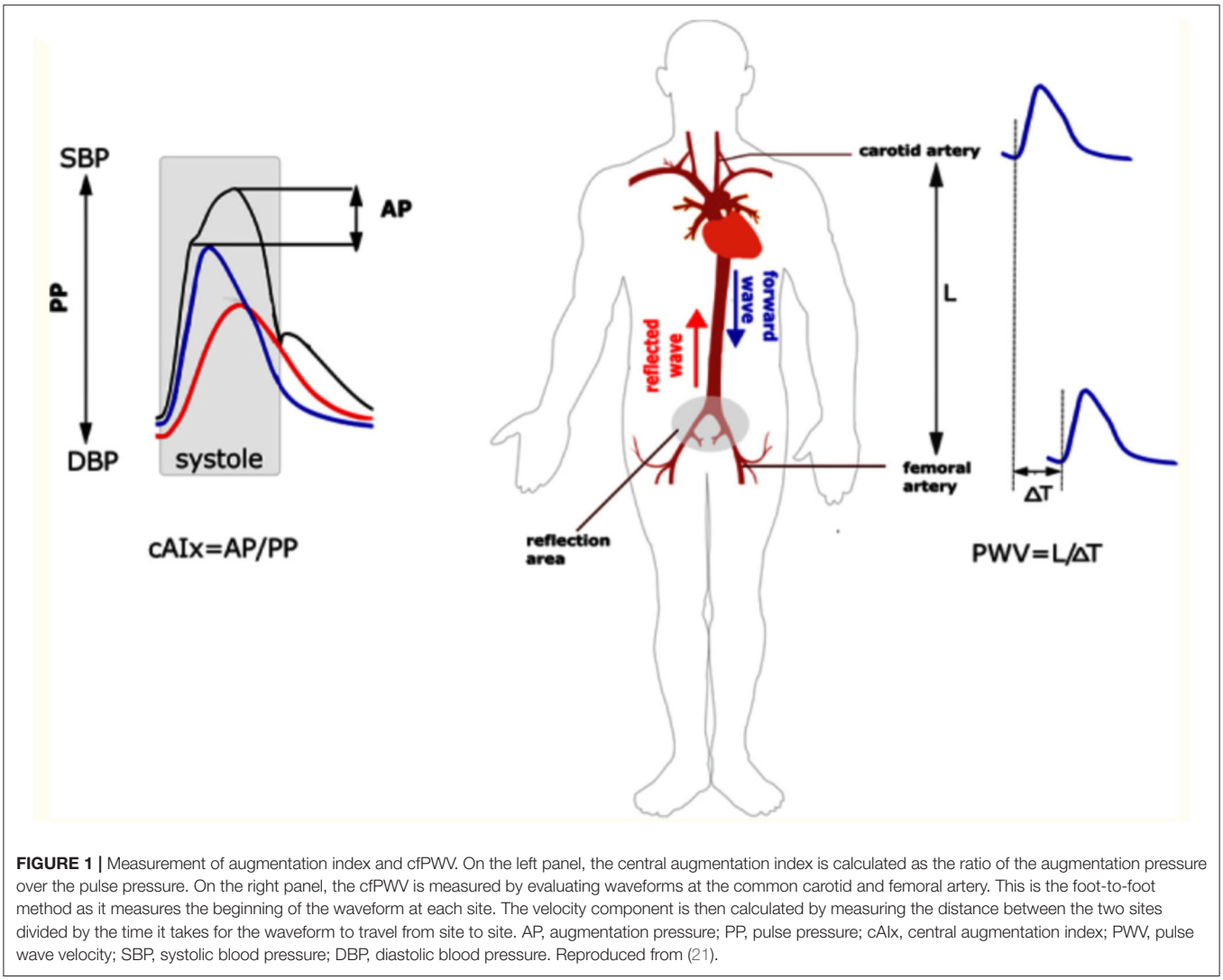

FIGURE 1 | Measurement of augmentation index and cfPWV. On the left panel, the central augmentation index is calculated as the ratio of the augmentation pressure over the pulse pressure. On the right panel, the cfPWV is measured by evaluating waveforms at the common carotid and femoral artery. This is the foot-to-foot method as it measures the beginning of the waveform at each site. The velocity component is then calculated by measuring the distance between the two sites divided by the time it takes for the waveform to travel from site to site. AP, augmentation pressure; PP, pulse pressure; cAIx, central augmentation index; PWV, pulse wave velocity; SBP, systolic blood pressure; DBP, diastolic blood pressure. Reproduced from (21).

NORMATIVE VALUES AND IMPACT OF DEMOGRAPHICS

Despite having known prognostic implications distinct from traditional cardiovascular risk factors, the clinical use of cfPWV has been limited due to lack of widespread use of population specific reference ranges. The 2007 ESC/ESH guidelines proposed a cut-off value of 12 m/s for elevated AoS based on clinical outcome data (30). Furthermore, multiple studies have sought to establish reference ranges for PWV. The Reference Values for Arterial Stiffness Collaboration Database was one of the first large-scale efforts to establish reference ranges for cfPWV in 16,867 European individuals across 13 centers (31). A subset of 11,092 individuals without prevalent CVD or use of anti-hypertensive or lipid-lowering medications were used to draw reference values presented in **Table 1**. However, a challenge with creating normative values is that experienced laboratories are needed for cfPWV measurement, and disparate measurement devices and methodologies can produce a variance in PWV affecting generalizability even within the same patient (32).

AGE, SEX, AND RACE

Age

A rise in AoS with age has been well-described in large, diverse groups free of clinical CVD (31, 33–35). Central artery stiffness results in a reduced arterial reservoir effect, augmenting pressure during systole and diminishing it during diastole (36). This is thought to be one mechanism for the observed age-related increase in systolic blood pressure and decline in diastolic blood pressure, which lead to adverse ventricular and vascular hemodynamics, poor cardiac perfusion, and cardiac remodeling (37, 38).

Several mechanisms may contribute to age-related arteriosclerosis. Intrinsic remodeling of arteries has been demonstrated with increasing intima media thickness with age (39). Changes in the mechanical properties of the vascular

TABLE 1 | Distribution of pulse wave velocity (PWV) values (m/s) in the reference value population (11,092 subject) according to age and blood pressure category.

Age category (years)	Blood pressure category				
	Optimal	Normal	High Normal	Grade I HTN	Grade II/III HTN
PWV as mean (±2SD)					
<30	6.1 (4.6–7.5)	6.6 (4.9–8.2)	6.8 (5.1–8.5)	7.4 (4.6–10.1)	7.7 (4.4–11.0)
30–39	6.6 (4.4–8.9)	6.8 (4.2–9.4)	7.1 (4.5–9.7)	7.3 (4.0–10.7)	8.2 (3.3–13.0)
40–49	7.0 (4.5–9.6)	7.5 (5.1–10.0)	7.9 (5.2–10.7)	8.6 (5.1–12.0)	9.8 (3.8–15.7)
50–59	7.6 (4.8–10.5)	8.4 (5.1–11.7)	8.8 (4.8–12.8)	9.6 (4.9–14.3)	10.5 (4.1–16.8)
60–69	9.1 (5.2–12.9)	9.7 (5.7–13.6)	10.3 (5.5–15.1)	11.1 (6.1–16.2)	12.2 (5.7–18.6)
≥70	10.4 (5.2–15.6)	11.7 (6.0–17.5)	11.8 (5.7–17.9)	12.9 (6.9–18.9)	14.0 (7.4–20.6)
PWV as median (10th−90th percentile)					
<30	6.0 (5.2–7.0)	6.4 (5.7–7.5)	6.7 (5.8–7.9)	7.2 (5.7–9.3)	7.6 (5.9–9.9)
30–39	6.5 (5.4–7.9)	6.7 (5.3–8.2)	7.0 (5.5–8.8)	7.2 (5.5–9.3)	7.6 (5.8–11.2)
40–49	6.8 (5.8–8.5)	7.4 (5.3–8.2)	7.7 (6.5–9.5)	8.1 (6.8–10.8)	9.2 (7.1–13.2)
50–59	7.5 (6.2–9.2)	8.1 (6.7–10.4)	8.4 (7.0–11.3)	9.2 (7.2–12.5)	9.7 (7.4–14.9)
60–69	8.7 (7.0–11.4)	9.3 (7.6–12.2)	9.8 (7.9–13.2)	10.7 (8.4–14.1)	12.0 (8.5–16.5)
≥70	10.1 (7.6–13.8)	11.1 (8.6–15.5)	11.2 (8.6–15.8)	12.7 (9.3–16.7)	13.5 (10.3–18.2)

Modified from Reference Values for Arterial Stiffness (31).
HTN, hypertension; SD, standard deviation.

media are also observed, with maladaptive remodeling with increased deposition of collagen (40). Age related arteriosclerosis that is independent of atherosclerosis is supported by the strong independent association between age and cfPWV that persists in those without aortic calcifications (41). The cumulative exposure to vascular risk factors including DM also contributes to increases in AoS with age (42).

Sex

The relationship between sex and AoS is complex and varies with age. Whereas pre-pubescent females have higher PWV than pre-pubescent males, this difference is abrogated post-puberty as the average PWV in females decreases but PWV in males increases (43). In the Jackson Heart Study, while adult men were more likely to have elevated cfPWV in the overall cohort, women had steeper rise in both cfPWV and forward wave amplitude with age >60 (35). Brachial-ankle PWV (baPWV) has been shown to be similar in males and females until about age 50–60 years old, at which point there is a greater proportional increase in female baPWV (44). This accelerated increase in the baPWV around age 50–60, when females are post-menopausal, provides further evidence that there is a hormonal component to the sex differences in AoS. Furthermore, when corrected for age and blood pressure, middle aged females with metabolic syndrome had higher aortic PWV as compared to males, again supporting the role of sex the relationship of age with PWV (45).

The mechanism behind sex differences in AoS may be related to downstream effects of sex hormones. Men with acquired hypogonadism have higher PWV compared to normal men, and treatment with testosterone therapy helps to lower PWV, supporting a possible role for testosterone in lowering AoS (46). Indeed, in animal models, testosterone induces endothelium-independent vasodilation of arterial beds (47). Sex hormones in women also seem to play roles in modulating AoS. Decreases in estradiol with menopause are associated with a proinflammatory state, which may be a cause of elevated AoS in women after menopause (48). Furthermore, female sex steroids such as 17 beta estradiol and progesterone promote elastin deposition, and thus withdrawal following menopause may also contribute to increased AoS during this time period (49).

Race

African Americans (AA) suffer a disproportionately increased risk of CVD, hypertension, and microvascular dysfunction compared to whites, highlighting the disparities in vascular morbidity and mortality (50–52). Data suggests that these differences may be driven by a difference in risk factor burden, sociodemographic factors including income, as well as intrinsic differences in mechanical properties of blood vessels and baseline AoS (53).

Differences in AoS between AA and whites have been observed in childhood. AA boys as young as 6–8 years old have elevated mean arterial pressure (MAP), intimal media thickness, and cfPWV compared to white boys (54). Sociodemographic factors including education, lower family income, and lower socioeconomic status were all associated with higher PWV (55). However, higher aortic PWV is seen in AA children compared to whites even after adjusting for age, sex, body mass index, mean arterial pressure, and socioeconomic status (56). This difference in AoS among children persists in adults. In the Multi-Ethnic Study of Atherosclerosis of multiple community cohorts, AA had a higher

prevalence of hypertension and lower aortic distensibility (57). In the Dallas Heart Study, both AA and Hispanic individuals had greater aortic arch PWV independent of cardiovascular risk factors including mean arterial pressure, heart rate, DM, and smoking (58).

However, other studies suggest that there may be confounding variables that account for the differences in AoS among races. In the ELSA-Brasil study, investigators noted that AAs had a higher burden of hypertension, DM, and obesity compared to the other racial groups and had higher unadjusted cfPWV compared to browns and whites who were similar. However, after adjusting for characteristics including mean arterial pressure, age, waist circumference, heart rate, and fasting glucose, the inter-group differences were abrogated. The results of this study indicate that ∼40% of the difference between cfPWV values could be explained by age and mean arterial pressure, suggesting less contribution by race itself to AoS. Though there may be a race-sex interaction in women, with AA and brown women having higher cfPWV than whites particularly in the highest quartiles of cfPWV, the strength of that relationship was much weaker than the effects of MAP and age (59).

Several mechanisms have been proposed to contribute to the differences of AoS among racial/ethnic groups. First, risk factor sensitivity may vary among different racial groups. For example, cfPWV progression is affected by risk factors such as diastolic blood pressure, glucose, and low-density lipoprotein cholesterol in AA women, while it was not in Caucasian women (60). Furthermore, it has been demonstrated that AAs living in the northern hemisphere likely suffer a greater burden of Vitamin D deficiency relative to white counterparts (61). Vitamin D has been proposed to improve vascular health by suppressing oxidative pathways and the sensitivity to renin-angiotensin-aldosterone system (RAAS) mediated remodeling. Vitamin D supplementation has been shown to decrease PWV in AAs with vitamin D deficiency (62). While the paucity of large-scale studies suggests the need for further research to determine the clinical utility of improving Vitamin D to improve vascular health, this modifiable risk factor creates a targetable treatment regimen for AAs.

Generalized endothelial dysfunction has also been posited as a mediator of progressive AoS in AAs compared to whites. Studies have demonstrated that AAs tend to have impaired nitric oxide signaling and thus more endothelial cell dysfunction at baseline and when compared to whites (63, 64). This impaired nitric oxide signaling in AAs compared to white Americans has been shown to be present even after adjusting for CVD risk factors, suggesting that impaired vascular function precedes incident disease (65). Whether additional intrinsic differences in the properties of vessels or unmeasured risk factors exist between racial/ethnic groups remains to be determined.

COMORBIDITIES ASSOCIATED WITH AoS

Hypertension

Hypertension demonstrates a very strong association with AoS compared to other cardiometabolic risk factors studied. A major shift has occurred regarding the understanding of directionality between hypertension on AoS and vice versa. The initial paradigm posited that arterial stress induced by elevated pressure and pulsatility-mediated breaks in elastin led to maladaptive remodeling by inducing inflammation (1, 66, 67). Both baseline blood pressure and blood pressure variability have been linked to increased vascular stiffness (68). Higher blood pressure variability is thought to promote vascular smooth muscle cell proliferation and atherosclerosis as well as increase oscillatory wall stress (69, 70). This increased variability may lead to increased AoS which in turn, with stiffer arteries, may increase blood pressure (71).

Clinical and experimental studies have demonstrated that the relationship between hypertension and AoS is interdependent (72–74). Elevated AoS preceding the development of overt hypertension has been demonstrated in population-based studies (3, 75). Additionally, Weisbrod et al. evaluated the temporal relationship between AoS and hypertension in a mouse model of diet induced obesity, demonstrating that AoS increased within 1 month while hypertension evolved in 5 months (76). Increased AoS and blood pressure were reversed with weight loss. Understanding this temporal relationship is of particular clinical significance, as AoS can be used as a marker for patients that are high risk to develop hypertension, prompting earlier risk factor modification and potential treatment.

Metabolic Syndrome

While hypertension alone can increase AoS, metabolic syndrome is also associated with increased AoS. Metabolic syndrome is a constellation of disorders consisting of obesity, insulin resistance, hypertension, and dyslipidemia. Investigators from the Bogalusa Heart Study showed that even in asymptomatic, young (ages 24–44) subjects, baPWV rose with increasing number of components of the metabolic syndrome (77). Multiple other studies have shown that metabolic syndrome components were associated with elevated PWV (78–80). Investigators of the CRAVE study also showed that patients with both hypertension and dyslipidemia had a four-fold increase in the annual progression of cfPWV compared to controls (80). There is also evidence to suggest that resolving metabolic syndrome is associated with lower PWV compared to those with current metabolic syndrome (81).

Diabetes Mellitus

Patients with DM are at a high risk for CVD (82, 83). Aortic PWV serves as an additional tool to help risk stratify patients as increased PWV has been shown to be associated with CVD in those with DM (84). An interesting dose dependent relationship between level of glucose dysregulation and elevation of cfPWV has also been described (85).

The pathogenesis of AoS in DM is likely to be mediated by the pro-inflammatory milieu generated by metabolic dysregulation and direct damage to the vascular wall. For example, high intake of advanced end glycation products, such as carboxy-methyl-lysine, have been associated with higher PWVs among those with DM (86). Furthermore, a trial of ALT-711, a non-enzymatic breaker of these products, decreased PWV in the elderly (87). Different genotypes of advanced end glycation products and their

TABLE 2 | Association of lifestyle risk factors with aortic stiffness.

	Population studied	Exposure	Effect
Diet	Adults 20–59 years of age	Salt consumption (varied)	An increase in urinary sodium excretion by >100 mmol over a 24-h period is associated with increased systolic pressures by 3–6 mm Hg and increased diastolic pressures by 0–3 mm Hg (90)
	11 adults aged 60 ± 2 years with elevated BP (139 ± 2 over 83±2 mmHg)	Low sodium (77 ± 2 mmol/d) vs. normal sodium (144 ± 7 mmol/d)	Low sodium group with 17% reduction in aortic PWV compared to normal sodium (7 ± 0.40 vs. 8.43 ± 0.36 m/s, $p = 0.001$) (91)
Exercise	Endurance trained males age 69 ± 2.5 years	Fitness level: VO2 max at least 1 SD above age matched sedentary counterparts	26% decrease in Aortic PWV relative to peers their age (92)
	Pre-menopausal women aged 31 ± 1 years and post-menopausal women age 59±2 years	6 ± 1 hour/week of endurance exercise	No significant difference in aortic PWV or AI between pre and post-menopausal women with exercise (suggesting age related increase in AoS is halted by exercise) (93)
	Systematic review/meta-analysis of 14 RCTs of adults with pre-hypertension and hypertension	Exercise types: aerobic/endurance, dynamic resistance, isometric resistance, combined exercise	Exercise significantly reduced PWV by 0.76 m/s (CI 1.05–0.47) (94)
Smoking	Healthy adults 33 ± 6 years of age	Acute: 5 min after smoking 1 cigarette	FMD % decreased from 13.5 ± 5 to 6.9 ± 4% (95)
	Adults 15–57 years of age	Chronic: 1–75 pack years	FMD 10±3.3% (4–22%) in controls vs. 4 ± 3.9% (0–17%) in smokers; FMD is inversely related to the duration of smoking (96)
	Males 30–64 years of age	Non-smokers, former smokers, and current smokers	Men who quit smoking <1 year prior had elevated AI (β 3.94, SE 1.54, $p = 0.011$) similar to current smokers (β 4.39, SE 0.74, $p < 0.001$) compared to non-smokers; those that quit 1– <10 years prior with AI similar to non-smokers (β 1.87, SE 0.94, $p < 0.047$) (97)
E-cigarettes	Adults 30 ± 8 years of age	5 min of usage and 30 min of usage	Smoking over 5 min increased cfPWV by 0.19 m/s after 15 min; over 30 min increased cfPWV by 0.36 m/s (98)
Alcohol	Males 40–80 years of age	4–10, 11–21, and 22–58 drinks/week	Compared to those consuming 0–3 drinks per week; decreased cfPWV by 0.77 m/s (4–10 drinks), 0.57 m/s (11–21 drinks), 0.14 m/s (22–58 drinks) (99)
	Post-menopausal women 50–74 years of age	1–3, 4–9, 10–14, and 15–35 drinks/week	Compared to non-drinkers: those consuming 1–3, 4–9, 10–14, and 15–35 drinks/week had the following difference in mean cfPWV 0.044 (95% CI −0.47–0.56), −0.085 (95% CI −0.59–0.43), −0.869 (95% CI −1.44–0.29), and −0.225 (95% CI −0.98–0.53) m/s (100)

AI, augmentation index; AoS, aortic stiffness; β, beta; BP, blood pressure; cfPWV, carotid-femoral pulse wave velocity; FMD, flow-mediated dilation; PWV, pulse wave velocity; RCT; randomized control trial; SD, standard deviation; SE, standard error.

receptors have also been associated with increased blood pressure and AoS in patients with DM (88). Therefore, modulation of advanced end glycation products remains an interesting target to halt disease progression. Furthermore, increased glucose may lead to increased activity of RAAS and thus the detrimental consequences as described in the section on RAAS below (89).

LIFESTYLE RISK FACTORS

The association of lifestyle risk factors with AoS detailed below are summarized in **Table 2**.

Alcohol

Much of the evidence for the association of alcohol with AoS is data derived from self-reported alcohol consumption in cross-sectional epidemiology studies. Interestingly, evidence suggests there may be a J shaped relationship of alcohol use to central aortic hemodynamics, with more favorable measures among those with light to moderate consumption compared with negligible and heavy drinkers. In young individuals, those who reported light alcohol consumption, 2–6 drinks per week, had lower central blood pressure than those who drank lower or greater amounts (101). Similar findings have been reported in middle aged to older adults. In men aged 40–80 years old, those who drank moderate to large amounts of 4–10 and 11–21 drinks per week had lower PWV than those who drank more or less than these groups (99). Additionally, in post-menopausal women aged 50–74 years, moderate alcohol intake was inversely related to PWV (100). Furthermore, in controlled experiments, alcohol ingestion appears to acutely decrease AoS. Even drinking 200 or 350 cc of beer leads to decreased baPWV and cfPWV compared to controls (102). There are many proposed mechanisms as to why low doses of alcohol can be beneficial

to the heart such as by increasing HDL, insulin sensitivity, and decreasing oxidative stress (103). More acutely, small amounts of alcohol may decrease PWV through alcohol induced increases in nitric oxide (104). Ultimately, future prospective studies will shed light on the ideal alcohol consumption with respect to long-term outcomes and recommended exposure for vascular health.

Smoking

Smoking is a major modifiable risk factor for CVD (105). One cigarette causes acute increases in brachial and aortic blood pressure, arterial wave reflection, and AoS (106). Even passive smoking has been shown to worsen the elasticity of the aorta (107). Cigarette smoking has been shown to have a dose-response relationship to elevated PWV, which is only reversed after prolonged smoking cessation >10 years (108). There is also evidence to suggest that e-cigarettes are detrimental to AoS (98). The effect of cigarettes on AoS may be due to endothelial cell damage and subsequent impaired vasodilatory capacity (95, 96). Additional mechanisms appear to be an increase in cholesterol, increased vascular remodeling and arterial calcification, increased vascular tone, and oxidative stress/inflammation (109).

Diet and Physical Activity

There is a growing body of evidence that lifestyle habits including smoking cessation, diet modification, and exercise/weight loss can reverse AoS (110). It is well-supported that high salt intake leads to higher blood pressures (90) and that reduction in salt intake leads to lower blood pressures (111). Low salt diets similarly have been associated with lower PWV independent of blood pressure (112). Furthermore, in men, over a period of 17.8 years, higher consumption of saturated fatty acids was associated with higher cfPWV and higher consumption of poly-unsaturated fatty acids was associated with lower cfPWV (113). Greater dairy consumption, particularly in those with DM, as well as increased intake of vegetables has also been associated with lower AoS (114–116).

Physical activity leads to lower central PWV and age-related increases in PWV can be mitigated by exercise in both men and women (92, 93). The Baltimore Longitudinal Study of Aging rigorously phenotyped adults and measured VO2 max in adults aged 21–96 years of age. These investigators demonstrated that with greater age in the entire cohort, augmentation index and aortic PWV increased out of proportion to the blood pressure increase. However, these measures of AoS were lower in endurance trained male athletes (defined by a VO2 max 1 standard deviation above their age matched non-trained controls), compared with sedentary individuals (defined as less than at least 20 min of aerobic exercise three times weekly) of similar age (92). Similarly, while sedentary post-menopausal women have higher augmentation index and PWV than comparable pre-menopausal women, these measures of AoS were similar in both pre- and post-menopausal active women who were physically active (performed endurance training, actively competing in running races, with average exercise of 6 +/– 1 hour of activity per week) (93). The effect of exercise on reducing AoS is thought to relate to exercise induced changes in vessel wall stress, a reduction in vasoconstrictors and ultimately vasodilation via increased nitric oxide activity (117, 118). These studies add to the growing body of evidence that improved lifestyle modifications could make a large impact on the development and progression of disease.

BIOMARKERS ILLUMINATING PATHOPHYSIOLOGY AND THERAPEUTICS

Given the association of AoS with adverse outcomes, serum biomarkers that correlate with AoS allow further insight into mechanisms of AoS, non-invasive detection and monitoring of AoS, and may highlight therapeutic targets. In this section, we will discuss key serum biomarkers that modulate AoS, and the associated evidence for therapies targeting these pathways.

Inflammatory Biomarkers

The presence of chronic inflammatory and infectious conditions is associated with elevated AoS. In patients with systemic lupus erythematosus, cfPWV was shown to be elevated even when traditional risk stratification categorized patients into low risk for CVD (119). Furthermore, higher aortic PWV has been seen in patients with inflammatory bowel disease and has been associated with disease duration (120). Many other inflammatory conditions have been associated with increased AoS such as rheumatoid arthritis (121, 122), psoriatic arthritis (123, 124), and Sjogren's syndrome (125, 126). The increase in AoS in those with autoimmune disorders and chronic inflammatory diseases is independent of more traditional risk factors and related to disease duration and the elevation in inflammatory markers, suggesting inflammation as a key player in this pathology (127).

Multiple inflammatory biomarkers have been associated with AoS. A prospective study that followed middle-aged Japanese men without hypertension for 9 years demonstrated that sustained elevations in serum C-reactive protein (CRP) were associated with a longitudinal increase in baPWV. Higher baPWV was in turn associated with higher blood pressures during follow-up (128). The accelerated vascular disease in this cohort at relatively low vascular risk suggests that chronic inflammation may contribute to progressive vascular stiffness and dysfunction. Though CRP is associated with several cardiovascular risk factors, models adjusting for these demonstrated a persistent linear association between CRP and AoS in the population-based Rotterdam Study (129). A potential mechanism may lie in endothelial dysfunction: in men with coronary artery disease with forearm blood flow response studied with venous occlusion plethysmography, CRP levels were associated with blunted endothelial vasodilator capacity in models including risk factors (130). Additionally, normalization of CRP levels was associated with improved blood flow response in these individuals. IL-6 is another inflammatory cytokine that has been shown to be associated with cfPWV in individuals with hypertension (131). Furthermore, there is research establishing a link between polymorphisms on IL-6 with increased cfPWV (132). These studies suggest that inflammation is associated

with AoS but more studies are needed to fully elucidate the mechanistic relationships.

The relationship between inflammatory states and CVD has been further elucidated by studies that have examined the effect of treatment of inflammatory diseases. Patients with rheumatoid arthritis treated with anti-tumor necrosis factor-a agents have shown significant declines in cfPWV after treatment (133). Furthermore, statins have been shown to decrease AoS in patients with inflammatory joint diseases, suggesting that controlling inflammation and possibly lowering lipids is beneficial in this population (134).

Klotho and Sirtuin-1

Klotho is predominantly expressed in the kidney and has been described as an anti-aging gene (135). When mice are deficient in Klotho, they have decreased lifespan and calcifications of multiple organs. Haplodeficiency of Klotho in mice leads to increased PWV and hypertension (136, 137). The association of Klotho levels with AoS has also been demonstrated in patients with chronic kidney disease (CKD) (138). Klotho appears to directly regulate SIRT1, a gene encoding a NAD+ dependent-deacetylase with anti-inflammatory and anti-oxidant effects and importance in endothelial cell function (139, 140). Klotho

TABLE 3 | Association of serum biomarkers with aortic stiffness.

Biomarker	Clinical relevance	Association with aortic stiffness
Key biomarkers with independent association with AoS		
Inflammatory biomarkers	• The presence of conditions like SLE (155), IBD (156), psoriasis (157), and HIV (158) are linked with high higher risk of CVD	• Elevated PWV in IBD patients (120) • Elevated carotid AI and PWV in SLE patients (159)
CRP	• Associated with insulin resistance (160), carotid intima-media thickness and markers of atherosclerosis (161)	• Sustained elevation in serum CRP correlated with increased baPWV and BP in middle aged Japanese men (128) • In Chinese general population baseline hs-CRP associated with baPWV (162)
Klotho	• Klotho levels lower in those with renovascular hypertension and essential hypertension compared to healthy controls (163) • Klotho levels lower in those with significant coronary artery disease (164)	• Haplodeficiency in Klotho in mice led to increased AoS (136, 137)
Aldosterone	• Increases insulin resistance, oxidative stress, inflammation (89) • Promotes vascular calcification (165)	• Associated with increased PWV (143) • Fibronectin accumulation (166)
Other biomarkers associated with AoS		
Adipocyte-Fatty-Acid-Binding protein (A-FABP)	• Elevated levels have been associated with endothelial dysfunction in patients with type 2 diabetes (167) • Elevated levels associated with diastolic dysfunction (168) and cardiovascular death (169)	• In patients with hypertension and metabolic syndrome, increased levels of A-FABP associated with increased cfPWV (170) • A-FABP levels positively correlated with cfPWV in patients with type 2 diabetes (171)
Leptin	• Leptin levels predicted ischemic heart disease in patients with type 2 diabetes (172) • Patients with coronary artery disease have higher levels of serum leptin (173)	• Higher leptin levels associated with increased cfPWV in patients with kidney transplants (174) and in geriatric patients on dialysis (175) • Meta-analysis demonstrated leptin is positively associated with cfPWV (176)
Natriuretic peptides	• Released in response to ventricular hypertrophy, inflammation, and fibrosis (177) • Predictor for heart failure or death in patients with an acute MI (178, 179)	• AoS is associated with NT-proBNP level and MR-proANP months after MI (180, 181)
Parathyroid hormone	• Parathyroid hormone is associated with atherosclerosis (182)	• Patients with mild hyperparathyroidism had increased cfPWV which then decreased after a thyroidectomy (183) • cfPWV increased independently with parathyroid hormone in Chinese patients with untreated hypertension (184)
Resistin	• Increased resistin associated with increased risk of heart failure, coronary heart disease, CVD (185)	• High levels of resistin associated with increased cfPWV in sample with high prevalence of untreated hypertension/obesity (186) • Serum resistin is an independent predictor of cfPWV in patients with coronary artery disease (187)
Uric Acid	• High levels of uric acid associated with acute myocardial infarction (188) cardiovascular events (189, 190) stroke (190)	• Association between higher uric acid and cfPWV in men after adjustment for confounders (191) • Overall positive association between uric acid and cfPWV at adjusted analysis in both males and females (192) • Serum uric acid is independently associated with cfPWV in post-menopausal women (193) • Significant association between uric acid cf PWV and carotid radial PWV in young Caucasian population (194)

AI, augmentation index; AoS, aortic stiffness; ba-PWV, brachial-ankle pulse wave velocity; CVD, cardiovascular disease; HIV, human immunodeficiency virus; hs-CRP, high sensitivity CRP; IBD, Inflammatory Bowel Disease; MI, myocardial infarction; PWV, pulse wave velocity; SLE, Systemic lupus erythematosus.

haplodeficiency downregulates SIRT1 in arterial endothelial and smooth muscle cells, with associated increased arterial wall collagen deposition and elastin fragmentation, both of which explain the association with AoS (137). Zhou et al. demonstrated that CYP11B2, a rate-limiting enzyme in aldosterone synthesis, is up-regulated in Klotho deficiency, and that treatment with eplerenone reversed increased AoS (141). Thus, another mechanism by which Klotho deficiency may mediate increased AoS is through the aldosterone pathway.

The interaction between Klotho and SIRT1 has illuminated a number of possible targets for therapies that modulate pro-oxidant and pro-inflammatory pathways. Further, improved calcium and phosphate homeostasis may be of increased importance in CKD patients where impaired calcium homeostasis and a pro-inflammatory milieu may accelerate vascular dysfunction. Thus, understanding these mechanisms provides opportunities for possible therapeutic interventions.

RAAS

The role of RAAS in the progression of AoS is supported by observational studies, clinical studies relating to modulation with therapeutics, biochemical studies demonstrating involvement in vascular remodeling, and mapping of related gene loci.

RAAS-associated AoS is proposed to be due to aldosterone and angiotensin II increased inflammation as well as vasoconstriction from activation of angiotensin I receptors and mineralocorticoid receptors (142). Aldosterone has been shown to be involved in many pathologic processes such as increased insulin resistance, increased oxidative stress, and increased inflammation (89). In multivariable adjusted models, serum aldosterone is linearly associated with PWV in hypertensive patients (143). The importance of RAAS is further highlighted by multiple studies that demonstrate a positive association between cfPWV and polymorphisms in the angiotensin II type 1 receptor (144, 145), angiotensin converting enzyme gene (146, 147) as well as in the aldosterone gene (148). Polymorphisms in RAAS may thus contribute to the highly heritable traits of AoS and blood pressure (149). Additional future work may determine the appropriate application of genetic testing to guide detection and management of AoS.

With respect to therapies, inhibiting aldosterone with spironolactone has been shown to decrease collagen density and thus AoS (150). London et al. demonstrated that central systolic blood pressure was decreased to a greater extent with perindopril/indapamide treatment compared to treatment with atenolol, implying a distinct role of RAAS modulation in central hemodynamics (151). This data on the role of RAAS inhibition in AoS may be useful to consider for physicians choosing an anti-hypertensive medication. When compared with atenolol, eplerenone has been shown to decrease AoS, decrease the collagen to elastin ratio, and decrease concentrations of inflammatory markers including MCP-1, basic fibroblast growth factor, and interleukin-10 (152). Furthermore, when comparing atenolol, nebivolol, aliskiren, and quinapril, the RAAS modulating agents demonstrated continued reductions of cfPWV, possibly implicating arterial remodeling rather than modulation of hemodynamics alone (153). Lastly, non-pharmacologic augmentation to the RAAS system is also important to consider. Decreased salt intake has been shown to decrease AoS independent of blood pressure reductions that may be mediated through RAAS modulation (154).

In addition to the above, other general biomarkers associated with AoS are presented in **Table 3**.

GENERALIZABILITY AND FUTURE DIRECTIONS

Despite data illuminating pathways important in AoS pathophysiology and the promising data for their modulation, there has been a paucity of data in this field. Controlled trials thus far have been of relatively small size with short duration, with possibly insufficient follow up time to adequately assess for aortic remodeling and change in AoS (195). However, encouraging data on the prognostic impact of PWV continues to emerge. In the past 2 years, a *post-hoc* analysis of 8,450 patients in the Systolic Blood Pressure Intervention Trial (SPRINT) demonstrated that reductions in PWV after 1 year of anti-hypertensive therapy were associated with 42% lower risk of death compared to individuals who did not have reductions in PWV, independent of Framingham Risk Score and blood pressure (196). Additionally, an innovative experiment performed on mice aortas *ex vivo* used a synthetic peptide targeted to a cytoskeletal protein known to be associated with AoS in human genome wide association studies (197). This study illustrated the proof of concept that such decoy peptides decreased cfPWV, illustrating that approaches targeted to AoS rather than blood pressure *per se*, may be able to be applied in the future. Ultimately, larger therapeutic trials that target AoS and demonstrate improved outcomes are needed to establish widespread clinical utility of AoS assessment and treatment.

CONCLUSION

AoS is a precursor to hypertension and an accepted risk factor for CVD independent of blood pressure. Despite its demonstrated prognostic value, thus far broad clinical applicability has been limited by measurement variation in multiple methodologies illustrated, lack of age and blood pressure specific reference values applicable to all populations, and effective therapeutics targeting AoS. AoS may be addressed indirectly through treating several lifestyle risk factors and associated comorbidities. Continued research will help to add to the illustrated biologic pathways of AoS. In the future, novel approaches and applications of existing drugs to specifically target pathways involved in modulating AoS may provide further support to its broader assessment and treatment to improve cardiovascular outcomes.

AUTHOR CONTRIBUTIONS

RA: drafted manuscript, manuscript editing, and figure copyright permissions. RM: drafted manuscript. CT: manuscript concept and editing. All authors contributed to the article and approved the submitted version.

FUNDING

This work was partially supported by NHLBI R03HL145195 and R01HL155717 (to CT).

ACKNOWLEDGMENTS

We would like to thank Matthew Borinshteyn for his assistance in drafting the tables.

REFERENCES

1. O'Rourke MF, Mancia G. Arterial stiffness. *J Hypertens.* (1999) 17:1065–72. doi: 10.1097/00004872-199917010-00001
2. Laurent S, Cockcroft J, Van Bortel L, Boutouyrie P, Giannattasio C, Hayoz D, et al. Expert consensus document on arterial stiffness: methodological issues and clinical applications. *Eur Heart J.* (2006) 27:2588–605. doi: 10.1093/eurheartj/ehl254
3. Kaess BM, Rong J, Larson MG, Hamburg NM, Vita JA, Levy D, et al. Aortic stiffness, blood pressure progression, incident hypertension. *JAMA.* (2012) 308:875–81. doi: 10.1001/2012.jama.10503
4. van Popele NM, Grobbee DE, Bots ML, Asmar R, Topouchian J, Reneman RS, et al. Association between arterial stiffness and atherosclerosis: the rotterdam study. *Stroke.* (2001) 32:454–60. doi: 10.1161/01.STR.32.2.454
5. Baumann M, Wassertheurer S, Suttmann Y, Burkhardt K, Heemann U. Aortic pulse wave velocity predicts mortality in chronic kidney disease stages 2-4. *J Hypertens.* (2014) 32:899–903. doi: 10.1097/HJH.0000000000000113
6. Feistritzer HJ, Klug G, Reinstadler SJ, Reindl M, Niess L, Nalbach T, et al. prognostic value of aortic stiffness in patients after st-elevation myocardial infarction. *J Am Heart Assoc.* (2017) 6:e005590. doi: 10.1161/JAHA.117.005590
7. Laurent S, Boutouyrie P, Asmar R, Gautier I, Laloux B, Guize L, et al. Aortic stiffness is an independent predictor of all-cause and cardiovascular mortality in hypertensive patients. *Hypertension.* (2001) 37:1236–41. doi: 10.1161/01.HYP.37.5.1236
8. Mitchell GF, Hwang SJ, Vasan RS, Larson MG, Pencina MJ, Hamburg NM, et al. Arterial stiffness and cardiovascular events: the framingham heart study. *Circulation.* (2010) 121:505–11. doi: 10.1161/CIRCULATIONAHA.109.886655
9. Mattace-Raso FU, van der Cammen TJ, Hofman A, van Popele NM, Bos ML, Schalekamp MA, et al. Arterial stiffness and risk of coronary heart disease and stroke: the rotterdam study. *Circulation.* (2006) 113:657–63. doi: 10.1161/CIRCULATIONAHA.105.555235
10. Sutton-Tyrrell K, Najjar SS, Boudreau RM, Venkitachalam L, Kupelian V, Simonsick EM, et al. Elevated aortic pulse wave velocity, a marker of arterial stiffness, predicts cardiovascular events in well-functioning older adults. *Circulation.* (2005) 111:3384–90. doi: 10.1161/CIRCULATIONAHA.104.483628
11. Willum-Hansen T, Staessen JA, Torp-Pedersen C, Rasmussen S, Thijs L, Ibsen H, et al. Prognostic value of aortic pulse wave velocity as index of arterial stiffness in the general population. *Circulation.* (2006) 113:664–70. doi: 10.1161/CIRCULATIONAHA.105.579342
12. Sarafidis PA, Loutradis C, Karpetas A, Tzanis G, Piperidou A, Koutroumpas G, et al. Ambulatory pulse wave velocity is a stronger predictor of cardiovascular events and all-cause mortality than office and ambulatory blood pressure in hemodialysis patients. *Hypertension.* (2017) 70:148–57. doi: 10.1161/HYPERTENSIONAHA.117.09023
13. Vlachopoulos C, Aznaouridis K, Stefanadis C. Prediction of cardiovascular events and all-cause mortality with arterial stiffness: a systematic review and meta-analysis. *J Am Coll Cardiol.* (2010) 55:1318–27. doi: 10.1016/j.jacc.2009.10.061
14. Ben-Shlomo Y, Spears M, Boustred C, May M, Anderson SG, Benjamin EJ, et al. Aortic pulse wave velocity improves cardiovascular event prediction: an individual participant meta-analysis of prospective observational data from 17,635 subjects. *J Am Coll Cardiol.* (2014) 63:636–46. doi: 10.1016/j.jacc.2013.09.063
15. Townsend RR, Wilkinson IB, Schiffrin EL, Avolio AP, Chirinos JA, Cockcroft JR, et al. Recommendations for improving and standardizing vascular research on arterial stiffness: a scientific statement from the American heart association. *Hypertension.* (2015) 66:698–722. doi: 10.1161/HYP.0000000000000033
16. Calabia J, Torguet P, Garcia M, Garcia I, Martin N, Guasch B, et al. Doppler ultrasound in the measurement of pulse wave velocity: agreement with the complior method. *Cardiovasc Ultrasound.* (2011) 9:13. doi: 10.1186/1476-7120-9-13
17. Jiang B, Liu B, McNeill KL, Chowienczyk PJ. Measurement of pulse wave velocity using pulse wave doppler ultrasound: comparison with arterial tonometry. *Ultrasound Med Biol.* (2008) 34:509–12. doi: 10.1016/j.ultrasmedbio.2007.09.008
18. Hickson SS, Butlin M, Broad J, Avolio AP, Wilkinson IB, McEniery CM. Validity and repeatability of the vicorder apparatus: a comparison with the SphygmoCor device. *Hypertens Res.* (2009) 32:1079–85. doi: 10.1038/hr.2009.154
19. Laurent S, Marais L, Boutouyrie P. The noninvasive assessment of vascular AGING. *Can J Cardiol.* (2016) 32:669–79. doi: 10.1016/j.cjca.2016.01.039
20. Wilkinson IB, Mäki-Petäjä KM, Mitchell GF. Uses of arterial stiffness in clinical practice. *Arterioscler Thromb Vasc Biol.* (2020) 40:1063–7. doi: 10.1161/ATVBAHA.120.313130
21. Jeroncic A, Gunjaca G, Mrsic DB, Mudnic I, Brizic I, Polasek O, et al. Normative equations for central augmentation index: assessment of inter-population applicability and how it could be improved. *Sci Rep.* (2016) 6:27016. doi: 10.1038/srep27016
22. Kim EJ, Park CG, Park JS, Suh SY, Choi CU, Kim JW, et al. Relationship between blood pressure parameters and pulse wave velocity in normotensive and hypertensive subjects: invasive study. *J Hum Hypertens.* (2007) 21:141–8. doi: 10.1038/sj.jhh.1002120
23. Van Bortel LM, Laurent S, Boutouyrie P, Chowienczyk P, Cruickshank JK, De Backer T, et al. Expert consensus document on the measurement of aortic stiffness in daily practice using carotid-femoral pulse wave velocity. *J Hypertens.* (2012) 30:445–8. doi: 10.1097/HJH.0b013e32834fa8b0
24. Cavalcante JL, Lima JA, Redheuil A, Al-Mallah MH. Aortic stiffness: current understanding and future directions. *J Am Coll Cardiol.* (2011) 57:1511–22. doi: 10.1016/j.jacc.2010.12.017
25. Hashimoto J, Imai Y, O'Rourke MF. Indices of pulse wave analysis are better predictors of left ventricular mass reduction than cuff pressure. *Am J Hypertens.* (2007) 20:378–84. doi: 10.1016/j.amjhyper.2006.09.019
26. Weber T, Auer J, O'Rourke M F, Kvas E, Lassnig E, Lamm G, et al. Increased arterial wave reflections predict severe cardiovascular events in patients undergoing percutaneous coronary interventions. *Eur Heart J.* (2005) 26:2657–63. doi: 10.1093/eurheartj/ehi504
27. Chun KH, Lee CJ, Oh J, Won C, Lee T, Park S, et al. Increased aortic augmentation index is associated with reduced exercise capacity after heart transplantation. *J Hypertens.* (2020) 38:1777–85. doi: 10.1097/HJH.0000000000002455
28. Sakurai M, Yamakado T, Kurachi H, Kato T, Kuroda K, Ishisu R, et al. The relationship between aortic augmentation index and pulse wave velocity: an invasive study. *J Hypertens.* (2007) 25:391–7. doi: 10.1097/HJH.0b013e3280115b7c
29. Yasmin, Brown MJ. Similarities and differences between augmentation index and pulse wave velocity in the assessment of arterial stiffness. *QJM.* (1999) 92:595–600. doi: 10.1093/qjmed/92.10.595
30. Mancia G, De Backer G, Dominiczak A, Cifkova R, Fagard R, Germano G, et al. 2007 guidelines for the management of arterial hypertension: the task force for the management of arterial hypertension of the European society of hypertension (ESH) and of the European society of cardiology (ESC). *J Hypertens.* (2007) 25:1105–87. doi: 10.1097/HJH.0b013e3281fc975a

31. Reference Values for Arterial Stiffness Collaboration. Determinants of pulse wave velocity in healthy people and in the presence of cardiovascular risk factors: 'establishing normal and reference values'. *Eur Heart J.* (2010) 31:2338–50. doi: 10.1093/eurheartj/ehq165
32. Rajzer MW, Wojciechowska W, Klocek M, Palka I, Brzozowska-Kiszka M, Kawecka-Jaszcz K. Comparison of aortic pulse wave velocity measured by three techniques: complior, SphygmoCor and arteriograph. *J Hypertens.* (2008) 26:2001–7. doi: 10.1097/HJH.0b013e32830a4a25
33. Khoshdel AR, Thakkinstian A, Carney SL, Attia J. Estimation of an age-specific reference interval for pulse wave velocity: a meta-analysis. *J Hypertens.* (2006) 24:1231–7. doi: 10.1097/01.hjh.0000234098.85497.31
34. Mitchell GF, Parise H, Benjamin EJ, Larson MG, Keyes MJ, Vita JA, et al. Changes in arterial stiffness and wave reflection with advancing age in healthy men and women: the framingham heart study. *Hypertension.* (2004) 43:1239–45. doi: 10.1161/01.HYP.0000128420.01881.aa
35. Tsao CW, Washington F, Musani SK, Cooper LL, Tripathi A, Hamburg NM, et al. Clinical correlates of aortic stiffness and wave amplitude in black men and women in the community. *J Am Heart Assoc.* (2018) 7:e008431. doi: 10.1161/JAHA.117.008431
36. Franklin SS, Gustin Wt, Wong ND, Larson MG, Weber MA, Kannel WB, et al. Hemodynamic patterns of age-related changes in blood pressure. The framingham heart study. *Circulation.* (1997) 96:308–15. doi: 10.1161/01.CIR.96.1.308
37. Saba PS, Roman MJ, Pini R, Spitzer M, Ganau A, Devereux RB. Relation of arterial pressure waveform to left ventricular and carotid anatomy in normotensive subjects. *J Am Coll Cardiol.* (1993) 22:1873–80. doi: 10.1016/0735-1097(93)90772-S
38. Cruickshank JM. The role of coronary perfusion pressure. *Euro Heart J.* (1992) 13:39–43. doi: 10.1093/eurheartj/13.suppl_D.39
39. Madhuri V, Chandra S, Jabbar A. Age associated increase in intima media thickness in adults. *Indian J Physiol Pharmacol.* (2010) 54:371–5.
40. Lakatta EG, Levy D. Arterial and cardiac aging: major shareholders in cardiovascular disease enterprises. *Circulation.* (2003) 107:139–46. doi: 10.1161/01.CIR.0000048892.83521.58
41. Tsao CW, Pencina KM, Massaro JM, Benjamin EJ, Levy D, Vasan RS, et al. Cross-sectional relations of arterial stiffness, pressure pulsatility, wave reflection, arterial calcification. *Arterioscler Thromb Vasc Biol.* (2014) 34:2495–500. doi: 10.1161/ATVBAHA.114.303916
42. Loboz-Rudnicka M, Jaroch J, Bociaga Z, Kruszynska E, Ciecierzynska B, Dziuba M, et al. Relationship between vascular age and classic cardiovascular risk factors and arterial stiffness. *Cardiol J.* (2013) 20:394–401. doi: 10.5603/CJ.2013.0098
43. Rossi P, Francès Y, Kingwell BA, Ahimastos AA. Gender differences in artery wall biomechanical properties throughout life. *J Hypertens.* (2011) 29:1023–33. doi: 10.1097/HJH.0b013e328344da5e
44. Tomiyama H, Yamashina A, Arai T, Hirose K, Koji Y, Chikamori T, et al. Influences of age and gender on results of noninvasive brachial-ankle pulse wave velocity measurement–a survey of 12517 subjects. *Atherosclerosis.* (2003) 166:303–9. doi: 10.1016/S0021-9150(02)00332-5
45. Protogerou AD, Blacher J, Aslangul E, Le Jeunne C, Lekakis J, Mavrikakis M, et al. Gender influence on metabolic syndrome's effects on arterial stiffness and pressure wave reflections in treated hypertensive subjects. *Atherosclerosis.* (2007) 193:151–8. doi: 10.1016/j.atherosclerosis.2006.05.046
46. Yaron M, Greenman Y, Rosenfeld JB, Izkhakov E, Limor R, Osher E, et al. Effect of testosterone replacement therapy on arterial stiffness in older hypogonadal men. *Eur J Endocrinol.* (2009) 160:839–46. doi: 10.1530/EJE-09-0052
47. Yue P, Chatterjee K, Beale C, Poole-Wilson PA, Collins P. Testosterone relaxes rabbit coronary arteries and aorta. *Circulation.* (1995) 91:1154–60. doi: 10.1161/01.CIR.91.4.1154
48. Pfeilschifter J, Köditz R, Pfohl M, Schatz H. Changes in proinflammatory cytokine activity after menopause. *Endocr Rev.* (2002) 23:90–119. doi: 10.1210/edrv.23.1.0456
49. Natoli AK, Medley TL, Ahimastos AA, Drew BG, Thearle DJ, Dilley RJ, et al. Sex steroids modulate human aortic smooth muscle cell matrix protein deposition and matrix metalloproteinase expression. *Hypertension.* (2005) 46:1129–34. doi: 10.1161/01.HYP.0000187016.06549.96
50. Muntner P, Lewis CE, Diaz KM, Carson AP, Kim Y, Calhoun D, et al. Racial differences in abnormal ambulatory blood pressure monitoring measures: results from the coronary artery risk development in young adults (CARDIA) study. *Am J Hypertens.* (2015) 28:640–8. doi: 10.1093/ajh/hpu193
51. Heffernan KS, Jae SY, Wilund KR, Woods JA, Fernhall B. Racial differences in central blood pressure and vascular function in young men. *Am J Physiol Heart Circul Physiol.* (2008) 295:H2380–7. doi: 10.1152/ajpheart.00902.2008
52. Hozawa A, Folsom AR, Sharrett AR, Chambless LE. Absolute and attributable risks of cardiovascular disease incidence in relation to optimal and borderline risk factors: comparison of African American with white subjects–atherosclerosis risk in communities study. *Arch Intern Med.* (2007) 167:573–9. doi: 10.1001/archinte.167.6.573
53. Din-Dzietham R, Couper D, Evans G, Arnett DK, Jones DW. Arterial stiffness is greater in African Americans than in whites: evidence from the forsyth county, north carolina, ARIC cohort. *Am J Hypertens.* (2004) 17:304–13. doi: 10.1016/j.amjhyper.2003.12.004
54. Mokwatsi GG, Schutte AE, Kruger R. Ethnic differences regarding arterial stiffness of 6-8-year-old black and white boys. *J Hypertens.* (2017) 35:960–7. doi: 10.1097/HJH.0000000000001267
55. Thurston RC, Matthews KA. Racial and socioeconomic disparities in arterial stiffness and intima media thickness among adolescents. *Soc Sci Med.* (2009) 68:807–13. doi: 10.1016/j.socscimed.2008.12.029
56. Lefferts WK, Augustine JA, Spartano NL, Atallah-Yunes NH, Heffernan KS, Gump BB. Racial differences in aortic stiffness in children. *J Pediatr.* (2017) 180:62–7. doi: 10.1016/j.jpeds.2016.09.071
57. Malayeri AA, Natori S, Bahrami H, Bertoni AG, Kronmal R, Lima JA, et al. Relation of aortic wall thickness and distensibility to cardiovascular risk factors [from the multi-ethnic study of atherosclerosis (MESA)]. *Am J Cardiol.* (2008) 102:491–6. doi: 10.1016/j.amjcard.2008.04.010
58. Goel A, Maroules CD, Mitchell GF, Peshock R, Ayers C, McColl R, et al. Ethnic difference in proximal aortic stiffness: an observation from the dallas heart study. *JACC Cardiovasc Imaging.* (2017) 10:54–61. doi: 10.1016/j.jcmg.2016.07.012
59. Baldo MP, Cunha RS, Ribeiro ALP, Lotufo PA, Chor D, Barreto SM, et al. Racial differences in arterial stiffness are mainly determined by blood pressure levels: results from the ELSA-Brasil study. *J Am Heart Assoc.* (2017) 6:e005477. doi: 10.1161/JAHA.117.005477
60. Birru MS, Matthews KA, Thurston RC, Brooks MM, Ibrahim S, Barinas-Mitchell E, et al. African-American ethnicity and cardiovascular risk factors are related to aortic pulse-wave velocity progression. *Am J Hypertens.* (2011) 24:809–15. doi: 10.1038/ajh.2011.57
61. Dong Y, Pollock N, Stallmann-Jorgensen IS, Gutin B, Lan L, Chen TC, et al. Low 25-hydroxyvitamin D levels in adolescents: race, season, adiposity, physical activity, and fitness. *Pediatrics.* (2010) 125:1104–11. doi: 10.1542/peds.2009-2055
62. Raed A, Bhagatwala J, Zhu H, Pollock NK, Parikh SJ, Huang Y, et al. Dose responses of vitamin D3 supplementation on arterial stiffness in overweight African Americans with vitamin D deficiency: a placebo controlled randomized trial. *PLoS ONE.* (2017) 12:e0188424. doi: 10.1371/journal.pone.0188424
63. Kalinowski L, Dobrucki IT, Malinski T. Race-specific differences in endothelial function: predisposition of African Americans to vascular diseases. *Circulation.* (2004) 109:2511–7. doi: 10.1161/01.CIR.0000129087.81352.7A
64. Campia U, Choucair WK, Bryant MB, Waclawiw MA, Cardillo C, Panza JA. Reduced endothelium-dependent and -independent dilation of conductance arteries in African Americans. *J Am Coll Cardiol.* (2002) 40:754–60. doi: 10.1016/S0735-1097(02)02015-6
65. Morris AA, Patel RS, Binongo JN, Poole J, Al Mheid I, Ahmed Y, et al. Racial differences in arterial stiffness and microcirculatory function between black and white Americans. *J Am Heart Assoc.* (2013) 2:e002154. doi: 10.1161/JAHA.112.002154
66. McEniery CM, Spratt M, Munnery M, Yarnell J, Lowe GD, Rumley A, et al. An analysis of prospective risk factors for aortic stiffness in men: 20-year follow-up from the caerphilly prospective study. *Hypertension.* (2010) 56:36–43. doi: 10.1161/HYPERTENSIONAHA.110.150896

67. Zieman SJ, Melenovsky V, Kass DA. Mechanisms, pathophysiology, and therapy of arterial stiffness. *Arterioscler Thromb Vasc Biol.* (2005) 25:932–43. doi: 10.1161/01.ATV.0000160548.78317.29
68. Tedla YG, Yano Y, Carnethon M, Greenland P. Association between long-term blood pressure variability and 10-year progression in arterial stiffness: the multiethnic study of atherosclerosis. *Hypertension.* (2017) 69:118–27. doi: 10.1161/HYPERTENSIONAHA.116.08427
69. Aoki Y, Kai H, Kajimoto H, Kudo H, Takayama N, Yasuoka S, et al. Large blood pressure variability aggravates arteriolosclerosis and cortical sclerotic changes in the kidney in hypertensive rats. *Circ J.* (2014) 78:2284–91. doi: 10.1253/circj.CJ-14-0027
70. Chappell DC, Varner SE, Nerem RM, Medford RM, Alexander RW. Oscillatory shear stress stimulates adhesion molecule expression in cultured human endothelium. *Circ Res.* (1998) 82:532–9. doi: 10.1161/01.RES.82.5.532
71. Shimbo D, Shea S, McClelland RL, Viera AJ, Mann D, Newman J, et al. Associations of aortic distensibility and arterial elasticity with long-term visit-to-visit blood pressure variability: the multi-ethnic study of atherosclerosis (MESA). *Am J Hypertens.* (2013) 26:896–902. doi: 10.1093/ajh/hpt040
72. Dernellis J, Panaretou M. Aortic stiffness is an independent predictor of progression to hypertension in nonhypertensive subjects. *Hypertension.* (2005) 45:426–31. doi: 10.1161/01.HYP.0000157818.58878.93
73. Franklin SS. Arterial stiffness and hypertension: a two-way street? *Hypertension.* (2005) 45:349–51. doi: 10.1161/01.HYP.0000157819.31611.87
74. Mitchell GF. Arterial stiffness and hypertension: chicken or egg? *Hypertension.* (2014) 64:210–4. doi: 10.1161/HYPERTENSIONAHA.114.03449
75. Najjar SS, Scuteri A, Shetty V, Wright JG, Muller DC, Fleg JL, et al. Pulse wave velocity is an independent predictor of the longitudinal increase in systolic blood pressure and of incident hypertension in the Baltimore longitudinal study of aging. *J Am Coll Cardiol.* (2008) 51:1377–83. doi: 10.1016/j.jacc.2007.10.065
76. Weisbrod RM, Shiang T, Al Sayah L, Fry JL, Bajpai S, Reinhart-King CA, et al. Arterial stiffening precedes systolic hypertension in diet-induced obesity. *Hypertension.* (2013) 62:1105–10. doi: 10.1161/HYPERTENSIONAHA.113.01744
77. Li S, Chen W, Srinivasan SR, Berenson GS. Influence of metabolic syndrome on arterial stiffness and its age-related change in young adults: the bogalusa heart study. *Atherosclerosis.* (2005) 180:349–54. doi: 10.1016/j.atherosclerosis.2004.12.016
78. Gomez-Sanchez L, Garcia-Ortiz L, Patino-Alonso MC, Recio-Rodriguez JI, Fernando R, Marti R, et al. Association of metabolic syndrome and its components with arterial stiffness in caucasian subjects of the MARK study: a cross-sectional trial. *Cardiovasc Diabetol.* (2016) 15:148. doi: 10.1186/s12933-016-0465-7
79. Safar ME, Thomas F, Blacher J, Nzietchueng R, Bureau JM, Pannier B, et al. Metabolic syndrome and age-related progression of aortic stiffness. *J Am Coll Cardiol.* (2006) 47:72–5. doi: 10.1016/j.jacc.2005.08.052
80. Terentes-Printzios D, Vlachopoulos C, Xaplanteris P, Ioakeimidis N, Aznaouridis K, Baou K, et al. Cardiovascular risk factors accelerate progression of vascular aging in the general population: results from the CRAVE Study (cardiovascular risk factors affecting vascular age). *Hypertension.* (2017) 70:1057–64. doi: 10.1161/HYPERTENSIONAHA.117.09633
81. Tomiyama H, Hirayama Y, Hashimoto H, Yambe M, Yamada J, Koji Y, et al. The effects of changes in the metabolic syndrome detection status on arterial stiffening: a prospective study. *Hypertens Res.* (2006) 29:673–8. doi: 10.1291/hypres.29.673
82. Haffner SM, Lehto S, Ronnemaa T, Pyorala K, Laakso M. Mortality from coronary heart disease in subjects with type 2 diabetes and in nondiabetic subjects with and without prior myocardial infarction. *N Engl J Med.* (1998) 339:229–34. doi: 10.1056/NEJM199807233390404
83. Kannel WB, McGee DL. Diabetes and glucose tolerance as risk factors for cardiovascular disease: the framingham study. *Diabetes Care.* (1979) 2:120–6. doi: 10.2337/diacare.2.2.120
84. Mansour AS, Yannoutsos A, Majahalme N, Agnoletti D, Safar ME, Ouerdane S, et al. Aortic stiffness and cardiovascular risk in type 2 diabetes. *J Hypertens.* (2013) 31:1584–92. doi: 10.1097/HJH.0b013e3283613074
85. Pietri P, Vlachopoulos C, Vyssoulis G, Ioakeimidis N, Stefanadis C. Macro- and microvascular alterations in patients with metabolic syndrome: sugar makes the difference. *Hypertens Res.* (2014) 37:452–6. doi: 10.1038/hr.2013.148
86. Di Pino A, Currenti W, Urbano F, Scicali R, Piro S, Purrello F, et al. High intake of dietary advanced glycation end-products is associated with increased arterial stiffness and inflammation in subjects with type 2 diabetes. *Nutr Metab Cardiovasc Dis.* (2017) 27:978–84. doi: 10.1016/j.numecd.2017.06.014
87. Kass DA, Shapiro EP, Kawaguchi M, Capriotti AR, Scuteri A, deGroof RC, et al. Improved arterial compliance by a novel advanced glycation end-product crosslink breaker. *Circulation.* (2001) 104:1464–70. doi: 10.1161/hc3801.097806
88. Engelen L, Ferreira I, Gaens KH, Henry RM, Dekker JM, Nijpels G, et al. The association between the−374T/A polymorphism of the receptor for advanced glycation endproducts gene and blood pressure and arterial stiffness is modified by glucose metabolism status: the hoorn and CoDAM studies. *J Hypertens.* (2010) 28:285–93. doi: 10.1097/HJH.0b013e3283330931
89. Lastra-Lastra G, Sowers JR, Restrepo-Erazo K, Manrique-Acevedo C, Lastra-Gonzalez G. Role of aldosterone and angiotensin II in insulin resistance: an update. *Clin Endocrinol.* (2009) 71:1–6. doi: 10.1111/j.1365-2265.2008.03498.x
90. Elliott P, Stamler J, Nichols R, Dyer AR, Stamler R, Kesteloot H, et al. Intersalt revisited: further analyses of 24 hour sodium excretion and blood pressure within and across populations. Intersalt cooperative research group. *BMJ.* (1996) 312:1249–53. doi: 10.1136/bmj.312.7041.1249
91. Jablonski KL, Fedorova OV, Racine ML, Geolfos CJ, Gates PE, Chonchol M, et al. Dietary sodium restriction and association with urinary marinobufagenin, blood pressure, aortic stiffness. *Clin J Am Soc Nephrol.* (2013) 8:1952–9. doi: 10.2215/CJN.00900113
92. Vaitkevicius PV, Fleg JL, Engel JH, O'Connor FC, Wright JG, Lakatta LE, et al. Effects of age and aerobic capacity on arterial stiffness in healthy adults. *Circulation.* (1993) 88:1456–62. doi: 10.1161/01.CIR.88.4.1456
93. Tanaka H, DeSouza CA, Seals DR. Absence of age-related increase in central arterial stiffness in physically active women. *Arterioscler Thromb Vasc Biol.* (1998) 18:127–32. doi: 10.1161/01.ATV.18.1.127
94. Lopes S, Afreixo V, Teixeira M, Garcia C, Leitão C, Gouveia M, et al. Exercise training reduces arterial stiffness in adults with hypertension: a systematic review and meta-analysis. *J Hypertens.* (2021) 39:214–22. doi: 10.1097/HJH.0000000000002619
95. Lekakis J, Papamichael C, Vemmos C, Nanas J, Kontoyannis D, Stamatelopoulos S, et al. Effect of acute cigarette smoking on endothelium-dependent brachial artery dilatation in healthy individuals. *Am J Cardiol.* (1997) 79:529–31. doi: 10.1016/S0002-9149(96)00805-3
96. Celermajer DS, Sorensen KE, Georgakopoulos D, Bull C, Thomas O, Robinson J, et al. Cigarette smoking is associated with dose-related and potentially reversible impairment of endothelium-dependent dilation in healthy young adults. *Circulation.* (1993) 88:2149–55. doi: 10.1161/01.CIR.88.5.2149
97. Lee GB, Shim JS, Kim HC. Dose-response association between smoking cessation and arterial stiffness: the cardiovascular and metabolic diseases etiology research center (CMERC) cohort. *Korean Circ J.* (2020) 50:361–9. doi: 10.4070/kcj.2019.0270
98. Vlachopoulos C, Ioakeimidis N, Abdelrasoul M, Terentes-Printzios D, Georgakopoulos C, Pietri P, et al. Electronic cigarette smoking increases aortic stiffness and blood pressure in young smokers. *J Am Coll Cardiol.* (2016) 67:2802–3. doi: 10.1016/j.jacc.2016.03.569
99. Sierksma A, Muller M, van der Schouw YT, Grobbee DE, Hendriks HF, Bots ML. Alcohol consumption and arterial stiffness in men. *J Hypertens.* (2004) 22:357–62. doi: 10.1097/00004872-200402000-00020
100. Sierksma A, Lebrun CE, van der Schouw YT, Grobbee DE, Lamberts SW, Hendriks HF, et al. Alcohol consumption in relation to aortic stiffness and aortic wave reflections: a cross-sectional study in healthy postmenopausal women. *Arterioscler Thromb Vasc Biol.* (2004) 24:342–8. doi: 10.1161/01.ATV.0000110784.52412.8f

101. Yu A, Cooke AB, Scheffler P, Doonan RJ, Daskalopoulou SS. Alcohol exerts a shifted u-shaped effect on central blood pressure in young adults. *J Gen Intern Med.* (2021) 36:2975–81. doi: 10.1007/s11606-021-06665-0
102. Nishiwaki M, Kora N, Matsumoto N. Ingesting a small amount of beer reduces arterial stiffness in healthy humans. *Physiol Rep.* (2017) 5:e13381. doi: 10.14814/phy2.13381
103. Gardner JD, Mouton AJ. Alcohol effects on cardiac function. *Compr Physiol.* (2015) 5:791–802. doi: 10.1002/cphy.c140046
104. Kuhlmann CR, Li F, Lüdders DW, Schaefer CA, Most AK, Backenköhler U, et al. Dose-dependent activation of Ca2+-activated K+ channels by ethanol contributes to improved endothelial cell functions. *Alcohol Clin Exp Res.* (2004) 28:1005–11. doi: 10.1097/01.ALC.0000130811.92457.0D
105. Centers for Disease Control and Prevention. Cigarette smoking among adults–United States, 2000. *MMWMorb Rep*. (2002) 51:642–5.
106. Mahmud A, Feely J. Effect of smoking on arterial stiffness and pulse pressure amplification. *Hypertension.* (2003) 41:183–7. doi: 10.1161/01.HYP.0000047464.66901.60
107. Stefanadis C, Vlachopoulos C, Tsiamis E, Diamantopoulos L, Toutouzas K, Giatrakos N, et al. Unfavorable effects of passive smoking on aortic function in men. *Ann Intern Med.* (1998) 128:426–34. doi: 10.7326/0003-4819-128-6-199803150-00002
108. Jatoi NA, Jerrard-Dunne P, Feely J, Mahmud A. Impact of smoking and smoking cessation on arterial stiffness and aortic wave reflection in hypertension. *Hypertension.* (2007) 49:981–5. doi: 10.1161/HYPERTENSIONAHA.107.087338
109. Doonan RJ, Hausvater A, Scallan C, Mikhailidis DP, Pilote L, Daskalopoulou SS. The effect of smoking on arterial stiffness. *Hypertens Res.* (2010) 33:398–410. doi: 10.1038/hr.2010.25
110. Tanaka H, Safar ME. Influence of lifestyle modification on arterial stiffness and wave reflections. *Am J Hypertens.* (2005) 18:137–44. doi: 10.1016/j.amjhyper.2004.07.008
111. He FJ, Li J, Macgregor GA. Effect of longer term modest salt reduction on blood pressure: Cochrane systematic review and meta-analysis of randomised trials. *BMJ.* (2013) 346:f1325. doi: 10.1136/bmj.f1325
112. Avolio AP, Clyde KM, Beard TC, Cooke HM, Ho KK, O'Rourke MF. Improved arterial distensibility in normotensive subjects on a low salt diet. *Arteriosclerosis.* (1986) 6:166–9. doi: 10.1161/01.ATV.6.2.166
113. Livingstone KM, Givens DI, Cockcroft JR, Pickering JE, Lovegrove JA. Is fatty acid intake a predictor of arterial stiffness and blood pressure in men? Evidence from the caerphilly prospective study. *Nutr Metab Cardiovasc Dis.* (2013) 23:1079–85. doi: 10.1016/j.numecd.2012.12.002
114. Crichton GE, Elias MF, Dore GA, Abhayaratna WP, Robbins MA. Relations between dairy food intake and arterial stiffness: pulse wave velocity and pulse pressure. *Hypertension.* (2012) 59:1044–51. doi: 10.1161/HYPERTENSIONAHA.111.190017
115. Petersen KS, Keogh JB, Meikle PJ, Garg ML, Clifton PM. Dietary predictors of arterial stiffness in a cohort with type 1 and type 2 diabetes. *Atherosclerosis.* (2015) 238:175–81. doi: 10.1016/j.atherosclerosis.2014.12.012
116. Aatola H, Koivistoinen T, Hutri-Kähönen N, Juonala M, Mikkilä V, Lehtimäki T, et al. Lifetime fruit and vegetable consumption and arterial pulse wave velocity in adulthood: the cardiovascular risk in young finns study. *Circulation.* (2010) 122:2521–8. doi: 10.1161/CIRCULATIONAHA.110.969279
117. Green D, Cheetham C, Mavaddat L, Watts K, Best M, Taylor R, et al. Effect of lower limb exercise on forearm vascular function: contribution of nitric oxide. *Am J Physiol Heart Circul Physiol.* (2002) 283:H899–907. doi: 10.1152/ajpheart.00049.2002
118. Green DJ, Bilsborough W, Naylor LH, Reed C, Wright J, O'Driscoll G, et al. Comparison of forearm blood flow responses to incremental handgrip and cycle ergometer exercise: relative contribution of nitric oxide. *J Physiol.* (2005) 562:617–28. doi: 10.1113/jphysiol.2004.075929
119. Sacre K, Escoubet B, Pasquet B, Chauveheid MP, Zennaro MC, Tubach F, et al. Increased arterial stiffness in systemic lupus erythematosus (SLE) patients at low risk for cardiovascular disease: a cross-sectional controlled study. *PLoS ONE.* (2014) 9:e94511. doi: 10.1371/journal.pone.0094511
120. Zanoli L, Boutouyrie P, Fatuzzo P, Granata A, Lentini P, Ozturk K, et al. Inflammation and aortic stiffness: an individual participant data meta-analysis in patients with inflammatory bowel disease. *J Am Heart Assoc.* (2017) 6. doi: 10.1161/JAHA.117.007003
121. Anyfanti P, Triantafyllou A, Gkaliagkousi E, Koletsos N, Aslanidis S, Douma S. Association of non-invasive hemodynamics with arterial stiffness in rheumatoid arthritis. *Scand Cardiovasc J.* (2018) 52:171–6. doi: 10.1080/14017431.2018.1453943
122. Maloberti A, Riva M, Tadic M, Valena C, Villa P, Boggioni I, et al. Association between atrial, ventricular and vascular morphofunctional alterations in rheumatoid arthritis. *High Blood Press Cardiovasc Prev.* (2018) 25:97–104. doi: 10.1007/s40292-017-0246-8
123. Costa L, Caso F, D'Elia L, Atteno M, Peluso R, Del Puente A, et al. Psoriatic arthritis is associated with increased arterial stiffness in the absence of known cardiovascular risk factors: a case control study. *Clin Rheumatol.* (2012) 31:711–5. doi: 10.1007/s10067-011-1892-1
124. Shen J, Shang Q, Li EK, Leung YY, Kun EW, Kwok LW, et al. Cumulative inflammatory burden is independently associated with increased arterial stiffness in patients with psoriatic arthritis: a prospective study. *Arthritis Res Ther.* (2015) 17:75. doi: 10.1186/s13075-015-0570-0
125. Sezis Demirci M, Karabulut G, Gungor O, Celtik A, Ok E, Kabasakal Y. Is there an increased arterial stiffness in patients with primary sjögren's syndrome? *Intern Med.* (2016) 55:455–9. doi: 10.2169/internalmedicine.55.3472
126. Ozisler C, Kaplanoglu H. Evaluation of subclinical atherosclerosis by ultrasound radiofrequency data technology in patients with primary Sjögren's syndrome. *Clin Rheumatol.* (2019) 38:709–17. doi: 10.1007/s10067-018-4330-9
127. Roman MJ, Devereux RB, Schwartz JE, Lockshin MD, Paget SA, Davis A, et al. Arterial stiffness in chronic inflammatory diseases. *Hypertension.* (2005) 46:194–9. doi: 10.1161/01.HYP.0000168055.89955.db
128. Tomiyama H, Shiina K, Matsumoto-Nakano C, Ninomiya T, Komatsu S, Kimura K, et al. The contribution of inflammation to the development of hypertension mediated by increased arterial stiffness. *J Am Heart Assoc.* (2017) 6:e05729. doi: 10.1161/JAHA.117.005729
129. Mattace-Raso FU, van der Cammen TJ, van der Meer IM, Schalekamp MA, Asmar R, Hofman A, et al. C-reactive protein and arterial stiffness in older adults: the rotterdam study. *Atherosclerosis.* (2004) 176:111–6. doi: 10.1016/j.atherosclerosis.2004.04.014
130. Fichtlscherer S, Rosenberger G, Walter DH, Breuer S, Dimmeler S, Zeiher AM. Elevated C-reactive protein levels and impaired endothelial vasoreactivity in patients with coronary artery disease. *Circulation.* (2000) 102:1000–6. doi: 10.1161/01.CIR.102.9.1000
131. Mahmud A, Feely J. Arterial stiffness is related to systemic inflammation in essential hypertension. *Hypertension.* (2005) 46:1118–22. doi: 10.1161/01.HYP.0000185463.27209.b0
132. Sie MP, Mattace-Raso FU, Uitterlinden AG, Arp PP, Hofman A, Pols HA, et al. The interleukin-6-174 G/C promoter polymorphism and arterial stiffness; the rotterdam study. *Vasc Health Risk Manag.* (2008) 4:863–9. doi: 10.2147/VHRM.S1693
133. Vlachopoulos C, Gravos A, Georgiopoulos G, Terentes-Printzios D, Ioakeimidis N, Vassilopoulos D, et al. The effect of TNF-a antagonists on aortic stiffness and wave reflections: a meta-analysis. *Clin Rheumatol.* (2018) 37:515–26. doi: 10.1007/s10067-017-3657-y
134. Ikdahl E, Rollefstad S, Hisdal J, Olsen IC, Pedersen TR, Kvien TK, et al. Sustained Improvement of arterial stiffness and blood pressure after long-term rosuvastatin treatment in patients with inflammatory joint diseases: results from the RORA-AS study. *PLoS ONE.* (2016) 11:e0153440. doi: 10.1371/journal.pone.0153440
135. Wang Y, Sun Z. Current understanding of klotho. *Ageing Res Rev.* (2009) 8:43–51. doi: 10.1016/j.arr.2008.10.002
136. Chen K, Zhou X, Sun Z. Haplodeficiency of klotho gene causes arterial stiffening via upregulation of scleraxis expression and induction of autophagy. *Hypertension.* (2015) 66:1006–13. doi: 10.1161/HYPERTENSIONAHA.115.06033
137. Gao D, Zuo Z, Tian J, Ali Q, Lin Y, Lei H, et al. Activation of SIRT1 attenuates klotho deficiency-induced arterial stiffness and hypertension by enhancing AMP-activated protein kinase activity. *Hypertension.* (2016) 68:1191–9. doi: 10.1161/HYPERTENSIONAHA.116.07709

138. Kitagawa M, Sugiyama H, Morinaga H, Inoue T, Takiue K, Ogawa A, et al. A decreased level of serum soluble Klotho is an independent biomarker associated with arterial stiffness in patients with chronic kidney disease. *PLoS ONE.* (2013) 8:e56695. doi: 10.1371/journal.pone.0056695
139. Zarzuelo MJ, Lopez-Sepulveda R, Sanchez M, Romero M, Gomez-Guzman M, Ungvary Z, et al. SIRT1 inhibits NADPH oxidase activation and protects endothelial function in the rat aorta: implications for vascular aging. *Biochem Pharmacol.* (2013) 85:1288–96. doi: 10.1016/j.bcp.2013.02.015
140. Fry JL, Al Sayah L, Weisbrod RM, Van Roy I, Weng X, Cohen RA, et al. Vascular smooth muscle sirtuin-1 protects against diet-induced aortic stiffness. *Hypertension.* (2016) 68:775–84. doi: 10.1161/HYPERTENSIONAHA.116.07622
141. Zhou X, Chen K, Wang Y, Schuman M, Lei H, Sun Z. Antiaging gene klotho regulates adrenal CYP11B2 expression and aldosterone synthesis. *J Am Soc Nephrol.* (2016) 27:1765–76. doi: 10.1681/ASN.2015010093
142. Neves MF, Cunha AR, Cunha MR, Gismondi RA, Oigman W. The role of renin-angiotensin-aldosterone system and its new components in arterial stiffness and vascular aging. *High Blood Press Cardiovasc Prev.* (2018) 25:137–45. doi: 10.1007/s40292-018-0252-5
143. Park S, Kim JB, Shim CY, Ko YG, Choi D, Jang Y, et al. The influence of serum aldosterone and the aldosterone-renin ratio on pulse wave velocity in hypertensive patients. *J Hypertens.* (2007) 25:1279–83. doi: 10.1097/HJH.0b013e3280f31b6e
144. Benetos A, Topouchian J, Ricard S, Gautier S, Bonnardeaux A, Asmar R, et al. Influence of angiotensin II type 1 receptor polymorphism on aortic stiffness in never-treated hypertensive patients. *Hypertension.* (1995) 26:44–7. doi: 10.1161/01.HYP.26.1.44
145. Lajemi M, Labat C, Gautier S, Lacolley P, Safar M, Asmar R, et al. Angiotensin II type 1 receptor-153A/G and 1166A/C gene polymorphisms and increase in aortic stiffness with age in hypertensive subjects. *J Hypertens.* (2001) 19:407–13. doi: 10.1097/00004872-200103000-00008
146. Dima I, Vlachopoulos C, Alexopoulos N, Baou K, Vasiliadou C, Antoniades C, et al. Association of arterial stiffness with the angiotensin-converting enzyme gene polymorphism in healthy individuals. *Am J Hypertens.* (2008) 21:1354–8. doi: 10.1038/ajh.2008.295
147. Taniwaki H, Kawagishi T, Emoto M, Shoji T, Hosoi M, Kogawa K, et al. Association of ACE gene polymorphism with arterial stiffness in patients with type 2 diabetes. *Diabetes Care.* (1999) 22:1858–64. doi: 10.2337/diacare.22.11.1858
148. Pojoga L, Gautier S, Blanc H, Guyene TT, Poirier O, Cambien F, et al. Genetic determination of plasma aldosterone levels in essential hypertension. *Am J Hypertens.* (1998) 11:856–60. doi: 10.1016/S0895-7061(98)00048-X
149. Laurent S, Boutouyrie P, Lacolley P. Structural and genetic bases of arterial stiffness. *Hypertension.* (2005) 45:1050–5. doi: 10.1161/01.HYP.0000164580.39991.3d
150. Nehme JA, Lacolley P, Labat C, Challande P, Robidel E, Perret C, et al. Spironolactone improves carotid artery fibrosis and distensibility in rat post-ischaemic heart failure. *J Mol Cell Cardiol.* (2005) 39:511–9. doi: 10.1016/j.yjmcc.2005.05.015
151. London GM, Asmar RG, O'Rourke MF, Safar ME. Mechanism(s) of selective systolic blood pressure reduction after a low-dose combination of perindopril/indapamide in hypertensive subjects: comparison with atenolol. *J Am Coll Cardiol.* (2004) 43:92–9. doi: 10.1016/j.jacc.2003.07.039
152. Savoia C, Touyz RM, Amiri F, Schiffrin EL. Selective mineralocorticoid receptor blocker eplerenone reduces resistance artery stiffness in hypertensive patients. *Hypertension.* (2008) 51:432–9. doi: 10.1161/HYPERTENSIONAHA.107.103267
153. Koumaras C, Tziomalos K, Stavrinou E, Katsiki N, Athyros VG, Mikhailidis DP, et al. Effects of renin-angiotensin-aldosterone system inhibitors and beta-blockers on markers of arterial stiffness. *J Am Soc Hypertens.* (2014) 8:74–82. doi: 10.1016/j.jash.2013.09.001
154. D'Elia L, Galletti F, La Fata E, Sabino P, Strazzullo P. Effect of dietary sodium restriction on arterial stiffness: systematic review and meta-analysis of the randomized controlled trials. *J Hypertens.* (2018) 36:734–43. doi: 10.1097/HJH.0000000000001604
155. Zeller CB, Appenzeller S. Cardiovascular disease in systemic lupus erythematosus: the role of traditional and lupus related risk factors. *Curr Cardiol Rev.* (2008) 4:116–22. doi: 10.2174/157340308784245775
156. Yarur AJ, Deshpande AR, Pechman DM, Tamariz L, Abreu MT, Sussman DA. Inflammatory bowel disease is associated with an increased incidence of cardiovascular events. *Am J Gastroenterol.* (2011) 106:741–7. doi: 10.1038/ajg.2011.63
157. Ahlehoff O, Gislason GH, Charlot M, Jorgensen CH, Lindhardsen J, Olesen JB, et al. Psoriasis is associated with clinically significant cardiovascular risk: a Danish nationwide cohort study. *J Intern Med.* (2011) 270:147–57. doi: 10.1111/j.1365-2796.2010.02310.x
158. Holloway CJ, Ntusi N, Suttie J, Mahmod M, Wainwright E, Clutton G, et al. Comprehensive cardiac magnetic resonance imaging and spectroscopy reveal a high burden of myocardial disease in HIV patients. *Circulation.* (2013) 128:814–22. doi: 10.1161/CIRCULATIONAHA.113.001719
159. Shang Q, Tam LS, Li EK, Yip GW, Yu CM. Increased arterial stiffness correlated with disease activity in systemic lupus erythematosus. *Lupus.* (2008) 17:1096–102. doi: 10.1177/0961203308092160
160. Yudkin JS, Stehouwer CD, Emeis JJ, Coppack SW. C-reactive protein in healthy subjects: associations with obesity, insulin resistance, and endothelial dysfunction: a potential role for cytokines originating from adipose tissue? *Arterioscler Thromb Vasc Biol.* (1999) 19:972–8. doi: 10.1161/01.ATV.19.4.972
161. van der Meer IM, de Maat MP, Bots ML, Breteler MM, Meijer J, Kiliaan AJ, et al. Inflammatory mediators and cell adhesion molecules as indicators of severity of atherosclerosis: the rotterdam study. *Arterioscler Thromb Vasc Biol.* (2002) 22:838–42. doi: 10.1161/01.ATV.0000016249.96529.B8
162. Xue H, Li JJ, Wang JL, Chen SH, Gao JS, Chen YD, et al. Changes in pulse pressure × heart rate, hs-CRP, and arterial stiffness progression in the Chinese general population: a cohort study involving 3978 employees of the Kailuan company. *J Geriatr Cardiol.* (2019) 16:710–6. doi: 10.11909/j.issn.1671-5411.2019.09.010
163. Park MY, Herrmann SM, Saad A, Eirin A, Tang H, Lerman A, et al. Biomarkers of kidney injury and klotho in patients with atherosclerotic renovascular disease. *Clin J Am Soc Nephrol.* (2015) 10:443–51. doi: 10.2215/CJN.07290714
164. Navarro-González JF, Donate-Correa J, Muros de Fuentes M, Pérez-Hernández H, Martínez-Sanz R, Mora-Fernández C. Reduced KLOTHO is associated with the presence and severity of coronary artery disease. *Heart.* (2014) 100:34–40. doi: 10.1136/heartjnl-2013-304746
165. Chirinos JA, Sardana M, Syed AA, Koppula MR, Varakantam S, Vasim I, et al. Aldosterone, inactive matrix gla-protein, and large artery stiffness in hypertension. *J Am Soc Hypertens.* (2018) 12:681–9. doi: 10.1016/j.jash.2018.06.018
166. Lacolley P, Labat C, Pujol A, Delcayre C, Benetos A, Safar M. Increased carotid wall elastic modulus and fibronectin in aldosterone-salt-treated rats: effects of eplerenone. *Circulation.* (2002) 106:2848–53. doi: 10.1161/01.CIR.0000039328.33137.6C
167. Aragones G, Ferre R, Lazaro I, Cabre A, Plana N, Merino J, et al. Fatty acid-binding protein 4 is associated with endothelial dysfunction in patients with type 2 diabetes. *Atherosclerosis.* (2010) 213:329–31. doi: 10.1016/j.atherosclerosis.2010.07.026
168. Fuseya T, Furuhashi M, Yuda S, Muranaka A, Kawamukai M, Mita T, et al. Elevation of circulating fatty acid-binding protein 4 is independently associated with left ventricular diastolic dysfunction in a general population. *Cardiovasc Diabetol.* (2014) 13:126. doi: 10.1186/s12933-014-0126-7
169. von Eynatten M, Breitling LP, Roos M, Baumann M, Rothenbacher D, Brenner H. Circulating adipocyte fatty acid-binding protein levels and cardiovascular morbidity and mortality in patients with coronary heart disease: a 10-year prospective study. *Arterioscler Thromb Vasc Biol.* (2012) 32:2327–35. doi: 10.1161/ATVBAHA.112.248609
170. Chen MC, Hsu BG, Lee CJ, Yang CF, Wang JH. High serum adipocyte fatty acid binding protein level as a potential biomarker of aortic arterial stiffness in hypertensive patients with metabolic syndrome. *Clin Chim Acta.* (2017) 473:166–72. doi: 10.1016/j.cca.2017.08.030
171. Tseng PW, Hou JS, Wu DA, Hsu BG. High serum adipocyte fatty acid binding protein concentration linked with increased aortic arterial

stiffness in patients with type 2 diabetes. *Clin Chim Acta.* (2019) 495:35–9. doi: 10.1016/j.cca.2019.03.1629
172. Vavruch C, Länne T, Fredrikson M, Lindström T, Östgren CJ, Nystrom FH. Serum leptin levels are independently related to the incidence of ischemic heart disease in a prospective study of patients with type 2 diabetes. *Cardiovasc Diabetol.* (2015) 14:62. doi: 10.1186/s12933-015-0208-1
173. Montazerifar F, Bolouri A, Paghalea RS, Mahani MK, Karajibani M. Obesity. Serum resistin and leptin levels linked to coronary artery disease. *Arq Bras Cardiol.* (2016) 107:348–353. doi: 10.5935/abc.20160134
174. Tsai JP, Lee MC, Chen YC, Ho GJ, Shih MH, Hsu BG. Hyperleptinemia is a risk factor for the development of central arterial stiffness in kidney transplant patients. *Transplant Proc.* (2015) 47:1825–30. doi: 10.1016/j.transproceed.2015.06.002
175. Kuo CH, Lin YL, Wang CH, Lai YH, Syu RJ, Hsu BG. High serum leptin levels are associated with central arterial stiffness in geriatric patients on hemodialysis. *Ci Ji Yi Xue Za Zhi.* (2018) 30:227–32. doi: 10.4103/tcmj.tcmj_10_18
176. D'Elia L, Giaquinto A, De Luca F, Strazzullo P, Galletti F. Relationship between circulating leptin levels and arterial stiffness: a systematic review and meta-analysis of observational studies. *High Blood Press Cardiovasc Prev.* (2020) 27:505–13. doi: 10.1007/s40292-020-00404-y
177. Clerico A, Giannoni A, Vittorini S, Passino C. Thirty years of the heart as an endocrine organ: physiological role and clinical utility of cardiac natriuretic hormones. *Am J Physiol Heart Circul Physiol.* (2011) 301:H12–20. doi: 10.1152/ajpheart.00226.2011
178. Khan SQ, O'Brien RJ, Struck J, Quinn P, Morgenthaler N, Squire I, et al. Prognostic value of midregional pro-adrenomedullin in patients with acute myocardial infarction: the LAMP (leicester acute myocardial infarction peptide) study. *J Am Coll Cardiol.* (2007) 49:1525–32. doi: 10.1016/j.jacc.2006.12.038
179. O'Malley RG, Bonaca MP, Scirica BM, Murphy SA, Jarolim P, Sabatine MS, et al. Prognostic performance of multiple biomarkers in patients with non-ST-segment elevation acute coronary syndrome: analysis from the MERLIN-TIMI 36 trial (metabolic efficiency with ranolazine for less ischemia in non-ST-elevation acute coronary syndromes-thrombolysis in myocardial infarction 36). *J Am Coll Cardiol.* (2014) 63:1644–53. doi: 10.1016/j.jacc.2013.12.034
180. Klug G, Feistritzer HJ, Reinstadler SJ, Krauter L, Mayr A, Mair J, et al. Association of aortic stiffness with biomarkers of myocardial wall stress after myocardial infarction. *Int J Cardiol.* (2014) 173:253–8. doi: 10.1016/j.ijcard.2014.02.038
181. Reinstadler SJ, Feistritzer HJ, Klug G, Mayr A, Huybrechts L, Hammerer-Lercher A, et al. Biomarkers of hemodynamic stress and aortic stiffness after STEMI: a cross-sectional analysis. *Dis Markers.* (2015) 2015:717032. doi: 10.1155/2015/717032
182. Hagstrom E, Michaelsson K, Melhus H, Hansen T, Ahlstrom H, Johansson L, et al. Plasma-parathyroid hormone is associated with subclinical and clinical atherosclerotic disease in 2 community-based cohorts. *Arterioscler Thromb Vasc Biol.* (2014) 34:1567–73. doi: 10.1161/ATVBAHA.113.303062
183. Schillaci G, Pucci G, Pirro M, Monacelli M, Scarponi AM, Manfredelli MR, et al. Large-artery stiffness: a reversible marker of cardiovascular risk in primary hyperparathyroidism. *Atherosclerosis.* (2011) 218:96–101. doi: 10.1016/j.atherosclerosis.2011.05.010
184. Cheng YB, Li LH, Guo QH, Li FK, Huang QF, Sheng CS, et al. Independent effects of blood pressure and parathyroid hormone on aortic pulse wave velocity in untreated Chinese patients. *J Hypertens.* (2017) 35:1841–8. doi: 10.1097/HJH.0000000000001395
185. Muse ED, Feldman DI, Blaha MJ, Dardari ZA, Blumenthal RS, Budoff MJ, et al. The association of resistin with cardiovascular disease in the multi-ethnic study of atherosclerosis. *Atherosclerosis.* (2015) 239:101–8. doi: 10.1016/j.atherosclerosis.2014.12.044
186. Norman G, Norton GR, Gomes M, Michel F, Majane OH, Sareli P, et al. Circulating resistin concentrations are independently associated with aortic pulse wave velocity in a community sample. *J Hypertens.* (2016) 34:274–81. doi: 10.1097/HJH.0000000000000792
187. Wang JH, Lee CJ, Yang CF, Chen YC, Hsu BG. Serum resistin as an independent marker of aortic stiffness in patients with coronary artery disease. *PLoS ONE.* (2017) 12:e0183123. doi: 10.1371/journal.pone.0183123
188. Krishnan E, Baker JF, Furst DE, Schumacher HR. Gout and the risk of acute myocardial infarction. *Arthritis Rheum.* (2006) 54:2688–96. doi: 10.1002/art.22014
189. Verdecchia P, Schillaci G, Reboldi G, Santeusanio F, Porcellati C, Brunetti P. Relation between serum uric acid and risk of cardiovascular disease in essential hypertension. The PIUMA study. *Hypertension.* (2000) 36:1072–8. doi: 10.1161/01.HYP.36.6.1072
190. Bos MJ, Koudstaal PJ, Hofman A, Witteman JC, Breteler MM. Uric acid is a risk factor for myocardial infarction and stroke: the rotterdam study. *Stroke.* (2006) 37:1503–7. doi: 10.1161/01.STR.0000221716.55088.d4
191. Baena CP, Lotufo PA, Mill JG, Cunha Rde S, Bensenor IJ. Serum uric acid and pulse wave velocity among healthy adults: baseline data from the brazilian longitudinal study of adult health (ELSA-Brasil). *Am J Hypertens.* (2015) 28:966–70. doi: 10.1093/ajh/hpu298
192. Rebora P, Andreano A, Triglione N, Piccinelli E, Palazzini M, Occhi L, et al. Association between uric acid and pulse wave velocity in hypertensive patients and in the general population: a systematic review and meta-analysis. *Blood Press.* (2020) 29:220–31. doi: 10.1080/08037051.2020.1735929
193. Park JS, Kang S, Ahn CW, Cha BS, Kim KR, Lee HC. Relationships between serum uric acid, adiponectin and arterial stiffness in postmenopausal women. *Maturitas.* (2012) 73:344–8. doi: 10.1016/j.maturitas.2012.09.009
194. Mehta T, Nuccio E, McFann K, Madero M, Sarnak MJ, Jalal D. Association of uric acid with vascular stiffness in the framingham heart study. *Am J Hypertens.* (2015) 28:877–83. doi: 10.1093/ajh/hpu253
195. Boutouyrie P, Chowienczyk P, Humphrey JD, Mitchell GF. Arterial stiffness and cardiovascular risk in hypertension. *Circ Res.* (2021) 128:864–886. doi: 10.1161/CIRCRESAHA.121.318061
196. Vlachopoulos C, Terentes-Printzios D, Laurent S, Nilsson PM, Protogerou AD, Aznaouridis K, et al. Association of estimated pulse wave velocity with survival: a secondary analysis of SPRINT. *JAMA Netw Open.* (2019) 2:e1912831. doi: 10.1001/jamanetworkopen.2019.12831
197. Nicholson CJ, Singh K, Saphirstein RJ, Gao YZ, Li Q, Chiu JG, et al. Reversal of aging-induced increases in aortic stiffness by targeting cytoskeletal protein-protein interfaces. *J Am Heart Assoc.* (2018) 7:e008926. doi: 10.1161/JAHA.118.008926

Conflict of Interest: The authors declare that the research was conducted in the absence of any commercial or financial relationships that could be construed as a potential conflict of interest.

Publisher's Note: All claims expressed in this article are solely those of the authors and do not necessarily represent those of their affiliated organizations, or those of the publisher, the editors and the reviewers. Any product that may be evaluated in this article, or claim that may be made by its manufacturer, is not guaranteed or endorsed by the publisher.

frontiers in Cardiovascular Medicine

ORIGINAL RESEARCH
published: 14 December 2021
doi: 10.3389/fcvm.2021.747803

An Robust Rank Aggregation and Least Absolute Shrinkage and Selection Operator Analysis of Novel Gene Signatures in Dilated Cardiomyopathy

*Xiao Ma, Changhua Mo, Liangzhao Huang, Peidong Cao, Louyi Shen and Chun Gui**

Department of Cardiology, First Affiliated Hospital of Guangxi Medical University, Nanning, China

Objective: Dilated cardiomyopathy (DCM) is a heart disease with high mortality characterized by progressive cardiac dilation and myocardial contractility reduction. The molecular signature of dilated cardiomyopathy remains to be defined. Hence, seeking potential biomarkers and therapeutic of DCM is urgent and necessary.

Methods: In this study, we utilized the Robust Rank Aggregation (RRA) method to integrate four eligible DCM microarray datasets from the GEO and identified a set of significant differentially expressed genes (DEGs) between dilated cardiomyopathy and non-heart failure. Moreover, LASSO analysis was carried out to clarify the diagnostic and DCM clinical features of these genes and identify dilated cardiomyopathy derived diagnostic signatures (DCMDDS).

Results: A total of 117 DEGs were identified across the four microarrays. Furthermore, GO analysis demonstrated that these DEGs were mainly enriched in the regulation of inflammatory response, the humoral immune response, the regulation of blood pressure and collagen–containing extracellular matrix. In addition, KEGG analysis revealed that DEGs were mainly enriched in diverse infected signaling pathways. Moreover, Gene set enrichment analysis revealed that immune and inflammatory biological processes such as adaptive immune response, cellular response to interferon and cardiac muscle contraction, dilated cardiomyopathy are significantly enriched in DCM. Moreover, Least absolute shrinkage and selection operator (LASSO) analyses of the 18 DCM-related genes developed a 7-gene signature predictive of DCM. This signature included ANKRD1, COL1A1, MYH6, PERELP, PRKACA, CDKN1A, and OMD. Interestingly, five of these seven genes have a correlation with left ventricular ejection fraction (LVEF) in DCM patients.

Conclusion: Our present study demonstrated that the signatures could be robust tools for predicting DCM in clinical practice. And may also be potential treatment targets for clinical implication in the future.

Keywords: dilated cardiomyopathy, Robust Rank Aggregation, novel gene signatures, Least absolute shrinkage and selection operator analysis, PERELP

OPEN ACCESS

Edited by:
Raffaele Maio,
University of Catanzaro, Italy

Reviewed by:
Paulo M. Dourado,
University of São Paulo, Brazil
Alfredo Jose Mansur,
Universidade de São Paulo, Brazil

****Correspondence:***
Chun Gui
guichun@yahoo.com

Specialty section:
This article was submitted to General Cardiovascular Medicine, a section of the journal Frontiers in Cardiovascular Medicine

Received: *21 August 2021*
Accepted: *17 November 2021*
Published: *14 December 2021*

Citation:
Ma X, Mo C, Huang L, Cao P, Shen L and Gui C (2021) An Robust Rank Aggregation and Least Absolute Shrinkage and Selection Operator Analysis of Novel Gene Signatures in Dilated Cardiomyopathy. Front. Cardiovasc. Med. 8:747803. doi: 10.3389/fcvm.2021.747803

INTRODUCTION

Dilated cardiomyopathy (DCM), characterized by left ventricular or bicentricular enlargement and myocardial systolic dysfunction, is the main cause of systolic heart failure and heart transplantation in about 40 million people worldwide (1, 2). The etiology of dilated cardiomyopathy is still not clear, and it is generally believed that people with genetic background of dilated cardiomyopathy are usually infected with Coxsackie virus, adenovirus and influenza virus, and then resulting cardiac inflammation and immune damage jointly lead to the occurrence and development of dilated cardiomyopathy (3, 4). In recent decades, many strategies including early diagnosis, more accurate typing, evidence-based treatment, rigorous follow-up, and the use of advanced anti-heart failure drugs, have improved the quality of life and long-term survival of patients with dilated cardiomyopathy (5, 6). However, patients with dilated cardiomyopathy presenting with symptoms of heart failure have a poor clinical prognosis, with a 5-year mortality rate of ∼20% in these patients (7, 8). At present, the pathogenesis of dilated cardiomyopathy is still poorly understood.

Advances in gene chips and high-throughput sequencing help to identify the key role of potential core genes and small molecule in the biological process of a variety of diseases (9, 10). Many studies have used microarray chip technology to measure the gene and non-coding RNA expression profile of dilated cardiomyopathy, providing the gene expression pattern of the myocardial tissue of dilated cardiomyopathy. For example, Zhang et al. used bioinformatics method to reanalyze gene expression profile and potential functional network in cardiac tissue of patients with dilated cardiomyopathy (11). Tao et al. also reported four hub lncRNAs in the DCM-related module, which helped to enhance the understanding of DCM pathophysiological process and reveal its potential treatment targets (12). However, most of the gene signatures were analyzed from a single data set,

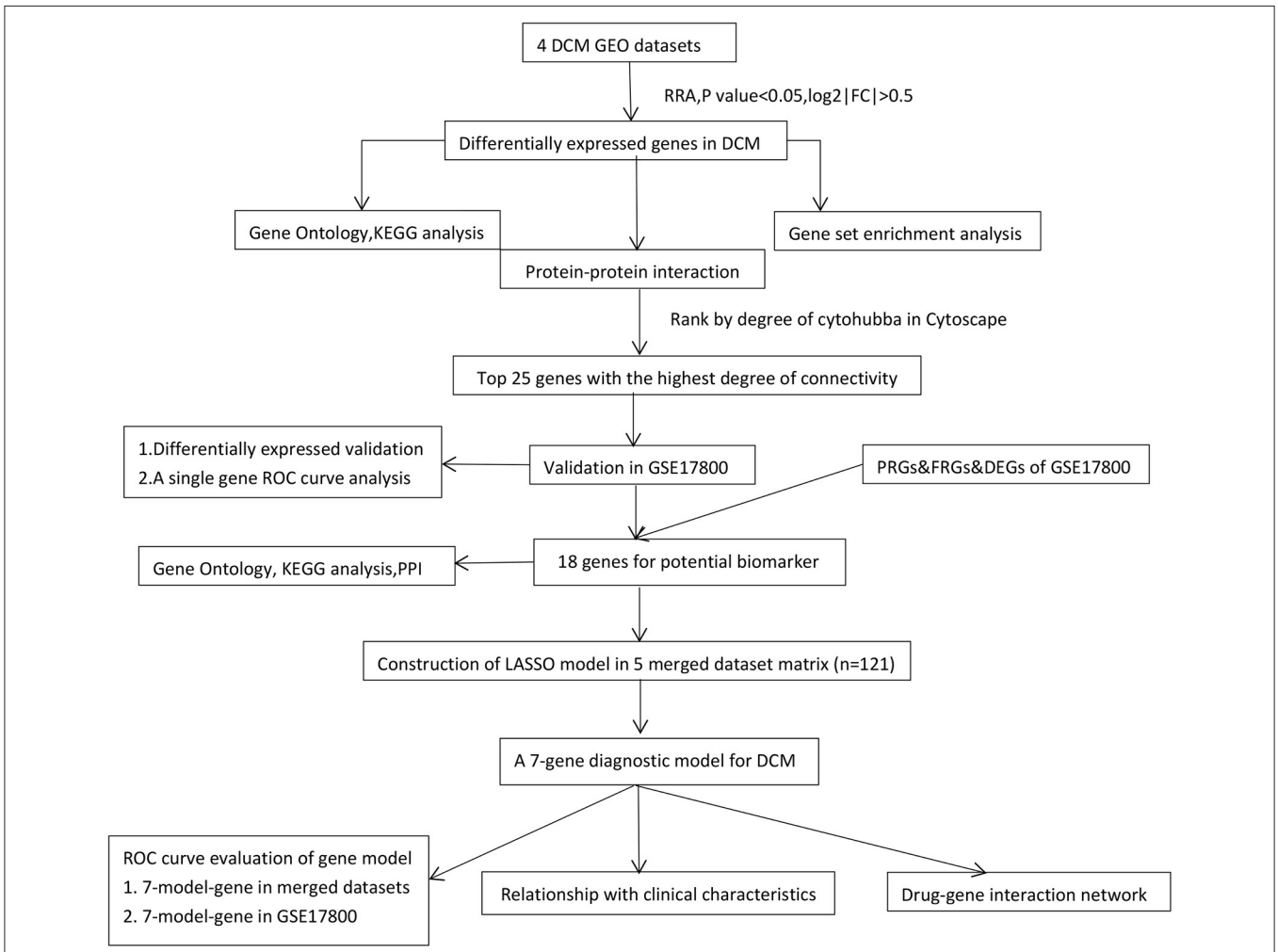

FIGURE 1 | The workflow of the study. DCM, dilated cardiomyopathy; RRA, Robust Rank Aggregation; LASSO, Least absolute shrinkage and selection operator; DEGs, differentially expressed genes; KEGG, Kyoto Encyclopedia of Genes and Genomes; PPI, protein-protein interaction; Con, control normal cardiac tissues; ROC, receiver operating characteristic; FRGs, ferroptosis-related genes; PRGs, pyroptosis-related genes.

and a limited number of patients have been included in most previous studies, which may compromise the prediction power or reliability. In-depth exploration of the public datasets can reveal disease related genes and develop a efficient risk gene signature in combination with clinicopathological characteristics (13), which can help to form a promising tool for predicting status of DCM and individualized therapy.

To explore potential pathogenesis and therapeutic targets of DCM, a series of analysis based on microarray chip data were performed. we developed a 7-gene DCM derived diagnosis signature (DCMDDS) distinguished DCM from NC with high specificity and sensitivity in both the training and validation cohorts. Besides, we performed gene-clinical feature correlation analysis on the 7-gene DCMDS, and predicted potential therapeutic targets via the DGIdb database. The present study provided new diagnostic markers and potential gene-based targeted treatment drug for DCM.

METHODS

Data Download

The workflow of the present study was shown in **Figure 1**. Four gene expression profiles of DCM, including GSE3585, GSE9800, GSE21610, and GSE42955, were downloaded from the Gene Expression Omnibus (GEO) (http://www.ncbi.nlm.nih.gov/geo accessed on 17 June 2021) and used to identify DEGs between DCM and normal cardiac (NC) tissue samples (**Table 1**). The criteria for selecting these datasets included: (1) Gene expression data must be available for both DCM and NCT samples, (2) at least 5,000 genes must be included when the microarray platform is used for expression profiling. In general, DCM is defined by patients with clinical features of a left ventricular end-diastolic diameter over than 56 mm and a left ventricular ejection fraction (LVEF) <50% (14). Exclusion criteria were genetic DCM or any cardiovascular, life-limiting systemic condition or an infectious or tumoral condition that may influence the definition of DCM. Of the five datasets (including the GSE17800 dataset below) with DCM, only four provided DCM definition (GSE3585 GSE17800, GSE21610 and GSE42955), and both datasets used the above criteria. In the GSE9800, a patient's DCM status was provided without specifying how it was defined. GEO belongs to public databases. The patients involved in the database have obtained ethical approval. Users can download these relevant data for free for research and publish relevant articles. A majority of data are based on open source data, so there are no ethical issues and other conflicts of interest.

Data Preprocessing and Identification of Robust Differentially Expressed Genes (DEGs)

R software (version 3.6.1) was performed to process and statistically analyze the expression files. We downloaded the series matrix files of datasets from GEO. The R package "limma" (15) was utilized to normalize the data and find DEGs, and a volcano map of DEGs was drawn using the "ggplot2" package (16) to show the DEGs. We then used RRA to integrate the results of those 4 datasets to find the most significant DEGs (17). The P value of each gene indicated its ranking in the final gene list, and genes with adjusted $P < 0.05$ and $\log2|FC| > 0.5$ were considered as significant DEGs in the RRA analysis.

Enrichment Analyses of GO and KEGG Pathway

Gene Ontology (GO) analysis and Kyoto Encyclopedia of Genes and Genomes (KEGG) analysis of DEGs were calculated using clusterProfiler package. clusterProfiler was a package of R software that was designed to compare and visualize functional profiles among gene clusters (18). A P value < 0.05 was considered to be significant, and the identified significant analyses were sorted by gene counts. Subsequently, the R package "RCircos" (version 1.2.1) (19) was used to visualize the expression patterns of different microarrays and chromosomal locations for the top 40 DEGs sorted by their P value.

Gene Set Enrichment Analysis

We performed gene set enrichment analysis (GSEA) using the gene expression matrix through the "clusterProfiler" package. "c2.cp.kegg.v7.0.symbols.gmt" was selected as the reference gene set (20). A false discovery rate (FDR) < 0.25 and $P < 0.05$ were considered significant enrichment.

TABLE 1 | The characteristic baseline of microarray.

Series accession	Normal(n)	DCM(n)	Samples	Platform	Author ref	Application
GSE3585	5	7	left ventricular tissue samples	GPL96 Affymetrix Human Genome U133A Array	Barth AS et al.	Integrated Analysis
GSE42955	5	12	left ventricle tissue samples	GPL6244 Affymetrix Human Gene 1.0 ST Array	Molina-Navarro MM et al.	Integrated Analysis
GSE9800	2	12	Left ventricular tissue samples	GPL887 Agilent-012097 Human 1A Microarray G4110B	Ohtsuki M et al.	Integrated Analysis
GSE21610	8	22	Left ventricular tissue samples	GPL570 [HG-U133_Plus_2] Affymetrix Human Genome U133 Plus 2.0 Array	Patrick Schwientek. et al.	Integrated Analysis
GSE17800	8	40	Myocardial biopsies tissue samples	GPL570 [HG-U133_Plus_2] Affymetrix Human Genome U133 Plus 2.0 Array	Sabine Ameling et al.	Validation and clinical relevance analysis

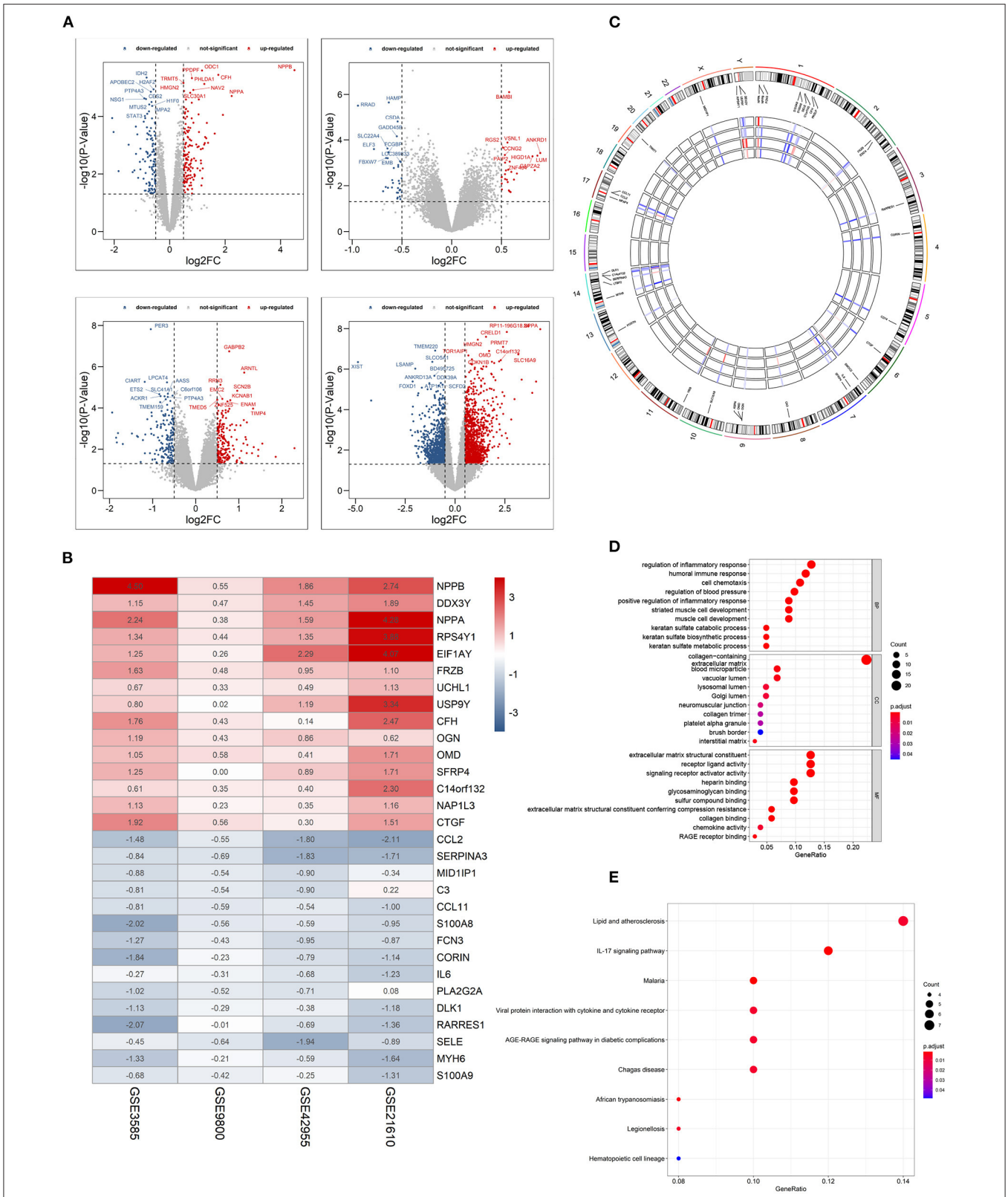

FIGURE 2 | Identification of differentially expressed genes (DEGs) between dilated cardiomyopathy cardiac and normal cardiac tissues samples from four unrelated cohorts. **(A)** Volcano plots of datasets GSE3585 and GSE9800 (upper panel), and GSE21610 and GSE42955 (lower panel) from the GEO database. DEGs with

(Continued)

FIGURE 2 | |log2 (Fold change)| > 0.5 would be listed, additionally. **(B)** Heatmap of the top 15 downregulated and the top 15 upregulated genes from Robust Rank Aggregation analysis of four datasets. Each column represents a dataset and each row a gene. The number in each rectangle represents the value of log2 (fold change). The gradual color ranging from blue to red represents the changing process from down- to up-regulation (DCM vs. Control). **(C)** Circular visualization of expression patterns and chromosomal positions of the top 40 DEGs. The outer circle represents chromosomes, and lines coming from each gene point to their specific chromosomal locations. **(D)** GO enrichment analyses of differentially expressed genes (DEGs) between localized DCM and normal cardiac samples. **(E)** KEGG pathway analyses of differentially expressed genes (DEGs) between localized DCM and normal cardiac samples. DCM, dilated cardiomyopathy; GO, Gene Ontology; KEGG, Kyoto Encyclopedia of Genes and Genomes. The size of each dot represents the count of genes, and the color represents the *p*-value.

Protein-Protein Interaction (PPI) Network

The PPI network was constructed with a threshold of medium confidence ≥0.4 through the Search Tool for the Retrieval of Interacting Genes (STRING) database (21). Cytoscape software (v3.6.1; http://www.cytoscape.org/) was used to visualize the network. Then, the top 25 genes with highest connectivity in the network were identified by DEGREE in cytoHubba (22).

The Identification and Validation of Hub Genes

The mRNA levels of high connectivity genes were verified in datasets GSE17800 and Student's *t* test was used to compare the expression levels of DCM and control groups. A list of 259 ferroptosis-related genes (FRGs) was identified through the ferroptosis database (FerrDb; http://www.zhounan.org/ferrdb) (23), a publicly available database of ferroptosis regulators, markers, and disease associations. A list of 34 pyroptosis-related genes (PRGs) from prior reviews and studies were also extracted (24, 25). The DEGs of GSE17800 was performed by limma package. And then, the DEGs in GSE17800 were intersected with FRGs/PRGs to obtain potential hub genes related to ferroptosis or pyroptosis. The high connectivity genes after validation and hub FRGs/PRGs were imported into the NCBI website for evaluating the expression abundance in normal human cardiac via high-throughput sequencing. Then, the gene expression with a threshold of RPKM in cardiac tissue ≥5 in NCBI Gene expression column was regarded as hub gene. To evaluate the identified ability of hub genes in DCM, ROC curve analysis were conducted in the GSE17800 data set through pROC package (26).

Construction of a Diagnostic Model and Correlation Analysis for DCM

To investigate whether the hub genes could be applied for predicting DCM occurrence, five datasets from the GEO database, GSE3585, GSE42955, GSE9800, GSE21610 and GSE17800, were pooled together, and the combined dataset was then adjusted for batch effect through the "ComBat" function of sva (version 3.34.0) R package (27) and assigned as the training set. The transcriptional profile of GSE17800 which included 40 DCM and 8 no-heart failure (NHF) samples, was used for the validation of the model. The predictability of the model was then evaluated by area under the curve (AUC) of ROC. The "ggstatsplot" package (https://indrajeetpatil.github.io/ggstatsplot/) was used to perform Spearman correlation analysis on diagnostic markers and the "ggplot2" package was used to visualize the results. A two-sided $p < 0.05$ was considered to be statistically significant.

RESULTS

Integrated Screening for Robust DCM-Associated Genes

Four GEO datasets were used for the identification of robust DCM-associated genes (**Table 1**). Using the "limma" R package, we normalized expression data from datasets GSE3585, GSE9800, GSE21610, and GSE42955, and identified 253, 60, 2078, and 370 DEGs between DCM and normal cardiac tissues respectively, with a cut-off of $p < 0.05$ and $\log2|FC| > 0.5$ (**Figure 2A**). Integration of all genes by the RRA method resulted in 117 DEGs ($|\log2FC| \geq 0.5$, $p < 0.05$), 100 of which were upregulated and 17 downregulated in DCM.

The top 15 upregulated and the top 15 downregulated genes in CRPC are shown as hierarchical cluster heatmaps (**Figure 2B**). For the top 40 DEGs between DCM and normal cardiac tissues, their expression patterns across the four datasets used for analysis, along with their chromosomal locations are shown in a circos plot (**Figure 2C**). The location of these 40 DEGs involves almost all chromosomes except for the 12, 15, 16, 18, 20, 21, 22 chromosome. The top three upregulated genes included NPPB, NPPA, and EIF1AY, and they are located on chromosomes 2, 6, 1, 17, and 2, respectively. The top three downregulated genes (CCL2, SERPINA3,RARRES1) are located on chromosomes 17, 14,and 3, respectively.

GO enrichment and KEGG pathway analyses were performed to further elucidate the potential biological function and the promising signaling pathways involving the entire 117 DEGs. With GO function analysis, we discovered that the DEGs are mostly enriched in biological process (BP), including the regulation of inflammatory response, the humoral immune response, the regulation of blood pressure, keratan sulfate metabolic process, and the striated muscle cell development. With regard to CC, the DEGs are enriched in the collagen–containing extracellular matrix, vacuolar lumen, blood microparticle, lysosomal lumen. As for molecular function, extracellular matrix structural constituent, signaling receptor activator activity, collagen binding and RAGE receptor binding (**Figure 2D**). In the KEGG pathway analysis, the DEGs participated in diverse infected signaling pathways, including Malaria, African trypanosomiasis, and Viral protein interaction with cytokine and cytokine receptor, Chagas disease and Legionellosis, and some immune-associated pathways such as the IL-17 signaling pathway (**Figure 2E**).

Gene Set Enrichment Analysis

Gene set enrichment analysis was also used to revealed the potential molecular mechanisms of DCM based on all gene

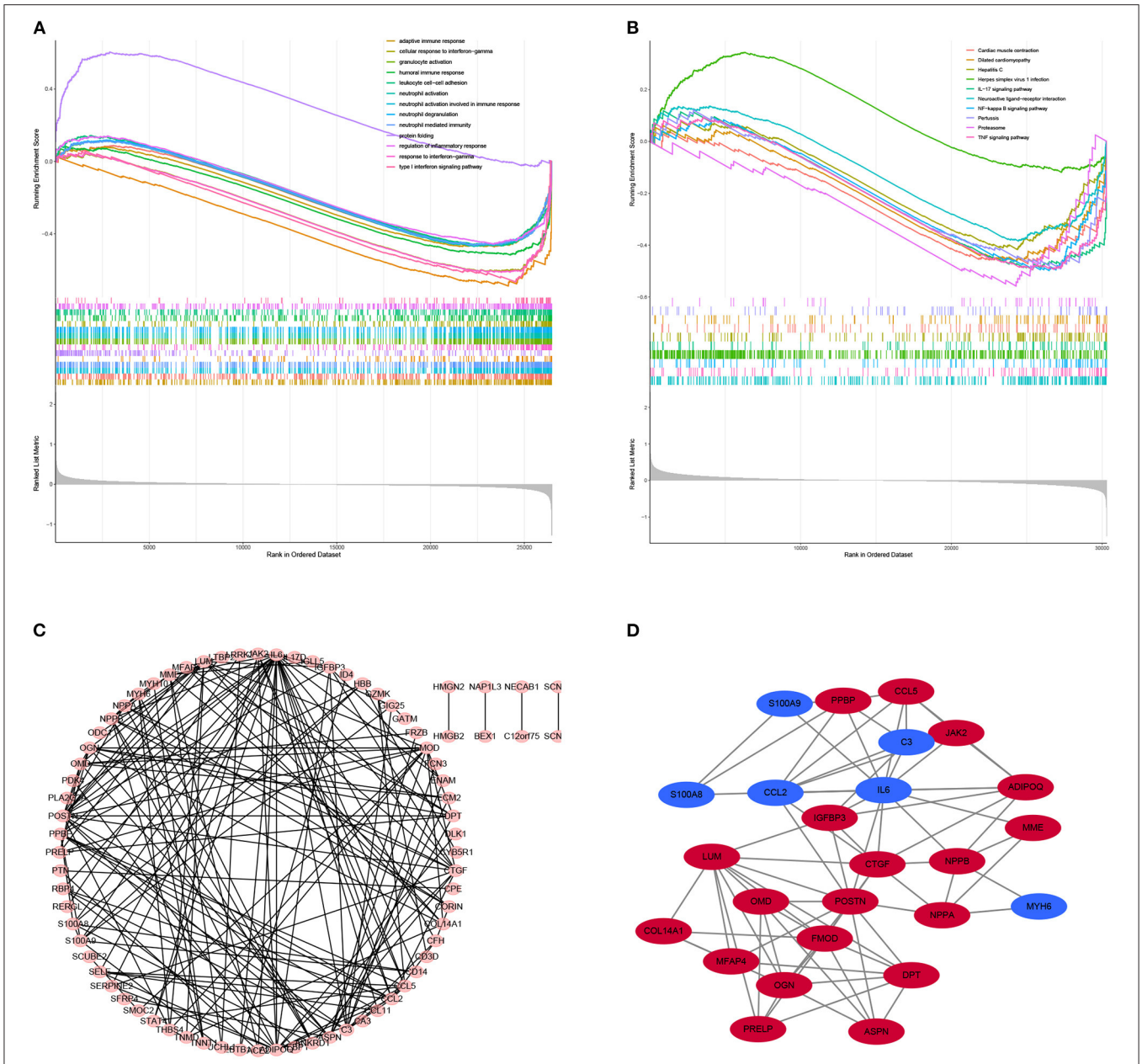

FIGURE 3 | Results of Gene Set Enrichment Analysis (GSEA) plots showing the most enriched gene sets of all detected genes in the DCM cardiac tissues and normal cardiac tissues in an integrated analysis of four datasets. **(A)** The top three most significant up-regulated enriched gene sets in the biological processes: protein folding, humoral immune response, regulation of inflammatory response. **(B)** The top three most significant up-regulated enriched gene sets in the Kyoto Encyclopedia of Genes and Genomes analysis: Herpes simplex virus 1 infection, Neuroactive ligand–receptor interaction, IL−17 signaling pathway. **(C)** PPI network of differentially expressed genes (DEGs). **(D)** Hub gene of differentially expressed genes.

information in the gene expression matrix. The enrichment analysis of gene sets revealed that compared to control samples, immune and inflammatory biological processes such as adaptive immune response, cellular response to interferon–gamma, neutrophil activation, protein folding, regulation of inflammatory response are significantly enriched in DCM (**Figure 3A**). The enriched KEGG pathways of GSEA showed that cardiac muscle contraction, dilated cardiomyopathy, hepatitis C, herpes simplex virus 1 infection and TNF signaling pathway are significantly enriched in DCM (**Figure 3B**).

PPI Network Analysis and Screening the Top 25 Genes With Highest Connectivity

STRING is an online tool for investigating and integrating interaction between proteins (21). PPI network of these genes was obtained after imputing the DEGs into the online tool STRING (**Figures 3C**, **4A**). In order to identify the top highest connectivity

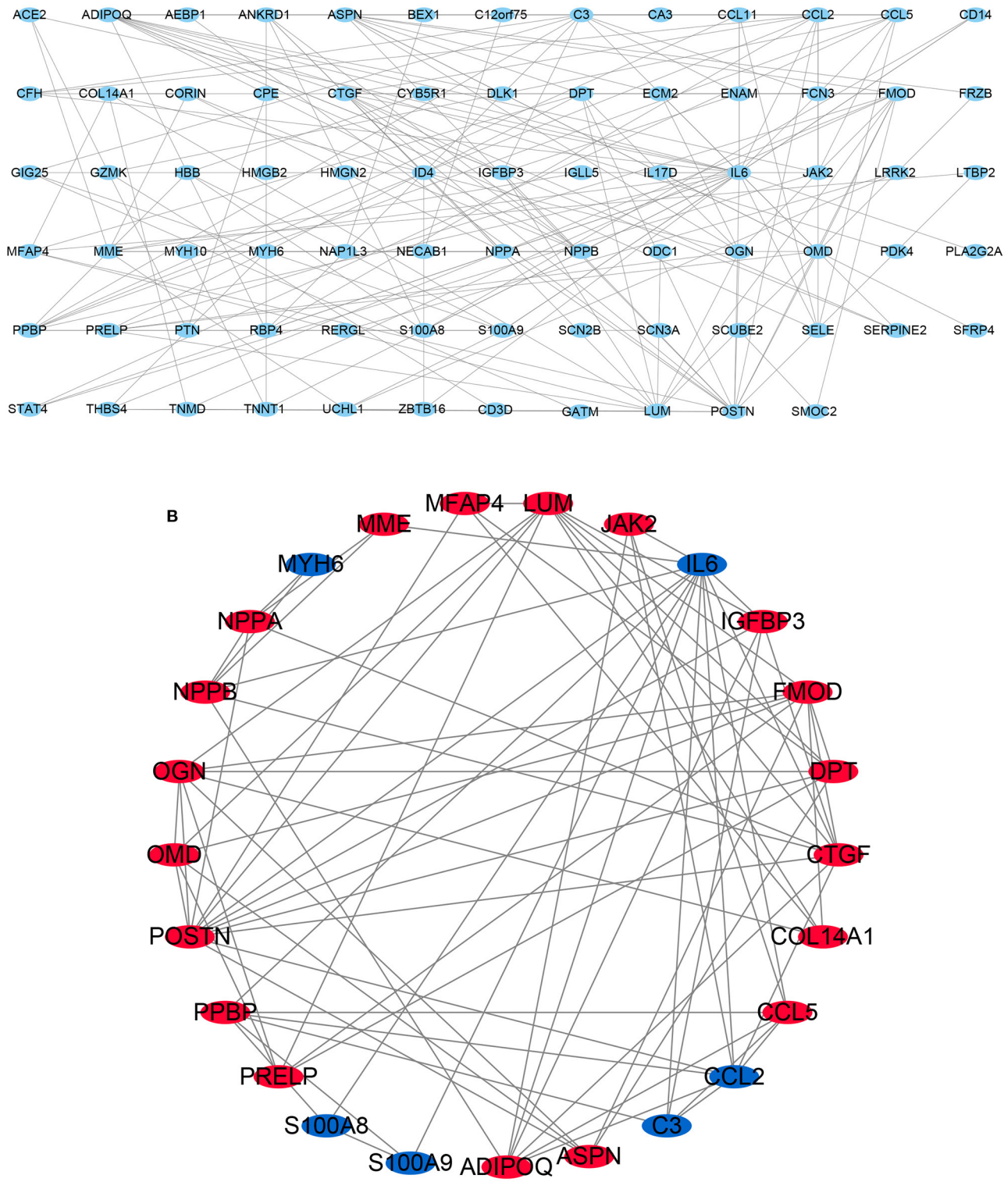

FIGURE 4 | Protein-protein interaction (PPI) network. **(A)** PPI network of 117 differentially expressed genes (DEGs). **(B)** subnetwork of top 25 genes with the highest degree of connectivity from the PPI network. Node color reflects the degree of connectivity (Red color represents a higher expression, and blue color represents a lower expression).

TABLE 2 | The clinical characteristics of GSE17800 in dilated cardiomyopathy.

Parameter	DCM group ($N = 40$)	Control group ($N = 8$)	*p* value
Age, years	50.21 ± 9.35	43.13 ± 14.76	0.084
Gender (Male/Female)	28/12	6/2	0.887
BMI, kg/m^2	27.88 ± 4.57	26.33 ± 5.26	0.303
LVEF, %	33.3 ± 6.4	59.8 ± 8.0	<0.001
LVIDD, mm	69.8 ± 8.0	51.4 ± 3.1	<0.001
Virus(Positive/Negative)	22/18	0/8	0.000
Inflammation	22 ± 23 or 18(12–22)	10 ± 3 or 10(8–13)	<0.001

BMI, body mass index; LVEF, left ventricular ejection fraction; LVIDD, left ventricular internal diameter at end-diastole.

25 genes in the network, the PPI network was imported into Cytoscape. And then, the top 25 genes with the highest degree of connectivity were calculated and extracted. Subsequently, the top 25 genes with the highest degree of connectivity were inputted into STRING to detect the interaction between proteins encoded by these genes (**Figures 3D**, **4B**).

Validation of the Expression of the Top 25 Genes With Highest Connectivity in Independent Patient Cohorts

There are 48 cardiac tissue samples including 40 DCM tissues and eight control tissues in GSE17800 dataset. This microarray also reported the information of patient's clinical features (**Table 2**). Independent patient cohorts fron GSE17800 dataset was used to verify the top 25 genes mRNA levels in DCM, which indicated that expression of ANKRD1, ASPN, CTGF, DPT, FMOD, MFAP4, OMD, JAK2, NPPA, NPPB and IGFBP3 was also significantly up-regulated and MYH6 was significantly down-regulated in DCM cardiac tissues as compared to normal cardiac tissues (**Figure 5**).

The Identification of Hub Genes and Functional Annotation Analysis

GSE17800 was also processed as previous. DEGs between DCM and normal cardiac tissues in GSE17800 were 1410. To explore potential ferroptosis or pyroptosis related genes in dilated cardiomyopathy, we intersected FRGs and PRGs with GSE17800's DEGS, and obtained 6 ferroptosis related differential genes including YY1AP1, CDKN1A, SRC, SESN2, CBS, and HSPB1 and 2 pyroptosis related differential genes including PRKACA and COL1A1 (**Figure 6A**). Next, the 13 high connectivity genes after validation and 8 FRGs/PRGs above were further import into NCBI respectively to test their expressive abundance in normal cardiac tissues. These genes with over than 5 mean RPKM were regarded as the hub genes (**Figure 6B**). To reveal potential biological process of these hub genes, GO and KEGG analyses were conducted. The most significant GO terms for biological process, keratan sulfate catabolic process, and keratan sulfate biosynthetic process, as well as KEGG pathways, were shown in **Figures 6C–G**. These analysis showed that these hub genes were mainly involved in keratan sulfate process, heart process and cGMP metabolic process. The PPI network of the 18 hub genes was also performed, which showed an interaction among them (except for YY1AP1) (**Figure 6H**).

Several Hub Genes Play a Diagnostic Role in DCM

A ROC curve analysis was performed to evaluated the diagnostic value of these hub genes in DCM. The results indicated that many genes, including ASPN ($AUC = 0.841$, $P < 0.0001$), COL1A2 ($AUC = 0.809$, $P < 0.0001$), DPT ($AUC = 0.844$, $P < 0.0001$), MYH6 ($AUC = 0.894$, $P < 0.0001$),NPPA ($AUC = 0.863$, $P < 0.0001$), NPPB ($AUC = 0.903$, $P < 0.0001$), PRELP ($AUC = 0.816$, $P < 0.0001$), PRKACA ($AUC = 0.822$, $P < 0.0001$) and YY1AP1 ($AUC = 0.891$, $P < 0.0001$), can efficiently distinguish DCM cardiac tissues from normal cardiac tissues (**Figures 7A–I**).

LAASO Model for Predicting DCM and Correlation of Clinicopathological Features and Model Genes

We extracted the expression profile of 18 hub genes from the merged datasets to construct LASSO model (**Figures 8A,B**). Through the LASSO, 7 genes were identified with non-zero regression coefficients, and the value of lambda.min = 0.03037093. ROC curve analysis indicated that the AUC of the 7-gene-based model was 0.938 in the merged gene set, which suggesting LASSO model may be used as a biomarker of DCM (**Figure 8C**). This model was further validated in a validation set (GSE17800) with AUC= 1 (**Figure 8D**).

Correlation heatmap of the 7 model genes and clinical factors revealed that LVEF had a significant positive correlation with MYH6 and had a significant negative correlation with LVIDD, ANKRD1, PRELP, COL1A1, CDKN1A. LVIDD had a significant negative correlation with MYH6 and had a significant positive correlation with inflammation, ANKRD1. Age and MYH6 had a significant negative correlation. The expression of MYH6 mRNA levels is associated with virus infection (**Figures 8E–J**).

Identification of the Potential Drugs

DGIdb was applied to determine the potential therapy drug that could reverse the expression of model gene in DCM. As shown in the drug–gene interaction network (**Figures 9A–D**), 18 drugs or molecular compounds included deoxycytidine, irinotecan hydrochloride, and cyclosporine, which differentially regulated the expression of ferroptosis-related gene CDKN1A. In addition, OMECAMTIV MECARBIL (INN), a cardiac specific myosin activator, was found to interact with MYH6. Further, collagenase clostridium histolyticum and antiplasmin regulated COL1A1 and 10 drugs or molecular compounds that included fasudil, SB-220025, SB-202190 and AST-487 regulated pyroptosis related gene PRKACA.

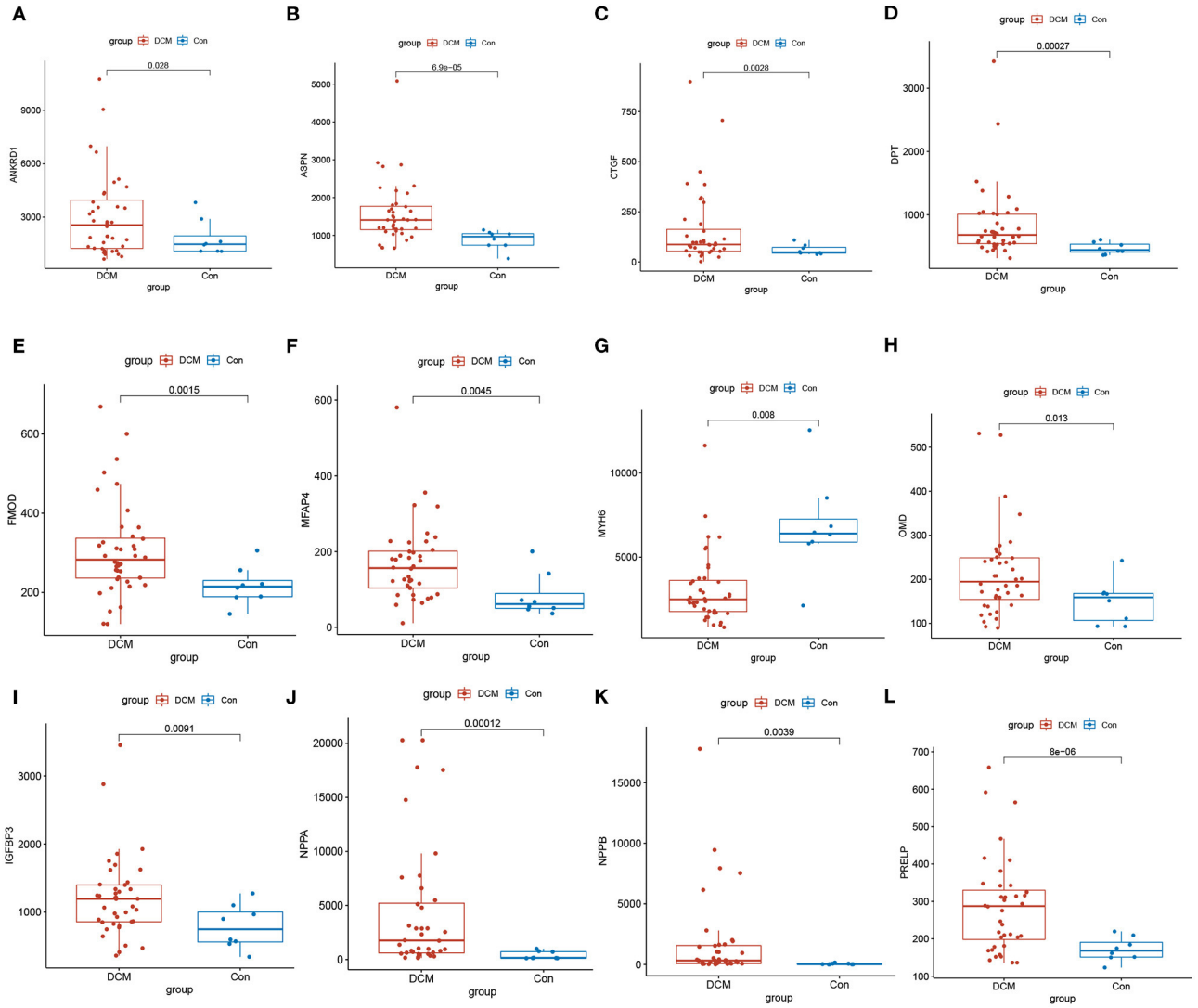

FIGURE 5 | Validation of top 25 genes with the highest degree of connectivity in GSE17800. The expression of genes **(A)** ANKRD1, **(B)** ASPN, **(C)** CTGF, **(D)** DPT, **(E)** FMOD1, **(F)** MFAP4, **(H)** OMD, **(I)** IGFBP3, **(J)** NPPA, **(K)** NPPB, **(L)** PRELP significantly upregulated, and **(G)** MYH6 significantly down regulated in the DCM in comparison to control group. DCM, dilated cardiomyopathy; Con, control group.

DISCUSSION

The pathogenesis of DCM, a complex and heterogeneous disease, remains unclear (28). Although many investigators have used microarray and RNA-seq to detect novel biomarkers and therapeutic targets for DCM, inconsistencies were seen between the DEGs found in different studies. To our knowledge, our work is the first to use RRA combined with LASSO regression model to explore novel hub genes associated with DCM. Previous studies compared gene expression profiles between DCM and non-heart failure samples for the dataset to explore hub gene and pathogenesis in DCM. However, these studies did not conduct link between gene expression and DCM clinical characteristics. This study integrated 4 qualified DCM datasets from GEO into the RRA method to identify DCM-associated genes and develop expression-based molecular signatures to predict DCM, some of which, such as NPPB (29) and ASPN (30), have been reported to be biomarkers of DCM or play an important role in its pathogenesis. In addition, associations of developed signatures with the clinicopathological characteristics of DCM were also evaluated.

Different from previous studies, GO analysis of differential genes in this study mainly involves the regulation of inflammatory response, immune response, keratinin sulfate processing and muscle cell contraction. And KEGG pathway analysis is mainly involved diverse infected signaling pathways, including Malaria, African trypanosomiasis, and Viral protein interaction with cytokine and cytokine receptor, Chagas disease and Legionellosis, and some immune-associated pathways such as the IL-17 signaling pathway. In addition, GSEA clarified a

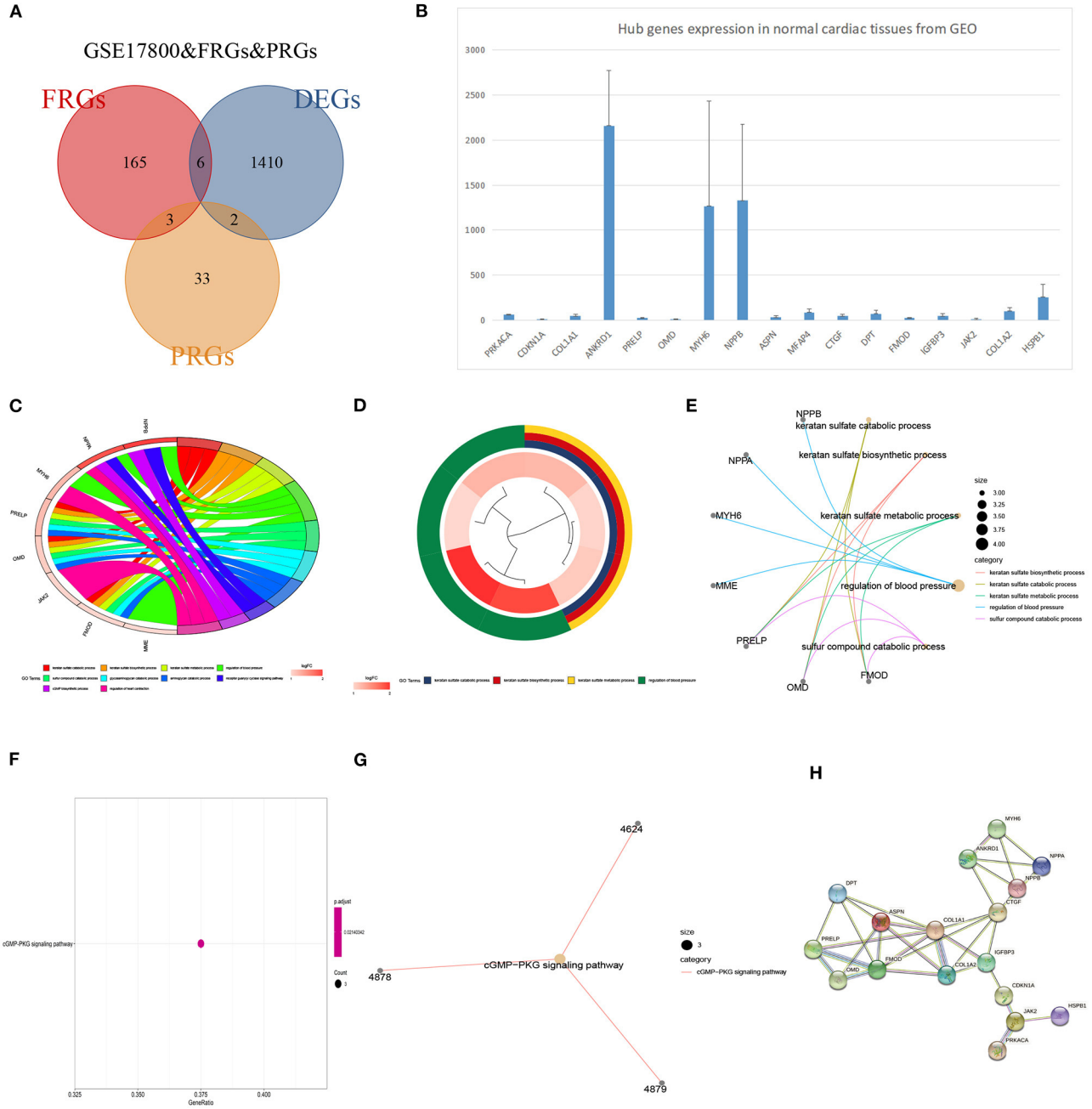

FIGURE 6 | The identification of DCM related genes and their functional analysis. **(A)** Venn diagram of ferroptosis-related genes, pyroptosis-related genes and DEGs in GSE17800. **(B)** The expression of potential biomarker genes including top 25 genes validated in GSE17800 and overlapping DEGs of ferroptosis-related genes, pyroptosis-related genes based on NCBI. **(C)** Chord plot shows the distribution of core genes in different GO-enriched functions. Symbols of core genes are presented on the left side of the graph with their fold change values mapped by color scale. **(D)** The top three significantly enriched Gene Ontology terms associated with potential biomarker genes. Gene involvement in the GO terms was determined by colored connecting lines. **(E)** Cluego network diagram shows the relationship between the potential biomarker genes and GO terms. **(F)** The bubble chart showed the KEGG pathway analyses of potential biomarker genes in DCM. **(G)** Cluego network diagram shows the relationship between the potential biomarker genes and KEGG terms. **(H)** PPI network of 18 potential biomarker genes.

new perspective for this study. It demonstrated that immune responses, such as adaptive immune response, cellular response to interferon–gamma, type I interferon signaling pathway, and inflammation responses including leukocyte cell-cell adhesion, neutrophil activation, neutrophil degranulation are involved in the pathophysiological process of dilated cardiomyopathy. Also, DCM process, some kinds of infections and two immune-related disease pathways that include IL-17 signaling pathway and TNF

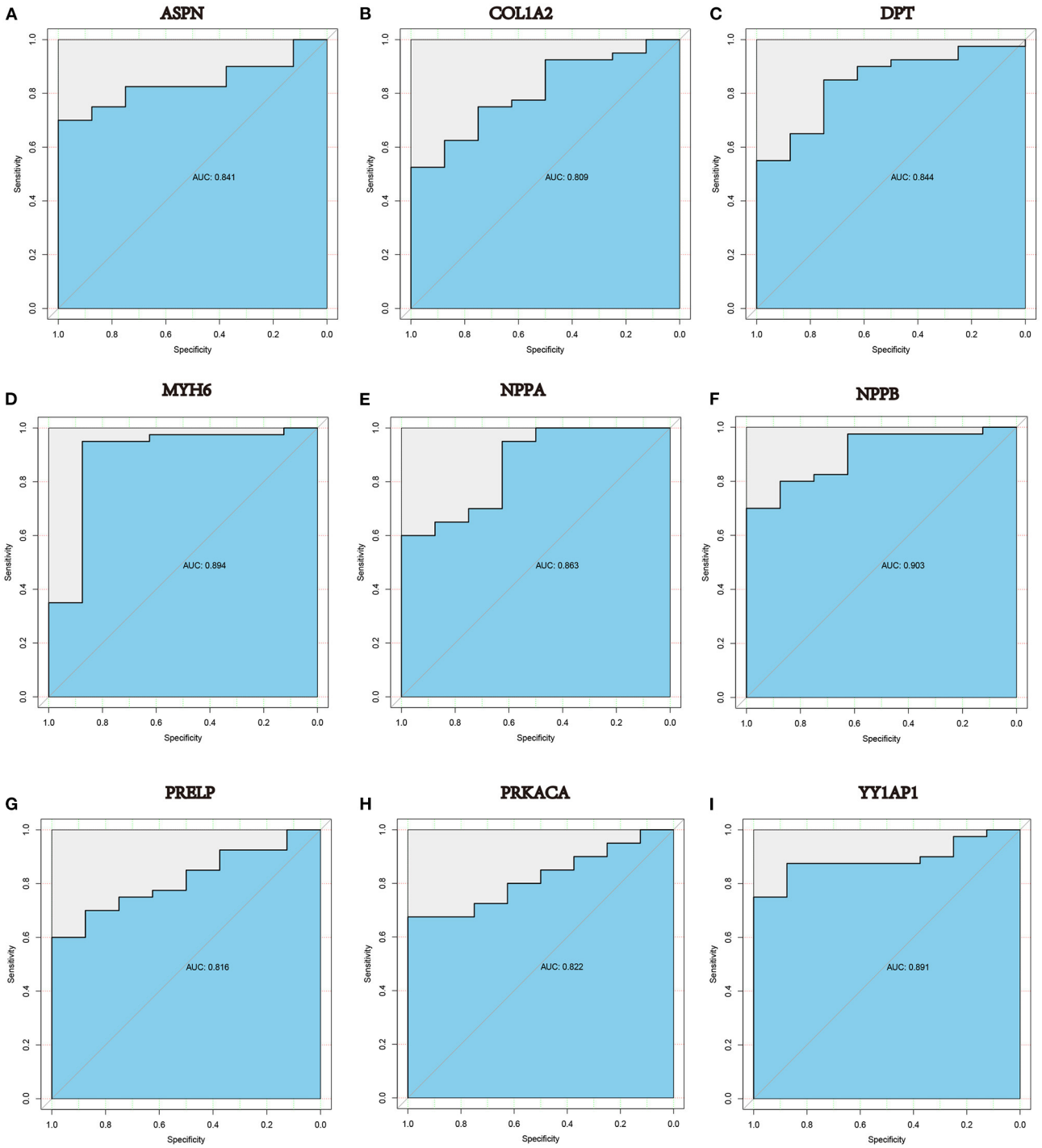

FIGURE 7 | ROC curve analysis in GSE17800 demonstrated that **(A)** ASPN, **(B)** COL1A2, **(C)** DPT, **(D)** MYH6, **(E)** NPPA, **(F)** NPPB, **(G)** PRELP, **(H)** PRKACA and **(I)** YY1AP1 may be diagnostic biomarkers in patients with DCM. AUC: area under the curve.

signaling pathway were involved. These confirmed that infection, inflammation and immune responses play important role in the development DCM.

Ferroptosis is reliant on a large number of cellular iron, interfering with the homeostasis of redox reactions, and eventually promoting cell death (31). Literature has indicated that iron-dependent ferroptosis is implicated in many cardiomyopathies (32). However, no studies have shown that ferroptosis is involved in the development of dilated cardiomyopathy; Moreover, pyroptosis is also another form

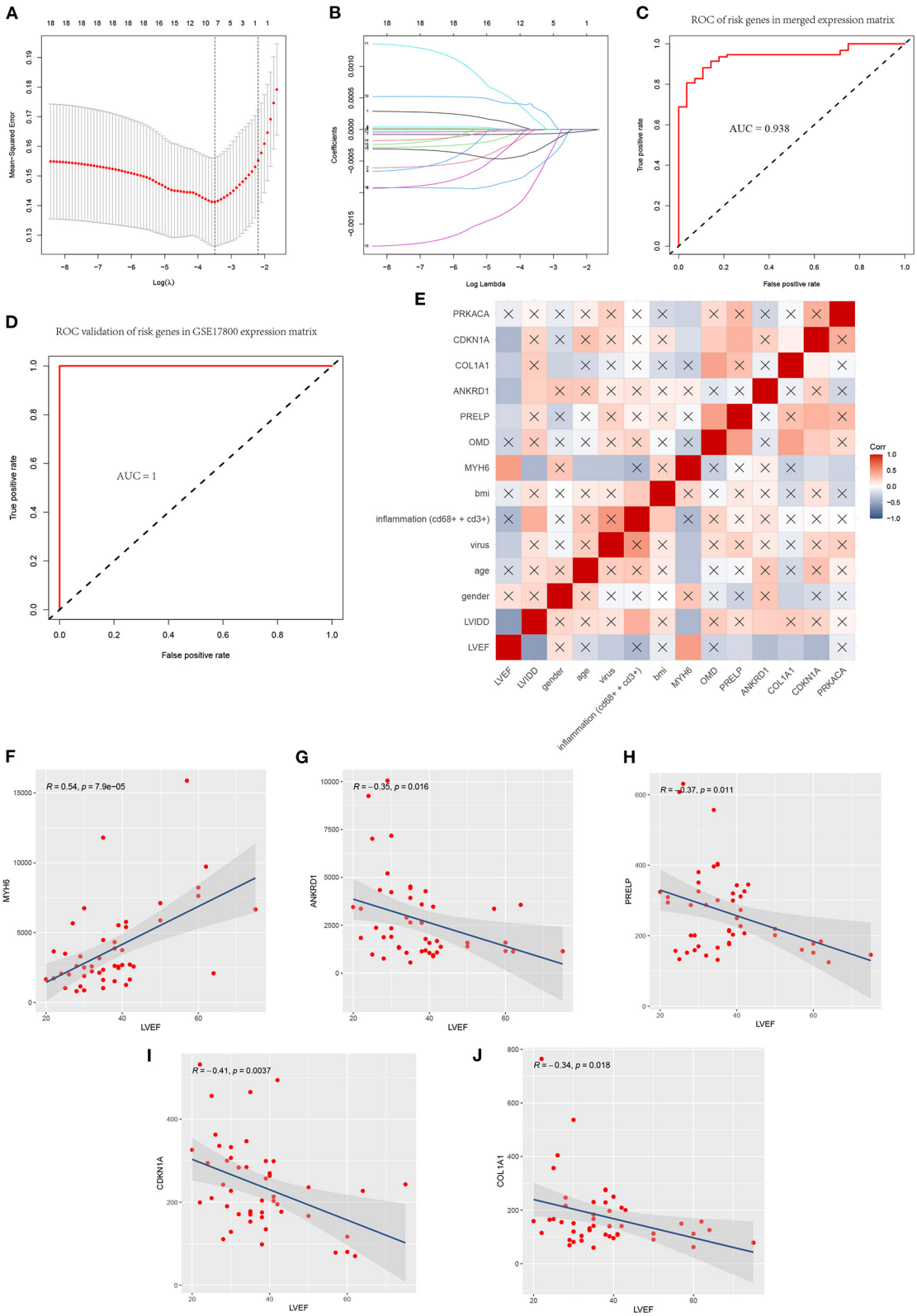

FIGURE 8 | A model for predicting DCM and correlation of clinicopathological features and model genes. **(A)** Least absolute shrinkage and selection operator (LASSO) logistic regression algorithm to screen diagnostic markers and risks genes in merged data matrix of five datasets. **(B)** Parameters of Lasso path and

(Continued)

FIGURE 8 | corresponding selected features of each fold. **(C)** ROC curve analysis of the 7-gene-based model in merged data matrix of five datasets (training set). **(D)** ROC curve analysis of the 7-gene-based model in GSE17800(validation set). **(E)** Correlation heat map of risks genes and clinicopathological features in datasets GSE17800. The depth of the color represents the strength of the correlation; red represents a positive correlation, blue represents a negative correlation. The "x" means irrelevance. Correlation analysis of left ventricular ejection fraction (LVEF) and **(F)** MYH6, **(G)** ANKRD1, **(H)** PRELP, **(I)** CDKN1A and **(J)** COL1A1.

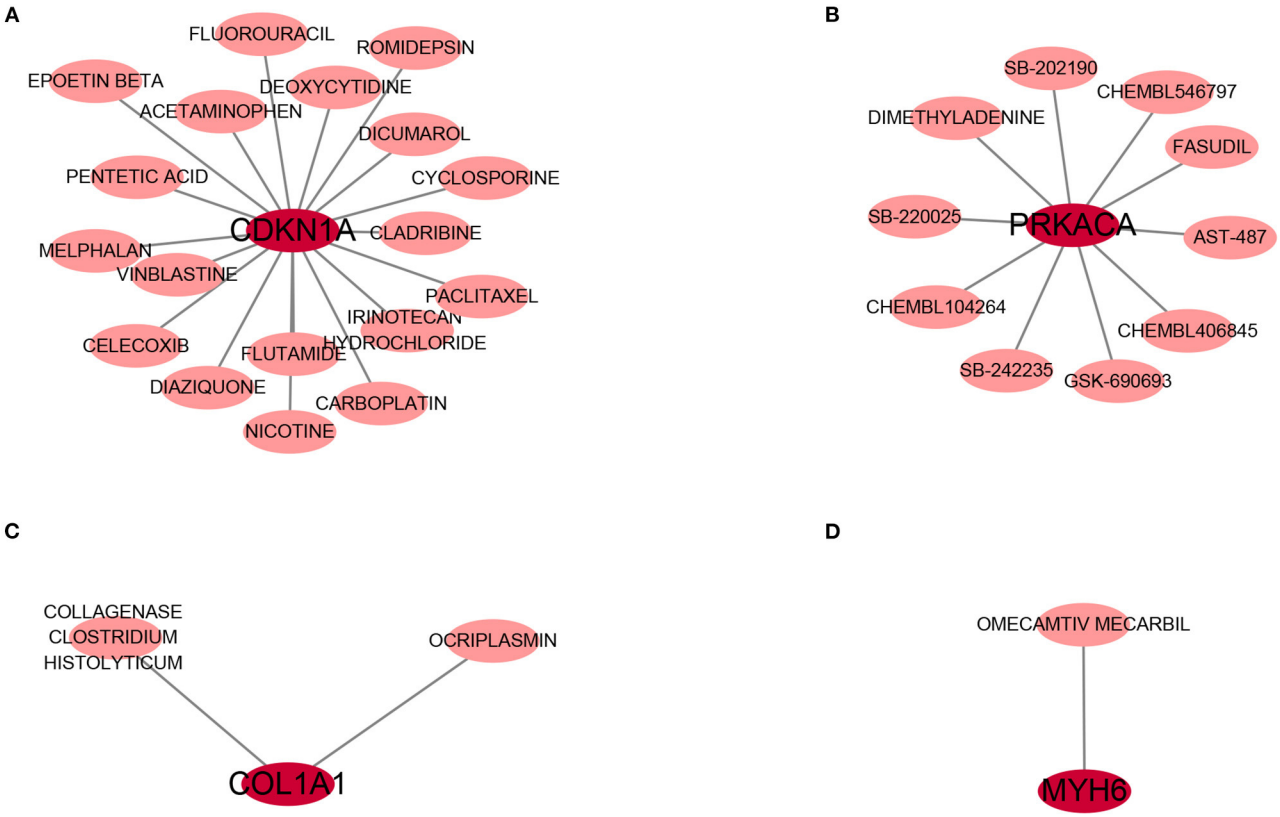

FIGURE 9 | The drug-gene interaction network. The dark red circle nodes in the center are the genes, and pale red nodes around are the drugs. **(A)** The interaction network of CDKN1A and its targeted compounds and drugs. **(B)** The interaction network of PRKACA and its targeted compounds and drugs. **(C)** The interaction network of COL1A1 and its targeted compounds and drugs. **(D)** The interaction network of MYH6 and its targeted compounds and drugs.

of cell death, which has only been shown in one study that NLRP3 inflammasome-mediated pyroptosis contributes to the pathogenesis of non-ischemic dilated cardiomyopathy (33). Therefore, the present study also for the first time reported ferroptosis related gene CDKN1A and pyroptosis related gene PRKACA may be involved in the development and progression of dilated cardiomyopathy.

We preliminarily obtained the possible core genes through protein interaction network and iron death or cell apoptosis related differential gene screening, and then carried out independent data set verification and expression abundance verification, and finally obtained the included 18 core genes. The 18 genes included up-regulated genes CDKN1A, COL1A1, ANKRD1, PRELP, OMD, NPPB, NPPA, ASPN, MFAP4, CTGF, DPT, FMOD, IGFBP3, JAK2, PRKACA and COL1A2, as well as down-regulated genes MYH6 and YY1AP1, which were mainly enriched in keratan sulfate process and cGMP–PKG signaling pathway through GO and KEGG analyses. some of them were demonstrated to exert essential roles in the pathogenesis of DCM (34–37). Among these hub genes, we further explore their diagnostic value in DCM, and found that nine genes have certain diagnostic value for dilated cardiomyopathy (AUC > 80%). Among them, NPPA (natriuretic peptide A) and NPPB (natriuretic peptide B) belong to the natriuretic peptide family, which encoded atrial natriuretic peptide (ANP) and brain natriuretic peptide (BNP) respectively (36). The natriuretic peptide family is a general name of a group of peptides secreted mainly by the cardiovascular system to regulate hydroelectrolyte balance, reduce cardiac afterload, and dilate blood vessels through natriuretic diuresis (38). In heart failure, NPPB is expressed at a high level in DCM, and patients with higher BNP level have a worse cardiac function (39, 40).

Combined LASSO and the forward stepwise selection analyses of the 18 genes resulted in the most robust model with the fewest genes capable of predicting DCM, a panel of seven genes including ANKRD1, PRELP, PRKACA, COL1A1, OMD, MYH6 and CDKN1A significantly correlates with DCM. This seven-gene panel was named DCM derived diagnostic signature

(DCMDDS), and the DCMDDS score is based on the seven genes' expression levels and regression coefficients. The model was validated in 5 patient cohorts, comprising more than 120 patients. Interestingly, five of the seven DCMDDS genes were associated with left ventricular ejection fraction based on their expression levels and correlation coefficients, as demonstrated by the Spearman correlation analysis. Among DCMDDS genes, MYH6, ANKRD1 and COL1A1 have been showed to participated in the development of DCM, while PRELP, PRKACA, CDKN1A and OMD seldomly reported.

PERELP, proline and arginine rich end leucine rich repeat protein, is a member of the leucine-rich repeat (LRR) family of extracellular matrix proteins in connective tissue (41). It is unclear whether PERELP plays a role in DCM and other cardiomyopathy. Data from the Human Protein Atlas (HPA) revealed that PRELP is secreted to the extracellular matrix and may anchor basement membranes to the underlying connective tissue (42), suggesting its potential function in maintaining normal cellular structure. Besides, previous studies have suggested that PERELP has prognostic value in hepatocellular carcinoma and regulates the extracellular matrix and collagen mineralization in the bone system (43, 44).

PRKACA is a gene encoding the cAMP-dependent protein kinase A (PKA) catalytic subunits alpha. PKA can directly phosphorylate the cytoplasmic receptor NLRP3 and attenuate its ATPase function, which showed a relationship to pyroptosis (45). Therefore, PRKACA was regarded as a pyroptosis-related gene (24). Prolonged and elevated cyclic adenylyl monophosphate (cAMP) levels have been observed in both heart failure and several cardiomyopathy, while PKA is promptly activated by increasing intracellular concentrations of cAMP synthesized by adenylyl Cyclases (46, 47). These revealed that regulating PKA phosphorylation may be a therapeutic strategy for certain stages of progressive and congestive heart failure (48). However, its role in DCM still not be reported.

CDKN1A (cyclin-dependent kinase inhibitor 1A) encodes p21, plays an important role in the pathological process of P53-mediated ferroptosis (49). CDKN1A is a potent cell cycle inhibitor that mediates post-natal cardiomyocyte cell cycle arrest. Although no reported in DCM, CDKN1A is implicated in LMNA-mediated cellular stress responses, and the mutation of LMNA is one of the important mechanisms DCM (50, 51). Moreover, Shah et al. also found the mutations in the CDKN1A gene in the blood of patients with heart failure (52).

OMD (Osteomodulin) is a leucine- and aspartic acid-rich keratan sulfate proteoglycan, which belongs to the small leucine-rich proteoglycan family (SLRP) family (53). A recent study shown that OMD could directly bind to Type I collagen, further regulating the diameter and shape of collagen fbrils (54). Interestingly, the results of the present study also suggest a positive correlation between OMD and COL1A1, and its functional analysis mainly involved in extracellular matrix processes. Extracellular matrix fibrosis is regarded as an important process in the development of DCM (55). Therefore, targeted OMD gene therapy may be a potential therapeutic strategy for dilated cardiomyopathy. Guo et al. also found that Osteomodulin is a potential genetic target for hypertrophic cardiomyopathy (56).

To found the potential effective therapy for DCM, DGIdb database was used to exam therapeutic agents that might reverse the abnormally expression of DCMDDS genes. OMECAMTIV MECARBIL (INN), previously codenamed CK-1827452, is a cardiac specific myosin activator. It is clinically tested for its role in the treatment of left ventricular systolic heart failure (57). In the present study, MYH6 was down-regulated in DCM, while OMECAMTIV MECARBIL can target and activate it. This means that MYH6 may be one of the important targeted gene of OMECAMTIV MECARBIL in the treatment of heart failure. COL1A1, one of the component collagen type I, is the main component of extracellular matrix. Elevated expression levels of COL1A1 will lead to fibrosis of extracellular matrix of cardiac muscle (58). Collagenase clostridium histolyticum and antiplasmin might be a effective anti-fibrosis therapy approach in DCM via targeting COL1A1. The roles of the drugs or molecular compounds above in DCM still need to be further explored as potential therapeutic targets.

There were several limitations in our study. First, due to limited conditions, myocardial biopsy tissue specimens were not obtained to carry out basic experiments for verification. Nevertheless, we used a multi-chip combined analysis method and validated in external DCM samples to ensure the accuracy of the bioinformatics analysis in the study. In addition, in our analysis results, NPPA, NPPB, COL1A2, ASPN, ANKRD1 and CTGF were all confirmed to be closely related to heart failure in dilated cardiomyopathy in various studies. Second, the sample size of our multi-chip combined analysis was significantly expanded. However, due to the difficulty and high risk of myocardial tissue biopsy, the sample size of the data set in our study was still relatively small. Third, although we explored the relationship between genes and clinical factors, we failed to obtain prognostic information from datasets, and we could not further explore the relationship between DCMDDS genes and patient outcomes.

In summary, by combining RRA, LASSO, and other bioinformatics tools, this study identified 117 robust DEGs between DCM and NFH samples, many of which were not reported in previous studies. A 7-gene panel derived from the 117 DCM-associated genes comprised of a diagnostic model predictive of DCM. Five of the seven genes were closely related to left ventricular ejection fraction. Therefore, these gene signatures may help develop DCM biomarkers via large-scale randomized clinical trials.

DATA AVAILABILITY STATEMENT

The datasets presented in this study can be found in online repositories. The names of the repository/repositories and accession number(s) can be found in the article/supplementary material.

AUTHOR CONTRIBUTIONS

XM, CM, and CG designed the present study, which was performed by XM, CM, and PC. XM and LH made substantial

contributions to acquisition and analysis of data. XM and LS also made contributions to interpretation of data. XM wrote the initial draft of the manuscript. LH revised it critically for important intellectual content. All authors have participated sufficiently in the work to take public responsibility for appropriate portions of the content and approved the manuscript, as well as agreed to be accountable for all aspects of the work. All authors read and approved the final manuscript.

FUNDING

The present study was supported by the National Nature Science Foundation of China (Grant No. 81770333).

ACKNOWLEDGMENTS

We acknowledge GEO database for providing their platforms and contributors for uploading their meaningful datasets.

REFERENCES

1. Merlo M, Cannatà A, Gobbo M, Stolfo D, Elliott PM, Sinagra G. Evolving concepts in dilated cardiomyopathy. *Eur J Heart Fail.* (2018) 20:228–39. doi: 10.1002/ejhf.1103
2. Tayal U, Prasad S, Cook SA. Genetics and genomics of dilated cardiomyopathy and systolic heart failure. *Genome Med.* (2017) 9:20. doi: 10.1186/s13073-017-0410-8
3. Verdonschot J, Hazebroek M, Merken J, Debing Y, Dennert R, Rocca HPBL, et al. Relevance of cardiac parvovirus B19 in myocarditis and dilated cardiomyopathy: review of the literature. *Eur J Heart Fail.* (2016) 18:1430–41. doi: 10.1002/ejhf.665
4. Ameling S, Herda LR, Hammer E, Steil L, Teumer A, Trimpert C, et al. Myocardial gene expression profiles and cardiodepressant autoantibodies predict response of patients with dilated cardiomyopathy to immunoadsorption therapy. *Eur Heart J.* (2013) 34:666–75. doi: 10.1093/eurheartj/ehs330
5. Merlo M, Pivetta A, Pinamonti B, Stolfo D, Zecchin M, Barbati G, et al. Long-term prognostic impact of therapeutic strategies in patients with idiopathic dilated cardiomyopathy: changing mortality over the last 30 years. *Eur J Heart Fail.* (2014) 16:317–24. doi: 10.1002/ejhf.16
6. Merlo M, Pyxaras SA, Pinamonti B, Barbati G, Di Lenarda A, Sinagra G. Prevalence and prognostic significance of left ventricular reverse remodeling in dilated cardiomyopathy receiving tailored medical treatment. *J Am Coll Cardiol.* (2011) 57:1468–76. doi: 10.1016/j.jacc.2010.11.030
7. Gulati A, Jabbour A, Ismail TF, Guha K, Khwaja J, Raza S, et al. Association of fibrosis with mortality and sudden cardiac death in patients with nonischemic dilated cardiomyopathy. *JAMA.* (2013) 309:896–908. doi: 10.1001/jama.2013.1363
8. Køber L, Thune JJ, Nielsen JC, Haarbo J, Videbæk L, Korup E, et al. Defibrillator implantation in patients with non ischemic systolic heart failure. *N Engl J Med.* (2016) 375:1221–30. doi: 10.1056/NEJMoa1608029
9. Li N, Wu H, Geng R, Tang Q. Identification of core gene biomarkers in patients with diabetic cardiomyopathy. *DisMarkers.* (2018) 2018:6025061. doi: 10.1155/2018/6025061
10. Chen R, Ge T, Jiang W, Huo J, Chang Q, Geng J, et al. Identification of biomarkers correlated with hypertrophic cardiomyopathy with co-expression analysis. *J Cell Physiol.* (2019) 234:21999–2008. doi: 10.1002/jcp.28762
11. Zhang H, Yu Z, He J, Hua B, Zhang G. Identification of the molecular mechanisms underlying dilated cardiomyopathy via bioinformatic analysis of gene expression profiles. *Exp Ther Med.* (2017) 13:273–9. doi: 10.3892/etm.2016.3953
12. Tao L,Yang L, Huang X, Hua F, Yang X. Reconstruction and analysis of the lncRNA-miRNA-mRNA network based on competitive endogenous RNA reveal functional lncrnas in dilated cardiomyopathy. *Front Genet.* (2019) 10:1149. doi: 10.3389/fgene.2019.01149
13. Liu X, Yin M, Liu X, Da J, Zhang K, Zhang X, et al. Analysis of hub genes involved in distinction between aged and fetal bone marrow mesenchymal stem cells by robust rank aggregation and multiple functional annotation methods. *Front Genet.* (2020) 11:573877. doi: 10.3389/fgene.2020.573877
14. Calderon-Dominguez M, Belmonte T, Quezada-Feijoo M, Ramos M, Calderon-Dominguez J, Campuzano O, et al. Plasma microrna expression profile for reduced ejection fraction in dilated cardiomyopathy. *Sci Rep.* (2021) 11:7517. doi: 10.1038/s41598-021-87086-1
15. Ritchie ME, Phipson B, Wu D, Hu Y, Law CW, Shi W, et al. limma powers differential expression analyses for RNA-sequencing and microarray studies. *Nucleic Acids Res.* (2015) 43:e47. doi: 10.1093/nar/gkv007
16. Raaphorst RV, Kjos M, Veening J. Bactmap: an r package for integrating, analyzing and visualizing bacterial microscopy data. *Mol Microbiol.* (2020) 113:297–308. doi: 10.1111/mmi.14417
17. Kolde R, Laur S, Adler P, Vilo J. Robust rank aggregation for gene list integration and meta-analysis. *Bioinformatics.* (2012) 28:573–80. doi: 10.1093/bioinformatics/btr709
18. Yu G, Wang L, Han Y, He Q. clusterProfiler: an R package for comparing biological themes among gene clusters. *OMICS.* (2012) 16:284–7. doi: 10.1089/omi.2011.0118
19. Zhang H, Meltzer P, Davis S. RCircos: an R package for Circos 2D track plots. *BMC Bioinformatics.* (2013) 14:244. doi: 10.1186/1471-2105-14-244
20. Liberzon A, Birger C, Thorvaldsdóttir H, Ghandi M, Mesirov JP, Tamayo P. The Molecular Signatures Database (MSigDB) hallmark gene set collection. *Cell Syst.* (2015) 1:417–25. doi: 10.1016/j.cels.2015.12.004
21. Szklarczyk D, Morris JH, Cook H, Kuhn M, Wyder S, Simonovic M, et al. The STRING database in 2017: quality-controlled protein-protein association networks, made broadly accessible. *Nucleic Acids Res.* (2017) 45:D362–8. doi: 10.1093/nar/gkw937
22. Hu J, Zhou L, Song Z, Xiong M, Zhang Y, Yang Y, et al. The identification of new biomarkers for bladder cancer: a study based on TCGA and GEO datasets. *J Cell Physiol.* (2019) 1–12. doi: 10.1002/jcp.28208
23. Zhou N, Bao J. FerrDb: a manually curated resource for regulators and markers of ferroptosis and ferroptosis-disease associations. *Database (Oxford).* (2020) 2020:baaa021. doi: 10.1093/database/baaa021
24. Ye Y, Dai Q, Qi H. A novel defined pyroptosis-related gene signature for predicting the prognosis of ovarian cancer. *Cell Death Discov.* (2021) 7:71. doi: 10.1038/s41420-021-00451-x
25. Zhang L, Zhang L, Huang Z, Xing R, Li X, Yin S, et al. αIncreased HIF-1 in knee osteoarthritis aggravate synovial fibrosis via fibroblast-like synoviocyte pyroptosis. *Oxid Med Cell Longev.* (2019) 2019:6326517. doi: 10.1155/2019/6326517
26. Robin X, Turck N, Hainard A, Tiberti N, Lisacek F, Sanchez JC, et al. pROC: an open-source package for R and S+ to analyze and compare ROC curves. *BMC Bioinformatics.* (2011) 12:77. doi: 10.1186/1471-2105-12-77
27. Parker HS, Leek JT, Favorov AV, Considine M, Xia X, Chavan S, et al. Preserving biological heterogeneity with a permuted surrogate variable analysis for genomics batch correction. *Bioinformatics.* (2014) 30:2757–63. doi: 10.1093/bioinformatics/btu375
28. Zecchin M, Merlo M, Pivetta A, Barbati G, Lutman C, Gregori D, et al. How can optimization of medical treatment avoid unnecessary implantable cardioverter-defibrillator implantations in patients with idiopathic dilated cardiomyopathy presenting with "SCD-HeFT criteria?" *Am J Cardiol.* (2012) 109:729–735. doi: 10.1016/j.amjcard.2011.10.033
29. Witt E, Hammer E, Dörr M, Weitmann K, Beug D, Lehnert K, et al. Correlation of gene expression and clinical parameters identifies a set of genes reflecting LV systolic dysfunction and morphological alterations. *Physiol Genomics.* (2019) 51:356–67. doi: 10.1152/physiolgenomics.00111.2018
30. Zhang K, Wu M, Qin X, Wen P, Wu Y, Zhuang J. Asporin is a potential promising biomarker for common heart failure. *DNA Cell Biol.* (2021) 40:303–15. doi: 10.1089/dna.2020.5995

31. Zhai Z, Zou P, Liu F, Xia Z, Li J. Ferroptosis Is a Potential Novel Diagnostic and Therapeutic Target for Patients With Cardiomyopathy. *Front Cell Dev Biol.* (2021) 9:649045. doi: 10.3389/fcell.2021.649045
32. Rosenbaum AN, Agre KE, Pereira NL. Genetics of dilated cardiomyopathy: practical implications for heart failure management. *Nat Rev Cardiol.* (2020) 17:286–97. doi: 10.1038/s41569-019-0284-0
33. Zeng C, Duan F, Hu J, Luo B, Huang B, Lou X, et al. NLRP3 inflammasome-mediated pyroptosis contributes to the pathogenesis of non-ischemic dilated cardiomyopathy. *Redox Biol.* (2020) 34:101523. doi: 10.1016/j.redox.2020.101523
34. Wittchen F, Suckau L, Witt H, Skurk C, Lassner D, Fechner H, et al. Genomic expression profiling of human inflammatory cardiomyopathy (DCMi) suggests novel therapeutic targets. *J Mol Med (Berl).* (2007) 85:257–71. doi: 10.1007/s00109-006-0122-9
35. Jordan E, Peterson L, Ai T, Asatryan B, Bronicki L, Brown E, et al. An Evidence-Based Assessment of Genes in Dilated Cardiomyopathy. *Circulation*. (2021) 144:7–19. doi: 10.1161/CIRCULATIONAHA.120.053033
36. Feng J, Perry G, Mori T, Hayashi T, Oparil S, Chen Y. Pressure-independent enhancement of cardiac hypertrophy in atrial natriuretic peptide-deficient mice. *Clin Exp Pharmacol Physiol.* (2003) 30:343–9. doi: 10.1046/j.1440-1681.2003.03836.x
37. Mihailovici AR, Deliu RC, Mărgăritescu C, Simionescu CE, Donoiu I, Istrătoaie O, Tudorașcu DR, Târtea EA, Gheonea DI. Collagen I and III, MMP-1 and TIMP-1 immunoexpression in dilated cardiomyopathy. *Rom J Morphol Embryol.* (2017) 58:777–81.
38. Kuhn M. Molecular physiology of natriuretic peptide signalling. *Basic Res Cardiol.* (2004) 99:76–82. doi: 10.1007/s00395-004-0460-0
39. Verstreken S, Delrue L, Goethals M, Bartunek J, Vanderheyden M. Natriuretic peptide processing in patients with and without left ventricular dysfunction. *Int Heart J.* (2019) 60:115–20. doi: 10.1536/ihj.18-012
40. Lemaître AI, Picard F, Maurin V, Faure M, Dos SP, Girerd N. Clinical profile and midterm prognosis of left ventricular thrombus in heart failure. *ESC Heart Fail.* (2021) 8:1333–41. doi: 10.1002/ehf2.13211
41. Bengtsson E, Neame PJ, Heinegård D, Sommarin Y. The primary structure of a basic leucine-rich repeat protein, PRELP, found in connective tissues. *J Biol Chem.* (1995) 270:25639–44. doi: 10.1074/jbc.270.43.25639
42. Uhlén M, Fagerberg L, Hallström BM, Lindskog C, Oksvold P, Mardinoglu A, et al. Proteomics. Tissue-based map of the human proteome. *Science.* (2015) 347:1260419. doi: 10.1126/science.1260419
43. Hong R, Gu J, Niu G, Hu Z, Zhang X, Song T, et al. PRELP has prognostic value and regulates cell proliferation and migration in hepatocellular carcinoma. *J Cancer.* (2020) 11:6376–89. doi: 10.7150/jca.46309
44. Sinkeviciute D, Skovlund GS, Sun S, Manon JT, Aspberg A, Önnerfjord P, et al. A novel biomarker of MMP-cleaved prolargin is elevated in patients with psoriatic arthritis. *Sci Rep.* (2020) 10:13541. doi: 10.1038/s41598-020-70327-0
45. Mortimer L, Moreau F, MacDonald JA, Chadee K. NLRP3 inflammasome inhibition is disrupted in a group of auto-inflammatory disease CAPS mutations. *Nat Immunol.* (2016) 17:1176–86. doi: 10.1038/ni.3538
46. Taskén K, Aandahl EM. Localized effects of cAMP mediated by distinct routes of protein kinase A. *Physiol Rev.* (2004) 84:137–67. doi: 10.1152/physrev.00021.2003
47. Hsiao YT, Shimizu I, Wakasugi T, Yoshida Y, Ikegami R, Hayashi Y, et al. Cardiac mitofusin-1 is reduced in non-responding patients with idiopathic dilated cardiomyopathy. *Sci Rep.* (2021) 11:6722. doi: 10.1038/s41598-021-86209-y
48. Liu Y, Chen J, Fontes SK, Bautista EN, Cheng Z. Physiological and pathological roles of protein kinase A in the heart. *Cardiovasc Res.* (2021) cvab008. doi: 10.1093/cvr/cvab008
49. Kang R, Kroemer G, Tang D. The tumor suppressor protein p53 and the ferroptosis network. *Free Radic Biol Med.* (2019) 133:162–8. doi: 10.1016/j.freeradbiomed.2018.05.074
50. Caron M, Auclair M, Donadille B, Béréziat V, Guerci B, Laville M, et al. Human lipodystrophies linked to mutations in A-type lamins and to HIV protease inhibitor therapy are both associated with prelamin A accumulation, oxidative stress and premature cellular senescence. *Cell Death Differ.* (2007) 14:1759–67. doi: 10.1038/sj.cdd.4402197
51. Pérez SA, Toro R, Sarquella BG, de Gonzalo CD, Cesar S, Carro E, et al. Genetic basis of dilated cardiomyopathy. *Int J Cardiol.* (2016) 224:461–72. doi: 10.1016/j.ijcard.2016.09.068
52. Shah S, Henry A, Roselli C, Lin H, Sveinbjörnsson G, Fatemifar G, et al. Genome-wide association and Mendelian randomisation analysis provide insights into the pathogenesis of heart failure. *Nat Commun.* (2020) 11:163. doi: 10.1038/s41467-019-13690-5
53. Tashima T, Nagatoishi S, Sagara H, Ohnuma SI, Tsumoto K. Osteomodulin regulates diameter and alters shape of collagen fibrils. *Biochem Biophys Res Commun.* (2015) 463:292–6. doi: 10.1016/j.bbrc.2015.05.053
54. Tashima T, Nagatoishi S, Caaveiro JMM, Nakakido M, Sagara H, Kusano AO, et al. Molecular basis for governing the morphology of type-I collagen fibrils by Osteomodulin. *Commun Biol.* (2018) 1:33. doi: 10.1038/s42003-018-0038-2
55. Wiśniowska SS, Dziewiecka E, Holcman K, Wypasek E, Khachatryan L, Karabinowska A, et al. Kinetics of selected serum markers of fibrosis in patients with dilated cardiomyopathy and different grades of diastolic dysfunction of the left ventricle. *Cardiol J.* (2020) 27:726–34. doi: 10.5603/CJ.a2018.0143
56. Guo W, Feng W, Fan X, HuangJ, Ou C, Chen M. Osteomodulin is a potential genetic target for hypertrophic cardiomyopathy. *Biochem Genet.* (2021) 59:1185–202. doi: 10.1007/s10528-021-10050-1
57. Zhang M, Mou T, Zhao Z, Peng C, Ma Y, Fang W, et al. Synthesis and 18F-labeling of the analogues of Omecamtiv Mecarbil as a potential cardiac myosin imaging agent with PET. *Nucl Med Biol.* (2013) 40:689–96. doi: 10.1016/j.nucmedbio.2013.02.013
58. Benitez AA, Samouillan V, Jorge E, Dandurand J, Nasarre L, et al. Identification of new biophysical markers for pathological ventricular remodelling in tachycardia-induced dilated cardiomyopathy. *J Cell Mol Med.* (2018) 22:4197–208. doi: 10.1111/jcmm.13699

Conflict of Interest: The authors declare that the research was conducted in the absence of any commercial or financial relationships that could be construed as a potential conflict of interest.

Publisher's Note: All claims expressed in this article are solely those of the authors and do not necessarily represent those of their affiliated organizations, or those of the publisher, the editors and the reviewers. Any product that may be evaluated in this article, or claim that may be made by its manufacturer, is not guaranteed or endorsed by the publisher.

frontiers in Cardiovascular Medicine

ORIGINAL RESEARCH
published: 15 February 2022
doi: 10.3389/fcvm.2021.683445

Diagnostic and Prognostic Value of Neutrophil Extracellular Trap Levels in Patients With Acute Aortic Dissection

Shuofei Yang[1†], Yongsheng Xiao[2†], Yuanfeng Du[3], Jiaquan Chen[1], Qihong Ni[1], Xiangjiang Guo[1], Guanhua Xue[1] and Xupin Xie[4*]*

[1] Department of Vascular Surgery, Renji Hospital, School of Medicine, Shanghai Jiaotong University, Shanghai, China, [2] Department of Vascular Surgery, Tianjin 4th Centre Hospital, The Fourth Central Hospital Affiliated to Nankai University, The Fourth Center Clinical College of Tianjin Medical University, Tianjin, China, [3] Department of Neurosurgery, School of Medicine, Affiliated Hangzhou First People's Hospital, Zhejiang University, Hangzhou, China, [4] Department of Vascular Surgery, School of Medicine, Affiliated Hangzhou First People's Hospital, Zhejiang University, Hangzhou, China

OPEN ACCESS

Edited by:
Alessio Molfino,
Sapienza University of Rome, Italy

Reviewed by:
Ruijing Zhang,
Second Hospital of Shanxi Medical University, China
Kumaravelu Jagavelu,
Central Drug Research Institute (CSIR), India

***Correspondence:**
Guanhua Xue
xueguanhua2018@163.com
Xupin Xie
xiexupin@163.com

[†] These authors have contributed equally to this work and share first authorship

Specialty section:
This article was submitted to General Cardiovascular Medicine, a section of the journal Frontiers in Cardiovascular Medicine

Received: 21 March 2021
Accepted: 10 September 2021
Published: 15 February 2022

Citation:
Yang S, Xiao Y, Du Y, Chen J, Ni Q, Guo X, Xue G and Xie X (2022) Diagnostic and Prognostic Value of Neutrophil Extracellular Trap Levels in Patients With Acute Aortic Dissection. Front. Cardiovasc. Med. 8:683445. doi: 10.3389/fcvm.2021.683445

Background: Acute aortic dissection (AAD) is a fatal disease demanding prompt diagnosis and proper treatment. There is a lack of serum markers that can effectively assist diagnosis and predict prognosis of AAD patients.

Methods: Ninety-six AAD patients were enrolled in this study, and 249 patients with chest pain due to acute myocardial infarction, pulmonary embolism, intramural hematoma, angina or other causes and 80 healthy controls were included as control group and healthy control group. Demographics, biochemical and hematological data and risk factors were recorded as baseline characteristics. The 1-year follow-up data were collected and analyzed. The diagnostic performance and ability to predict disease severity and prognosis of NET components in serum and aortic tissue were evaluated.

Results: Circulating NET markers, citH3 (citrullination of histone 3), cell-free DNA (cfDNA) and nucleosomes, had good diagnostic value for AAD, with superior diagnostic performance to D-dimer in discriminating patients with chest pain due to other reasons in the emergency department. Circulating NET marker levels (i.e., citH3, cfDNA and nucleosomes) of AAD patients were significantly higher than that of control group and healthy control group. In addition, circulating NET markers levels were closely associated with the disease severity, in-hospital death and 1-year survival of AAD patients. Systolic blood pressure < 90 mmHg and serum citH3 levels were identified as independent risk factors for 1-year survival of AAD patients. Excessive NET components (i.e., neutrophil elastase and citH3) in the aortic tissue of AAD patient were significantly higher than that of healthy donor aortic tissue. The expression levels of granules and nuclear NET components were significantly higher in aortic tissue from AAD patients than controls.

Conclusions: Circulating NET markers, citH3, cfDNA and nucleosomes, have significant diagnostic value and predictive value of disease severity and prognosis of AAD patients. The NETs components may constitute a useful diagnostic and prognostic marker in AAD patients.

Keywords: neutrophil extracellular trap, acute aortic dissection, serum biomarker, diagnostic marker, prognostic marker

INTRODUCTION

Acute aortic dissection (AAD) is a fatal aortic disease with high mortality and morbidity that demands prompt diagnosis and proper treatment (1). Despite recent advances in diagnostic imaging methods, AAD remains a challenge to diagnose. A widely available and cost-effective measure such as a blood test that can rule in and/or rule out the disease would indeed aid in quick diagnosis, benefiting patients and caregivers. Several major diseases that cause chest pain, such as acute myocardial infarction (AMI), pulmonary embolism (PE), intramural hematoma and angina, require differential diagnosis with AAD. Moreover, there is still a lack of effective markers to accurately predict the in-hospital and long-term outcomes of patients with AAD after surgical repair.

Neutrophils are the most abundant cell type in leukocytes and play a crucial role in the innate immune system (2). Neutrophils are also involved in the pathological mechanism of aortic dissection (AD) (3). AAD is initiated by neutrophil infiltration of the aortic intima, and local neutrophil recruitment and activation in response to AAD can lead to aortic rupture (4, 5). In patients with AAD receiving surgical repair, the neutrophil to lymphocyte ratio may be used to predict worse outcomes and hospital mortality (6). In the inflammatory response, neutrophils play critical roles through the release of neutrophil extracellular traps (NETs), which are extracellular neutrophil-derived web-like structures that constitute a DNA backbone containing histones and neutrophil granule proteins. A critical step in NET release is the citrullination of histone 3 (citH3), a process mediated by protein deiminase 4, and citH3 is considered one of the most specific markers for NET formation assessment (7). Initially, NETs were thought to provide defense against pathogens (8). In recent years, NETs have been implicated in a number of cardiovascular diseases (9). By immunophenotypic analysis, NETs were found to participate in the tissue repair of AD (10).

NETs could be used as a new circulating marker for several cardiovascular diseases, such as acute coronary syndrome, acute ischemic stroke, myocardial infarction, and deep venous thrombosis (11–13). Data on NET presence in the serum and tissue of AAD patients and the association between NET levels and clinical outcomes are scarce. Hence, this study sought to determine whether NETs may serve as disease biomarkers in AAD patients. Specifically, our aims were to examine the diagnostic value of NETs for AAD and the predictive significance of NETs for disease severity, in-hospital mortality and 1-year survival in AAD patients receiving surgical repair.

Abbreviations: AAD, acute aortic dissection; AMI, acute myocardial infarction; AD, aortic dissection; PE, pulmonary embolism; NETs, neutrophil extracellular traps; citH3, citrullination of histone 3; CTA, computed tomography angiography; MRA, magnetic resonance angiography; TAAD, type A aortic dissection; TABD, type B aortic dissection; APACHE II, the Acute Physiology, Age, Chronic Health Evaluation II; cfDNA, cell-free DNA; NE, neutrophil elastase; ROC, receiver operating characteristic curve; AUR, area under the ROC; NET, neutrophil extracellular trap; SBP, systolic blood pressure; TF, tissue factor.

PATIENTS AND METHODS

Patients

The study was approved by the ethical committee of Renji Hospital, School of Medicine, Shanghai Jiaotong University (No. RA2020-253). All patients or their proxies provided written informed consent. Ninety-six consecutive patients with AAD hospitalized in Renji Hospital between May 01, 2016, and April 04, 2019, were enrolled in this study. Diagnoses were made based on computed tomography angiography (CTA), digital subtraction angiography and, when appropriate, magnetic resonance angiography (MRA). The Stanford classifications of AAD were evaluated at the time of diagnosis. Stanford type A aortic dissection (TAAD) involves the ascending aorta, whereas type B aortic dissection (TABD) involves the descending aorta only. The severity of disease was measured by the Acute Physiology, Age, Chronic Health Evaluation II (APACHE II) score at hospital entrance and discharge. The detection risk score of AD was calculated at admission to the emergency department according to the guidelines (14). During the same time period, 249 patients admitted to the emergency chest pain center with a diagnosis of AMI, PE, angina or others were included in the control group. In addition, 80 healthy controls were included in this study. Demographics, biochemical and hematological data, clinical history, and risk factors were recorded as baseline patient characteristics. Clinical follow-up was performed 1 year after hospital discharge in all AAD patients. This was conducted by reviewing the electronic records in clinics or by telephone contact. Follow-up records included reoperation information, CTA or MRA follow-up information, mortality, and cause and date of death.

Citrated-anticoagulated venous blood was obtained from all the patients within 3 h of diagnosis and on the last morning before discharge. Platelet-poor plasma was prepared by centrifugation of the blood (2,500 × g) for 10 min at 22°C, and the plasma was stored at −80°C until analysis. Aortic tissue samples were obtained from 45 AAD patients included in this study who received open surgery. Twenty normal aortic tissues were obtained from organ donors (crash victims or brain-dead patients). Tissue samples were stored at −80°C until analysis.

NET Markers

We evaluated three different markers of NETs [i.e., cfDNA (cell-free DNA), nucleosomes and citH3]. citH3 is currently considered to be the most specific marker, as H3 citrullination is required for chromatin decondensation in neutrophils. Detection of cfDNA and nucleosomes was performed as described previously (13). For cfDNA determination, plasma was diluted 1:10 with phosphate-buffered saline and mixed with an equal volume of 1 mM SytoxGreen (Invitrogen, Carlsbad, CA, USA; No. S7020) in PBS. Fluorescence was determined in a fluorescence microplate reader (Gemini XPS; Molecular Devices, Sunnyvale, CA, USA). A calibration curve was generated with calf thymus DNA (Invitrogen; No. 15633019) in PBS. Nucleosomes were measured with the Cell Death Detection ELISAPLUS kit (Roche Diagnostics, Madrid, Spain; No. 11774425001) according to the manufacturer's instructions. Determination of citH3 was

TABLE 1 | Baseline characteristics of chest pain patients included in this study.

Characteristics	AAD ($n = 96$)	Controls ($n = 249$)	*P*-value
Age, mean (range)	59.1 (35–85)	60.3 (40–92)	0.45
Male sex, *n* (%)	53 (55.2)	128 (51.4)	0.53
Medical history and risk factors, n (%)			
Hypertension	72 (75.0)	129 (51.8)	<0.05
Diabetes	44 (45.8)	109 (43.8)	0.62
Stroke	28 (29.2)	80 (32.1)	0.60
Hyperlipidemia	48 (50.0)	135 (54.2)	0.48
Smoking	55 (57.3)	125 (50.2)	0.24
Marfan syndrome	12 (12.5)	1 (0.4)	<0.01
Atrial fibrillation	28 (29.2)	63 (25.3)	0.47
Valvulopathy	20 (20.8)	42 (16.9)	0.39
Diagnosis, n (%)			
TAAD	42 (43.8)	/	/
TBAD	54 (56.3)	/	/
IH	/	10 (4.0)	/
AMI	/	63 (25.3)	/
PE	/	42 (16.9)	/
Angina	/	66 (26.5)	/
Others	/	68 (27.3)	/
Biochemical and hematological data, mean ± SD			
Glucose, mg/dL	130.3 ± 52.4	125.4 ± 44.2	0.42
Creatinine, μmol/L	148.7 ± 33.6	142.9 ± 40.7	0.36
Uric acid, mg/dL	6.1 ± 2.4	5.9 ± 2.9	0.37
Cholesterol, mg/dL	178.3 ± 39.2	183.2 ± 29.9	0.72
Triglycerides, mg/dL	182.1 ± 88.4	189.1 ± 79.2	0.60
AST, U/L	28.2 ± 13.4	30.2 ± 20.2	0.13
ALT, U/L	38.3 ± 16.7	39.6 ± 26.3	0.22
Bilirubin, mg/dL	1.9 ± 1.6	1.8 ± 0.8	0.82
Hematocrit, %	41.3 ± 6.3	39.4 ± 5.6	0.63
Platelets, $10^3/\mu L$	248.3 ± 56.4	256.6 ± 47.2	0.20
Leukocytes, $10^3/\mu L$	6.4 ± 3.4	6.8 ± 3.9	0.74
Lymphocytes, %	26.3 ± 9.2	27.5 ± 8.4	0.20
Neutrophils, %	74.4 ± 18.3	73.9 ± 19.8	0.48
Monocytes, %	8.8 ± 4.2	9.0 ± 7.3	0.33
D-dimer, ng/ml	2080.5 ± 1131.9	1867.3 ± 2007.3	<0.05

AAD, acute aortic dissection; TAAD, type A aortic dissection; TBAD, type B aortic dissection; IH, intramural hematoma; AMI, acute myocardial infarction; PE, pulmonary embolism; SD, standard deviation; AST, aspartate transaminase; ALT, alanine aminotransferase.

performed as previously described (15). Briefly, plasma samples were mixed with a monoclonal mouse anti-histone biotinylated antibody in a streptavidin-coated plate. A rabbit polyclonal anti-histone-H3 (citrullinated R17 + R2 + R8) (Abcam Inc., MA, USA; No. ab81797) antibody was used in the second step. Detection was performed with a peroxidase-linked antibody (GE Biosciences, Barcelona, Spain; No. A1783). Values were normalized to a pool of samples from normal subjects. Values are expressed as individual absorption values. The neutrophil elastase (NE) concentration was measured using commercially available ELISA kits.

Proteomics Analysis

In this study, we built a custom pathway of NET-associated proteins as described previously (16). To build a custom "NETosis" pathway, twenty-three proteins that belonged to five subcellular compartments (nucleus, granules, cytoplasm/cytoskeleton, enzymes, and plasma membrane) were identified by a literature screen for detailed characterization of NET proteins (17, 18). According to a Gene Set Enrichment Analysis heat map, the custom NETosis pathway was enriched in aortic tissue from AAD patients vs. normal controls. Samples were reduced, alkylated and trypsin-digested according to the iTRAQ manufacturer's instructions (AB Sciex Inc., MA, USA). To diminish any potential variation introduced by the labeling reaction, samples from AAD patients and normal controls were split into two aliquots of 60 μg to perform two technical replicates with tag swapping. Each peptide solution was labeled at room temperature for 1 h with one iTRAQ reagent vial. To verify the labeling efficiency, 1 μg of each labeled sample was individually analyzed by liquid chromatography-tandem mass spectrometry (LC-MS/MS) as specified below. Acquired data were searched against the Mascot database, setting iTRAQ labeling as the variable modification. No unmodified peptides were identified from the search, and all the peptides were correctly modified at the N-terminus and at each lysine residue. Finally, the four iTRAQ-labeled samples were combined in a 1:1:1:1 ratio, and the pool was vacuum dried in a SpeedVac system.

Immunofluorescence

NET identification in tissue samples was performed by immunofluorescence staining. The NE/citH3 pair was researched in paraffin-embedded, 3-μm-thick sections. The slides were incubated with the primary antibodies (anti-NE antibody, MAB91671, R&D Systems, Minneapolis, USA; anti-H3Cit antibody, ab5103, Abcam, Cambridge, UK; both 1:50 dilution) at 4°C overnight after blocking with goat serum. Then, the sections were incubated with secondary antibodies (Alexa Fluor 488, green, ab150077; Alexa Fluor 647, red, ab150075; both from Abcam, Cambridge, UK) for 1 h at room temperature. DAPI was used for nuclear staining (ZSGB Biotech, Beijing, China; No. ZLI-9577). The slides were analyzed with a confocal laser scanning microscope (TCS-SP5; Leica, Wetzlar, Germany). The average numbers of NE and H3Cit double-positive cells were calculated by two independent researchers counting five random microscopic fields.

Statistics

Data are expressed as the means ± SEM of absolute values or as percentages. Continuous variables were analyzed with the Mann-Whitney test. Discrete variables were evaluated with a contingency χ^2 test. By the Shapiro-Wilk test, the value of citH3, cfDNA and nucleosomes were found to be normally distributed. The Spearman coefficient (r) was used to quantify the correlations between variables. Compared with D-dimer, the diagnostic performance of NET markers for distinguishing AAD from all other diseases, AMI, PE, or angina was assessed using receiver operating characteristic curve (ROC) analysis. The area under the ROC (AUR),

TABLE 2 | NETs and risk factors before the onset of the acute event.

Characteristics		citH3 (ng/ml)	*P*	cfDNA (AU)	*P*	Nucleosomes (AU)	*P*
Hypertension	Yes	0.46 ± 0.23	0.73	698.82 ± 306.28	0.11	1.56 ± 0.82	0.82
	No	0.47 ± 0.26		788.13 ± 438.75		1.58 ± 0.88	
Diabetes	Yes	0.46 ± 0.23	0.56	692.48 ± 317.45	0.31	1.53 ± 0.85	0.75
	No	0.47 ± 0.25		745.40 ± 365.98		1.59 ± 0.83	
Smoking	Yes	0.48 ± 0.24	0.12	749.98 ± 355.40	0.21	1.61 ± 0.85	0.32
	No	0.44 ± 0.24		682.46 ± 328.01		1.50 ± 0.82	
Marfan syndrome	Yes	0.47 ± 0.21	0.52	664.25 ± 210.41	0.04	1.52 ± 0.74	0.21
	No	0.47 ± 0.24		729.27 ± 359.05		1.57 ± 0.85	
Atrial fibrillation	Yes	0.49 ± 0.25	0.44	757.68 ± 359.99	0.09	1.57 ± 0.80	0.71
	No	0.45 ± 0.24		706.10 ± 338.55		1.56 ± 0.85	

citH3, citrullination of histone 3; cfDNA, cell-free DNA; AU, arbitrary units.

sensitivity, specificity, accuracy, positive predictive value, and negative predictive value were calculated. The Wald test was used to assess the significance of the difference between areas under the ROC curve. The optimal cutoff point from the study was the threshold leading to the maximum summation of sensitivity and specificity. Univariate logistic regression analysis was used to assess the association between risk factors and in-hospital death or 1-year survival, and a multivariate Cox regression analysis was performed using variables with $P \leq 0.20$ in univariate analysis. A two-sided *P*-value <0.05 was considered statistically significant. Statistical analyses were performed with SPSS 20 (SPSS, Inc., Chicago, IL, USA).

RESULTS

Baseline Demographic Information and Hematological Parameters

A total of 96 patients, 42 TAADs and 54 TBADs, were enrolled in the AAD group. Another 249 patients were enrolled in the control group, including 10 IH cases, 63 AMI cases, 42 PE cases, 66 angina cases and 68 cases with other causes. The baseline demographic information, medical history, risk factors, and biochemical and hematological data are shown in **Table 1**. The demographic information, biochemical and hematological data of 80 healthy controls are shown in **Supplementary Table 1**. The rates of hypertension and Marfan syndrome were significantly higher in the AAD group than in the control group. Moreover, AAD patients had significantly higher levels of D-dimer than patients in the control group. There was no significant difference between the two groups regarding other parameters. The AAD patients were stratified according to classical risk factors. No significant differences among any of the three NET markers were observed between patients with or without hypertension, diabetes, smoking history and atrial fibrillation. The cfDNA levels in patients with Marfan syndrome were significantly higher than those in patients without Marfan syndrome. However, the levels of citH3 and nucleosomes were comparable between patients with or without Marfan syndrome (**Table 2**).

Diagnostic Performance of Circulating NET Markers for Discriminating AAD

The values of citH3, cfDNA and nucleosomes in patients with AAD were significantly higher than those in the control group or healthy controls (**Figure 1A**) Circulating levels of citH3, cfDNA, and nucleosomes were positively correlated with the detection risk score of AD (**Figure 1B**). In the ROC curve, the AURs in patients with AAD vs. all control patients were 0.87 for citH3, 0.95 for cfDNA, 0.92 for nucleosomes, and 0.64 for D-dimer (**Figure 1C**). Thus, circulating NET markers showed superior overall diagnostic performance compared with D-dimer when sudden-onset chest pain was present in the emergency department. cfDNA at cutoff levels of 403.5 ng/ml and D-dimer at 2015 ng/ml were the thresholds leading to the maximum summation of sensitivity and specificity in discriminating AAD from all other diagnoses. The corresponding sensitivities were 77.08% for cfDNA and 57.29% for D-dimer, and the specificities were 100% for cfDNA and 84.74% for D-dimer, resulting in 93.62% of patients for cfDNA and 55.61% of patients for D-dimer being correctly classified (**Supplementary Table 2**).

The time course was also examined in the AAD group using box plot analysis according to the admission time from symptom onset. The peak NET marker levels occurred within 12–24 h after symptom onset (**Figure 1D**). In addition, no significant difference in circulating NET markers was found between patients with TAAD and TBAD or among different subsets of the control group. There was no correlation between age and circulating levels of NET markers (**Supplementary Figure 1**).

Association Between Circulating NET Markers and Disease Severity of AAD at Onset and Discharge

There was a positive correlation between the APACHE II score and the levels of all three NET markers at disease onset (**Figure 2A**). When patients were classified according to the APACHE II score into four groups, those with higher scores had significantly higher levels of all three NET markers (**Figure 2B**). At discharge, the levels of all three NET markers were also positively correlated with the APACHE II score (**Figure 2C**). Classified by APACHE II score into three groups, patients with

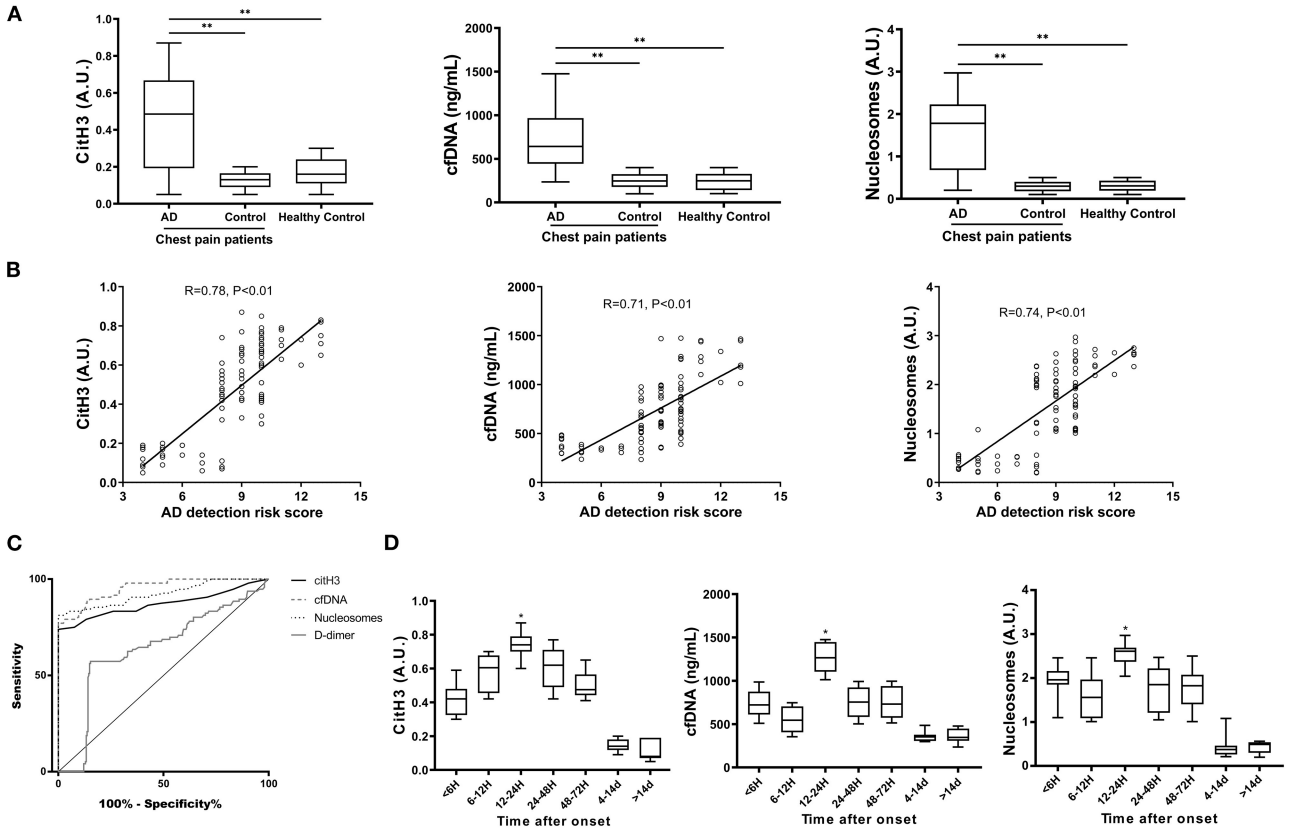

FIGURE 1 | The diagnostic performance of circulating NET markers for discriminating AAD. **(A)** Serum levels of citrullinated H3 (citH3), cell-free DNA (cfDNA), and nucleosomes were evaluated in 96 patients with AAD and 249 patients in the control group. CitH3 and nucleosomes are expressed in arbitrary units (AU). The cfDNA concentration (ng/mL) was determined based on a calibration curve of calf thymus DNA. All three markers were significantly higher in the AAD group than in the control group. **(B)** Serum levels of citH3, cfDNA and nucleosomes were positively correlated with the detection risk score of AD. **(C)** ROC curve for the diagnosis of AAD. Circulating NET markers showed superior overall diagnostic performance compared with D-dimer when sudden-onset chest pain was present in the emergency department. **(D)** The time course of NET markers was examined in patients with AAD according to the admission time from symptom onset. The peak NET marker levels occurred within 12–24 h of symptom onset. $^{*}P < 0.05$, $^{**}P < 0.01$.

greater disease severity showed significantly higher levels of the three NET markers (**Figure 2D**). These results demonstrated the association between circulating levels of NET markers and disease severity at both admission and discharge.

Prognostic Significance of Circulating NET Markers for Predicting In-hospital Death and 1-year Survival of Patients With AAD

The results in **Figure 3A** show that the levels of NET markers in patients with in-hospital death were significantly higher than those in patients without in-hospital death. AAD patients with the highest quartiles of citH3, cfDNA, or nucleosome levels presented significantly lower survival rates by 1 year than patients with the lower three quartiles of citH3 (**Figure 3B**). Based on the ROC curve, three circulating NET markers showed superior predictive ability for 1-year survival compared with D-dimer (**Figure 3C**). The AURs were 0.72 for citH3, 0.76 for cfDNA, 0.73 for nucleosomes, and 0.51 for D-dimer. The cfDNA at cutoff levels of 1,052 ng/ml and D-dimer at 915 ng/ml were threshold values. The corresponding sensitivities were 46.15% for cfDNA and 26.92% for D-dimer, and the specificities were 94.29% for cfDNA and 82.86% for D-dimer (**Supplementary Table 3**).

Risk Factor Analysis of 1-year Survival in AAD Patients

We next examined whether NET markers were independently associated with the 1-year survival of AAD patients. By univariate and multivariate risk factor analysis, systolic blood pressure (SBP) < 90 mmHg and citH3 levels were identified as independent risk factors for 1-year survival ($p < 0.05$) (**Figure 4A** and **Supplementary Table 4**). AAD patients with SBP < 90 mmHg had significantly increased circulating NET markers compared with patients with SBP > 90 mmHg (**Figure 4B**).

Excess NET Components in Aortic Tissue and Their Association With Disease Severity and Prognosis in Patients With AAD

The expression levels of granule and nuclear NET components were significantly higher, and non-granular enzymes and

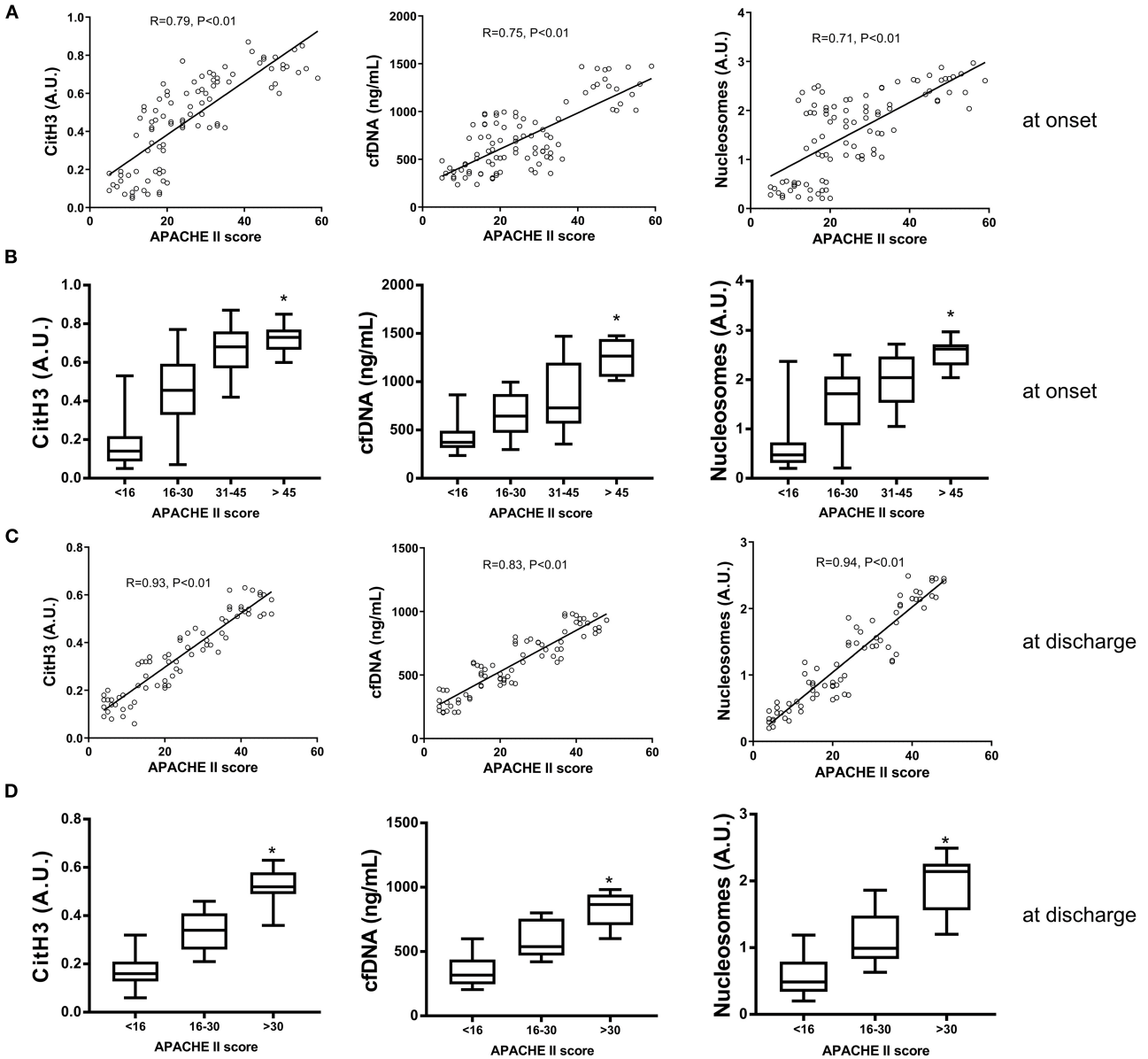

FIGURE 2 | The association between NET markers and disease severity of AAD at onset and discharge. **(A)** Serum levels of citH3, cfDNA and nucleosomes were positively correlated with the APACHE II score at disease onset. **(B)** AAD patients were classified into four groups according to APACHE II score. Patients with higher scores had significantly higher levels of all three NET markers. **(C)** The levels of all three NET markers were positively correlated with the APACHE II score at discharge. **(D)** AAD patients with greater disease severity showed significantly higher levels of NET markers. *$P < 0.05$.

membrane components were mildly enriched in aortic tissue from AAD patients compared with normal controls (**Figures 5A,B**). The expression of neutrophil elastase, the prototypical NET marker, was significantly higher in aortic tissue from the AAD group than in aortic tissue from the control group (**Figure 5C**). Additionally, the elastase level in patients with in-hospital death or without 1-year survival was significantly higher than that in patients without in-hospital death or with 1-year survival (**Figures 5D,E**).

Local NETosis was detected in the aortic samples from AAD patients, as colocalization of NE with citH3 was observed by confocal microscopy (**Figure 6A**). Compared with healthy donor aortic tissue, the numbers of NETs formed per field in the tissue samples from AAD patients were significantly increased (**Figure 6B**). Moreover, the number of NETs formed per field was positively correlated with the detection risk score of AD and the APACHE II score (**Figures 6C,D**). The number of NETs formed per field in patients with in-hospital death or death within 1-year was significantly higher than that in patients without in-hospital death or death within 1-year (**Figures 6E,F**). These results indicated that excess NET components in aortic tissue samples are associated with the disease severity and prognosis of AAD.

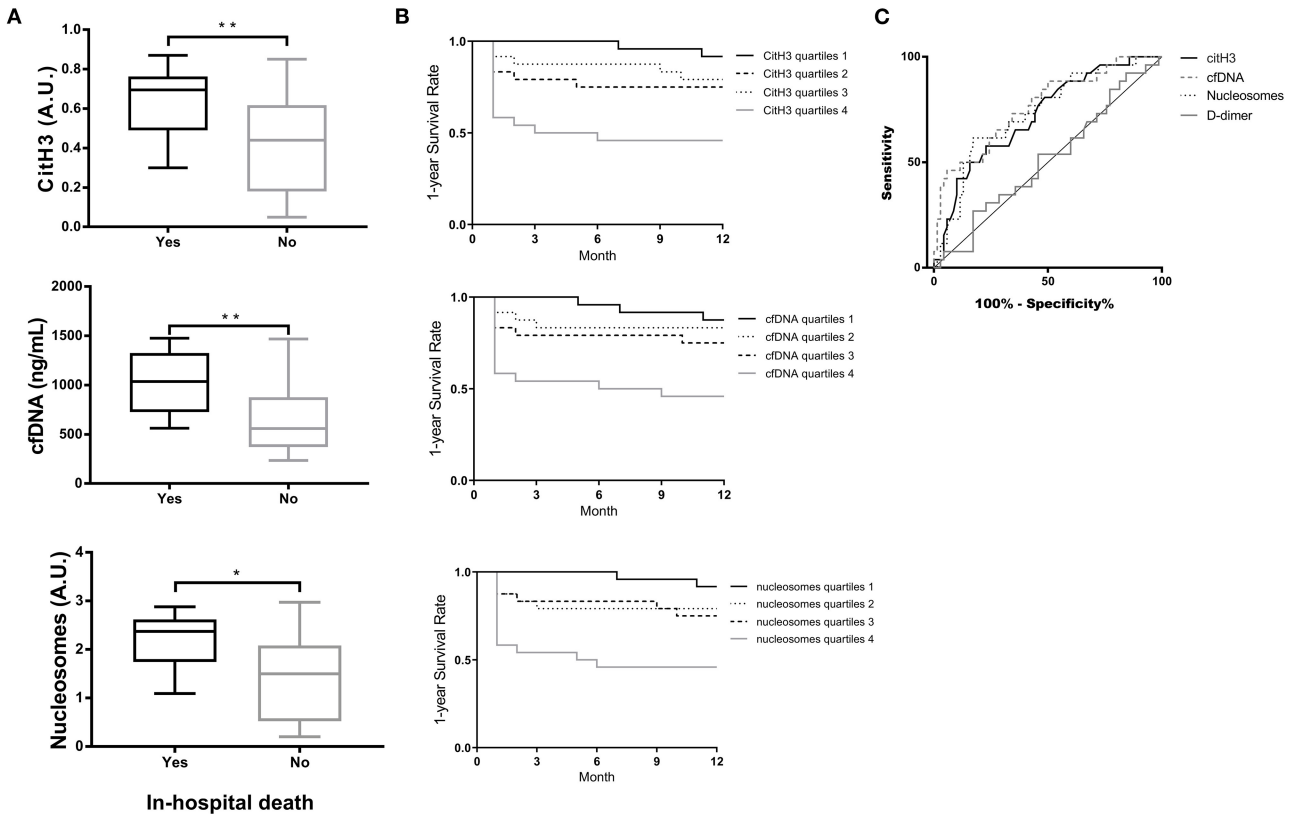

FIGURE 3 | Prognostic significance of circulating NET markers for predicting in-hospital death and 1-year survival of AAD patients. **(A)** Serum levels of citH3, cfDNA and nucleosomes in patients with in-hospital death were significantly higher than those in patients without in-hospital death. **(B)** AAD patients with the highest quartiles of citH3, cfDNA or nucleosome levels presented significantly lower survival rates by 1 year than patients with the lower three quartiles of citH3. **(C)** Based on the ROC curve, three circulating NET markers showed superior prediction ability of 1-year survival compared with D-dimer. $^{*}P < 0.05$, $^{**}P < 0.01$.

DISCUSSION

To the best of our knowledge, this is the first time that the diagnostic and prognostic value of NETs has been evaluated in patients with AAD. In this study, the major findings were that: (a) circulating NET markers had reliable diagnostic value of AAD, with superior diagnostic performance to discriminate patients with chest pain from other reasons in the emergency department compared with D-dimer; (b) circulating NET markers were independently associated with the disease severity, in-hospital death and 1-year survival of patients with AAD; and (c) excessive NET components in the aortic tissue were associated with the disease severity and prognosis of AAD patients.

It is well-known that neutrophils are the first line of defense against infections by pathogens. Neutrophils are also pivotal as primary effector cells at sites of inflammation, but through regulation of their survival by means of regulated cell death, these cells are also involved in the resolution of inflammation (19). Significant neutrophilic infiltration was found not only in early but also in later stages of organizing dissections and not only in the clot but also in adventitial fat (10, 20). This could reflect an upregulation of neutrophil survival to maintain the intense tissue remodeling required for the repair of the arterial wall. In both surgical and autopsy cases of AAD, immunohistochemical staining for citH3 revealed a massive presence of NETs in the clot and in the adventitia in the subacute stage and less abundantly in early organizing stage dissections (10). It is worth noting that aortic tissue samples were collected during surgery in this study. However, in surgical cases, awareness of the pattern of margination, transmigration and extravasation around microvessels that may occur due to robust handling during surgery should be considered to avoid overinterpration of the more diffuse patterns of neutrophil infiltration and NET release related to dissection.

Our results elucidated that the three markers of NETs are significantly elevated in patients with AAD compared with the corresponding levels in subjects from the control group. Recent reports have documented the association of NETs with the severity of stroke evaluated by clinical indexes (21, 22). Our study showed for the first time that the three markers of NETs were in line with the disease severity score of AAD at onset and discharge. However, the APAHE II scoring system is predictive of disease severity only when specific baseline and wound characteristics are accounted for. A plasma marker that can be easily and quickly

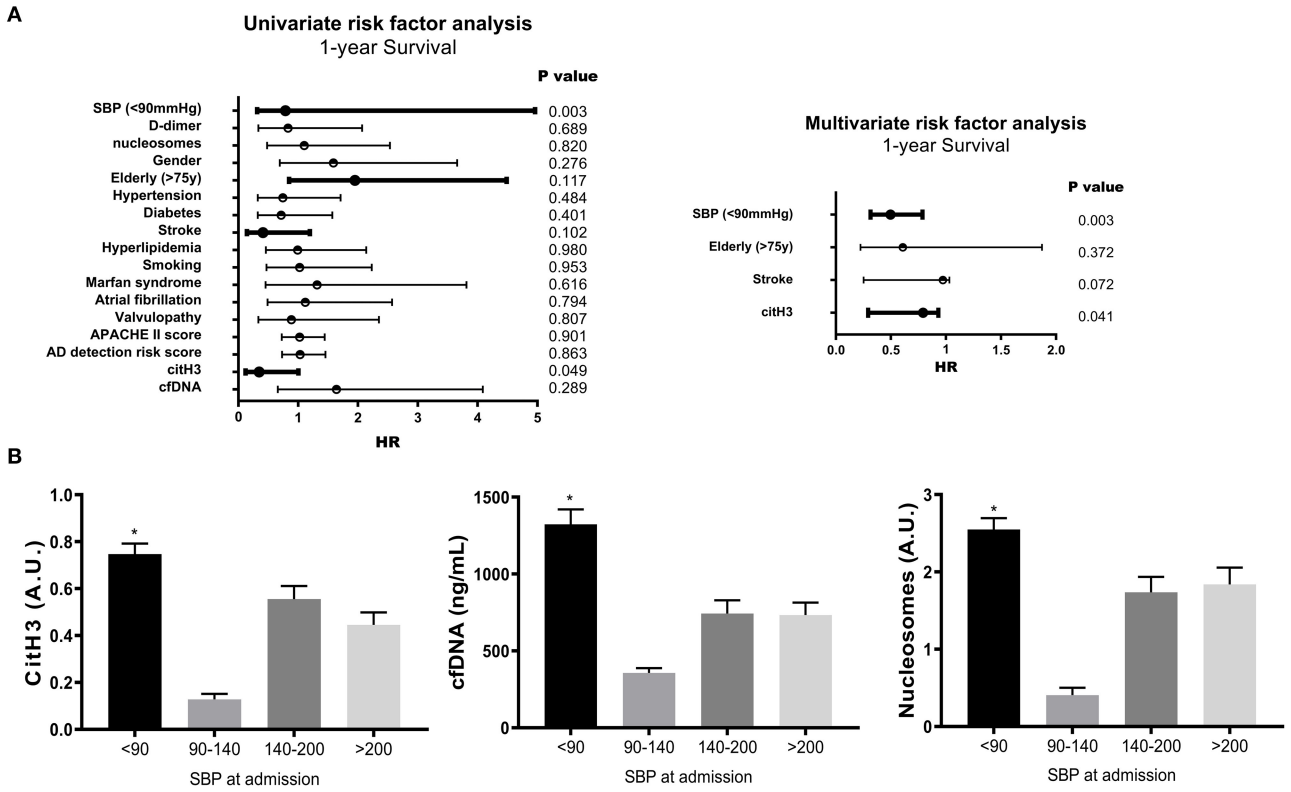

FIGURE 4 | Risk factor analysis of 1-year survival in AAD patients. **(A)** By univariate and multivariate risk factor analysis, systolic blood pressure (SBP) < 90 mmHg and citH3 levels were identified as independent risk factors for 1-year survival. **(B)** AAD patients with SBP < 90 mmHg had significantly increased circulating NET markers compared with patients with SBP > 90 mmHg. *$P < 0.05$.

tested to stratify patients with different risks of mortality is of great prognostic significance.

In this study, a time course study of NET markers was performed in AAD patients according to the admission time from symptom onset. The levels of all three NET markers peaked within 12–24 h after symptom onset. However, the concentrations of NET markers were measured using leftover samples of the patients from initial presentation. However, strictly speaking, the time after the actual onset of disease might be different for each patient. It would be beneficial to study the changes in concentrations according to time course or disease progression intraindividually. In addition, the time window for NET concentrations returning to the baseline level after surgery also needs to be determined. This will provide a stable time horizon for the testing of NET markers to predict the outcome of treatment for patients with AAD.

The mechanism underlying the increased NET formation in AAD remains unknown. AAD is considered an active inflammatory process that occurs in response to endothelial damage through high shear stress. Neutrophils and NETs are emerging as important mediators of pathogenic inflammation in the aorta (23). When aortic dissection occurs, disruption of the aortic media immediately changes aorta hemodynamics, with intramural hemorrhage leading to propagation and tracking of blood within the media, which will overactivate the coagulation system. Currently, there is increasing awareness that NETs are linked to thrombosis since they may shift the hemostatic balance toward excessive coagulation (24). AAD exhibits high concentrations of tissue factor (TF) in serum, and the ability of neutrophils to expose functional TF on NETs is considered a link between inflammation and coagulation (25, 26).

In the last two decades, much progress has been made to make effective biochemical diagnoses of AAD, which is an unmet need with lifesaving value. Several promising biomarkers have emerged. Vinculin, lumican, MMP-12 and high levels of ischemia-modified albumin have been considered potential AAD-related serum markers that may assist in the diagnosis and prediction of the in-hospital mortality of patients with AAD (27–30). However, most of these biomarkers are still clinically unavailable. In real-world clinical practice, in patients with acute chest pain and elevated D-dimer, a diagnosis of AAD should be considered. D-dimer might be a useful complementary tool to the current diagnostic work-up of patients with suspected AAD (31, 32). D-dimer levels may be useful in risk-stratifying patients with potential AD to rule out AD if used within the first 24 h after symptom onset (33). Nevertheless, D-dimers are not always elevated in patients with AAD (34). The results of this study demonstrated that circulating NET markers showed

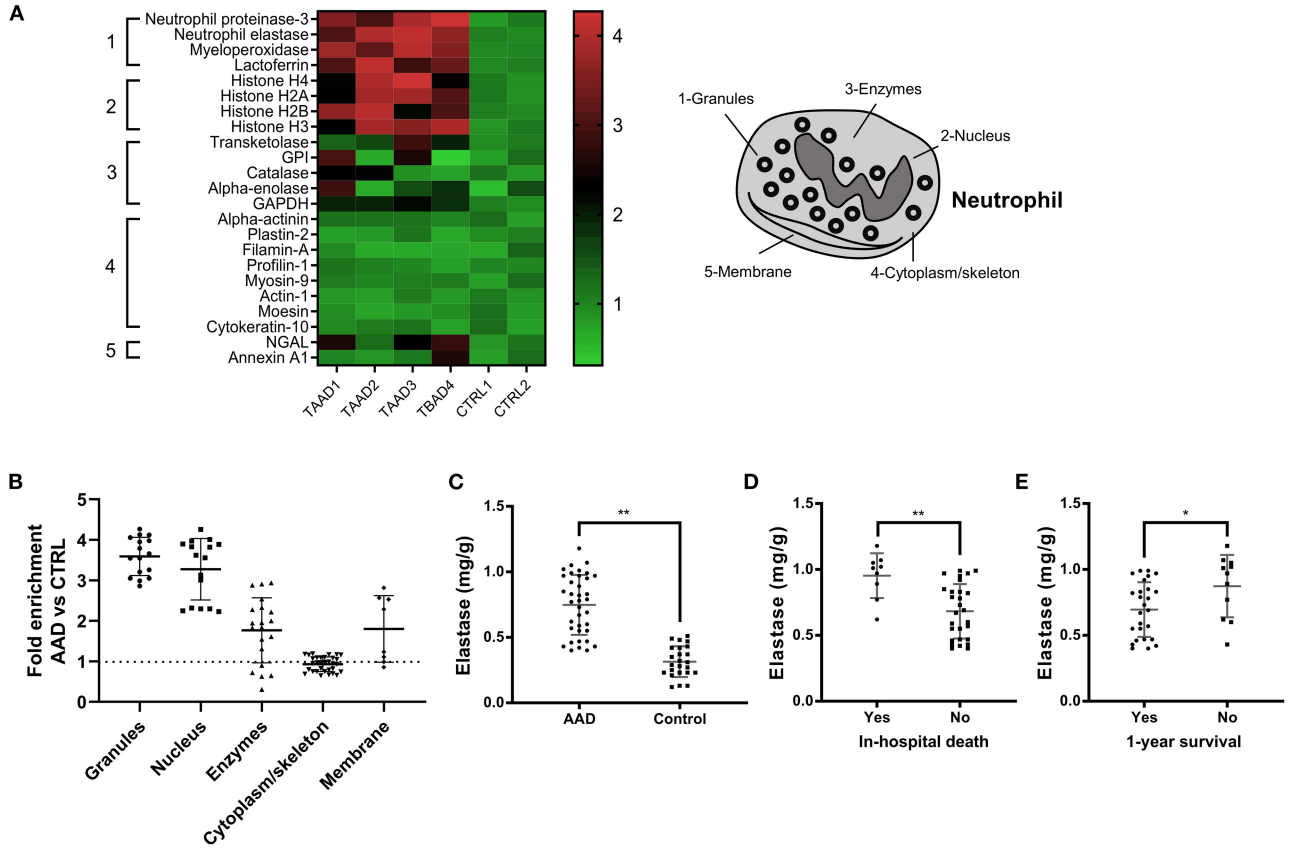

FIGURE 5 | Custom proteomic analysis of aortic tissue lysates from AAD patients. **(A)** Twenty-three proteins that belonged to five subcellular compartments (nucleus, granules, cytoplasm/cytoskeleton, enzymes, and plasma membrane) were identified to build a custom "NETosis" pathway. Profile plot from the Gene Set Enrichment Analysis (GSEA) showing highly significant enrichment of most proteins in the custom NETosis pathway in the 4 replicates (TAAD1-3, TBAD 4) compared with negative control subjects (CTRL1-2). The false discovery rate–adjusted P value for this analysis, according to GSEA output, was < 0.01. **(B)** The expression of granules and nuclear NET components was significantly higher, and non-granular enzymes and membrane components were mildly enriched in aortic tissue from AAD patients. **(C)** Neutrophil elastase was significantly higher in aortic tissue from the AAD group than in aortic tissue from the control group. **(D,E)** The elastase level in patients with in-hospital death or without 1-year survival was significantly higher than that in patients without in-hospital death or with 1-year survival. $^{*}P < 0.05$, $^{**}P < 0.01$.

significantly superior diagnostic performance compared with D-dimer to discriminate AAD patients with chest pain due to other reasons.

Despite acceptable reproducibility, as indicated by interassay cutoff values, the variability of the data makes clinically relevant cutoffs infeasible, and causality cannot be addressed. Although we used methods in line with current standards, the observed results highlight the need for improved methods when quantifying circulating NET markers (35). However, the inconsistent findings among the levels of cfDNA, citH3 and nucleosomes call into question their specificity in terms of reflecting NETosis. Previous studies have used various methods for evaluating the suitability of NETs as biomarkers in different clinical conditions, in which the main analytical targets were cfDNA, histones, and other components of NETs, such as neutrophil elastase or myeloperoxidase in plasma (36). cfDNA has repeatedly been described as a NET marker due to the objectivity of DNA quantification methods, yet its source is ambiguous, as non-neutrophil cells also release chromatin through cell death processes (35). The citrullination of histone 3 is a necessary step in the formation of NETs, as demonstrated by genetic and pharmacological approaches (37). Thus, citH3 appears to be the most specific marker of NETs, and it has been used to test for the presence of NETs in plasma. Importantly, citH3 has been reported to be independently associated with all-cause mortality during the 1-year follow-up in patients with acute ischemic stroke (21). In this study, citH3 was also identified as an independent risk factor for 1-year survival in patients with AAD.

Some limitations should be considered in the interpretation of our results. First, this is a single-center study with a relatively small number of subjects. Potential selection biases are not negligible. Future research on this topic should aim to include a larger study population. Secondly, a long-term follow-up period would be necessary to obtain statistically significant results in the prediction of disease prognoses. In this study, we reported major outcomes observed during the 1-year follow-up. Analysis of the changes in circulating levels of NETs during the follow-up period is also meaningful. Thirdly, our study was mostly descriptive, whereas the specific mechanism of NETs in circulation or aortic tissue promoting the occurrence and progression of AAD was not

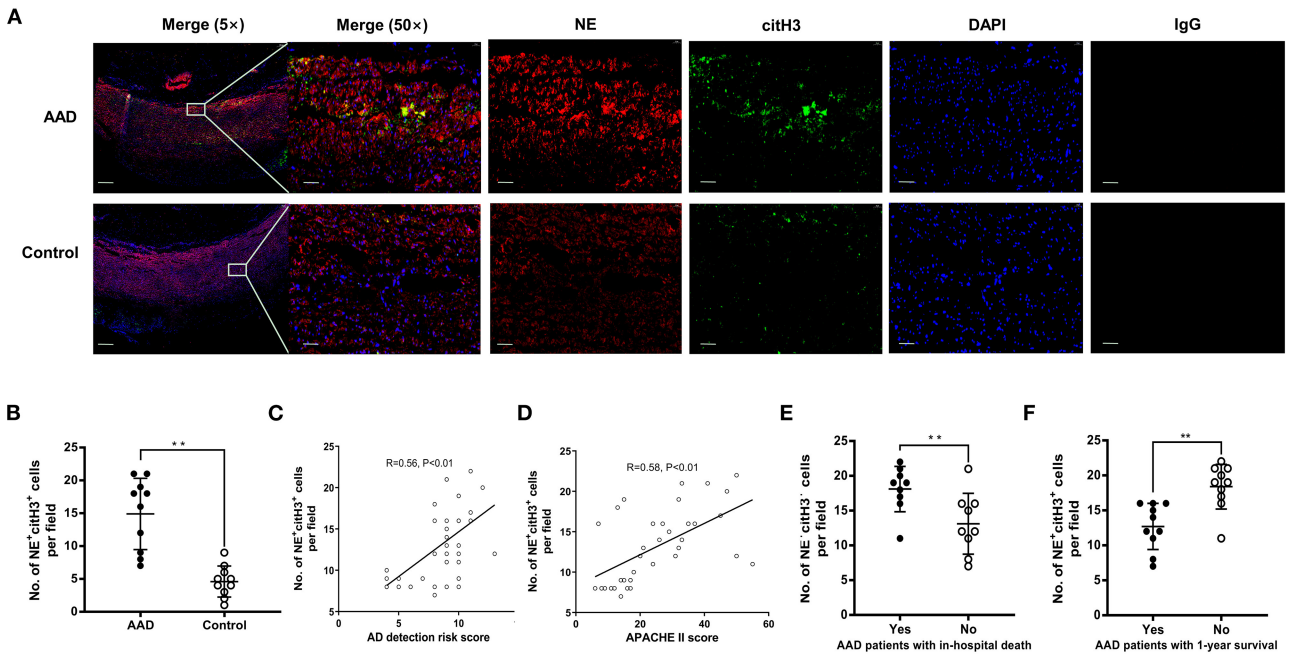

FIGURE 6 | The association between excess NETs in aortic tissue and disease severity or prognosis of patients with AAD. **(A)** Local NETosis was detected in aortic samples from AAD patients, as colocalization of NE with citH3 was observed by confocal microscopy. NE was stained green (Alexa Fluor 488) and citH3 was stained red (Alexa Fluor 647). DAPI staining was used to mark nucleus (blue fluorescence). **(B)** Compared with normal controls, the number of NETs formed per field in the tissue samples from AAD patients was significantly increased. **(C,D)** The number of NETs formed per field was positively correlated with the detection risk score of AD and the APACHE II score. **(E)** The number of NETs formed per field in patients with in-hospital death was significantly higher than that in patients without in-hospital death. **(F)** The number of NETs formed per field in patients with 1-year survival was significantly lower than that in patients without 1-year survival. $^{**}P < 0.01$.

addressed in this study. Further research is needed to determine whether NET components could be used as potential therapeutic targets for AAD.

In conclusion, the present study demonstrates that circulating NET markers have significant diagnostic value for AAD with good diagnostic performance to discriminate patients with chest pain from other causes. NET markers, in both the serum and aortic tissue, are associated with disease severity and the prognosis of AAD patients at the 1-year follow-up. Our results suggest that NETs may constitute a useful diagnostic and prognostic marker in patients with AAD and open new avenues for future drug therapy for AAD.

DATA AVAILABILITY STATEMENT

The raw data supporting the conclusions of this article will be made available by the authors, without undue reservation. The data presented in the study are deposited in the (http://proteomecentral.proteomexchange.org) repository, accession number (PXD001603).

ETHICS STATEMENT

The studies involving human participants were reviewed and approved by the Ethical Committee of Renji Hospital, School of Medicine, Shanghai Jiaotong University. The patients/participants provided their written informed consent to participate in this study.

AUTHOR CONTRIBUTIONS

Study conception and design and drafting of article were performed by SY and YX. Data collection was performed by JC and QN. Analysis and interpretation of data was performed by SY, YD, and XG. Critical revision was performed by GX and XX. All authors contributed to the article and approved the submitted version.

FUNDING

This work was supported by Grants from the National Science Foundation of China (Grant No. 81700423 and No. 81873526), Clinical Research Innovation and Cultivation Fund of Renji Hospital (Grant No. PYIII-17-003), Shanghai Outstanding Young Doctor Training Program from Shanghai Municipal Commission of Health and Family Planning (to SY), Shanghai Jiaotong University Medical Engineering Cross Fund (Grant No. YG 2016QN57), scientific research project of Shanghai municipal commission

of health and family planning (Grant No. 20164Y0058), Shanghai Jiao Tong University School of Medicine Nursing Research Key Project (Grant No. Jyhz1901), and Hangzhou science and technology development project (Grant No. 20201203B195).

SUPPLEMENTARY MATERIAL

The Supplementary Material for this article can be found online at: https://www.frontiersin.org/articles/10.3389/fcvm.2021.683445/full#supplementary-material

REFERENCES

1. Bossone E, LaBounty TM, Eagle KA. Acute aortic syndromes: diagnosis and management, an update. *Eur Heart J*. (2018) 39:739–49d. doi: 10.1093/eurheartj/ehx319
2. Nathan C. Neutrophils and immunity: challenges and opportunities. *Nat Rev Immunol*. (2006) 6:173–82. doi: 10.1038/nri1785
3. Yoshida S, Yamamoto M, Aoki H, Fukuda H, Akasu K, Takagi K, et al. STAT3 activation correlates with adventitial neutrophil infiltration in human aortic dissection. *Ann Vasc Dis*. (2019) 12:187–93. doi: 10.3400/avd.oa.19-00007
4. Anzai A, Shimoda M, Endo J, Kohno T, Katsumata Y, Matsuhashi T, et al. Adventitial CXCL1/G-CSF expression in response to acute aortic dissection triggers local neutrophil recruitment and activation leading to aortic rupture. *Circ Res*. (2015) 116:612–23. doi: 10.1161/CIRCRESAHA.116.304918
5. Kurihara T, Shimizu-Hirota R, Shimoda M, Adachi T, Shimizu H, Weiss SJ, et al. Neutrophil-derived matrix metalloproteinase 9 triggers acute aortic dissection. *Circulation*. (2012) 126:3070–80. doi: 10.1161/CIRCULATIONAHA.112.097097
6. Kalkan ME, Kalkan AK, Gündeş A, Yanartaş M, Oztürk S, Gurbuz AS, et al. Neutrophil to lymphocyte ratio: a novel marker for predicting hospital mortality of patients with acute type A aortic dissection. *Perfusion*. (2017) 32:321–7. doi: 10.1177/0267659115590625
7. Li P, Li M, Lindberg MR, Kennett MJ, Xiong N, Wang Y. PAD4 is essential for antibacterial innate immunity mediated by neutrophil extracellular traps. *J Exp Med*. (2010) 207:1853–62. doi: 10.1084/jem.20100239
8. Brinkmann V, Reichard U, Goosmann C, Fauler B, Uhlemann Y, Weiss DS, et al. Neutrophil extracellular traps kill bacteria. *Science*. (2004) 303:1532–5. doi: 10.1126/science.1092385
9. Döring Y, Libby P, Soehnlein O. Neutrophil extracellular traps participate in cardiovascular diseases: recent experimental and clinical insights. *Circ Res*. (2020) 126:1228–41. doi: 10.1161/CIRCRESAHA.120.315931
10. Visonà SD, de Boer OJ, Mackaaij C, de Boer HH, Pertiwi KR, de Winter RW, et al. Immunophenotypic analysis of the chronological events of tissue repair in aortic medial dissections. *Cardiovasc Pathol*. (2018) 34:9–14. doi: 10.1016/j.carpath.2018.01.009
11. Lim HH, Jeong IH, An GD, Woo KS, Kim KH, Kim JM, et al. Evaluation of neutrophil extracellular traps as the circulating marker for patients with acute coronary syndrome and acute ischemic stroke. *J Clin Lab Anal*. (2020) 34:e23190. doi: 10.1002/jcla.23190
12. Novotny J, Oberdieck P, Titova A, Pelisek J, Chandraratne S, Nicol P, et al. Thrombus NET content is associated with clinical outcome in stroke and myocardial infarction. *Neurology*. (2020) 94:e2346–60. doi: 10.1212/WNL.0000000000009532
13. Yang S, Qi H, Kan K, Chen J, Xie H, Guo X, et al. Neutrophil extracellular traps promote hypercoagulability in patients with sepsis. *Shock*. (2017) 47:132–9. doi: 10.1097/SHK.0000000000000741
14. Hiratzka LF, Bakris GL, Beckman JA, Bersin RM, Carr VF, Casey DE Jr, et al. 2010 ACCF/AHA/AATS/ACR/ASA/SCA/SCAI/SIR/STS/SVM Guidelines for the diagnosis and management of patients with thoracic aortic disease. A Report of the American College of Cardiology Foundation/American Heart Association Task Force on Practice Guidelines, American Association for Thoracic Surgery, American College of Radiology, American Stroke Association, Society of Cardiovascular Anesthesiologists, Society for Cardiovascular Angiography and Interventions, Society of Interventional Radiology, Society of Thoracic Surgeons, and Society for Vascular Medicine. *J Am Coll Cardiol*. (2010) 55:e27–129. doi: 10.1016/j.jacc.2010.02.010
15. Borissoff JI, Joosen IA, Versteylen MO, Brill A, Fuchs TA, Savchenko AS, et al. Elevated levels of circulating DNA and chromatin are independently associated with severe coronary atherosclerosis and a prothrombotic state. *Arterioscler Thromb Vasc Biol*. (2013) 33:2032–40. doi: 10.1161/ATVBAHA.113.301627
16. Fadini GP, Menegazzo L, Rigato M, Scattolini V, Poncina N, Bruttocao A, et al. NETosis delays diabetic wound healing in mice and humans. *Diabetes*. (2016) 65:1061–71. doi: 10.2337/db15-0863
17. Ravindran M, Khan MA, Palaniyar N. neutrophil extracellular trap formation: physiology, pathology, and pharmacology. *Biomolecules*. (2019) 9:365. doi: 10.3390/biom9080365
18. Papayannopoulos V. Neutrophil extracellular traps in immunity and disease. *Nat Rev Immunol*. (2018) 18:134–47. doi: 10.1038/nri.2017.105
19. Witko-Sarsat V, Mocek J, Bouayad D, Tamassia N, Ribeil J-A, Candalh C, et al. Proliferating cell nuclear antigen acts as a cytoplasmic platform controlling human neutrophil survival. *J Exp Med*. (2010) 207:2631–45. doi: 10.1084/jem.20092241
20. del Porto F, Proietta M, Tritapepe L, Miraldi F, Koverech A, Cardelli P, et al. Inflammation and immune response in acute aortic dissection. *Ann Med*. (2010) 42:622–9. doi: 10.3109/07853890.2010.518156
21. Valles J, Lago A, Santos MT, Latorre AM, Tembl JI, Salom JB, et al. Neutrophil extracellular traps are increased in patients with acute ischemic stroke: prognostic significance. *Thromb Haemost*. (2017) 117:1919–29. doi: 10.1160/TH17-02-0130
22. Tsai NW, Lin TK, Chen SD, Chang WN, Wang HC, Yang TM, et al. The value of serial plasma nuclear and mitochondrial DNA levels in patients with acute ischemic stroke. *Clin Chim Acta*. (2011) 412:476–9. doi: 10.1016/j.cca.2010.11.036
23. Liu Y, Carmona-Rivera C, Moore E, Seto NL, Knight JS, Pryor M, et al. Myeloid-specific deletion of peptidylarginine deiminase 4 mitigates atherosclerosis. *Front Immunol*. (2018) 9:1680. doi: 10.3389/fimmu.2018.01680
24. Gould TJ, Lysov Z, Liaw PC. Extracellular DNA and histones: double-edged swords in immunothrombosis. *J Thromb Haemost*. (2015) 13(Suppl. 1):S82–91. doi: 10.1111/jth.12977
25. Kambas K, Chrysanthopoulou A, Vassilopoulos D, Apostolidou E, Skendros P, Girod A, et al. Tissue factor expression in neutrophil extracellular traps and neutrophil derived microparticles in antineutrophil cytoplasmic antibody associated vasculitis may promote thromboinflammation and the thrombophilic state associated with the disease. *Ann Rheum Dis*. (2014) 73:1854–63. doi: 10.1136/annrheumdis-2013-203430
26. Gao Z, Pei X, He C, Wang Y, Lu J, Jin M, et al. Oxygenation impairment in patients with acute aortic dissection is associated with disorders of coagulation and fibrinolysis: a prospective observational study. *J Thorac Dis*. (2019) 11:1190–201. doi: 10.21037/jtd.2019.04.32
27. Gu G, Cheng W, Yao C, Yin J, Tong C, Rao A, et al. Quantitative proteomics analysis by isobaric tags for relative and absolute quantitation identified Lumican as a potential marker for acute aortic dissection. *J Biomed Biotechnol*. (2011) 2011:920763. doi: 10.1155/2011/920763
28. Proietta M, Tritapepe L, Cifani N, Ferri L, Taurino M, Del Porto F. MMP-12 as a new marker of Stanford-A acute aortic dissection. *Ann Med*. (2014) 46:44–8. doi: 10.3109/07853890.2013.876728
29. Yang G, Zhou Y, He H, Pan X, Chai X. Ischemia-modified albumin, a novel predictive marker of in-hospital mortality in acute aortic dissection patients. *Front Physiol*. (2019) 10:1253. doi: 10.3389/fphys.2019.01253
30. Wang HQ, Yang H, Tang Q, Gong YC, Fu YH, Wan F, et al. Identification of vinculin as a potential diagnostic biomarker for acute aortic dissection using label-free proteomics. *Biomed Res Int*. (2020) 2020:7806409. doi: 10.1155/2020/7806409
31. Ohlmann P, Faure A, Morel O, Petit H, Kabbaj H, Meyer N, et al. Diagnostic and prognostic value of circulating D-Dimers

in patients with acute aortic dissection. *Crit Care Med*. (2006) 34:1358–64. doi: 10.1097/01.CCM.0000216686.72457.EC
32. Marill KA. Serum D-dimer is a sensitive test for the detection of acute aortic dissection: a pooled meta-analysis. *J Emerg Med*. (2008) 34:367–76. doi: 10.1016/j.jemermed.2007.06.030
33. Suzuki T, Distante A, Zizza A, Trimarchi S, Villani M, Salerno Uriarte JA, et al. Diagnosis of acute aortic dissection by D-dimer: the International Registry of Acute Aortic Dissection Substudy on Biomarkers (IRAD-Bio) experience. *Circulation*. (2009) 119:2702–7. doi: 10.1161/CIRCULATIONAHA.108.833004
34. Paparella D, Malvindi PG, Scrascia G, de Ceglia D, Rotunno C, Tunzi F, et al. D-dimers are not always elevated in patients with acute aortic dissection. *J Cardiovasc Med*. (2009) 10:212–4. doi: 10.2459/JCM.0b013e32831c849e
35. Masuda S, Nakazawa D, Shida H, Miyoshi A, Kusunoki Y, Tomaru U, et al. NETosis markers: quest for specific, objective, and quantitative markers. *Clin Chim Acta*. (2016) 459:89–93. doi: 10.1016/j.cca.2016.05.029
36. Jorch SK, Kubes P. An emerging role for neutrophil extracellular traps in noninfectious disease. *Nat Med*. (2017) 23:279–87. doi: 10.1038/nm.4294
37. Martinod K, Demers M, Fuchs TA, Wong SL, Brill A, Gallant M, et al. Neutrophil histone modification by peptidylarginine deiminase 4 is critical for deep vein thrombosis in mice. *Proc Natl Acad Sci USA*. (2013) 110:8674–9. doi: 10.1073/pnas.1301059110

Conflict of Interest: The authors declare that the research was conducted in the absence of any commercial or financial relationships that could be construed as a potential conflict of interest.

Publisher's Note: All claims expressed in this article are solely those of the authors and do not necessarily represent those of their affiliated organizations, or those of the publisher, the editors and the reviewers. Any product that may be evaluated in this article, or claim that may be made by its manufacturer, is not guaranteed or endorsed by the publisher.

Advantages of publishing in Frontiers

OPEN ACCESS
Articles are free to read for greatest visibility and readership

FAST PUBLICATION
Around 90 days from submission to decision

HIGH QUALITY PEER-REVIEW
Rigorous, collaborative, and constructive peer-review

TRANSPARENT PEER-REVIEW
Editors and reviewers acknowledged by name on published articles

Frontiers
Avenue du Tribunal-Fédéral 34
1005 Lausanne | Switzerland

Visit us: www.frontiersin.org
Contact us: frontiersin.org/about/contact

REPRODUCIBILITY OF RESEARCH
Support open data and methods to enhance research reproducibility

DIGITAL PUBLISHING
Articles designed for optimal readership across devices

FOLLOW US
@frontiersin

IMPACT METRICS
Advanced article metrics track visibility across digital media

EXTENSIVE PROMOTION
Marketing and promotion of impactful research

LOOP RESEARCH NETWORK
Our network increases your article's readership